

27 May 2005

Science

Vol. 308 No. 5726
Pages 1209–1360 \$10

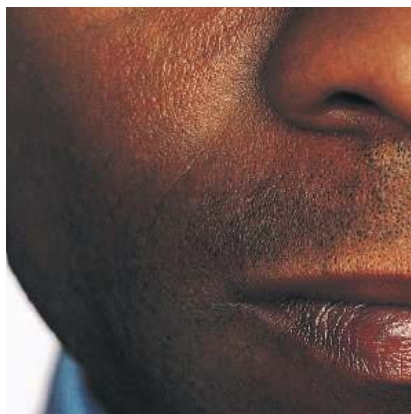
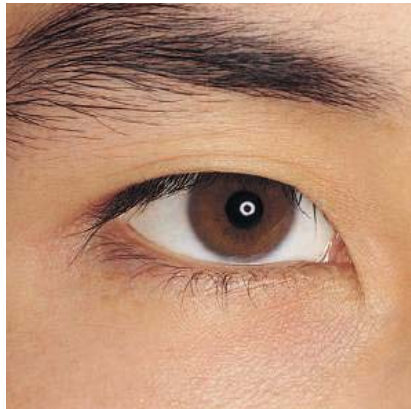


125
YEARS OF GLOBAL
Science

AAAS

WIN \$5,000 in FREE PRODUCT!

Visit www.cambrex.com/promotion/05CBIO for details.



Successful research is important to all of us.

Use Clonetics® Melanocyte Cell Systems.



Clonetics® Melanocyte Cell Systems contain normal human epidermal neonatal melanocytes (*shown on left*) and optimized media for their growth. Each system can quickly generate

melanocyte cultures for the study of pigmentation (melanogenesis), cellular differentiation, viral-induced transformation, antigen expression and cell adhesion. Clonetics Melanocyte Cell Systems are convenient and easy to use, allowing the researcher to focus on results.

Normal Human Epidermal Melanocyte Cell System **NEW**

- Cells are >90% functional based on verification of melanocyte conversion of L-dopa into dopa-melanin.
- New optimized media kit for melanocyte proliferation is superior to existing commercial media products.
- Guaranteed purity of >85% using immunofluorescent labeling of Mel-5.
- Cells, medium and reagents are quality tested together and guaranteed to give optimum performance as a complete “cell system”.

Cambrex, the source for Clonetics® and Poietics™ Cell Systems, BioWhittaker™ Classical Media, SeaPlaque® and NuSieve® Agarose, and PAGEr® Precast Gels.

For more information contact us at:
www.cambrex.com/prod.NHEM

U.S. 800-638-8174 | Europe 32 (0) 87 32 16 11

All trademarks herein are marks of Cambrex Corporation or its subsidiaries.
For Research Use Only. Not for Use in Diagnostic Procedures.

Cambrex Bio Science Walkersville, Inc.
8830 Biggs Ford Road | Walkersville, MD 21793

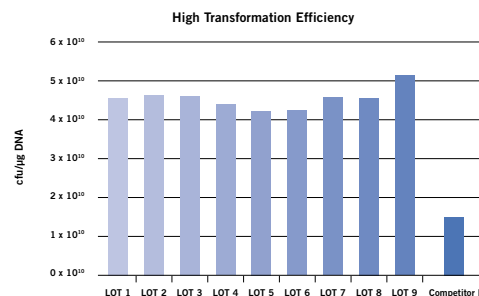


Innovation. Experience. Performance.



Three times more competent than the competition.
ElectroTen-Blue® cells give you the highest efficiency competent cells available.

Stratagene's newly improved ElectroTen-Blue® electrocompetent cells* offer the highest available transformation efficiencies of $\geq 3.0 \times 10^{10}$ cfu/ μ g of supercoiled pUC DNA. The high efficiency electroporation (Hee) phenotype improves the cell's ability to take up large and ligated plasmids. High efficiency, ease-of-use, and the Hee phenotype make ElectroTen-Blue electrocompetent cells ideal for your most demanding cloning applications.



We compared transformation efficiencies across several lots of ElectroTen-Blue® electroporation-competent cells and one lot of competitor cells. Consistent lot to lot results ensure success in all of your cloning projects.

Need More Information? Give Us A Call:

Stratagene USA and Canada
Order: (800) 424-5444 x3
Technical Services: (800) 894-1304

Stratagene Europe
Order: 00800-7000-7000
Technical Services: 00800-7400-7400

Stratagene Japan K.K.
Order: 03-5159-2060
Technical Services: 03-5159-2070

www.stratagene.com

Ask Us About These Great Products:

ElectroTen-Blue® Electroporation-Competent Cells 5 x 0.1-ml 200159



*U.S. Patent Nos. 6,635,457, 6,586,249, 6,338,965, 6,040,184 and patents pending.



Amersham
Biosciences

Part of GE Healthcare

Before you put our radionucleotides to the test

We put them to the test

Radionucleotides from GE Healthcare are made to perform. Our ^{32}P and ^{33}P nucleotides are tested in DNA-labeling experiments before shipping, so you can be confident they'll work in your application. But what's more, they're manufactured frequently and dispensed from local sites, so you can always rely on rapid delivery of the freshest material. For your convenience, they're available in a variety of pack sizes and formats, which can be customized to your specific needs. All of which adds up to a refreshingly easy way to ensure the best results in your research.

Visit www.amershambiosciences.com/radiochemicals



imagination at work



COVER A collage, based on botanical drawings of the 17th to 19th centuries, illustrating the different categories of rapid plant movement: *Dionea muscipula* uses a snap buckling movement to capture prey; *Astomeria* uses an explosive fracture to disperse its seeds ballistically; and *Pharbitis nil* twirls its tendrils in search of support through swelling. Also shown are formulas (see page 1308) for the physical limits of rapid plant and fungal movements. [Image: Ellen Skotheim]

DEPARTMENTS

- 1219 SCIENCE ONLINE
- 1221 THIS WEEK IN SCIENCE
- 1225 EDITORIAL by Peter Crane and Ann Kinzig
Nature in the Metropolis
- 1227 EDITORS' CHOICE
- 1230 CONTACT SCIENCE
- 1233 NETWATCH
- 1272 AAAS NEWS AND NOTES
- 1327 NEW PRODUCTS
- 1338 SCIENCE CAREERS

NEWS OF THE WEEK

- 1234 **INFECTIOUS DISEASES**
Genetic Analyses Suggest Bird Flu Virus Is Evolving
- 1234 **TOXICOLOGY**
House Would Foil Human Pesticide Studies
- 1235 **SMALLPOX**
WHA Gives Yellow Light for Variola Studies
- 1237 **PLANETARY SCIENCE**
Voyager 1 Crosses a New Frontier and May Save Itself From Termination
- 1237 SCIENCE SCOPE
- 1238 **NUMBER THEORY**
Third Time Proves Charm for Prime-Gap Theorem
- 1239 **SOCIOLOGY**
Controversial Study Suggests Seeing Gun Violence Promotes It
related Report page 1323
- 1240 **BIOCHEMISTRY**
Plant Hormone's Long-Sought Receptor Found
- 1241 **2006 BUDGET**
Physics Research Gets a Boost and a Warning From Its Funders
- 1241 **SCIENCE AND THE LAW**
Butler Gets Break on Pending Appeal
- 1243 **FRENCH SCIENCE**
Cracks in the Monolith: CNRS Begins a Long-Awaited Reform

NEWS FOCUS

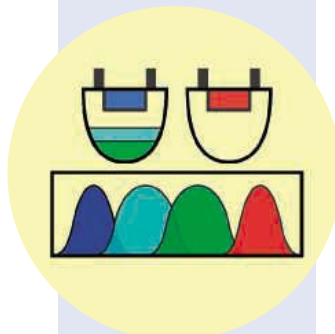
- 1244 **NATIONAL LABS**
A Bidding War for Los Alamos
- 1247 **PLANETARY SCIENCE**
Comet Crackup Will Spur Science, Whatever the Result
- 1248 **CANCER**
Encouraging Results for Second-Generation Antiangiogenesis Drugs
- 1249 **ASTRONOMY**
Turbulent Orion Nebula Shows a Flare for the Dramatic



1244



1261



1263 &
1274

- 1251 **ECOLOGY**
Israeli Controversy Blossoms Over Protecting Gilboa Iris
- 1253 RANDOM SAMPLES

LETTERS

- 1257 The Future of Farming and Conservation
J. Vandermeer and I. Perfecto. Response R. E. Green et al. Fossil Horses and Rate of Evolution K. R. Dronamraju. Response B. J. MacFadden. HIV and Smallpox R. A. Gruters and A. D. M. E. Osterhaus. Response D. Nolan et al. How Similar Are Poxviruses? R. Mezeencev and K. Mereish
- 1260 Corrections and Clarifications

BOOKS ET AL.

- 1261 **ANTHROPOLOGY**
When They Severed Earth from Sky How the Human Mind Shapes Myth
E. W. Barber and P. T. Barber, reviewed by A. A. Baird
- 1262 **NEUROSCIENCE**
Brain Fiction Self-Deception and the Riddle of Confabulation
W. Hirstein, reviewed by A. Schnider

POLICY FORUM

- 1263 **ENVIRONMENT**
The Specter of Fuel-Based Lighting
E. Mills
related Review page 1274

PERSPECTIVES

- 1265 **ASTRONOMY**
The Link Between Supernovae and Gamma Ray Bursts
B. Schmidt
related Report page 1284
- 1266 **CELL BIOLOGY**
Lessons in Rational Drug Design for Protein Kinases
N. G. Ahn and K. A. Resing
related Report page 1318
- 1267 **GEOCHEMISTRY**
When Do Rocks Become Oil?
B. F. Schaefer
related Report page 1293
- 1268 **MATERIALS SCIENCE**
Designing Superhard Materials
R. B. Kaner, J. J. Gilman, S. H. Tolbert
- 1269 **BIOMEDICINE**
Hamiltonian Medicine: Why the Social Lives of Pathogens Matter
K. R. Foster

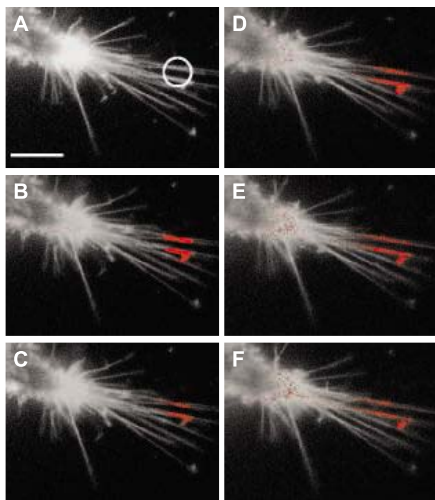
REVIEW

- 1274 **APPLIED PHYSICS**
Solid-State Light Sources Getting Smart
E. F. Schubert and J. K. Kim
related Policy Forum page 1263

TAGGED



EVROGEN
www.evrogen.com



Use of the photoactivatable protein PS-CFP to track dopamin transporter traffic in cell filopodia.

Unique collection of fluorescent proteins:

- bright fluorescence ranging in color from cyan to far-red
- successful performance in various fusions
- proven availability for creating stably transfected cell lines
- photoactivatable tags to track cellular events in real-time
- broad spectrum of expression vectors for research and commercial use

DNA technologies for gene hunters:

- cDNA normalization: kits and service
- custom cDNA subtractive hybridization
- custom cDNA library construction
- custom RACE
- custom genome walking
- custom gene synthesis and mutagenesis
- all kinds of DNA cloning

Cost-effective licensing program
Prompt and friendly support
Convenient service
Wide list of international distributors
Flexible discount programs

Evrogen JSC
Miklukho-Maklaya str, 16/10,
117997, Moscow, Russia
Tel: +7(095) 429 8020
Fax: +7(095) 429 8520
E-mail: order@evrogen.com
Licensing: license@evrogen.com

Qs & AAAS



www.sciencedigital.org/subscribe

For just US\$130, you can join AAAS TODAY and start receiving *Science* Digital Edition immediately!

Qs & AAAS



www.sciencedigital.org/subscribe

For just US\$130, you can join AAAS TODAY and start receiving *Science* Digital Edition immediately!

SCIENCE EXPRESS www.scienceexpress.org

MEDICINE: Protection from Experimental Asthma by an Endogenous Bronchodilator

L. G. Que, L. Liu, Y. Yan, G. S. Whitehead, S. H. Gavett, D. A. Schwartz, J. S. Stamler

A nitric oxide-carrying molecule protects against hyperreactivity of lung airways in a model of asthma.

CELL BIOLOGY: MicroRNA Expression in Zebrafish Embryonic Development

E. Wienholds, W. P. Kloosterman, E. Miska, E. Alvarez-Saavedra, E. Berezikov, E. de Bruijn, H. R. Horvitz, S. Kauppinen, R. H. A. Plasterk

miRNA expression patterns in embryonic vertebrate development are exquisitely complex. Maps of RNA expression in zebrafish embryos indicate that small noncoding RNAs participate widely in the later stages of development, controlling tissue differentiation and identity.

ASTRONOMY: Discovery of Pulsed OH Maser Emission Stimulated by a Pulsar

J. M. Weisberg, S. Johnston, B. Koribalski, S. Stanimirović

Photons from a pulsar produce stimulated emission in an interstellar molecular cloud, the same fundamental process that generates light in a laser.



TECHNICAL COMMENT ABSTRACTS

1260 **NEUROSCIENCE**

Comment on "The Involvement of the Orbitofrontal Cortex in the Experience of Regret"

D. M. Eagleman

[full text at www.sciencemag.org/cgi/content/full/308/5726/1260b](http://www.sciencemag.org/cgi/content/full/308/5726/1260b)

Response to Comment on "The Involvement of the Orbitofrontal Cortex in the Experience of Regret"

G. Coricelli, N. Camille, P. Pradat-Diehl, J.-R. Duhamel, A. Sirigu

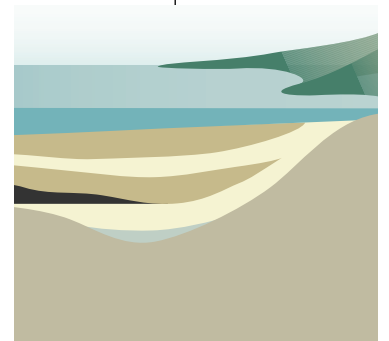
[full text at www.sciencemag.org/cgi/content/full/308/5726/1260c](http://www.sciencemag.org/cgi/content/full/308/5726/1260c)

BREVIA

1279 **CHEMISTRY: High-Resolution NMR Spectroscopy with a Portable Single-Sided Sensor**

J. Perlo, V. Demas, F. Casanova, C. A. Meriles, J. Reimer, A. Pines, B. Blümich

A nuclear magnetic resonance spectrometer is adapted for use in the field by compensating for the variation in the field produced by a one-sided probe.



RESEARCH ARTICLE

1280 **ECOLOGY: Bottom-Up Ecosystem Trophic Dynamics Determine Fish Production in the Northeast Pacific**

D. M. Ware and R. E. Thomson

Satellite imaging of chlorophyll shows that local areas with more phytoplankton in the ocean off northwestern North America also contain larger fish populations.

REPORTS

1284 **ASTRONOMY: An Asymmetric Energetic Type Ic Supernova Viewed Off-Axis, and a Link to Gamma Ray Bursts**

P. A. Mazzali, K. S. Kawabata, K. Maeda, K. Nomoto, A. V. Filippenko, E. Ramirez-Ruiz, S. Benetti, E. Pian, J. Deng, N. Tominaga, Y. Ohyama, M. Iye, R. J. Foley, T. Matheson, L. Wang, A. Gal-Yam

Observations of supernova SN2003jd suggest a strongly aspherical explosion that could have produced gamma ray bursts. *related Perspective page 1265*

1287 **PHYSICS: Scaling in the Time Domain: Universal Dynamics of Order Fluctuations in Fe₃Al**
C. Mocuta, H. Reichert, K. Mecke, H. Dosch, M. Drakopoulos

Focusing a brilliant x-ray beam on a small sample spot allows imaging of how atomic order fluctuates in a crystal during a phase transition.

1291 **PLANETARY SCIENCE: Amalthea's Density Is Less Than That of Water**

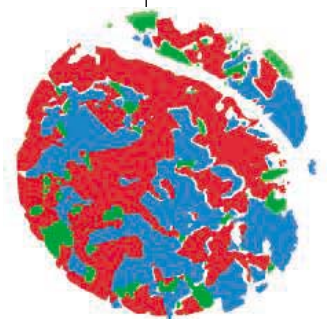
J. D. Anderson, T. V. Johnson, G. Schubert, S. Asmar, R. A. Jacobson, D. Johnston, E. L. Lau, G. Lewis, W. B. Moore, A. Taylor, P. C. Thomas, G. Weinwurm

Jupiter's small inner moon Amalthea seems to be mostly porous ice, implying that it formed in a cold region of space and was later captured by the giant planet.

1293 **GEOCHEMISTRY: Direct Radiometric Dating of Hydrocarbon Deposits Using Rhenium-Osmium Isotopes**

D. Selby and R. A. Creaser

Rhenium-osmium dating in oil reveals when petroleum migrates to a reserve and shows that the giant Alberta oil sands formed 112 million years ago. *related Perspective page 1267*

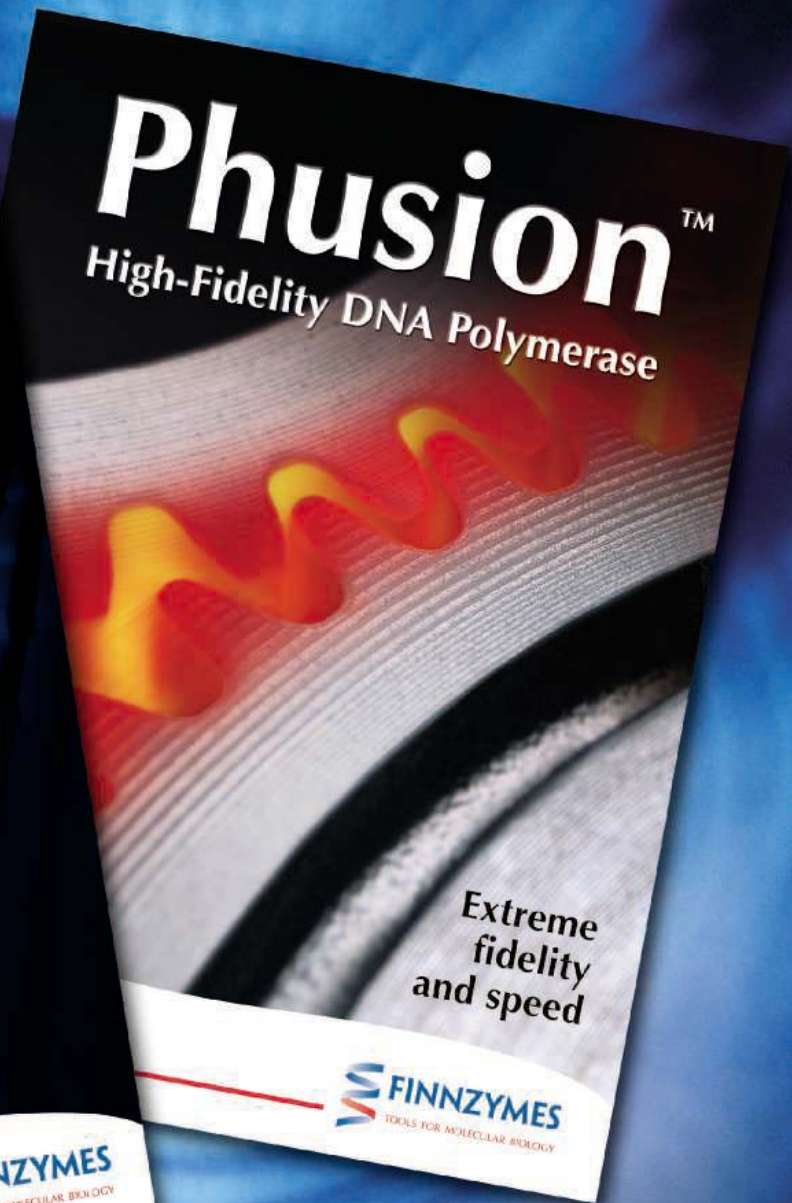
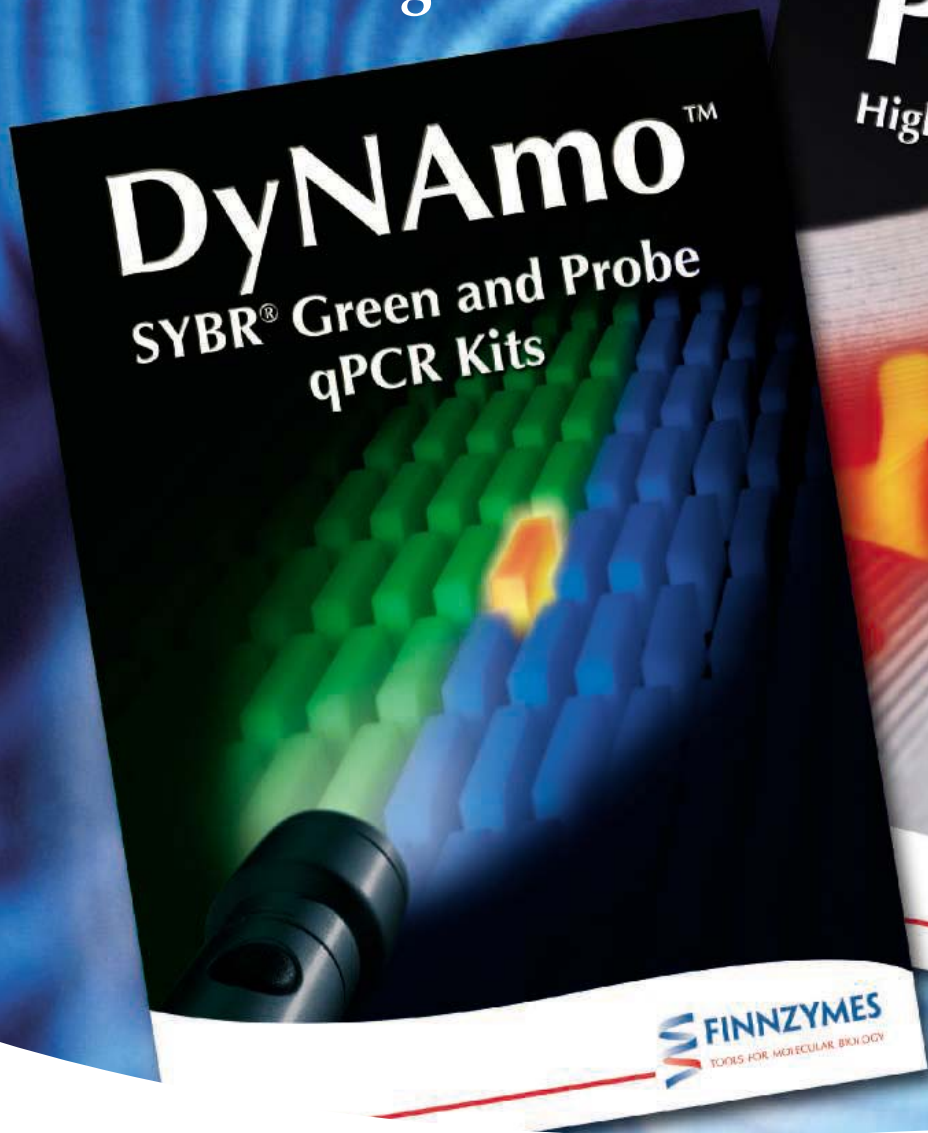


1267 &
1293

1303

Contents continued ►

Synergy
exceptional products,
outstanding service



Finnzymes and New England Biolabs Working Together to Advance PCR and qPCR Technology

New England Biolabs (NEB) is now the exclusive distributor of Finnzymes' PCR-licensed products: Phusion™ High-Fidelity DNA Polymerase, DyNAmo™ SYBR® Green qPCR Kits, and DyNAzyme™ DNA Polymerases in the United States and Canada. Together, the expertise of Finnzymes

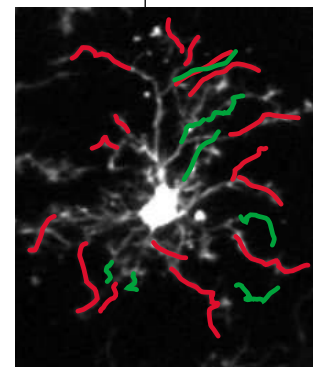
and NEB delivers an unsurpassed product offering for researchers utilizing modern molecular biology techniques. Finnzymes and NEB, state-of-the-art products, exceptional quality and outstanding service. That's synergy. For more information, visit www.finnzymes.com or www.neb.com



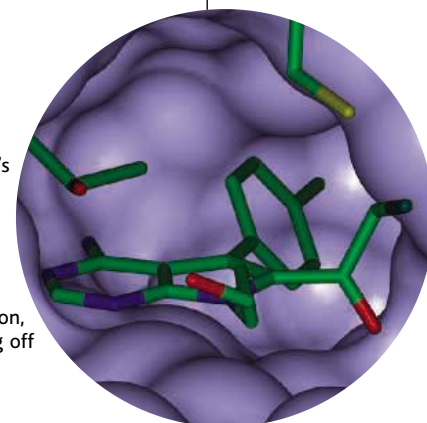
Phusion, DyNAmo and DyNAzyme are trademarks of Finnzymes Oy. SYBR is a registered trademark of Molecular Probes. PCR license notice: These products are sold under licensing arrangements of Finnzymes Oy with E.Hoffman-La Roche LTD, Roche Molecular Systems, Inc. and The Perkin-Elmer Corporation. The purchase of these products is accompanied by a limited licence to use them in the Polymerase Chain Reaction (PCR) process in conjunction with a thermal cycler whose use in the automated performance of the PCR process is covered by the up-front fee, either by payment to Perkin-Elmer or as purchased, i.e. an authorized thermal cycler.

REPORTS CONTINUED

- 1296 **APPLIED PHYSICS:** Simultaneous Inhibition and Redistribution of Spontaneous Light Emission in Photonic Crystals
M. Fujita, S. Takahashi, Y. Tanaka, T. Asano, S. Noda
 A two-dimensional photonic crystal combined with high refractive index material can simultaneously inhibit and redistribute spontaneous light emission from selected defects in the photonic crystal.
- 1299 **CHEMISTRY:** Identifying Vibrations That Destabilize Crystals and Characterize the Glassy State
G. N. Greaves, F. Meneau, O. Majérus, D. G. Jones, J. Taylor
 A structural origin for the low-frequency boson mode in glasses has been identified from a vibrational study of an amorphized zeolite.
- 1303 **MATERIALS SCIENCE:** The Importance of Threading Dislocations on the Motion of Domain Boundaries in Thin Films
F. El Gabaly, W. L. W. Ling, K. F. McCarty, J. de la Figuera
 Direct observations show that grain boundaries move unevenly but in preferred directions in a thin film until they become fixed, in part by atomic defects.
- 1305 **MICROBIOLOGY:** A Microbial Arsenic Cycle in a Salt-Saturated, Extreme Environment
R. S. Oremland, T. R. Kulp, J. S. Blum, S. E. Hoefft, S. Baesman, L. G. Miller, J. F. Stolz
 Using only inorganic electron donors, an anaerobic bacterium helps drive a full biogeochemical cycle of arsenic in highly contaminated Searle's Lake, California.
- 1308 **PLANT SCIENCE:** Physical Limits and Design Principles for Plant and Fungal Movements
J. M. Skotheim and L. Mahadevan
 Movement in plants leads to insights into how hydraulically driven systems operate.
- 1310 **EVOLUTION:** The Effects of Artificial Selection on the Maize Genome
S. I. Wright, I. V. Bi, S. G. Schroeder, M. Yamasaki, J. F. Doebley, M. D. McMullen, B. S. Gaut
 The early domestication of maize from the wild grass teosinte selected genes that affect the plant's growth habit, many of which are also now agriculturally important loci.
- 1314 **NEUROSCIENCE:** Resting Microglial Cells Are Highly Dynamic Surveillants of Brain Parenchyma in Vivo
A. Nimmerjahn, F. Kirchhoff, F. Helmchen
 Imaging of resident immune cells in the living mouse brain reveals that they are always in motion, continuously sending out processes and protuberances and reacting quickly to damage by sealing off the injured area.
- 1318 **BIOCHEMISTRY:** Structural Bioinformatics-Based Design of Selective, Irreversible Kinase Inhibitors
M. S. Cohen, C. Zhang, K. M. Shokat, J. Taunton
 Analysis of the apparently similar catalytic sites of two ubiquitous enzymes enables the design of small molecules that inhibit only one of them, and therefore may be useful as targeted drugs.
related Perspective page 1266
- 1321 **BIOCHEMISTRY:** Global Topology Analysis of the *Escherichia coli* Inner Membrane Proteome
D. O. Daley, M. Rapp, E. Granseth, K. Melén, D. Drew, G. von Heijne
 Visible markers attached to one end of each membrane protein facilitate its assignment as facing the cytoplasm or the periplasm.
- 1323 **SOCIOLOGY:** Firearm Violence Exposure and Serious Violent Behavior
J. B. Bingenheimer, R. T. Brennan, F. J. Earls
 If adolescents are exposed to firearm violence, the odds increase that they will perpetrate violence within a few years. *related News story page 1239*



1314



1266 &
1318



ADVANCING SCIENCE. SERVING SOCIETY

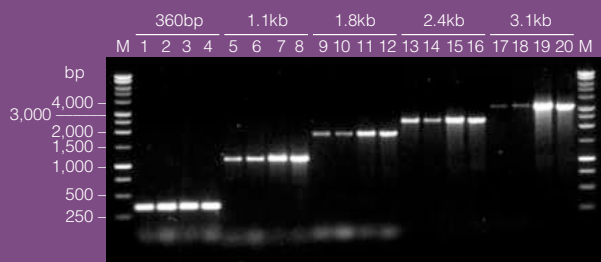
SCIENCE (ISSN 0036-8075) is published weekly on Friday, except the last week in December, by the American Association for the Advancement of Science, 1200 New York Avenue, NW, Washington, DC 20005. Periodicals Mail postage (publication No. 484460) paid at Washington, DC, and additional mailing offices. Copyright © 2005 by the American Association for the Advancement of Science. The title SCIENCE is a registered trademark of the AAAS. Domestic individual membership and subscription (51 issues): \$135 (\$74 allocated to subscription). Domestic institutional subscription (51 issues): \$550; Foreign postage extra: Mexico, Caribbean (surface mail) \$55; other countries (air assist delivery) \$85. First class, airmail, student, and emeritus rates on request. Canadian rates with GST available upon request, GST #1254 88122. Publications Mail Agreement Number 1069624. Printed in the U.S.A.

Change of address: allow 4 weeks, giving old and new addresses and 8-digit account number. Postmaster: Send change of address to Science, P.O. Box 1811, Danbury, CT 06813-1811. Single copy sales: \$10.00 per issue prepaid includes surface postage; bulk rates on request. Authorization to photocopy material for internal or personal use under circumstances not falling within the fair use provisions of the Copyright Act is granted by AAAS to libraries and other users registered with the Copyright Clearance Center (CCC) Transactional Reporting Service, provided that \$15.00 per article is paid directly to CCC, 222 Rosewood Drive, Danvers, MA 01923. The identification code for Science is 0036-8075/83 \$15.00. Science is indexed in the Reader's Guide to Periodical Literature and in several specialized indexes.

Contents continued ►



Get remarkably robust DNA amplification. Again and again and again.



Regular *Taq* vs. GoTaq DNA Polymerase over a wide range of target sizes. In each set the left two lanes are *Taq* DNA Polymerase and the right two lanes are GoTaq DNA Polymerase.

Reap the benefits of consistent, robust performance every time you amplify with GoTaq® Polymerases.

- Harvest spectacular yields with optimal enzyme and buffer
- See faster results with the all-in-one reaction buffer that doubles as a gel loading buffer
- Perform perfect gel tracking with the GoTaq Green buffer – tracks small fragments and bumper products
- Enjoy the Promega PCR Performance Guarantee

Prove it to yourself...again and again and again.

To learn more, visit www.promega.com/gotaq

PROMEGA CORPORATION • www.promega.com

©2004 Promega Corporation 12362-AD-MD

Certain applications of this product are covered by patents issued and applicable in certain countries. Because purchase of this product does not include a license to perform any patented application, users of this product may be required to obtain a patent license depending upon the particular application and country in which the product is used.



Promega

The Quake That Shook the World

December's Sumatran earthquake triggered small events across the globe.

What Price Recollection?

Forming long-term memories shortens life in fruit flies.

Any Stegosaurus 'Round These Parts?

Dinos' plates and spikes may have helped creatures recognize each other.



Too much time in one lab?

science's next wave www.nextwave.org CAREER RESOURCES FOR YOUNG SCIENTISTS

UK: Time to Change Lab *CareerDoctor*

How long can you stay in the same lab before it becomes damaging to your career?

UK: Standing in the Welfare Line *P. Dee*

A scientist is haunted by failure as he ponders his first few weeks out of work.

US: A Grim Outlook for American Scientists *B. Benderly*

A generally pessimistic picture emerged at the annual AAAS Forum on Science and Technology.

US: Educated Woman, Chapter 39—Who Am I? *M. P. DeWhyse*

No test will tell you where to go, what to do, and whom to do it for.

MISciNET: Narrowing the Diversity Gap in Marine Science *E. Francisco*

A program at Western Washington University exposes minority students to careers in marine science.

science's sage ke www.sageke.org SCIENCE OF AGING KNOWLEDGE ENVIRONMENT

REVIEW: Nitric Oxide and Oxidative Stress in Cardiovascular Aging *S. V. Y. Raju, L. A. Barouch, J. M. Hare*

Researchers say NO thanks to oxidative stress.

NEWS Focus: The Skeleton Goes to Pot *R. J. Davenport*

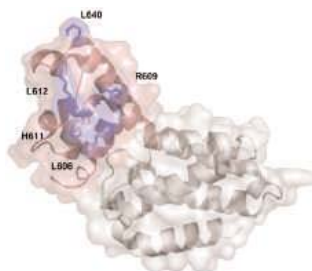
Prodding marijuana receptors spurs bone loss.

NEWS Focus: Hush, Little Gene *M. Leslie*

Mystery molecule helps gene-quieting protein mothball DNA.



Bones go up in flames.



SAM domain (pink) for binding RNA.

science's stke www.stke.org SIGNAL TRANSDUCTION KNOWLEDGE ENVIRONMENT

REVIEW: The Many Faces of SAM *F. Qiao and J. U. Bowie*

The protein module known as a SAM domain provides many signaling proteins with an interface for interaction with diverse functional partners.

TEACHING RESOURCE: Nuclear Receptors *R. Taneja*

Prepare a graduate-level class covering nuclear receptor activation and regulation.

Separate individual or institutional subscriptions to these products may be required for full-text access.

Confidence in FLAG® Fusion Protein Detection – Now Even Better!

Introducing our NEW and IMPROVED Affinity Purified ANTI-FLAG® M2 Antibody

- *Enhanced Specificity*
- *Superior Sensitivity*
- *Improved Stability*

Consistent with Sigma's goal to continually improve our product offerings, we have developed a **New and Improved ANTI-FLAG M2 Antibody**, a proven system for your most demanding applications! Whether performing Western blots, dot blots, ELISAs, immunoprecipitation, or immunocytochemistry, our new affinity purified ANTI-FLAG M2 antibody provides increased specificity with no detectable background. This new ANTI-FLAG M2 antibody offers superior sensitivity in its ability to

detect less than 1 ng of recombinant protein. Also, the new 50% glycerol formulation offers improved stability avoiding damage caused by freeze/thaw cycles.

Let Sigma be your partner in innovation. As a **true leader** in recombinant protein detection, we're confident we can make your protein detection easier.

Product Code	Description
F1804	Monoclonal ANTI-FLAG M2 Affinity Purified Antibody

See for yourself!

For more information about our New and Improved ANTI-FLAG M2 antibody, visit us at:

sigma-aldrich.com/antiflag

Lighting's Latest Leitmotif

Conventional incandescent and fluorescent light sources are being replaced at a growing rate by illumination technologies such as light-emitting diodes. **Schubert and Kim** (p. 1274; see the Policy Forum by **Mills**) review the principles and applications of solid-state lighting. Not only can solid-state devices provide greater energy efficiency, but the nature of emission can be custom tailored—for example, indoor lighting could be programmed to change in its color spectrum just as the Sun's does during the day.

An Icy Realm

Amalthea is one of Jupiter's small inner moons whose orbit is within that of Io. The Galileo spacecraft passed close enough to Amalthea to obtain an estimate of its mass from radio Doppler data. Using estimates of its size from both Voyager and Galileo observations, **Anderson et al.** (p. 1291) calculate that its density is less than 1000 kilograms per cubic meter, which suggests that it is composed of mostly porous ice. These results are consistent with Amalthea having formed elsewhere and later captured by Jupiter.

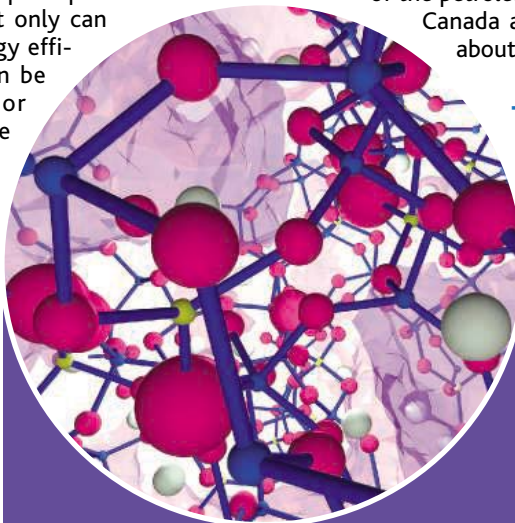
Asymmetrical Supernovae

When a star exhausts its nuclear fuel, gravitational forces cause the remaining stellar material to collapse, triggering a supernova explosion. Some of these events have been linked to very bright gamma ray bursts, an unusual and still not understood high-energy astrophysical phenomenon. Gamma ray bursts, however, require strongly asymmetric jet-like explosions, whereas supernovae have been thought to be mostly spherical explosions. **Mazzali et al.** (p. 1284) report recent supernova observations with the Subaru and Keck telescopes in which spectral lines of stellar material show an unusual double-peak structure indicative of an aspherical explosion. The results suggest that gamma ray bursts may be produced in supernovae, but they can remain unseen on Earth if they point in the wrong direction.

Direct Oil Dating

Petroleum deposits typically form when oil generated from source rocks collects beneath or in some geologic trap, such as under relatively impermeable rocks. Migration usually occurs long after the source rocks are deposited, and establishing the timing of migration and identifying the source rocks are critical for further exploration. Most isotopic dating systems, however,

date the history of the rock rather than the oil. **Selby and Creaser** (p. 1293; see the Perspective by **Schaefer**) now show that oil contains enough rhenium and osmium, inherited from organic-rich source rocks, to provide important direct ages on the history of the petroleum. Data for the great oil sand deposits of Canada all plot along a single isochron dating to about 112 million years ago.



Boson Peaks and Glass Formation

The origin of a characteristic feature in the vibrational spectra of glasses, a broadband of low-frequency modes (between 20 to 50 wavenumbers or 4 to 12 millielectron volts) called the Boson peak, has been a matter of debate; many explanations invoke collective modes reminiscent of phonon modes in crystals. **Greaves et al.** (p. 1299) have used high-resolution inelastic neutron scattering to follow the decay of low-frequency features in zeolite Y as they amorphize this open framework material to varying degrees. They identified vibrations that destabilize the crystalline state, and they can attribute the Boson peak to the coupling of oscillations between rings within the structures that have a range of sizes.

Timing Light Emission

One goal of photonic band gap engineering is to control the spontaneous decay rate of optical excitations. In practice, however, fabrication of high-quality samples with a fully three-dimensional (3D) bandgap is highly challenging. It was suggested that the strict requirements of a 3D bandgap could be relaxed by combining a 2D bandgap and a high-dielectric material. **Fujita et al.** (p. 1296) have prepared a series of such samples and show that spontaneous emission of an embedded emitter can indeed be inhibited. Simultaneously, the energy stored in the system can be redistributed and emitted from a specifically designed defect in the crystal structure.

Stalking Stacking Domains

When a metal is deposited onto a substrate that has a different lattice spacing, a domain texture will form, but the mechanism for forming this texture has been much debated. **El Gabaly et al.** (p. 1303) present a real-time study of the microscopic domain structure of a heteroepitaxial thin film of copper on a ruthenium substrate. By combining bright- and dark-field low-energy electron microscopy images, they could map both the stacking and rotational domains of the film and follow their temporal evolution on the

time scale of seconds. The boundaries between stacking domains within a given rotational domain move quickly and smoothly but get stuck at the rotational boundaries. Thus, the mobility of the stacking domains depends on the orientation and boundaries of the rotational domains, where threading dislocations represent an effective barrier for the gliding atomic planes.

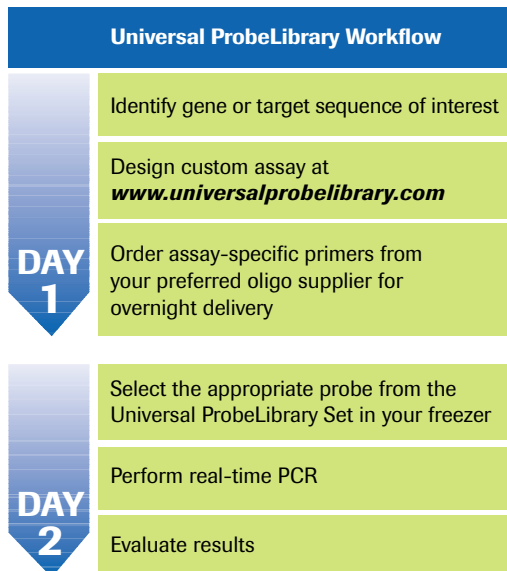
Plant Life in the Fast and Slow Lanes

The movements of plants vary in speed from the slow curling of a tendril to the rapid snapping of a Venus flytrap. **Skotheim and Mahadevan** (p. 1308; see the cover) have analyzed the diversity of plant movements and find certain guiding principles to the



Roche Applied Science
Universal ProbeLibrary

Design Your Gene-Expression Assay Today— *Run it Tomorrow!*



Significantly reduce assay design time – In just seconds, design specific, intron-spanning real-time qPCR assays for human, mouse, rat, *Drosophila*, *Arabidopsis*, *C. elegans*, and primates.

Create cost-effective assays with high specificity for your gene of interest – The Universal ProbeLibrary provides you with probe specificity at prices comparable to SYBR Green I.

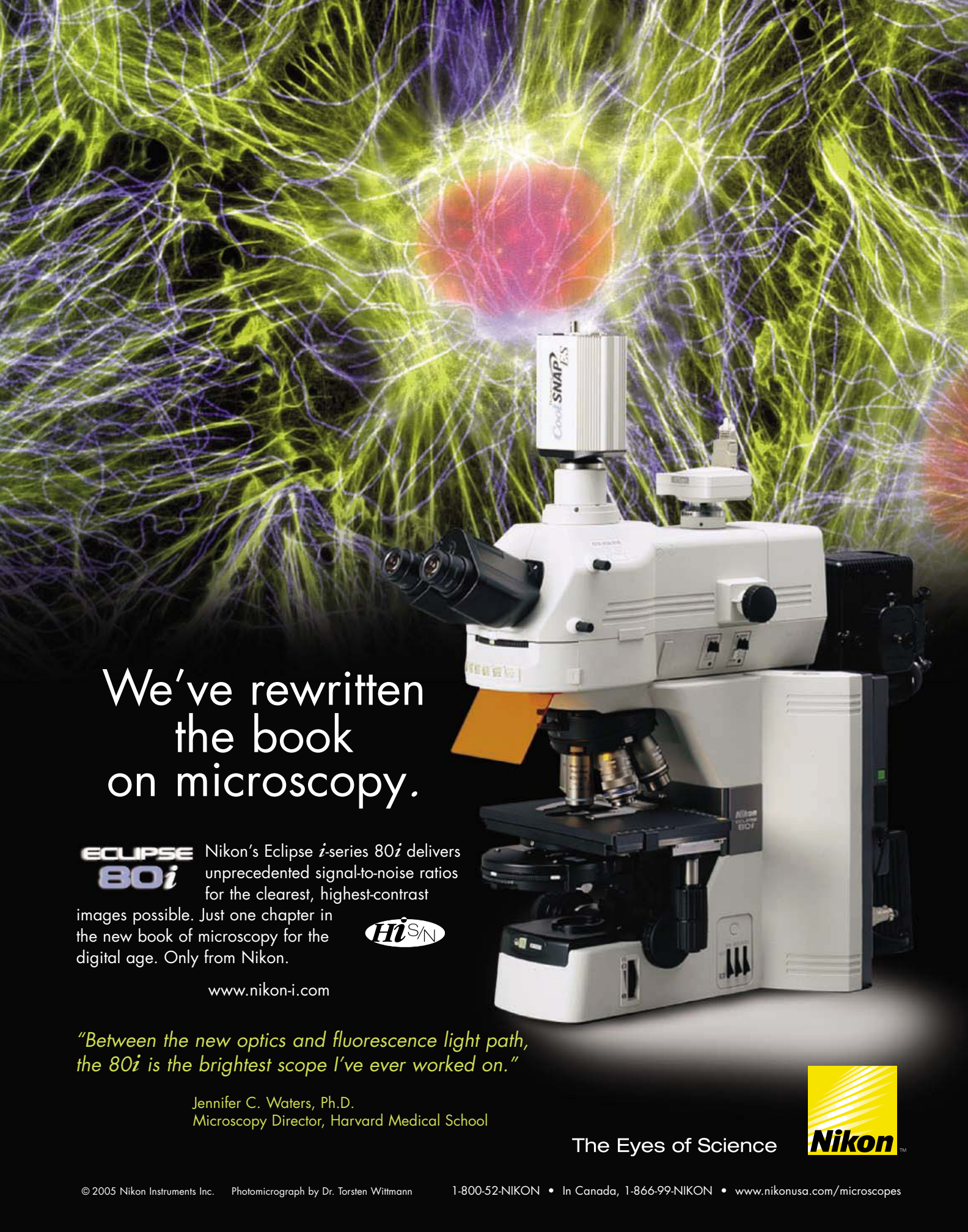
Why wait 1–4 weeks for an assay or custom probe? Create a functional, highly specific, optimized assay overnight using pre-validated Universal ProbeLibrary probes. Choose individual probes or a complete set of 90 probes stored in your freezer.

No special hardware or unique reaction conditions required – Employ standard PCR protocols on any real-time PCR instrument.

For detailed information on the Universal ProbeLibrary and to design your next qPCR assay, visit www.universalprobelibrary.com



Diagnostics



We've rewritten the book on microscopy.

**ECLIPSE
80i**

Nikon's Eclipse *i*-series 80*i* delivers unprecedented signal-to-noise ratios for the clearest, highest-contrast images possible. Just one chapter in the new book of microscopy for the digital age. Only from Nikon.



www.nikon-i.com

"Between the new optics and fluorescence light path, the 80i is the brightest scope I've ever worked on."

Jennifer C. Waters, Ph.D.
Microscopy Director, Harvard Medical School

The Eyes of Science



Nature in the Metropolis

World Environment Day 2005 might be just the moment to highlight some pristine location that showcases what we most value about our environment: clean air, pure water, uncluttered landscapes, and rich plant and animal life. But instead, the United Nations (UN) Environment Programme turns to a city, San Francisco, as the focus for its celebrations. The reason is simple: Cities are where people concentrate, and what we find there—business, universities, government, and media—shapes public perceptions and political agendas.

This June, mayors from around the world will gather in San Francisco to discuss “green cities” and what sustainability means in the urban environment. The topic is timely because we are witnessing a key moment in the history of our species. For the first time, more people are living in cities than outside them. Now and into the future, we will be *Homo urbanus*: the city dweller.

This transition is profound. For one thing, it seems likely to be irreversible, at least under any scenario we would care to witness. For another, it is a manifestation of a relentless trend. It has taken a few millennia for the number of people living in cities to reach 3 billion. It will take only about 50 years to double that number. According to UN projections, cities will absorb nearly all of the growth in the human population over the next three decades. At the beginning of the 20th century, the three most populous cities were London (6.5 million), New York (4.2 million), and Paris (3.3 million). By 2015, Tokyo, Mumbai, and Delhi will top the list with populations between 20 and 37 million residents. But it isn't only the megacities that fuel the growth in urban populations. The number of urban areas with over 1 million people is expected to grow by over 40% between 2000 and 2015. The vast majority of this growth will be in middle- and low-income countries.



In some respects, cities are good for the environment. They concentrate half the world's population on about 2% of Earth's land surface, and they are undeniably centers of innovation and economic growth. However, they are also centers for the production of heat, waste, and pollution. The activities and demands of their residents can shape both nearby wilderness and globally distant sites, with better or worse environmental outcomes. If city mayors are to set out some steps on the path to sustainability, they will need to address these and many other interconnected issues as they seek to enhance the quality of life of urban residents, particularly the poor, in an environmentally sustainable fashion.

A further subtle but important consequence of increased urbanization is that most of the world's people will have much of their direct contact with nature in an urban rather than rural setting. We don't know what the long-term effect of this might be, but one likely outcome is increasing urban-versus-rural disagreement on priorities for the urban hinterland. For instance, what constitutes appropriate wildlife or habitat management? It seems very likely that our environmental ethic will gradually change.

Whatever the future of our environmental ethic, one thing is clear: What remains of habitats and biodiversity within the city is of disproportionate importance. And, perhaps surprisingly, these may also be of national or even global significance. São Paulo, Brazil, contains important fragments of the Atlantic Rain Forest embedded within its conurbation. Significant remnants of the unique Cape Floristic Province persist within and around Cape Town in South Africa. Even in London, there are still superb opportunities to connect with nature, from the restored wetlands of Barn Elms to the acid grasslands of Richmond Park.

If World Environment Day is anything, it is a day of reflection, and hopefully a day for commitment. Excellent partnerships for managing nature in the city are already under way, such as the Chicago Wilderness Consortium in the United States, which comprises 172 public and private organizations working together to protect, restore, and manage Chicago's natural resources. Such efforts need to be emulated. Extending them further will also require an integrated science of urbanization that is today woefully inadequate. We must move quickly. And we must remember that nature in the metropolis needs to be nurtured, not only for its value now, but even more for its importance in the future.

Peter Crane and Ann Kinzig

Peter Crane is director of the Royal Botanic Gardens, Kew, UK. Ann Kinzig is an associate professor of Urban Ecology at Arizona State University, USA.

10.1126/science.1114165

IDT *Breaking all the Barriers!*



© Photo property of United States Government.

IDT is breaking all the barriers with our new **Express DLP™** synthesis service! The *fastest turnaround* time coupled with the *lowest price* available, gives researchers the opportunity to receive their dual-labeled probes in just *two working days!* All **Express DLPs™** are HPLC purified and quality control checked by mass spectrometry. As always, the QC data is available FREE on our website.

Reporter: 5' 6-FAM™

Quencher	Guaranteed Yield	Price
3' Iowa Black™ FQ	10 nmole	\$99!
3' Black Hole Quencher®-1	10 nmole	\$99!
3' TAMRA™	10 nmole	\$99!

Express DLP™ Specifications:

Next day shipping!

HPLC Purified

QC verified by mass spectrometry

Innovation & Precision in Nucleic Acid Synthesis

1710 Commercial Park
Coralville, IA 52241 USA
800.328.2661 fax: 319.626.8444
www.idtdna.com

XXE IDT
INTEGRATED **DNA**
TECHNOLOGIES, INC.

edited by Gilbert Chin

GEOPHYSICS

Experimenting in the Kitchen

The surfaces of basaltic lavas commonly exhibit two kinds of textures: Pāhoehoe flows form a ropy and relatively smooth surface, and 'a'ā flows look like jumbled, sharp, angular blocks. It is generally thought that these types reflect an interaction between the viscosity of the lava, which varies as it cools and crystals form, and the shear rate of the flow. Many flows change their morphology from pāhoehoe to 'a'ā, and a few change back.

To investigate this transition, Soule and Cashman carried out a series of laboratory experiments using corn syrup (diluted to the viscosity of hot basaltic magma) and rice (which has the same density as the diluted syrup and represents the lava crystals). They observed four different regimes: With increasing amounts of rice (corresponding to



Pāhoehoe (above) and 'a'ā (left) lavas.

increasing viscosity), flow is laminar; the rice grains aggregate into clumps; shear zones form between the clumps; and finally, a thin film of rice-free syrup appears along the flow boundary, perhaps by cavitation, and the main flow is thus detached. This evolution and the abrupt transitions between these regimes are consistent with field measurements of the pāhoehoe-to-'a'ā transition. — BH

Geology 33, 361 (2005).

tionalize alkanes under mild conditions. For poly(2-butene), which can be thought of as polyethylene with a methyl branch at every third carbon, grafting occurred at the tertiary carbons. For random copolymers of ethylene and 1-octene, grafting occurred primarily at the secondary carbons and was controlled by the ratio of polymer to graft monomer. The authors also showed that they could also functionalize polypropylene, primarily at the secondary carbons, without any of the chain scission problems that plague the traditional radical-initiated methods. — MSL

Macromolecules 10.1021/ma050626f (2005).

PSYCHOLOGY

A Sliding Scale

How hiring decisions are made is, not surprisingly, a topic of broad and continuing interest in view of their impact on people, individually in everyday life and collectively in societal debates about opportunity and outcome. Uhlmann and Cohen describe a trio of experiments showing how shifting standards might contribute to discrimination. In a pair of roughly mirror-image situations, male and female subjects were asked to assess male and female applicants for high-ranking stereotypically male- and female-dominated jobs (police chief and women's studies professor). Contrasting sets of skills (physical fitness versus media savvy) and achievements (publications versus advocacy) were evenly distributed among the applicants, and subjects did in fact evaluate applicant strength on the basis of credentials and not as a function of applicant gender. Male subjects, however, rated media savvy as being a more

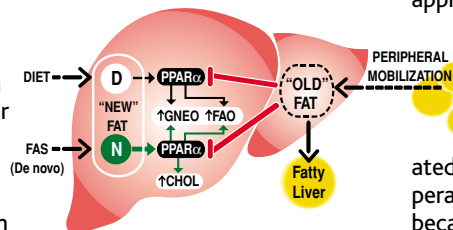
BIOMEDICINE

New Fat, Old Fat

Pursuing good health may mean including enough fat in your diet. Fat that is either consumed or synthesized de novo in cells is considered new, whereas old fat is stored in adipose tissue, waiting to be used. According to Chakravarthy *et al.*, the liver discriminates between these sources as it coordinates nutrient and energy homeostasis.

Fatty acids serve as the natural ligands for PPAR α , a hepatocyte nuclear receptor that regulates genes involved in the metabolism of glucose, fatty acids, and cholesterol. When fed a diet with no fat, mice lacking fatty acid synthase (FAS) developed hypoglycemia due to a failure in activating target genes of PPAR α that control gluconeogenesis (GNEO). Paradoxically, the livers in these mice became fat-laden because of the mobilization of peripheral fat and the inability of the liv-

ers to express PPAR α target genes involved in fatty acid oxidation (FAO). Adding dietary fat or an agonist of PPAR α reversed these symptoms. Mice lacking FAS also had low serum and liver cholesterol levels due to decreased hepatic cholesterol synthesis (CHOL). The authors propose that new fat may activate a distinct pool of PPAR α in the liver to maintain



Model for PPAR α pathways in the liver.

normal levels of glucose, fat and cholesterol. Metabolic abnormalities associated with obesity and diabetes might be treated by pharmacologically activating these distinct receptor pools. — LDC

Cell Metab. 1, 309 (2005).

CHEMISTRY

Better Grafting

Polyolefins, such as polyethylene and polypropylene, have many uses, including shopping bags and hip replacements. To improve the solvent resistance or to make them more adhesive to polar surfaces, it is advantageous to graft polar groups onto the polymer backbone. However, current approaches to adding polar groups are either much slower than commercial polyolefin polymerization methods or are initiated by radicals at high temperatures and pressures because they are not compatible with the use of metal catalysts. Ideally, one would like to add side groups in a controlled secondary process, something that is easy to do for polymers with unsaturated bonds in the backbone, but is much more challenging for polyolefins. Díaz-Requejo *et al.* examined a copper-based catalytic system, which they had used to func-

CONTINUED ON PAGE 1229



Targetron™

Gene Knockout System

Genetic Engineering that is Right on Target!

The Targetron™ Gene Knockout System is a revolutionary method for rapid and specific disruption of genes in prokaryotic organisms. Utility of the technology has been demonstrated for prokaryotic genetic engineering, systems biology and functional genomics approaches.

The method exploits the retrohoming ability of group II introns and utilizes a simple PCR step to “re-target” the Targetron group II intron for specific insertion into the host genome. Gene knockout using the Targetron system has been validated in a broad range of bacterial strains such as *Escherichia coli*, *Staphylococcus aureus*, *Lactococcus lactis*, *Clostridium perfringens*, *Shigella flexneri* and *Salmonella typhimurium*.

- Targeted and permanent gene disruption
- Simple, streamlined protocol; Knockouts in 3 days or less
- Minimal screening to isolate mutants.
- No cell conjugation or specific host factor requirements
- >90% successful targeted insertion

Product	Description	Unit
TA0100	Targetron™ Gene Knockout System	3EA 10EA

For additional details and product availability, please visit www.sigma-aldrich.com/s1target

This product and its use are the subject of one or more of U.S. Patent Nos. 5,698,421, 5,804,418, 5,869,634, 6,027,895, 6,001,608, and 6,306,596 and/or other pending U.S. and foreign patent applications controlled by InGex, LLC.

important criterion for success as a police chief when ranking male applicants who had that skill; similarly, female subjects emphasized advocacy as being crucial when considering female applicants who had been activists for the professorship. These differences then translated into hiring choices, where men favored men in the first competition and women favored women in the second. The simple manipulation of committing to hiring criteria before evaluating the applicants largely mitigated gender bias in the outcomes. — GJC

Psychol. Sci. 16, 474 (2005).

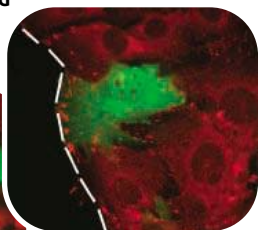
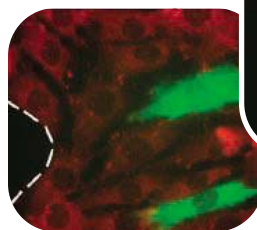
CELL BIOLOGY

Defocusing with Dynamin

In mammalian cells, actin-rich focal adhesions form at places where the cell membrane protein integrin interacts with the extracellular matrix. When adherent cells move across a surface, they lay down focal adhesions at the front of the cell and disassemble adhesions at the back. Much is known about focal adhesion assembly, but less about disassembly.

Ezratty *et al.* targeted molecules specifically involved in focal adhesion disassembly by adding a drug that induced microtubule disassembly and then removing the drug to allow microtubules to regrow, during which time focal adhesions disassembled in a

An inactive form of dynamin (green, left) interferes with migration toward a wound (dashed line) as compared with cells with wild-type dynamin (right).



synchronous fashion. They found that adhesion disassembly required focal adhesion kinase and dynamin, which localized to the adhesions, and inhibiting dynamin activity prevented cell migration. Thus, the disassembly of focal adhesions involves a pair of molecular entities, microtubules and dynamin, neither of which are used in the assembly process. — SMH

Nat. Cell Biol. 10.1038/ncb1262 (2005).

IMMUNOLOGY

A Regulatory Effect of Tax

Regulatory T (T-reg) cells are central moderators of the immune system, restraining overexuberant T cells and those that have a tendency to react against the body's own components. Consequently, perturbing the function of T-reg cells could have deleterious effects on the health of an individual.

Yamano *et al.* have extended previous observations that T-reg cells represent a preferential reservoir for the human T cell lymphotropic virus (HTLV-1) in infected individuals. These patients develop an immunity-based neurologic disease, in which large numbers of virus-specific CD8⁺ cytotoxic T cells invade the central nervous system. Virus-infected T-reg cells were severely diminished in their ability to suppress T cell responses and in the expression of the transcription factor Foxp3. These deficits were traced to the expression of a viral transcriptional repressor, Tax, and could be recapitulated by transfecting the tax gene into uninfected T-reg cells. Although some autoimmune effects have been reported in this group of HTLV-1 patients, it is interesting that such a profound T-reg cell defect does not appear to result in a broader impairment of normal immune function. — SJS

J. Clin. Invest. 115, 1361 (2005).

APPLIED PHYSICS

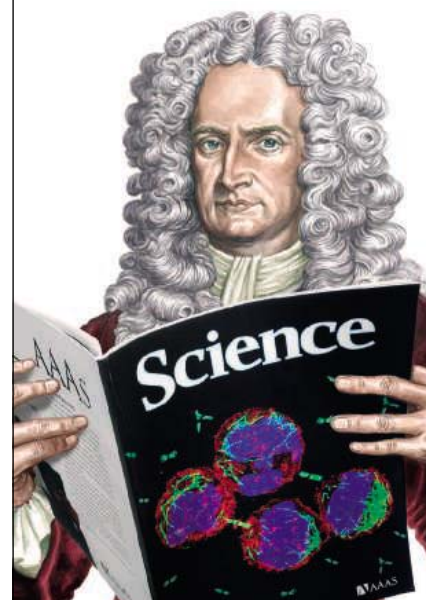
Quantum Networking

The ability to send single photons down optical fibers offers the possibility of secure communications over existing fiber networks. One challenge has been to find single-photon sources that emit at the telecom wavelengths of 1300 nm. The emission wavelength of quantum dots can be tuned by controlling their size, making them ideal candidates for further study. On the other hand, infrared communication wavelengths would require the dots to be relatively large; under typical growth conditions, this would require a longer growth time, resulting in a high density of dots on the surface and a large number of single-photon sources. By carefully adjusting the growth conditions, Ward *et al.* show that they can whittle down and isolate the number of emitters to just one, thereby providing a practical source of single photons for quantum communication over fiber-optic networks. — ISO

Appl. Phys. Lett. 86, 201111 (2005).

Looking for a career that defies the law of gravity?

Then talk to someone who knows science.



Isaac Newton

1642–1727

If you want to head upward in science, don't leave your career to chance. At ScienceCareers.org we know science. We are committed to helping you find the right job, and to delivering the advice you need. So if you want your career to bear fruit, trust the specialist in science.



ScienceCareers.org

We know science



1200 New York Avenue, NW
 Washington, DC 20005
 Editorial: 202-326-6550, FAX 202-289-7562
 News: 202-326-6500, FAX 202-371-9227

Bateman House, 82-88 Hills Road
 Cambridge, UK CB2 1LQ
 +44 (0) 1223 326500, FAX +44 (0) 1223 326501

SUBSCRIPTION SERVICES For change of address, missing issues, new orders and renewals, and payment questions: 800-731-4939 or 202-326-6417, FAX 202-842-1065. Mailing addresses: AAAS, P.O. Box 1811, Danbury, CT 06813 or AAAS Member Services, 1200 New York Avenue, NW, Washington, DC 20005

INSTITUTIONAL SITE LICENSES please call 202-326-6755 for any questions or information

REPRINTS Ordering/Billing/Status 800-635-7171; Corrections 202-326-6501

PERMISSIONS 202-326-7074, FAX 202-682-0816

MEMBER BENEFITS Bookstore: AAAS/BarnesandNoble.com bookstore www.aaas.org/bn; Car purchase discount: Subaru VIP Program 202-326-6417; Credit Card: MBNA 800-847-7378; Car Rentals: Hertz 800-654-2200 CDP#343457, Dollar 800-800-4000 #AA1115; AAAS Travels: Betchart Expeditions 800-252-4910; Life Insurance: Seabury & Smith 800-424-9883; Other Benefits: AAAS Member Services 202-326-6417 or www.aaasmember.org.

science_editors@aaas.org (for general editorial queries)
 science_letters@aaas.org (for queries about letters)
 science_reviews@aaas.org (for returning manuscript reviews)
 science_bookrevs@aaas.org (for book review queries)

Published by the American Association for the Advancement of Science (AAAS), *Science* serves its readers as a forum for the presentation and discussion of important issues related to the advancement of science, including the presentation of minority or conflicting points of view, rather than by publishing only material on which a consensus has been reached. Accordingly, all articles published in *Science*—including editorials, news and comment, and book reviews—are signed and reflect the individual views of the authors and not official points of view adopted by the AAAS or the institutions with which the authors are affiliated.

AAAS was founded in 1848 and incorporated in 1874. Its mission is to advance science and innovation throughout the world for the benefit of all people. The goals of the association are to: foster communication among scientists, engineers and the public; enhance international cooperation in science and its applications; promote the responsible conduct and use of science and technology; foster education in science and technology for everyone; enhance the science and technology workforce and infrastructure; increase public understanding and appreciation of science and technology; and strengthen support for the science and technology enterprise.

INFORMATION FOR CONTRIBUTORS

See pages 135 and 136 of the 7 January 2005 issue or access www.sciencemag.org/feature/contribinfo/home.shtml

EDITOR-IN-CHIEF **Donald Kennedy**
 EXECUTIVE EDITOR **Monica M. Bradford**
 DEPUTY EDITORS NEWS EDITOR
R. Brooks Hanson, Katrina L. Kelner Colin Norman

EXECUTIVE PUBLISHER **Alan I. Leshner**
 PUBLISHER **Beth Rosner**

EDITORIAL SUPERVISORY SENIOR EDITORS Barbara Jasny, Phillip D. Szurmi; **SENIOR EDITORS** Gilbert J. Chin, Lisa D. Chong, Pamela J. Hines, Paula A. Kiberstis (Boston), Beverly A. Purnell, L. Bryan Ray, Guy Riddihough (Manila), H. Jesse Smith, Valda Vinson, David Voss; **ASSOCIATE EDITORS** Marc S. Lavine, Jake S. Yeston; **ONLINE EDITOR** Stewart Willis; **CONTRIBUTING EDITOR** Ivan Amato; **ASSOCIATE ONLINE EDITOR** Tara S. Marathe; **BOOK REVIEW EDITOR** Sherman J. Suter; **ASSOCIATE LETTERS EDITOR** Etta Kavanagh; **INFORMATION SPECIALIST** Janet Kegg; **EDITORIAL MANAGER** Cara Tate; **SENIOR COPY EDITORS** Jeffrey E. Cook, Harry Jack, Barbara P. Ordway; **COPY EDITORS** Cynthia Howe, Alexis Wynne Mogul, Sabrah M. n'hRaven, Jennifer Sills, Trista Wagoner; **EDITORIAL COORDINATORS** Carolyn Kyle, Beverly Shields; **PUBLICATION ASSISTANTS** Chris Filiatreau, Jol S. Granger, Jeffrey Hearn, Lisa Johnson, Scott Miller, Jerry Richardson, Brian White, Anita Wynn; **EDITORIAL ASSISTANTS** Ramatoulaye Diop, E. Annie Hall, Patricia M. Moore, Brendan Nardozi, Michael Rowedag; **EXECUTIVE ASSISTANT** Sylvia S. Kihara; **ADMINISTRATIVE SUPPORT** Patricia F. Fisher

NEWS SENIOR CORRESPONDENT Jean Marx; **DEPUTY NEWS EDITORS** Robert Coontz, Jeffrey Mervis, Leslie Roberts, John Travis; **CONTRIBUTING EDITORS** Elizabeth Cullotta, Polly Shulman; **NEWS WRITERS** Yudhijit Bhattacharjee, Jennifer Couzin, David Grimm, Constance Holden, Jocelyn Kaiser, Richard A. Kerr, Eli Kintisch, Andrew Lawler (New England), Greg Miller, Elizabeth Pennisi, Charles Seife, Robert F. Service (Pacific NW), Erik Stokstad; **AMITABH AVASTHI (intern); CONTRIBUTING CORRESPONDENTS** Marcia Barinaga (Berkeley, CA), Barry A. Cipra, Adrian Cho, Jon Cohen (San Diego, CA), Daniel Ferber, Ann Gibbons, Robert Lion, Mitch Leslie (NetWatch), Charles C. Mann, Evelyn Strauss, Gary Taubes, Ingrid Wickelgren; **COPY EDITORS** Linda B. Felaco, Rachel Curran, Sean Richardson; **ADMINISTRATIVE SUPPORT** Scherraine Mack, Fannie Groom **BUREAUS:** Berkeley, CA: 510-652-0302, FAX 510-652-1867, New England: 207-549-7755, San Diego, CA: 760-942-3252, FAX 760-942-4979, Pacific Northwest: 503-963-1940

PRODUCTION DIRECTOR James Landry; **SENIOR MANAGER** Wendy K. Shank; **ASSISTANT MANAGER** Rebecca Doshi; **SENIOR SPECIALISTS** Vicki J. Jorgensen, Jessica K. Moshell; **SPECIALISTS** Jay R. Covert, Stacey Ferebee; **PREFLIGHT DIRECTOR** David M. Tompkins; **MANAGER** Marcus Spiegler; **SPECIALIST** Jessie Mudjittaba;

ART DIRECTOR Joshua Moglia; **ASSOCIATE ART DIRECTOR** Kelly Buckheit; **ILLUSTRATOR** Katharine Sutliff; **SENIOR ART ASSOCIATES** Holly Bishop, Laura Creveling, Preston Huey, Julie White; **ASSOCIATE** Nayomi Kevitiyagala; **PHOTO RESEARCHER** Leslie Blizard

SCIENCE INTERNATIONAL

EUROPE science@science-int.co.uk **EDITORIAL: INTERNATIONAL MANAGING EDITOR** Andrew M. Sugden; **SENIOR EDITOR/PERSPECTIVES** Julia Fahrenkamp-Uppenbrink; **SENIOR EDITORS** Caroline Ash (Geneva: +41 (0) 222 346 3106), Stella M. Hurlley, Ian S. Osborne, Peter Stern; **ASSOCIATE EDITOR** Stephen J. Simpson; **EDITORIAL SUPPORT** Emma Westgate; **EDITOR** Dennis Dennison **ADMINISTRATIVE SUPPORT** Janet Clements, Phil Marlow, Jill White; **NEWS: INTERNATIONAL NEWS EDITOR** Eliot Marshall **DEPUTY NEWS EDITOR** Daniel Cury; **CORRESPONDENT** Gretchen Vogel (Berlin: +49 (0) 30 2809 3902, FAX +49 (0) 30 2809 8365); **CONTRIBUTING CORRESPONDENTS** Michael Balter (Paris), Martin Enserink (Amsterdam and Paris); **INTERN MANAGER** Inman ASIA Japan Office: Asca Corporation, Eiko Ishioka, Fusako Tamura, 1-8-13, Hirano-cho, Chuo-ku, Osaka-shi, Osaka, 541-0046 Japan; +81 (0) 6 6202 6272; FAX +81 (0) 6 6202 6271; asca@os.gulf.or.jp **JAPAN NEWS BUREAU:** Dennis Normile (contributing correspondent, +81 (0) 3 3391 0630, FAX 81 (0) 3 5936 3531; dnormile@gol.com); **CHINA REPRESENTATIVE** Hao Xin, +86 (0) 10 6307 4439 or 6307 3676, FAX +86 (0) 10 6307 4358; haoxin@earthlink.net; SOUTH ASIA Pallava Bagla (contributing correspondent +91 (0) 11 2271 2896; pbagla@vsnl.com); **CENTRAL ASIA** Richard Stone (+7 3272 6413 35, rstone@aaas.org)

FULFILLMENT & MEMBERSHIP SERVICES (membership@aaas.org) **DIRECTOR** Marlene Zendeck; **MANAGER** Waylon Butler; **SENIOR SPECIALIST** Pat Butler; **SPECIALISTS** Laurie Baker, Tamara Alfton, Karena Smith, Andrew Vargo; **MARKETING ASSOCIATE** Deborah Stromberg

BUSINESS OPERATIONS AND ADMINISTRATION **DIRECTOR** Deborah Rivera-Wienhold; **BUSINESS MANAGER** Randy Yi; **SENIOR FINANCIAL ANALYST** Lisa Donovan; **BUSINESS ANALYST** Jessica Tierney; **FINANCIAL ANALYST** Farida Yeastmir; **RIGHTS AND PERMISSIONS: ADMINISTRATOR** Emilie David; **ASSOCIATE** Elizabeth Sandler; **MARKETING: DIRECTOR** John Meyers; **MEMBERSHIP MARKETING MANAGER** Darryl Walter; **MARKETING ASSOCIATE** Julianne Wielga; **RECRUITMENT MARKETING MANAGER** Allison Pritchard; **ASSOCIATES** Mary Ellen Crowley, Amanda Donathen, Catherine Featherston; **DIRECTOR OF INTERNATIONAL MARKETING AND RECRUITMENT ADVERTISING** Deborah Harris; **INTERNATIONAL MARKETING MANAGER** Wendy Sturley; **MARKETING/MEMBER SERVICES EXECUTIVE** Linda Rusk; **JAPAN SALES AND MARKETING MANAGER** Jason Hannaford; **SITE LICENSE SALES: DIRECTOR** Tom Ryan; **SALES AND CUSTOMER SERVICE** Mehan Dossani, Catherine Holland, Adam Banner, Yaniv Snir; **ELECTRONIC MEDIA: INTERNET PRODUCTION MANAGER** Lizabeth Harman; **ASSISTANT PRODUCTION MANAGER** Wendy Stengel; **SENIOR PRODUCTION ASSOCIATES** Sheila Mackall, Amanda K. Skelton, Lisa Stanford; **PRODUCTION ASSOCIATE** Nichele Johnston; **LEAD APPLICATIONS DEVELOPER** Carl Saffell

PRODUCT ADVERTISING (science_advertising@aaas.org); **MIDWEST** Rick Bongiovanni: 330-405-7080, FAX 330-405-7081 • **WEST COAST** WY, CANADA B. Neil Boylan (Associate Director): 650-964-2266, FAX 650-964-2267 • **EAST COAST/E. CANADA** Christopher Breslin: 443-512-0330, FAX 443-512-0331 • **UK/SCANDINAVIA/France/Italy/BELGIUM/NETHERLANDS** Andrew Davis (Associate Director): +44 (0) 1782 750111, FAX +44 (0) 1782 751999 • **GERMANY/SWITZERLAND/AUSTRIA** Tracey Peers (Associate Director): +44 (0) 1782 752530, FAX +44 (0) 1782 752531 **JAPAN** Masuyoshi Yoshikawa: +81 (0) 33235 5961, FAX +81 (0) 33235 5852 **ISRAEL** Jessica Nachlas +9723 5449123 • **TRAFFIC MANAGER** Carol Mardo; **SALES COORDINATOR** Deandra Simms

CLASSIFIED ADVERTISING (advertise@sciencecareers.org); **U.S. SALES DIRECTOR** Gabrielle Boguslawski: 718-491-1607, FAX 202-289-6742; **INTERNET SALES MANAGER** Beth Dwyer: 202-326-6534; **INSIDE SALES MANAGER** Daryl Anderson: 202-326-6543; **WEST COAST/MIDWEST** Kristine von Zedlitz: 415-956-2531; **EAST COAST** Jill Downing: 631-580-2445; **LINE AD SALES** Ermet Tesfaye: 202-326-6740; **SENIOR SALES COORDINATOR** Erika Bryant; **SALES COORDINATORS** Rohan Edmonson, Christopher Normile, Joyce Scott, Shirley Young; **INTERNATIONAL SALES MANAGER** Tracy Holmes: +44 (0) 1223 326255, FAX +44 (0) 1223 326532; **SALES** Christina Harrison, Suilana Barnes; **SALES ASSISTANT** Helen Moroney; **JAPAN** Jason Hannaford: +81 (0) 52 789 1860, FAX +81 (0) 52 789 1861; **PRODUCTION: MANAGER** Jennifer Rankin; **ASSISTANT MANAGER** Deborah Tompkins; **ASSOCIATE** Amy Hardcastle; **SENIOR TRAFFICKING ASSOCIATE** Christine Hall; **SENIOR PUBLICATIONS ASSISTANT** Robert Buck; **PUBLICATIONS ASSISTANT** Natasha Pinol

AAAS BOARD OF DIRECTORS **RETIRED PRESIDENT, CHAIR** Shirley Ann Jackson; **PRESIDENT** Gilbert S. Ornien; **PRESIDENT-ELECT** John P. Holdren; **TREASURER** David E. Shaw; **CHIEF EXECUTIVE OFFICER** Alan I. Leshner; **BOARD** Rosina M. Bierbaum; John E. Burris; John E. Dowling; Lynn W. Enquist; Susan M. Fitzpatrick; Richard A. Meserve; Norine E. Noonan; Peter J. Stang; Kathryn D. Sullivan



ADVANCING SCIENCE. SERVING SOCIETY

SENIOR EDITORIAL BOARD

John I. Brauman, Chair, Stanford Univ.
Richard Losick, Harvard Univ.
Robert May, Univ. of Oxford
Marcia McNutt, Monterey Bay Aquarium Research Inst.
Linda Partridge, Univ. College London
Vera C. Rubin, Carnegie Institution of Washington
Christopher R. Somerville, Carnegie Institution

BOARD OF REVIEWING EDITORS

R. McNeill Alexander, Leeds Univ.
Richard Amasino, Univ. of Wisconsin, Madison
Kristi S. Anseth, Univ. of Colorado
Cornelia I. Bargmann, Univ. of California, SF
Brenda Bass, Univ. of Utah
Ray H. Baughman, Univ. of Texas, Dallas
Stephen J. Benkovic, Pennsylvania St. Univ.
Michael J. Bevan, Univ. of Washington
Ton Bisseling, Wageningen Univ.
Peer Bork, EMBL
Dennis Bray, Univ. of Cambridge
Stephen Buratowski, Harvard Medical School
Jillian M. Buriak, Univ. of Alberta
Joseph A. Burns, Cornell Univ.
William P. Butz, Population Reference Bureau
Doreen Cantrell, Univ. of Dundee
Mildred Cho, Stanford Univ.
David Clapham, Children's Hospital, Boston
David Clary, Oxford University
J. M. Claverie, CNRS, Marseille
Jonathan D. Cohen, Princeton Univ.
Robert Colwell, Univ. of Connecticut
Peter Crane, Royal Botanic Gardens, Kew
F. Fleming Crim, Univ. of Wisconsin

William Cumberland, UCLA
Caroline Dean, John Innes Centre
Judy DeLoache, Univ. of Virginia
Robert Desimone, NIMH, NIH
John Diffley, Cancer Research UK
Dennis Discher, Univ. of Pennsylvania
Julian Downward, Cancer Research UK
Dennis Duboule, Univ. of Geneva
Christopher Dye, WHO
Richard Ellis, Cal Tech
Gerhard Ertl, Fritz-Haber-Institut, Berlin
Douglas H. Erwin, Smithsonian Institution
Barry Everitt, Univ. of Cambridge
Paul G. Falkowski, Rutgers Univ.
Tom Fenchel, Univ. of Copenhagen
Barbara Finlayson-Pitts, Univ. of California, Irvine
Jeffrey S. Flier, Harvard Medical School
Chris D. Frith, Univ. College London
R. Gadagkar, Indian Inst. of Science
Mary E. Galvin, Univ. of Delaware
Don Ganem, Univ. of California, SF
John Gearhart, Johns Hopkins Univ.
Jennifer M. Graves, Australian National Univ.
Christian Haas, Ludwig Maximilians Univ.
Dennis L. Hartmann, Univ. of Washington
Chris Hawkesworth, Univ. of Bristol
Martin Heimann, Max Planck Inst., Jena
James A. Hendler, Univ. of Maryland
Ary A. Hoffmann, La Trobe Univ.
Evelyn L. Hu, Univ. of California, SB
Meyer B. Jackson, Univ. of Wisconsin Med. School
Stephen Jackson, Univ. of Cambridge
Bernhard Keimer, Max Planck Inst., Stuttgart
Alan B. Krueger, Princeton Univ.
Antonio Lanzavecchia, Inst. of Res. in Biomedicine
Anthony J. Leggett, Univ. of Illinois, Urbana-Champaign

Michael J. Lenardo, NIAID, NIH
Norman L. Letvin, Beth Israel Deaconess Medical Center
Richard Losick, Harvard Univ.
Andrew P. MacKenzie, Univ. of St. Andrews
Raul Madariaga, École Normale Supérieure, Paris
Rick Maizels, Univ. of Edinburgh
Eve Marder, Brandeis Univ.
George M. Martin, Univ. of Washington
William McGinnis, Univ. of California, San Diego
Virginia Miller, Washington Univ.
Edvard Moser, Norwegian Univ. of Science and Technology
Naoto Nagaosa, Univ. of Tokyo
James Nelson, Stanford Univ. School of Med.
Roland Nolte, Univ. of Nijmegen
Eric N. Olson, Univ. of Texas, SW
Erin O'Shea, Univ. of California, SF
Malcolm Parker, Imperial College
John Pendry, Imperial College
Josef Perner, Univ. of Salzburg
Phillippe Poulin, CNRS
David J. Read, Univ. of Sheffield
Colin Renfrew, Univ. of Cambridge
Trevor Robbins, Univ. of Cambridge
Nancy Ross, Virginia Tech
Edward M. Rubin, Lawrence Berkeley National Labs
David G. Russell, Cornell Univ.
Gary Ruvkun, Mass. General Hospital
J. Roy Sambles, Univ. of Exeter
Phillippe Sansonetti, Institut Pasteur
Dan Schrag, Harvard Univ.
Georg Schulz, Albert-Ludwigs-Universität
Paul Schulze-Lefert, Max Planck Inst., Cologne
Terrence J. Sejnowski, The Salk Institute
George Somero, Stanford Univ.
Christopher R. Somerville, Carnegie Institution
Joan Steitz, Yale Univ.

Edward I. Stiefel, Princeton Univ.
Thomas Stocker, Univ. of Bern
Jerome Strauss, Univ. of Pennsylvania Med. Center
Tomoyuki Takahashi, Univ. of Tokyo
Glenn Telling, Univ. of Kentucky
Marc Tessier-Lavigne, Genentech
Craig B. Thompson, Univ. of Pennsylvania
Michiël van der Klis, Astronomical Inst. of Amsterdam
Derek van der Kooy, Univ. of Toronto
Bert Vogelstein, Johns Hopkins
Christopher A. Walsh, Harvard Medical School
Christopher T. Walsh, Harvard Medical School
Graham Warren, Yale Univ. School of Med.
Fiona Watt, Imperial Cancer Research Fund
Julia R. Weertman, Northwestern Univ.
Daniel M. Wegner, Harvard University
Ellen D. Williams, Univ. of Maryland
R. Sanders Williams, Duke University
Ian A. Wilson, The Scripps Res. Inst.
Jerry Workman, Stowers Inst. for Medical Research
John R. Yates II, The Scripps Res. Inst.
Martin Zatz, NIMH, NIH
Walter Ziegglansberger, Max Planck Inst., Munich
Huda Zoghbi, Baylor College of Medicine
Maria Zuber, MIT

BOOK REVIEW BOARD

David Bloom, Harvard Univ.
Londa Schieberger, Stanford Univ.
Richard Shwartz, Univ. of Chicago
Robert Slower, MIT
Ed Wasserman, DuPont
Lewis Wolpert, Univ. College, London

SAMPLE TRACKING

**We'll Help You Keep Track
Of Pretty Much Everything.**

Except Your Mother's Birthday.



Take Advantage Of The Industry's Largest Selection Of Sample Tracking Solutions.

Calendars. Date books. Electronic organizers. There are plenty of ways to keep track of things in your personal life. Fortunately, now you have access to just as many in your lab.

At Matrix, we offer the most complete selection of drug discovery solutions in the industry – from instrumentation to consumables – including the widest range of innovations for shipping, storing and tracking samples.

Whether you need the versatility to quickly trace hundreds, thousands or millions of individually marked tubes or the flexibility to add customized bar codes to your microplates, blocks or tube racks, we have the perfect solution.

For more information, visit us at www.matrixtechcorp.com/sc5 or call toll-free, (800) 345-0206. Either way, you may suddenly get the feeling like today's *your* birthday.

To learn more about Matrix tracking solutions, please visit us at
www.matrixtechcorp.com/sc5

MATRIX
fluid thinking.

HANDHELD PIPETTING

AUTOMATED PIPETTING

CONSUMABLES

Custom AQUA Peptides

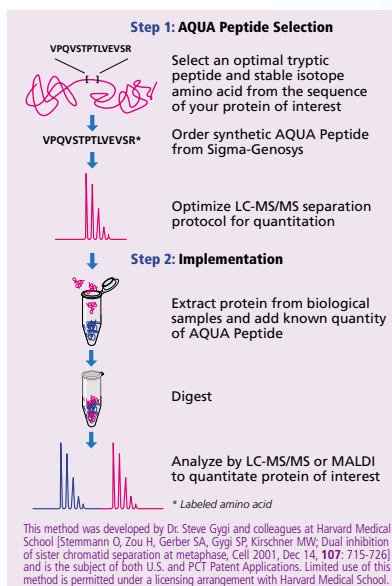
The Ultimate Method for Biomarker Quantitation

Unrivaled Sensitivity To:

- Accurately quantitate low abundance proteins
- Measure phosphorylation states and splice variants
- Validate RNAi knockdown

Protein-AQUA™ is a powerful, enabling technology that facilitates focused, quantitative studies of not only specific protein expression, but specific amino acid modification as well. The Protein-AQUA strategy, originally presented in 2003 by Dr. Steve Gygi and his team, enables absolute protein quantitation using stable isotope labeled peptides, and mass spectrometry. Protein-AQUA is based on a common principle: the use of a labeled molecule as an internal standard. By applying this technique to protein and peptide analysis, Gygi's team has advanced the abilities of protein researchers to study complex biological samples quantitatively, and has provided a valuable new tool for Proteomics!

To meet the specific requirements of AQUA experimentation, Sigma has developed a specialized custom peptide offering. Custom AQUA Peptides are synthesized using fully labeled 98 atom% ¹³C and 98 atom% ¹⁵N enriched amino acids (one labeled amino acid per peptide), and are stringently tested to ensure high purity (HPLC), accurate molecular weight (MALDI-TOF MS), and specific peptide content. Custom AQUA Peptides are available in small (5 x 1 nmol) package sizes to enable convenient sample preparation, and provide an appropriate peptide quantity.



To learn more about AQUA Peptides, visit our Web site at: sigma-aldrich.com/aqua5

To order your AQUA Peptides today, visit our Web site at: sigma-genosys.com/order.asp

sigma-aldrich.com

LEADERSHIP IN LIFE SCIENCE, HIGH TECHNOLOGY AND SERVICE
SIGMA-ALDRICH CORPORATION • BOX 14508 • ST. LOUIS • MISSOURI 63178 • USA

SIGMA[®]
GENOSYS

IN PARTNERSHIP WITH THE
SIGMA[®] AND ISOTEC[®] BRANDS

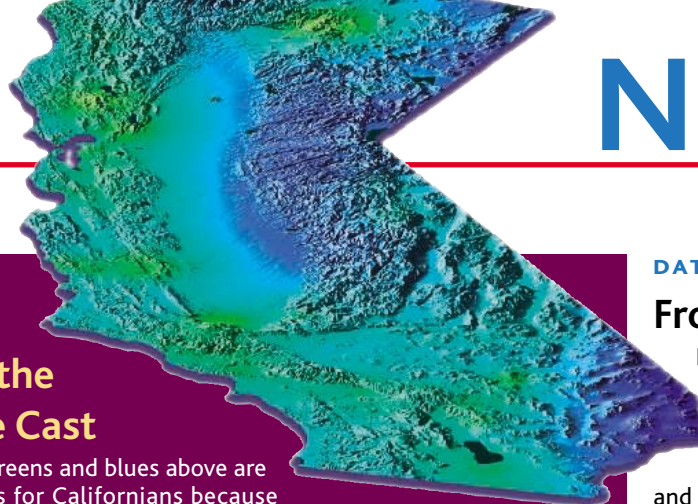
IMAGES

Tune In for the Quake Cast

The cool greens and blues above are good news for Californians because they signify a low risk of earthquakes. Worried residents and curious visitors can now check the local quake forecast throughout the state, thanks to a new online map that's updated hourly. The site won't tell people when a big quake is imminent, but it can predict the probability of aftershocks, which can still cause substantial damage.

The map is the brainchild of seismologist Matt Gerstenberger of the U.S. Geological Survey in Pasadena, California, and colleagues. Their procedure, published in last week's issue of *Nature*, uses all the known faults in the state and records of past earthquakes to generate a baseline historical level of risk. Whenever an earthquake occurs, the program estimates the likely locations and sizes of aftershocks and maps them. Blue signifies a one-in-a-million chance of intensity 6 shaking (forceful enough to break windows and crack plaster), whereas red indicates a greater than one in 10 chance.

pasadena.wr.usgs.gov/step



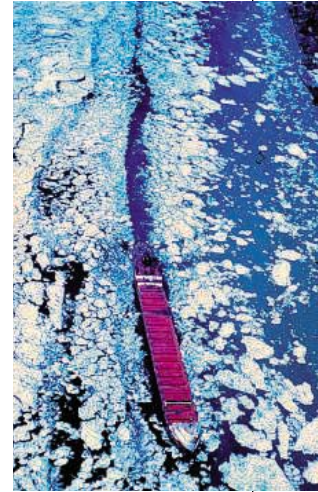
DATABASE

Frozen in Time

Researchers are keeping an eye on the world's ice for signs of climate change. For data on one warming spot, glide over to the Great Lakes Ice

Atlas by Raymond Assel of the National Oceanic and Atmospheric Administration. The archive charts ice cover on the lakes from 1973 to 2002, combining measurements from satellites, aircraft, shipboard observers, and other sources. You can summon weekly maps of ice extent or watch animations that portray the waxing and waning of lake ice for each winter. Visitors can also download data such as daily ice cover values. The records suggest that like much of the world's frozen water, Great Lakes ice is dwindling. For example, between 1853 and 1972, Grand Traverse Bay on Lake Michigan didn't freeze over during 17 winters. But between 1973 and 2002, it remained open in 16 years.

www.glerl.noaa.gov/data/ice/atlas

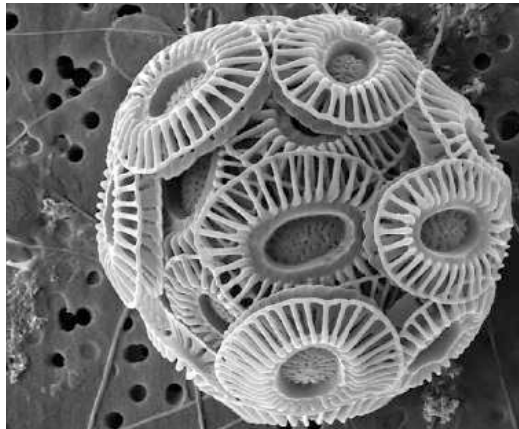


EDUCATION

Gems of the Ocean

Individual cells of the protist *Emiliana huxleyi* (below) are so tiny that researchers can barely see them with a light microscope. But *E. huxleyi*, or "Ehux" for short, has a disproportionately large impact on the planet. This Ehux site from oceanographer Toby Tyrrell of Southampton University in the United Kingdom offers backgrounders by experts on the cells' anatomy, reproduction, ecology, and other topics. The creatures' calcium carbonate armor scatters light and can color large swaths of the ocean turquoise. By making the surface water more reflective, Ehux reduces the amount of light penetrating into the ocean and cools the lower layers. Although the cells are photosynthetic, they might worsen global warming, the site explains, because their changes

to water chemistry boost the amount of dissolved carbon dioxide. The site also includes a gallery of delicate Ehux shells, a bibliography, and a link to NASA satellite photos of Ehux blooms.



www.noc.soton.ac.uk/soes/staff/tt/eh/index.html

ARCHIVE

Evolution's Big Hitter

Stephen Jay Gould dubbed R. A. Fisher "the Babe Ruth of statistics and evolutionary theory." A British geneticist and mathematician, Fisher (1890–1962) earned the rave review with achievements from inventing the analysis of variance to helping mesh natural selection and genetics, which many scientists in the early 1900s believed were incompatible.

To delve into Fisher's complex and eclectic work, click over to the R. A. Fisher Digital Archive from the University of Adelaide Library in Australia. Readers can browse more than 170 of Fisher's publications, which probe questions such as the origin of dominant genes and the inheritance of the Rh blood groups. A stack of Fisher's correspondence lets you follow along as he discusses heredity, natural selection, and other topics with thinkers such as Charles Darwin's son Leonard, a soldier and scientist. Fisher's papers also reveal what Gould called one of his "major-league errors," his campaign to discredit the link between smoking and lung cancer. A pipe smoker, Fisher argued that we needed stronger evidence "before plant[ing] fear in the minds of perhaps 100 million smokers around the world."

www.library.adelaide.edu.au/digitised/fisher

Send site suggestions to netwatch@aaas.org. Archive: www.sciencemag.org/netwatch



INFECTIOUS DISEASES

Genetic Analyses Suggest Bird Flu Virus Is Evolving

New genetic analyses of samples from recent human H5N1 avian influenza patients reinforce epidemiological evidence suggesting that new strains of the virus may be emerging in northern Vietnam. But an expert report detailing the genetic analyses, posted on the Web site of the World Health Organization (WHO) last week, cautions that data are too limited to draw firm conclusions. Even so, the report urges heightened surveillance, increased preparedness, and further research, warning that H5N1 poses “a continuing and potentially growing pandemic threat.”

At a meeting to review data at the request of WHO, held in Manila on 6 and 7 May, scientists also concluded that human-to-human transmission of the virus may be more common than previously thought. The meeting—attended by 40 or so epidemiologists, virologists, public and animal health experts, and representatives from Cambodia, Thailand, and Vietnam—came on the heels of a visit by a three-person WHO team to Vietnam in late April.

Lance Jennings, a clinical virologist for the Canterbury District Health Board in New Zealand and a member of the WHO team, says epidemiological evidence, some of it previously reported (*Science*, 22 April, p. 477), indicates a changing virus: Clusters



Fighting back. Nguyen Si Tuan is among a growing number of bird flu survivors in Vietnam whose recoveries may suggest that the virus is becoming more infectious but less deadly.

of infection are larger and more numerous than seen previously, and there is often a time lag between the onset of symptoms in the first case and subsequent cases within clusters. Among those infected were three infants, ruling out poultry tending as a route of infection in those cases. And in a few other cases, exposure to poultry could not be traced. Although

these findings suggest that human-to-human transmission is occurring, Jennings adds that “there are other possible explanations.” The virus could have acquired the ability to persist longer in the environment, or perhaps resistant poultry are now shedding the virus without signs of sickness.

The new genetic data, reviewed by scientists for the first time at the Manila meeting, comes from the U.S. Centers for Disease Control and Prevention (CDC) in Atlanta, Georgia, and Japan’s National Institute of Infectious Diseases. Partial sequencing of viral isolates revealed a number of differences between samples recovered this year in northern Vietnam and previous samples, particularly in the hemagglutinin gene. Hemagglutinin (which is the H in virus designations, such as H5N1) codes for a surface glycoprotein that binds the virus to cells in the animal or human host. Some of the sequence changes are near the protein’s binding site; others are near a site associated with pathogenicity.

Conceivably, these genetic changes could be affecting the virus’s ability to bind to human cells and its deadliness, which is lower among recent cases in northern Vietnam than elsewhere, the report notes. But there isn’t enough epidemiological or experimental evidence to be sure. “We need more studies and possibly animal experiments to determine the characteristics of ▶

TOXICOLOGY

House Would Foil Human Pesticide Studies

In a surprising move, the U.S. House of Representatives has voted to prevent the Environmental Protection Agency (EPA) from using studies that deliberately expose human volunteers to pesticides.

The amendment is the latest twist in a 7-year debate about so-called human dosing experiments, in which companies pay volunteers to ingest tiny amounts of pesticides to help determine safe exposure levels. Companies began conducting more such studies after a 1996 law required that EPA tighten pesticide safety levels to protect children. But the agency held off on using them after an advocacy group complained that they were unethical and later requested

a study by the National Academies’ National Research Council (NRC). That panel found that some human pesticide dosing studies were acceptable (*Science*, 27 February 2004, p. 1272). Three months ago, EPA announced it would once again begin considering data from such experiments.

Last week’s vote would halt EPA’s plans. An amendment to a spending bill by Representatives Hilda Solis (D–CA) and Timothy Bishop (D–NY) prohibits EPA from using its 2006 budget to review third-party pesticide dosing studies or conduct its own studies, which they call “reprehensible and unethical.” The move comes a few weeks after Congress persuaded EPA

to kill a Florida study that would have monitored children’s exposure to pesticides in homes where they are routinely used (*Science*, 15 April, p. 340).

Jay Vroom of CropLife America, an industry group in Washington, D.C., says he’s “profoundly disappointed” that lawmakers would block the use of “essential” safety data. But the NRC panel’s chair, ethicist James Childress of the University of Virginia in Charlottesville, thinks the move is fine. “A lot of us [on the NRC panel] were troubled” by the dosing studies, he notes, and “personally, my view is that [the House amendment is] within the range of ethically justifiable responses.”

—JOCELYN KAISER

CREDIT: HOANG DINH NAM/AP/GETTY IMAGES

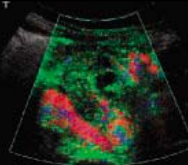
1244

Los Alamos: soon to be under new management



1248

Antiangiogenesis drugs show promise



1249

Orion's stellar nursery



these new strains,” says Hitoshi Oshitani, leader of the disease outbreak team at WHO’s regional office in Manila. Such studies have been hampered because the new strains are proving difficult to culture. “We don’t know why, perhaps because of the way it is changing, but even the CDC can’t get some of these recent viruses to grow, even though the patients were positive” by other tests, Oshitani says.

The genetic analyses also turned up one viral isolate that exhibited some resistance to oseltamivir, the drug considered a first line of defense against the virus. Jennings cautions, however, against extrapolating too much from a single isolate, as it is already known that a certain percentage of individuals develop resistance to oseltamivir.

Meanwhile, both human cases and avian outbreaks continue to be reported in Vietnam,

Indonesia, and China, even though at this time last year the virus seemed to have gone into remission.

Although the recent findings raise many questions, Jennings says it is clear that exposure to infected poultry is still the primary route of infection, including to the index cases of clusters. “Controlling H5N1 in poultry is the key to keeping it out of humans,” he says.

—DENNIS NORMILE

SMALLPOX

WHA Gives Yellow Light for Variola Studies

PARIS—After the smoke had cleared, both sides declared victory last week in a debate about the most dreaded virus on the planet. Proponents of further research with variola, the virus that causes smallpox, won approval at the World Health Assembly (WHA) to expand the scope of the studies. But those opposing it—including two vocal advocacy groups—say the surprisingly lively debate showed that opposition to the work is mounting.

At the meeting, the 192 member countries of the World Health Organization (WHO) rejected one study proposal, urged extra care with others, and questioned the composition of the panel overseeing the research.

The meeting was the latest round of discussions, managed by WHO, about variola’s fate. After its eradication in the 1970s, plans to destroy the last remaining virus stocks, now officially stored at only one Russian and one U.S. lab, have been postponed repeatedly to allow the development of new diagnostics, vaccines, and drugs to defend against bioterror attacks. Both the United States and Russia have stepped up their research programs since 9/11.

Last November, WHO’s Advisory Committee on Variola Virus Research recommended giving researchers more leeway by allowing, among other things, the transfer of DNA snippets of up to 500 base pairs among labs, the production of gene chips containing variola DNA, insertion of a gene for green fluorescent protein into the variola genome, and splicing variola genes into the genomes of other orthopoxviruses (*Science*, 19 November 2004, p. 1270).

The proposal to transfer variola genes to other species ran into opposition from WHO Director-General Lee Jong-wook, who urged WHA last month to send it back to the Advisory Panel and ask for additional biosafety

and biosecurity measures. During the WHA debate, on 19 and 20 May, almost a dozen countries, from South Africa to China to Tonga and the Netherlands, aired concerns about the research. Some worried about accidental escapes from the lab, others asked for a firm deadline for the final destruction of the virus; some also argued that the Advisory Committee is dominated by northern countries and by researchers with vested interests in continuing the research.

Because WHA didn’t vote or adopt a resolution, WHO’s secretariat must interpret what exactly it decided. WHO smallpox program officer Daniel Lavanchy says the assembly agreed to ban the gene-transfer studies for now but gave the green light to the other work. To allay concerns, the Advisory

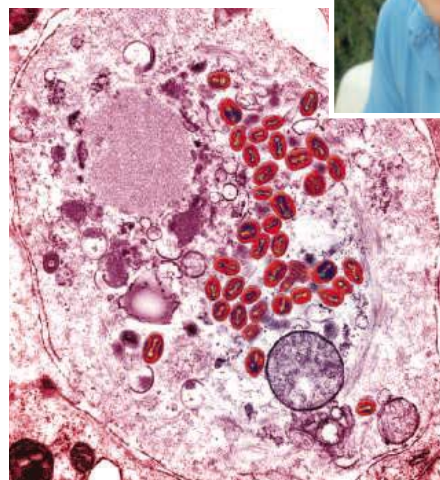
Committee will scrutinize individual proposals even more exhaustively, he says. WHO will also “certainly try to address the [committee’s] geographical imbalance,” says Lavanchy, who agrees that the United States has been a dominant force.

The debate this year was stoked by a new phenomenon: Two advocacy groups, the Sunshine Project in Austin, Texas, and the Third World Network, with headquarters in Penang, Malaysia, had campaigned aggressively against the new research. Lavanchy says the lobbying had little impact, but Jonathan Tucker of the Monterey Institute’s Center for Nonproliferation Studies in Washington, D.C., says the campaign was “remarkably successful” in raising the heat.

The underlying question is if—and when—work with variola will ever be completed. The goals of the research program—which include developing safer vaccines and two different smallpox drugs—give Russia and the United States an excuse to hold on to the virus almost indefinitely, says Edward Hammond, director of the Sunshine Project. Not so, says Lavanchy, who estimates that the research should take “a couple of years.”

D. A. Henderson, the former leader of the global eradication campaign and a long-time champion of variola destruction, also considers WHO’s timetable highly unrealistic. Given the time needed to develop antiviral drugs, the added problems of working in maximum-containment labs, and the lack of a good animal model for smallpox, he says, “this could take 20, 30, or even 50 years.”

—MARTIN ENSERINK



Advocate for destruction. Edward Hammond of the Sunshine Project campaigned against new experiments with the smallpox virus.

**100% heat inactivation in 5 minutes.
very cool.**



Antarctic Phosphatase

RECOMBINANT AND 100% HEAT LABILE — A BETTER ENZYME THAN SAP AT A BETTER PRICE

For many years, BAP, CIP and SAP were the only options for dephosphorylation protocols. Now, New England Biolabs introduces Antarctic Phosphatase – a superior reagent that saves time because you can ligate without purifying vector DNA, and since it's recombinant, you are guaranteed the quality and value you've grown to expect from New England Biolabs.

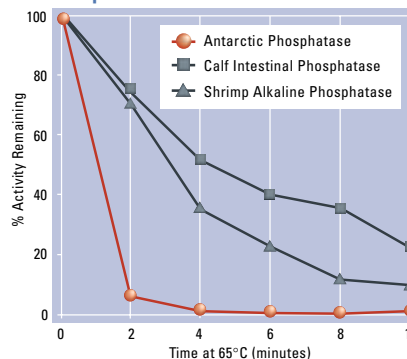
To Order:

M0289S 1,000 units \$58 (US)
M0289L 5,000 units \$232 (US)

Advantages:

- 100% heat inactivated in 5 minutes
- ligate without purifying vector DNA
- recombinant enzyme for unsurpassed purity and consistency; no nuclease contamination
- active on DNA, RNA, protein, dNTPs and pyrophosphate
- active on all DNA ends: blunt, 5' and 3' overhangs

Phosphatase Heat Inactivation



10 units of each phosphatase were incubated under recommended reaction conditions (including DNA) for 30 minutes and then heated at 65°C. Remaining phosphatase activity was measured by p-nitrophenyl-phosphate (pNPP) assay.

PRODUCTS YOU TRUST. TECHNICAL INFORMATION YOU NEED. www.neb.com

- **New England Biolabs Inc.** 32 Tozer Road, Beverly, MA 01915 USA 1-800-NEB-LABS Tel. (978) 927-5054 Fax (978) 921-1350 info@neb.com
- **Canada** Tel. (800) 387-1095 info@ca.neb.com
- **Germany** Tel. 0800/246 5227 info@de.neb.com
- **UK** Tel. (0800) 318486 info@uk.neb.com
- **China** Tel. 010-82378266 beijing@neb-china.com

DISTRIBUTORS: Argentina (11) 4372 9045; Australia (07) 5594-0299; Belgium (0800)1 9815; Brazil (11) 3622 2320; Czech Rep. 0800 124683; Denmark (39) 56 20 00; Finland (09) 584-121; France (01) 34 60 24 24; Greece (010) 5226547; Hong Kong 2649-9988; India (044) 220 0066; Israel (3) 9021330; Italy (02) 381951; Japan (03) 5820-9408; Korea (02) 556-0311; Malaysia 603-80703101; Mexico 52 5525 5725; Netherlands (033) 495 00 94; Norway 23 17 60 00; Singapore 2731066; Spain 902.20.30.70; Sweden (08) 30 60 10; Switzerland (061) 486 80 80; Taiwan (02) 28802913

 **NEW ENGLAND
BioLabs[®] Inc.**
the leader in enzyme technology

Voyager 1 Crosses a New Frontier and May Save Itself From Termination

Talk about timing. Only last March, NASA managers had decided that the Voyager 1 spacecraft—28 years and 14 billion kilometers out from Earth—might have outlived its usefulness (*Science*, 11 March, p. 1541). It didn't seem worth the expense of waiting for Voyager to find something more interesting than the now-monotonous hum of the solar wind as the spacecraft glided into the void far beyond the farthest planets. Then this week, Voyager scientists announced that their craft had just entered a new realm, one long hypothesized but never observed, that marks the doorstep to true interstellar space. "I hope this will just reinforce the exploratory nature of what Voyager is doing," says Voyager team member Edward Stone of the Jet Propulsion Laboratory in Pasadena, California. It's already excited space physicists, who now have a whole new playground to explore.

At first the play wasn't entirely harmonious. In 2003, dueling papers appeared in *Nature* arguing over recent data from Voyager 1. Space physicist Stamatios Krimigis of the Applied Physics Laboratory (APL) in Laurel, Maryland, and colleagues reported that in 2002, their instrument on Voyager had detected a large increase in energetic charged particles at a distance of 85 times the distance between Earth and the sun (85 astronomical units, or AU). That rise, they said, implied that Voyager had passed beyond the supersonic solar wind that bathes all the planets and had entered the region called the heliosheath, where the solar wind has slowed to subsonic speeds. The heliosheath constitutes the outer reaches of the teardrop-shaped bubble, called the heliosphere, that the solar wind inflates in the near-vacuum of interstellar space.

By that interpretation, Voyager 1 was the first humanmade object to cross the solar system's termination shock—the region where the solar wind abruptly slows before it collides with the more distant interstellar medium, behaving much as air does when it piles up in front of a supersonic plane. Six months later, Voyager seemed to cross back into high-speed

solar wind, perhaps as the solar wind gusted.

Space physicist Frank McDonald of the University of Maryland, College Park, Stone, and colleagues had a different take on their own 2002 Voyager data. Like the APL team's instruments, theirs reported an increase in charged particles—in this case, cosmic ray particles. But that was to be expected before reaching the termination shock, they said, not after crossing it. The debate has since continued without a resolution.

Researchers may be a long time settling whether Voyager 1 crossed the termination shock in 2002. But this week Norman Ness, principal investigator on the magnetometer subsystem at



Outward bound. Voyager 1 has entered the outer reaches of the sun's realm, which resembles this region around the star LL Ori.

the University of Delaware, Newark, declared, without fear of contradiction, "We have entered the heliosheath." Ness and the rest of the Voyager magnetometer team reported at this week's Joint Assembly of the American Geophysical Union (AGU) in New Orleans that last December the feeble magnetic field dragged along by the charged particles of the solar wind intensified by a factor of 3 at a distance of about 94 AU. That increase is the key marker of a termination-shock crossing, Stone says, because slowing and thus compressing the solar wind ought to intensify its magnetic field. Instruments showed no such intensification during the supposed 2002 crossing, Stone notes.

Also at the AGU meeting, Voyager principal investigator Donald Gurnett of the University of Iowa in Iowa City added more evidence of a crossing. He reported that on 15 December, Voyager detected the same sort of plasma-wave oscillations that spacecraft ►

Manhattan Showered With Stem Cell Gifts

Philanthropists are pouring money into three New York City biomedical institutions to support stem cell research.

The latest gift comes from the Starr Foundation, which is dividing \$50 million over 3 years among Rockefeller University, Memorial Sloan-Kettering Cancer Center, and Weill Medical College of Cornell University. Last year Weill received \$15 million from the Houston, Texas-based Ansary Foundation to establish a center for stem cell therapeutics, and earlier this month Mount Sinai School of Medicine took in \$10 million from donors for its own stem cell institute (*Science*, 13 May, p. 937).

The Starr Foundation was established by Cornelius Vander Starr, founder of the financial and insurance companies called American International Group Inc. Its Tri-Institutional Stem Cell Initiative will focus on a wide range of stem cell projects, involving cells from embryos, adult tissues, and cancerous tumors, says Sloan-Kettering President Harold Varmus. He says the gift is already influencing recruitments at Sloan-Kettering, and he hopes it might lessen the possible lure of California's \$3 billion in public funding. "We don't want people leaving or young people to ignore the fact that we have a lot of support for this research in New York," he says. Weill Dean Antonio Gotto hopes some of the funds will allow researchers at its large fertility clinic to produce new stem cell lines from cloned human embryos.

—GRETCHEN VOGEL

Quality Check for Australia's Research

Australia is beginning a \$2.8 million study of how the government funds research that is expected to put greater emphasis on scientific productivity.

As the first step in the process, a government-appointed panel has been asked to develop a method of ranking university departments based on the impact of publications by faculty members. The panel, led by Gareth Roberts of Wolfson College in Oxford, U.K., is looking closely at a U.K. system adopted in 1986 as well as reviewing comments from stakeholders. A 6-month trial of the new system will begin in September.

—JACOPO PASOTTI

have always encountered just before running into shock waves in the solar wind upstream of planets. Shortly after the oscillations, Voyager was in the new solar wind regime of heightened magnetic field. Everyone, including Krimigis, now agrees that this new regime is the heliosheath.

Now that they are in it, researchers are eager to understand the heliosheath. They missed recording the actual passage through the shock because it occurred during one of the gaps in Voyager monitoring by the big radio telescopes of the Deep Space Network. But they will be studying the heightened tur-

bulence within the heliosheath and how the turbulence helps deflect galactic cosmic rays. The spacecraft's reports from the heliosheath should also help scientists understand similar shock-bounded "astrospheres" seen around other, more energetic stars.

Researchers are also looking outward toward the next Voyager milestone: leaving the heliosphere entirely. Estimates of the distance to the heliopause—where solar wind ends and the interstellar medium begins—vary widely. Gurnett's interpretation of radio signals emanating from that frontier place it anywhere from 116 AU to 177 AU. But

Voyager 1 will run short of power from its radioisotope thermal generator as early as 2020 and go silent about 147 AU out.

Now, knowing where the termination shock is, researchers are suggesting 125 AU as a best estimate of the distance to the heliopause. "That's a comforting number," says Gurnett, because it would get Voyager 1 there around 2014. Perhaps NASA managers will be equally comforted and remove Voyager 1 and its lagging companion Voyager 2 from the list of space physics missions to be considered this fall for termination.

—RICHARD A. KERR

NUMBER THEORY

Third Time Proves Charm for Prime-Gap Theorem

Dan Goldston feels much better. Two years ago the number theorist at San Jose State University in California suffered a discouraging setback. He and Cem Yildirim of Boğaziçi University in Istanbul, Turkey, had announced a dramatic breakthrough in the theory of prime numbers, only to learn that their proof contained a fatal error (*Science*, 4 April 2003, p. 32; 16 May 2003, p. 1066). But now, with the help of János Pintz of the Alfréd Rényi Mathematical Institute in Budapest, Hungary, Goldston and Yildirim have unveiled a new proof of their breakthrough result. This time experts who have examined it say the proof is rock-solid—in part because it is much simpler than the earlier attempt.

"It's of enormous importance," says Brian Conrey, director of the American Institute of Mathematics in Palo Alto, California. "It's going to open the door to lots of stuff." Andrew Granville of the University of Montreal, Quebec, whose work helped torpedo the original flawed proof, agrees. "It's quite a turning point," he says.

Goldston and Yildirim were studying the way one prime number follows another. Prime numbers—positive integers such as 2, 3, 5, 7, 11, and 13, which can't be broken down into smaller factors—become rarer as numbers get larger. On average, the gap between a large prime p and the next prime number is approximately the natural logarithm of p , written $\log p$. But the actual gap

between two primes may be far from average. Number theorists long ago proved that there is no upper limit on how large the gap can grow, relative to $\log p$. What Goldston and Yildirim claimed—and, together with Pintz, have now proved—is that the smallest possible gap also continues to shrink relative to $\log p$, as the numbers increase.

The original proof foundered when Granville and Kannan Soundararajan of the University of Michigan, Ann Arbor, spotted a mistake in a single, technical subsection of the proof, known as a lemma. The rest of the proof was fine, and part of it immediately enabled two other mathematicians to make a major breakthrough in studying arithmetic progressions of primes (*Science*, 21 May 2004, p. 1095). Goldston and Yildirim also salvaged a weaker result about prime gaps that improved on previous researchers' work.

Goldston kept hoping to make the proof work but finally gave up. "I had come to terms with not getting a good result," he recalls. Then, about a year ago, he had an idea for a new approach. He worked out the details and presented his new proof last summer at the mathematical conference center in Oberwolfach, Germany. He woke up the next morning, however, knowing he had made another mistake, this time in the very last step of the proof. "I really felt jinxed by the whole thing," he recalls.

Pintz, however, took a close look at the flawed proof and came up with the key insight for the ultimate fix. He contacted Goldston and Yildirim last December, and the three number theorists had a complete proof by early February. This time, they were more cautious about announcing the result. "We all thought it was wrong," Goldston says. They circulated the manuscript to a handful of experts, including Granville and Soundararajan, asking them to probe it for any new or remaining errors.

In addition to finding nothing wrong, the ad hoc jury also discovered ways to simplify the proof. "It's been simplified so much there's not much room for an error to be hiding," says Conrey. One of the experts, Yoichi Motohashi of Nihon University in Japan, found a shortcut that led to a surprisingly short proof of the basic, qualitative result. He and the three lead authors have posted this proof, running a mere eight pages, at the arXiv preprint server (www.arxiv.org). The more-detailed paper with Pintz is being rewritten to incorporate some of the simplifications. Goldston gave a public presentation on the new proof at a number theory conference held from 18 to 21 May at the City University of New York.

In itself, the basic result is not a surprise. But it may help mathematicians tackle the famous "twin prime" conjecture, which probably dates back as far as mathematicians have thought about prime numbers. The conjecture holds that there are infinitely many primes for which the gap is 2. The list of twin primes starts with (3, 5), (5, 7), and (11, 13), and has been tabulated by now into the trillions. No one knows whether twin primes ever stop appearing. The new proof is still a far cry from the twin prime conjecture, but it offers a glimmer of hope that number theorists may eventually get there—perhaps a lot sooner than they ever expected. "The twin prime conjecture doesn't seem impossible to prove anymore," Goldston says.

—BARRY CIPRA



Comeback kid. Goldston despaired of rescuing his proof, but a bright idea saved the day.

Controversial Study Suggests Seeing Gun Violence Promotes It

A longitudinal study of Chicago adolescents has concluded that even a single exposure to firearm violence doubles the chance that a young person will later engage in violent behavior. The study may once again stoke up the debate over juvenile violence; it has already triggered criticism over the unusual statistical method it employs.

The work is part of the decade-old Project on Human Development in Chicago Neighborhoods, run by Harvard University psychiatrist Felton J. Earls. On page 1323, Earls and

The authors then went to great lengths to weed out confounding factors. Subjects were ranked according to “propensity” scores: a cumulative tally of 153 risk factors that estimated the probability of exposure to gun violence. They were then divided up according to whether or not they had reported such exposure and whether or not they had subsequently engaged in violent behavior. Those with the same propensity scores but different exposures were compared with each other. In this way, the authors claim, they controlled for a host of individual, family, peer, and neighborhood variables.

Even with this analysis, exposure to gun violence predicted a doubling of the risk for violent behavior—from 9% for unexposed to 18% among the subjects who reported exposure, says Bingenheimer. And it didn’t take repeated exposures—“the vast majority” of subjects reported only one, he says. Can a single experience of seeing someone shoot at someone else make an individual more violence-prone? “That doesn’t seem improbable to me,” says Bingenheimer. “It could be for only a minority, but a very large effect for that minority.”

Developmental psychologist Jeanne Brooks-Gunn of Columbia University, one of the scientific directors of the Chicago neighborhoods project, agrees that a single exposure might have a profound effect, even on a hitherto nonviolent individual. “Nobody’s done this kind of analysis before,” she says, and nobody has focused just on gun violence, which “clearly is a very extreme type of violence.”

But a number of other scholars have deep misgivings about both the study findings and the methodology. Psychiatrist Richard Tremblay of the University of Montreal in Canada says the study does not demonstrate that “those who are nonviolent to begin with will become violent.” Indeed, the authors didn’t address this point directly because a lack of subjects in the lowest-risk category led them to eliminate it from their analysis. ▶

Violence debate. A study of Chicago adolescents indicates that seeing a murder may lead to later gun violence by the observer.

two health statisticians describe how they used a relatively new technique called “propensity score stratification” to create, through statistical means, a randomized experiment on propensity toward violence from observational data.

Over a 5-year period, the researchers conducted three interviews with more than 1000 adolescents initially aged 12 to 15. In the first, they gathered extensive data on variables such as family structure, temperament, IQ, and previous exposure to violence. Halfway through the study, the subjects were asked if, in the prior 12 months, they had been exposed to firearm violence—defined as being shot or shot at or seeing someone else shot or shot at. Then at the end of the period, the 984 subjects remaining were asked if they had engaged in any violence—defined as participation in a fight in which anyone got hurt as well as firearm-related incidents, including carrying a gun.

“If you just compare exposed and unexposed, the exposed were three or four times as likely to be [violence] perpetrators,” says lead author Jeffrey B. Bingenheimer, a Ph.D. candidate at the University of Michigan School of Public Health in Ann Arbor.



New Reporting Regs for Globe-Trotting Diseases

The world has a new set of rules for dealing with diseases, such as flu or SARS, that cross borders easily. On Monday, the World Health Assembly, an annual meeting of 192 governments in Geneva, Switzerland, approved regulations making it mandatory for countries to detect and respond to infectious diseases within their borders, notify the World Health Organization (WHO) within 24 hours of any outbreak that could threaten other countries, and collaborate in investigating and controlling such outbreaks.

Similar International Health Regulations have existed for half a century. But even the latest version from 1981 was widely considered outdated; for one, it didn’t cover newly emerging infections. The revised treaty, which will formally take effect in 2007, has been debated for more than 10 years. The issue became more urgent in 2003, when China risked a wide spread of SARS by hiding the extent of its outbreak—behavior that would violate the new rules. Although WHO has no sanctions for countries that violate the new regimen, “this gives us much clearer ground rules,” says WHO’S Max Hardiman.

—MARTIN ENSERINK

Embattled Berkeley Ecologist Wins Tenure

Ignacio Chapela, an ecologist whose views on biotechnology have attracted controversy, has won tenure at the University of California, Berkeley, after appealing an earlier rejection.

Chapela caused a stir with a 2001 report in *Nature* that promoter genes from genetically modified corn had been detected in traditional kinds of corn in Mexico—a finding the journal later disavowed (*Science*, 12 April 2002, p. 236). He also was a persistent critic of a \$25 million deal with Novartis in 1998 for exclusive licensing of plant and microbial research.

Chapela claimed that the university denied him tenure in 2003 because of his opposition to the Novartis deal (*Science*, 19 December 2003, p. 2065). Last month, he sued the university, claiming it had also discriminated against him because he was born in Mexico. Berkeley, meanwhile, was reexamining the case as part of an earlier consent agreement, and a nine-member panel voted thumbs-up. “This was a case in which reasonable reviewers could disagree,” says spokesperson George Strait. After learning of his victory, Chapela e-mailed supporters that he now fears tenure “may become a [self-imposed] muzzle.” —ERIK STOKSTAD

Because the remaining subjects already had some violence risk factors, the results don't surprise Tremblay. He compares the work to looking at whether alcoholics are more likely to drink if they are exposed to alcohol. It is already well known, he says, that "if individuals at a high risk of violence are in an environment with violence, they're more likely to be violent."

Economist Steven Durlauf of the Univer-

sity of Wisconsin, Madison, calls the study an "implausible modeling of violence exposure." The authors assume that two individuals with the same propensity rankings are equally likely to encounter violence, he says. But such exposure may not be random; rather, it probably stems from "something that has not been measured"—such as recklessness, says Durlauf. Nobel Prize-winning economist James Heckman of the University of

Chicago agrees, calling the study "potentially very misleading." Adds Heckman: "This is why you find out orange juice causes lung cancer one week and cures it the next."

But Brooks-Gunn defends the innovative study. The propensity scoring technique "comes the closest we have to any experiment, which is why I think the results are so strong," she says. —CONSTANCE HOLDEN

BIOCHEMISTRY

Plant Hormone's Long-Sought Receptor Found

In all of nature, few molecules do more. The plant hormone auxin helps plants grow toward light, grow upward rather than branch out, and grow their roots down. It helps plants flower and bear fruit. Now, more than 70 years after auxin was first discovered, biologists have finally identified its major receptor—a crucial step toward understanding how the hormone works.

"It's really exciting for auxin biology to know how auxin can be perceived," says plant geneticist Bonnie Bartel of Rice University in Houston, Texas.

In the 26 May issue of *Nature*, two teams, led by Ottoline Leyser of the University of York, U.K., and Mark Estelle of Indiana University, Bloomington, independently report that auxin binds to a protein called TIR1. When auxin attaches, TIR1 helps mark for destruction another protein that represses a set of genes that are known to be activated by auxin's presence; when the cell destroys that protein, the genes turn on.

For decades, biochemists fished around in extracts of growing plants for proteins that bound to auxin (also known as indole-3-acetic acid). Plants lacking one such protein, auxin-binding protein 1 (ABP1), die, demonstrating that it is essential. But ABP1 does not resemble other hormone receptors, and it doesn't seem to turn genes on or off, a property that's needed to explain auxin's myriad effects, Estelle says. So beginning in the mid-1980s, he and his co-workers began anew, identifying lines of a small plant called *Arabidopsis thaliana* (wall cross) that respond abnormally to auxin. They reasoned that the defective genes in these mutant lines might be part of the machinery that enables the plant to respond to auxin.

One such defective gene encoded an F-box protein, a family of proteins found in plants and animals that tag other proteins with a molecule called ubiquitin, which signals the cell to destroy the tagged proteins. That sug-

gested that the plant auxin response involved protein degradation, and that this particular F-box protein, called TIR1, played a key role. By 2001, Estelle and Leyser, a former postdoc of Estelle's who by then ran her own laboratory, had shown that auxin causes a protein complex containing TIR1 to bind to so-called Aux/IAA proteins, which repress certain genes known to be triggered by auxin. Auxin apparently activates genes by marking Aux/IAA proteins for destruction.

To establish precisely how, the two teams first spent several years running down "a lot of blind alleys," Estelle says. It turned out that

and showed that it bound to purified TIR1 complexes but not to Aux/IAA proteins.

Stefan Kepinski, a postdoc in Leyser's laboratory, also took the gene encoding TIR1 and injected it into hundreds of frog embryos in order to mass-produce the protein. After purifying TIR1 from the ground-up embryos, Kepinski showed that the auxin caused the protein to bind to a purified piece of an Aux/IAA protein. Nihal Dharmasiri, a postdoc in Estelle's group, did similar experiments with TIR1 protein produced in insect cells and got similar results. Because no other plant proteins

were present in either case, the work shows that TIR1 is an auxin receptor, Estelle says.

"We're happy to have a receptor for auxin," says plant biologist Joanne Chory of the Salk Institute for Biological Studies in La Jolla, California. "Auxin has been such an enigma."

What's more, according to results from Estelle's group that will appear in *Developmental Cell*, TIR1 is just one of four related F-box proteins, each of which functions as an auxin receptor; when all four are missing, a plant's development is severely damaged. These results suggest that a family of TIR1-like proteins, working with a family of Aux/IAA proteins, could direct many of the diverse physiological responses to auxin.

The discovery of this auxin receptor may also shed light on additional plant signaling pathways. Plants have roughly 700 F-box proteins, but little is known about them. Researchers suggest that some of them may mediate responses to other hormones, such as jasmonate, which mediates plant defenses, and the gibberellins, which promote germination and stem growth. "It's a whole new type of receptor," Bartel says. That's "the big story."

—DAN FERBER



Hormone helper. Two teams, one led by Mark Estelle (above), have finally identified a key receptor that enables the hormone auxin to guide plant growth.

the pathway was a lot simpler than assumed, Leyser says. They'd expected an auxin receptor to activate genes the way other hormone receptors do: through a signal cascade involving a series of enzymes in which the last one activates gene-regulating protein. Both teams isolated TIR1-containing complexes from plant extracts, thinking they'd have to find and add back other enzymes to allow the complexes to detect auxin and bind Aux/IAA. But nothing else was needed. To prove the point, both teams added radioactively tagged auxin

2006 BUDGET

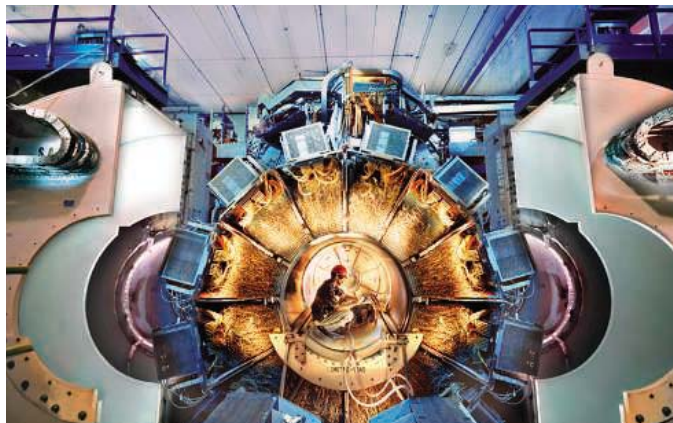
Physics Research Gets a Boost and a Warning From Its Funders

A spending committee of the U.S. House of Representatives has restored many of the cuts proposed by President George W. Bush to the Department of Energy's (DOE's) 2006 science budget, including those in its high-energy and nuclear physics programs. But that ray of sunshine was quickly clouded over by an agency request for scientists to evaluate the consequences of shutting down yet another key accelerator.

House appropriators last week added \$200 million to the president's request, which would have taken a 4% bite out of the department's \$3.6 billion Office of Science. Along with \$39 million more for an advanced computing initiative, \$70 million for biological and environmental research (including \$35 million in earmarks), and a \$5.6 million boost for fusion science, high-energy and nuclear physics were brought back roughly to fiscal year (FY) 2005 levels. The \$22 million increase for high-energy physics would be split between neutrino physics and linear collider work, and the 10% boost for nuclear physics would prevent threatened cuts in run times at two nuclear physics labs, as well as providing funding for research into a new nuclear-physics facility, the Rare Isotope Accelerator, that has been stalled.

But those increases, which require concurrence from the Senate, don't mean that DOE-funded scientists are in the clear. The House Appropriations committee did not reverse DOE's decision to cancel a high-energy physics project, BTeV, at Fermilab (*Science*, 1 April, p. 38). Nor did it give any comfort to a nuclear-physics panel created this spring to weigh which of the two flagship nuclear-physics facilities in the United States—CEBAF at the Thomas Jefferson National Accelerator Facility in Virginia or RHIC at Brookhaven National Laboratory in Upton, New York—should be shut down (*Science*, 29 April, p. 615). Its report is due next month.

The commentary on the appropriations bill heaps praise upon the Office of Science and its endeavors—and should bolster scientists who feel the squeeze of tightening budgets. “High-energy physics is the cornerstone of our understanding of the physical universe,” the committee writes. And although the Senate appropriators have not yet produced their own numbers, in the past few years they, too, have supported an Office



B sting? A tight DOE budget could claim the BaBar detector at the Stanford Linear Accelerator Center.

of Science budget significantly above the presidential request.

Still, last week's meeting of the High Energy Physics Advisory Panel (HEPAP) for DOE and the National Science Foundation brought more bad news. The panel agreed to evaluate the costs and benefits of shutting down the Tevatron accelerator at Fermilab in Illinois or the B Factory at the Stanford Linear Accelerator Center in California—or both—

as early as the end of FY 2006. That would be 3 years and 2 years earlier, respectively, than the current timetables. “Will the resources now invested in [these accelerators] have a greater scientific impact if they are to be employed otherwise?” asked DOE high-energy head Robin Staffin, who said that the beneficiaries would likely be the proposed International Linear Collider as well as new (and smaller) initiatives in high-energy physics.

“This way of doing business is making me very jumpy,” responded Peter Meyers, a Princeton physicist and member of HEPAP. “When you proposed [2008 and 2009] end dates to the [B Factory and Tevatron] projects, everyone gritted their teeth and said OK. But now, even when the projects are going really, really well, you're still going to evaluate whether to sweep them away.”

Panel members say it's appropriate to look at what facilities they must sacrifice to keep the field alive. “We shouldn't be scared of asking ourselves hard questions,” says physicist Steven Ritz of NASA Goddard Space Flight Center in Greenbelt, Maryland, a HEPAP member. But the exercises are still stressful, says Meyers: “Boy, do they make me feel uncomfortable.”

—CHARLES SEIFE

SCIENCE AND THE LAW

Butler Gets Break on Pending Appeal

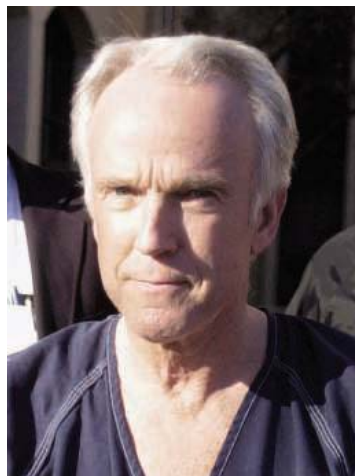
Infectious-disease researcher Thomas Butler will be back in the headlines next month when a federal appeals court in New Orleans, Louisiana, hears his request to overturn his conviction for fraud and mishandling plague samples. Butler, who was sentenced to 2 years in prison, became a cause célèbre for scientists worried about the government's zeal to combat bioterrorism. Legal experts say his appeal faces an uphill fight. But it's less risky than it once seemed now that the federal government has dropped a counter-appeal seeking an even stiffer sentence.

Butler, 63, was arrested in January 2003 after he reported that 30 vials of plague bacteria were missing

from his lab at Texas Tech University in Lubbock, and the incident escalated into a bioterror scare. He was later charged with 69 criminal counts, including mishandling samples, tax evasion, and lying to investigators. A jury acquitted him of 22 charges but

convicted him of violating export rules on shipping a package of bacteria and of steering clinical research payments to himself rather than to Texas Tech (*Science*, 19 December 2003, p. 2054). In March 2004, a federal judge, citing Butler's contributions to humanity, sentenced him to 2 years rather than the 9-year term specified by federal sentencing guidelines.

In August, Butler asked the appeals court to overturn the conviction or order a new trial. The move triggered a cross-appeal from prosecutors arguing that his reduced sen- ▶



Back in court. Thomas Butler's appeal will be heard 8 June.

eppendorf
PhysioCare
Concept criteria
3 and 4

- 30% less weight
- Single handed volume setting
- Ergonomic studies
- Ergonomics approved by TÜV



eppendorf® is a registered trademark.

Less strain – more efficiency.

Optimized form and function – Perfectly balanced

PhysioCare Concept pipettes.

The more strain you experience, the less energy you have. And because energy is a very precious and exhaustible resource, we try to use it as efficiently as possible.

So why aren't more manufacturers doing it? Probably because it's not that easy.

TÜV Rheinland approved our manual pipettes as: ergonomic, user-friendly and user tested.



Check out how good your pipette really is!
PhysioCare Concept™ website
www.physiocare-concept.info

eppendorf
In touch with life

Your local distributor: www.eppendorf.com/worldwide · Application Hotline: +49 180-3 66 67 89

Eppendorf AG · Germany · +49 40 538 01-0 • Eppendorf North America, Inc. 800-645-3050

tence violated federal sentencing guidelines (*Science*, 22 October 2004, p. 590). Fortunately for Butler, the U.S. Supreme Court in January declared that the sentencing guidelines are not mandatory. The decision, *United States v. Booker*, led the government to withdraw its cross-appeal, which was dismissed on 1 March. However, Butler could still receive a longer sentence if a new jury reaches different conclusions, notes Larry Cunningham, a Texas Tech law professor. "It's not a given that he would be entitled to a better sentence," he says.

Butler's supporters are hoping for vindication. In a commentary in the 1 June issue of *Clinical Infectious Diseases*, 14 scientists and physicians call for his release so that "com-

mon sense [can] prevail." Lead author Barbara E. Murray of the University of Texas Medical School in Houston worries that a similar fate could befall any researcher. "We're in an environment in which if somebody wanted to get us, they could," she says.

In his appeal, Butler argues that the trial was flawed by six "legal errors," including trying him on charges related to his handling of the plague samples and his financial dealings simultaneously, relying on vague university policies to find criminal fraud, and refusing to allow certain university e-mails and testimony. The government responded that the charges were "properly joined" because they showed a "scheme" to defraud the university and that the testi-

mony and documents were "immaterial." Its brief also asserts that the university policies weren't critical to his fraud conviction because Butler's "secretive, self-serving conduct was ample to show he had the intent to defraud." Cunningham says that "very few criminal cases get reversed" by the Fifth Circuit Court.

Meanwhile, Butler's attorneys and family are hoping that he will be released by Christmas. A legal defense fund is helping to support his appeal, which is being handled at a reduced rate by Jonathan Turley of George Washington University Law School in Washington, D.C., and attorneys from Bryan Cave LLP. The initial trial cost Butler's family \$1 million, Turley notes. —JOCELYN KAISER

FRENCH SCIENCE

Cracks in the Monolith: CNRS Begins a Long-Awaited Reform

PARIS—The chiefs of France's CNRS—the largest basic research agency in Europe—have adopted a plan to shake the place to its foundations. The new scheme will halve the number of the agency's departments and merge many of its directly supported labs, reducing their number from 1200 to "perhaps 800," according to CNRS director Bernard Larroutourou, who presented the plan at a 23 May press conference.

Although many agreed that reform was overdue, it has taken more than a year of tough negotiations between the government and research unions to bring it off. Some observers were worried that the government might gut CNRS. The agency has grown massively since its creation in 1939; it now employs 11,600 researchers and 14,400 engineers, technicians, and administrative staff. It has never had a major organizational overhaul. The government wants to maintain the institution, not eviscerate it, Larroutourou said. He acknowledged, however, that CNRS's role will be changed. The plan "goes way beyond an [internal] reorganization [and] will bolster the CNRS as a research operator," he said.

Larroutourou peppered his presentation with references to the Max Planck Gesellschaft, saying he admires the German agency's focus on the core activity of research. He believes one of CNRS's roles is to be a "client" of the National Research Agency (ANR), the controversial French organization that was created this year to fund research projects and that some researchers fear will finance targeted projects at the expense of open-ended basic research. Larroutourou said it will be important to maintain a balance between ANR and other institutions.

The new plan calls for CNRS to reduce its thematic science departments from eight to four: chemistry, social sciences, life sciences,

and a giant grouping of math, computer science, physics, and science of the planets and the universe. Two new crosscutting departments will be created for environment/sustainable development and engineering. CNRS will also create a general science



New agenda. More change ahead, says CNRS director Bernard Larroutourou.

directorate to assist the director and five inter-regional divisions (DIRs).

Larroutourou said that the shakeout, to be in place by next January, was needed to clarify CNRS's mission, to improve career prospects for young researchers, to foster university research, and to be part of the "training-research-innovation continuum." CNRS will do all this, he said, by encouraging closer links between public and private-

sector research and the transfer of knowledge and technology. Larroutourou also said CNRS should play a key role in developing pan-European research, promoting research in French regions, and breaking down barriers between disciplines, a goal Larroutourou admits was pursued by at least seven of his predecessors. He does not rule out ending support for some disciplines if CNRS has a minor presence but says no decisions have yet been made: "Thinking about it is already a revolution."

The leading research union to which French/CNRS scientists belong, SNCS, is unhappy—both with specific changes and with Larroutourou's "polite arrogance," said Jacques Fossey, general secretary of SNCS and a member of the CNRS board. Fossey opposes the reform on several points, including its "lack of scientific coherence in the overdiversified" math-physical sciences department and the extra layer of complexity the DIRs will bring.

The changes at CNRS are part of a broad government agenda to improve French science, including a reform bill that has been delayed for months in a standoff between the government and researchers (*Science*, 11 February, p. 829). Recently, government officials made new promises in an attempt to break the impasse. Education and Research Minister François Fillon said 3000 scientific posts would be created in 2007—in addition to those pledged for 2006—in step with "implementation of the law," or cooperation from the labs. The final draft bill, Fillon has said, will be out by 15 June. That pledge did not stop several thousand scientists—who object to the government's reluctance to commit to specific jobs and cash figures—from marching in protest last week.

—BARBARA CASASSUS

Barbara Casassus is a writer in Paris.

Defense contractors will play a larger role in the next contract to manage Los Alamos National Lab, which has spent 62 years under academic reins

A Bidding War for Los Alamos

Can a scientific icon of the atomic age find happiness with a bottom-line industrialist? That's a question the Department of Energy (DOE) will soon have to grapple with: Last week, the department announced a competition to manage Los Alamos National Laboratory, and industrial companies are expected to be partners on the leading bids (see next page). Many scientists are worried that the wrong answer could tarnish the crown jewel of the country's nuclear weapons complex.

Perched atop several mesas in northern New Mexico, Los Alamos has long been known as a place where classified weapons research coexists happily with academic traditions such as open publication and peer review. That culture has been nurtured by the University of California (UC), which has run the lab since 1943 through a succession of no-bid contracts. But after a series of security and management scandals, Congress forced DOE to hold an open competition for the next 7-year contract to run the \$2.2-billion-a-year lab, which DOE has sweetened by increasing the yearly fee from \$9 million to an incentives-laden \$79 million. Some of the rules under which UC has operated have also been changed. But many lab scientists are fearful that the new boss might stifle the scientific enterprise in the course of tightening oversight.

The question of who should control the science of atomic warfare dates back to the lab's origins. Civilian scientists prevailed over the military's attempt to manage nuclear weapons research after World War II. Yet DuPont and Dow Chemical were among early corporate managers of various nuclear industrial facilities—often for no fee. Since 1993, Lockheed has received mostly good reviews for its management of neighboring Sandia National Laboratories, which focuses on nuclear engineering.

In contrast, UC's stewardship of Los Alamos has been increasingly rocky. The university was widely criticized for its investigation into alleged espionage by computer scientist Wen Ho Lee in the 1990s and for various security breaches, both real and imagined. In 2003, DOE announced that it would put the lab up for bids after UC's contract expired on 30 September 2005.

Although UC has been coy about its intentions, this week its Board of Regents was expected to announce that it would join with Bechtel in bidding for the contract.

Shoring up safety and security are central to DOE's stated rationale for opening up the contract to competition. But officials say science is also a priority. The National Nuclear Security Administration (NNSA), which oversees the labs, has announced that one-third of each applicant's score will be based on "science," including the ability to foster "an environment of scientific skepticism and peer review" and collaborative research. "Good management is not the enemy of good science," says Tyler Przybylek, head of the NNSA board that will evaluate proposals. "There are things corporate managers do very well."

The current system isn't perfect, scientists concede. Many scientists say management is "too bureaucratized," says former

and maintains nuclear power plants and military installations. In addition to Sandia, Lockheed Martin, which has teamed with UT, runs the Knolls Atomic Power Laboratory in upstate New York, which conducts research for the Navy. Northrop Grumman manages the nation's nuclear ballistic missiles and studies radiological power for space flight. Some, like White House science adviser John Marburger, point to Sandia—as well as Oak Ridge National Laboratory in Tennessee—as proof that a nonacademic contractor can deliver great science and sound management.

But many scientists feel that the study of nuclear weapons gives Los Alamos a unique mission that could be degraded by a company concerned about its bottom line. Sigma Xi director John Ahearne, who sits on an unpaid UC advisory council, thinks handing over control to a defense contractor is "just too big a risk." Says Philip Coyle, former deputy to the director of Lawrence Livermore National Laboratory, which has an identical mission, "the design weapons labs have to be honest brokers about these weapons, be clear about what they know and don't know, and not make money on it." The current debate over the effectiveness of the W-76 warhead, a military mainstay, illustrates how that system works, says Thomas Meyer, former Los Alamos associate director for strategic

research. "This is an example of people without economic bias or interest sitting down and looking at a crucial problem," he says.

Experts point to several ways in which Los Alamos's culture is conducive to top research despite the restrictions. A 2004 report by the National Research Council (NRC) lauded its "easy and open communication on unclassified [research]," plenty of postdocs and visiting students, seminars, ample publishing, and blunt critiques. That culture is foreign to industry, says Timothy Thompson, former head of design engineering at Los Alamos: "At an aerospace company, you always feel like you're competing with the guy next door."



Los Alamos science policy adviser Anne Fitzpatrick, now at the Federation of American Scientists in Washington, D.C. A defense contractor, says Roy Schwitters, a physicist at the University of Texas (UT), Austin, "allows the physicists to think about physics—not scheduling programs." He says the failed Superconducting Super Collider lab in Waxahachie, Texas, which he directed, suffered from "tensions" between its scientific and industrial teams, although he feels the arrangement generally worked.

The likely bidders certainly have hefty technical management experience. Bechtel National, an equal partner with UC, builds

Getting ready. Los Alamos scientists prepare for a subcritical experiment last year at the underground Nevada Test Site.

Many Los Alamos scientists also worry that a corporate boss, seeking to avoid controversy, might interfere with the lab's annual review that leads to a letter assuring the president of a "safe, secure, and reliable" nuclear stockpile. Some complain that the current UC bureaucracy already stifles dissent, but lab chief science officer Thomas Bowles says an emphasis on "academic integrity" allows working scientists to raise concerns. Peer review at the lab currently ranges from internal "red teams" that assess science programs to regular review of laboratory-administered grants. "It's not the kind of practice industry is used to doing," says Meyer, who left the lab in the wake of a laser accident last year.

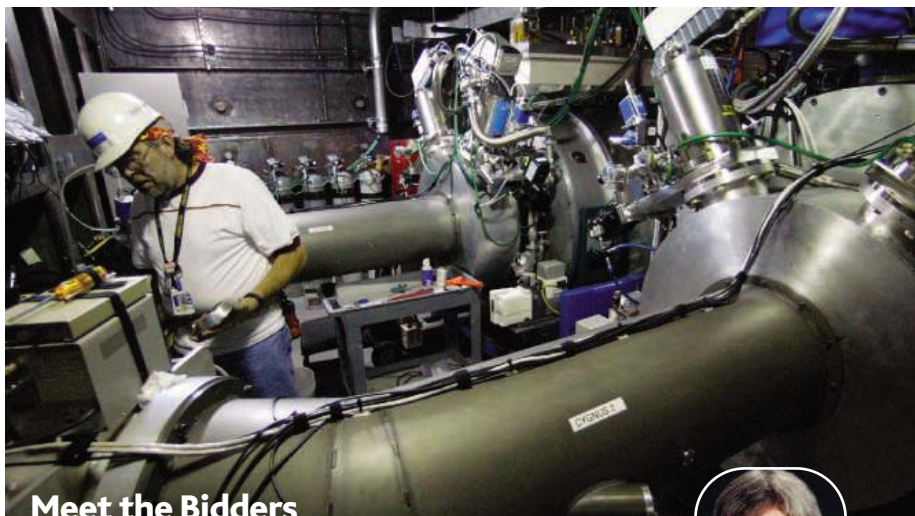
The leeway to pursue basic science not directly related to the lab's national-security mission is another aspect that some see as imperiled. Basic work on proton radiography, says Bowles, has led to a new way to image weapons material. Former lab postdoc Gavin Lawes, now at Wayne State University in Detroit, Michigan, was impressed by the freedom given scientists to pursue personal interests. "In the morning they'll do their own research outside the fence, and in the afternoon they go inside," he says.

The way internal funds are distributed for projects proposed by lab scientists is also at risk, says Sidney Drell, a current Los Alamos consultant and longtime DOE adviser. A goals-driven industrial philosophy, he warns, could result in a "too tightly programmed" lab-directed research and development (LDRD) account—a potential problem at a number of DOE labs.

The account, which amounts to 6% of the lab's budget, also plays a key role in recruiting and retaining staff, says the NRC panel, because "it offers the possibility of following their most promising ideas to fruition, even if there is a high risk of failure." The existence of such funds could also stem what some administrators fear will be a flood of retirements if UC doesn't win the bid.

Not surprisingly, scientists on the teams bidding for the contract take quite a different view of industry's ability to run the storied laboratory. C. Paul Robinson has served as director of Sandia under Lockheed management since 1995 and would lead Los Alamos were Lockheed to prevail. "We don't let anybody put Lockheed Martin's interest in front of the national interest," he says.

Robinson says curiosity-driven research would thrive under his leadership, adding that well-managed LDRD projects at Sandia led to breakthroughs in bomb-disablement techniques and mobile sensors. He also cites the yearly "deans' days" at Sandia



Meet the Bidders

UNIVERSITY OF CALIFORNIA/BECHTEL

Minor partners: BWX Technologies, Washington Group International

Team Leader: Michael Anastasio ▶

Relevant Experience: Current manager of Los Alamos, Lawrence Livermore, and Lawrence Berkeley national laboratories

What They're Saying: Sure, UC has a long track record. But does adding Bechtel erase concerns about lab safety and management?



NORTHROP GRUMMAN INFORMATION TECHNOLOGY

Academic partners: Not yet named

Team Leader: Not yet named

Relevant Experience: Management of ICBM fleet, Newport News shipyard

What They're Saying: Running want ads in *The Washington Post* suggests that Northrop hasn't played in this league. Are they up for the challenge?

LOCKHEED MARTIN

Minor partners: University of Texas

Team Leader: C. Paul Robinson ▶

Relevant Experience: Current manager of Sandia National Laboratories

What They're Saying: Lockheed gets high marks for Sandia, which conducts weapons engineering. But what about nuclear physics and design?



as a way to foster "strategic partnerships" with universities.

Drell, a Stanford physicist, takes issue with the proposed role of UT, which is partnering with Lockheed. Under the arrangement, officials say, Lockheed will manage the lab's classified research, and UT would provide peer review for some of the projects. "That's not a way to get the work done," says Drell, who fears that it will lead to barriers between managers. Robinson disagrees, saying that the lab will perform "as one entity."

As for Northrop, officials say its academic partners, not yet announced, will maintain peer-review traditions and the academic atmosphere. The company has worked with NASA on sensors and cosmology, and Northrop's vice president for business development for technical services, Al Ferrari, says that good science is also good business. "We want to be getting high-performance marks, leading to money, which is value for stockholders," he says,

referring to goal-based awards NNSA has built into the contract.

If UC were to win, officials say the university will preserve what has worked well and carve out an "equal" role for Bechtel. Los Alamos currently has the sole U.S. facility for building weapons components called plutonium pits. A secondary UC partner on the bid, BWXT, runs NNSA's Y-12 nuclear manufacturing facility in Oak Ridge, raising worries among some that production capabilities would take priority under a new contract with UC.

UT's Schwitters, who is not connected to the Lockheed bid, knows the importance of a good public face for a scientific project. He thinks better management could help the lab with its yearly battles on Capitol Hill. "You've failed [if you don't] convince the stockholders," he says, referring to the ultimate source of the lab's funding. Soon, however, Los Alamos may have a set of real investors to satisfy.

—Eli KINTISCH



HUMAN FRONTIER SCIENCE PROGRAM

12 Quai Saint-Jean, 67080 Strasbourg Cedex, FRANCE
Phone: +33 (0)3 88 21 51 27/34 Fax: +33 (0)3 88 32 88 97
E-mail: fellow@hfsp.org Web site: <http://www.hfsp.org>

OPPORTUNITIES FOR POSTDOCTORAL TRAINING ABROAD

The Human Frontier Science Program (HFSP) **promotes basic research in the life sciences**. Special emphasis is given to **novel and interdisciplinary research** aimed at **elucidating the complex mechanisms of living organisms**. The HFSP fellowship program provides support for training of postdoctoral researchers across national boundaries. To answer fundamental questions in the life sciences investigators should be able to span more than one scientific discipline. Applicants are therefore **encouraged to explore new areas of experimental research**.

Researchers from one of the supporting member countries can apply to work in any other country, while other nationals can apply for training only in a supporting country. Current supporting members are: Australia*, Canada, the European Union, France, Germany, Italy, Japan, the Republic of Korea*, Switzerland, the United Kingdom, and the United States of America (* new supporting members starting in award year 2006).

Important deadlines:

Compulsory pre-registration for password: **25 August 2005**

Submission of applications: **1 September 2005**

Long-Term Fellowships

Long-Term Fellowships are intended for postdoctoral fellows with a Ph.D. degree in the life sciences. Applicants are expected to **broaden their horizon and to move into a new research field that is different from their doctoral studies or previous postdoctoral training**.

Cross-Disciplinary Fellowships

Cross-Disciplinary Fellowships are intended for postdoctoral fellows with a Ph.D. degree in the physical sciences, chemistry, mathematics, engineering or computer sciences who **wish to receive training in the life sciences**. Applicants are expected to **move into a new research field through a significant change in discipline**.

Both programs provide up to 3 years of support for fellows to train in an outstanding laboratory of their choice in another country. Fellows can utilize their final year of postdoctoral support in the home country. Only the fellows who choose to return to their home country can defer their final year for up to two years while they are funded through other sources. The final year can then be used for an additional year of research training in the home country. Former HFSP fellows returning to their home country will be eligible to apply for a Career Development Award designed to establish themselves as independent young investigators.

The online system to submit applications will become available in summer 2005 on the HFSP web site.

Short-Term Fellowships

Short-Term Fellowships are intended for researchers early in their careers and provide up to 3 months of support to **learn techniques in a new area of research or establish new collaborations in another country**. Applications are accepted throughout the year.

Guidelines for all fellowships are available on the HFSP web site (www.hfsp.org).

Comet Crackup Will Spur Science, Whatever the Result

Almost anything could happen when Deep Impact smashes into comet Tempel 1, but whether the impact is a boom or a bust, science should come out a winner

Despite a natural urge to poke things to see what they're like, planetary scientists usually have to content themselves with merely watching the planetary bodies they study. Not this Fourth of July. On American Independence Day, controllers of the U.S. Deep Impact mission will smash a copper "bullet" nearly half a ton in mass into an icy, 14-kilometer-long comet nucleus at 100 times the speed of a .22-caliber rifle bullet, just to see what the inside is like.

"We don't have a clue what's going to happen, to be honest," says Deep Impact principal investigator Michael A'Hearn of the University of Maryland, College Park. The reason is a double dose of mystery: Despite decades of impact studies and comet flybys, researchers still know nothing at all about the nature of a comet's interior and too little about the physics of hypervelocity impact. For all they know, Deep Impact might blast out a classic impact crater, vanish into the comet with nary a trace, or, at the other extreme, reduce the comet to rubble with a single blow. To maximize the new science from Deep Impact, as well as the fun, team member Jay Melosh of the University of Arizona, Tucson, is just "hoping we will be baffled."

The Deep Impact concept could have been taken from piñata bashing: Hit it as hard as you can to get the goodies out. Twenty-four hours before arriving at Tempel 1, the spacecraft will release the 1-meter-diameter, 1-meter-high impactor on a collision course with the comet. Fine-tuning its course as it goes, the camera-equipped impactor will collide with Tempel 1 at 05:44 Universal Time on the Fourth at a closing speed of 36,720 kilometers per hour. Meanwhile, for the best view of the impact, the flyby spacecraft will dodge to pass safely 500 kilometers from the nucleus.

Team members are hoping Deep Impact will give them a clear view of the stuff comets—and planets—were made from. Planets have altered their starting materials beyond recognition, but comets preserve the dust, organic matter, and ice that went into the

outer planets—and bombarded the nascent Earth. Unfortunately for comet researchers, sunlight vaporizes the ices on an active comet's surface and largely destroys the chemical compounds that vaporization releases, leaving comet researchers with a



Splat. Deep Impact watches its impactor form a conventional crater—enlarged for illustration—on 14-kilometer-long comet Tempel 1.

"Humpty Dumpty" problem of putting it all back together again. But if Deep Impact exposes fresh, unaltered material in ejecta and a broad crater, the flyby spacecraft's spectrometer should return data on the composition of primordial stuff. That knowledge, in turn, should shed light on where and under what conditions solar system ingredients first came together.

The impact will also help explain how comets formed and how they have evolved under the sun's glare. That information would come in handy if a threatening comet had to be nudged out of Earth's path. Knowing the impactor's size, mass, and velocity—the reasoning goes—team members will be able to infer the density, strength, and porosity of the comet from the breadth and depth of the crater and the behavior of the ejecta. The team is most often quoted as expecting that Deep Impact will blast out a conventional crater about 100 meters wide and 25 meters to 30 meters deep while throwing up sheets of pristine comet debris, ideal for flyby observations.

Whatever the team is hoping for, no impact expert on or off the team is confident that's

what they'll see on the Fourth. The prediction of a broad, deep crater assumes—on the basis of computer simulations and extrapolations from lab experiments—that comet material is so fragile that most of the impact's energy will go into lifting it out to form the crater. That may be so, say impact specialists Kevin Housen of The Boeing Company in Seattle, Washington, and Keith Holsapple of the University of Washington, Seattle. But they suspect comets are strong enough that more energy will be needed to break up the material, leaving less for crater excavation. If so, says Housen, the crater could be as small as 10 meters or 20 meters across with far less ejecta. That's less than ideal for the flyby camera and spectrometer, which will have a resolution ranging from 85 meters down to 7 meters.

Things could get even worse. If comets are highly porous and compressible like Styrofoam, as some models would have it, much of the impactor's energy could go into compressing the material ahead of it, with little or none of the energy excavating anything. (The same sort of cushioning allows aerogel—the ultralow-density "frozen smoke" flown on the Stardust spacecraft—to snag high-velocity dust particles without vaporizing them.) Cratering researcher and team member Peter Schultz of Brown University in Providence, Rhode Island, expects to see such deep, craterless penetration, but with a redeeming twist. At some point inside the comet, the impactor would disintegrate like a meteor detonating in the atmosphere, says Schultz, shooting debris back up the hole like a Roman candle and blowing off plates of any rigid comet crust.

Melosh imagines another extreme scenario. "There's a possibility the impact could disintegrate the comet," he says, "which would be wonderful." Comets tend to fall apart, he notes. In July 1994, comet Shoemaker-Levy 9 broke into 21 large pieces when it passed too close to Jupiter. Comet LINEAR broke into six pieces with no apparent provocation shortly after its discovery in 1999. Melosh suspects that such breakups are driven by the pressure of solar-heated gas within a comet's interior. Break through the few meters or tens of meters of sun-baked crust holding the pressure in, and the whole comet might burst open like a pricked balloon.

With all the possibilities, only one thing seems certain for the Fourth of July. Says Housen: "Every time we look at an asteroid or comet [close up], we're always surprised."

—RICHARD A. KERR

Encouraging Results for Second-Generation Antiangiogenesis Drugs

The strategy of denying growing tumors a blood supply continues to show clinical promise as new and improved drugs move through the pipeline

The development of cancer drugs that stifle tumor growth by blocking the formation of the blood vessels they need seems to have turned the corner. Early last year, the U.S. Food and Drug Administration approved the first cancer drug, an antibody called Avastin, that is specifically designed to prevent this tumor angiogenesis, as the new blood vessel growth is called. Avastin may soon have company, if presentations last week at the annual meeting of the American Society of Clinical Oncology (ASCO) in Orlando, Florida, are any indication.

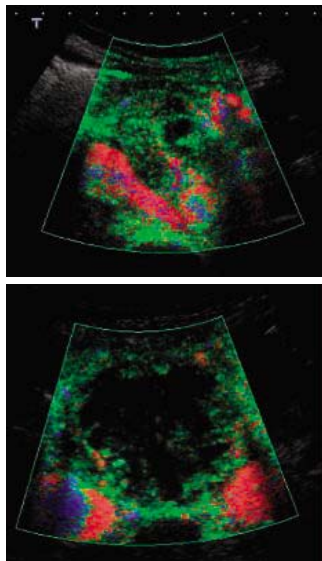
One advanced clinical trial showed that a new antiangiogenesis drug called sorafenib significantly slows metastatic kidney cancer, and another drug, known as Sutent, proved its mettle in treating a digestive system cancer called GIST (gastrointestinal stromal tumor). In contrast to Avastin, which must be injected because it's a protein, both of these drugs are small molecules that can be taken in pill form. Perhaps even more important, the new drugs take aim at multiple molecular targets, only some of which are related to blood-vessel growth. The results from this novel drug class "mark the dawn of a new era in antiangiogenesis therapy," says William Li, director of the Angiogenesis Foundation in Boston, Massachusetts.

Despite their chemical differences, Avastin and the new drugs share a common purpose: starving tumors of blood. Avastin is designed to bind to and block the activity of an angiogenesis-promoting protein called vascular endothelial growth factor (VEGF). Sorafenib, which is being developed by Bayer Corp. and Onyx Pharmaceuticals, and Sutent, under development by Pfizer Corp., also block VEGF action, but in a different way. The receptors through which VEGF works are so-called tyrosine kinases, which add phosphate groups to certain proteins. The new drugs block this kinase activity, thus inhibiting receptor action.

In addition, they inhibit other tyrosine kinase enzymes within cells. This means the drugs may block tumor cell growth directly, as well as by inhibiting angiogenesis. "These are

like Gatling guns; Avastin is like a sniper," is how Li puts it.

Sorafenib was originally identified on the basis of its ability to inhibit a tyrosine kinase called Raf, a member of a major cellular growth control pathway—one that often contributes to the runaway cell division of cancer cells due to mutations that cause it to be overactive. But the drug also inhibits additional tyrosine kinases, including the receptors for VEGF and for platelet-derived growth factor (PDGF) and the products of the *KIT* and *FLT-3* oncogenes.



Slow flow. Blood flow to a kidney tumor (*top*, green) is reduced (*bottom*) by an angiogenesis inhibitor.

Sorafenib, which was discovered 4 years ago, moved quickly through animal and preliminary clinical studies. By early 2004, investigators had begun a large phase III trial of the drug's effectiveness in patients with metastatic kidney cancer. This double-blind trial included some 900 patients at multiple medical centers who had not responded to previous therapy and who were given either sorafenib or a placebo.

At the ASCO meeting, Bernard Escudier of the Institute Gustave Roussy in Villejuif, France, reported that sorafenib "very significantly" increased the length of time before the treated patients' cancers grew visibly, from 3 months in the placebo group to 6 months. "This was the best data we have seen in kidney cancer with any drug so far," Escudier says. The improvement was so striking that the review committee for the trial unblinded the results early so that the controls could also receive the drug.

Despite the drug's targeting of multiple tyrosine kinases, side effects, which included rashes, hair loss, nausea, diarrhea, and high blood pressure, were relatively mild. Still to be determined, however, is whether the delayed progression will translate into improved sur-

vival for the patients. But periodic imaging of the tumor's blood flow did suggest that at least part of sorafenib's effects were due to its ability to block angiogenesis. "Tumor vascularization was decreased" in patients who received the drug, Escudier says.

Sutent, identified about 5 years ago by Julie Cherrington, then at SUGEN Inc. in South San Francisco, California, and her colleagues, is also moving quickly through clinical testing. (SUGEN has since been acquired by Pfizer.) This drug also targets a broad set of tyrosine kinases. The fact that it inhibits the protein produced by the *KIT* oncogene suggested that it might be a good drug for treating GIST. "GIST cells are totally addicted to that [KIT] signal" for growth, says George Demetri of Harvard's Dana-Farber Cancer Institute in Boston, who led the phase III clinical trial of Sutent for GIST reported at the meeting.

One proof of that came with the discovery that this kind of tumor responds to the anti-cancer drug Gleevec, which inhibits both KIT and another kinase that drives a leukemia called CML. The current trial included more than 300 GIST patients for whom Gleevec no longer worked. Again the results were so striking that the trial was unblinded early so that the controls could receive treatment.

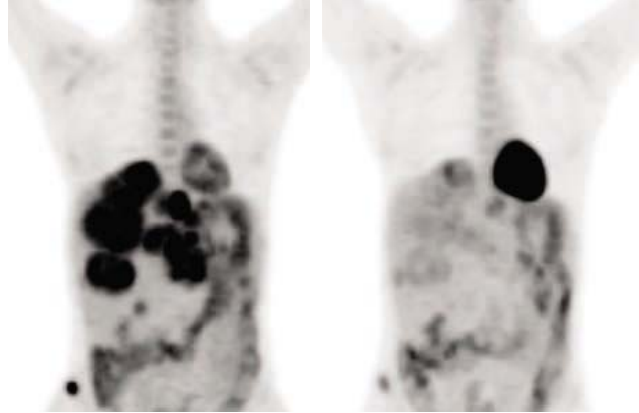
Sutent delayed the time of tumor progression on average from 1.5 to 6.3 months and also significantly reduced the death rate, even at this early stage of analysis. And like sorafenib, Sutent may be effective against kidney tumors. Robert Motzer of Memorial Sloan-Kettering Cancer Center in New York City described the results of two smaller studies, including 169 patients with metastatic kidney cancer. Roughly two-thirds of the patients responded to the drug with either tumor shrinkage or delayed progression.

In addition, Kathy Miller of Indiana University, Indianapolis, reported that in a small phase II trial, about 14% of breast cancer patients who failed previous chemotherapy treatments responded to Sutent. "It doesn't sound like much, but in this group of heavily pretreated patients, this is very good," she says.

Not all the large studies of second-generation antiangiogenesis drugs reported at ASCO produced clear results, however. The drug known as PTK/ZK, which is being developed by Novartis and Schering, targets most of the same tyrosine kinases as sorafenib and Sutent. Although it did produce a 12% increase in progression-free survival in a trial including nearly 1200 patients with metastatic colon cancer, that improvement did not attain statistical significance.

As for Avastin, the first-generation angiogenesis inhibitor continues to show promise. Although it is currently approved only for treating colon cancer, results pre-

sented at the ASCO meeting show that when given with more conventional chemotherapeutic drugs, Avastin can work on other cancers as well. In an earlier trial on patients with advanced breast cancer, Avastin combined with chemotherapy did not produce a statistically significant improvement over the results of chemotherapy alone. But at the meeting, Indiana's Miller, who also led the earlier study, reported on a new phase III trial in which Avastin was combined with the chemotherapy drug paclitaxel. This time, the news was good. Patients who got both drugs experienced significant increases in progression-free survival and overall survival compared to those on paclitaxel alone.



Quick reaction. A gastrointestinal tumor (left, dark areas) rapidly shrinks (right) after 1 week of treatment with the drug Sutent.

Avastin may have worked better this time, Miller says, because those in the current trial had not previously been treated with chemotherapy and thus their cancers may have been less advanced than those in the earlier trial, who had all undergone—and failed—several rounds of chemotherapy. Genentech, the company that makes Avastin, got other

good news at the ASCO meeting. In another phase III trial, described by Alan Sandler of Vanderbilt University School of Medicine in Nashville, Tennessee, the addition of Avastin to a chemotherapy regimen slowed tumor progression in patients with one form of nonsmall cell lung cancer.

Although second-generation antiangiogenesis drugs such as sorafenib and Sutent, unlike Avastin, have shown promise when given alone, researchers are also beginning to test the drugs in combination with other therapies. The idea, they say, is to mix drugs that hit different aspects of the pathological changes that drive tumor growth. An antiangiogenesis drug might be combined, for example, with a drug that blocks the cell growth-stimulating activity of epidermal growth factor. “We’re getting smarter,” Demetri says. “We’re going to be able to profile the tumor and pick and choose [anticancer] drugs just like we pick and choose antibiotics for treating life-threatening infections.”

—JEAN MARX

Astronomy

Turbulent Orion Nebula Shows A Flare for the Dramatic

A deep x-ray scan of a crowded star-forming cloud suggests that our solar system's youth was far from serene

On crisp winter nights, the stars of Orion, the Hunter, rule the Northern Hemisphere's sky. But deep within the Orion Nebula, the constellation's famous stellar nursery, conditions are anything but chilly. Fierce and persistent flares from baby stars pierce the nebula with x-rays, according to unprecedented studies released this month. The spasms light up the cloud “like an x-ray Christmas tree flashing on and off,” says astronomer Eric Feigelson of Pennsylvania State University, University Park.

The pyrotechnics were revealed by the Chandra Orion Ultradeep Project (COUP), in which NASA's Chandra X-ray Observatory stared at the nebula for nearly 2 weeks in January 2003. The penetrating scan captured the early lives of more than 1400 young stars, ranging from titans to dwarfs. The results turn back the clock to the infancy of our own sun, which may have formed in a similar nursery 4.6 billion years ago among siblings that have long since dispersed.

COUP's international team of 37 scientists, led by Feigelson, found that the eruptions unleashed by Orion's stars are thousands of times stronger than the worst our sun can dole out today. The biggest flares probably extend out far enough to strike the disks of gas and dust around the young stars from which planets may form. No one knows the impacts of such giant magnetic short-circuits. But in one intriguing scenario, they churn circumstellar disks enough to keep newborn planets from spiraling into their suns.

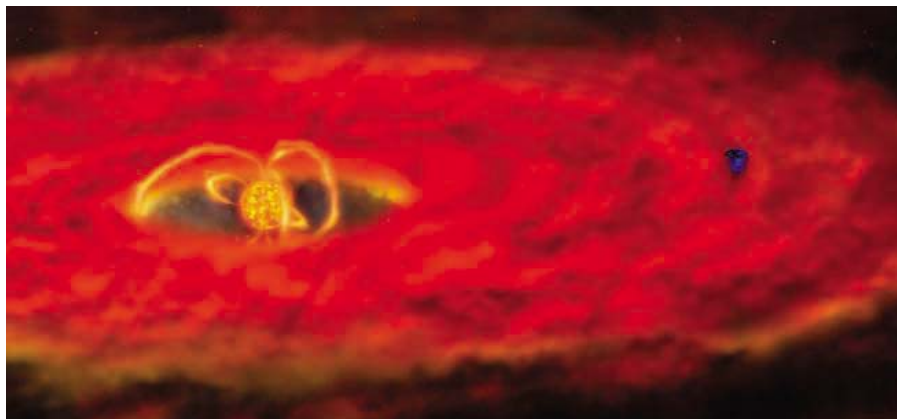
If that happened in our solar system's youth, it would be an ironic twist on our conception of x-ray flares as dangerous, Feigelson says: “They may have protected Earth from early destruction.”

This statement became the catch phrase of a NASA briefing for reporters on 10 May, even though it stretches current theory, Feigelson readily admits. But for the first time, he says, the 13 papers* from COUP give theorists the data they need to understand the full range of high-energy tantrums from the youngest stars.

The perfect target

The Orion Nebula is ideal to study so many stars in one fell swoop, says astrophysicist Fabio Favata of the European Space Agency's R&D center ESTEC in Noordwijk, the Netherlands. “If you were to design a nebula from scratch as a target for

* To appear in *Astrophysical Journal Supplement Series*, available at www.astro.psu.edu/coup



Magnetic turmoil. Giant flares may spark turbulence in disks around newborn stars.

Chandra, Orion is the perfect one," he says. At its distance of about 1500 light-years, the grand nebula fits nicely onto Chandra's electronic detectors. The telescope's sharp vision resolves individual stars and picks up enough x-rays to peer into the cloud's deepest recesses, Favata notes.

Indeed, the feeblest COUP sources reveal about 70 brand-new protostars that even the largest near-infrared telescopes on the ground can't see. Those objects—detected by as few as five x-ray photons—are valuable probes of the nebula's structure, says optical astronomer C. Robert O'Dell of Vanderbilt University in Nashville, Tennessee. "Going to x-rays gives you the advantage of looking into highly obscured regions and seeing just how much atomic material is along the line of sight," he says.

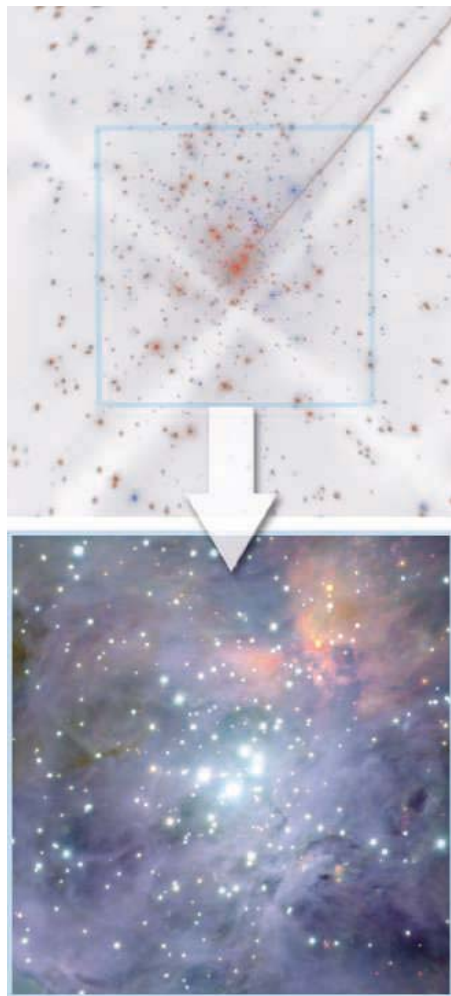
Orion's nursery, consisting of molecular hydrogen and heavier elements, is far larger than the glowing nebula. We see the nebula as a "thin blister of ionized gas," O'Dell says, its atoms stripped of electrons by ultraviolet radiation from a handful of hot stars born in the past 100,000 to 1 million years. In the most active knot, called the Trapezium cluster, stars jam together 20,000 times more densely than in our part of the galaxy, and their radiation blasts the entire nebula. The brightest star, 45 times as massive as our sun, sears the center of Chandra's image with diffracted and scattered x-rays.

To see both the dazzling beacons and the barely perceptible blips, COUP researchers took pains to point the telescope in precisely the same direction and orientation during six exposures. About 15 hours of down time truncated each exposure as the satellite passed through Earth's radiation belts. With the exact aim, x-rays from each source always hit the same spot on the detector. During analysis, a team led by Penn State astronomer Konstantin Getman adjusted for the glare of bright objects by extracting data from the edges of their x-ray imprints rather than the overexposed centers.

The study's length sets it apart from previous examinations of star-birth regions, including two 12-hour Chandra observations of Orion in 1999 and 2000. The COUP team caught hundreds of flares that lasted from hours to several days. The longer events—many captured from start to finish—show young stars at their most extreme. "This was a whole category of energy release and physics that we just couldn't study before," says astronomer Scott Wolk of the Harvard-Smithsonian Center for Astrophysics in Cambridge, Massachusetts.

Flares by the millions

Wolk led the analysis for 27 stars in Orion with nearly the same mass as our sun. Chan-



Two views. Baby stars in Orion sparkle in both x-rays (top) and near-infrared light (inset, bottom).

dra saw 41 x-ray flares from these objects, some lasting as long as 2.5 days. The rate suggests that young sunlike stars emit powerful flares once a week on average, Wolk says. Each one spews as much energy as thousands of today's solar flares.

If a typical disk of dust and gas around a star lasts for millions of years, it will experience hundreds of millions of flares, Wolk notes: "That's enough to really cook the disk in several different ways." For instance, such repeated doses of fierce x-rays in our young solar system arguably produced the melted mineral inclusions, called chondrules, that pepper the insides of meteorites. Astrophysicist Frank Shu, now president of National Tsing Hua University in Hsinchu, Taiwan, and others first proposed that idea in *Science* (15 March 1996, p. 1545) to explain the origins of chondrules.

To test the hypothesis, COUP scientists tried to gauge how the biggest Orion flares might affect circumstellar disks, which the Hubble Space Telescope sees scattered throughout the nebula. In particular, the astronomers looked for signs that giant

magnetized loops of hot plasma stretch from young stars to their disks. A team led by Favata modeled the sizes of the outbursts based on their duration and their blazing temperatures, perhaps exceeding 200 million degrees Celsius. Small flares quickly dwindle, but others linger for days. For such hot flares to remain stable above a rapidly spinning star for so long, they must cascade along magnetic loops 5 to 10 times larger than the stars and physically connect to disks, the group deduced. By comparison, our sun's biggest storms spit out magnetic loops just 1/3 to 1/2 of the sun's size.

Another COUP study reports tantalizing hints of burn marks in the disks. Penn State astronomer Masahiro Tsujimoto and his colleagues saw traces of iron atoms fluorescing at a key wavelength. Such a glow is normally seen when x-rays irradiate disks that whirl around neutron stars and black holes. The team argues that x-rays from Orion's stars torch the surrounding disks in the same way, ionizing some of the gas.

What happens next is anyone's guess. Theoretical work by astrophysicists Steven Balbus and John Hawley of the University of Virginia, Charlottesville, maintains that ionizing a magnetized circumstellar disk makes the gas unstable and turbulent, like disrupting a smooth whirlpool by boiling the water. If planets are coalescing within the disks, turbulence sparked by x-ray flares might jostle their orbits. That, in turn, might prevent gravitational drag forces from pulling the planets ever inward toward their hungry parent stars.

"Turbulence may play a role in the architecture of planetary systems," says astronomer Joan Najita of the National Optical Astronomy Observatory in Tucson, Arizona. "Planetary cores can scatter off lumpy turbulent fluctuations, somewhat like boats tossed about by waves in a storm."

Might x-ray flares from our sun have saved Earth from fiery doom in this way? Feigelson thinks this "planetary protection" picture, in a phrase coined by NASA, needs a better theoretical anchor before anyone hops aboard that boat. "The story is not necessarily persuasive because of the complexities of planet formation, but it's very tempting," he says. "COUP gives us much more confidence that our young sun was very magnetically active. I am not as confident about the other steps in the argument."

As theorists ponder the influences of hyperactive young stars, they will draw upon COUP for years, Wolk believes. No proposed x-ray study will scrutinize so many objects in a stellar nursery at this level of detail—even with a new generation of space telescopes. "For the next quarter-century, this is it," Wolk says. "The data set is that good and that rich."

—ROBERT IRION

Israeli Controversy Blossoms Over Protecting Gilboa Iris

A proposed eco-friendly settlement on Mount Gilboa has enraged Israeli scientists, who say it will trample on a beloved national icon

MOUNT GILBOA, ISRAEL—Every March, tourists clog the narrow road snaking up this mountain to enjoy the spectacular blooming of the purple Gilboa iris. But this year the rare flower, a national icon unique to the ridge, has also become a major bone of contention between settlers of a proposed eco-friendly town and Israeli scientists who call the settlement “an ecological crime.” The fight is part of a larger battle over preserving open spaces in a country where environmental concerns often take a back seat to an Israeli imperative to build on the ancient land.

The new settlement, called Michal, would sit atop the Gilboa ridge in northeastern Israel, just east of the West Bank. Two years ago, Israel’s Nature and Parks Authority approved a plan to build 120 housing units on 0.15 square kilometers after the regional government agreed to set aside 63 sq. km., including the eastern slope of the ridge, as a permanent nature preserve. “Nature gets a lot,” said an authority spokesperson. Settlers say they want to implement ambitious plans for energy-efficient homes, recycling, and the use of native plants. “We want to live with nature,” says software engineer Aviv Harary, a community leader who notes that each iris in the path of the new settlement will be transplanted before construction begins.

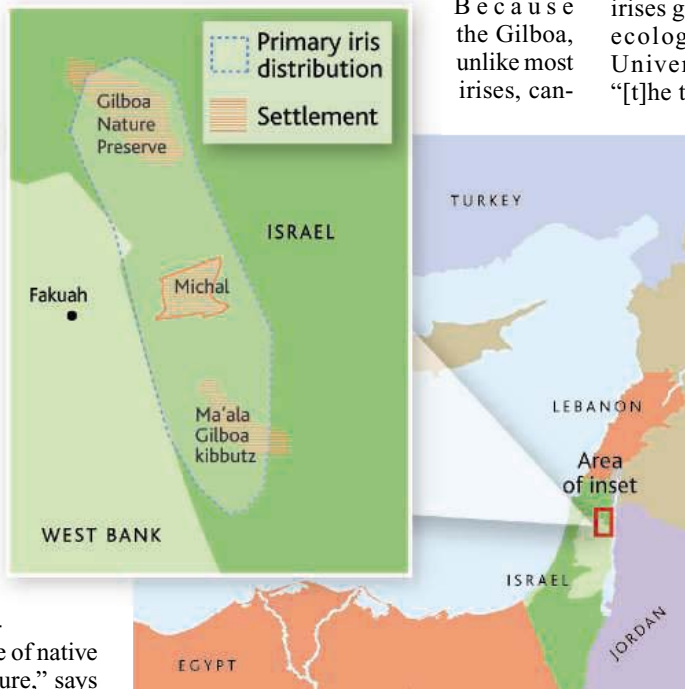
But a coalition of Israeli scientists has filed an official objection to the settlement, arguing that any construction, however benign, risks “total extinction” of the iris. They hope to influence the deliberations of Israel’s national planning council, the last in a series of bureaucratic hurdles that must be cleared before construction can begin. The scientists are joined by the Society for Protection of Nature in Israel, which uses the iris in its logo and says the flower is one part of a distinctive blend of desert, steppe, and Mediterranean conditions on the mountain.

Encouraged to come to the area by a regional government seeking new residents,

the settlers chose this site because they were attracted by the region’s beauty. They hope that Michal—through its domestic use of rainwater, buildings faced with recycled materials, and south-facing structures—will serve as a model for ecological living in Israel.

Despite the green engineering of its buildings, opponents fear that the settlement will damage the local ecology.

Because the Gilboa, unlike most irises, can-



Flower power. Environmentalists want Israeli government to pay more heed to the Gilboa iris.

not self-pollinate, the settlement will reduce crucial genetic diversity by isolating clusters of irises to the north and south, worries plant ecologist Yuval Sapir of Indiana University, Bloomington. In a letter leaked to the Israeli paper *Ha'aretz* last year, Nature and Parks Authority board science committee chair Tamar Dayan attacked the plans,

saying that the light, pets, gardens, and utilities from the settlement could affect an area on the mountain 10 times larger than its footprint of homes. For example, the flower’s pollinating insects might be forced to compete with other insects introduced by imported gardens and agriculture, says Michael Avishai, scientific director of the Jerusalem Botanical Gardens.

Michal planner Chaim Shenhar replies that residents plan to protect the irises in their midst and that the settlement’s footprint was even modified to avoid affecting areas of higher density. He also says that homeowners plan to cultivate local plants.

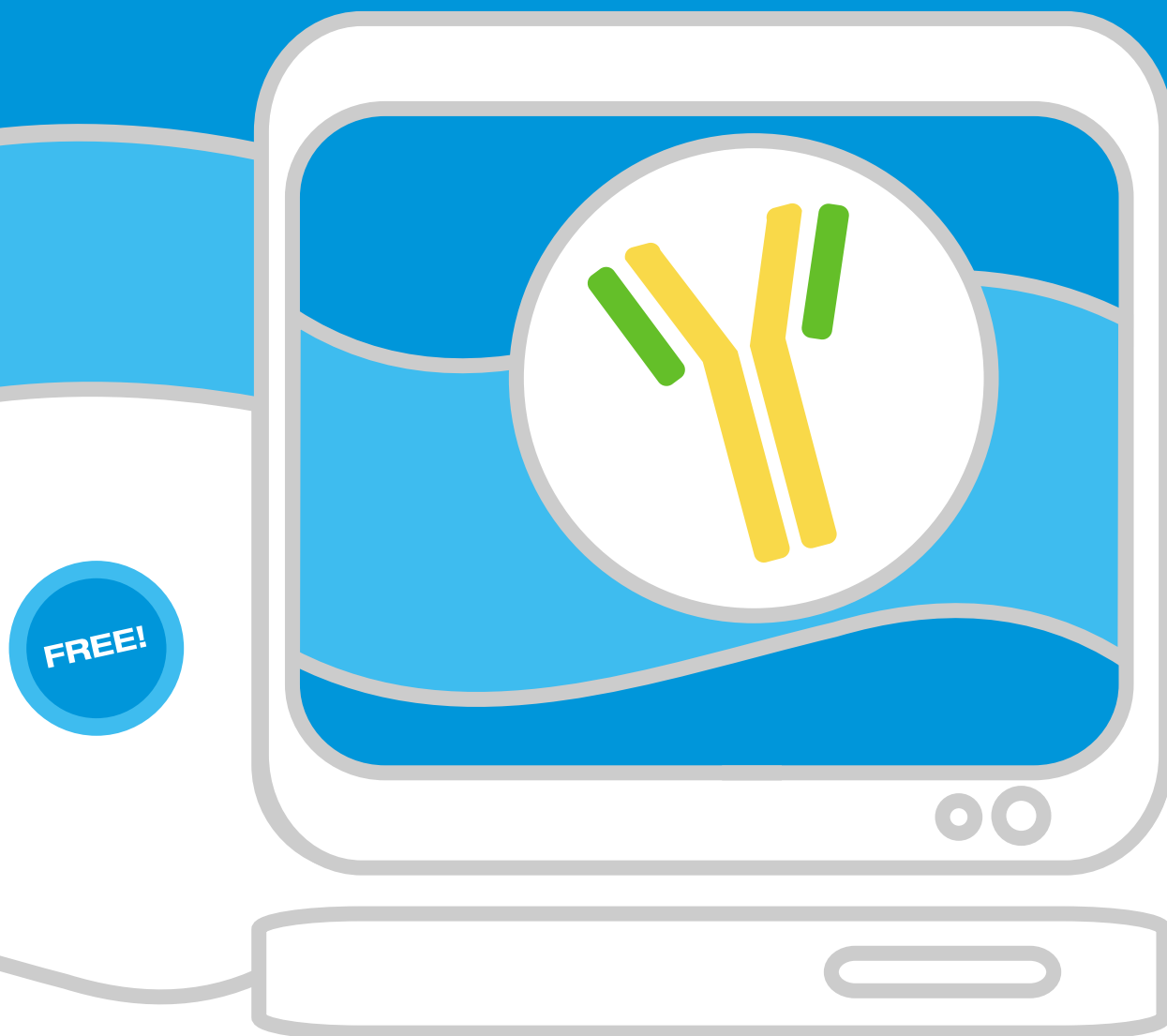
Scientists are also unhappy with the arrangement to set aside land along the slopes of the mountain. They note that few irises grow in the protected areas. From an ecological perspective, says Tel Aviv University ecologist Yoram Yom-Tov, “[t]he top of the Gilboa is more important than the slopes.” The leaked Dayan document asserted that the deal, approved by the authority’s politically appointed board, was made “without scientific or professional backing.” In response, the authority says it followed its normal practice on consultations.

The proliferation of the irises along the streets and lawns of the nearby kibbutz Ma’ale Gilboa shows that humans and flowers can co-exist, says Dani Kamari, deputy head of the Bet She’an regional council, which welcomes the new settlement as a way to make existing education, health care, and garbage services more cost-efficient. “Some scientist sitting in Tel Aviv doesn’t understand how people here live,” he adds. Kamari acknowledges that the kibbutz, an Orthodox community, and two other nearby towns could use additional residents. But he notes that the Michal group prefers to live in its own, secular town.

Opponents are asking prominent lawmakers to pressure the planning council, which is now reviewing comments before making a final decision. Likud legislator Omri Sharon, son of the prime minister, has already signaled his support. But in a country where development is a national priority, opponents of Michal fear the traffic on Mount Gilboa will soon be getting worse—and that the Gilboa iris will pay the price.

—ELI KINTISCH

Spend less time looking for antibodies
and more time doing research...



Find Antibodies Online

Search over 130,000 antibodies from over
100 companies by antigen, species reactivity,
and application... free and online.

- Over 130,000 Antibodies
- Over 100 Antibody Companies
- No Registration Required
- Full Product Specifications
- Over 225,000 Research Products and Instruments
- Direct Access to Product Pages on Company Websites



The Buyer's Guide for Life Scientists™

www.biocompare.com



One-size-does-not-fit-all.

Especially not in medicines.

Individuals can have very different responses to the same medicine based on both genetic and environmental factors. Now, personalizing medicine based on a patient's unique genetic characteristics is possible.

By analyzing millions of unique genetic variations in thousands of patients, Perlegen finds the genetic differences that are associated with efficacy and side effects. We can predict how people will respond to a given medicine, so physicians and pharmaceutical companies can make sure the right medicines get to the right patients.

Providing a better therapeutic fit results in increasing market share, getting drugs from development to market faster, and even moving second line therapies to first line choices – all while making sure patients feel a little less exposed.

To learn more, contact:
Partnerships41@perlegen.com
www.perlegen.com

Targeting today's drugs.
Discovering tomorrow's.™



Edited by Yudhijit Bhattacharjee

PIONEERS

Simulated step. Hall Train may have dropped out of high school, but the 48-year-old Canadian inventor is applying his artistic and mechanical talents to help paleontologists explain and conduct their research.

Train has built numerous models of dinosaurs, from a cable-controlled *Tyrannosaurus rex* head used in TV documentaries to a massive, 8-meter-long robotic *Triceratops* at Universal Studios Theme Park in Orlando, Florida. Earlier this month, the latest of Train's creations—one he describes as his "masterpiece"—debuted in New York City at the American Museum of Natural History. The museum's new dinosaur exhibit features his 2-meter model of a *T. rex* skeleton that walks in place. Train spent 6 months in his Toronto studio building the mechanism; the little toes alone required 50 moving parts each.

The model's eerily realistic walk is "a powerful tool for explaining locomotion," says John Hutchinson, a paleontologist at the Royal Veterinary College in North Mymms, U.K. Hutchinson suspects that the model may even reveal some new aspects of how joints function. Train is currently helping researchers at Stanford build a remote-controlled pterosaur that can fly.



FACE OFFS

Jabbing the old guard. Richard Horton, the prickly editor of *The Lancet*, showed again last week that he enjoys a good fight—even if he has to start it himself. In the 21 May issue of the journal, he delivers a scorching editorial attack on the Royal Society (RS)



of London, the world's oldest scientific club. Beginning with the question, "What is the Royal Society for?," Horton writes that it has become "a lazy institution, resting on its historical laurels" and "little more than a shrill and superficial cheerleader for British science." As far as medicine is concerned, he adds, its "marbled cupboards are largely bare." He recommends a housecleaning.

The riposte came quickly in a statement released by RS Executive Secretary Stephen Cox. It decries the "personal campaign that Richard Horton ... has been conducting against the Royal

Society." The editorial is "wholly inaccurate," says Cox, who cites other examples of Horton's errors including "the recent embarrassment ... in which [*The Lancet*] had to publish a partial retraction" of a paper that linked childhood vaccination with autism. The contretemps is unlikely to end with this exchange.

AWARDS

Stellar mentors. A blind graduate student taught computer scientist Richard Ladner that the intensely graphical content of science and engineer-

ing was completely inaccessible to the blind. So Ladner, a professor at the University of Washington, Seattle, launched a project to automate the conversion of two-dimensional graphics into embossed images comprehensible by touch. The research is part of a broader effort by Ladner to help students with disabilities pursue graduate studies.

Last week, that effort earned him a 2004 Presidential Award for Excellence in Science, Mathematics, and Engineering Mentoring. Eight other academics received the \$10,000 prize: Lenore Blum of Carnegie

Mellon University; Barbara Burke of California State Polytechnic University; Charlena Grimes of Washington State University; Jeffrey Russell of the University of Wisconsin; Herb Schroeder of the University of Alaska; John Warner of the University of Massachusetts; Steven Watkins of Louisiana State University and A&M College; and Elizabeth Yanik of Emporia State University in Kansas. Five institutions also were honored at the Washington, D.C., ceremony.

Got any tips for this page? E-mail people@aaas.org

NONPROFIT WORLD

Learning curve. After more than 20 victories on the U.S. professional golf tour, including the 2004 Master's Tournament, Phil Mickelson is swinging for a new target: getting children excited about math and science.

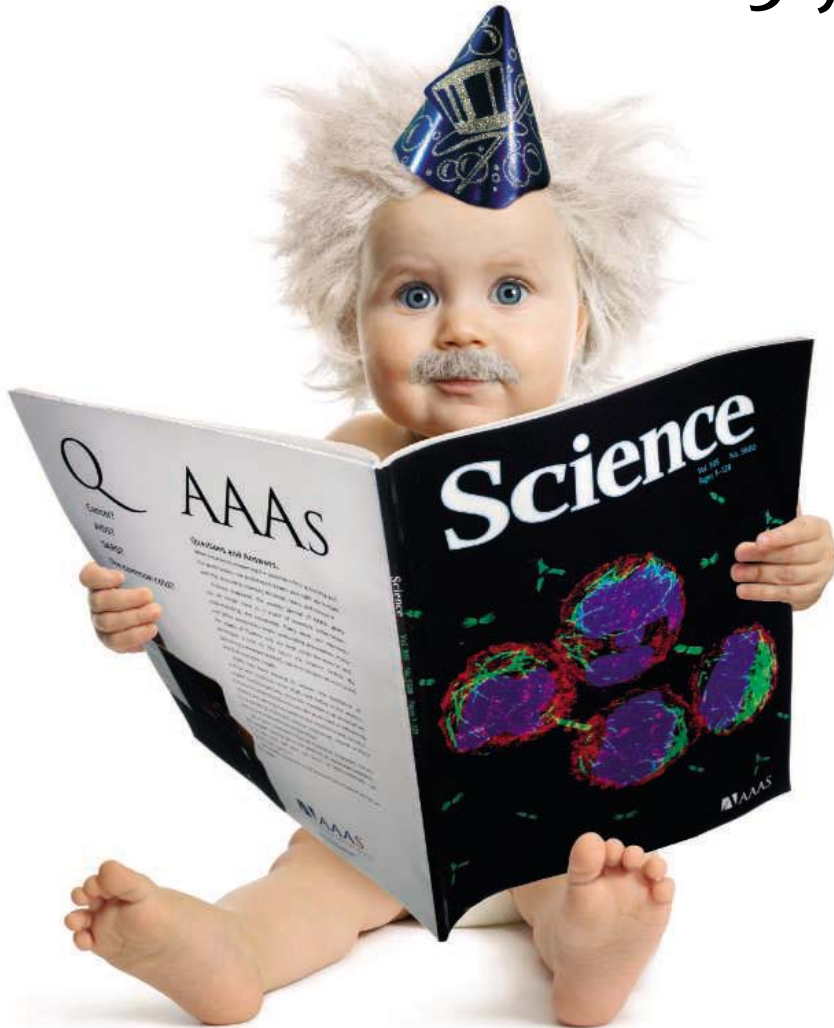
Mickelson and his wife Amy have teamed up with ExxonMobil to train elementary school teachers in math and science instruction. In July, the Mickelson ExxonMobil Teachers Academy will enroll 200 teachers from across the country for a 5-day workshop on innovative teaching methods aimed at creating a sense of inquiry and problem-solving ability in students. The program, to be held at an ExxonMobil site in Fairfax, Virginia, may become an annual feature depending on its success this year. For more information, see www.exxonmobil.com/corporate/Sponsorships/sponsor_home.asp.



CREDITS (TOP TO BOTTOM): RICK EDWARDS/AMNH; SOURCE: ROYAL COLLEGE OF PHYSICIANS; REUTERS

Q: Guess who's turning 125?

A: Join us to celebrate
125 years of **Science!**



You are invited to join the editors and staff of *Science* to celebrate this occasion at a cocktail reception at the Natural History Museum in London on Thursday 14 July 2005.

Drinks and canapés will be served.

Guests of honor will include Dr. Donald Kennedy
Editor-in-Chief of Science Magazine.

7:00 - 11:00 p.m.
Thursday 14 July 2005

Earth Galleries
Natural History Museum
Cromwell Road
London SW7 5BD

RSVP required

You can learn more about the venue and find directions at www.nhm.ac.uk/museum/earthgalleries

All are welcome to attend but we require that you RSVP. To RSVP or for further information, please email: 125th@science-int.co.uk.

More information can be found on our website at promo.aaas.org/kn_marketing/125anniversary.shtml



Qs & AAAS



www.sciencedigital.org/subscribe

For just US\$130, you can join AAAS TODAY and start receiving *Science* Digital Edition immediately!

Qs & AAAS



www.sciencedigital.org/subscribe

For just US\$130, you can join AAAS TODAY and start receiving *Science* Digital Edition immediately!

The Future of Farming and Conservation

THE RESEARCH ARTICLE BY R. E. GREEN ET AL. “Farming and the fate of wild nature” (28 Jan., p. 550) adds to the already burgeoning literature on agroecosystems and conservation. The authors are to be commended for their attempt to develop a model that could be of use in decision-making about agricultural development and wildlife conservation. Unfortunately, this work contains some critical errors, conceptual flaws, and missing literature that invalidate its conclusions. We list here a few such problems.

1) The assertion is made that existing agri-environment schemes depend on farmers receiving large amounts of financial compensation from the government. Although a popular vision in Europe, this is not true throughout the world. A growing number of wildlife-friendly schemes rely on premium prices paid by consumers for environmental services (e.g., organic certification or the Smithsonian Bird Friendly Certification for coffee). This also brings up an issue of which the authors seem unaware, the hidden costs of conventional intensive agriculture, which have been widely exposed and documented over the past 20 years (1–5).

2) Given the extensive literature on the effects of pesticides and fertilizers on non-target organisms and wildlife outside farming areas (6–8), ignoring this in the construction of the model is not justified and could be very misleading to policy-makers.

3) The unwarranted assumption is made that wildlife-friendly agriculture (which includes a wide variety of practices and techniques) reduces yield. However, there is accumulating evidence that organic farming can produce as much, if not more in some cases, as conventional agriculture (9, 10).

4) Most conservation biologists have gone beyond the simplistic idea that there is “wild habitat” and “agricultural land.” Most land is subjected to some sort of human interference, and the goal for conservation is to preserve as much biodiversity as possible in landscapes that include mosaics of different types of land use.

5) Almost all landscapes are currently fragmented, with patches of more or less native vegetation interspersed among a matrix of different land-use systems, including agriculture. Metapopulation and metacommunity structures are likely to exist among those patches (11–13) and organisms need to migrate from patch to patch to maintain these structures. If the so-called high-productivity

agriculture includes monoculture and/or the use of biocides, this may result in the death of many organisms attempting that interpatch migration, which is necessary to avoid what almost all agree will be the inevitable extinctions from the patches that, on their own, are almost certainly too small to sustain most populations.

6) Green *et al.*'s assumptions about food needs and how to meet them are largely political. Not all experts agree on how future food needs should be met—many focus on equity and food security rather than production.

Although the issue of agriculture and biodiversity preservation is certainly an important one, Green *et al.* present an analysis that is misleading to those not familiar with recent literature.

JOHN VANDERMEER^{1,2} AND IVETTE PERFECTO²

¹Department of Ecology and Evolutionary Biology, ²School of Natural Resources and Environment, University of Michigan, Ann Arbor, MI 48109, USA. E-mail: jvander@umich.edu, perfecto@umich.edu

References

1. P. A. Matson, W. J. Parton, A. G. Power, M. J. Swift, *Science* **277**, 504 (1997).
2. D. Pimentel *et al.*, *Science* **267**, 1117 (1995).
3. D. Pimentel *et al.*, *Oikos* **34**, 126 (1980).
4. D. Tilman, *Proc. Natl. Acad. Sci. U.S.A.* **96**, 5995 (1999).
5. National Research Council, *Alternative Agriculture* (National Research Council, Washington, DC, 1989).
6. P. M. Vitousek, H. A. Mooney, J. Lubchenco, J. M. Melillo, *Science* **277**, 494 (1997).
7. D. Pimentel, C. A. Edwards, *Bioscience* **32**, 595 (1982).
8. K. Freemark, C. Boutin, *Agric. Ecosyst. Environ.* **52**, 67 (1995).
9. M. Altieri, *Environ. Dev. Sustainabil.* **1**, 197 (1999).
10. J. Pretty, R. Hine, *Reducing Food Poverty with Sustainable Agriculture: A Summary of New Evidence* (Centre for Environment and Society, Essex University, UK, 2001).
11. K. McCann, P. Yodzis, *Am. Nat.* **144**, 873 (1994).
12. I. Hanski, *Metapopulation Ecology* (Oxford Univ. Press, Oxford, 1999).
13. S. Nee, R. M. May, *J. Anim. Ecol.* **61**, 37 (1992).

Response

VANDERMEER AND PERFECTO RAISE SEVERAL points that require clarification. They assert that we assume that wildlife-friendly farming is always associated with yield penalties. We explicitly say the opposite. We state in our section describing wildlife-friendly farming that it is clearly beneficial if it does not involve yield penalties. We also explore a very wide range of shapes of species-specific density-yield functions in our model,

including ones in which density increases or remains constant with respect to yield, at least over some interval. Our paper is an argument for the need to know, for a wide range of organisms and farming systems, what the relationships between species density, farming methods, and yield actually are. Vandermeer and Perfecto imply that the answers are already known and that, for many farming systems, species densities and province-wide species persistence are neutral to increases in yield. However, the literature they cite does not provide the quantitative evidence required to establish this, and the widespread need for agri-environment payments and price premiums suggests that yield penalties are instead commonplace. Moreover, price premiums can only be levied on produce that is sold to wealthy consumers, so they are not applicable to the rising productivity needed to meet food demand from poorer nations.

Vandermeer and Perfecto are concerned that we concentrate on food production rather than distribution. Hunger is undeniably linked to equity of access, but given that food demand is likely to at least double by 2050, it is essential to consider how production can be increased.

Vandermeer and Perfecto raise important points about our model not addressing the external effects of intensive farming on wildlife in nonfarmed areas, and its movement between habitat patches. We agree that these are serious limitations, and we raised them at some length in our paper as needing further research. However, as we pointed out, both high-yielding and low-yielding agriculture can have negative effects on biodiversity in nonfarmed land, and those effects associated with low-yielding agriculture, while they may be lower per unit area of farmed land, can have a severe effect if they require farming of a larger area. We are producing an extended version of our model, which incorporates negative externalities and effects of habitat fragmentation, and hope that this will suggest practical ways of better quantifying the relevant effects.

In sum, we maintain that the key to identifying how best to reconcile food production and biodiversity conservation is through explicit models guiding systematic data collection, rather than by qualitative inference.

RHYS E. GREEN,^{1,2*} STEPHEN J. CORNELL,^{1,3} JÖRN P. W. SCHARLEMANN,^{1,2} ANDREW BALMFORD^{1,4}



A woman prepares the ground for planting in Mozambique.

LETTERS

¹Department of Zoology, University of Cambridge, Downing Street, Cambridge, CB2 3EJ, UK. ²Royal Society for the Protection of Birds, The Lodge, Sandy, SG19 2DL, UK. ³The Faculty of Biological Sciences, University of Leeds, Leeds, LS2 9JT, UK. ⁴Percy FitzPatrick Institute of African Ornithology, University of Cape Town, Private Bag, Rondebosch 7701, South Africa.

*To whom correspondence should be addressed. E-mail: reg29@hermes.cam.ac.uk

Fossil Horses and Rate of Evolution

IN HIS DISCUSSION OF THE EVOLUTION OF fossil horse teeth ("Fossil horses—evidence for evolution," Perspectives, 18 Mar., p. 1728), B. J. MacFadden does not mention the interesting suggestion of J. B. S. Haldane (1) that these fossil data could be used for measuring the unit of evolutionary rate, for example, a darwin, for an increase or decrease of size by a factor of e per million years, or an increase or decrease of 1/1000 per 1000 years. The horse rates would range around 40 millidarwins. Haldane wrote that the unit for the character may be a unit increase in the natural logarithm of a variate, or alternatively one stan-

dard deviation of the character in a population at a given horizon.

KRISHNA R. DRONAMRAJU
Foundation for Genetic Research, Post Office Box 27701-0, Houston, TX 77227, USA. E-mail: kdronamraj@aol.com

Reference

1. J. B. S. Haldane, *Evolution* 3, 51 (1949) [reprinted in *The Selected Genetic Papers of J.B.S. Haldane*, K. R. Dronamraju, Ed. (Garland Publishing, New York, 1990), pp. 127–132].

Response

DRONAMRAJU CORRECTLY POINTS OUT THAT quantitative rates of morphological evolution have been calculated from the fossil record. Haldane (1) originally proposed the "darwin" (d) to compare morphological rates of evolution in dinosaurs, fossil horses, and fossil humans. Since Haldane's time, over a half-century ago, more key fossils have been found and the precision of geological dating has vastly improved. Gingerich (2) analyzed rates of morphological change in many fossil groups ranging from invertebrates to mammals. He found relatively high rates (>1 d) within adaptive radiations of some primitive mammals. Using tooth measurements in ancestral-descendant pairs of fossil horses from North America, I (3) found that morphological rates of evolution vary widely in differ-

ent variates; for example, tooth crown height evolves more rapidly (~ 0.1 d) than tooth length (~ 0.03 d) in some extinct grazing horses, an example of mosaic evolution (4). With some important caveats (2), Haldane's method is an effective way to compare morphological rates evidenced from the fossil record, including the Family Equidae.

BRUCE J. MACFADDEN

Florida Museum of Natural History, University of Florida, Gainesville, FL 32611, USA. E-mail: bmacfadd@flmnh.ufl.edu

References

1. J. B. S. Haldane, *Evolution* 3, 51 (1949).
2. P. D. Gingerich, *Science* 222, 159 (1983).
3. B. J. MacFadden, *Biol. J. Linn. Soc.* 35, 37 (1988).
4. G. de Beer, *Adv. Sci.* 42, 1 (1954).

HIV and Smallpox

IN THEIR PERSPECTIVE "HIV: EXPERIENCING the pressures of modern life," D. Nolan *et al.* depict the complex interaction of this pathogen with us humans as its host (4 Mar., p. 1422). The authors conclude that HIV is highly adaptable. As an example of a less adaptable organism, they mention vaccinia virus as the cause of smallpox. Although under certain conditions, vaccinia virus infection may cause lesions similar to those of smallpox in humans (1), smallpox in

PACIFIC NORTHWEST NATIONAL LABORATORY

Northwest Symposium for SYSTEMS BIOLOGY 2005

TOWARD A PREDICTIVE SCIENCE

June 20-21 ■ Richland, WA

Special keynote presentation by **Dr. David Galas**
V.P., Chancellor, Chief Scientific Officer, Professor
Keck Graduate Institute
V.P., Chief Scientific Officer for Biological and Life Sciences
Battelle Memorial Institute

- ▶ *Generating the Data Needed for Prediction*
- ▶ *Generating Models that Predict*
- ▶ *Applications: Brave New World*

Attend **NSSB 2005** to discover and discuss cutting-edge technologies in Systems Biology for the 21st century.

REGISTER ON-LINE @
www.pnl.gov/northwestsymposium

BioMolecular Systems Initiative
www.sysbio.org

Pacific Northwest National Laboratory
Operated by Battelle for the U.S. Department of Energy
www.pnl.gov

Is Albumin Getting in the Way of Your Biomarker Detection?

Reveal Your Biomarkers with ProMax Albumin Removal Kit

- **Fast Removal of Albumin in 30 minutes or less**
- **Easy-to-Use Kit supplied with Optimized Protocols and Reagents**
- **Patented Magnetic Particle Technology Requires No Columns or Centrifugation**

Receive more information on the ProMax Albumin Removal Kit by visiting www.PSIinfo.com/13 or call 1-800-430-9415

Polysciences, Inc.
Chemistry beyond the ordinary

400 Valley Road • Warrington, PA 18976

humans was caused by variola virus, which was eradicated in the late 1970s (2).

ROB A. GRUTERS AND ALBERT D. M. E. OSTERHAUS
Department of Virology, Erasmus MC, Dr. Molewaterplein 50, 3015 GE Rotterdam, Netherlands. E-mail: r.gruters@erasmusmc.nl, a.osterhaus@erasmusmc.nl

References

1. R. R. Redfield *et al.*, *N. Engl. J. Med.* **316**, 673 (1987).
2. J. G. Breman, I. Arita, *N. Engl. J. Med.* **303**, 1263 (1980).

Response

GRUTERS AND OSTERHAUS ARE CORRECT IN pointing out that the virus responsible for smallpox was variola. Vaccinia is a relatively nonpathogenic virus that has served as the basis for smallpox vaccination since Jenner's first fortuitous discovery. Knowledge of the diversity and adaptability of naturally occurring variola virus is limited, with only two of the 200 variola proteins characterized (1), although it is presumed that the high degree of homology between these related poxviruses—as well as their lack of diversity—have contributed to the success of this global vaccination strategy. The variola virus may also be relevant to the genetics of the chemokine receptor 5 (CCR5)-HIV interaction (2), as variola encodes a high-affinity secreted chemokine-binding protein that binds CC-chemokine

receptors (1). This virus, now extinct in its natural form, may have been responsible for enriching (3, 4) or maintaining (5) the *CCR5Δ32* mutation within Northern European populations, thus providing their descendants more than a thousand years later with relative protection against HIV infection and disease progression (2, 6).

DAVID NOLAN, IAN JAMES, SIMON MALLAL

Centre for Clinical Immunology and Biomedical Statistics, Murdoch University, Perth, Western Australia 6000, Australia.

References

1. L. R. Dunlop *et al.*, *Microbes Infect.* **5**, 1049 (2003).
2. D. Nolan *et al.*, *AIDS* **18**, 1231 (2004).
3. A.P. Galvani, M. Slatkin, *Proc. Natl. Acad. Sci. U.S.A.* **100**, 15276 (2003).
4. F. Libert *et al.*, *Hum. Mol. Genet.* **7**, 399 (1998).
5. S. R. Duncan *et al.*, *J. Med. Genet.* **42**, 205 (2005).
6. M. Samson *et al.*, *Nature* **382**, 722 (1996).

How Similar Are Poxviruses?

IN HIS ARTICLE "UNNOTICED AMENDMENT bans synthesis of smallpox virus" (News of the Week, 11 Mar., p. 1540), M. Enserink refers to the October 2004 Act to reform the intelligence community of the United States, which outlawed, *inter alia*, "knowing production, engineering, synthesis, acquisition, pos-

session, usage or threatening to use variola virus," specified in the bill as "a virus that can cause human smallpox or any derivative of variola virus that contains more than 85% of the gene sequence of the variola major or variola minor virus." In connection with the Act, Peter Jahrling from USAMRIID points out that many poxviruses, including vaccinia virus, have genomes more than 85% identical to variola major, and suggests that overzealous interpretation of the Act would put a lot of poxvirologists in jail.

It is undisputable that many poxviruses share high degree of similarity of their nucleotide sequences; however, this similarity is pertinent only to specific portions of their genomes and not to the overall genomes. Alignments of variola major virus strain Bangladesh-1975, camelpox virus strain CMS, and vaccinia virus strain Copenhagen were shown to share nucleotide identity 91% throughout the conserved central region of their genomes (1). Nevertheless, for the interpretation of the Act, the global alignment of the whole genomes would be more appropriate than the local alignment of their conserved portions. Global alignment by Lalign program with scoring matrix *dna.mat* and gap penalties -14/-4 (2) shows that variola major virus



JPT

Innovative Custom Peptide Solutions

Micro-Scale Peptide Sets

- Flexible: thousands of individual peptides in micro plates
- Speed: 10 000 peptides in 2 weeks
- Amount: up to 250 nmol per peptide
- Purity: av. 70%; QC available
- Proprietary Technology guarantees lowest prices: US \$ 1.29/per residue

Specialty Peptides

- Any modification, challenge us!
- Substrate peptides for kinases, phosphatases, proteases
- Pilot scale synthesis of peptides
- DIN EN ISO 9001:2000 certified
- Systematic peptide optimization
- Over 10 years experience with top references

Custom Peptide Arrays

- Fast and flexible peptide array production
- Any peptide collection on membranes or chips
- Up to 10 000 peptides/chip
- Multiple copies, chip series to order
- Speed: 5 000 peptides/chip in 2 weeks
- Over 200 peer reviewed papers



LETTERS

(NC_001611) shares identity of only 28.2% with variola minor Garcia-1966, 28% with vaccinia virus WR, and 27.9% with Camelpox virus CMS.

ROMAN MEZENECV AND KAY MEREISH

United Nations, 866 United Nations Plaza at 48th Street, New York, NY 10017, USA.

References

1. C. Gubser, G. L. Smith, *J. Gen. Virol.* **83**, 855 (2002).
2. E. W. Myers, W. Miller, *Comput. Appl. Biosci.* **4**, 11 (1988).

CORRECTIONS AND CLARIFICATIONS

News Focus: "Ibogaine therapy: A 'vast, uncontrolled experiment'" by B. Vastag (15 Apr., p. 345). The article incorrectly described work by Deborah Mash's group at the University of Miami. The brain bank she runs is sponsored by the National Parkinson Foundation and is primarily devoted to that disease. Her research on cocaine and alcohol did not demonstrate brain damage, but that the two drugs combine to form a lethal metabolite. Ibogaine has been shown to slow the heart only in cocaine-dependent patients with depleted blood volume. Mash holds no patent on ibogaine but has patents on the use of its metabolite, noribogaine. This metabolite, not ibogaine, was described as acting like "super-sticky long-acting Prozac." Mash says she has not published all her data on noribogaine because they are proprietary. In addition, Dorit Ron and colleagues at the University of California, San Francisco conducted research on mice addicted to alcohol, not opiates. Robert Burke and colleagues at Columbia University

did the work on mice overproducing glial cell line-derived neurotrophic factor and suggested that GDNF maintains and possibly repairs dopamine receptors. Kenneth Alper is not at Columbia but is associate professor of psychiatry and neurology at the New York University School of Medicine.

ScienceScope: "Alaskan coral preserved" (18 Feb., p. 1027). The image credit was incorrect. It should have been "Alberto Lindner/NOAA."

News Focus: "RNAi shows cracks in its armor" by J. Couzin (12 Nov. 2004, p. 1124). The story inadvertently omitted mention of Sumedha D. Jayasena at Amgen. His team helped explain how small interfering RNA molecules unwind, which plays a role in how they target genes.

TECHNICAL COMMENT ABSTRACTS

COMMENT ON "The Involvement of the Orbitofrontal Cortex in the Experience of Regret"

David M. Eagleman

Camille *et al.* (Reports, 21 May 2004, p. 1167) hypothesized that regret is useful for steering decision-making. They sought to show that patients with lesions of the orbitofrontal cortex perform more poorly on a gambling task because they do not experience regret. However, choices in the task design raise questions about their interpretation.

Full text at www.sciencemag.org/cgi/content/full/308/5726/1260b

RESPONSE TO COMMENT ON "The Involvement of the Orbitofrontal Cortex in the Experience of Regret"

Giorgio Coricelli, Nathalie Camille, Pascale Pradat-Diehl, Jean-René Duhamel, Angela Sirigu

We recently showed that in contrast to normal subjects, patients with orbitofrontal lesions do not experience the emotion of regret. Eagleman argues that the task parameters we used may have provoked frustration, rather than regret. We demonstrate that this alternative explanation fails to consider several of our findings and is therefore implausible.

Full text at www.sciencemag.org/cgi/content/full/308/5726/1260c

Letters to the Editor

Letters (~300 words) discuss material published in *Science* in the previous 6 months or issues of general interest. They can be submitted through the Web (www.submit2science.org) or by regular mail (1200 New York Ave., NW, Washington, DC 20005, USA). Letters are not acknowledged upon receipt, nor are authors generally consulted before publication. Whether published in full or in part, letters are subject to editing for clarity and space.

Analytical Instruments

affordably
Now you can [^]monitor
Biomolecular Binding
Reactions in real time.

SR7000 New Surface Plasmon Resonance Instrument:

- High quality, kinetic data
- Flexible: you design it to do your work
- Affordable: a fraction of other instruments
- Easy to set up and use

Uses/Features:

- Response vs. time and reflectivity data
- For kinetics (on, off, equilibrium), relative affinity, sequence recognition, concentration, ligand fishing
- For epitope screening and mapping
- For method development...before running more expensive tests
- Extremely sensitive: Savitzky Golay Smoothed Data rms Noise = 0.45 μ RIU = 0.33 RU = 3.3e-05 deg. (Raw Data rms Noise = 0.97 μ RIU = 0.71 RU = 7.1e-05 deg)
- Excellent baseline stability: Maximum drift 3.1 μ RIU/hour [1 μ RIU = 0.73 RU = 7.3e-05 Deg]
- Given ready chemistry (slide with surface and analyte to test against it), the instrument can be up and producing data within an hour out of the box.
- Uses off-the-shelf HPLC fluidics

NOW AVAILABLE
Autosampler
ADDS TO
Flexibility & Throughput



Reichert
Analytical Instruments

Reichert, Inc.
3374 Walden Avenue • Depew, NY 14043
Toll Free: 888-849-8955 • Tel: (716) 686-4500
Fax: (716) 686-4545 • Email: info@reichert.com
www.reichertai.com

Imagine the perfect SPR instrument for you.

ANTHROPOLOGY

Sifting Myths for Truths About Our World

Abigail A. Baird

The Indonesian island of Simeule is the closest inhabited land to the epicenter of the 26 December 2005 Sumatran earthquake. Its inhabitants were the first to experience the full force of the subsequent tsunami, which killed more than 150,000 people. Within 30 minutes of the initial seismic activity, the tsunami slammed into the island's northern coast. Waves 10-m high left little behind. Yet when all was said and done, only seven of the island's 75,000 inhabitants had died. Unlike hundreds of thousands of others who thought the worst was over when the earthquake's shuddering stopped, the people of Simeule—remembering a story passed down from their grandparents—fled to higher ground, thus saving their lives. The story describes angry gods who shake the ground and then produce giant waves called “smong.” Interestingly, this oral history is believed to result from accounts of an actual tsunami that struck in 1907 and killed thousands of islanders.

It has been suggested that language-dominated cognition among human beings enables a “mythic culture” whose primary function is to pass collective knowledge about survival through a vast mythic heritage, complete with oral lore, totemic art, mimetic song, dance, and ritual (1). In *When They Severed Earth from Sky*, Elizabeth Wayland Barber and Paul T. Barber effectively argue that myths, while enabling survival, also serve as carriers of important information about real events and observations. To this end, the authors (2) provide not only a compelling and highly readable collection of mythic interpretations but also a framework through which to decode those stories and uncover seismic, geological, astrological, or other natural events that preceded written history.

Previous scholarship has described myth as an aesthetic device for bringing the imaginary but powerful world of preternatural forces into a manageable collaboration with the objective, experienced facts of life in such a way as to excite a sense of reality amenable to both the

unconscious passions and the conscious mind (3). To this end, humans have been equipped with an ability, which lies somewhere between curiosity and compulsion, to discern meaning in our experience. Although this ability is largely useful, problems with accuracy can result from the fact “that our brains are constructed to seek out patterns so avidly that they will happily pounce onto single cases” and give them causes or meanings. Barber and Barber give the example of a reaction to finding a corpse in the kitchen: spatial proximity may lead one to conclude

When They Severed Earth from Sky
How the Human Mind Shapes Myth
 by Elizabeth Wayland Barber and Paul T. Barber
 Princeton University Press, Princeton, NJ, 2004. 310 pp. \$29.95, £18.95. ISBN 0-691-09986-3.

therefore that the cook did it—*prope hoc, ergo propter hoc*. The problem of accuracy also arises in regard to the human quest for meaning; there are few occurrences, either natural or otherwise, that are devoid of meaning to human beings. For example, you might think that you did not get the job because it was not meant to be or the tsunami was meant to reflect the gods' anger.

The authors' discussion of the problems with accuracy is but one example of the way that they deftly deal with human cognition in the presence of actual events. The Barbers' technique, the “stripping procedure,” facilitates the discernment of the true original events by removing the offered explanations (“meaning making”) from the story, more clearly singling out the observations.

In one of the book's highlights, the authors unpack myths involving fire-breathing dragons. Working with the text of *Beowulf* (among other legends), they use their stripping procedure to interpret the myth. In the story of *Beowulf*, they identify six usable observations: (i) “Someone steals a cup from an old barrow” (a burial mound in the ground). (ii) “Fire erupts from the barrow and spreads.” (iii) “Near the stone entrance, our hero stabs blindly at the

source of flames.” (iv) “It smells bad.” (v) “People stab deeper, and eventually the flame goes out.” (vi) “Inside the barrow is treasure but no trace of a dragon's body.”

Barber and Barber offer an integrated interpretation of these data points: People do steal from tombs, which often do smell bad and contain valuable items. Because these tombs were well constructed, it was often the case that the gasses from the decomposing bodies were held within the tombs, creating large amounts of horrible smelling, and highly flammable, methane (or “marsh gas”). If a tomb thief has broken in at night with a lantern or torch in hand, a fire is likely to start. Stabbing at the mound, as *Beowulf* did, likely further aerated the barrow and provoked larger fiery bursts, until all combustible material was gone and the fire and dragon were no more. Through the authors' framework, *Beowulf's* fight with a dragon is revealed as the natural properties of a burial mound.

Although this account is both compelling and convincing, it also reflects the book's principal weakness. Throughout the text, the authors pay little attention to the human psyche itself—more specifically, to the importance of these myths in identity and personality. Jerome Bruner has described myth as the synergistic blend of external reality and the internal vicissitudes of man (4). His account effectively emphasizes the importance of the individual in both the construction and propagation of myth. In addition to their value as repositories of natural history, myths also speak to us about who we are and help us as individuals make sense of both our external



The Churning of the Ocean of Milk (circa 1785, Pahari school, Kangra, India). In Hindu and Buddhist mythology, the axis around which Earth and sky are organized is analogized as the shaft of a churn that gods and demons use to stir the Milky Way.

CREDIT: SAN DIEGO MUSEUM OF ART (EDWIN BINNEY 3RD COLLECTION)

The reviewer is at the Department of Psychological and Brain Sciences, Dartmouth College, 6207 Moore Hall, Hanover, NH 03755, USA. E-mail: abigail.a.baird@dartmouth.edu

and internal worlds. Given these other values, it is possible for myths to reveal important data about what character traits and virtues were desirable at different points in history. It is clear that the framework provided by Barber and Barber is able to excavate natural facts from linguistically based myth. It would have been interesting to see the same type of approach applied to social or individual processes. However, those questions clearly lie beyond the scope set out by the authors, and that they were ignored detracts in no way from the flow or impact of the book.

Quite simply, the Barbers' book is for people who prefer "just because" to "just so" stories. In the tradition of books by Merlin Donald (1) and Daniel Schacter (5), *When They Severed Earth from Sky* provides an intellectually challenging and parsimonious new framework. It not only sheds light on the planet's natural history but also offers alluring insights about human cognition.

References and Notes

1. M. Donald, *Origins of the Modern Mind: Three Stages in the Evolution of Culture and Cognition* (Harvard Univ. Press, Cambridge, MA, 1991).
2. E. W. Barber is a professor of linguistics and archaeology at Occidental College; P. T. Barber is a research associate with the Fowler Museum of Cultural History at the University of California, Los Angeles.
3. R. V. Chase, *Quest for Myth* (Louisiana State Univ. Press, Baton Rouge, LA, 1949).
4. J. S. Bruner, *On Knowing: Essays for the Left Hand* (Harvard Univ. Press, Cambridge, MA, 1962).
5. D. L. Schacter, *The Seven Sins of Memory: How the Mind Forgets and Remembers* (Houghton Mifflin, Boston, 2001).

10.1126/science.1111126

NEUROSCIENCE

One Cause for All Confabulations?

Armin Schnider

Even though it is no shame to fabricate stories—and some make a living doing so—the term “confabulation,” which means exactly this, has always had a negative connotation. It was toward the end of the 19th century that clinicians first described the curious tendency of certain memory-impaired subjects to make up stories about their recent doings (1). Some patients appeared to believe in their stories; others produced them only when questioned. To some observers, the significance of these stories—soon termed confabulations—rapidly appeared obvious: the patients desired to fill gaps in memory (2). Variants of this idea have survived to the pres-

The reviewer is in the Division of Rehabilitation, Department of Clinical Neurosciences and Dermatology, University Hospital, Avenue de Beau-Séjour 26, 1211 Geneva 14, Switzerland. E-mail: armin.schnider@hcuge.ch

ent, and new hypotheses positing defective “monitoring” processes have been added. Interpreting confabulations has become more delicate with the observation that even healthy people may unknowingly confabulate. Memory is now considered a reconstructive process in which memories are constantly reactivated, associated, and again encoded. In his magnificent book, Daniel Schacter describes the imperfections of normal memory as “the seven sins of memory” (3). These sins are particularly pertinent in the context of legal testimony.

Fabricated stories also occur as a result of inaccurate perception. I vividly recall a patient, blinded by a stroke of the back part of her brain, watching emptily into the room and complimenting me on my “yellow tie with pink spots.” I knew she was blind, and I would never wear such a tie, but she was totally unaware of her blindness. Similar confabulations, mostly with unawareness of deficit, also occur in other disorders of perception and language (4).

On this background—with multiple forms of confabulations emanating from diverse lesions and reflecting failures of memory or perception—the idea of reducing all confabulations to one specific mechanism appears quite unlikely. In *Brain Fiction*, William Hirstein, a philosophy professor at Elmhurst College, takes a different stand: “The apparent diversity of confabulation syndromes invites a search for something they have in common.”

Working primarily with extracts from the recent literature, Hirstein first gathers evidence pinpointing the orbitofrontal cortex at the base of the anterior brain as the critical area for the occurrence of confabulations. This area has recently received much attention because damage to it may produce socially inappropriate behavior or flagrant confabulation. Patients with acute lesions may invent stories about their doings and act according to plans for the future that completely disregard their current brain damage, a disorder called spontaneous confabulation (5). However, other false productions from memory have no comparable anatomical specificity. Hirstein extends the thesis of a frontal origin of confabulations to cover those emanating from false perception. Although this idea is shared by some neurologists, the argument runs aground when one considers, for example, the confabulations of patients who have visual defects following isolated posterior brain damage. The author's suggestion that right hemisphere damage would be particularly critical for the occurrence of confabulation also holds only as long as one forgets confabulations produced by patients

with visual agnosia after left hemisphere damage: who see objects but fail to understand their meaning, misname them, and sometimes even use them according to this false name.

What would be a common mechanism for all forms of confabulation? Hirstein proposes that confabulations result from disinhibition like that responsible for socially inappropriate remarks. Confabulators would be unaware that it is socially inappropriate to provide false information and would fail to notice that others disapprove of their false statements. Thus, their common problem would be a failure to read the mind of others. As the author notes, this explanation has difficulty in accounting for the confabulations in the first place, before listeners hear the false statements. In more general terms, he

suggests that “confabulation occurs when a perceptual or mnemonic process fails and the failure is not detected by frontal processes.” How could this be checked? “If you combine a representation-evaluating process with a behavior-inhibiting process, the combination can function as a checking process.” The idea is reminiscent of previous monitoring hypotheses, now applied to all forms of confabulation. Unfortunately, Hirstein offers no suggestion of an experimental approach to test it.

Brain Fiction offers one of the most extensive accounts of false memories and perceptions, although it leaves out important forms, including those occurring in healthy subjects. Hirstein proposes that one mechanism (a mind-reading difficulty based on frontal-lobe dysfunction) accounts for all forms of confabulations. It is inspiring to consider such a wide-ranging thought-monitoring process, but the book also shows to what degree current neurobiological evidence has to be selected and generalized to maintain such a unitary concept. At a time when neuropsychological experimentation and modern imaging technologies allow us to dissect cognitive processes ever more finely, some might prefer a more evidence-driven, analytical approach to the all-inclusive, hypothetical one Hirstein takes.

References

1. S. S. Korsakow, *Allg. Z. Psychiat. Psych. Med.* **47**, 390 (1892).
2. K. Bonhoeffer, *Die Akuten Geisteskrankheiten des Gewohnheitstrinkers: Eine Klinische Studie* (Gustav Fischer, Jena, Germany, 1901).
3. D. L. Schacter, *The Seven Sins of Memory; How the Mind Forgets and Remembers* (Houghton Mifflin, Boston, 2001).
4. O. J. Grüsser, T. Landis, *Visual Agnosias and Other Disturbances of Visual Perception and Cognition*, vol. 12 in *Vision and Visual Dysfunction*, J. Cronly-Dillon, Ed. (Macmillan, London, 1991).
5. A. Schnider, *Nat. Rev. Neurosci.* **4**, 662 (2003).

10.1126/science.1112149

Brain Fiction Self-Deception and the Riddle of Confabulation by William Hirstein

MIT Press, Cambridge, MA, 2005. 301 pp. \$35, £22.95. ISBN 0-262-08338-8. Philosophical Psychopathology: Disorders in Mind.

ENVIRONMENT

The Specter of Fuel-Based Lighting

Evan Mills

Thomas Edison's seemingly forward-looking statement that "we will make electricity so cheap that only the rich will burn candles" (1) was true for the industrialized world, but it did not anticipate the plight of 1.6 billion people (2)—more than the world's population in Edison's time—who

Enhanced online at www.sciencemag.org/cgi/content/full/308/5726/1263

more than a century later still lack access to electricity (see figure, this page). While electricity was becoming available in the wealthier countries, leaders of the oil industry (3, 4) promoted lighting-oil products in China and elsewhere. The legacy of costly and low-grade lighting for the world's poor remains. For those without access to electricity, lighting is derived from a diversity of sources, including kerosene, diesel, propane, biomass, candles, and yak butter. Many of the 35 million people living in camps for refugees and internally displaced people have no light at all.

Throughout the developing world, 14% of urban households and 49% of rural households were without electricity as of the year 2000 (2). In extreme cases, e.g., Ethiopia and Uganda, only ~1% of rural households are electrified (5). An unknown additional number of people have intermittent access to electricity in their homes or lack it altogether in their workplaces, markets, schools, or clinics (6). The number and proportion of people lacking electricity is growing in sub-Saharan Africa and parts of Latin America and the Caribbean, the Middle East, and South Asia (7). Population growth, stalling rates of electrification, and declining household sizes (8) exacerbate the problem. The number of people without access to electricity globally is projected to decline at only 0.4%/year over the next 3 decades (2).

Illumination is one of the core end-use energy services sought by society and is today obtained by some at efficiencies on the order of 100 lumens per watt and by others at well below 1 lumen per watt (9). Compounding this disparity, the least efficient sources also deliver less—and less uniform—light: A simple wick lantern provides about 1 lux (lumens/m²) at 1 meter from the source,

compared with levels on the order of 500 lux routinely provided in industrialized countries (figs. S1 to S3).

Although the energy performance of individual fuel-based light sources has been analyzed previously (9, 10), the global dimensions have not been quantified. We estimate that fuel-based lighting is responsible for annual energy consumption of 77 billion liters of fuel worldwide (or 2800 petajoules, PJ), at a cost of \$38 billion/year or \$77 per household (table S1). This equates to 1.3 million barrels of oil per day, on a par with the total production of Indonesia, Libya, or Qatar, or half that of pre-war Iraq. Consumption of lighting fuel is equivalent to 33% of the total primary energy (electricity plus fuel) used for household lighting globally and 12% of that across all lighting sectors (11).

Used 4 hours a day, a single kerosene lantern emits over 100 kg of the greenhouse gas carbon dioxide into the atmosphere each year. The combustion of fuel for lighting consequently results in 190 million metric tonnes per year of carbon dioxide emissions, equivalent to one-third the total emissions from the U. K.

Although about one in four people obtain light exclusively from fuel, representing about 17% of global lighting energy costs, they receive only 0.1% of the resulting lighting energy services (lumen hours). Despite the paucity of lighting services obtained, individual unelectrified households in the developing world spend a comparable amount of money on illumination as do households in the industrialized world.

Fuel-based lighting embodies enormous economic and human inequities. The cost per useful lighting energy services (\$/lux-hour of light, including capital and operating costs) for fuel-based lighting is up to ~150 times that for premium-efficiency fluorescent lighting (see figure, next page). The total annual light output (about 12,000 lumen-hours) from a simple wick lamp is equivalent to that produced by a 100-watt incandescent bulb in a mere 10 hours.

By virtue of its inefficiency and poor quality, fuel-based light is hard to work or read by, poses fire and burn hazards, and compromises indoor air quality. Women and children typically have the burden of obtaining fuel (12, 13). Availability of lighting is linked to improved security, literacy, and income-producing activities in the home (14). Fuel prices can be highly volatile (15), and fuels are often rationed, which leads to political and social unrest, hoarding, and scarcity.

Although sometimes driven by good intentions such as reducing demand for fuel wood, fuel subsidies divert public sector funds from other uses. In India, where nearly 600 million people are without electricity, kerosene and liquid propane gas subsidies are of the same magnitude as those for education

(16). Subsidies also create price distortions that discourage conservation and encourage dangerous and polluting fuel adulteration in the domestic and transport sectors (17, 18).

Centralized rural electrification has its own problems, not the least of which is the cost of distribution in rural areas with low load densities, coupled with the high capital costs and low efficiencies associated

with thermal power generation. Power theft levels reach 40% in some countries (2).

Off-Grid Solid-State Lighting: An Opportunity for Technological Leapfrogging

As they modernize, developing countries can select better technologies and in so doing surpass levels of efficiency typical of industrialized countries (19). The latest improvement in lighting energy efficiency is the solid-state white light-emitting diode (WLED) (20), distinguished from other lighting technologies by a continuing trend toward increasing light output, declining costs per unit of output, and rising efficiencies.

WLED technologies provide more and better illumination (with easier optical control) than do fuels (fig. S4), dramatically reducing operating costs (table S2) and greenhouse gas emissions, while increasing the quality and quantity of lighting services. Efficiencies of only five delivered lumens per watt in the mid-1990s are moving toward 100 lumens per watt (compared with 0.1 lumens per watt for a flame-based lantern). Relative



Tailor working by candlelight in an "electrified" village in India.

light output (assuming 1-watt WLEDs) would be 5 lumens, 100 lumens, and 40 lumens, respectively. Coupled with inexpensive dif-fusers or optics, today's best WLEDs deliver 10 to 100 times as much light to a task as do traditional fuel-based lanterns.

Commercially available 1-watt WLEDs require 80% less power than the smallest energy-efficient compact fluorescent lamps and can be run on AA batteries charged by a solar array the size of a paperback novel. Rapid efficiency gains have made such systems affordable (fig. S5). With long service life, direct current operation, ruggedness, portability, and ability to utilize inexpensive and readily available batteries, WLED lanterns are well suited for developing country applications. Early demonstrations of primitive WLED systems were well received in the developing world (21), and more advanced prototypes were later developed at Stanford University. When evaluated in terms of total cost of ownership (purchase plus operation), WLED systems emerge as the most cost-effective solution for off-grid applications (table S3). In fact, WLEDs can also provide very substantial savings when compared with the often inefficiently applied electric lighting in the grid-connected homes (see SOM).

Entrepreneurs and charities have deployed relatively complex large-scale

solar-fluorescent systems in the developing world with some success. But, at least partly because of cost, market penetration is only 0.1%. In the absence of a service infrastructure, these systems often fall into disrepair (22, 23, 24). Innovative financing and service strategies are now emerging.

Although less costly WLED systems are well suited for task- and narrow-area ambient lighting, these larger systems or solar-fluorescent lanterns certainly have an important role to play in meeting the broader demand for electricity and for wide-area lighting applications in households that can afford them.

Some have begun to cultivate the enormous potential for self-contained solar-WLED alternatives, which should come to market at a relatively affordable price of about US\$25, without subsidy, and pay for themselves in 1 year or less (fig. S6). The fuel savings represent an ongoing annuity, equal to a month's income each year for the 1 billion people who live on less than \$1/day.

Solutions to the problem of fuel-based lighting are emblematic of the notion that end-use energy efficiency is integral to providing energy services at least cost. As demonstrated in the case of lighting, attaining a higher standard of living does not require increased energy use. Yet, the specter of fuel-based lighting—linked tightly with energy security,

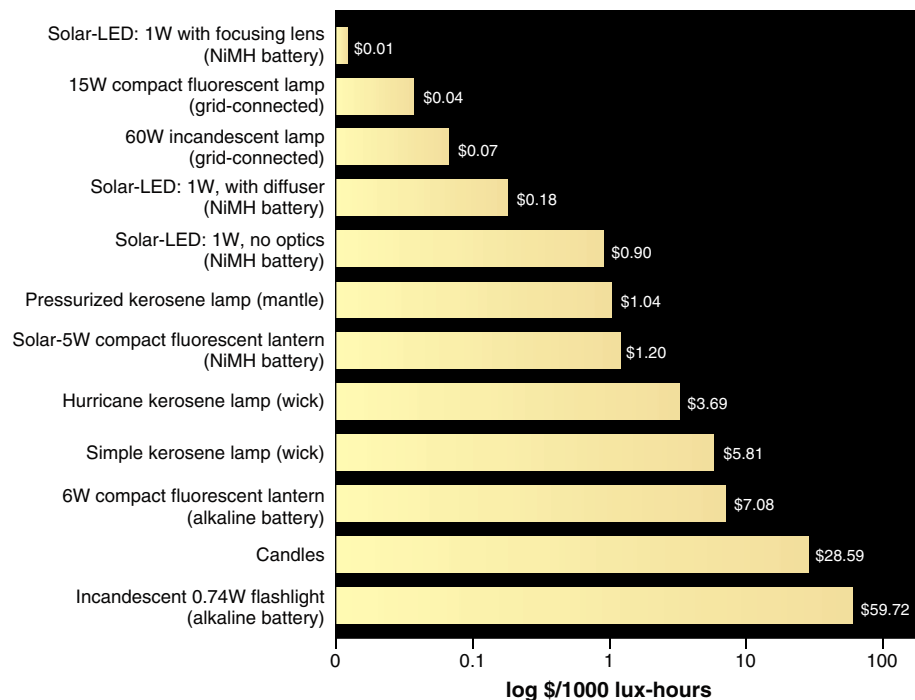
equity, and development concerns—remains a largely unmet challenge for policy-makers. If current trends continue, lighting energy demand and greenhouse gas emissions will increase sharply as countries develop and replace a relatively small number of fuel-based lanterns with more and more grid-connected electric light (25, 26). Or, with a reversal of the technical double standard seen prevailing since Edison's day we could see the use of WLEDs for illumination take hold first in the developing countries, where the need and potential benefits are greatest.

References and Notes

1. D. N. Langenberg, *Science* **272**, 1721 (1996).
2. International Energy Agency (IEA), in *Outlook 2002* (IEA, Paris, 2002), chap. 13.
3. www.kenai-peninsula.org/archives/000326.html.
4. www.shell.com, choose Shell directory, China, about Shell China, who we are.
5. S. Karekezi, J. Kimani, *Energy Sustain Dev.* **8** (4), 10 (2004).
6. According to the IEA (2), in the Indian state of Madhya Pradesh, more than 90% of rural electrified households use kerosene as a backup fuel for lighting.
7. S. Karekezi et al., *Energy Sustain Dev.* **8** (4), 3 (2004).
8. J. Lui et al., *Nature* **421**, 530 (2003).
9. R. J. Van der Plas, A. B. de Graaff, "A comparison of lamps for domestic lighting in developing countries" (Energy Ser. Pap. 6, Industry and Energy Department, World Bank, Washington, DC, 1988).
10. G. S. Dutt, *Energy Sustain Dev.* **1** (1), 23 (1994).
11. E. Mills, *Proceedings of the 5th International Conference on Energy-Efficient Lighting*, Nice, France, June 2002 [International Association for Energy-Efficient Lighting (IAEEL), Stockholm, 2004], pp. 368–385.
12. S. Batliwala, A. K. N. Reddy, *Energy Sustain Dev.* **7** (3), 33 (2003).
13. V. Laxmi, et al., *Energy Sustain Dev.* **7** (1), 50 (2003).
14. W. Floor, R. Massé, "Peri-urban electricity consumers, a forgotten but important group: What can we do to electrify them?" [ESM249, Joint U.N. Development Programme (UNDP)/World Bank Energy Sector Management Assistance Program (ESMAP) Report, 2001].
15. Unsubsidized Arabian Gulf kerosene price fluctuated by a factor of 3.5 between Jan. 1998 and Jan. 2001.
16. UNDP/World Bank, "India: Access of the poor to clean household fuels" (ESM263, UNDP/ESMAP, 2001).
17. M. Kojima, R. Bacon (World Bank), *Public Policy for the Private Sector Note No. 237* (2001).
18. A. K. N. Reddy, *Annu. Rev. Energy Environ.* **27**, 23 (2002).
19. J. T. Goldemberg et al., *Ambio* **14** (4–5), 190 (1985).
20. E. J. Schubert, J. K. Kim, *Science* **308**, 1274 (2005).
21. S. A. Craine, D. Irvine-Haliday, *Proc. SPIE Int. Soc. Opt. Eng.* **4445**, 39 (2001).
22. J. E. Goldemberg et al., *Energy Sustain. Dev.* **8** (4), 86 (2004).
23. O. Davidson, S. A. Mwakasonda, *Energy Sustain Dev.* **8** (4), 26 (2004).
24. D. Jianping et al., *Proceedings of the Sixth International Conference on Energy-Efficient Lighting*, Shanghai, China, 9 to 11 May 2005 (IAEEL and Novem, Sittard, 2005), pp. 397–400.
25. E. Mills, *Light Eng.* **10** (4), 5–10.36 (2002).
26. D. Gately, S. S. Streifel, "The demand for oil products in developing countries" (World Bank Discuss. Pap. No. 359, World Bank, Washington, DC, 1997).
27. Sponsored by the International Energy Agency and by the U.S. Department of Energy under Contract No. DE-AC03 76SF00098. S. Johnson, J. Galvin, R. Clear, E. Page, M. Siminovitich, D. Kelley, J. Patell, B. Behrman, N. Borg, S. Selkowitz, S. Wiel, M. Levine, C. Setchell, R. Sturm, A. Rosenfeld, and J. Livingston provided encouragement, useful discussions, and/or assistance.

Supporting Online Material

www.sciencemag.org/cgi/content/full/308/5726/1263/DC1



Total cost of illumination services. Costs include equipment purchase price amortized over 3 years, fuel, electricity, wicks, mantles, replacement lamps, and batteries. Performance characteristics of light sources vary; values shown reflect common equipment configurations (see table S3) and include dirt depreciation factors for fuel lanterns and standard service depreciation factors for electric light per Illuminating Engineering Society of North America. Assumptions are 4 hours/day operation over a 1-year period in each case, \$0.1/kWh electricity price, \$0.5/liter fuel price. NiMH, nickel metal hydride. (Range of market prices for kerosene shown in table S5.) We estimate an average of 11 liters (7) of lighting fuel per household per month; observed values vary from 2 to 20 liters (table S4).

10.1126/science.1113090

The Link Between Supernovae and Gamma Ray Bursts

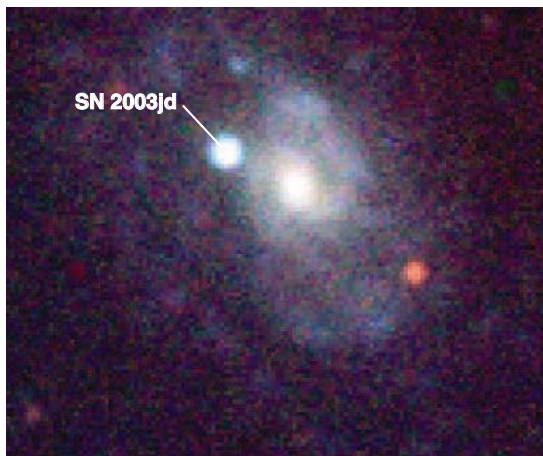
Brian Schmidt

Gamma ray bursts (GRBs) were first discovered in 1967 by American military satellites. The discovery was declassified in 1973; within months, more ideas were published about the origin of these cosmic explosions than there were detected bursts. Since then, observations of thousands of these objects have yielded a deeper understanding of GRBs, but questions remain. For example, it is known that supernovae underlie some GRBs, but how some supernovae produce GRBs remains unclear.

On page 1284 of this issue, Mazzali *et al.* (1) shed some light on the link between GRBs and supernovae. They report that supernova 2003jd (see the figure) appears to have been disrupted by a highly asymmetric process, similar to the jets that produce GRBs. Thus, supernova 2003jd may itself be a GRB, with its jets pointed away from Earth when it exploded. This is the first time that researchers have found a supernova that might be a GRB, rather than a GRB that might be a supernova.

The data revolution for GRBs started in 1991 with the launch of NASA's Compton Gamma Ray Observatory. This satellite and its dedicated GRB instrument, BATSE (Burst and Transient Source Experiment), detected more than 8000 bursts until it was sent into the Pacific Ocean in 2000. Before BATSE, models for GRBs ranged from collisions of objects in our solar system to mergers of black holes on the other side of the universe. BATSE observations showed that GRBs are distributed uniformly across the sky, providing strong evidence that they must be occurring in the distant universe (2), because it is only at great distances that the sky begins to look uniform.

However, although BATSE was very sensitive to high-energy photons, it could not discern the location of a burst to better than a few degrees uncertainty—an area of sky too large to pinpoint the location of individual explosions. Without a smoking



A cosmic explosion 250 million light years away. Observations of supernova (SN) 2003jd show it to be a highly energetic explosion, similar to the hypernovae associated with GRBs. Mazzali *et al.* (1) argue that this object was ripped apart by something like a jet, suggesting that SN 2003jd might have been a GRB with its jets directed away from Earth.

gun, theorists could still bend their models of nearby bursts to fit the observations.

In 1996, the Italian-Dutch BeppoSAX satellite was launched. This satellite was not as sensitive as BATSE to gamma rays, but—inspired by predictions that lower-energy x-rays would persist long after the burst of gamma rays—it was able to point an x-ray detector onto a GRB within a few hours of the burst. Beppo-SAX's x-ray detectors could localize these x-ray emissions to much less than 1° uncertainty. This precision was sufficient for optical and radio telescopes to follow up individual objects and look for these explosions.

This strategy paid off when a GRB detected on 28 February 1997 was localized in x-rays; astronomers using the William Herschel Telescope in the Canary Islands then found a fading optical afterglow in a distant galaxy at this location (3). This discovery confirmed the cosmological origin of GRBs. Another event detected on 8 May 1997 was determined to be more than 7 billion light years away—halfway across the visible universe (4). The huge distance implied an enormous energy. GRBs were thus proclaimed to be the largest bangs in the universe since the big one.

On 25 April 1998, BeppoSAX yielded another surprise. Optical observations of an apparently normal GRB showed a young, very energetic exploding star—a type Ic supernova—at a distance of 80 million light years, one-hundredth the distance of typical GRBs (5). The optical brightness of the supernova, named 1998bw, was high for an object at this distance, but its gamma ray, x-ray, optical, and radio brightnesses are several orders of magnitude fainter than for any other GRB observed to date.

Type Ic supernovae are thought to occur when stars 10 to 100 times the mass of the Sun, which have been stripped of their outer layers of hydrogen and helium, run out of nuclear fuel in their center and collapse into neutron stars or black holes. If the dying star that formed supernova 1998bw had lost its outer layers as a result of a merger with another star, it should have been spinning rapidly at the time of its death. Theorists therefore proposed that a jet, produced by the collapse of a rapidly rotating massive star into a black hole, created supernova 1998bw and could produce typical GRBs (6).

The jet produces observable gamma rays if it points toward the observer; the resulting expanding debris looks like a very energetic type Ic supernova—a so-called hypernova. This model could explain supernova 1998bw, but its relevance to the rest of the GRB population was unclear because of the very different energies of supernova 1998bw and other more distant GRBs.

Since the discovery of 1998bw, much effort has been put into studying the connection between GRBs and hypernovae. The HETE-2 (High Energy Transient Explorer Mission) satellite, launched in 2000, and the Swift Gamma Ray Burst Explorer, launched in 2004, are providing accurate GRB positions for astronomers to chase on an almost daily basis. The light associated with a GRB jet fades quickly, whereas the brightness of a supernova tends to brighten for 1 to 3 weeks. Therefore, 2 weeks past an explosion, a supernova should in most cases outshine a GRB's jet. Observations of nearby GRBs have shown that some objects exhibit supernova-like features as their brightness evolves over time.

The GRB-hypernova connection was confirmed directly on 29 March 2003, when HETE-2 discovered an object one-

The author is in the Research School of Astronomy and Astrophysics, Mount Stromlo Observatory, Australian National University, Weston, ACT 2611, Australia. E-mail: brian@mso.anu.edu.au

third as distant as any other cosmological GRB to that date. As the object faded, spectra taken with optical telescopes revealed an underlying supernova—an object almost identical to supernova 1998bw (7, 8), but with a gamma ray energy a thousand times higher.

The connection between GRBs and hypernovae thus seems secure, but important questions remain. The GRB jet of supernova 1998bw is much less energetic than that associated with any other GRB to date, and no consensus has emerged as to how a single mechanism could produce supernova 1998bw and the much more powerful bursts in the distant universe.

In addition, the jets of most GRB-hypernovae should aim away from Earth; although not visible in gamma rays, these “misdirected” GRBs should be seen at radio wavelengths (9). By comparing the numbers of hypernovae and GRBs in the uni-

verse, one can gauge the fraction of hypernovae that are misdirected GRBs. Current data suggest that this fraction should be substantial (10). To date, relatively few hypernovae have been discovered in the nearby universe, but none seem to show the intense radio emission expected for misdirected GRBs.

Mazzali *et al.*'s observations of supernova 2003jd, a hypernova at a distance of 250 million light years (see the figure), may resolve the latter problem. The authors provide evidence for the gross asymmetries that are expected for a GRB-hypernova. After the discovery of 2003jd, observers used the Very Large Array radio telescope to look at it, but did not detect it at radio wavelengths. Mazzali *et al.* argue that better radio or x-ray observations are needed to reveal whether this hypernova had a GRB jet. Even if subsequent observations fail to find jets associated with supernova 2003jd, the observations

reported in (1) provide substantial evidence that the engine that powered supernova 2003jd to become a hypernova is the same that creates GRBs in the distant universe.

With two dedicated GRB telescopes and many programs scanning the sky for supernovae, the next few years promise many more GRB-hypernova connections. These results should help astronomers to further untangle the mysteries of GRBs.

References

1. P. A. Mazzali *et al.*, *Science* **308**, 1284 (2005).
2. C. A. Meegan *et al.*, *Nature* **355**, 143 (1992).
3. J. van Paradijs *et al.*, *Nature* **386**, 686 (1997).
4. M. R. Metzger *et al.*, *Nature* **387**, 878 (1997).
5. T. J. Galama *et al.*, *Nature* **395**, 670 (1998).
6. A. I. MacFadyen, S. E. Woosley, *Astrophys. J.* **524**, 262 (1999).
7. K. Z. Stanek *et al.*, *Astrophys. J.* **591**, L17 (2003).
8. J. Hjorth *et al.*, *Nature* **423**, 847 (2003).
9. E. Berger *et al.*, *Astrophys. J.* **599**, 408 (2003).
10. P. Podsiadlowski *et al.*, *Astrophys. J.* **607**, L17 (2004).

10.1126/science.1112928

CELL BIOLOGY

Lessons in Rational Drug Design for Protein Kinases

Natalie G. Ahn and Katheryn A. Resing

How do you design a drug that selectively recognizes one enzyme from among hundreds, all of which share the same substrate? This is the challenge confronting biochemists when developing small-molecule inhibitors of protein kinases, enzymes that regulate cellular growth, homeostasis, and signal transduction. Fifteen years ago, intracellular kinases were considered too ubiquitous to be useful drug targets. But with mounting evidence for highly specific function in many kinases, many pharmaceutical endeavors today have screening programs for inhibitors of this class of enzymes.

Since the mid-1990s, three kinase inhibitors have been approved by the U.S. Food and Drug Administration (FDA) for treatment of chronic myelogenous leukemia, gastrointestinal stromal tumors, and lung tumors (1, 2), and many others are in clinical trials. Each drug works by competitively displacing adenosine 5'-triphosphate (ATP), the nucleotide that binds to the active site of protein kinases. However, because all kinases share molecular recognition determinants in their conserved nucleotide binding pocket, no ATP analog has been found

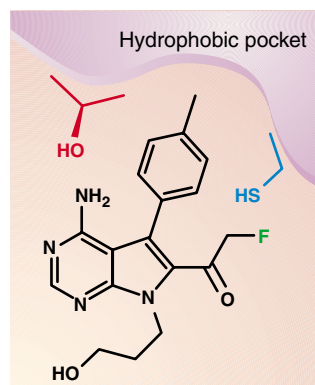
that selectively inhibits a single enzyme. This complicates strategies for developing protein kinase inhibitors. It is difficult to identify small-molecule compounds with high specificity for a single kinase. One must further verify that cellular responses to drug treatment are caused by inhibition of the targeted enzyme.

Enter rational drug design, combining structural determination and computational modeling to identify small molecules that complement amino acid residues within the active site of a target enzyme. So far, only a few successful lead compounds have been developed based on principles of molecular recognition, as opposed to random screening. However, bioinformatics strategies have added new tools to the arsenal, enabling researchers to predict variations in nucleotide and protein sequence that may serve as specificity determinants.

On page 1318 in this issue, Cohen *et al.* (3) describe such an approach to designing small-molecule inhibitors of p90 ribosomal S6 kinases (RSKs) by selectively targeting two determinants, or “selectivity filters,” in the ATP binding pocket. One selectivity filter, the “gatekeeper,” is a residue that flanks a highly variable hydrophobic pocket at the rear of the ATP binding site (4). When the side chain of the gatekeeper residue occupies a small volume, the hydrophobic pocket is empty. This allows bulky groups on adenine ring analogs to fit into the pocket. On the other hand, a gatekeeper

residue with a large side chain precludes binding of bulky substituents. This mechanistic understanding of selectivity enables candidate inhibitors to be identified by comparing aligned sequences at the gatekeeper position.

The second selectivity filter is a reactive cysteine residue within the active site. The strategy of targeting active-site cysteine residues was previously successful in developing irreversible inhibitors for the epidermal growth factor (EGF) receptor (5). However, cysteine residues within active sites of kinases are relatively rare. Using bioinformatics analysis, Cohen *et al.* showed that only 11 kinases among a set of 491 had cysteine residues within the conserved gly-



Proposed binding mode of a rationally designed inhibitor of p90 RSK. Two “selectivity filters” in the ATP binding site are required for potent inhibition. A threonine residue (red) in the gatekeeper position allows the inhibitor (black) to access a hydrophobic pocket. A poorly conserved cysteine (blue; valine in many kinases) is positioned for attack by the electrophilic fluoromethylketone substituent of the inhibitor (F; green).

The authors are in the Department of Chemistry and Biochemistry, University of Colorado, Boulder, CO 80309, USA. E-mail: natalie.ahn@colorado.edu

CREDIT: M. COHEN AND R. BATEMAN

cine loop, a region that forms close contacts with bound ATP. Of these, only three kinases, all members of the RSK family, also contained a gatekeeper residue that presented an empty hydrophobic pocket. Thus, by judiciously placing fluoromethylketone or chloromethylketone groups onto adenine ring analogs that were also modified with bulky substituents, the authors designed molecules that could both occupy the hydrophobic pocket and irreversibly alkylate the cysteine residue (see the figure).

The resulting compounds showed remarkable specificity toward RSK family members. When the authors administered the fluoromethylketone-modified molecule to cells in culture, only RSK1 and RSK2 were identified as covalently associated proteins. Treatment with the drug also efficiently suppressed cellular responses controlled by RSK, whereas other kinases that contained only one of the two selectivity filters were unaffected. Cohen *et al.* then engi-

neered both selectivity filters into MSK1 and Src, two enzymes that contain either the cysteine or gatekeeper residues, respectively. Both enzymes were beautifully converted into inhibitor-responsive enzymes. Thus, only two filters were necessary and sufficient to confer selectivity of inhibitor binding to the ATP binding site.

The approach developed by Cohen *et al.* has broad implications for the rational design of kinase inhibitors, where the ability to distinguish between members of closely related enzyme families is key to drug selectivity. In principle, only a few molecular substituents are required for specificity, provided that their chemical and structural properties are sufficient to distinguish variations among amino acid residues within a conserved protein active site. However, this rosy picture breaks down when drug-resistant mutations arise in the kinases, as observed with the current FDA-approved inhibitors to the tyrosine kinases EGF receptor [Iressa (gefitinib),

Tarceva (erlotinib)] and BCR-ABL [Gleevec (imatinib)]. Intriguingly, resistance mutations include alterations at the gatekeeper residue that eliminates access to the hydrophobic pocket (6–8). Presumably, these resistance mutations were selected by their ability to interfere with inhibitor recognition while retaining ATP binding. By using strategies for combinatorial recognition based on sequence variations, additional selectivity filters may be identified that can be exploited in the design of new inhibitors.

References

1. W. Pao, V. A. Miller, *J. Clin. Oncol.* **23**, 2556 (2005).
2. M. Deininger, E. Buchdunger, B. J. Druker, *Blood* **105**, 2640 (2005).
3. M. S. Cohen, C. Zhang, K. M. Shokat, J. Taunton, *Science* **308**, 1318 (2005).
4. Y. Liu *et al.* *Chem. Biol.* **6**, 671 (1999).
5. A. J. Bridges, *Curr. Med. Chem.* **6**, 825 (1999).
6. S. Kobayashi *et al.*, *N. Engl. J. Med.* **352**, 786 (2005).
7. W. Pao *et al.*, *PLoS Med.* **2**, e73 (2005).
8. M. E. Gorre *et al.*, *Science* **293**, 876 (2001).

10.1126/science.1113707

GEOCHEMISTRY

When Do Rocks Become Oil?

Bruce F. Schaefer

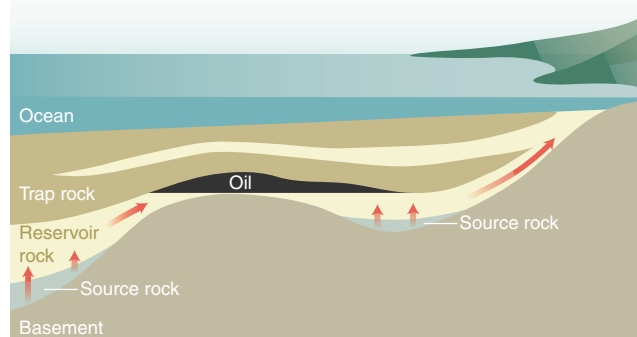
Hydrocarbons and their derivative products are central to today's society. We know that the source of these petroleum products is buried ancient plants and animals. Less clear is how hydrocarbons, such as oil and gas, form and how they are trapped in petroleum systems large enough to be exploited. Now, on page 1293 of this issue, Selby and Creaser (*1*) have precisely dated the time at which hydrocarbons migrated and accumulated within a large petroleum system in Canada.

Oil and gas formation relies on a series of fortuitous events to produce a field large enough for extraction to be economically viable. Unraveling the competing processes and their resulting signatures in the oils produced is notoriously difficult. Different types of organic material can contribute, as can any number of different organic-rich source sediments. On top of this, hydrocarbons such as oil and gas almost invariably migrate through geological strata until they either escape to Earth's surface or are trapped and accumulate into petroleum fields (see the figure). Generally the process of migration obliterates the memory of where the hydrocarbons have come from and when they formed. This complicates

predictive exploration for hydrocarbons, as Earth scientists have only limited information regarding potential source rocks that may contribute to specific geological traps.

Selby and Creaser (*1*) addressed the question of the origin of hydrocarbons by taking account of the naturally occurring ^{187}Re - ^{188}Os decay scheme. Although both rhenium and osmium are present only in trace amounts in Earth's crust (typically parts per trillion) (*2*), they are effectively sequestered into organic

compounds when sedimentation occurs in highly reducing, organic-rich conditions. Such enrichment in Re and Os produces a wide range of $^{187}\text{Re}/^{188}\text{Os}$ ratios in the sediments that over time result in high $^{187}\text{Os}/^{188}\text{Os}$ ratios. By analyzing both ratios, it is possible to determine the age of the material sampled and to obtain the initial $^{187}\text{Os}/^{188}\text{Os}$ isotopic ratio (the ratio all the samples had the last time they were mobile and thus in isotopic equilibrium). Selby and Creaser (*1*) used Os isotopic ratios to determine the last time that the hydrocarbons in the giant oil sand deposits of Alberta, Canada, were mobile, and hence have measured the age of the petroleum deposits [112 ± 5.3 million years ago (Ma) (*1*)]. They also measured the initial Os isotopic ratio, which acts as a fingerprint for the specific rocks that the oil came from—a kind of forensic signature linking the deposits with the scene of hydrocarbon formation. In this case, it appears that the bulk of the hydrocarbons within this giant petroleum system derive from a single package of source rocks, rather than a number of different sources with a range of ages. This supports organic biomarker studies predicting a common source for the bulk of the oil sands in western Canada (*3*).



Growth of an oil field. Schematic summary of the critical elements in a hydrocarbon generation and accumulation system. Organic-rich source rocks are buried to depths sufficient for hydrocarbon generation to begin. If the surrounding rocks are sufficiently porous and permeable, hydrocarbons are able to migrate through them to sites where they either are trapped by impermeable trap rocks and accumulate, or escape to Earth's surface where they are rapidly oxidized. Millions of years can elapse between sedimentary deposition and the subsequent generation, migration, and accumulation of hydrocarbons.

The author is in the School of Geosciences, Monash University, Clayton, Victoria 3800, Australia. E-mail: bruce.schaefer@sci.monash.edu.au

Why are these two observations important? First, for petroleum explorers, knowing the origin of hydrocarbons in a sedimentary basin places constraints on where they might be able to accumulate, or whether they are able to accumulate at all. With oil exploration drillholes costing multiple millions of dollars, every piece of data informing site location is of immense worth.

Second, knowing when hydrocarbons migrated offers a unique perspective into the thermal state of the upper crust at the time. Often, petroleum formation takes place in geologically quiet circumstances, driven by the gradual accumulation of sediments causing burial of older sediments beneath them. Sometimes, however, hydrocarbon generation can be driven by later external processes, such as mountain building or crustal thickening. Previous models had suggested hydrocarbon migration into

the Alberta giant oil sands at ~60 Ma (4). The earlier time of migration suggested by Selby and Creaser is comparable to the age of the rocks that host the oil sand deposits, and appears to rule out younger oil generation associated with a mountain-building event, the Late Cretaceous Laramide Orogeny, at ~60 Ma. Instead, Selby and Creaser argue that source rocks as old as ~200 Ma could have provided hydrocarbons that migrated and accumulated at 112 ± 5.3 Ma.

The Selby and Creaser study represents an innovative application of a radiogenic isotopic technique, one that is generally applied to so-called “hard rock” geology (5), to a longstanding issue of great importance for the petroleum industry. A host of other questions have long awaited answers. How important is mountain building in driving hydrocarbon generation? Can mul-

multiple source rocks contribute to a single hydrocarbon accumulation, but at different times? What is the minimum amount of time that must elapse between deposition of sediment and the generation of hydrocarbons—in other words, how long does it take to produce oil from buried plants and animals? With the Re-Os geochronometer, Earth scientists are at last in a position to provide answers.

References

1. D. Selby, R. A. Creaser, *Science* **308**, 1293 (2005).
2. B. K. Esser, K. K. Turekian, *Geochim. Cosmochim. Acta* **57**, 3093 (1993).
3. P. W. Brooks, M. G. Fowler, R. W. Macqueen, *Org. Geochem.* **12**, 519 (1988).
4. S. Creany, J. Allan, *Am. Assoc. Petrol. Geol. Mem.* **55**, 279 (1992).
5. S. B. Shirey, R. J. Walker, *Annu. Rev. Earth Planet. Sci.* **26**, 423 (1998).

10.1126/science.1113158

MATERIALS SCIENCE

Designing Superhard Materials

Richard B. Kaner, John J. Gilman, Sarah H. Tolbert

Ultrahard materials are used in many applications, from cutting and polishing tools to wear-resistant coatings. Diamond remains the hardest known material, despite years of synthetic (1, 2) and theoretical (3) efforts to improve upon it. However, even diamond has limitations. It is not effective for cutting ferrous metals, including steel, because of a chemical reaction that produces iron carbide. Cubic boron nitride—the second-hardest material, with a structure analogous to that of diamond—can be used to cut ferrous metals. However, it does not occur naturally and must be synthesized under conditions of extreme pressure and temperature, making it quite expensive. New superhard materials are thus not only of great scientific interest, but also could be very useful.

To design new superhard materials, we must understand what makes diamond special. In diamond, tetrahedrally bonded sp^3 carbon atoms form a three-dimensional, covalent network of high symmetry. Other carbon-based materials have shorter and stronger carbon bonds, but not in three dimensions. For

example, the trigonal sp^2 bonds in graphite form sheets with shorter and stronger carbon-carbon bonds. But only weak van der Waals interactions hold the sheets together, allowing layers of graphite to cleave readily. A three-dimensional network composed of short, strong bonds is thus critical for hardness.

In thinking about new ultrahard materials, it is useful to consider the types of structural changes that a material can undergo under load. These changes can be divided into elastic (reversible) and plastic (irreversible) deformations.

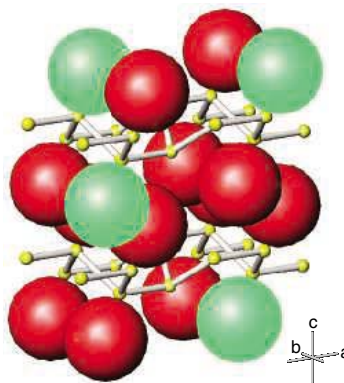
A material is considered stiff if it is difficult to compress elastically. Such a material has a large bulk modulus (it is resistant to volume compression) and/or Young's modulus (it is resistant to linear compression).

Elastic deformation in a direction different from that of the applied load results in shape rather than volume changes; these motions are measured by the shear modulus. In all elastic distortions, the basic relations between atoms do not change.

A material is considered hard if it resists plastic deformation. In contrast to elastic deformation, plastic deformation usually

involves irreversible motion of the atoms with respect to each other, often via the creation and movement of dislocations.

It is a source of substantial confusion that high modulus and high hardness are often discussed together, even though the underlying deformations are fundamentally different. This grouping occurs because the processes can be correlated: If a material shows large elastic changes under small load (low modulus), it tends to respond to larger loads by deforming plastically (low hardness). This is particularly true for shear motions, which are required to scratch or indent a material; a good correlation has been found between shear modulus and hardness (1–3). Highly directional bonding is needed to withstand both elastic and plastic deformations. Purely covalent bonding (such as in diamond) is best,



Toward superhard materials. By combining metals with a high density of valence electrons, such as osmium, iridium, or rhenium, with small, covalent bond-forming atoms such as boron, ultra-incompressible, hard materials may be created. Mixed metals, as shown in this orthorhombic structure predicted for $(Os, Ir)_B_2$, can act as barriers to the movement of dislocations. Osmium is shown in red, iridium in green, and boron in yellow.

and some ionic character is acceptable. However, highly ionic or metallic bonding is the same in all directions and therefore poor at resisting either plastic or elastic shape deformations.

With these ideas in mind, efforts to design superhard materials can be divided into two main approaches. In the first, light elements, including boron, carbon, nitro-

R. B. Kaner is in the Department of Chemistry and Biochemistry and Department of Materials Science and Engineering, University of California, Los Angeles, CA 90095, USA. E-mail: kaner@chem.ucla.edu J. J. Gilman is in the Department of Materials Science and Engineering, University of California, Los Angeles, CA 90095, USA. E-mail: gilman@seas.ucla.edu S. H. Tolbert is in the Department of Chemistry and Biochemistry, University of California, Los Angeles, CA 90095, USA. E-mail: tolbert@chem.ucla.edu

gen, and/or oxygen, are combined to form short covalent bonds. In the second, elements with very high densities of valence electrons are included to ensure that the materials resist being squeezed together.

The first approach gained favor in the late 1980s, when calculations suggested that the hypothetical compound C_3N_4 may be even less compressible than diamond (4). However, after years of experiments, further calculations indicated that even for the least compressible C_3N_4 structure, the shear modulus would only be 60% of the diamond value (5). New forms of carbon, including fullerenes and nanotubes, generated great excitement in the 1990s, when high-pressure processing produced very hard substances (1). However, these substances, which fall under the rubric of diamondlike coatings, can approach but never reach the hardness of diamond (6); furthermore, squeezing fullerenes and nanotubes is unlikely to be an inexpensive, practical synthetic route to diamondlike carbon. Three-dimensional boron-rich compounds, including B_4C , B_6O , their solid solutions, and B/C/N phases, are very hard materials that deserve continued study. However, this approach is unlikely to produce materials with hardnesses exceeding those of boron nitride/diamond solid solutions, which are intermediate in hardness between diamond and cubic boron nitride (1, 2, 7).

In the second approach, transition metals that have a high bulk modulus but low hardness are combined with small, covalent bond-forming atoms such as boron, carbon, nitrogen, and/or oxygen. In this way, a material that can maintain both volume and shape can be created. This idea has led to highly incompressible phases such as RuO_2 (8), WC, and Co_6W_6C (9). Unfortunately, these materials do not even approach the hardness of cubic boron nitride, owing to the partially ionic character of the Ru-O bond and the metallic nature of the W-W and Co-W interactions (3). Borides may be a better choice to achieve the required covalent bonding. Transition metal borides such as the tungsten borides WB_4 , WB_2 , and WB are promising (1, 2). Elements with a higher density of valence electrons (and thus high bulk modulus) such as rhenium, osmium, and iridium also have the potential to form very hard borides (10); mixed-metal borides could be even harder (see the figure).

Once the best combination of elements is found, hardness could be increased by controlling the underlying nanostructure. For example, if the motion of dislocations in a material is hindered, hardness can be increased. This phenomenon is well known to occur in an ultrafine-grained diamond called carbonado (11). More recently, nanoceramics with a grain size of ~ 10 nm have exhibited the same phenomenon (12). Superlattices of TiN/AlN or carbon nitride/TiN with a perio-

dicity of 6 to 8 nm also exhibit hardnesses two to three times as great as that of the bulk crystalline form of these materials (13, 14). In all these materials, the interfaces between the nanometer-scale components act as barriers to the movement of dislocations.

Despite all the research activity into synthesizing superhard materials, many opportunities remain unexplored. For example, the lightest element that could produce three-dimensional structures, beryllium, has been neglected, perhaps because it is toxic and may require specialized high-pressure equipment. Ternary phases of beryllium with other light elements—boron, carbon, nitrogen, and oxygen—could have exciting properties in their own right or in combination with high-valence electron density metals.

Despite their potential, new materials are unlikely to replace diamond altogether, because in addition to its hardness, diamond possesses many other amazing properties. It is the most incompressible material, has one of the highest indices of refraction, and has a room-temperature thermal conductivity five times as large as that of the best metals. The scientific challenge of finding a superhard

material that surpasses diamond in any of these properties will keep the field energized for years to come. Combining high hardness with other properties, such as chemical inertness and low-cost synthesis, could quickly yield practical benefits, for example, by providing a replacement for cubic boron nitride for cutting and polishing steel.

References

1. V. V. Brazhkin, A. G. Lyapin, R. J. Hemley, *Philos. Mag. A* **82**, 231 (2002).
2. J. Haines, J. M. Léger, G. Bocquillon, *Annu. Rev. Mater. Res.* **31**, 1 (2001).
3. D. M. Teter, *Mater. Res. Soc. Bull.* **23**, 22 (January 1998).
4. A. L. Liu, M. L. Cohen, *Science* **245**, 841 (1989).
5. D. M. Teter, R. J. Hemley, *Science* **271**, 53 (1996).
6. M. Weiler *et al.*, *Phys. Rev. B* **53**, 1594 (1996).
7. T. Sasaki *et al.*, *Chem. Mater.* **5**, 695 (1993).
8. J. Haines, J. M. Léger, *Phys. Rev. B* **48**, 13344 (1993).
9. N. A. Dubrovinskaia *et al.*, *J. Alloys Compd.* **285**, 242 (1999).
10. R. W. Cumberland *et al.*, *J. Am. Chem. Soc.* **127**, 7264 (2005).
11. Y. L. Orlov, *The Mineralogy of the Diamond* (Wiley, New York, 1977).
12. S. Yip, *Nature* **391**, 532 (1998).
13. D. Li, X. Chu, S.-C. Cheng, X.-W. Li, V. P. Dravid, *Appl. Phys. Lett.* **67**, 203 (1995).
14. S. Barnett, A. Madan, *Phys. World* **11**, 45 (1998).

10.1126/science.1109830

BIOMEDICINE

Hamiltonian Medicine: Why the Social Lives of Pathogens Matter

Kevin R. Foster*

Brushing your teeth is an experiment in social evolution. Brushing mixes bacteria that were previously surrounded by their clonemates with unrelated bacteria from another part of your mouth. This mixing reduces the relatedness among adjacent bacteria, which can in turn affect their behavior and, ultimately, whether they harm you. This argument is at the center of recent work suggesting that the social behavior of pathogens may be important in understanding disease virulence and antibiotic resistance.

Only some pathogens are dangerous. Understanding what causes virulent pathogens to emerge is a priority for both biologists and physicians (1). A key factor affecting the evolution of virulence is the number of different pathogen strains that infect a host (2–4). It was first thought that the

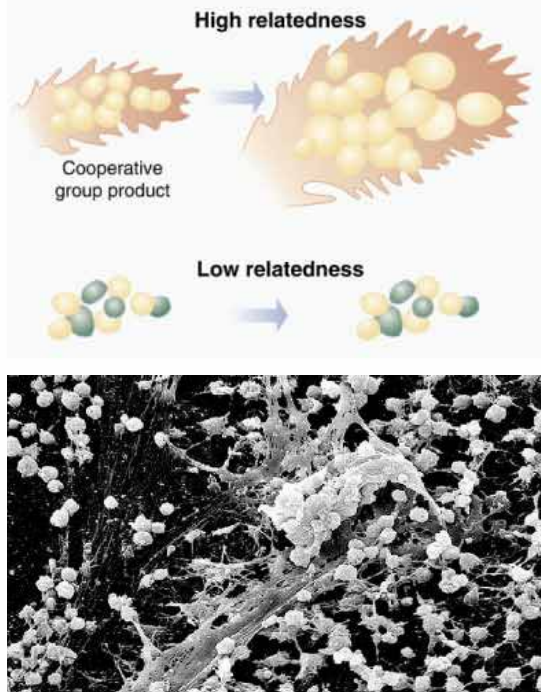
more strains there are in the host, the more virulent they should become. Frank (2) modeled the effect of multiple strains using Hamilton's kin selection theory (5). Originally developed to explain animal social behavior, kin selection theory revolutionized thinking by showing that related individuals cooperate with one another because of their shared genes (5). This approach can be applied to disease because multiple infections reduce relatedness among pathogens; kin selection then predicts that multiple infections should also decrease cooperation. The pathogens in Frank's model were not cooperating in a truly social sense but simply were solving the problem of how quickly to divide and reproduce. Frank predicted that low relatedness would make strains divide rapidly in competition, which would harm the host and increase virulence (2). Despite the elegant theory, many pathogens refused to cooperate with predictions. Studies on viral, bacterial, and plasmodial diseases found that mixed infection often favors the less virulent strain, showing that, contrary to Frank's theory, reduced relatedness often reduces virulence (3, 4, 6).

The author is in the Department of Ecology and Evolutionary Biology, Rice University MS 170, 6100 Main Street, Houston, TX 77005, USA. E-mail: krfoster@rice.edu

*Present address: Wissenschaftskolleg zu Berlin, Institute for Advanced Study, Wallotstrasse 19, 14193, Berlin, Germany.

This failure to cooperate with the theory is now being explained by the ability of related pathogens to cooperate with each other and to make use of shared products in their battle to overcome a host (see the figure) (4). For example, many bacteria collectively release feeding enzymes to break down host tissues, and the protein coats that protect viruses are shared, after manufacture, among all viruses in a cell. Shared products require cooperation because they can be exploited by selfish individuals who could use the product of others without making it themselves. Incorporating such products into Frank's model reverses the predictions: Lowered relatedness is now predicted to decrease virulence because it reduces the total amount of the virulence causing products (see the figure) (4). Griffin *et al.* (6) recently used the pathogenic bacterium *Pseudomonas aeruginosa* to test this hypothesis. *P. aeruginosa* infects almost any injured human tissue and is a problem in diseases such as cystic fibrosis, pneumonia, and meningitis. As is true for many pathogenic bacteria, growth of *P. aeruginosa* in vivo is limited by iron uptake because hosts actively withhold iron in order to combat infection. As a result, bacterial growth (and hence virulence) is linked to the cooperative release of iron-binding agents known as siderophores, which scavenge iron and increase bacterial growth. In a wonderful verification of the theory, bacteria living with other highly related bacteria evolved to produce more siderophores than bacteria living with unrelated individuals (6).

Bacterial cooperation can also increase virulence by reducing infighting (7, 8). Many bacteria kill nonclonemates with toxins known as bacteriocins, which reduce virulence by decreasing bacterial density. Interestingly, kin selection theory indicates that such chemical warfare is most likely to occur when the bacterial population has an intermediate level of relatedness (7). At high relatedness, there are too few nonclonemates to make the production of bacteriocins worthwhile; at low relatedness, each clone is too rare to significantly affect the other bacteria. Highest virulence, therefore, is predicted at either very high or very low levels of relatedness, owing to the low levels of bacteriocins. Massey *et al.* (8) simulated intermediate relatedness among bacteria by inoculating caterpillars with two species of bacteria that are known to harm each other with bacteriocins. As predicted, less harm came to



The benefits of living among relatives. (Upper panel) Highly related groups of pathogens (top) are better than low relatedness groups (bottom) at making shared group products—such as feeding enzymes, iron-scavenging siderophores, and protective slime. These facilitate growth and virulence or antibiotic resistance of the whole population. Dark and light ovals, two unrelated strains of bacteria. **(Lower panel)** Scanning electron micrograph of a *Staphylococcus* biofilm on medical equipment. The round objects are cells; a large amount of secreted slime is visible in the middle of the image. [Image: J. Carr, Centers for Disease Control and Prevention]

the caterpillars bearing mixed infections than to those with clonal infections. For this range of relatedness, therefore, the conclusions are the same as for the siderophore system: Lowering relatedness reduces virulence (8).

The concept of cooperation among pathogens is also emerging in studies of biofilms and antibiotic resistance. The idea that microbes spend their lives haplessly floating around has been superseded by the realization that they often live in highly organized biofilm communities attached to surfaces (see the figure) (9–11). Biofilms are involved in more than 60% of bacterial infections treated in the developed world and can contaminate almost any biological or industrial surface (9). The success of a biofilm depends on the production of slimy protective chemicals, a mix of polysaccharides, proteins, and nucleic acids. This collectively produced goop helps bacteria to adhere to surfaces, provides structural support, and can confer considerable protection from antibiotics (9,10). Slime production, therefore, is key to understanding the ecological success of biofilms. A recent simulation showed that biofilm formation was critically dependent

on high relatedness among the bacteria because slime, like siderophores, is a cooperative product (10). High relatedness also allows bacteria in biofilms to attain an optimal growth rate (10,11). With low relatedness, selfish competition is predicted to cause rapid and wasteful reproduction, which reduces the ultimate size and success of the biofilm (11). High relatedness may be common in biofilms if slime production reduces cell motility and thereby limits clonal mixing. Another interesting possibility is that low cell motility may itself evolve in order to raise relatedness and enable cooperation (11).

The recognition that pathogens can cooperate against us may greatly improve our understanding of disease. Nevertheless, many open questions remain. An important next step is to establish just how related pathogens usually are. Infections with multiple strains certainly occur, but particularly in biofilms there may still be high relatedness locally (9–11).

Is it typical for highly related pathogens to be more harmful? To date, high virulence has been associated with both low and high levels of relatedness (3) and, empirically, we know little about the relationship between relatedness and antibiotic resistance. Another question is whether, beyond the targeted killing by bacteriocins, pathogens can detect and respond to kinship in the short term. Finally, it is important to look at pathogen cooperation among species, because pathogens can exist in species-rich communities (10).

To recognize the growing significance of these ideas, we might view them as a distinct subset of Darwinian medicine (12) known as “Hamiltonian medicine” to reflect W. D. Hamilton’s seminal contribution to social evolution (5). The implications are clear: Medical strategies that alter relatedness among pathogens can affect both virulence and antibiotic resistance. When next brushing your teeth, consider that you may be suppressing plaque by making your bacteria fight each other instead of you.

References

1. P. W. Ewald, *Evolution of Infectious Disease* (Oxford Univ. Press, New York, 1994).
2. S. A. Frank, *Q. Rev. Biol.* **71**, 37 (1996).
3. A. F. Read, L. H. Taylor, *Science* **292**, 1099 (2001).
4. S. P. Brown, M. E. Hochberg, B. T. Grenfell, *Trends Microbiol.* **10**, 401 (2002).
5. W. D. Hamilton, *J. Theor. Biol.* **7**, 1 (1964).
6. A. S. Griffin, S. A. West, A. Buckling, *Nature* **430**, 1024 (2004).
7. A. Gardner, S. A. West, A. Buckling, *Proc. R. Soc. London B* **271**, 1529 (2004).
8. R. C. Massey, A. Buckling, R. French-Constant, *Proc. R. Soc. London B* **271**, 785 (2004).
9. C. A. Fux, J. W. Costerton, P. S. Stewart, P. Stoodley, *Trends Microbiol.* **13**, 34 (2005).
10. J. Krefl, *Microbiology* **150**, 2751 (2004).
11. J. Krefl, S. Bonhoeffer, *Microbiology* **151**, 637 (2005).
12. G. C. Williams, R. M. Nesse, *Q. Rev. Biol.* **66**, 1 (1991).

ADVANCED TRAINING COURSE IN BIOMEDICAL RESEARCH

Genomic and Post-genomic Approaches to Study Virus-Host Cell Interactions

October 5–21, 2005, Cuernavaca, Morelos, Mexico

Instituto de Biotecnologia/UNAM

Applications are invited for this HHMI-sponsored international course for graduate students, postdoctoral fellows, and junior faculty.

The aim of this hands-on course is to recognize and understand the complexity of the interactions that occur between a virus and its host cell and to review modern global approaches—including transcriptomics, proteomics, and RNA interference—for studying these interactions.

Application deadline: July 8, 2005

More information:

www.hhmi.org/grants/courses

HHMI

HOWARD HUGHES MEDICAL INSTITUTE

International Program

Looking for a JOB?

- Job Postings
- Job Alerts
- Resume/CV Database
- Career Advice
- Career Forum — **NEW**

ScienceCareers.org

We know science



IAS 2005

3rd IAS Conference on HIV Pathogenesis and Treatment Rio de Janeiro

24–27 July 2005

Standard
Registration Fee
Deadline
10 June

Late Breakers
Abstract
Submission
25 May–15 June

Letter of Invitation Request Deadline: 10 July

Special Registration Rate
for Delegates from
Non-OECD Countries!

Bringing Together the World of HIV Science to Address the Challenges of Research, Prevention and Treatment



To read more about the
Conference programme and to
register on-line, visit

www.ias-2005.org



Scientists and Health Care Workers
Committed to HIV/AIDS

Co-Sponsors



Sociedade Brasileira de
Infecç es, SBI



Universidade Federal do
Rio de Janeiro, UFRJ



SCIENCE AND POLICY

Deep Concerns Aired at AAAS's 30th S&T Policy Forum

When U.S. Representative Rush Holt took the stage at the AAAS Forum on Science and Technology Policy, he offered a critical view of the state of the union between science and policy-makers: The federal government is underinvesting in "almost every sector" of S&T research. Energy policy remains focused on oil, despite high prices and the impact of global warming. Young students enter school open to the excitement of science, he said, but "we beat it out of them over the years."

Holt's view was sobering, but it captured the prevailing mood among scientists and science policy experts during the 2-day gathering in Washington, D.C. Despite the broad contributions of science to American well-being, many speakers said, it is finding diminished support from policy-makers and from much of the public on issues ranging from climate change to development of the S&T workforce.

The AAAS Forum on Science and Technology Policy annually features some of the nation's most influential policy-makers and experts. More than 550 people attended the 30th annual Forum, held 21 to 22 April.

This year, no issue attracted more scrutiny than the federal budget.

John H. Marburger III, the White House science adviser, opened the Forum with a firm defense of President George W. Bush's record. The administration has proposed \$132.3 billion for R&D spending in fiscal 2006, up 45% from 2001. That "very clearly shows a strong commitment to science and technology," Marburger concluded.

But Kei Koizumi, director of the AAAS R&D Budget and Policy Program, said the 2006 plan would raise R&D spending only 0.1% over 2005; while many agencies will see their budgets cut, most will lose ground to inflation.

Paul Posner, managing director of federal budget issues for the U.S. Government Accountability Office, said budget deficits, outstanding debt, and other liabilities total \$150,000 for every U.S. resident. Without reforms in Social Security and health care or major increases in federal revenues, Posner said, federal deficits and debt will grow to levels unsustainable for the U.S. economy.

Under one scenario where the administration's tax cuts are made permanent and discretionary spending grows with the economy, the deficit by 2040 would be so severe that the government would have only enough



White House science adviser John H. Marburger III offered a firm defense of federal research and development spending.

income to cover interest payments—but nothing for ongoing government programs.

Other speakers saw the conflicts over embryonic stem cell research and teaching evolution in public schools as evidence of stress between science and society.

John Gearhart, a professor in the School of Medicine at Johns Hopkins University, has been a pioneer in embryonic stem cell research. Though his work someday might help tens of millions of people suffering from chronic disease and severe injury, he described in a subdued voice how he has been jostled, shoved, subjected to demonstrations, and called a Nazi. In one visit to Capitol Hill, Gearhart recalled, he was asked how it "felt to kill the littlest Americans."

Robert Klein, the guiding force behind the victorious California initiative to invest \$3 billion in stem cell research, was pointedly critical of one new bill in Congress, saying it would subject parents who seek embryonic stem cell therapies for their children to arrest and imprisonment.

Eugenie Scott, executive director of the National Center for Science Education, dissected the arguments of anti-evolution

leaders, detailing their misconceptions. She recounted the experience of a physical anthropologist she knows who taught evolution to a group of religious students in a community college in the South. Several of the students approached their teacher after a few weeks of class and readily acknowledged that species change over time. "You mean that's what evolution is?" they asked. "We thought evolution meant you can't believe in God."

Scott and others urged respectful relations with opponents and a willingness to listen. Gearhart said he has visited churches, temples, and social clubs to talk about embryonic stem cell research. Likewise, physicist and author Lawrence Krauss of Case Western Reserve University in Ohio said he has discussed evolution during visits to churches and religious schools.

"I am not under the illusion that I will ever be able to convince ardent opponents of evolution," Krauss said after the forum. "I am more

interested in the vast middle—those people who haven't thought about the issue and are willing to listen openly, or to young people who have been propagandized, but who can learn from being exposed to honest and respectful assessments of reality."

EDUCATION

NSF/AAAS Report Hails Inquiry-Based Learning

The engineering program at Itasca Community College doesn't generate the national buzz of MIT or Caltech; even in Minnesota and the Dakotas, it's probably not as well known as bigger state schools. But for Tom Calgaro, the decision to attend Itasca a few years ago was a crucial step in his early development.

Itasca has successfully followed a model of "inquiry-based learning," one of the programs cited in a new AAAS-National Science Foundation report on the most innovative new approaches to teaching science, engineering, and related fields. For Calgaro, inquiry-based learning is no

AAAS NEWS AND NOTES

mere pedagogical fashion—it was an immersion in learning that prepared him for a career in avionics, and for life, too.

Members of the Itasca engineering faculty “have a passion for their work, and they pass it along to their students,” said Calgaro, who spent 2 years at the school in Grand Rapids, on the western edge of Minnesota’s Iron Range. “They foster a team atmosphere by creating an environment and teaching style called a ‘learning community,’ in which students become part of a group, with ties similar to those of family.”

The new AAAS/NSF report is called “Invention and Impact: Building Excellence in Undergraduate Science, Technology, Engineering and Mathematics (STEM) Education.” It explores what schools can do to draw from the broadest and most diverse student body and to educate them in a way that imparts not just skills, but the deeper understanding, passion, and commitment that will help them thrive.

Itasca is a “wonderful example” of how schools are working to retain students in STEM fields, said Rosemary R. Haggett, director of the NSF’s Division of Undergraduate Education within the Directorate for Education and Human Resources. “With U.S. enrollments in these fields declining, it’s more important than ever to keep every student engaged in learning.”

According to Ronald Ulseth, director of the Itasca engineering program, learning communities are especially effective at educating women in the field. Overall, Ulseth said, more than 90% of all graduates go on to obtain their bachelor’s degrees in engineering.

As detailed in the new report, inquiry-based learning takes various forms, including “peer-led team teaching,” which makes even large classes seem intimate as student-leaders direct workshops, creative faculty-development methods, case study-based learning, and virtual laboratories.

The report “is the first truly comprehensive volume on what’s happening in terms of undergraduate educational reform efforts across all the STEM fields,” said co-author Yolanda George, deputy director of Education and Human Resources at AAAS.

“Invention and Impact” is based on an April 2004 conference at which some 400 participants exchanged data and experience about new teaching methods resulting from NSF’s Course, Curriculum, and Laboratory Improvement (CCLI) program. The program, established 5 years ago, has supported 1750 innovative teaching projects at 600 institutions, involving 1.4 million students and 25,000 faculty members.

Calgaro is a strong proponent. This month, he graduated with honors from North Dakota State University, earning a degree in electrical engineering. He already has logged substantial work experience in aviation engineering, and he has his pilot’s license. He’s accepted a post as a systems engineer at the aviation electronics firm Rockwell Collins in Cedar Rapids, Iowa. “This is about as close to my dream job as I could have imagined,” he said.

The new report is online at www.aaas.org/publications/books_reports/CCLI/. A limited supply of print copies are available for \$19.95 by e-mailing ehr@aaas.org.

—GINGER PINHOLSTER CONTRIBUTED TO THIS REPORT

SCIENCE AND SOCIETY

Science, Religion Intersect at Neuroethics Forum

The idea of using technology to boost brain performance makes Christian moral theologian Brent Waters a little wary. The goal of technology is to improve the quality of human lives, and “better brains don’t necessarily mean better people,” he said at “Our Brains and Us: Neuroethics, Responsibility and the Self,” a recent conference cosponsored by AAAS and held at MIT.

“Better brains don’t necessarily mean worse people either,” countered brain researcher Paul Gold of the University of Illinois at Urbana-Champaign.

Ultimately, Gold and Waters, a professor at Garrett-Evangelical Theological Seminary, agreed on many points, such as the idea that it is how performance-enhancing brain technologies are used—rather than the technologies themselves—that is good or bad. Throughout the conference, speakers from the scientific, ethics, and religious communities often shared common ground, but some differences did emerge.

“Neuroscientists have an obsession with pushing the forefront of knowledge, while religious practitioners have a deep commitment to understanding the nature of the self in the context of how to improve the human condition. So, both perspectives have important forward-looking points and drawbacks,” said MIT neuroscientist Christopher Moore.

“The multidisciplinary and multireligious engagement of the participants at the intersection of science, ethics, and religion was a model for the kind of civil discourse needed as we make decisions that will shape the human future,” said Jim Miller, senior program associate for AAAS’s Dialogue on Science, Ethics, and Religion.

COMMUNICATION

Two Selected for New Minority Internship

AAAS and Science have named two California students as the first recipients of the new Minority Science Writers Internship for undergraduates pursuing science journalism careers.

Genevra Ann Ornelas of California State University-Fresno and Cathy Tran of the University of California-Santa Barbara, both graduating seniors, will begin their 10-week internships in June at the Washington, D.C., headquarters of *Science*. Tran majored in biopsychology, Ornelas in biology.

They will help reporters gather information for news stories, attend hearings and briefings, and work on their own stories for *Science* or *Science Now*, the journal’s daily online news service.

A common question raised by speakers from the religious communities was how neuroscience might affect people’s conceptions of the soul and the spirit, since, as Dr. Roger Pitman of Harvard Medical School said, most neuroscientists believe that “everything that happens in the mind happens in the brain.”

The theologians, ethicists, and neuroscientists returned often to common questions. Will humans try to perfect themselves through neuroscience-based enhancements? How does a society draw the line between enhancement and therapy? How can society guard against the risk that new technologies could widen disparities among socioeconomic groups?

Much of the research that is provoking these questions is still in the early stages. The speakers discussed studies showing that certain chemicals can enhance memory and that we can influence each other’s memories as well as our own experience of pain.

Others described the potential for using brain scanning in everything from criminal trials to soda marketing research. Researchers are also making progress with prosthetic devices controlled by the brain and in understanding how a specialized set of “mirror neurons” in the brain may form at least a partial basis for empathy.

The conference took place 17 to 19 April in Cambridge, Massachusetts, and was cosponsored by AAAS’s Dialogue on Science, Ethics, and Religion; MIT’s Department of Brain and Cognitive Sciences; the Technology and Culture Forum at MIT; and the Boston Theological Institute.—KATHY WREN

Solid-State Light Sources Getting Smart

E. Fred Schubert and Jong Kyu Kim

More than a century after the introduction of incandescent lighting and half a century after the introduction of fluorescent lighting, solid-state light sources are revolutionizing an increasing number of applications. Whereas the efficiency of conventional incandescent and fluorescent lights is limited by fundamental factors that cannot be overcome, the efficiency of solid-state sources is limited only by human creativity and imagination. The high efficiency of solid-state sources already provides energy savings and environmental benefits in a number of applications. However, solid-state sources also offer controllability of their spectral power distribution, spatial distribution, color temperature, temporal modulation, and polarization properties. Such "smart" light sources can adjust to specific environments and requirements, a property that could result in tremendous benefits in lighting, automobiles, transportation, communication, imaging, agriculture, and medicine.

The history of lighting has taken several rapid and often unexpected turns (1). The first commercial technology for lighting was based on natural gas that served thousands of streets, offices, and homes at the end of the 19th century.

As a result of the competition from Edison's incandescent lamp, gaslights were strongly improved by the use of mantles soaked with the rare-earth compound thorium oxide, which converted the gas flame's heat energy and ultraviolet (UV) radiation into visible radiation. Ultimately, however, the gaslights shown in Fig. 1 were displaced by incandescent light bulbs first demonstrated in 1879. Fluorescent tubes and compact fluorescent lamps became widely available in the 1950s and early 1990s, respectively. Along with high-intensity discharge lamps, they offer a longer life and lower power consumption than incandescent sources, and have become the mainstream lighting technology in homes, offices, and public places.

The efficiency of fluorescent lamps based on mercury vapor sources is limited to about 90 lm/W by a fundamental factor: the loss of

energy incurred when converting a 250-nm UV photon to a photon of the visible spectrum. The efficiency of incandescent lamps is limited to about 17 lm/W by the filament tem-

perature that has a maximum of about 3000 K, which results, as predicted by blackbody radiation theory, in the utter dominance of invisible infrared emission. In contrast, the present efficiency of solid-state light sources is not limited by fundamental factors but rather by the imagination and creativity of engineers and scientists who, in a worldwide concerted effort, are longing to create the most efficient light source possible.

Several promising strategies to create white light with the use of inorganic sources, organic sources, and phosphors are shown in Fig. 2,

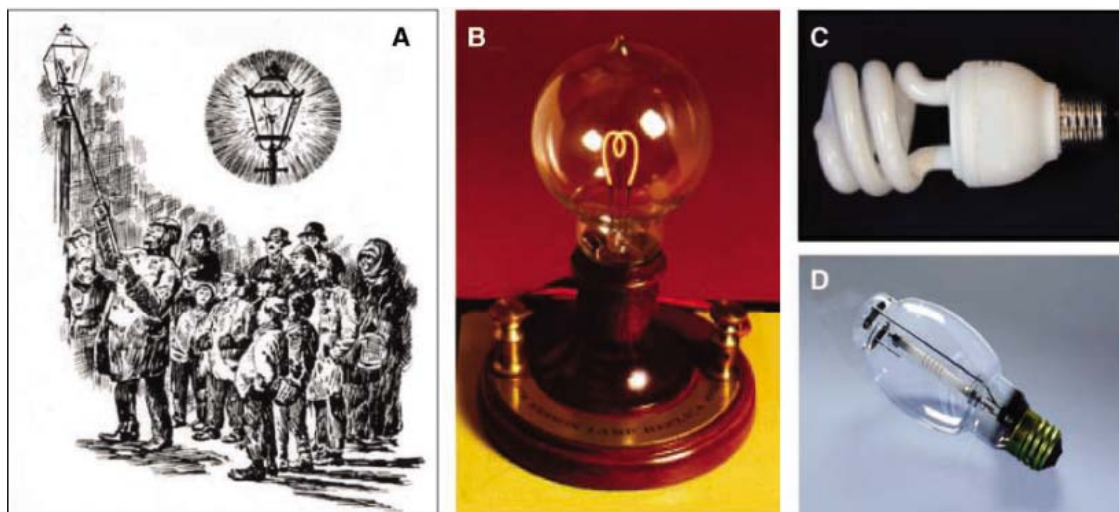


Fig. 1. (A) 1880s illustration of the nightly illumination of a gaslight with a thorium oxide-soaked mantle. (B) Replica of Edison's lamp. (C) Contemporary compact fluorescent lamp. (D) High-pressure sodium lamp.

perature that has a maximum of about 3000 K, which results, as predicted by blackbody radiation theory, in the utter dominance of invisible infrared emission. In contrast, the present efficiency of solid-state light sources is not limited by fundamental factors but rather by the imagination and creativity of engineers and scientists who, in a worldwide concerted effort, are longing to create the most efficient light source possible.

Bergh *et al.* (2) discussed the huge potential benefits of solid-state light sources, in particular reduced energy consumption, dependence on foreign oil, emission of greenhouse

gases (CO₂), emission of acid rain-causing SO₂, and mercury pollution. Solid-state lighting could cut the electricity used for lighting, currently at 22%, in half. Although tremendous energy savings have already materialized [e.g., traffic lights that use light-emitting diodes (LEDs) consume only one-tenth the power of incandescent ones], there is a sobering possibility that energy savings may be offset by increased energy consumption: More wasteful usage patterns, abundant use of displays, and an increase in accent and artistic lighting may keep the use of electricity for lighting at its current level [11% in private homes, 25% in commercial use, and 22% overall (3)].

Department of Electrical, Computer, and Systems Engineering and Department of Physics, Applied Physics, and Astronomy, Rensselaer Polytechnic Institute, Troy, NY 12180, USA.

poorly render the colors of objects when illuminated by the dichromatic source. Tetrachromatic sources have excellent color rendering capabilities but have a lower luminous efficacy than dichromatic or trichromatic sources. Trichromatic sources can have both good color rendering properties and high luminous efficacies (>300 lm/W).

Figure 2 also shows several phosphor-based white light sources. Such sources use optically active rare-earth atoms embedded in an inorganic matrix. Cesium-doped yttrium-aluminum-garnet (YAG) is a common yellow phosphor. However, phosphor-based white light sources suffer from an unavoidable Stokes energy loss due to the conversion of short-wavelength photons to long-wavelength photons. This energy loss can reduce by 10 to 30% the overall efficiency of systems based on phosphors optically excited by LEDs. Such loss is not incurred by white light sources based exclusively on semiconductor LEDs. Furthermore, phosphor-based sources do not allow for the extensive tunability afforded by LED-based sources, particularly in terms of spectral composition and temporal modulation (YAG phosphorescence radiative lifetime is in the millisecond range).

The luminous efficiency of a light source is a key metric for energy savings considerations. It gives the luminous flux in lumens (light power as perceived by the human eye) per unit of electrical input power. Luminous efficiencies of 425 lm/W and 320 lm/W could potentially be achieved with dichromatic and trichromatic sources, respectively, if solid-state sources with perfect characteristics could be fabricated. Perfect materials and devices would allow us to generate the optical flux of a 60-W incandescent bulb with an electrical input power of 3 W.

Besides luminous efficiency, color rendering is an essential figure of merit for a light source used in illumination applications. It is a very common misconception that the color of an object depends only on the properties of the object. However, as George Palmer first found in 1777, the perceived color of an object equally strongly depends on the illumination source [for Palmer's original paper, see (4)]. Illuminating colored test samples with different light sources, he found that "red appears orange" and, more strikingly, "blue appears

green." Thus, the "true color" of an object requires that we have a certain reference illuminant in mind. Today, a procedure similar to Palmer's is used: The apparent color of a set of sample objects is assessed (quantitatively in terms of chromaticity coordinates, no longer just qualitatively as Palmer did) under illumination by the test light source and then by the reference light source. The color differences of a set of eight standardized color samples are added. The sum, weighted by a prefactor, is then subtracted from 100. This gives the color rendering index (CRI), a key metric for light sources. A high CRI value indicates that a light source will accurately render the colors of an object.

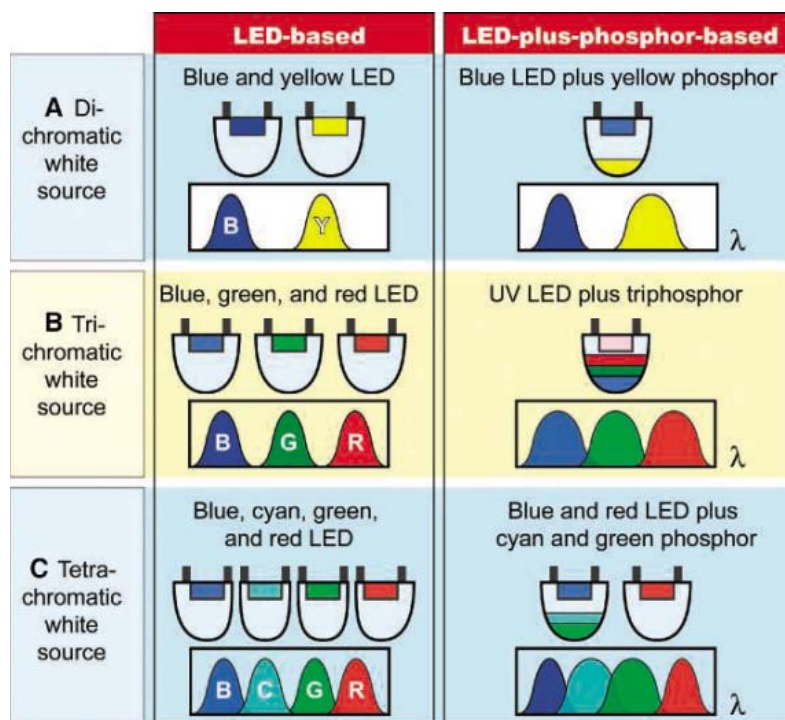


Fig. 2. LED-based and LED-plus-phosphor-based approaches for white light sources implemented as di-, tri-, and tetrachromatic sources. Highest luminous source efficiency and best color rendering are obtained with dichromatic and tetrachromatic approaches, respectively. Trichromatic approaches can provide very good color rendering and luminous source efficiency.

Although trichromatic sources already give very good CRI values, tetrachromatic sources give excellent CRI values suitable for essentially any application. The emission spectrum, luminous efficacy, and color rendering properties of a tetrachromatic white LED-based source with color temperature of 6500 K are shown in Fig. 3. Color temperature may appear to be a somewhat surprising quantity, as color and temperature would not seem to have a direct relationship with each other. However, the relationship is derived from Planck's blackbody radiator; at increasing temperatures it glows in the red, orange, yellowish white, white, and ultimately bluish white. The color temperature is the tempera-

ture of a blackbody radiator that has the same chromaticity as the white light source considered. Figure 3 shows that a favorable wavelength combination is $\lambda = 450, 510, 560,$ and 620 nm, giving a luminous efficacy of 300 lm/W and a CRI of 95. Such a CRI makes tetrachromatic light sources suitable for practically any application.

However, the emission power, peak wavelength, and spectral width of inorganic LEDs vary with temperature, a major difference from conventional lighting sources. LED emission powers decrease exponentially with temperature; low-gap red LEDs are particularly sensitive to ambient temperature. As a result, the chromaticity point, correlated color tempera-

ture, CRI, and efficiency of LED-based light sources drift as the ambient temperature of the device increases. An example of the change in chromaticity point with junction temperature is shown in Fig. 4 for a trichromatic LED-based light source (5); the chromaticity changes by about 0.02 units, thereby exceeding the 0.01-unit limit that is considered the maximum tolerable change by the lighting industry. Furthermore, the CRI changes from 84 to 72. To avoid this change, corrective action must be taken by tuning the relative electrical input powers of the LEDs. Energy-efficient adaptive drive electronics with integrated temperature compensation are already under development. White sources that use phosphor, particularly UV-pumped phosphor sources, have great color stability and do not suffer from the strong change in chromaticity and color rendering. This is because the intra-rare-earth atomic transitions occurring in phosphors do not depend on temperature.

Technological Challenges

What specific advances will be required to move solid-state light sources from their current performance closer to their fundamental limits? What are the "bottlenecks" that will need to be overcome to enable specific types of control for smart lighting systems? The major technical challenges in solid-state lighting can be categorized into three groups:

- Epitaxial and bulk crystal growth; materials including nanomaterials and substrates; phosphors

- Device physics; device design and architecture; low-cost processing and fabrication technologies

- Packaging; integration of components into lamps and luminaires; smart lighting systems

We next discuss several important technical issues involved in meeting these challenges. Additional challenges and a roadmap with specific goals were presented by Tsao (6) and Rohwer and Srivastava (7). Here, we emphasize inorganic materials and devices, which at this time are more advanced in terms of luminance and reliability than organic devices.

Internal efficiency. The development of efficient UV emitters (<390 nm), green emitters (515 to 540 nm), yellow-green emitters (540 to 570 nm), and yellow emitters (570 to 600 nm) is a major challenge. The internal quantum efficiency (photons created per electron injected) of some of these emitters, particularly in the deep UV, can be below

package is complicated because this light tends to be generated near metallic ohmic contacts that have low reflectivity and are partially absorbing. Either totally reflective or totally transparent structures are desirable. This insight has driven the replacement of absorbing GaAs substrates with transparent GaP substrates, and it has also spurred the development of new omnidirectional reflectors with angle-integrated transverse electric–transverse magnetic (TE-TM) averaged mirror losses that are 1% those of metal reflectors. Sophisticated chip shapes and photonic crystal structures are becoming commonplace. Another fruitful strategy is to reduce deterministic optical modes trapped in the chip and the package by introducing indeterministic optical elements such as diffuse reflective and transmissive surfaces.

Chip and lamp power. Although substantial progress has been achieved in LED optical output power, an order of magnitude increase

emission can be accomplished by micromirrors that redirect waveguided modes toward the surface-normal direction of the chip.

The scaling of the current density requires strong confinement of carriers to the active region. Such confinement reduces carrier escape out of the active region and carrier overflow. Changes in device design will be required, including the use of electron and hole blocking layers that prevent carriers from escaping from the active region.

Semiconductors with band gap energies corresponding to the visible spectral range, in particular wide-gap III-V nitrides, exhibit great temperature stability. However, common epoxy encapsulants limit the maximum temperature of operation to about 120°C. Silicone, mostly known as a common household glue, offers mechanical flexibility (reducing stress) and great stability up to temperatures of about 190°C.

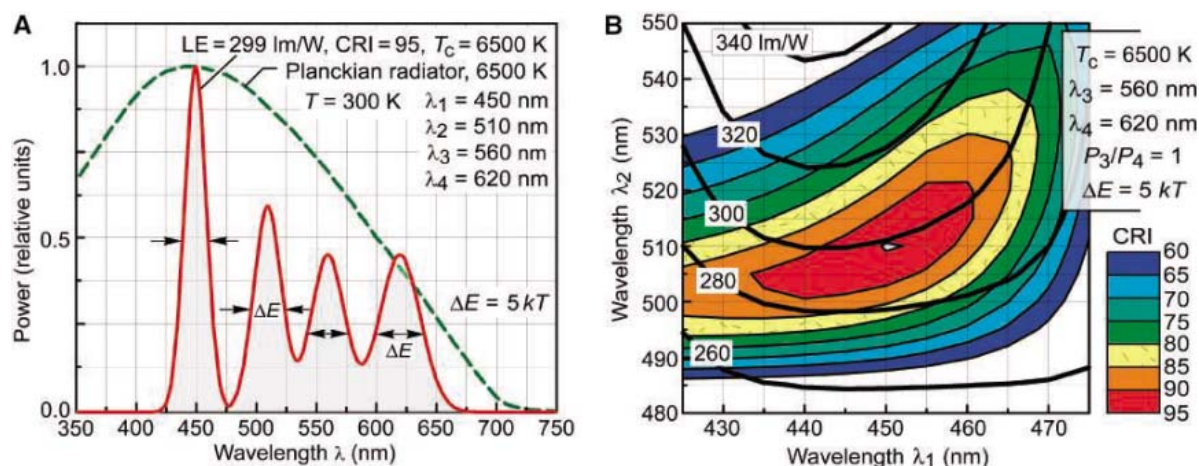


Fig. 3. Spectrum (A) and contour plot (B) showing luminous efficiency of radiation and CRI of tetrachromatic LED-based white light source with peak emission wavelength λ_1 , λ_2 , λ_3 , and λ_4 and a spectral width of $\Delta E = 5 kT$ (~ 125 meV), as is typical for light-emitting active regions consisting of ternary alloy semiconductors. The power ratio is chosen to obtain a chromaticity location on the Planckian locus with a color temperature of 6500 K.

1%. A better understanding of the materials physics—in particular, defects, dislocations, and impurities—will be required to attain efficient emitters in this wavelength range. Novel epitaxial growth approaches, including growth on pseudo-matched substrates and growth on nano-structured substrates (8, 9), will be required to overcome these limitations.

Phosphors. Hundreds of phosphors are available for excitation at 250 nm, the dominant emission band of Hg lamps. In solid-state lighting, however, the excitation wavelength is much longer, typically in the range 380 to 480 nm. New high-efficiency phosphors, which can be efficiently excited at these wavelengths, are now being developed. Whereas high-efficiency yellow phosphors are readily available (e.g., cesium-doped YAG phosphors), the efficiency of red phosphors still lags.

Extraction efficiency. The efficient extraction of light out of the LED chip and the

in power per package is still required. Several strategies are being pursued simultaneously, including (i) scaling up the chip area, (ii) scaling up the current density, and (iii) increasing the maximum allowable operating temperature.

Scaling of the chip area is particularly interesting because it reminds us of the scaling in Si microelectronics technology that for decades has been governed by Moore's law. Whereas feature sizes are shrinking in Si technology, die sizes are growing in solid-state lighting devices. However, the increase in chip area is frequently accompanied by a reduced efficiency (scaling losses) due to absorption losses of waveguided modes propagating sideways within the semiconductor. New scalable geometries and high-reflectivity omnidirectional reflectors are being developed by several research groups. Surface-emitting devices are generally more scalable, as they do not suffer from waveguide losses. Surface

Thermal issues. In conventional packages, LED chips driven at high currents quickly heat up. This is because the thermal resistance of “5-mm packages,” which have been around for decades, is greater than 200 K/W. Active cooling (with a fan or thermoelectric device) is not an option for most applications, as such cooling reduces the power efficiency. Advanced packaging methods use a direct thermal path: a metallic slug that extends from the LED chip through the package to a larger heat sink (such as a printed circuit board) that spreads the heat. Such packages will have thermal resistances < 5 K/W, nearly two orders of magnitude lower than conventional packages.

Polarization control. Polarization control would be useful for a number of applications. For example, a backlighting power saving of up to 50% in liquid crystal display applications would result from the ability to

control polarization. Photonic crystal structures, which can have a photonic gap for only one polarization, offer a unique capability for achieving this goal. Superluminescent structures offer an alternative way to enhance one polarization.

High-luminance/high-radiance devices and control of far field. Flexible optical designs require high-luminance devices with small, very bright surfaces (high luminance and radiance). Such high-radiance point sources can be imaged with greater precision and enable flexible optical designs with precise steering of beams. LEDs emitting through all side surfaces and the top surface are not well suited for point-source applications. New structures that completely lack side emission will need to be developed for such applications;

of electricity to operate the lamp, would appear most relevant, the lamp purchase price, measured in “\$ per lumen,” is the cost that prominently appears on the price tag to the consumer. A high lamp purchase price is a barrier for the broad adoption of solid-state lighting.

Substantial cost reductions are to be expected mostly through scaling of LED chips, lamps, and packages. In silicon technology, scaling of integrated circuits has reduced the cost of a logic gate by more than six orders of magnitude. Similarly, the scaling up of the LED chip size (analogous to geometric scaling in Si integrated circuits) and of the current density (analogous to current-density scaling in Si integrated circuits) will enable substantial cost reductions that, in the years to come, will

human eye, more than 150 years after the discovery of the rod cells and the red-, green-, and blue-sensitive cone cells (10–12). The fifth type of photoreceptor, the ganglion cell, had been believed to be merely a nerve interconnection and transmitter cell. Such cells are now believed to be instrumental in the regulation of the human circadian (wake-sleep) rhythm. Because ganglion cells are most sensitive in the blue spectral range (460 to 500 nm, Fig. 5), they act as a “blue-sky receptor,” that is, as a high-color-temperature receptor. Indeed, during midday periods natural daylight has color temperatures ranging from 6000 K under overcast conditions to as high as 20,000 K under clear blue-sky conditions. However, in the evening hours, the color temperature of the Sun decreases to only 2000 K. This periodic var-

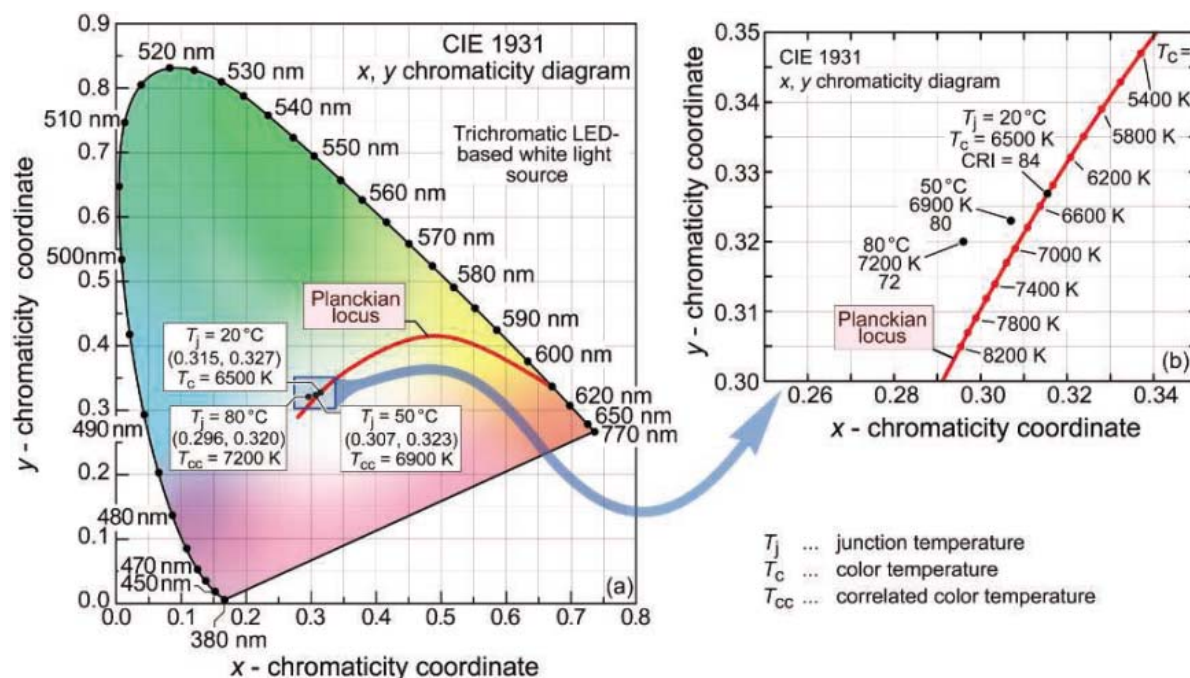


Fig. 4. Change in chromaticity coordinate, correlated color temperature, and CRI of trichromatic LED light source for junction temperatures of $T_j = 20^\circ$, 50° , and 80°C represented in the (x, y) chromaticity diagram.

photonic band gap structures and the use of reflectors will be required. Furthermore, specific arrangements of phosphors will allow for chromatically dispersive emission patterns (i.e., patterns that exhibit a correlation between emission color and direction).

Cost. Although cost is a *conditio sine qua non* from a point of view that focuses on the replacement of conventional sources, it is of lesser importance for smart lighting applications. The benefits of smart lighting add another dimension to the economics of lighting, as these benefits derive from the possibility of temporal, spatial, spectral, and polarization control, a feature that conventional lighting technologies are unable to offer. Whereas the “cost of ownership,” which includes the cost of lamp purchase and cost

bring LEDs into offices, homes, and maybe even the chandeliers of dining rooms.

Smart Lighting

In addition to the energy savings and positive environmental effects promised by solid-state lighting, solid-state sources—in particular, LED-based sources—offer what was inconceivable with conventional sources: controllability of their spectral, spatial, temporal, and polarization properties as well as their color temperature. Technologies currently emerging are expected to enable tremendous benefits in lighting, automobiles, transportation, communication, imaging, agriculture, and medicine.

Recently, a remarkable discovery was made: A fifth type of photoreceptor had first been postulated and then identified in the retina of the

human eye, more than 150 years after the discovery of the rod cells and the red-, green-, and blue-sensitive cone cells (10–12). The fifth type of photoreceptor, the ganglion cell, had been believed to be merely a nerve interconnection and transmitter cell. Such cells are now believed to be instrumental in the regulation of the human circadian (wake-sleep) rhythm. Because ganglion cells are most sensitive in the blue spectral range (460 to 500 nm, Fig. 5), they act as a “blue-sky receptor,” that is, as a high-color-temperature receptor. Indeed, during midday periods natural daylight has color temperatures ranging from 6000 K under overcast conditions to as high as 20,000 K under clear blue-sky conditions. However, in the evening hours, the color temperature of the Sun decreases to only 2000 K. This periodic var-

iation of the color temperature of natural light synchronizes the human circadian rhythm. Figure 5 shows that the circadian and visual efficacies are vastly different (orders of magnitude), particularly in the red spectral range. Inappropriate lighting conditions were shown in mammals to upset the body chemistry and to lead to deleterious health effects, including cancer (13). Thus, circadian light sources with tunability of color temperature would be beneficial to human health, well-being, and productivity. Furthermore, such circadian lights could lead to a reduced dependence on sleep-inducing pharmaceuticals. For this reason, sources replicating the Sun’s high color temperature during the midday period and low color temperatures during early morning and at night would be a wonderful illumination

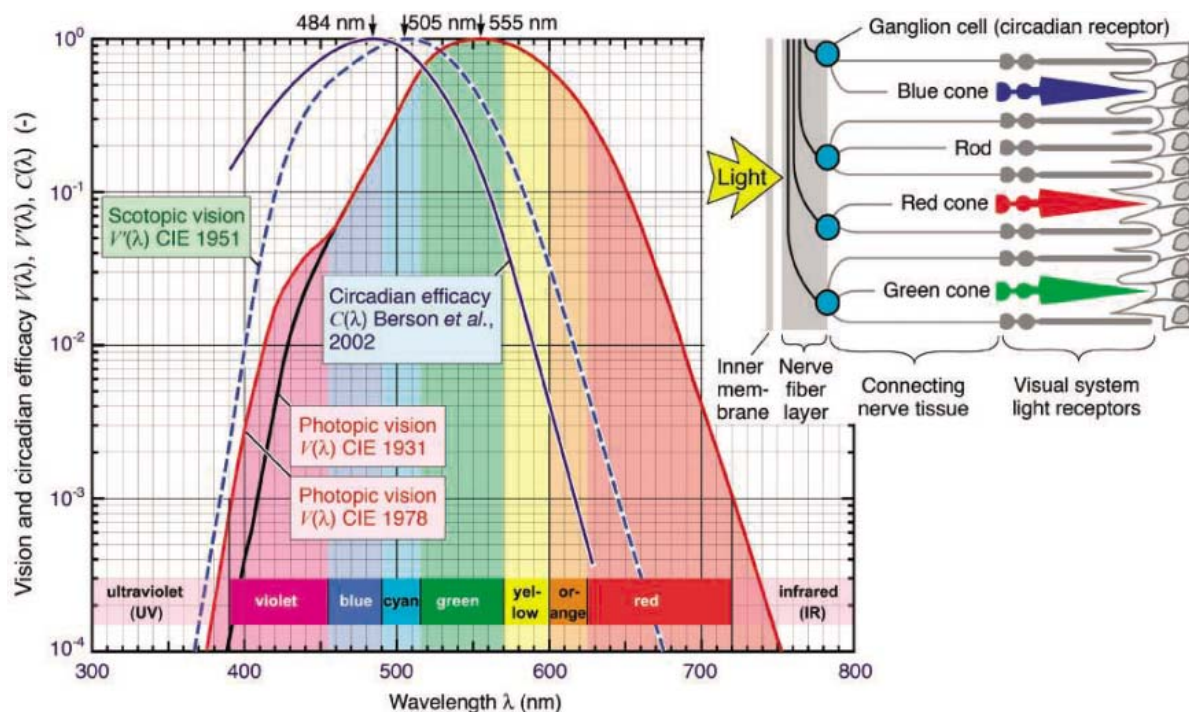


Fig. 5. CIE eye sensitivity function $V(\lambda)$ for the photopic vision regime mediated by retinal cone and rod cells. Also shown is the eye sensitivity function for the scotopic vision regime, $V'(\lambda)$, that applies to low ambient light levels, and the circadian efficacy curve $C(\lambda)$ derived from retinal ganglion cell photoreponse.

source, given that we humans adapted to such a circadian source during evolution. Alternatively, we may want to influence and manipulate the human circadian rhythm: If circadian lights (e.g., blue automotive dashboard lights) could reduce driver fatigue, the number of traffic accidents and fatalities caused by this condition could be reduced as well.

Another potential benefit of smart lighting originates in the ability to rapidly modulate the output power of LED-based light sources, thereby enabling communication features. New modes of communication based on room-light sources would help to reduce the overcrowding of the radio frequency bands. Of course, the visual appearance of such communicative light sources would be indistinguishable from conventional sources. In automotive communication applications, brake lights could communicate an emergency braking maneuver to a following car. Headlights could inform a red traffic light of an approaching car while fully maintaining their normal function as headlights. Smart road signs could flash warnings specifically to drivers that approach a dangerous curve with excessive speed. Room lights could broadcast messages, alarms, and other types of information, without any noticeable change in the illumination quality. Modulation rates in the megahertz range are possible, with the limiting factor being the device resistance and capacitance (RC time) of high-power devices. The large-area junction capacitance means that such devices would be limited by RC time rather than by spontaneous lifetime.

Smart lighting could be used in headlights that are spectrally and spatially dispersive, with peripheral regions having a spectrum different from that of the center. It is well known that the spectral sensitivity of the cone cell-rich central vision region of the retina is different from the rod cell-rich peripheral vision region of the retina. It is also well known that human vision has a photopic (daytime vision) regime with peak sensitivity at 555 nm and a scotopic (nighttime vision) regime with peak sensitivity at 505 nm. Although it is too early to guess at the magnitude of safety enhancements, advances in automotive lighting enabled by solid-state sources would certainly reduce accidents.

Plant growth in northern countries and during non-native seasons is already supported by artificial illumination. However, spectral distributions are not yet optimized. Smart lighting would allow one to select the most efficacious spectral composition, thereby enabling plant growth in the most energy-efficient way.

In microscopy applications, smart lighting with infrared, visible-spectrum, and UV illumination sources with specific spectral compositions, polarizations, and color temperatures (for white illumination) could render microscopic objects more clearly than a conventional light bulb could. Smart sources could enable real-time identification, counting, and sorting of biological cells. During surgical procedures, the real-time enhanced rendering of specific cells, tissues, and organs could be very helpful.

Other applications are awaiting the arrival of smart sources for imaging, microscopy, and

visualization. For television sets, computer monitors, and outdoor displays, smart light sources promise a huge color gamut, brilliant colors, and again, large energy savings. Solid-state light sources are already the type of source manufactured in the greatest numbers. They have enjoyed double-digit growth rates for more than a decade. The opportunities discussed above will ensure that this trend will be sustained for years to come.

References and Notes

1. B. Bowers, *Lengthening the Day* (Oxford Univ. Press, Oxford, 1998).
2. A. Bergh, G. Craford, A. Duggal, R. Haitz, *Phys. Today* **54** (no. 12), 42 (2001).
3. J. Kelso, *Buildings Energy Databook* (U.S. Department of Energy, January 2005 revision).
4. D. L. MacAdam, Ed., *Selected Papers on Colorimetry—Fundamentals*, vol. 77 of *SPIE Milestone Series* (SPIE Press, Bellingham, WA, 1993).
5. S. Chhajed, Y. Xi, Y.-L. Li, E. F. Schubert, *J. Appl. Phys.* **97**, 054506 (2005).
6. J. Y. Tsao, *IEEE Circuits & Devices* **20** (no. 3), 28 (2004).
7. L. S. Rohwer, A. M. Srivastava, *Electrochemical Society Interface* **12** (no. 2), 36 (2003).
8. D. Zubia, S. D. Hersee, *J. Appl. Phys.* **85**, 6492 (1999).
9. X. Y. Sun et al., *J. Appl. Phys.* **84**, 1450 (2004).
10. G. C. Brainard et al., *J. Neurosci.* **21**, 6405 (2001).
11. D. M. Berson, F. A. Dunn, M. Takao, *Science* **295**, 1070 (2002).
12. S. Hattar, H.-W. Liao, M. Takao, D. M. Berson, K.-W. Yau, *Science* **295**, 1065 (2002).
13. D. E. Blask, R. T. Dauchy, L. A. Sauer, J. A. Krause, G. C. Brainard, *Breast Cancer Res. Treat.* **79**, 313 (2003).
14. Supported by NSF grant 0401075, the U.S. Army Research Office, Samsung Advanced Institute of Technology (Suwon, Korea), and Crystal IS Corporation (Watervliet, NY).

10.1126/science.1108712

High-Resolution NMR Spectroscopy with a Portable Single-Sided Sensor

Juan Perlo,¹ Vasiliki Demas,^{2,3,4*} Federico Casanova,¹
 Carlos A. Meriles,⁵ Jeffrey Reimer,^{3,4} Alexander Pines,^{2,4}
 Bernhard Blümich^{1*}

Unlike absorption and fluorescence spectrometers, nuclear magnetic resonance (NMR) instruments are not easily miniaturized for field use. Portable NMR systems have been built, with open single-sided probes for arbitrarily sized samples (1). However, the unavoidable spatial inhomogeneity of the static magnetic field has precluded the use of these devices for high-resolution spectroscopy. These field variations are usually orders of magnitude larger than those created by the microscopic structure of the molecules to be detected, so no chemical shift information can be extracted from the spectra. Thus far, the systems have mainly yielded relaxation times as a crude estimate of material composition, but more detailed information would benefit a broad range of fields, from medical diagnosis to archaeological analysis.

Recently, a solution to this *ex situ* challenge has been proposed (2). The strategy compensates for the main field inhomogeneity by using parallel variations in the applied radio frequency (rf) field. For spins with the same chemical shift, different Larmor frequencies throughout the sample give rise to progressive dephasing during a free evolution period. At any stage, this loss of coherence can be reversed if a proper position-dependent phase correction is applied. However, when this is done, phase differences accumulated during the evolution and arising from the chemical shift differences must be maintained. Such a position-dependent phase correction can be accomplished by the use of *z*-rotation pulses (3). In the presence of matched rf and static field profiles, these pulses induce echoes with a phase sensitive only to chemical shift differences. Sampling of the echo maxima occurring after incremental periods of free evolution leads to high-resolution NMR spectra (4). (Discussion of the underlying theory is available as supporting online material.) Unlike other approaches (5–8), this method can be used at low magnetic field strengths and does not rely on any special properties of a given substrate, such as intramolecular interactions.

Here we describe a portable single-sided sensor that functions on the above principle. Two concentric, U-shaped NdFeB magnets inducing opposing magnetic fields were arranged to create a sweet spot 7 mm above the magnet (Fig. 1A). In this region, the magnetic field was parallel to the magnet surface and reached 0.2 T. The dimensions of a rectangular surface

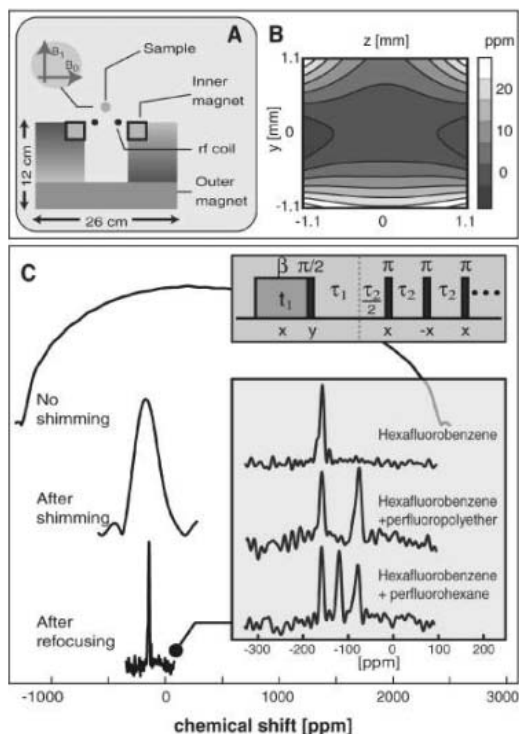


Fig. 1. (A) Schematic. The inner shimming magnet opposes the field of the outer magnet to give a sweet spot 7 mm above the magnet surface. A 3-mm³ sample tube (inner diameter = 1 mm) placed at this site was oriented parallel to the magnet gap (the *x* axis). B_0 , static magnetic field; B_1 , rf field. (B) Field map of the difference (as a fraction of B_0) between the magnitudes of the static and normalized rf fields in the region of the sweet spot, which sets the attainable resolution. The reference frame has the *z* axis parallel to B_0 and the *y* axis parallel to B_1 . (C) (Upper inset) A spatially inhomogeneous rf *z* rotation induces an echo after a period of free evolution τ_1 . The echo position is incremented by varying the duration t_1 of the pulse β . A train of π pulses with separation $\tau_2 = 1.5$ ms improves the signal to noise ratio. Rf phases are labeled. (Main) Spectra of C_6F_6 before and after we optimized the position of the inner magnet and after we used the refocusing sequence. (Lower inset) Chemical shift-resolved spectra for different samples.

rf coil and the position of the inner magnet were finely adjusted to optimize the correspondence between the static and rf magnetic fields (Fig. 1B). The final configuration did not minimize the static field variations. Rather, a remnant static gradient perpendicular to the magnet surface was retained to better reproduce the natural field inhomogeneity of the rf coil.

We reconstructed a well-resolved spectrum by sequentially incrementing the length of the initial (spatially dependent) pulse β (Fig. 1C). The pulse train after the first echo was used simply to increase detection sensitivity (4). As a proof of principle, we acquired ¹⁹F spectra of several fluorinated hydrocarbons. Optimization of the coil and magnet geometry provided a preliminary linewidth of 2500 Hz, which further narrowed to 65 Hz when the pulse sequence was applied (Fig. 1C). This resolution, corresponding to a chemical shift of 8 parts per million (ppm), required only 3 min of acquisition time. These results suggest that proton chemical shift resolution could be achieved in the near future (the ¹H chemical shift range is 12 ppm).

References and Notes

- B. Blümich, *NMR Imaging of Materials* (Clarendon, Oxford, 2000).
- C. A. Meriles, D. Sakellariou, H. Heise, A. Moule, A. Pines, *Science* **293**, 82 (2001).
- R. R. Ernst, G. Bodenhausen, A. Wokaun, *Principles of Nuclear Magnetic Resonance in One and Two Dimensions* (Clarendon, Oxford, 1994).
- Materials and methods are available as supporting material on Science Online.
- D. P. Weitekamp, J. R. Garbow, J. B. Murdoch, A. Pines, *J. Am. Chem. Soc.* **103**, 3578 (1981).
- J. J. Balbach *et al.*, *Chem. Phys. Lett.* **277**, 367 (1997).
- L. D. Hall *et al.*, *J. Am. Chem. Soc.* **109**, 7579 (1987).
- W. Richter, S. Lee, W. S. Warren, Q. He, *Science* **267**, 654 (1995).
- We thank D. Sakellariou for helpful discussion during the course of this work. Supported by the Deutsche Forschungsgemeinschaft, Forschergruppe FOR333, "Surface NMR of Elastomers and Biological Tissue," and by the U.S. Department of Energy under contract no. DE-AC03-76SF00098.

Supporting Online Material

www.sciencemag.org/cgi/content/full/1108944/DC1

Materials and Methods

Figs. S1 to S4

References and Notes

20 December 2004; accepted 8 March 2005

Published online 7 April 2005;

10.1126/science.1108944

Include this information when citing this paper.

¹Institut für Technische Chemie und Makromolekulare Chemie, RWTH-Aachen, D-52056, Germany. ²Department of Chemistry, ³Department of Chemical Engineering, University of California, Berkeley, CA 94720, USA. ⁴Materials Sciences Division, Lawrence Berkeley National Laboratory, Berkeley, CA 94720, USA. ⁵Department of Physics, City College of New York, City University of New York, NY 10031, USA.

*To whom correspondence should be addressed. E-mail: bluemich@mc.rwth-aachen.de (B.B.); vdemas@berkeley.edu (V.D.)

Bottom-Up Ecosystem Trophic Dynamics Determine Fish Production in the Northeast Pacific

Daniel M. Ware^{1,2,3} and Richard E. Thomson^{4,2,5*}

We addressed the question of bottom-up versus top-down control of marine ecosystem trophic interactions by using annual fish catch data and satellite-derived (SeaWiFS) chlorophyll *a* measurements for the continental margin of western North America. Findings reveal a marked alongshore variation in retained primary production that is highly correlated with the alongshore variation in resident fish yield. The highest productivity occurs off the coasts of Washington and southern British Columbia. Zooplankton data for coastal British Columbia confirm strong bottom-up trophic linkages between phytoplankton, zooplankton, and resident fish, extending to regional areas as small as 10,000 square kilometers.

It remains unclear whether long-term sustainable fish catches from continental margin ecosystems are controlled largely by the primary production rate (bottom-up processes) or by predatory-prey interactions at higher trophic levels, including fisheries (top-down processes). Comparative cross-system analy-

ses (1) suggest that bottom-up control is the principal mechanism. However, other studies (primarily of lake ecosystems, where it is easier to experimentally manipulate fish production) have found that top-down processes may prevail (2). Although it is certain that, at some high harvest level, a fishery will begin to exert a controlling influence on fish production, the rate of removal at which this level occurs is uncertain. We used satellite-derived estimates of mean annual chlorophyll *a* (chl-*a*) concentration to test the hypothesis that long-term average fish production and yield within large-scale fishing zones along the continental margin of western North America are mainly controlled by phytoplankton production.

Satellite observations of surface chl-*a* concentration (Fig. 1), a proxy measure of the

surface phytoplankton concentration (3), are available at a spatial resolution of 1.1 km through the water-leaving radiance (reflectance) measurements provided by the standard Seaviewing Wide Field-of-view Sensor (SeaWiFS) (4). The surface concentration of chl-*a* is also directly related to the rate of primary production (5). At the larger spatial scales examined in this study (average surface area, 67,157 km²), we calculated the mean annual chl-*a* concentrations for the years 1998 to 2003 for the 11 North Pacific Anadromous Fish Commission (NPAFC) statistical fishing areas (6). The NPAFC areas span the continental margin from southern California to western Alaska (Table 1 and Fig. 1). We also calculated smaller scale (average area, 18,830 km²) mean concentrations for six oceanographically distinct fishing areas identified (7) for western British Columbia (Fig. 1). Extensive zooplankton time series for British Columbia (8) further made it possible to examine regional-scale trophic coupling between phytoplankton and zooplankton and between zooplankton and fish.

The mean chl-*a* values used in this study are those for which the negative water leaving radiance (NWLRL) filter (9) was not applied (NWLRL-Off). For the regions we studied, the correlation between the “filter-on” and “filter-off” versions of the mean annual chl-*a* data (Table 1) is near unity (10), so we arrive at the same conclusions regardless of which data set is compared with the fish catch data. The mean annual yields (catch in metric tons per km²) of resident and highly migratory fish species for the northeast Pacific continental margin were calculated from long-term

¹Aquatic Ecosystem Associates, 3674 Planta Road, Nanaimo, BC V9T 1M2, Canada. ²Department of Earth and Ocean Sciences, University of British Columbia, Vancouver, BC, Canada. ³School of Resource and Environmental Management, Simon Fraser University, Burnaby, BC, Canada. ⁴Institute of Ocean Sciences, 9860 West Saanich Road, Sidney, BC V8L 4B2, Canada. ⁵School of Earth and Ocean Science, University of Victoria, Victoria, BC, Canada.

*To whom correspondence should be addressed. E-mail: thomsonr@pac.dfo-mpo.gc.ca

Table 1. Mean annual chl-*a* concentrations (with temporal coefficients of variation shown in parentheses) and long-term annual yields of resident and highly migratory fish for various regions along the western continental margin of North America. Latitude denotes the central coastal location of each area. Migratory fish yields for Conception are not estimated because the fish stocks are distributed over a large, poorly defined area off southern California.

Region (latitude °N)	Surface area (km ²)	Chl- <i>a</i> (NWLRL-Off) (mg m ⁻³)	Chl- <i>a</i> (NWLRL-On) (mg m ⁻³)	Resident fish yield (metric tons km ⁻²)	Migratory fish yield (metric tons km ⁻²)	Total fish yield (metric tons km ⁻²)
<i>NPAFC Areas</i>						
Conception (34.3°N)	60,046	1.38 (0.57)	1.06 (0.44)	0.06	–	–
Monterey (38.3°N)	41,613	2.29 (0.54)	1.42 (0.40)	0.45	0.39	0.84
Eureka (41.8°N)	18,692	2.20 (0.86)	1.47 (0.66)	0.66	0.88	1.54
Columbia (45.3°N)	36,573	3.24 (0.68)	2.02 (0.60)	0.88	2.65	3.53
Vancouver (49.0°N)	34,688	5.15 (0.66)	2.81 (0.57)	1.97	1.43	3.40
Charlotte (52.5°N)	82,769	2.16 (0.69)	1.45 (0.53)	0.79	0.01	0.80
Southeast Alaska (56.1°N)	43,342	2.79 (0.80)	1.62 (0.52)	0.60	0	0.60
Yakutat (58.5°N)	76,430	1.57 (0.63)	1.39 (0.43)	0.27	0	0.27
Kodiak (57.4°N)	144,911	2.00 (0.62)	1.50 (0.43)	0.63	0	0.63
Chirikof (54.9°N)	83,590	1.83 (0.79)	1.35 (0.55)	0.65	0	0.65
Shumagin (53.3°N)	116,074	1.66 (1.20)	1.21 (0.84)	0.36	0	0.36
<i>British Columbia</i>						
BCF1 (48.5°N)	11,312	4.26 (0.70)	2.48 (0.62)	2.39	2.93	5.32
BCF2 (49.6°N)	10,099	3.30 (0.71)	1.91 (0.63)	0.85	0	0.85
BCF3 (49.4°N)	8,803	6.92 (0.57)	3.56 (0.47)	3.19	0	3.19
BCF4 (51.6°N)	31,408	2.00 (0.71)	1.34 (0.55)	0.92	0.03	0.95
BCF5 (53.1°N)	44,158	2.41 (0.68)	1.61 (0.48)	0.80	0	0.80
BCF6 (53.0°N)	7,203	1.10 (0.69)	0.86 (0.56)	1.03	0	1.03

landing statistics compiled by the International North Pacific Fisheries Commission (INPFC) and NPAFC for the period 1960 to 1998. For the six British Columbia fishing regions, long-term fish catch data are available for the period 1960 to 1991 (11). Resident species, such as herring and groundfish, are defined as those populations that occupy the continental margin year-round and undertake only spatially limited seasonal migrations. In contrast, highly migratory species are present in some fishing regions for only a short time each year. For example, sockeye, pink, and chum salmon undertake extensive northward migrations as juveniles along the continental margins of British Columbia and Alaska, before entering the Gulf of Alaska. These species return several years later as adults to spawn in their natal rivers. In the southern NPAFC regions, components of the Pacific hake, sardine, and mackerel populations migrate northward from southern California in the spring as far as British Columbia, where they spend the summer foraging. These species migrate back to southern California in the fall to spawn.

Large-scale trophic coupling. Table 1 presents the mean annual satellite-derived estimates of chl-a for the NWLR-Off (and, for comparison, the NWLR-On) data, together with the corresponding fish yields for the 11 large-scale NPAFC statistical areas spanning western North America. Biweekly chl-a concentrations were most variable in the Shumagin and Eureka regions and least variable in the Monterey and Conception regions (Table 1). There is a highly significant linear correlation (Fig. 2) between the long-term average resident fish yield (LTY , in metric tons km^{-2}) and the mean annual chl-a concentration (in mg m^{-3}), such that $LTY = 0.436 \times \text{chl-a}(\text{NWLR-Off}) - 0.38$, with adjusted squared correlation coefficient $r^2 = 0.87$. Thus, spatial variability in the annual chl-a concentration accounts for 87% of the spatial variance in the long-term yield of resident fish. These findings, combined with the observation that primary production is a function of the surface chl-a concentration, confirm a strong linkage between large-scale, area-specific rates of phytoplankton production and fish yield in the northeast Pacific.

From both an oceanographic and biological perspective, the NPAFC region can be divided into a coastal upwelling domain, which spans NPAFC areas from Conception to Vancouver, and a coastal downwelling domain, which spans the areas from Charlotte to Shumagin (12). An analysis of covariance of the resident fish yield and chl-a revealed that neither the type of domain nor the domain-chlorophyll interaction effects were significant. As a consequence, the relationship between fish yield and chl-a concentration in both domains is explained by a common intercept and slope.

Within the coastal upwelling domain, annual offshore (seaward) Ekman transport, which is forced by the upwelling-favorable alongshore winds that prevail over the continental margin (13), is highest in the south and diminishes with latitude, reaching near-zero values at the northern limit of the upwelling domain near 50°N (Fig. 3). Coincidentally, there is a significant poleward increase in the average surface chl-a concentration, with the chl-a concentration at the spatial scale of the NPAFC

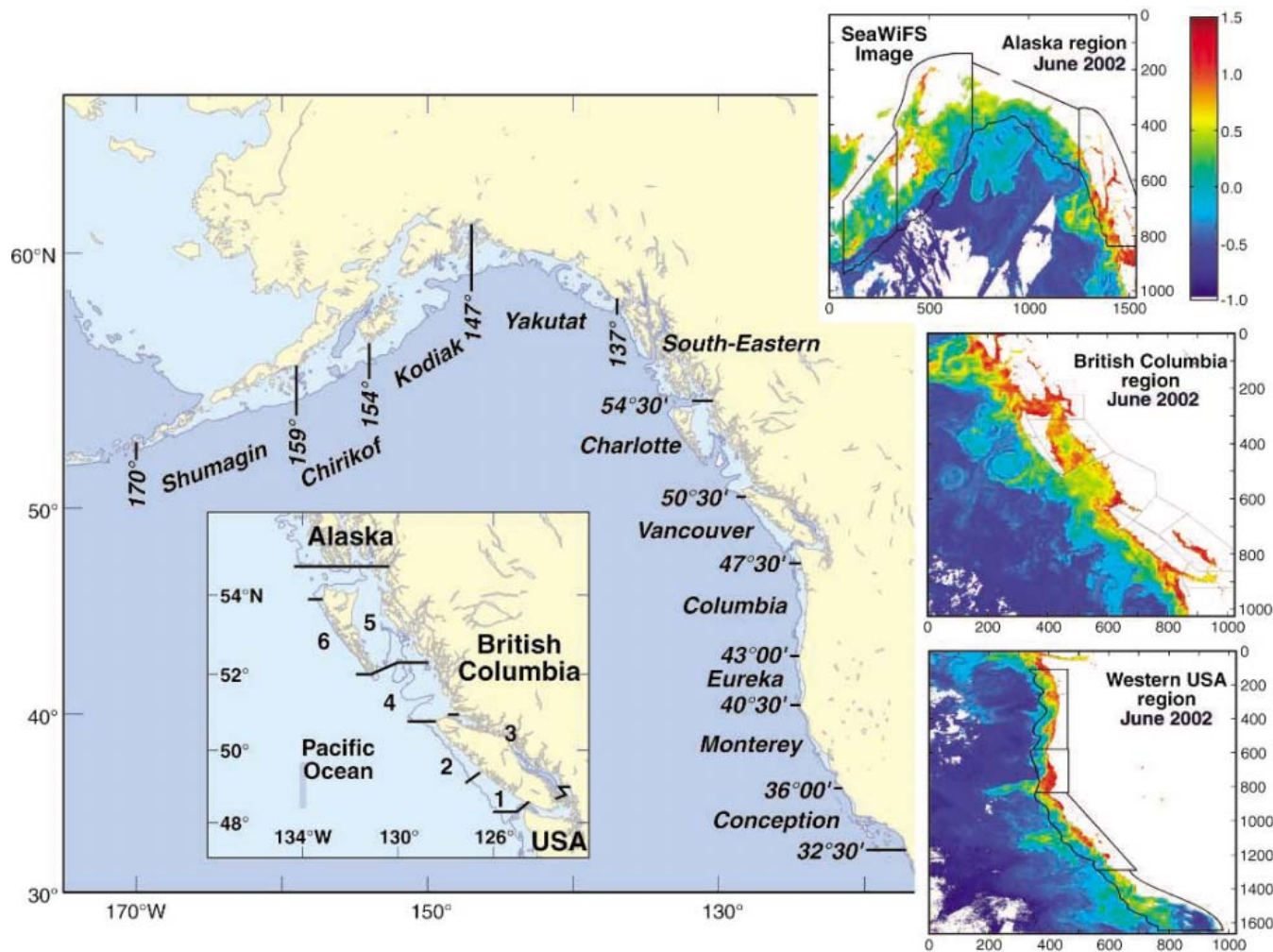


Fig. 1. Map of the 11 NPAFC regions, extending from Conception off California to Shumagin off western Alaska. (Left inset) The areas covered by the six British Columbia subregions. (Right insets) Examples of monthly

mean SeaWiFS chl-a maps for the Alaska, British Columbia, and western U.S. regions; grids are in pixels, at 1.1 km/pixel; the color bar denotes concentration in $\log(\text{chl-a in } \text{mg m}^{-3})$.

regions negatively correlated ($P = 0.011$) with the annual cumulative seaward Ekman transport. The negative sign of this correlation is counterintuitive (in that decreasing seaward Ekman transport is normally thought to produce reduced primary productivity) and indicates that factors other than wind-induced upwelling are important for plankton productivity. For example, from spring to fall in the southern NPAFC regions, upwelling is frequently punctuated by flow events (14), which cause the seaward transport of plankton from the narrow (10-km scale) shelf to the deep ocean. As a consequence, a substantial fraction of the primary production in the coastal region from Pt. Conception to 43°N becomes unavailable to the resident fish ecosystem.

Factors other than seaward export also contribute to the alongshore variation in primary productivity. In particular, the northward increase in coastal runoff from major rivers in the northeast Pacific leads to increased stability and shoaling of the upper layer, as well as an increase in the supply of land-derived nutrients. Accordingly, the highest annual average chl-*a* concentrations occur in the Washington–southern British Columbia region, where there is moderate upwelling and substantial year-round freshwater flux (from the Columbia and Fraser rivers). The latter provides both stability and micronutrients. The continental margin off the British Columbia–Washington coast is also wider than that off Oregon–California, so that more of the primary production remains on the shelf (15), where it is cycled through the pelagic and benthic food webs to the resident fish community.

In the coastal downwelling domain from northern British Columbia to western Alaska, the large volume of fresh water entering the coastal ocean from major rivers continues to be a major source of micronutrients and upper ocean stability (16, 17). Macronutrients are supplied through current-induced upwelling, coastal eddies, and winter upwelling winds. Thus, chl-*a* concentrations remain moderately high despite the absence of summer upwelling.

Pacific hake is currently the most abundant migratory pelagic fish species in the northeast Pacific. The largest hake catches occur between 42°N and 50°N (Table 1), which is also the region of the highest chl-*a* concentrations (Fig. 3). Components of the hake population are clearly migrating northward each spring from southern California to the most productive areas along the continental margin, where, in summer, they feed primarily on euphausiids and small forage fish, such as herring (18). As with resident fish stocks, the alongshore biomass of highly migratory fish stocks is strongly linked to primary productivity. However, because of the way the fishery for migratory species is conducted, the area-specific catch of hake is not proportional to the amount of food hake consumed

in each area during their annual migration. Consequently, there is more scatter in the linear regression linking migratory fish yields to chl-*a* concentration (Table 1).

Regional-scale trophic linkages. To determine if the significant correlation found for the NPAFC fishing areas holds at smaller spatial scales, we calculated the annual mean concentrations of chl-*a* and resident fish yield for the six British Columbia coastal fishing areas. Between 1998 and 2003, the period for which annual SeaWiFS records are available, the highest mean annual chl-*a* concentration occurred in the Strait of Georgia (site BCF3), and the lowest concentrations were in areas BCF4 and BCF6 off the outer northwest coast (Fig. 1 and Table 1). Biweekly chl-*a* concentrations are least variable in the Strait of Georgia (site BCF3) and most variable off the west coast of Vancouver Island (sites BCF1, BCF2, and BCF4) (Table 1).

As with the NPAFC regions, the smaller scale British Columbia regions show a significant linear correlation between the mean annual chl-*a* concentration (mg m^{-3}) and the mean annual resident fish yield (metric tons km^{-2}), with $LTY = 0.437 \times \text{chl-}a(\text{NWLR-Off}) + 0.08$, with adjusted $r^2 = 0.76$ ($P = 0.015$) (Table 1). Based on an analysis of covariance for the British Columbia areas, the

mean resident fish yield versus chl-*a* regression has the same slope as the LTY -chl-*a* regression for the large-scale NPAFC areas (Fig. 2).

Zooplankton abundance time series for coastal British Columbia enabled us to extend our analysis to regional-scale coupling between primary productivity (Fig. 4A) and secondary (zooplankton) productivity (Fig. 4B) (19). Consistent with bottom-up trophic control, the mean annual zooplankton and chl-*a* concentrations for the six British Columbia regions are highly correlated through the power-law function $Zoo = 46.57 \times (\text{chl-}a)^{0.488}$, with adjusted $r^2 = 0.85$; here, Zoo denotes zooplankton concentration (in mg of dry weight per m^3) and the mean chlorophyll concentration (NWLR Filter-Off) is in mg m^{-3} . This relationship is nonlinear, presumably because zooplankton are unable to graze the larger concentrations of phytoplankton produced in the more fertile areas with the same trophic efficiency. In productive continental shelf regions, an increasing proportion of the phytoplankton biomass settles to the sea floor and is ultimately transferred to the shelf fish community through the benthic food web. The relationship between resident fish yield and zooplankton in British Columbia is linear (Fig. 4B): $LTY = 0.055 \times Zoo - 1.98$, with adjusted $r^2 = 0.79$ ($n = 6$ catch areas, $P = 0.01$). Small zooplankton are an important

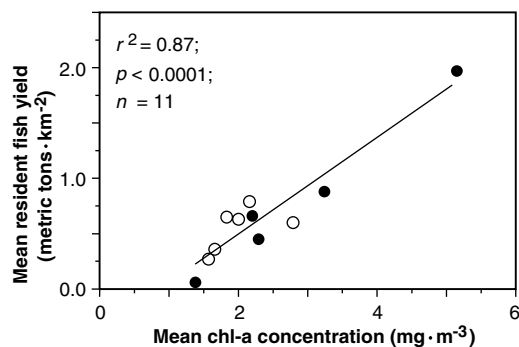


Fig. 2. Large-scale trophic linkage between the annual mean chl-*a* concentration (NWLR-Off) and the long-term annual yield of resident fish for each of the 11 NPAFC regions. Solid circles denote upwelling regimes; open circles, downwelling regimes.

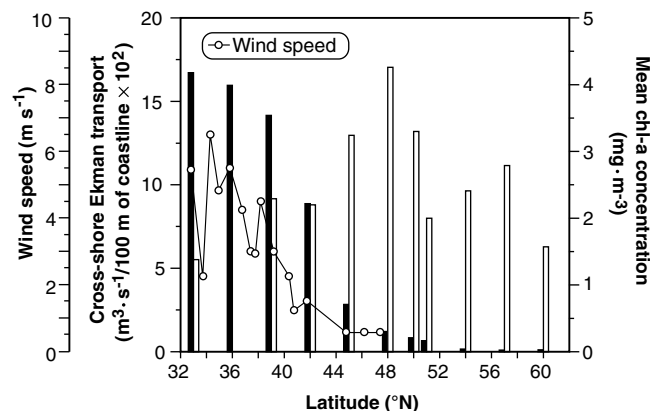


Fig. 3. South-to-north variation in the mean annual seaward component of cumulative Ekman transport (30) given positive (upwelling) values only (black bars) and the mean annual chl-*a* concentration from SeaWiFS (white bars), averaged over the scale of the NPAFC regions. Observations span the period January 1998 to December 2003. Connected circles represent the 10-year mean components of the alongshore wind speed from coastal

meteorological buoys along the west coast of the United States, taken from table 2 of Dorman and Winant (29). Mean winds are roughly alongshore (equatorward), except for the three sites north of 44°N, where mean annual winds are predominantly poleward. The especially low wind speed at 33°42' is for buoy National Data Buoy Center 25, located well within the sheltered region of the Southern California Bight.

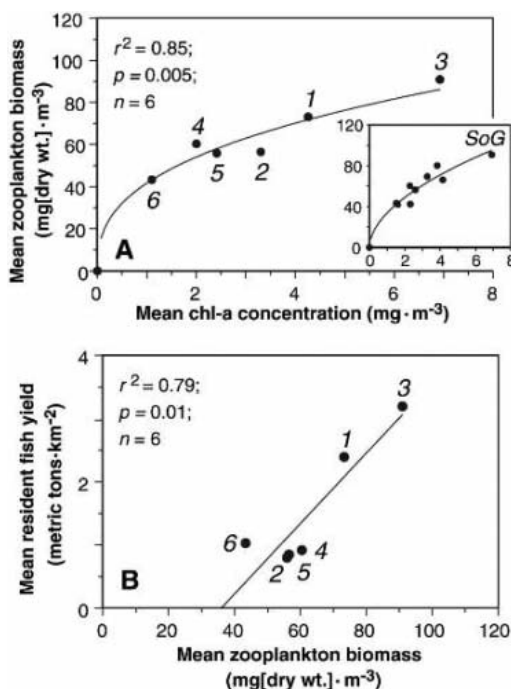
food source for the early life history stages of all resident fish species, and larger zooplankton are an important food for many juvenile and adult resident fish.

Our analysis leads to several fundamental conclusions concerning marine food web interactions along the west coast of North America. Within the large-scale (67,000 km²) NPFAC fishing areas extending from southern California to western Alaska, a large proportion (87%) of the spatial variation in long-term, averaged, resident fish production is controlled by bottom-up trophic interactions. On average, high regional primary productivity (represented by SeaWiFS chl-a data) produced high fishery yields. Plankton and fisheries data for coastal British Columbia further reveal that this linkage also extends to much smaller spatial scales (19,000 km²). Regression of the long-term, averaged, resident fish yield against chl-a concentration yielded the same regression slope for both the coastal upwelling and coastal downwelling domains, a highly unexpected result because the biological diversities of the zooplankton and the migratory and resident fish communities in these domains are quite distinct. The similar regression slopes for both the intense upwelling and intense downwelling regions demonstrates that the available primary production is channeled through the pelagic and benthic food webs to the resident fish community with approximately the same conversion efficiency in each domain. We further found that the resident fish yields in summer upwelling regions increase poleward, in inverse proportion to the annual accumulative Ekman transport seaward over the continental margin, and reach a maximum in southern British Columbia near the north-

ern limit (50°N) of the coastal upwelling domain. The highly productive areas of southern British Columbia and northern Washington—corresponding to the transition region between the low annual coastal runoff of California and the high coastal discharge of Alaska—are also near the northern foraging limit of the migratory Pacific hake and sardine populations in the northeast Pacific. Resident fish yields continue to remain relatively high northward along the Alaskan coast, despite the absence of substantial coastal upwelling. Consequently, the tightly coupled phytoplankton-fish relationship we observed for the west coast of North America must be maintained by either an onshore nutrient supply, late-winter “preconditioning” of the surface ocean (20), or upper ocean stability associated with freshwater discharge from major rivers along the coast.

The resident fish catch time series for the Conception to Columbia region indicates that fish yields increased in the 1960s and 1970s, peaked in the early 1980s, and have since declined. A climatic regime shift, characterized by warmer upper ocean temperatures, occurred in the northeast Pacific in 1976. About the same time, zooplankton concentrations started to decline off southern California (21). These observations suggest that, in addition to harvesting, a coincident decline in zooplankton biomass (and production) may have contributed to the recent downward trend in fish yield in this region. This possibility is in broad agreement with Richardson and Schoeman (22), who found that an increase in water temperatures in warmer regions in the northeast Atlantic leads to a decrease in phytoplankton abundance.

Fig. 4. Small-scale trophic linkages for each of the six British Columbia sub-regions. (A) Linkage between the mean annual concentrations of chl-a and zooplankton. (Inset) An almost identical relationship appears when the British Columbia zooplankton and chl-a data are analyzed at an even smaller spatial scale. SoG denotes the value for the Strait of Georgia (BCF3). (B) The corresponding linkage between mean annual zooplankton biomass and the long-term mean annual resident fish yield.



References and Notes

- R. L. Iverson, *Limnol. Oceanogr.* **35**, 1593 (1990).
- M. Scheffer, S. Rinaldi, Y. A. Kuznetsov, *Can. J. Fish. Aquat. Sci.* **57**, 1208 (2000).
- Satellite-based phytoplankton pigment (chl-a) estimates were derived from water-leaving radiance at near-infrared frequency bands after correction for atmospheric optical properties (23). Except for highly turbid coastal waters, where the optical properties of inorganic suspended matter and colored dissolved organic matter can be problematic (24), the calibrated radiance data are a proxy for surface phytoplankton concentration.
- Chl-a concentrations were derived from the ratio of radiance at the 510- and 555-nm frequency bands by the SeaWiFS sensor aboard the SeaStar spacecraft launched in August 1997.
- In the Columbia region, the depth-integrated daily rate of primary production is linearly correlated with the surface chl-a concentration (15).
- Long-term average fish catches were compiled from data summarized in the INPFC/NPAFC statistical yearbooks for the period 1960 to 1998 (25) and in the California Cooperative Oceanic Fisheries Investigations report series. The catch time series indicate that the fisheries were well developed by 1960 in every area, except Yakutat, Chirikof, and Shumagin, which had developed by 1966, and Columbia and Kodiak, developed by 1975. Long-term mean catches were estimated for each area for the period starting with the aforementioned years to 1998 (the most recent data available). For each region, the catch was partitioned into resident species and highly migratory species. Resident species (of which there are >20 interacting species in the northeast Pacific) inhabit the continental margin and undergo limited along-shelf and cross-shelf seasonal movements. In contrast, in the five southern NPAFC areas, Pacific hake, sardine, and mackerel undergo extensive annual north-south migrations. Accordingly, these species, plus the mobile anchovy populations, were classified as highly migratory. In the five northern NPAFC areas (Shumagin to Charlotte), the entire catch consisted of resident species, primarily groundfish and herring. In the five southern areas, the resident fish community also includes herring and groundfish (but not hake). However, a substantial fraction of the total catch in this region consisted of highly migratory species (Table 1). Regional resident and highly migratory fish yields were estimated by dividing the respective catches by the surface area of each region.
- B. J. Waddell, D. M. Ware, *Can. Tech. Rep. Fish. Aquat. Sci.* **2030** (1995).
- Monthly mean estimates of total zooplankton concentrations (mg of dry weight per m³) were derived for the six coastal regions in British Columbia. The data (mostly collected between 1992 and 2002) were obtained from the Institute of Ocean Sciences in Sidney, British Columbia (26). The raw data were sorted into bins according to the coastal region where the samples were collected. The original 53 zooplankton species groups were reduced to eight functional groups. An analysis of variance indicated a highly significant night-day sampling effect for euphausiids: Euphausiid night biomasses were 2.8 to 5.4 times higher than day biomasses. The night/day ratio was species-specific. Accordingly, we corrected euphausiid samples collected during the day by multiplying the day biomass by the species-specific night/day correction factor. We found no significant day-night sampling effect on the other seven functional groups in our data set. We obtained the total biomass for plankton in each sample by adding the biomasses of the eight functional groups and obtained monthly estimates by averaging all the samples collected in the same month.
- Near the coast, SeaWiFS can overestimate the atmospheric correction, giving physically unrealistic negative reflectance values, particularly at 412 nm, the shortest wavelength. Negative radiance at 412 nm implies that the values at 510 and 555 nm are likely too small, so the ratio will tend to give chl-a values that are too large. As a consequence, a filter is typically used to remove negative radiance values. For coastal British Columbia, we found that the average chl-a values for NWLR-On estimates are more similar to historical in situ measurements of mean chl-a concentrations. However, comparison of the NWLR-On versus the NWLR-Off chl-a estimates for British Columbia reveals that, although the NWLR-On data may represent more accurate es-

- imates of the annual mean chl-a biomass, the NWLR-Off data yield more realistic estimates of the seasonal variability (i.e., spring and fall blooms) and the expected seasonal cycle in surface chl-a concentrations. This comparison implies that the NWLR filter eliminates high chl-a estimates too severely and retains low chl-a estimates too conservatively (27).
- For the mean chl-a data applied to the 11 NPFAC fishing regions in Table 1, we found the linear regression relation for the NWLR-On and NWLR-Off data to be $chl-a(NWLR-On) = 0.440 \times chl-a(NWLR-Off) + 0.523$, with $r^2 = 0.96$ ($n = 11$ regions; $P < 0.0001$). For all chl-a data (including the British Columbia data in Table 1), $chl-a(NWLR-On) = 0.449 \times chl-a(NWLR-Off) + 0.487$ with $r^2 = 0.98$ ($n = 17$, all fishing regions; $P < 0.0001$).
 - Long-term fish catch data are available for the six fishing regions in British Columbia (7) for the period 1920 to 1991. The fisheries, particularly for groundfish, were still developing in British Columbia before 1960. Therefore, we calculated the average, long-term catch of resident species for each region for the period 1960 to 1991 (Table 1). The long-term average yield (metric tons km^{-2}) was estimated by dividing the catch by the surface area of each region (28).
 - D. M. Ware, G. A. McFarlane, *Can. Spec. Publ. Fish. Aquat. Sci.* **108**, 359 (1989).
 - Table 2 of (29) presents observed 10-year mean wind speeds for meteorological buoys moored along the west coast of the United States. Because of the Coriolis effect, winds blowing equatorward parallel to the west coast of North America generate a net seaward transport in the surface Ekman layer. This transport is compensated by a net onshore transport at depth, which gives rise to upwelling conditions over the continental slope.
 - P. T. Strub, P. M. Kosro, A. Huyer, *J. Geophys. Res.* **96**, 14743 (1991).
 - M. J. Perry, J. P. Bolger, D. C. English, in *Coastal Oceanography of Washington and Oregon*, M. R. Landry, B. M. Hickey, Eds. (Elsevier, Amsterdam, 1989), pp. 117–138.
 - T. C. Royer, *J. Geophys. Res.* **87**, 2017 (1982).
 - P. J. Stabeno *et al.*, *Continental Shelf Res.* **24**, 859 (2004).
 - R. W. Tanasichuk, D. M. Ware, W. Shaw, G. A. McFarlane, *Can. J. Fish. Aquat. Sci.* **48**, 2118 (1991).
 - Because there are sufficient data to obtain reasonably accurate estimates of the average annual zooplankton and chl-a concentrations, we were able to divide the six British Columbia fishing regions into 10 smaller subareas. The inset in Fig. 4A shows the relationship between these two variables [$Zoo = 33.9 \times (chl-a)^{0.531}$, adjusted $r^2 = 0.81$; $P = 0.001$].
 - E. A. Logerwell, N. Mantua, P. W. Lawson, R. C. Francis, V. N. Agostini, *Fish. Oceanogr.* **12**, 554 (2003).
 - J. A. McGowan, D. R. Cayan, L. M. Dorman, *Science* **281**, 210 (1998).
 - A. J. Richardson, D. S. Schoeman, *Science* **305**, 1609 (2004).
 - S. Tassan, *Applied Optics* **33**, 2369 (1994).
 - K. G. Ruddick, F. Ovidio, M. Rijkeboer, *Applied Optics* **39**, 897 (2000).
 - M. V. H. Lynde, *NOAA Technical Memo., NMFS/NWC-103* (1986).

- Institute of Ocean Sciences, unpublished data.
- W. W. Gregg, N. W. Casey, *Remote Sens. Environ.* **93**, 463 (2004).
- Materials and methods are available as supporting material on Science Online.
- C. E. Dorman, C. D. Winant, *J. Geophys. Res.* **100**, 16029 (1995).
- Time series of Ekman transport are available from the Pacific Fisheries Environmental Laboratory at www.pfeg.noaa.gov.
- We thank J. Gower and J. Wallace for providing us with SeaWiFS imagery from the Department of Fisheries and Oceans satellite facility, L. Beauchemin and B. Wallace for processing the SeaWiFS data for the fish catch areas, D. McQueen and S. Romaine for assisting with the zooplankton data, C. Wright and P. Kimber for helping prepare the manuscript, B. Hickey for consulting with us on the validity of variously derived wind fields for the California coastal region, and three reviewers for comments on the manuscript.

Supporting Online Material

www.sciencemag.org/cgi/content/full/1109049/DC1

Materials and Methods
References and Notes

22 December 2004; accepted 15 April 2005

Published online 21 April 2005;

10.1126/science.1109049

Include this information when citing this paper.

REPORTS

An Asymmetric Energetic Type Ic Supernova Viewed Off-Axis, and a Link to Gamma Ray Bursts

Paolo A. Mazzali,^{1,2,3,4*} Koji S. Kawabata,⁵ Keiichi Maeda,⁶
Ken'ichi Nomoto,^{1,2*} Alexei V. Filippenko,⁷ Enrico Ramirez-Ruiz,⁸
Stefano Benetti,⁹ Elena Pian,⁴ Jinsong Deng,^{10,12}
Nozomu Tominaga,¹ Youichi Ohyama,^{11,12} Masanori Iye,^{1,13,14}
Ryan J. Foley,⁷ Thomas Matheson,¹⁵ Lifan Wang,¹⁶
Avishay Gal-Yam¹⁷

Type Ic supernovae, the explosions after the core collapse of massive stars that have previously lost their hydrogen and helium envelopes, are particularly interesting because of their link with long-duration gamma ray bursts. Although indications exist that these explosions are aspherical, direct evidence has been missing. Late-time observations of supernova SN 2003jd, a luminous type Ic supernova, provide such evidence. Recent Subaru and Keck spectra reveal double-peaked profiles in the nebular lines of neutral oxygen and magnesium. These profiles are different from those of known type Ic supernovae, with or without a gamma ray burst, and they can be understood if SN 2003jd was an aspherical axisymmetric explosion viewed from near the equatorial plane. If SN 2003jd was associated with a gamma ray burst, we missed the burst because it was pointing away from us.

When a massive star reaches the end of its life and exhausts its nuclear fuel, the core itself collapses to form a compact remnant (a neutron star or a black hole). Although the exact mechanism is not well understood, the resulting release of energy leads to the ejection of the envelope of the star at high velocities, producing a supernova (SN).

Typically, a massive star has a large H-rich envelope, making it difficult to observe the innermost part, where the action takes place. However, there are some cases where the H envelope, and also the inner He envelope, were lost before the star exploded, through either a stellar wind or, more likely, binary interaction (1). These SNe, called type Ic, offer a view

close to the core, and so they are particularly interesting as tools to study the properties of the collapse and of the SN ejection.

Some type Ic SNe, characterized by a very high kinetic energy (2, 3), have been observed to be linked with the previously unexplained phenomenon of gamma ray bursts (GRBs), which are brief but extremely bright flashes of hard (γ -ray and x-ray) radiation that had baffled astronomers for decades (4–8). The link between type Ic SNe and GRBs is probably not accidental. If a jet is produced by a collapsing star, it can only emerge and generate a GRB if the stellar envelope does not interfere with it (9).

In view of this link, we have searched among known type Ic SNe for the counterpart of a property that is typical of GRBs: asphericity. A jet-like explosion is required for GRBs from energetics considerations; if they were spherically symmetric, GRBs would involve excessively large energies, comparable to the rest mass of several suns. The best evidence for asphericity in the GRB-associated SNe (GRB/SNe) to date has come from the fact that iron seems to move faster than oxygen in the ejected material. Evidence of this is seen in spectra obtained several months after the explosion, when the ejected material has decreased in density and behaves like a nebula. The GRB/SN 1998bw (10) showed strong emission lines of [O I] (a forbidden line of neutral oxygen), as do normal type Ic SNe, but also of [Fe II] (a forbidden line of singly ionized iron), which are weak in normal type Ic SNe. The [Fe II] lines near 5100 Å in SN 1998bw are broader than the [O I] 6300 and 6363 Å blend.

Asphericity can explain this peculiar situation (11). In a typical spherical SN explosion, heavier elements are produced in deeper layers of the progenitor star. As a consequence of the hydrodynamical properties of the explosion, the heavier elements are given less kinetic energy per unit mass than are the external layers, which typically contain lighter elements. However, in a jet-like explosion, the heavier elements (in particular, ^{56}Ni) are probably synthesized near the jet at the time of core collapse and are ejected at high velocities. Lighter elements such as oxygen, which are not produced in the explosion but rather by the progenitor star during its evolution, are ejected near the equatorial plane with a smaller kinetic energy and are distributed in a disc-like structure.

Given this scenario, the observed line profiles depend on the orientation of the explosion with respect to our line of sight. Iron can be observed to be approaching us at a higher velocity than is oxygen, if we view the explosion near the jet direction, which is also the requirement for the GRB to be observed (10, 11). The [O I] line, on the other hand, will appear narrow and sharp in the case of a polar view, because in that case, oxygen moves almost perpendicular with respect to our line of sight (the case of SN 1998bw); however, it will show a broader double-peaked profile for an equatorial view, because a large fraction of the oxygen would then be moving either toward or away from the observer (11).

¹Department of Astronomy, ²Research Center for the Early Universe, School of Science, University of Tokyo, Bunkyo-ku, Tokyo 113-0033, Japan. ³Max-Planck-Institut für Astrophysik, Karl-Schwarzschild Strasse 1, D-85748 Garching, Germany. ⁴Instituto Nazionale di Astrofisica (INAF)-Osservatorio Astronomico di Trieste, Via Tiepolo 11, I-34131 Trieste, Italy. ⁵Hiroshima Astrophysical Science Center, Hiroshima University, Hiroshima 739-8526, Japan. ⁶Department of Earth Science and Astronomy, Graduate School of Arts and Sciences, University of Tokyo, Komaba 3-8-1, Meguro-ku, Tokyo 153-8902, Japan. ⁷Department of Astronomy, University of California, Berkeley, CA 94720-3411, USA. ⁸Institute for Advanced Study, Einstein Drive, Princeton, NJ 08540, USA. ⁹INAF-Osservatorio Astronomico di Padova, vicolo dell'Osservatorio 5, 35122 Padova, Italy. ¹⁰National Astronomical Observatories, CAS, 20A Datun Road, Chaoyang District, Beijing 100012, China. ¹¹Department of Infrared Astrophysics, Institute of Space and Astronautical Science, Japan Aerospace Exploration Agency, 3-1-1 Yoshinodai, Sagami-hara, Kanagawa, 229-8510, Japan. ¹²Subaru Telescope, National Astronomical Observatory of Japan (NAOJ), 650 North A'ohoku Place, Hilo, HI 96720, USA. ¹³Optical and Infrared Astronomy Division, National Astronomical Observatory, Mitaka, Tokyo 181-8588, Japan. ¹⁴Department of Astronomical Science, School of Physical Sciences, Graduate University for Advanced Studies, Osawa, Mitaka, Tokyo 181-8588, Japan. ¹⁵National Optical Astronomy Observatory, 950 North Cherry Avenue, Tucson, AZ 85719-4933, USA. ¹⁶Lawrence Berkeley National Laboratory, 50-232, 1 Cyclotron Road, Berkeley, CA 94720, USA. ¹⁷Department of Astronomy, California Institute of Technology, Pasadena, CA 91125, USA.

*To whom correspondence should be addressed. E-mail: mazzali@ts.astro.it (P.A.M.); nomoto@astron.s.u-tokyo.ac.jp (K.N.)

Although this picture seems well established for GRB/SNe, it is important to determine whether it may be common to other type Ic SNe. Measurements of the relative widths of the Fe and O lines are difficult for fainter type Ic SNe because the Fe lines are weak. However, the [O I] line is always rather strong, and it can be expected that given a sufficiently large sample, variations will be seen in its profile reflecting different viewing angles.

Until recently, the evidence for these variations was missing (12), but recent observations of SN 2003jd seem to close this gap. SN 2003jd, discovered on 25 October 2003 (13) (universal time), is a type Ic SN at a distance of ~ 80 million parsecs (Mpc) and reached a rather bright maximum. Assuming a galactic extinction $E(B - V)_{\text{Gal}} = 0.06$ mag-

nitudes (mag) (where E is the magnitude difference between the amount of light absorbed in two photometric bands, B is the blue band, and V is the visual band) (14), and a host extinction $E(B - V)_{\text{Host}} = 0.09$ mag, as derived from the strength of the interstellar Na I D absorption (15), we derive the absolute blue-band magnitude (M_B) at maximum light to be $M_B(\text{max}) \approx -18.7$ mag. This is much more luminous than the normal type Ic SN 1994I (1, 16) and is comparable to the GRB/SNe 1998bw (4) and 2003dh (6). Spectroscopically, however, SN 2003jd shows narrower lines than the hyper-energetic GRB/SNe (Fig. 1), and it appears to be intermediate between those and the normal type Ic SN 1994I (16). The closest analog may be the energetic SN 2002ap (17, 18).

Fig. 1. The near-maximum optical spectrum of SN 2003jd compared with spectra of other type Ic SNe at a similar phase (F_λ is the flux per unit wavelength). The dates are the days relative to the optical maximum (i.e., the minus sign means before the maximum light). Spectra are ordered by increasing line width (implying increasing kinetic energy per unit mass), ranging from the normal SN 1994I (16), to the energetic SN 2002ap (17, 18), to the hyper-energetic GRB/SN 1998bw (30). The absorption line near 7600 Å in the spectrum of SN 1998bw is telluric.

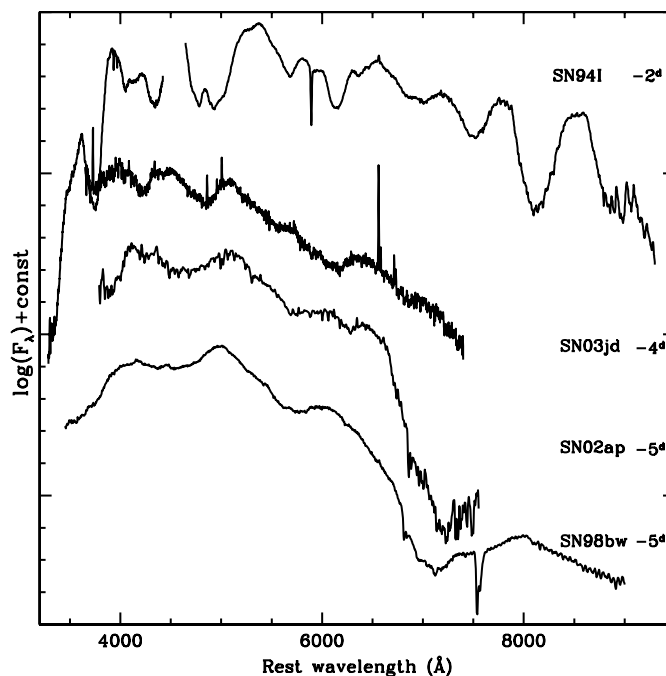
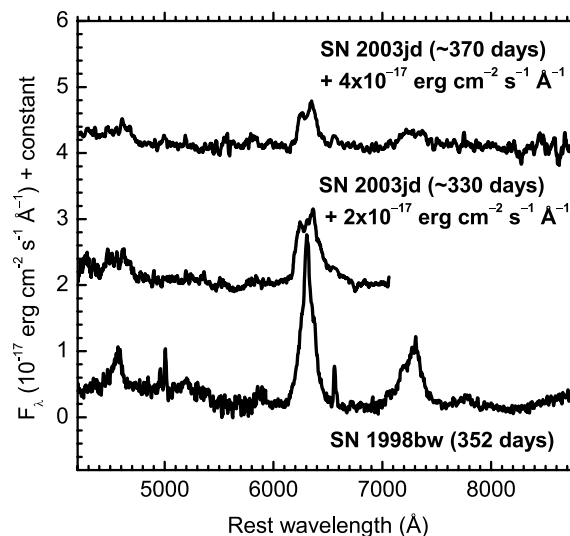


Fig. 2. Nebular spectra of type Ic SNe. The bottom curve shows the nebular spectrum of SN 1998bw (30) taken 337 days after maximum light (352 days after the explosion). Note the Mg I], [Fe II], [O I], and [Ca II] lines near 4570, 5100, 6300, and 7300 Å, respectively. The middle curve shows the Subaru FOCAS spectrum of SN 2003jd ~ 330 days after the putative time of explosion. The top curve shows the Keck spectrum of SN 2003jd at an epoch of ~ 370 days. The [O I] 6300, 6363 Å line in SN 2003jd clearly exhibit a double-peaked profile. Marginal evidence of a double peak is also present in the profiles of Mg I] at 4570 Å and [Ca II] at 7300 Å. The spectrum of SN 1998bw has been shifted in flux to make it consistent with the distance of SN 2003jd.



We observed SN 2003jd in the nebular phase with the Japanese 8.2-m Subaru telescope on 12 September 2004 (19) using the Faint Object Camera and Spectrograph (FOCAS) (20), and with the 10-m Keck-I telescope on 19 October 2004 using the Low Resolution Imaging Spectrograph (LRIS) (21). These dates correspond to SN ages of ~ 330 and ~ 370 days after explosion, respectively. In both spectra (Fig. 2), the nebular line [O I], at wavelengths of 6300 and 6363 Å, clearly has a double-peaked profile with full width at half maximum (FWHM) ≈ 8000 km s $^{-1}$. The semiforbidden Mg I line at 4570 Å shows a similar profile. Magnesium is formed near oxygen in the progenitor star. The [Fe II] blend near 5100 Å is quite weak.

Late-phase emission is created by the release of the heat deposited by γ rays and positrons, both of which are emitted in the decay chain $^{56}\text{Ni} \rightarrow ^{56}\text{Co} \rightarrow ^{56}\text{Fe}$. Therefore, the mass of ^{56}Ni can be determined indirectly through the strength of the emission lines. Because SN 2003jd was not as luminous as SN 1998bw, we rescaled the synthetic spectra to the appropriate ^{56}Ni mass, the best value for which was ~ 0.3 the mass of the Sun (M_{\odot}). This value is actually very similar to that derived for the GRB/SN 2003dh (22, 23) and much larger than in the non-GRB type Ic SNe (17).

We computed nebular spectra of two-dimensional (2D) explosion models for various asphericities and orientations (11). We found that a spherical model produces a flat-topped [O I] profile, which is not compatible with either SN 1998bw or SN 2003jd. The flat-topped emission is a typical characteristic of emission from a shell. Indeed, the emission from any spherically distributed material should have a maximum at the wavelength of the line transition between 6300 and 6363 Å, taking into account the line blending. On the other hand, Fig. 3 shows that a highly aspherical model can explain the [O I] line profiles in both SN 1998bw and SN 2003jd. To reproduce the double-peaked profile of the [O I] line in SN 2003jd, we found that SN 2003jd must be oriented $\geq 70^{\circ}$ away from our line of sight. In contrast, for SN 1998bw, this angle was only $\sim 15^{\circ}$ to 30° (11), and it was even smaller for SN 2003dh (24). Less aspherical models do not produce sufficiently sharp [O I] in SN 1998bw.

This result confirms that SN 2003jd was a highly aspherical explosion, and it raises the interesting question of whether SN 2003jd was itself a GRB/SN. A GRB was not detected in coincidence with SN 2003jd (25).

If the explosion was very off-axis, we presume that we would not have been able to detect γ rays. However, a GRB is expected to produce a long-lived radiative output through synchrotron emission. X-ray and radio emissions are produced by the deceleration of the relativistic jet as it expands into the wind emitted by the progenitor star before it ex-

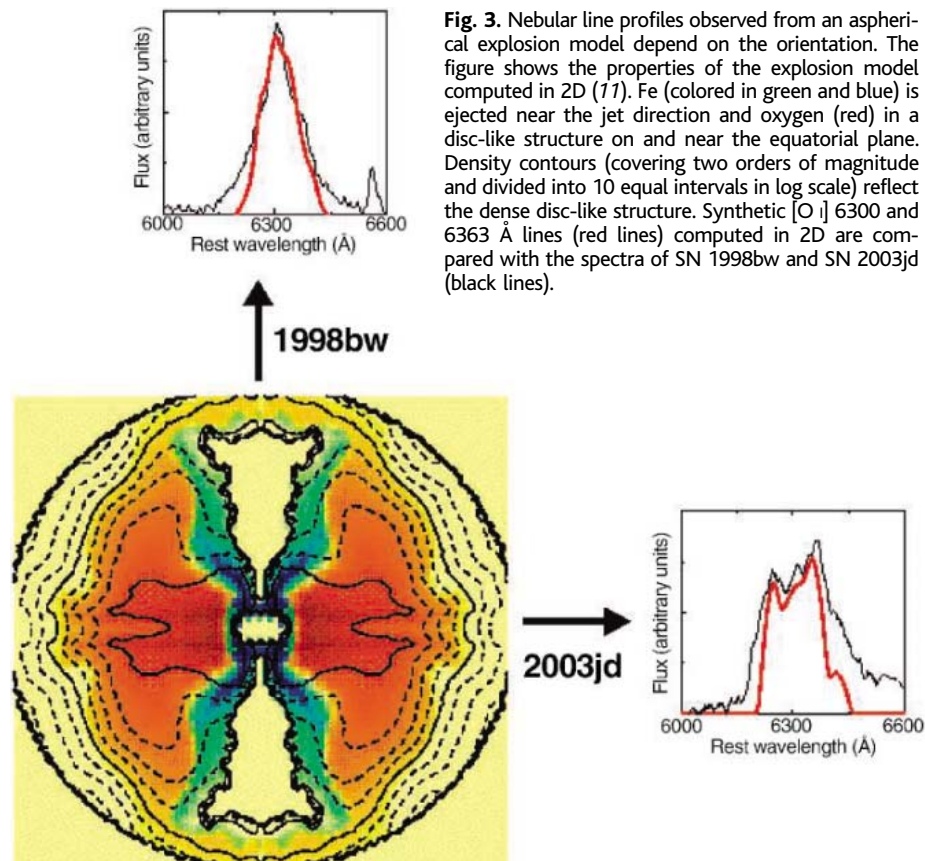


Fig. 3. Nebular line profiles observed from an aspherical explosion model depend on the orientation. The figure shows the properties of the explosion model computed in 2D (11). Fe (colored in green and blue) is ejected near the jet direction and oxygen (red) in a disc-like structure on and near the equatorial plane. Density contours (covering two orders of magnitude and divided into 10 equal intervals in log scale) reflect the dense disc-like structure. Synthetic [O I] 6300 and 6363 Å lines (red lines) computed in 2D are compared with the spectra of SN 1998bw and SN 2003jd (black lines).

ploded. This afterglow emission is very weak until the Doppler cone of the beam intersects our line of sight, making off-axis GRB jets directly detectable only months after the event, and at long wavelengths.

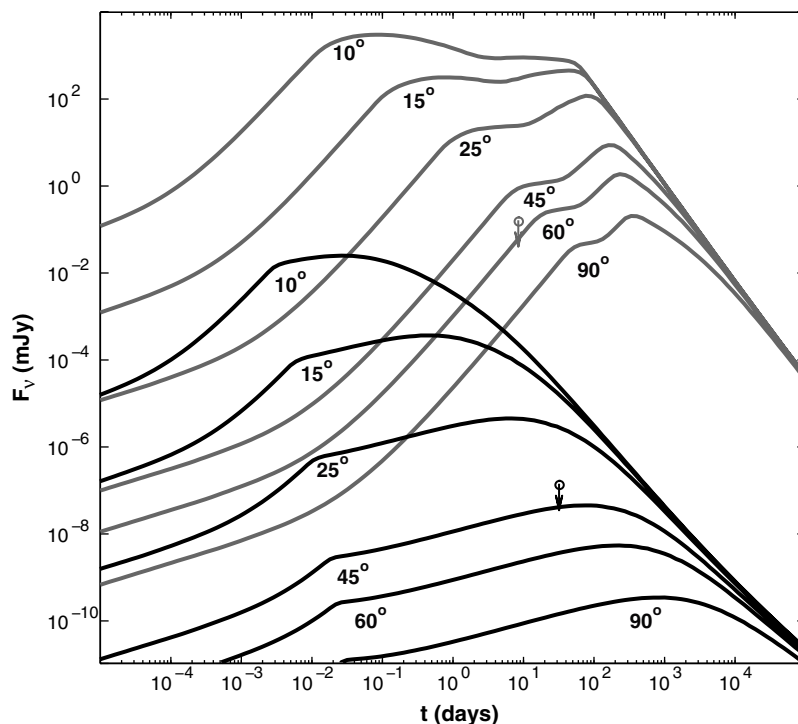
SN 2003jd was observed in x-rays with Chandra on 10 November 2004, about 30 days after the explosion, and was not detected to an x-ray limit $L_x \leq 3.8 \times 10^{38}$ erg s $^{-1}$ in the energy interval 0.3 to 2 keV (26). It was also observed in the radio regime (8.4 GHz) 9 days after the explosion, and again not detected to a radio limit $L_r \leq 10^{27}$ erg s $^{-1}$ Hz $^{-1}$ (27).

These nondetections may suggest that SN 2003jd did not produce a GRB. However, absence of evidence is not necessarily evidence of absence. Let us consider the standard jet associated with typical GRBs, that is, a sharp-edged uniform jet with $E = 10^{51}$ erg and a 5° opening angle, expanding laterally at the local sound speed (see Fig. 4 legend for other parameters) (28, 29). If the jet expands in a wind with density $\dot{M}/v = 5 \times 10^{11}$ g cm $^{-1}$ (for example, a mass-loss rate $\dot{M} = 10^{-6} M_{\odot}$ per year and velocity $v = 2000$ km s $^{-1}$), it would give rise to the x-ray and radio light curves shown in Fig. 4. If the SN made a large angle ($\geq 60^{\circ}$) with respect to our line of sight, its associated GRB jet, if present, would not have been detected in the x-rays or radio. Furthermore, the afterglow emission can be fainter for a lower jet energy and/or for a lower wind density.

Although this does not by itself prove that SN 2003jd produced a GRB, it is certainly a possibility, because quantities such as the ejected mass of ^{56}Ni are comparable to those typical of GRB/SNe (22). Moreover, our observations confirm that the energetic SN 2003jd is an aspherical explosion, reinforcing the case for a link with a GRB. It could also be the case for other energetic type Ic SNe. The lack of x-ray and radio emission does not place stringent constraints on the intrinsic kinetic energy carried by the SN as long as the ejecta experience little deceleration before ~ 30 days. The expansion velocity (which need not be isotropic) must be $\lesssim 0.2 A_*^{-1/3} (\epsilon_e/0.1)^{-1/3} c$ (where ϵ_e is the fraction of the total blast energy that goes into shock-accelerated electrons, A_* is wind density (\dot{M}/v), and c is the speed of light) in order to produce $L_x (t \approx 30 \text{ days}) \leq 3.8 \times 10^{38}$ erg s $^{-1}$ for a standard 10^{51} -erg SN shell expanding into a wind with density $A_* = (\dot{M}/v)/(5 \times 10^{11} \text{ g cm}^{-1}) = 1$ (28). The average expansion velocity along our line of sight can be estimated from the early-time spectra; for SN 2003jd, this is about $0.05c$. In an aspherical explosion, however, the kinetic energy must be considerably larger near the rotation axis of the stellar progenitor, with bulk expansion velocities close to $\sim 0.1c$.

The bright SN 2003jd is the first type Ic SN that shows double peaks in the [O I] line (12), which suggests that the degree of asphericity is

Fig. 4. Afterglow emission from a sharp-edged uniform jet in SN 2003jd. X-ray (0.3 to 2 keV, black) and radio (8.4 GHz, gray) light curves are calculated for various viewing angles, θ_{obs} , for a GRB with the standard parameters $E_{\text{jet}} = 10^{51}$ erg, $\epsilon_e = 0.1$, $\epsilon_B = 0.1$, $\theta_0 = 5^\circ$, and $A_* = 1$ (where E_{jet} is the energy in the jet, ϵ_e and ϵ_B are the fraction of the internal energy in the electrons and magnetic field, respectively, and θ_0 is the opening half-angle of the jet). The synchrotron spectrum is taken to be a piecewise power law with the usual self-absorption, cooling, and injection frequencies calculated from the cooled electron distribution and magnetic field (28, 29). The observed radio and x-ray upper limits for SN 2003jd are marked by open circles. Cosmological parameters taken in the model are $\Omega_m = 0.27$, $\Omega_\Lambda = 0.73$, and $H_0 = 72 \text{ km s}^{-1} \text{ Mpc}^{-1}$, where Ω_m is the matter density of the universe, Ω_Λ is the energy density of the universe, and H_0 is the Hubble constant.



not the same in all type Ic SNe. The GRB/SNe 1998bw and 2003dh, which are probably highly aspherical, have been discovered thanks to a GRB trigger; their orientation is therefore such that the [O I] profile must be single-peaked. For normal type Ic SNe, which are on average closer and easier to discover, the lack of observed double-peaked profiles suggests that they are not as strongly aspherical. SN 2003jd appears to share many of the properties (energetics and luminosity) of the GRB/SNe, but it was discovered independent of a GRB, and it is likely to be an aspherical SN viewed off-axis. There have been three energetic type Ic SNe without a GRB trigger (therefore less biased)—SNe 1997dq, 1997ef, and 2002ap—whose nebular spectra did not show the double peaks in the [O I] 6300 Å line. Given the small sample, the number (one out of four) is not inconsistent with our interpretation that the viewing angle $\gtrsim 70^\circ$ results in the double-peaked [O I].

Additional sensitive radio and x-ray observations of SN 2003jd are strongly encouraged, because a jet with the standard parameters could still be detectable by deep observations (Fig. 4). The result should provide valuable tests for the presence of an off-axis GRB with the typical parameters and would further constrain the viewing angle and the mass-loss rate.

References and Notes

1. K. Nomoto *et al.*, *Nature* **371**, 227 (1994).
2. K. Iwamoto *et al.*, *Nature* **395**, 672 (1998).
3. K. Nomoto *et al.*, in *Stellar Collapse*, C. L. Fryer, Ed. (Kluwer Academic, Dordrecht, Netherlands, 2004), pp. 277–325.
4. T. J. Galama *et al.*, *Nature* **395**, 670 (1998).
5. C. Stanek *et al.*, *Astrophys. J.* **591**, L17 (2003).
6. T. Matheson *et al.*, *Astrophys. J.* **599**, 394 (2003).
7. J. Hjorth *et al.*, *Nature* **423**, 847 (2003).
8. J. Malesani *et al.*, *Astrophys. J.* **609**, L5 (2004).
9. A. E. MacFadyen, S. E. Woosley, *Astrophys. J.* **524**, 262 (1999).
10. P. A. Mazzali *et al.*, *Astrophys. J.* **559**, 1047 (2001).
11. K. Maeda *et al.*, *Astrophys. J.* **565**, 405 (2002).
12. T. Matheson *et al.*, *Astron. J.* **121**, 1648 (2001).
13. J. Burket, B. Swift, W. Li, *Int. Astron. Union Circ.* **8232** (2003).
14. D. Schlegel, D. Finkbeiner, M. Davis, *Astrophys. J.* **500**, 525 (1998).
15. S. Benetti *et al.*, in preparation.
16. A. V. Filippenko *et al.*, *Astrophys. J.* **450**, L11 (1995).
17. P. A. Mazzali *et al.*, *Astrophys. J.* **572**, L61 (2002).
18. R. J. Foley *et al.*, *Publ. Astron. Soc. Pac.* **115**, 1220 (2003).
19. K. Kawabata *et al.*, *Int. Astron. Union Circ.* **8410** (2004).
20. N. Kashikawa *et al.*, *Publ. Astron. Soc. Jpn.* **54**, 819 (2002).
21. J. B. Oke *et al.*, *Publ. Astron. Soc. Pac.* **107**, 375 (1995).
22. P. A. Mazzali *et al.*, *Astrophys. J.* **599**, L95 (2003).
23. J. Deng *et al.*, *Astrophys. J.* **624**, 898 (2005).
24. E. Ramirez-Ruiz *et al.*, in press (<http://arxiv.org/abs/astro-ph/0412145>).
25. K. Hurley *et al.*, *GRB Coord. Network Circ. Serv.* **2003**, no. 2439 (2003).
26. D. Watson, E. Pian, J. N. Reeves, J. Hjorth, K. Pedersen, *GRB Coord. Network Circ. Serv.* **2003**, no. 2445 (2003).
27. A. M. Soderberg, S. R. Kulkarni, D. A. Frail, *GRB Coord. Network Circ. Serv.* **2003**, no. 2435 (2003).
28. E. Ramirez-Ruiz, P. Madau, *Astrophys. J.* **608**, L89 (2004).
29. J. Granot, E. Ramirez-Ruiz, *Astrophys. J.* **609**, L9 (2004).
30. F. Patat *et al.*, *Astrophys. J.* **555**, 900 (2001).
31. This work is based on data collected at the Subaru telescope, operated by the NAOJ, and at the Keck telescopes made possible by the W. M. Keck Foundation. This research is supported in part by the Japan Society for the Promotion of Science and the Ministry of Education, Culture, Sports, Science, and Technology in Japan and by NSF in the USA. E.R.-R. is a Chandra Fellow and A.G.-Y. is a Hubble Fellow.

22 February 2005; accepted 18 April 2005
10.1126/science.1111384

Scaling in the Time Domain: Universal Dynamics of Order Fluctuations in Fe₃Al

Cristian Mocuta,^{1*} Harald Reichert,^{1†} Klaus Mecke,^{1‡}
Helmut Dosch,^{1,2} Michael Drakopoulos^{3§}

By focusing a highly brilliant synchrotron x-ray beam to a micrometer spot on a sample, we measured in real time the x-ray intensity fluctuations associated with order fluctuations in crystalline materials. We applied this method to the binary alloy Fe₃Al near its continuous A2-B2 phase transformation and determined a specific four-point time correlation function for the order parameter. From a detailed theoretical analysis, dynamical scaling in the time domain with a transition from noncritical to critical dynamics is disclosed.

A premier objective of condensed matter research is to understand and predict how a material reacts upon external fields—such as

temperature, pressure, and magnetic or electric fields—especially near a phase transition. The macroscopic response functions χ

(susceptibilities) of a given many-body system are intimately related to a set of local fluctuations $\delta\mu(\mathbf{r})$ of a thermodynamic quantity μ (such as volume, entropy, or sublattice order) at location \mathbf{r} , which are exploring all possible neighboring states of the system. More rigorously, the average static susceptibility χ is determined by

$$\chi = \lim_{\mathbf{q} \rightarrow 0} \langle |\delta\mu_{\mathbf{q}}|^2 \rangle / k_B T \quad (1)$$

that is, by the long-wavelength limit of the power spectrum $\langle |\delta\mu_{\mathbf{q}}|^2 \rangle = \Sigma g_2(\mathbf{r}) \exp(i\mathbf{q}\mathbf{r})$, where $g_2(\mathbf{r}) = \langle \delta\mu(\mathbf{r})\delta\mu(0) \rangle$, k_B is Boltzmann's constant, and T is temperature. Here, $g_2(\mathbf{r})$ is the well-known two-point correlation function which is, to lowest order, given for $d = 3$ (where d is number of dimensions) in the Ornstein-Zernicke form $g_2(r) \sim \exp(-r/\xi)/r$, with ξ being a system-inherent correlation length (Fig. 1A).

Materials that undergo continuous phase transformations have been of particular interest, because the correlation length $\xi = \xi_0|\theta|^{-\nu}$ diverges as the associated critical temperature, T_c , is approached, where $\theta = (T - T_c)/T_c$ is the reduced temperature and the critical exponent $\nu = 0.67$ (1, 2). The resulting unlimited growth of the range of fluctuations leads to a “quasi long-ranged” power law behavior $g_2(r) = r^{-(2-d-\eta)}$ (critical exponent $\eta = 0.036$) (3), and in this manner, leads to universal macroscopic response functions that depend only on d and the symmetry of the system. These fluctuations render the system ultrasensitive to external fields near $\theta = 0$. In conventional x-ray or neutron scattering experiments, the observed diffuse scattering distribution $I_{\mathbf{q}} \sim \langle |\delta\mu_{\mathbf{q}}|^2 \rangle$ directly maps the Fourier transform of the spatial correlation function $g_2(\mathbf{r})$. Starting with the pioneering scattering experiments by Als-Nielsen and Dietrich on β -CuZn (4), many experimental tests of the concept of criticality have been performed. Today, the entire body of x-ray and neutron-scattering evidence has led to a rather comprehensive and consistent picture of the static critical behavior of crystalline matter, both in the bulk as well as at the surface of matter (5–7).

However, local fluctuations are dynamic in nature, i.e., $\delta\mu = \delta\mu(\mathbf{r}, t)$, where t is time. Thus, our microscopic understanding of fluctuations is fundamentally incomplete as long as we do not have experimental access to the temporal behavior of thermal fluctuations.

¹Max-Planck-Institut für Metallforschung, 70569 Stuttgart, Germany. ²Institut für Theoretische und Angewandte Physik, Universität Stuttgart, 70569 Stuttgart, Germany. ³European Synchrotron Radiation Facility, 38043 Grenoble, France.

*Present address: European Synchrotron Radiation Facility, 38043 Grenoble, France.

†To whom correspondence should be addressed. E-mail: reichert@mf.mpg.de

‡Present address: Universität Erlangen-Nürnberg, Staudtstrasse 7, 91058 Erlangen, Germany.

§Present address: Diamond Light Source, Chilton Didcot, Oxon, OX11 0DE, UK.

During the past four decades, the theory of dynamical critical phenomena, as they emerge at T_c , has been worked out and many universal predictions have been put forward (8, 9). In particular, a dynamic power-law behavior

$$g_2(t) \sim t^{-(d-2+\eta)/z} \quad (2)$$

has been proposed to appear at T_c (9), governed by the universal dynamic exponent z . The origins of the power law (Eq. 2) are temporal critical fluctuations that emerge at all time scales. The exact value of z should depend on, in addition to the dimension and symmetry of the system, only very general conservation laws (9), where $z = 4$ is found for systems with a so-called conserved order parameter and $z = 2$ for systems with a nonconserved order parameter (in the mean-field approximation with $\eta = 0$). We focus on systems exhibiting a continuous order-disorder transition, i.e., a nonconserved order parameter. Near T_c , $g_2(t)$ should exhibit in Gaussian approximation the asymptotic form (9)

$$g_2(t) \sim e^{-t/t_\xi} (t/t_\xi)^{-3/2} \quad (3)$$

implying that the universal power-law behavior (Eq. 2) should be visible only within a time window

$$t_\xi \sim \xi^z \quad (4)$$

where t_ξ can be pictured as the lifetime of a fluctuation of typical size ξ (Fig. 1A). This critical slowing-down phenomenon has been observed in the energy width of neutron-

scattering signals (10). The functional form of $g_2(t)$ is shown in the critical regime near T_c (dotted line in Fig. 1C, $t_\xi = 10^5$). Conventional x-ray diffraction with a large probing beam performs a spatial and temporal average over the sample. In turn, it provides the time-independent probability distribution of the fluctuations, and the dynamic nature of the fluctuations is inherently not accessible by this diffraction scheme (11). The direct observation of the microscopic critical dynamics in the time domain in crystalline materials turned out to be a challenge in experimental physics. Dynamic scaling has been observed so far only in the dynamic light scattering from density fluctuations in fluids near T_c (12).

In recent years, x-ray intensity fluctuation spectroscopy has been developed that exploits the fully coherent part of the x-ray beam provided by modern synchrotron radiation sources (13). In this scheme, the sample is illuminated by a coherent x-ray beam and produces a “speckle” diffraction pattern that is uniquely related to the exact spatial arrangement of the disorder, which fluctuates in time (14). Thus, through proper time resolution, this speckle pattern carries the information on the dynamic part of the fluctuations. However, because of the limited coherent flux of current synchrotron radiation sources, the scenario of universal critical dynamics could not be tested in such experiments.

Here we propose and present a different scheme to observe dynamic fluctuations on a

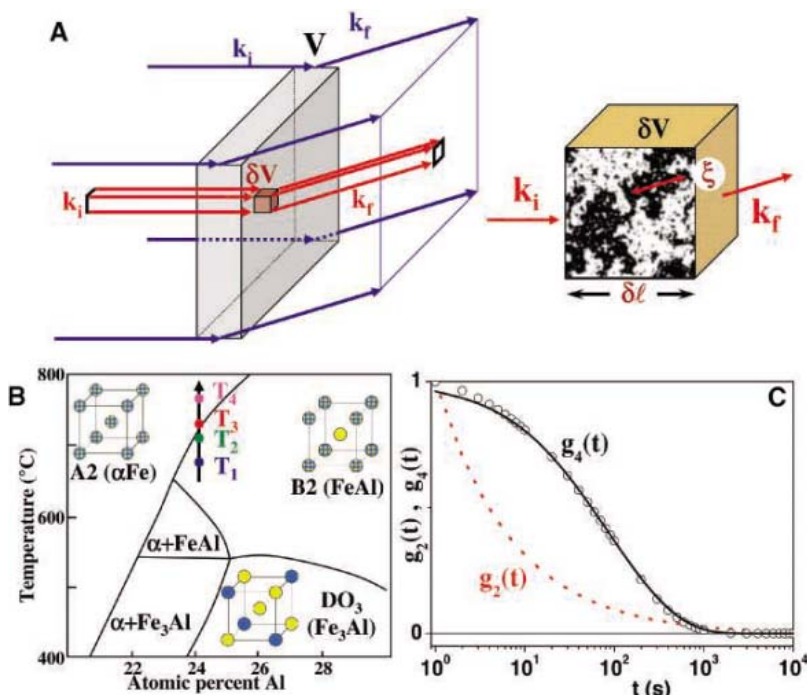


Fig. 1. (A) Principle for a diffraction microscope. A microbeam illuminates a small-volume sample δV in Fe_3Al that is kept close to a phase transition temperature T_c , producing a fluctuating diffraction intensity. (B) The phase diagram of Fe_3Al (yellow, Fe; blue, Al) with the continuous transitions DO_3 -B2 and B2-A2 (four measured temperatures are indicated). (C) The functional form of the two-point and four-point autocorrelation.

microscopic scale. This scheme allows us to test the existence of a universal power-law range in the dynamics of order-disorder fluctuations, which we will demonstrate for the binary alloy, Fe_3Al , close to T_c . Consider a material with fluctuations of size ξ (Fig. 1A). In a given volume V , the average number of fluctuations N can be estimated by $\langle N \rangle = V/\xi^3$. Even for a fixed temperature, N fluctuates with time; that is, $N(t) = \langle N \rangle + \delta N(t)$. However, when V is of macroscopic size, $\langle N \rangle$ is a very large number; in turn, the relative number fluctuation $\delta N/\langle N \rangle$ is much smaller than the shot noise in the x-ray beam and thus not accessible. For a scattering volume δV of such small size that only a few fluctuations are tested by the x-ray beam, the diffraction experiment no longer performs an ensemble average, but should exhibit a fluctuating diffraction intensity that directly reflects the dynamics of the thermal fluctuation. Because this x-ray scheme does not require a fully coherent beam, the incident beam is strongly focused to a small spot size at the sample position to preserve to a large extent the number of incident photons.

In such microdiffraction experiments (15), the required minimum length scale δl of the microdiffraction volume δV must be properly adjusted to the critical fluctuation length scale $\xi \approx \xi_0 \theta^{-1/2}$, which is determined by the experimental temperature uncertainty $\theta = \Delta T/T_c$. We assume here for simplicity that $\nu \approx 0.5$ and $\xi_0 \approx a_0$ (where a_0 is the lattice constant). The condition that the intensity contribution

of the critical fluctuations, $(\Delta I/I)_{\text{fluc}} = N^{-1/2}$, to the overall x-ray intensity fluctuation should exceed a minimum value α (as given by the shot noise in the x-ray beam) leads to the experimental constraint

$$\delta l \leq \alpha^{-2/3} \theta^{-1/2} a_0 \quad (5)$$

If we can control ΔT to 0.1 K, and setting $\alpha \approx 0.01$ (typical shot noise level in the experiment), we obtain (with $T_c \approx 10^3$ K and $a_0 \approx 0.5$ nm) $\delta l \leq 1$ to 2 μm . With the development of hard x-ray focusing devices, such x-ray microdiffraction experiments have now become possible at third-generation synchrotron radiation sources (16). We describe the prototype of such an experimental scheme and an x-ray microdiffraction study of the alloy system Fe_3Al near T_c of the continuous B2-A2 phase transition (Fig. 1B). The experiment was performed at the ID22 beamline of the European Synchrotron Radiation Facility (ESRF) in Grenoble.

A hard x-ray beam (energy $E = 16.5$ keV) was focused to the sample position by an Al compound-refractive lens composed of 56 individual lenses (16). The focused hard x-ray beam limits the diffraction volume δV in two dimensions to 1.5 μm by 1.7 μm . To reduce the third dimension, we used a specimen preparation procedure, originally developed for high-resolution transmission electron microscopy (TEM). A disk-shaped sample was mechanically thinned to 0.4-mm thickness, and then a small hole was produced in the center of the sample by chemical etching. The rim of

the hole shows a wedge-like shape and thus a variable thickness in the micrometer range, depending on the distance from the rim. By using precise sample positioning devices, we selected a microdiffraction volume δV according to the aforementioned experimental conditions (thickness = 1.5 μm) (17).

The Fe-Al system has a body-centered cubic lattice and exhibits a variety of ordered and partially ordered phases (Fig. 1B) (18). The order-disorder transitions DO₃-B2 and B2-A2 (shown in red at T_3) occur on different sublattices and are continuous (19, 20). We focus on the B2-A2 order-disorder transition, which occurs at higher temperatures and which gives rise to fluctuations up to a time scale of a few tens of seconds. In the time-resolved x-ray microdiffraction experiments, the (2,2,6) superstructure reflection with typical intensities on the order of 10^3 counts/s was measured as a direct diffraction signal of the B2-A2 order-disorder fluctuations. A typical set of experimental results is shown in Fig. 2C, where time-resolved (2,2,6) intensities are shown for various temperatures. All time series were normalized to a constant incident beam intensity. We find that the Bragg intensities exhibit strong fluctuations in time and are most pronounced for $T = T_c$. The amplitude of the fluctuations exhibits the characteristic λ -shape as a function of T , indicative of critical dynamics at T_c (Fig. 2B).

To test the nature of the observed x-ray intensity fluctuations, we performed a detailed statistical analysis of the data, based on the use of time-time correlation functions (Fig. 3). Using the time-averaged intensity $\bar{I} = N^{-1} \sum I(t_i)$, we calculate the (time-dependent) intensity correlation function

$$C_1(t) = \frac{1}{t_{\text{max}} - t} \times \sum_{i=1}^{t_{\text{max}} - t} [I(t_i) - \bar{I}] [I(t_i + t) - \bar{I}] \quad (6)$$

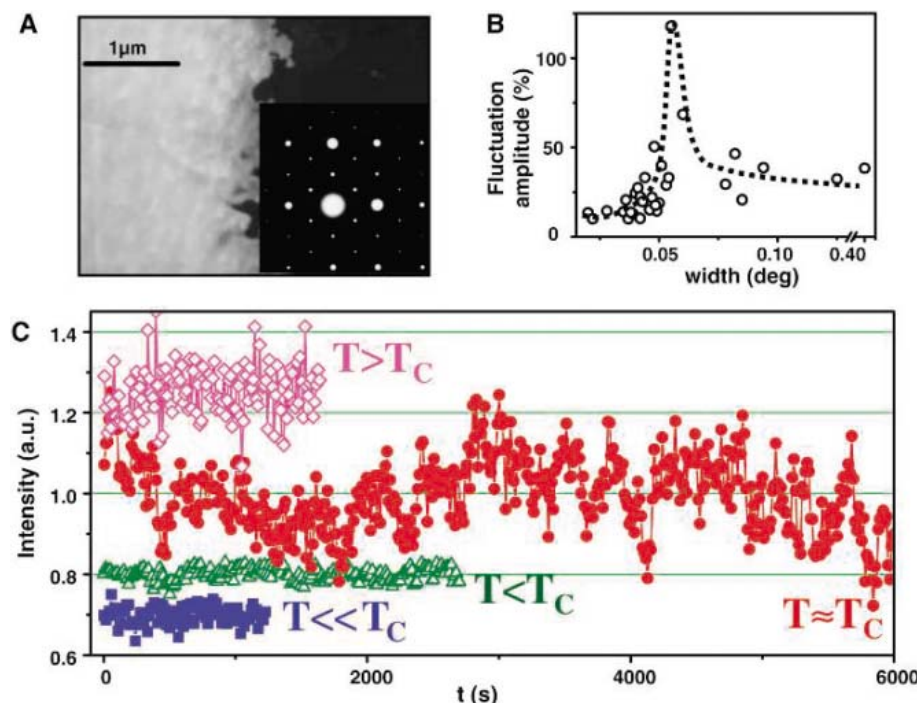


Fig. 2. (A) A TEM micrograph of the Fe_3Al sample kept in an ultrahigh-vacuum chamber. (B) Fluctuation amplitude versus width of the diffraction peak revealing a typical λ -like behavior (the dotted line is a guide for the eye) across the phase transformation, which can be used to localize T_c . (C) Time-resolved (2,2,6) diffraction intensities are shown for four different temperatures across the phase transformation. All time series are normalized to a mean value 1 and shifted vertically.

displayed in Fig. 3A for the four time-resolved intensity curves depicted in Fig. 2. In the following we use $C_1^*(t) = C_1(t)/\sigma^2$, which is normalized by the variance $\sigma^2 = C_1(0)$. A direct and unambiguous way to test the existence of correlations between the fluctuations as observed in the time-resolved intensity measurements is through so-called lag plots, where $I(t_i + \Delta t)$ is plotted as a function of $I(t_i)$. For a given time lag Δt , strong correlations manifest themselves in a highly anisotropic distribution, as shown in Fig. 3B for $T \sim T_c$ and $\Delta t = 1$ s, whereas a random signal, as we find for $T > T_c$ (Fig. 3C), exhibits an isotropic distribution.

In addition, we find a Gaussian distribution (black line in Fig. 3D) of intensities for all temperatures with no signature of nonlinearity in the time series. Thus, the data are consistent with a Gaussian stochastic process. Because the

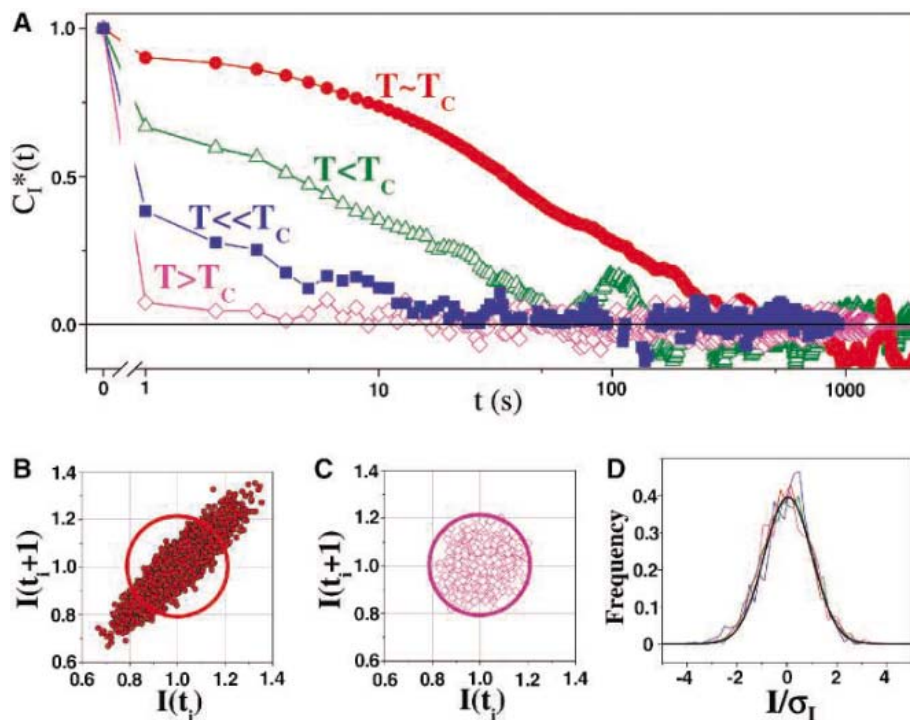


Fig. 3. Statistical analysis of the time-resolved diffraction data. **(A)** Full intensity-intensity correlation functions $C_1^*(t)$ for the observed time series shown in Fig. 2C. **(B and C)** Lag plots, i.e., $I(t_i + \Delta t)$ versus $I(t_i)$, for two selected temperatures ($T \approx T_c$ and $T > T_c$, respectively) with $\Delta t = 1$ s. The absence of temporal correlations in an isotropic distribution of data points is associated with $T > T_c$, whereas the ellipse-shaped distribution associated with data $T \approx T_c$ is characteristic for strong temporal correlations in the measured intensity fluctuations. **(D)** Frequency distributions of the measured intensities. They exhibit a Gaussian shape for all temperatures, confirming that the intensity fluctuations occur in the regime of linear response.

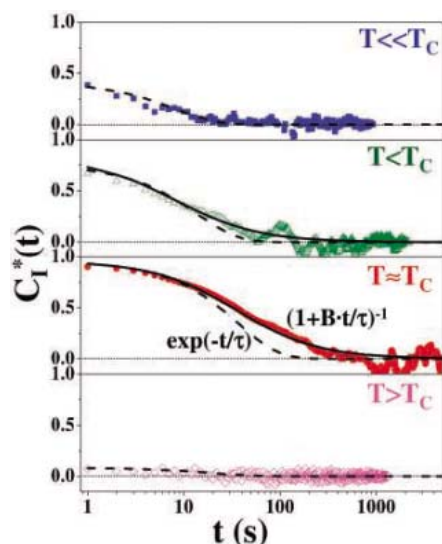


Fig. 4. Fits to the measured correlation functions using exponential (dashed lines) and power-law (solid lines) decay, demonstrating the crossover form close to T_c .

measured intensity $I(\mathbf{q}, t)$ is already a two-point function of the order parameter $\mu(\mathbf{q}, t)$, i.e., $I_{\mathbf{q}}(t) \sim \mu_{\mathbf{q}}(t)\mu_{\mathbf{q}}^*(0)$, the quantity $C_1^*(t) + 1$ is governed by the four-point correlation function $g_4(\mathbf{r}, t) \sim \int d\mathbf{q} g_4(\mathbf{q}, t) \exp(i\mathbf{q}\mathbf{r})$. The

quantity $g_4(\mathbf{q}, t) = \langle \mu_{\mathbf{h}}(t_0)\mu_{\mathbf{h}+\mathbf{q}}(t_0)\mu_{\mathbf{k}}(t_0 + t)\mu_{\mathbf{k}+\mathbf{q}}(t_0 + t) \rangle$ relates four (fluctuating) order parameter components as they emerge at different reciprocal lattice vectors (\mathbf{h} and \mathbf{k}) and times with time resolution t_0 , which has been set to $t_0 = 1$ s in the x-ray experiment described above. \mathbf{q} is the reduced momentum transfer in the first Brillouin zone. Intensity fluctuation spectroscopy generally does not yield the dynamical two-point autocorrelation function $g_2(t)$ (Eq. 3) directly, but rather the more elaborate four-point autocorrelation function $C_1^*(t) = g_4(t) - 1$.

In the experimental scheme described above, we have deduced the self-correlation of the B2 superlattice intensity measured at the (2,2,6) reciprocal lattice vector [$\mathbf{h} = \mathbf{k} = (2,2,6)$] and have isolated the scattering at $\mathbf{q} = 0$, which describes the temporal behavior of the long-range fluctuations as they become dominant near critical points. A detailed theoretical analysis of this situation (21) shows that the finite time resolution t_0 enters $C_1^*(t)$, which then decomposes into two parts

$$C_1^*(t) = (k_B T / 4\pi\xi^2) \exp(2t_D/t_\xi) (t_\xi/t_0)^2 \{C^{(2)}[(t + t_D + t_0)/t_\xi] - C^{(2)}[(t + t_D)/t_\xi]^2\} \quad (7a)$$

with

$$C^{(2)}(s) = (s/\pi)^{1/2} e^{-s} - \{s + 1/2\} [1 - \text{erf}(s^{1/2})] \quad (7b)$$

We also identified a second time scale $t_D = (L/\xi)^2 t_\xi$ (diffusion time) in our scheme that depends on the ratio L/ξ , where L is the cross section of the x-ray microbeam (22). Equation 7 carries the power-law behavior of the critical dynamics in a rather implicit manner. Near T_c , a noticeable deviation from a simple exponential behavior can be detected. However, a detailed analysis shows that the asymptotic behavior of $C_1^*(t)$ (Eq. 7) at temperatures $T \neq T_c$ is well-reproduced by the empirical function (21)

$$C_1^*(t) = \begin{cases} Ae^{-2t/t_\xi} & T < T_c \quad (8a) \\ A/[1 + B(t/t_D)^m] & T \approx T_c \quad (8b) \end{cases} \quad \text{for}$$

that recovers a power-law behavior closest to T_c with $m = 2(d - 2 + \eta)/z \approx 1$ (associated with $z \approx 2$ and $\eta \approx 0$) (where A and B are constants, and t_D is the diffusion time), as shown in Fig. 1C (solid line), which compares Eq. 7 (open circles) with a fit using Eq. 8b (solid line). In the off-critical regime, the lifetime of a fluctuation is expected to be much shorter than t_D , because $L/\xi \ll 1$.

In Fig. 4, the experimental data of Figs. 2 and 3 are now compared with this theoretical scheme for a series of temperatures ranging from $T \ll T_c$, $T < T_c$, and $T \approx T_c$ to a final temperature $T > T_c$, where we use the phenomenological expressions in Eq. 8. In the critical regime only, we find an algebraic decay of the correlation function with an experimentally determined exponent $m = 1 \pm 0.2$, which provides an experimental confirmation of the universal critical order fluctuation scenario in the time domain and experimental evidence for the crossover from noncritical to critical dynamics in solid binary alloys. We find from the analysis that the C_1^* correlation time increases to $t_\xi = 70$ s upon approaching T_c . By comparing the value of t_ξ with the microscopic time scale of 10^{-7} s for the single jump of an Fe atom (23), we find that a scaling behavior must be present that bridges eight orders of magnitude in the time domain.

References and Notes

1. M. E. Fisher, in *Critical Phenomena*, M. S. Green, Ed. (Academic Press, London, 1971), pp. 1–99.
2. M. E. Fisher, R. J. Burford, *Phys. Rev.* **156**, 583 (1967).
3. A. Pelissetto, E. Vicari, *Phys. Rep.* **368**, 549 (2002).
4. J. Als-Nielsen, O. W. Dietrich, *Phys. Rev.* **153**, 706 (1967).
5. K. Binder, in *Phase Transitions and Critical Phenomena*, C. Domb, J. L. Lebowitz, Eds. (Academic Press, New York, 1983), vol. 8, pp. 1–144.
6. H. W. Diehl, in *Phase Transitions and Critical Phenomena*, C. Domb, J. L. Lebowitz, Eds. (Academic Press, New York, 1986), vol. 10, pp. 75–267.
7. H. Dosch, *Critical Phenomena at Surfaces and Interfaces, Tracts in Modern Physics* (Springer, Berlin, 1992), vol. 126.

8. B. I. Halperin, P. C. Hohenberg, *Phys. Rev. Lett.* **19**, 700 (1967).
9. P. C. Hohenberg, B. I. Halperin, *Rev. Mod. Phys.* **49**, 435 (1977).
10. O. W. Dietrich, J. Als-Nielsen, L. Passell, *Phys. Rev. B* **14**, 4923 (1976).
11. B. Park, G. B. Stephenson, S. M. Allen, K. F. Ludwig, *Phys. Rev. Lett.* **68**, 1742 (1992).
12. A. Onuki, *Phase Transition Dynamics* (Cambridge Univ. Press, Cambridge, 2002).
13. S. Brauer et al., *Phys. Rev. Lett.* **74**, 2010 (1995).
14. M. Sutton et al., *Nature* **352**, 608 (1991).
15. J. Wang et al., *Phys. Rev. Lett.* **80**, 1110 (1998).
16. B. Lengeler et al., *Appl. Phys. Lett.* **74**, 3924 (1999).
17. The Fe₃Al single crystal was grown by a float-zone technique and then prepared as described. The single-crystal quality and the local composition at the rim of the center hole have been checked carefully by TEM (Fig. 2A). By local chemical energy dispersive x-ray analysis a composition of Fe_{71.5 ± 0.5} Al_{28.5 ± 0.5} was found. The electron diffraction confirmed a crystalline well-ordered alloy. The sample was then pre-aligned and mounted in a mobile ultrahigh-vacuum diffraction chamber with a precise heating control (± 80 mK) which was then shipped to the ESRF.
18. M. Allen, J. W. Cahn, *Scripta Met.* **10**, 451 (1976).
19. L. Guttman, H. C. Schnyders, G. J. Arai, *Phys. Rev. Lett.* **22**, 517 (1969).
20. L. Guttman, H. C. Schnyders, *Phys. Rev. Lett.* **22**, 520 (1969).
21. K. Mecke et al., unpublished results.
22. The diffusion time t_D can be interpreted as the time for a fluctuation of size ξ to diffuse through the cross section of the microbeam.
23. S. M. Mehrer et al., *Mat. Sci. Eng.* **A239-240**, 889 (1997).

21 January 2005; accepted 4 April 2005
 Published online 21 April 2005;
 10.1126/science.1110001
 Include this information when citing this paper.

Amalthea's Density Is Less Than That of Water

John D. Anderson,^{1*} Torrence V. Johnson,¹ Gerald Schubert,^{2,3}
 Sami Asmar,¹ Robert A. Jacobson,¹ Douglas Johnston,¹
 Eunice L. Lau,¹ George Lewis,¹ William B. Moore,²
 Anthony Taylor,^{1†} Peter C. Thomas,⁴ Gudrun Weinwurm^{5‡}

Radio Doppler data from the Galileo spacecraft's encounter with Amalthea, one of Jupiter's small inner moons, on 5 November 2002 yield a mass of $(2.08 \pm 0.15) \times 10^{18}$ kilograms. Images of Amalthea from two Voyager spacecraft in 1979 and Galileo imaging between November 1996 and June 1997 yield a volume of $(2.43 \pm 0.22) \times 10^6$ cubic kilometers. The satellite thus has a density of 857 ± 99 kilograms per cubic meter. We suggest that Amalthea is porous and composed of water ice, as well as rocky material, and thus formed in a cold region of the solar system, possibly not at its present location near Jupiter.

After Galileo's discovery of Jupiter's four largest satellites, Io (JI), Europa (JII), Ganymede (JIII), and Callisto (JIV), it took another 282 years of telescope development before a fifth satellite, Amalthea (JV), was discovered by Barnard with the 36-inch refractor at Lick Observatory on Mt. Hamilton (I). This small moon orbits Jupiter at an altitude of only 110,000 km. All five satellites are in synchronous rotation with their orbital periods, and all five are in nearly circular orbits in Jupiter's equatorial plane. [A compilation of satellite data can be found in (2)]. Barnard concluded that because Amalthea's orbit lies in the plane of Jupiter's equator, the satellite is an old member of Jupiter's family. After Barnard's discovery, seven more small satellites were discovered between 1904

and 1951, although these have distant and irregular orbits and possibly represent captured comets or asteroids. Many more distant satellites were discovered after 1951, but only three more, Thebe (JXIV), Adrastea (JXV), and Metis (JXVI), were discovered orbiting close to Jupiter in nearly circular orbits in Jupiter's equatorial plane (3–7).

The Galileo spacecraft encountered Amalthea with a closest-approach distance r_0 of about 244 km and flyby velocity v_0 of 18.3951 km s⁻¹. The primary goal of the encounter was the determination of Amalthea's mass and mean density through Doppler tracking. However, the spacecraft lost phase lock with the uplink S-Band radio signal during the flyby, so backup one-way Doppler, referenced to the ultrastable oscillator (USO), was recorded by an open-loop radio science receiver at DSS63 for an interval from closest approach to Amalthea (E) minus 684 s to E plus 455 s. We extracted the received carrier frequency from the one-way data at a sample interval of 1.0 s (1140 Doppler samples).

The one-way Doppler data can be fit with a simple flyby model for the Doppler velocity v_r , given by (8, 9)

$$v_r = -\frac{\mu}{rr_0v_0}(\alpha v_0 t - \beta r_0) \quad (1)$$

where μ is equal to the gravitational constant G times the mass of Amalthea, α is the direction cosine of the line of sight on the Amalthea-centered radius vector at closest ap-

proach, β is the direction cosine of the line of sight on the Amalthea-centered velocity vector at closest approach, and r is the Amalthea-spacecraft distance, approximated by

$$r = \sqrt{r_0^2 + v_0^2 t^2} \quad (2)$$

where t is measured from the time of closest approach t_0 . All parameters except r_0 and μ are well-known from the nominal flyby trajectory, with $\alpha = -0.585775$ and $\beta = -0.460834$.

We reduced the samples of received frequency ν to Doppler velocity by the conversion factor $v_r = -c\nu/v_0$, with the reference S-Band frequency ν_0 equal to 2.29513 GHz and c the speed of light. Next, a cubic polynomial was removed from the v_r data, and the resulting residuals were smoothed with a 10-point moving average. Finally, the residuals were isolated to the flyby region, ± 100 s from closest approach. The resulting reduced data are shown in Fig. 1. The solid line represents the minimum-variance fit for a quadratic polynomial plus the flyby model of Eq. 1. The polynomial accounts for drift in the USO over the 200-s interval and also for an integration constant for the velocity as derived from the μ/r^2 Newtonian acceleration projected on the line of sight. The results for the three flyby parameters of the fitting model are $\mu = 0.130 \pm 0.029$ km³ s⁻², $r_0 = 251 \pm 41$ km, and $t_0 = 1.99 \pm 0.89$ s, where the formal standard errors have been multiplied by $\sqrt{10}$ to account for the 10-point smoothing (formal errors are a factor of $\sqrt{10}$ too small because smoothed points are not independent). The quadratic polynomial is required to model the USO's random walk in frequency over the 200-s interval of the one-way data. A linear polynomial leaves systematic residuals, whereas a cubic polynomial does not improve the fit over the quadratic polynomial, in the sense that χ^2 for the residuals is not reduced. Although Amalthea is elongated, with a gravitational field approximated by a homogeneous ellipsoid, the residuals inferred from Fig. 1 show that there is no hope of inferring any gravity parameters other than the mass from the one-way Doppler data. No systematic signal in the residuals nearest to closest approach could possibly be attributed to higher degree gravity harmonics.

We also pursued a determination of the Amalthea mass by accounting for its effect on

¹Jet Propulsion Laboratory, California Institute of Technology, Pasadena, CA 91109–8099, USA. ²Department of Earth and Space Sciences, University of California, Los Angeles, CA 90095–1567, USA. ³Institute of Geophysics and Planetary Physics, Los Angeles, CA 90095–1567, USA. ⁴Center for Radio Physics and Space Research, Cornell University, Ithaca, NY 14853–4901, USA. ⁵Institute of Geodesy and Geophysics, Vienna University of Technology, A-1040 Vienna, Austria.

*To whom correspondence should be addressed. E-mail: john.d.anderson@jpl.nasa.gov

†Present address: Kinex, Inc. Space Navigation and Flight Dynamics, 21 West Easy Street, Suite 108, Simi Valley, CA 93065–1694, USA.

‡Present address: Austrian Research Centers, Seibersdorf Research GmbH, 2444 Seibersdorf, Austria.

Galileo's orbit, using only the two-way data recorded outside the closest approach. The result was similar to that obtained with the closest-approach data. We explored similar approaches with both the one-way and two-way data for several weeks after the encounter. However, the most comprehensive approach involved combining the Amalthea Doppler data with ground-based astrometric data, spacecraft-based astrometric data, and Deep Space Network Doppler data for a determination of parameters of the entire Jupiter system, including the orbits of the Galilean satellites and the four inner moons. One advantage of this approach is that the relative locations of Amalthea and the Galileo spacecraft are determined from the data, with an implicit determination of the closest-approach distance r_0 . The mass determination results from a statistical combination of both the 200-s one-way data at encounter and the two-way data outside the flyby region. The result yields a mass μ equal to $0.139 \pm 0.010 \text{ km}^3 \text{ s}^{-2}$, which we adopt. The error estimate is consistent with a value of χ^2 equal to the number of data points; hence, it is a realistic estimate of standard deviation for the parameters, including Amalthea's mass. The mass error is about a factor of 2 smaller than the determination from the one-way data alone. However, all three determinations, one-way only, two-way only, and combined one-way and two-way, are useful for purposes of cross-checking. The closest-approach distance is

obtained by subtracting the Amalthea inertial position from the spacecraft inertial position and finding the minimum distance. This yields a value of $244 \pm 11 \text{ km}$ for r_0 , consistent with the results from the one-way data alone. The time of closest approach, corresponding to r_0 , is 0.67 s later than the nominal closest-approach distance of Fig. 1.

Amalthea's volume was determined by imaging data from the two Voyager spacecraft and from Galileo (10). A digital topographic map was generated in the form of a table of radius versus latitude and longitude. From this table, we determined the volume to be $(2.43 \pm 0.22) \times 10^6 \text{ km}^3$. Division of μ by G (11) yields a mass of $(2.08 \pm 0.15) \times 10^{18} \text{ kg}$. The mass and volume yield a density of $(857 \pm 99) \text{ kg m}^{-3}$, where the error is a realistic estimate of the standard deviation on the density measurement. The possibility that Amalthea is solid water ice with a density of 930 kg m^{-3} is unlikely. If the measured density and its error bar are interpreted in terms of a normal probability density function, there is a 23% probability that Amalthea's density is greater than 930 kg m^{-3} . The probability that its density is greater than 1050 kg m^{-3} , typical of "dirty" water ice, is even smaller, only 2.6%. We thus suggest that Amalthea has a porous internal structure. Amalthea is highly elongated, with the principal axes having radial dimensions $a > b > c$, 125 by 73 by 64 km (10). The long axis always points to Jupiter. Although the

rotational centrifugal acceleration and Jupiter tidal forces reduce the surface acceleration appreciably near the sub- and antijovian points, the surface acceleration g is everywhere directed inward, even for a density as small as 750 kg m^{-3} . The topographic data show that the escape velocity from the surface varies widely from a minimum of 1 m s^{-1} to a maximum of 90 m s^{-1} . Here, escape is defined by ejecta that can reach a distance of 1000 km, remain detached long enough to mix with other ejecta, and eventually reimpact on the surface as homogenized ejecta. Amalthea has three areas with prominent brighter markings near the antijovian end (12). The coarse sampling of the shape model is unable to correlate these bright markings with low gravity and low escape velocity, but their locations are consistent with low g and a corresponding enhanced removal of materials.

Knowledge of the bulk density (also called mean density or simply density) places a strong constraint on the composition and internal structure of any planetary body. For smaller satellites and asteroids with low gravity, the role of porosity or void space is the major complicating factor in interpreting density information. Whether substantial porosity exists is also closely connected to a body's ability to maintain a nonspherical shape, because both depend on internal stresses and strengths of material (13). Satellites with volumes less than $\sim 10^7 \text{ km}^3$ have arbitrary and highly irregular shapes, with the ratio a/c of the long axis a to the short axis c ranging from 1.1 to 2.0 (14). In contrast, the dozen or so satellites with higher volumes are quite spherical ($a/c < 1.1$). The same pattern is evident in asteroids. The seven largest asteroids having volumes greater than $\sim 2 \times 10^7 \text{ km}^3$ are relatively spherical. One object, 511 Davida, does have $a/c = 1.4$ (15–17), but small asteroids such as Eros, with a volume of only $2.5 \times 10^3 \text{ km}^3$, are in general highly irregular (18).

This transition can be related to internal pressure and strength. A spherical object with 10^7 km^3 volume has a central pressure of $\sim 2.5 \text{ MPa}$ if composed of ice and $\sim 30 \text{ MPa}$ if made of anhydrous rock (density 3500 kg m^{-3}). The compressive strength of natural ice depends on its structure and impurities but is between ~ 1 and 5 MPa (19, 20). Rock strengths range from ~ 50 to 300 MPa (21). Thus, objects below a volume of $\sim 10^7 \text{ km}^3$ have pressures throughout their interiors that are much less than the strength of their constituent materials, whereas those with larger volumes have internal pressures capable of crushing or deforming icy materials. Amalthea's volume of $2.43 \times 10^6 \text{ km}^3$ and our reported density give an equivalent central pressure of $< 1 \text{ MPa}$, consistent with its shape and a/c of nearly two and implying that its internal stresses are considerably lower than the strength of even weak ice.

We thus suggest that Amalthea's low density results from both a relatively low-density materi-

Fig. 1. Reduced one-way radio Doppler data. The time tags for the plot are referenced to a nominal Amalthea closest-approach time of 5 November 2002, 07:02:25.95 UTC, ground receive time. The solid curve represents the best-fit flyby model with Amalthea mass μ , closest-approach distance r_0 , and closest-approach time t_0 as free parameters.

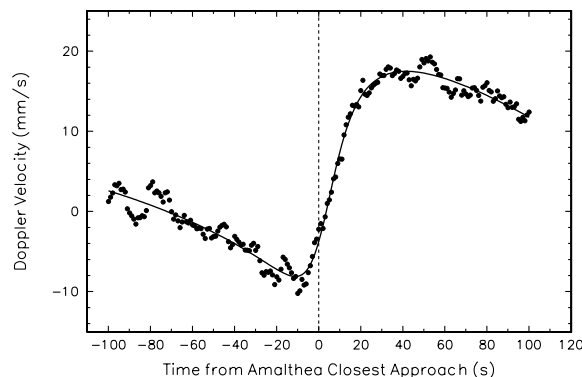
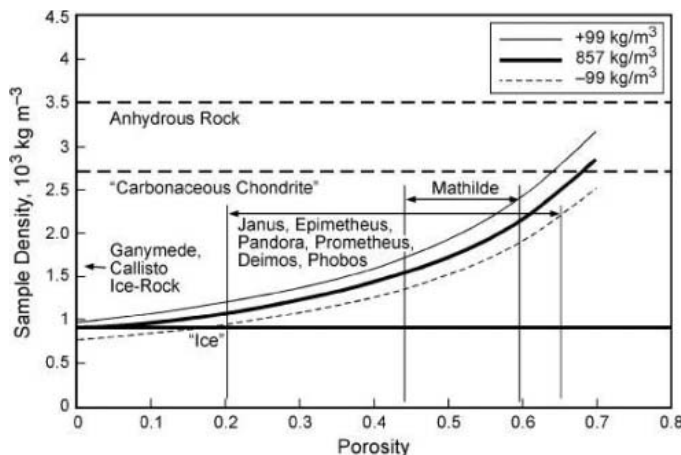


Fig. 2. Sample density versus porosity over a range of reasonable values for Amalthea. The heavy solid line represents the measured density, and the light lines indicate the ± 1 SD limits.



al composition, almost certainly icy, and bulk porosity, as shown in Fig. 2. As can be seen, a pure ice composition would require a low porosity (<0.1), whereas a rocky Amalthea would imply a porosity >0.7 . Both these end members are probably unrealistic. The range of plausible porosities known from other small satellites and asteroids would allow for an actual sample density for Amalthea from ~ 1200 to 2000 kg m^{-3} .

In all cases, water ice must be a major constituent, even for high porosity choices. Calculations of rock/ice ratios for Ganymede and Callisto imply an uncompressed density of $\sim 1600 \text{ kg m}^{-3}$ for the rock-ice material that formed these satellites, near the mid-range of plausible values for Amalthea.

Current Jupiter subnebula models imply that temperatures were high at Amalthea's current position when the Galilean satellites formed, inconsistent with their formation from water ice (22). We thus suggest that Amalthea was formed in a colder region. One possibility is that it formed later than the major satellites; another is that it formed farther from Jupiter, either beyond the orbit of Europa or in the solar nebula at or beyond Jupiter's po-

sition, and was then dynamically transported to or captured in its current inner orbit. Either alternative poses challenges for models of giant planet satellite formation.

References and Notes

- E. E. Barnard, *Astron. J.* **12**, 81 (1892).
- D. J. Tholen, V. G. Tejfel, A. N. Cox, in *Allen's Astrophysical Quantities Fourth Edition*, A. N. Cox, Ed. (Springer-Verlag, New York, 2000), pp. 302–310.
- D. C. Jewitt, G. E. Danielson, S. P. Synnott, *Science* **206**, 951 (1979).
- S. P. Synnott, *Science* **210**, 786 (1980).
- S. P. Synnott, *Science* **210**, 1392 (1980).
- S. P. Synnott, *Science* **212**, 191 (1981).
- S. P. Synnott, *Icarus* **58**, 178 (1984).
- J. D. Anderson, in *Physical Studies of Minor Planets*, T. Gehrels, ed. (NASA, Washington, DC, 1971), pp. 577–581.
- J. D. Anderson, G. Giampieri, *Icarus* **138**, 309 (1999).
- P. C. Thomas *et al.*, *Icarus* **135**, 360 (1998).
- Six measurements of G published after 1995 can be found in Gundlach and Merkowitz (23). We use their most accurate measurement of $G = (6.674215 \pm 0.000092) \times 10^{-11} \text{ m}^3 \text{ kg}^{-1} \text{ s}^{-2}$. The standard error includes both systematic error sources and statistical error for a total relative uncertainty of 13.7 parts per million.
- D. P. Simonelli *et al.*, *Icarus* **147**, 353 (2000).
- T. V. Johnson, T. R. McGetchin, *Icarus* **18**, 612 (1973).
- P. C. Thomas, J. Ververka, S. Dermott, in *Satellites*, J. A. Burns, M. S. Matthews, Eds. (University of Arizona Press, Tucson, AZ, 1986), pp. 802–835.
- J. D. Drummond, K. Hege, in *Asteroids II*, R. P. Binzel, T. Gehrels, M. S. Matthews, Eds. (University of Arizona Press, Tucson, AZ, 1989), pp. 171–191.
- R. L. Millis, D. W. Dunham, in *Asteroids II*, R. P. Binzel, T. Gehrels, M. S. Matthews, Eds. (University of Arizona Press, Tucson, AZ, 1989), pp. 148–170.
- C.-I. Lagerkvist, A. W. Harris, V. Zapala, in *Asteroids II*, R. P. Binzel, T. Gehrels, M. S. Matthews, Eds. (University of Arizona Press, Tucson, AZ, 1989), pp. 1162–1179.
- J. Veverka *et al.*, *Science* **289**, 2088 (2000).
- D. Deimand, V. Klovok, A Method for Producing Fine-Grained Ice from Snow by Compaction, ERDC/CRREL TR-01-12, U.S. Army Corps of Engineers (2001).
- Snow, Ice, and Permafrost Research Establishment, SIPRE Report 4, U.S. Army Corps of Engineers (1951).
- D. A. Lockner, in *A Handbook of Physical Constants, Rock Physics, and Phase Relations*, vol. 3, T. J. Ahrens, Ed. (American Geophysical Union, Washington, DC, 1995), pp. 127–147.
- R. M. Canup, W. R. Ward, *Astron. J.* **124**, 3404 (2002).
- J. H. Gundlach, S. M. Merkowitz, *Phys. Rev. Lett.* **85**, 2869 (2000).
- We thank the Galileo Mission Team for making this Amalthea experiment possible. We especially thank A. Anabtawi for coordinating the experiment and for leading the radio science operations. The JPL part of this work was performed at the Jet Propulsion Laboratory, California Institute of Technology, under contract with NASA. G.S. and W.B.M. acknowledge support from NASA grants through the Planetary Geology and Geophysics program.

31 January 2005; accepted 29 March 2005
10.1126/science.1110422

Direct Radiometric Dating of Hydrocarbon Deposits Using Rhenium-Osmium Isotopes

David Selby^{1,2*} and Robert A. Creaser¹

Rhenium-osmium (Re-Os) data from migrated hydrocarbons establish the timing of petroleum emplacement for the giant oil sand deposits of Alberta, Canada, at 112 ± 5.3 million years ago. This date does not support models that invoke oil generation and migration for these deposits in the Late Cretaceous. Most Re-Os data from a variety of deposits within the giant hydrocarbon system show similar characteristics, supporting the notion of a single source for these hydrocarbons. The Re-Os data disqualify Cretaceous rocks as the primary hydrocarbon source but suggest an origin from older source rocks. This approach should be applicable to dating oil deposits worldwide.

Uncertainties regarding the timing of emplacement and the source of major global hydrocarbon accumulations are common exploration questions (1). The decay of ^{187}Re to ^{187}Os is a useful chronometer and tracer (2, 3), and both elements are highly enriched in black shales (4–6), which are the crustal source rocks of many crude oils. We show that sufficient amounts of Re and Os are present in hydrocarbons to make the ^{187}Re - ^{187}Os radioisotope

system viable to constrain the timing of emplacement, and potentially the source, of migrated oils and their biodegraded products (oil sands). Thus, this method has widespread application to global petroleum systems.

We focused our study on the giant hydrocarbon deposits of the Western Canada Sedimentary Basin (WCSB), the world's second-largest oil sand reserve ($258.9 \times 10^9 \text{ m}^3$) (Fig. 1). The timing of generation and migration of oil across the WCSB and the identity of the source rocks have been uncertain and much debated (7–15). The oil sands and heavy oil deposits of the WCSB are hosted in the Lower Cretaceous Manville Group or equivalent sedimentary rocks [Aptian to Albian age, ~ 120 to 100 million years ago (Ma)] (16) (Fig.

1) and include the Athabasca-Wabasca, Peace River, Cold Lake, and Provost deposits. Heavy oil deposits are hosted by Cretaceous reservoirs at Lloydminster and in reservoirs of Paleozoic carbonate rocks beneath the Cretaceous rocks, known as the carbonate trend, which include the Grosmont deposit (Fig. 1). Oil is generally thought to have migrated from west to east in the WCSB as a result of the late Cretaceous Laramide orogeny (7–9, 17–19). Other studies predict that oil migration occurred tens of millions of years earlier (10, 11).

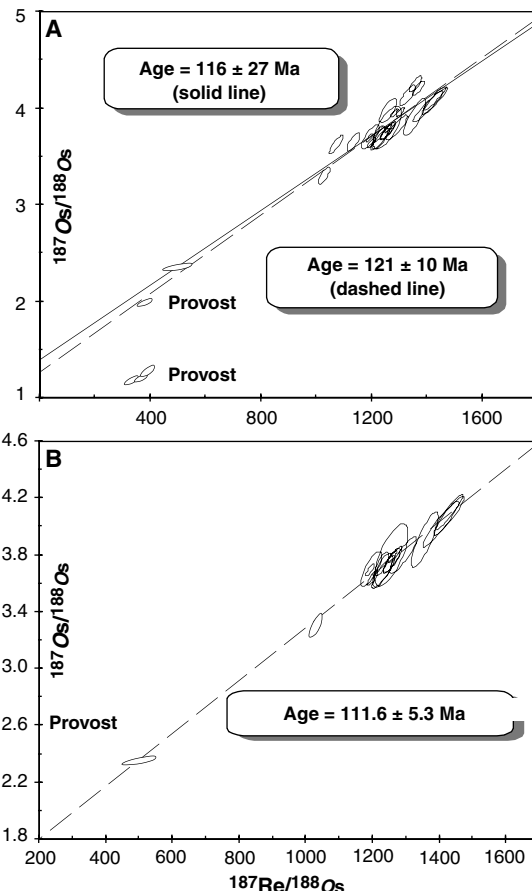
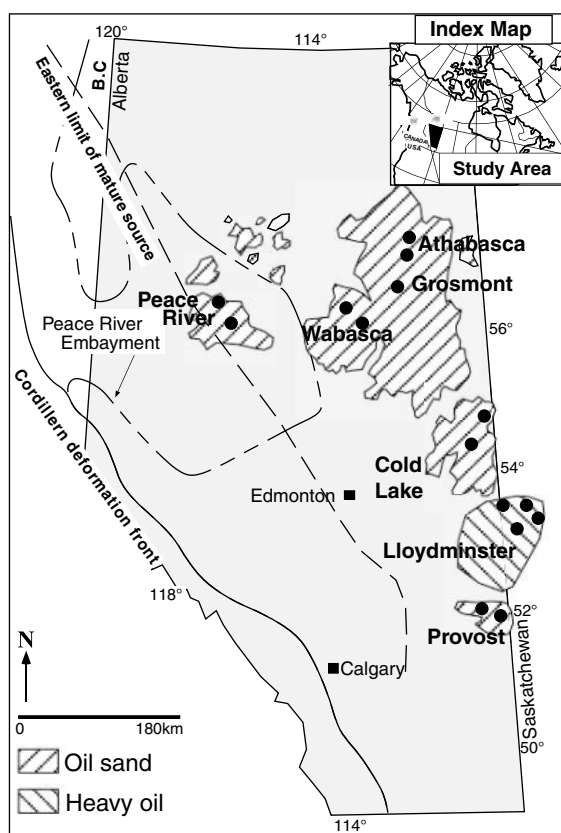
We collected samples from seven regional deposits within the larger giant oil sands deposit. We sampled and analyzed the same core interval or used an aliquant of material previously collected for organic geochemistry (Fig. 1 and table S1) (14, 20). The distinctive organic geochemistries of the samples have been interpreted to indicate the same or similar sources for all hydrocarbons, possibly the Paleozoic Exshaw Formation (21). Provost samples 1418 and 1431 also contain minor amounts of the so-called Q compounds [unusual polycyclic alkane and aromatic compounds (22)], known only from the Early Cretaceous Ostracode Zone source rocks, which suggests that the Provost deposit contains minor Ostracode Zone oil in addition to oil from the dominant source (22).

Our samples contain 3 to 50 parts per billion (ppb) Re and 25 to 290 parts per thousand (ppt) Os (table S1), which are abundances similar to typical organic-rich shale sources of crude oil [crustal abundances of silicate rocks are ~ 1 to 2 ppb Re and ~ 50 ppt Os (4–6, 23, 24)]. These findings lead us to infer that these elements

¹Department of Earth and Atmospheric Science, University of Alberta, Edmonton, Alberta, T6G 2E3, Canada. ²Department of Earth Sciences, University of Durham, Durham DH1 3LE, UK.

*To whom correspondence should be addressed. E-mail: dselby@ualberta.ca

Fig. 1 (left). Location map of the Alberta oil sand deposits. Black circles mark the sample locations. **Fig. 2 (right).** Re-Os isochron diagrams for the Alberta oil sand oil. **(A)** Regression of Re-Os data, not including that for Provost, yields a model 3 Re-Os date of 116 ± 27 Ma ($n = 24$, MSWD = 21, 2σ uncertainty) with an initial $^{187}\text{Os}/^{188}\text{Os}$ ratio of 1.40 ± 0.56 (solid line). By including Provost samples 1418 and 1431, an Re-Os date of 121 ± 10 Ma ($n = 26$, MSWD = 21, 2σ uncertainty, model 3) with an initial $^{187}\text{Os}/^{188}\text{Os}$ ratio of 1.29 ± 0.21 is determined (dashed line). **(B)** Seventeen samples have Os_{110} values of 1.4 to 1.5, which yield a date of 111.6 ± 5.3 Ma (MSWD = 2.2, model 3), with an initial $^{187}\text{Os}/^{188}\text{Os}$ ratio of 1.43 ± 0.11 (20).



are inherited from their organic-rich source rocks during oil generation and do not originate from crustal units during migration. In shale source rocks, Re and Os are known to be associated with organic matter (25), but the specific binding compounds are not known. Hydrocarbons analyzed for Re and Os in our samples were isolated by means of organic solvents and filtered to remove any mineral impurities (20). Thus, we also infer that Re and Os in oil are organically bound, possibly in the asphaltene fraction of oil in which many metals reside (26).

The $^{187}\text{Re}/^{188}\text{Os}$ ratios in our samples are high (350 to 1450), and the Os isotopic composition is radiogenic ($^{187}\text{Os}/^{188}\text{Os} \sim 1.2$ to 4.2; table S1). With the exception of samples from Provost that form two clusters with low $^{187}\text{Re}/^{188}\text{Os}$ ratios, all other samples from six deposit areas cluster with similar $^{187}\text{Re}/^{188}\text{Os}$ and $^{187}\text{Os}/^{188}\text{Os}$ ratios of 1000 to 1450 and 3.3 to 4.1, respectively, and these clusters define a shallow slope on an Re-Os isochron diagram (Fig. 2A). Regression of the latter Re-Os data, with the exception of the Provost samples, yields an Re-Os date of 116 ± 27 Ma [$n = 24$ samples, mean square weighted deviation (MSWD) = 21, 2σ uncertainty, model 3], with an initial $^{187}\text{Os}/^{188}\text{Os}$ ratio of 1.40 ± 0.56 (Fig. 2A). Two of the samples from Provost also plot close to this regression and, if included, the isochron age is 121 ± 10 Ma ($n = 26$,

MSWD = 21, 2σ) and the initial $^{187}\text{Os}/^{188}\text{Os}$ ratio is 1.29 ± 0.21 (Fig. 2A).

The high MSWD value (21) for the regressions indicates that scatter about the regression exists in excess of analytical uncertainties that relate to geological processes. For the requirements of an isochron to be met, the sample set must have formed at the same time, having the same initial Os isotope ratio and not having experienced disturbance by the gain or loss of Re and/or Os since formation (27). Given the high abundance of Re and Os in the hydrocarbons and the highly reducing nature of this substrate, disturbance of the Re-Os systematics in the hydrocarbon is unlikely. It is more plausible that given the giant size of this petroleum system, the processes of hydrocarbon migration did not fully homogenize the Re-Os isotope systematics of the produced and migrated oil. However, many samples have a similar initial $^{187}\text{Os}/^{188}\text{Os}$ value at 110 Ma (Os_{110}), which is the approximate age of the upper Manville Group reservoir units (28) and the age indicated by the Re-Os data. Seventeen of the samples have Os_{110} values of 1.4 to 1.5 (Fig. 3), and together yield a date of 111.6 ± 5.3 Ma (MSWD = 2.2, Model 3), with an initial $^{187}\text{Os}/^{188}\text{Os}$ value of 1.43 ± 0.11 (Fig. 2B). The date is within uncertainty of the date from all the Re-Os data but is more precise. Eight samples from several of the oil sand deposits have Os_{110} values >1.5 , which may

reflect another generation and migration history for the petroleum in these deposits or minor variation in source rock Re-Os characteristics. These eight samples yield a nominally older date, although it is within uncertainty of the ~ 112 -Ma date (126 ± 35 Ma, MSWD = 14). Three samples from Provost have considerably lower $^{187}\text{Re}/^{188}\text{Os}$ ratios and less radiogenic Os compositions, and they have lower Os_{110} values of 0.5 to 0.6; limited variation in the Re-Os data precludes determination of a date (table S1). However, samples 1418 and 1431 also have a similar organic geochemistry to that of the wider sample set, suggesting a predominant Exshaw source (14, 22). These complexities may suggest that hydrocarbons at Provost were generated in part from different sources. In addition, burial models predict that hydrocarbon generation began in the region west of Calgary at ~ 60 Ma (10, 11).

We suggest that the Re-Os data reflect emplacement of the giant hydrocarbon deposits of the eastern WCSB at ~ 112 Ma, and this implies that the oil found in the Paleozoic and Cretaceous reservoirs is primarily of the same generation and source. However, the specific mechanisms of isotopic resetting and equilibration for Re and Os isotopes in migrated hydrocarbons are not fully known. During oil generation, Re and Os sourced in the shale must have been partly transferred to the produced oil in order to record the high abundances of Re and

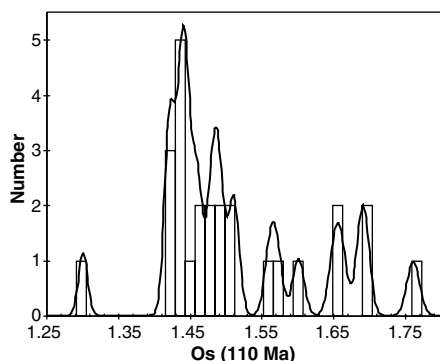


Fig. 3. A cumulative probability plot of Os_{110} values, including a 2σ absolute uncertainty of 0.01.

Os measured here. For shales that have generated oils, the process of hydrocarbon maturation does not grossly disturb the Re-Os isotope systematics of the matured shale source (5, 25, 29). Thus, no large fractionation of Re from Os between oil and the shale source likely occurs during oil generation, unless the Re and Os mass balance is dominated by retention of these elements in the shale, rendering detection of changes in Re/Os difficult. We suggest that the process of oil migration could be a mechanism for homogenizing any differences in $^{187}Re/^{188}Os$ and $^{187}Os/^{188}Os$ values of produced oil, reflecting small-scale source rock Re/Os variations (4–6, 25, 30), thereby effectively resetting the isotopic chronometer at this time. The ~112-Ma observed date reflects the time elapsed since this homogenization, but in turn requires the presence of a mechanism, perhaps organically based, that can fractionate Re/Os ratios in migrated hydrocarbons to some extent.

The date of ~112 Ma precludes the generation and migration of hydrocarbons and heavy oil during the late Cretaceous Laramide Orogeny at ~60 Ma (7–9, 13). The Re-Os date does support models of the burial history of west-central Alberta and British Columbia that predict petroleum generation and migration from Paleozoic strata source rocks in the Peace River Embayment area at ~110 Ma (10, 11). Numerical transport simulations of oil migration for the Athabasca oil sands (28) found that it would not be possible to migrate enough hydrocarbons to the oil sand reservoirs as a dissolved phase in the time after maximum burial in the Laramide (60 Ma), and that either hydrocarbon migration began earlier or oil transport was through a separate phase mechanism (or both).

The Re-Os emplacement age of ~112 Ma also indicates that the generation and migration of hydrocarbons in the Peace River Embayment in western WCSB were contemporaneous with Aptian-to-Albian sedimentation of the reservoir rocks more than 200 km to the east. This observation supports the inference that reservoir filling by hydrocarbons hampered or prevented lithification of the host rocks (10), and it implies

that the arrival of oil into the Cretaceous reservoir may have preceded deposition of the regional seal, the late Albian Joli Fou Shale (31). Further, the implied shallow depth of reservoir filling may have promoted biodegradation of oils within these unlithified reservoirs. This in turn may explain the lower levels of biodegradation of Lloydminster oils hosted by lithified Manville Group reservoirs, which are slightly older than other deposits to the north, based on palynomorph biostratigraphy (32).

Both single and multiple sources from both Mesozoic and Paleozoic strata have been proposed for WCSB oil. Most of the Re-Os data from deposits other than Provost are similar, supporting a predominantly single source (10, 11). The Cretaceous Clearwater black shale has been suggested as a source (12, 33), although it is considered unlikely because of mass balance calculations (34). During Cretaceous time, the $^{187}Os/^{188}Os$ ratio of seawater, which is recorded in deposited source shales and subsequently in migrated hydrocarbons, varied from ~0.3 to 0.8 (35). However, the Cretaceous Re-Os age indicated for oil of the WCSB hydrocarbon deposits is accompanied by a high initial $^{187}Os/^{188}Os$ value (~1.4), which requires that the source rock of these hydrocarbons be significantly older than Early Cretaceous (112 Ma) in order for the Os isotopic composition to evolve from typical Paleozoic-Mesozoic seawater values [~0.3 to 0.6 (35)] to ~1.4. More than 100 million years is required, on the basis of the typical range in $^{187}Re/^{188}Os$ and initial $^{187}Os/^{188}Os$ values for Paleozoic and Mesozoic black shales of western Canada. These data preclude Cretaceous shale as a source for the oil sands.

References and Notes

- B. St. John, *Sedimentary Basins of the World and Giant Hydrocarbon Accumulations* (American Association of Petroleum Geologists, Tulsa, OK, 1980).
- C. L. Allegre, J. M. Luck, *Earth Planet. Sci. Lett.* **48**, 148 (1980).
- S. B. Shirey, R. J. Walker, *Annu. Rev. Earth Planet. Sci. Lett.* **26**, 423 (1998).
- A. S. Cohen, A. L. Coe, J. M. Bartlett, C. J. Hawkesworth, *Earth Planet. Sci. Lett.* **167**, 159 (1999).
- R. A. Creaser, P. Sannigrahi, T. Chacko, D. Selby, *Geochim. Cosmochim. Acta* **66**, 3441 (2002).
- G. Ravizza, K. K. Turekian, *Geochim. Cosmochim. Acta* **53**, 3257 (1989).
- S. Cao, S. Bachu, *Use of a Quantitative Basin Analysis System in the Evaluation of Hydrocarbon Generation, Migration and Accumulation* (Proceedings of the World Petroleum Congress, Wiley, Chichester, UK, 1992).
- S. Creaney, J. Allan, in *Classic Petroleum Provinces*, J. Brooks, Ed. (Geological Society Special Publication, Blackwell Scientific, London, 1990), vol. 50, pp. 189–202.
- S. Creaney, J. Allan, in *Foreland Basins and Fold Belts*, R. W. MacQueen, D. A. Leckie, Eds. (American Association of Petroleum Geologists Memoir, 1992), vol. 55, pp. 279–308.
- D. Barson et al., *Hydrogeology of Heavy Oil and Tar Sand Deposits: Water Flow and Supply, Migration and Degradation, Field Trip Notes* (Geological Survey of Canada, 2000), Open File Report 3946.
- C. Riediger, S. Ness, M. Fowler, T. Akpulat, *GeoCanada 2000 CD Archive* (2000).

- G. Deroo, T. G. Powell, B. Tissot, R. G. McCrossan, *Geol. Surv. Can. Bull.* **262**, 136 (1977).
- S. Creaney et al., in *Geological Atlas of the Western Canada Sedimentary Basin*, G. D. Mossop, I. Shetsen, Eds. (Canadian Society of Petroleum Geologists and Alberta Research Council, Calgary, Canada, 1994), pp. 455–468.
- P. W. Brooks, M. G. Fowler, R. W. MacQueen, *Org. Geochem.* **12**, 519 (1988).
- P. W. Brooks, M. G. Fowler, R. W. MacQueen, in *Proceedings Eastern Oil Shale Symposium, November 15–17*, D. J. Lazar, Ed. (Institute for Mining and Minerals Research, University of Kentucky, Lexington, KY, 1989), pp. 104–111.
- J. W. Kramers, G. D. Mossop, *Geological Association of Canada/Mineralogical Association of Canada Annual Meeting, May 25–27* (1987), p. 48.
- M. T. Cioppa, I. S. Al-Aasm, D. T. A. Symons, K. P. Gillen, *Am. Assoc. Petrol. Geol. Bull.* **87**, 71 (2003).
- D. T. A. Symons, H. Pan, D. F. Sangster, E. C. Jowett, *Can. J. Earth Sci.* **30**, 1028 (1993).
- D. R. Issler, S. D. Willett, C. Beaumont, R. A. Donelick, A. M. Grist, *Bull. Can. Petrol. Geol.* **47**, 475 (1999).
- Materials and methods are available as supporting material on Science Online.
- The distinctive biomarker compositions of many samples used here, such as the carbon number distribution of steroidal alkanes (C27, C28, C29 diasteranes); the presence of 28,30-bisnorhopanes; and the relative abundances of 28,30-bisnorhopanes and gammacerane, as compared with 17 α (H)-hopanes (14), are interpreted to indicate the same or similar source for hydrocarbons (10, 11, 22).
- C. L. Riediger, M. G. Fowler, L. R. Snowdon, R. MacDonald, M. D. Sherwin, *Bull. Can. Petrol. Geol.* **47**, 43 (1999).
- W. Sun, V. C. Bennett, S. M. Eggins, V. S. Kamenetsky, R. J. Arculus, *Nature* **422**, 294 (2003).
- B. K. Esser, K. K. Turekian, *Geochim. Cosmochim. Acta* **57**, 3093 (1993).
- D. Selby, R. A. Creaser, *Chem. Geol.* **200**, 225 (2003).
- D. A. C. Manning, A. P. Gize, *The Role of Organic Matter in Ore Transport Processes*, M. H. Engel, S. A. Macko, Eds. (Plenum, New York, 1993).
- A. Dickin, *Radiogenic Isotope Geology* (Cambridge Univ. Press, Cambridge, 1995).
- J. J. Adams, B. J. Rostron, C. A. Mendoza, *Can. J. Earth Sci.* **41**, 1077 (2004).
- D. Selby, R. A. Creaser, *Geology*, in press.
- B. S. Kendall, R. A. Creaser, G. M. Ross, D. Selby, *Earth Planet. Sci. Lett.* **222**, 729 (2004).
- J. Allan, S. Creaney, *Bull. Can. Petrol. Geol.* **39**, 107 (1991).
- E. T. Burden, in *The Mesozoic of Middle North America*, D. F. Stott, D. J. Glass, Eds. (Canadian Society of Petroleum Geologists Memoir, Canada, 1984), vol. 9, pp. 249–269.
- J. A. Masters, in *Elmworth—Case Study of a Deep Basin Gas Field*, J. A. Masters, Ed. (American Association of Petroleum Geologists Memoir, Tulsa, OK, 1984), vol. 38, pp. 1–33.
- S. O. Moshier, D. W. Waples, *Am. Assoc. Petrol. Geol. Bull.* **69**, 161 (1985).
- B. Peucker-Ehrenbrink, G. Ravizza, *Terra Nova* **12**, 205 (2000).
- We thank C. Riediger, M. Fowler, J. Adams, and B. Rostron for sample donations and insightful discussions; three reviewers for helpful comments; and K. Nixon and S. Hagen for technical assistance. This research was supported by a Natural Sciences and Engineering Research Council (NSERC) Discovery Grant and an American Chemical Society Petroleum Research Fund Grant to R.A.C. and by NSERC and Alberta Ingenuity Postdoctoral Fellowships and Grants to D.S. The Radiogenic Isotope Facility at the University of Alberta is supported in part by an NSERC Major Facilities Access Grant.

Supporting Online Material

www.sciencemag.org/cgi/content/full/308/5726/1293/DC1

Materials and Methods

Table S1

References

15 February 2005; accepted 29 March 2005
10.1126/science.1111081

Simultaneous Inhibition and Redistribution of Spontaneous Light Emission in Photonic Crystals

Masayuki Fujita, Shigeki Takahashi, Yoshinori Tanaka, Takashi Asano, Susumu Noda*

Inhibiting spontaneous light emission and redistributing the energy into useful forms are desirable objectives for advances in various fields, including photonics, illuminations, displays, solar cells, and even quantum-information systems. We demonstrate both the “inhibition” and “redistribution” of spontaneous light emission by using two-dimensional (2D) photonic crystals, in which the refractive index is changed two-dimensionally. The overall spontaneous emission rate is found to be reduced by a factor of 5 as a result of the 2D photonic bandgap effect. Simultaneously, the light energy is redistributed from the 2D plane to the direction normal to the photonic crystal.

Spontaneous light emission is a fundamental factor (or bottleneck) limiting the performance of devices in various fields, including photonics (1), illuminations (2), displays (3), solar cells (4), and quantum-information systems (5). For example, in light-emitting diodes, spontaneous emission that is not extracted from the device contributes to losses. Similarly, in lasers, spontaneous emission that does not couple to the lasing mode results in both losses and noise. Therefore, inhibiting undesirable spontaneous light emission and redistributing (6) the energy into useful forms will allow advances in these fields. Three-dimensional (3D) photonic crystals (7–13),

which have a 3D periodic refractive-index distribution that eliminates the optical modes in all 3D directions via the photonic bandgap (PBG) effect, have been used to demonstrate the inhibition of spontaneous light emission (11, 13). However, redistribution of the energy has yet to be demonstrated.

Here, we investigate both the “inhibition” and “redistribution” of spontaneous light emission using 2D photonic crystals (14–19). These crystals are predicted to provide a

mechanism for controlling spontaneous emission, which reflects their 2D nature (14): The overall spontaneous emission rate is expected to decrease as a result of the inhibition of optical modes in all 2D directions by the 2D PBG effect, whereas the emission efficiency for the direction normal to the crystal (in which the 2D PBG effect does not appear) should increase via redistribution of the saved energy. Although an experimental trial has been reported recently (20), it is not clear whether the spontaneous emission is inhibited by the 2D PBG effect.

Spontaneous emission originates from fluctuations in the vacuum field. Under a weak light–matter coupling regime, the rate of spontaneous emission (R_{spont}) is given by Fermi’s golden rule (21) and is determined by the number of optical modes. In order to control spontaneous light emission, the optical modes must therefore be manipulated. Figure 1 shows the 2D photonic crystal used, in which a triangular-lattice 2D photonic crystal is formed in a semiconductor (GaInAsP) slab. The structure incorporates a single quantum well (QW) as the light-emitting material, emitting light with a transverse-electric (TE) polarization in which the dipole moment is orientated parallel to the slab plane (22). The optical modes in the thin slab can be categorized into two modes: “slab modes,” which are confined to

Department of Electronic Science and Engineering, Kyoto University, Katsura, Nishikyo-Ku, Kyoto 615-8510, Japan.

*To whom correspondence should be addressed. E-mail: snoda@kuee.kyoto-u.ac.jp

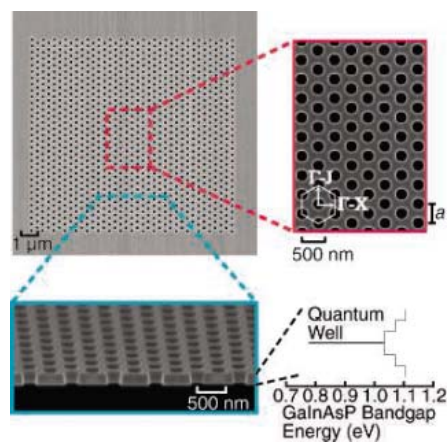


Fig. 1. The semiconductor (GaInAsP) 2D photonic-crystal slab. A scanning electron micrograph is shown. The 2D photonic-crystal slab has a triangular lattice structure with an air-hole radius r of $0.29a$ (lattice constant $a = 300$ to 500 nm) and a thickness of 245 nm. A 5 -nm-wide single QW is inserted at the center of the slab to form the light-emitting layer.

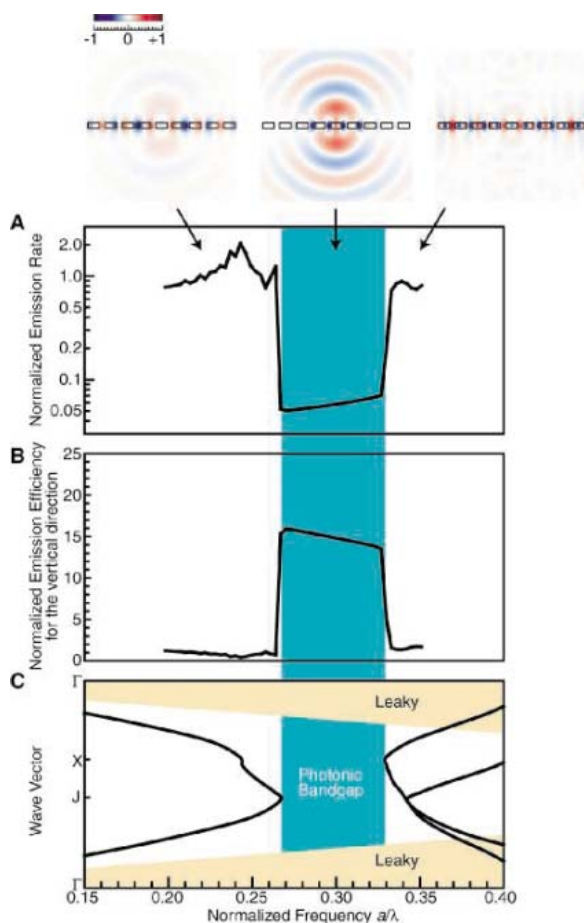


Fig. 2. Theoretical analyses of the effects of the 2D photonic-crystal slab (Fig. 1) on spontaneous-emission inhibition and energy redistribution. A flat semiconductor (GaInAsP) slab on a semiconductor (InP) substrate is used as a reference. The refractive index and thickness of the semiconductor slab are 3.27 and $0.6a$, respectively. The refractive index of the substrate and air are 3.13 and 1.0 , respectively. (A) Calculated spontaneous emission rate as a function of frequency, normalized by the result calculated for the reference structure. (B) Emission efficiency in the vertical direction for various frequencies, normalized by the results calculated for the reference. (Top) Schematic views illustrate how emission is controlled by the 2D PBG effect. The arrow denotes the corresponding frequency region. (C) Photonic-band diagram calculated by 3D FDTD using periodic boundary conditions. The solid lines show the dispersion relation of the 2D slab modes. The frequency region between 0.267 and 0.330 corresponds to the 2D PBG region. “Leaky” refers to the region in which the TIR condition is not satisfied and light is emitted outside the crystal surface.

the 2D plane by satisfying the total internal reflection (TIR) condition for the vertical direction, and “vertical modes,” which do not satisfy the TIR condition and are emitted outside the slab. Excited carriers that are confined in the QW generate spontaneous emission coupled to both slab and vertical modes, and the spontaneous emission rate (R_{spon}) can be expressed by

$$R_{\text{spon}} = R_{\text{slab}} + R_{\text{vertical}} \quad (1)$$

Here, R_{slab} and R_{vertical} denote the spontaneous emission rate for slab modes and vertical modes, respectively. For a semiconductor slab with a large refractive index that is surrounded by low-refractive index air cladding (Fig. 1), light is strongly confined within the slab, and the condition $R_{\text{slab}} \gg R_{\text{vertical}}$ is satisfied. Therefore, spontaneous emission from the QW is mostly coupled to the slab modes. However, when a 2D photonic-crystal structure is incorporated in the slab, R_{slab} is expected to be strongly reduced, whereas basically no modification of R_{vertical} occurs. As a result, a marked reduction in R_{spon} is expected through the reduction of R_{slab} . The 2D PBG is responsible for inhibiting emission into the slab modes so that photons emitted from the QW can only couple into the vertical

modes. Therefore, the efficiency of spontaneous emission in the vertical direction, which can be detected, will increase. These two effects—the reduction of R_{spon} due to the inhibition of spontaneous emission into 2D slab modes within the PBG and the increased emission efficiency of the vertical modes—will occur simultaneously. This implies that the 2D photonic crystal effectively redistributes the light energy from the 2D plane to the vertical direction.

We quantitatively investigated the spontaneous emission modification and energy redistribution within the 2D photonic-crystal structure. For these purposes, we calculated the spontaneous emission rate and the emission efficiency in the vertical direction using the 3D finite-difference time-domain (FDTD) method (23, 24) and normalized the results using values calculated for an equivalent structure without a photonic crystal. The details of the FDTD calculation are described in the supporting text (25). Figure 2, A and B, show the results, and Fig. 2C illustrates the corresponding photonic band diagram for the 2D photonic-crystal slab. Figure 2A shows that the spontaneous emission rate is reduced by more than a factor of 15 within the PBG region (blue region) compared with that outside the PBG

region. Simultaneously, the emission efficiency for the direction normal to the crystal (Fig. 2B) increases by more than a factor of 15 within the PBG region compared with that outside the PBG region. Schematic views of the cross-sectional electric field on such situations are shown also in Fig. 2, where a dipole oscillator is placed at one point on the slab and is continuously excited so that the total power emitted in all directions becomes constant for each case. When the emission wavelength is outside the PBG, emission normal to the crystal is weak because $R_{\text{slab}} \gg R_{\text{vertical}}$ and the energy is distributed mostly in the 2D slab modes. However, when the wavelength is within the PBG, emission normal to the crystal is increased notably, despite the small value of R_{vertical} , because emission into 2D slab modes is inhibited ($R_{\text{slab}} \sim 0$) and the energy is redistributed into vertical emission modes.

Our samples were fabricated using a combination of epitaxial growth, electron-beam lithography, plasma etching, and chemical etching (26). A series of samples were prepared on the same wafer, with the lattice constants a ranging from 300 to 500 nm in 10-nm intervals, in order to investigate a wide normalized-frequency range. The samples were optically pumped using a Ti-Al₂O₃ laser emitting at 980 nm with a pulse width of 2 ps and a repetition frequency of 2 MHz. The PBG region was at first estimated for each sample under a sufficiently strong excitation condition (10 W/cm² on average) (27). Then, the average laser power was reduced to 0.5 W/cm² so that only recombination processes in the QW involving emission of TE polarized light could occur, in order to satisfy the assumption made in the calculation. If the optical absorption coefficient of the slab is assumed to be 2×10^4 cm⁻¹, the excited-carrier density is estimated as $\sim 8 \times 10^{17}$ cm⁻³. Under the weak excitation condition, time-integrated emission spectra (Fig. 3A), which indicate the emission efficiency in the vertical direction, were measured at 4 K using a multichannel GaInAs detector system. Then, time-resolved emission measurements (Fig. 3B) were made at the same temperature using a time-correlated single-photon-counting system (28) incorporating a photomultiplier detector, where we collected spectra across the whole emission wavelength range, in order to measure the overall emission rate.

When the emission wavelength is within the PBG region (Fig. 3, A and B) ($a = 390$ to 480 nm), the spontaneous emission lifetime (which corresponds to $1/R_{\text{spon}}$) increases compared with that observed in structures not incorporating photonic crystals. Simultaneously, the emission efficiency increases in the direction normal to the crystal compared with that in structures not incorporating photonic crystals. In contrast, when the emission wave-

Fig. 3. Experimental results. (A) Time-integrated emission spectra for samples with a range of lattice constants between 350 and 500 nm. The blue cross-hatching denotes the PBG region. (B) Time-resolved photoluminescence measurements for various samples. When the spontaneous-emission spectrum lies within the PBG region, the emission lifetime increases by a factor of 5 relative to that observed when the spectrum lies outside the PBG region (and compared with that of the sample without a photonic-crystal structure). A corresponding increase in the light-emission efficiency in the vertical direction, where the PBG effect does not occur, is clearly observed in the PBG region, as seen in (A).

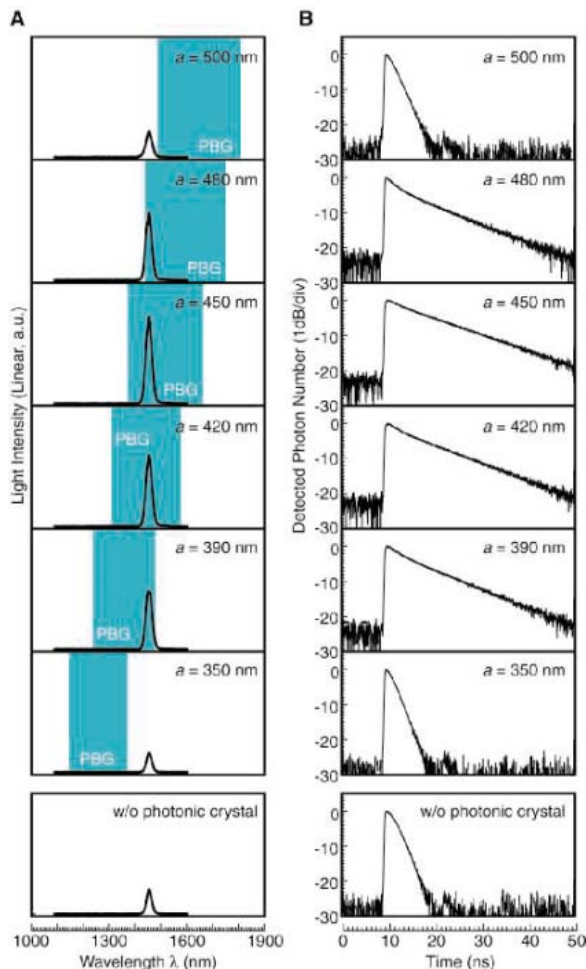
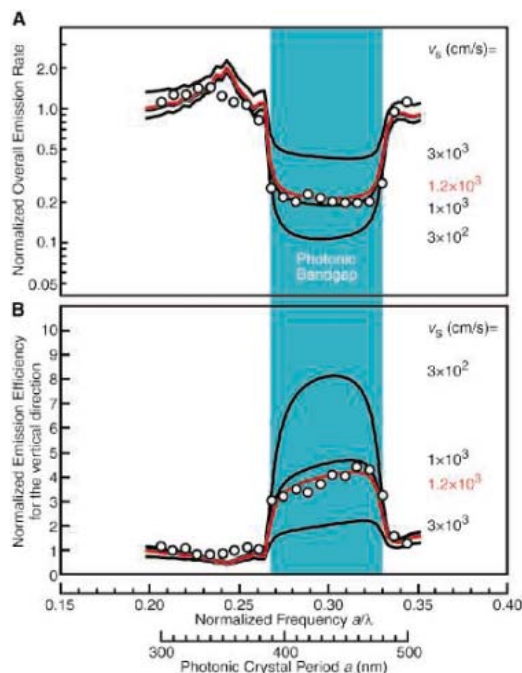


Fig. 4. Plots of the experimental results for a wide range of normalized frequencies (open circles). **(A)** Overall spontaneous-emission decay rates. **(B)** Emission efficiency in the direction normal to the crystal. The results were normalized by those for the reference sample without photonic crystals. The solid lines represent theoretically fitted results for a range of values of v_s . The experimentally observed inhomogeneous broadening of the emission spectra is accounted for in the calculation. The closest correspondence between the experimental results and theoretical curves is obtained for $v_s = 1.2 \times 10^3$ cm/s.



length lies outside the PBG (Fig. 3, A and B) ($a = 350$ and 500 nm), the spontaneous emission lifetime and the emission efficiency in the normal direction are both comparable to those observed in structures without photonic crystals. Figure 4 summarizes these results over a range of normalized frequencies (open circles) with the emission lifetimes converted to corresponding emission rates. The 2D PBG effect is clearly seen in Fig. 4A. The overall emission rate decreases by a factor of 5 within the PBG region compared with those outside the PBG region, and the increase in emission efficiency in the direction normal to the crystal is clearly seen in Fig. 4B. These results are in good agreement with the theoretical analyses shown in Fig. 2. Therefore, simultaneous inhibition and redistribution of spontaneous emission are successfully demonstrated by this experiment.

We also fitted the experimental results more quantitatively by considering the energy loss due to nonradiative recombination of excited carriers in the QW layer. Surface recombination is the most likely mechanism for nonradiative relaxation, and the rate (R_{non}) is proportional to the ratio of the exposed QW surface area (S_w) to its overall volume (V_w) (22), which is expressed as

$$R_{\text{non}} = \frac{S_w}{V_w} v_s = \frac{4\pi r}{\sqrt{3}a^2 - 2\pi r^2} v_s \quad (2)$$

Here, v_s is the surface-recombination velocity and r is the air-hole radius. The total recombination rate (R_T) is therefore expressed as

$$R_T = R_{\text{spon}} + R_{\text{non}} \quad (3)$$

The experimentally observed rate should be proportional to R_T . Similarly, the emission

efficiency for the direction normal to the photonic crystal can be modified in light of this nonradiative recombination process. Under these conditions, the experimental results can be fitted, as shown in Fig. 4, A and B. Lines have been drawn for various values of v_s . There is good agreement between the theoretical calculation and the experimental results for $v_s = 1.2 \times 10^3$ cm/s. This is a factor of 10 lower than typical values for GaInAsP (22) at room temperature and is consistent with the effects of sample cooling. We believe that similar values of v_s will be attainable at room temperature, with special treatment of the surface (29). The use of high-quality crystalline silicon, with surface-recombination velocities of less than 1 cm/s (30), might also be advantageous for the suppression of nonradiative processes, because it will lead to the realization of high-quality silicon-based photonic devices. Furthermore, applications for the control of thermal (or black body) emission would no longer be affected by surface-recombination processes.

We believe that our demonstration of simultaneous inhibition and redistribution of spontaneous light emission in photonic crystals is an important step toward the evolution of photonic devices and systems in various fields, including photonics, illuminations, displays, solar cells, and even quantum-information systems.

References and Notes

- B. E. A. Saleh, M. C. Teich, *Fundamentals of Photonics* (Wiley, New York, 1991).
- D. A. Steigerwald et al., *IEEE J. Sel. Top. Quantum Electron.* **8**, 310 (2002).
- K. Ziemelis, *Nature* **399**, 408 (1999).
- M. Grätzel, *Nature* **414**, 338 (2001).
- H. Mabuchi, A. C. Doherty, *Science* **298**, 1372 (2002).
- The term "redistributing" is used here to indicate that the energy, which is otherwise utilized (or

distributed) for undesirable spontaneous emission, is (re)distributed in more useful forms. In light-emitting diodes, this energy, which is otherwise distributed in spontaneous emission that cannot be extracted from a device, is (re)distributed in emission that can be extracted from the device. In lasers, the energy is redistributed into the lasing mode. In solar cells, the energy is redistributed for use as electrical energy.

- E. Yablonovitch, *Phys. Rev. Lett.* **58**, 2059 (1987).
- S. John, *Phys. Rev. Lett.* **58**, 2486 (1987).
- S. Noda, K. Tomoda, N. Yamamoto, A. Chutinan, *Science* **289**, 604 (2000).
- A. Blanco et al., *Nature* **405**, 437 (2000).
- S. Ogawa, M. Imada, S. Yoshimoto, M. Okano, S. Noda, *Science* **305**, 227 (2004).
- M. Qi et al., *Nature* **429**, 538 (2004).
- P. Lodahl et al., *Nature* **430**, 654 (2004).
- S. Fan, P. R. Villeneuve, J. D. Joannopoulos, *Phys. Rev. Lett.* **78**, 3294 (1997).
- O. Painter et al., *Science* **284**, 1819 (1999).
- M. Boroditsky et al., *J. Lightwave Technol.* **17**, 2096 (1999).
- S. Noda, A. Chutinan, M. Imada, *Nature* **407**, 608 (2000).
- S. Noda, Y. Yokoyama, M. Imada, A. Chutinan, M. Mochizuki, *Science* **293**, 1123 (2001).
- Y. Akahane, T. Asano, B. S. Song, S. Noda, *Nature* **425**, 944 (2003).
- H. Y. Ryu, Y. H. Lee, R. Sellin, D. Bimberg, *Appl. Phys. Lett.* **79**, 3573 (2001).
- R. Loudon, *The Quantum Theory of Light* (Oxford Univ. Press, New York, 2000).
- L. A. Coldren, S. W. Corzine, *Diode Lasers and Photonic Integrated Circuits* (Wiley, New York, 1995), pp. 148–153, 518–525.
- J. K. Hwang, H. Y. Ryu, Y. H. Lee, *Phys. Rev. B* **60**, 4688 (1999).
- R. K. Lee, Y. Xu, A. Yariv, *J. Opt. Soc. Am. B* **17**, 1438 (2000).
- The details of the FDTD method are presented as supporting material on Science Online.
- M. Fujita, A. Sugitatsu, T. Uesugi, S. Noda, *Jpn. J. Appl. Phys. Part 2* **43**, L1400 (2004).
- The PBG region is identified as follows. At the edges of the PBG (the upper and lower boundaries of the PBG region), the group velocity of light approaches zero and waves propagating in different directions in the slab couple in a type of 2D cavity resonator, resulting in standing-wave formation. Under sufficiently strong excitation, above the population-inversion threshold, a resonant peak is observed at the photonic band edge as a result of stimulated emission. In these experiments, we used an excitation intensity of 10 W/cm², which is 20 times as high as that used in the spontaneous emission-lifetime measurement, to obtain such a population inversion. In this way, we detected resonant peaks corresponding to the photonic band edges over a broad wavelength range. It was possible to fit the relation between the band-edge wavelength and the photonic-crystal period using a linear function, obtaining $\lambda_s = 2.28a + 350$ (nm) for the shorter wavelength band edge and $\lambda_l = 2.90a + 357$ (nm) for the longer wavelength band edge. These results are consistent with the 3D FDTD photonic band-diagram calculation.
- D. O' Connor, D. Phillips, *Time-Correlated Single Photon Counting* (Academic Press, London, 1985).
- E. Yablonovitch, C. J. Sandroff, R. Bhat, T. Gmitter, *Appl. Phys. Lett.* **51**, 439 (1987).
- E. Yablonovitch, D. L. Allara, C. C. Chang, T. Gmitter, T. B. Bright, *Phys. Rev. Lett.* **57**, 249 (1986).
- This work was partly supported by a Grant-in-Aid (no. 15GS0209) and an IT project grant from the Ministry of Education, Culture, Sports, Science and Technology of Japan, and by the Japan Science and Technology Corporation (CREST). M.F. was supported by a Research Fellowship of the Japan Society for the Promotion of Science (no. 15004417).

Supporting Online Material

www.sciencemag.org/cgi/content/full/308/5726/1296/DC1

SOM Text

Figs. S1 and S2

References and Notes

31 January 2005; accepted 4 April 2005
10.1126/science.1110417

Identifying Vibrations That Destabilize Crystals and Characterize the Glassy State

G. N. Greaves,¹ F. Meneau,^{1,2} O. Majérus,^{1,3} D. G. Jones,¹ J. Taylor⁴

High-resolution inelastic neutron scattering was used to identify major sources of low-frequency vibrations in zeolite crystals. Dispersed and nondispersed modes were found, both of which are prominent in the early stages of compressive amorphization but decline dramatically in strength once a glass of conventional density is created. By identifying the dispersed modes with the characteristic vibrations of the various secondary building units of zeolitic structures, the Boson peak, a characteristic of the glassy state, can be attributed to vibrations within connected rings of many different sizes. The nondispersed phonon features in zeolites, retained in the amorphized glass, were also replicated in silica. These modes are librational in origin and are responsible for destabilizing the microporous crystalline structure, for converting the resulting glass from a low- to a high-density phase, and for the associated changes in network topology that affect the Boson peak.

Vibrational states of crystals can be understood as phonon modes (*1*), but the origin and nature of vibrations in glasses are less well understood (*2*). However, crystalline and amorphous solids differ in a number of important ways, particularly in the low-frequency vibrational modes of these materials and the replacement of a periodic atomic potential by a complex energy landscape (*3*). For example, the excess specific heat of glasses at very low temperatures (<1 K) as compared with crystals can be understood in terms of tunneling states (*4, 5*). Formalized as two-level systems (TLSs), these are anharmonic modes and in silica glass can be modeled as librational vibrations (hindered rotations) coupling groups of tetrahedra (*6, 7*). At higher temperatures, however, the same motion enabled by the aperiodicity can be used to explain anharmonic relaxation processes with vibrational energies of 1 to 2 meV (*7*).

Another characteristic difference between crystals and glasses is the presence in the latter of a broad band of harmonic modes (between 4 and 12 meV in silica glass) called the Boson peak (BP) (*8*) that is rarely seen in crystals. Many spectroscopies (*4, 8–11*) reveal how the low-frequency vibrational density of states (VDOS) is enhanced compared to the Debye model (*12*), all of which have been variously attributed to large clusters (*13*), nanoparticles (*14*), floppy modes (*15*), mismatched rings (*16*), and the rocking of small tetra-

hedral groups (*11*). Common to many of these approaches is the anharmonic motion of atoms inherent in TLSs (*2, 3, 7, 16, 17*). Within the same band of frequencies, the BP evokes a rich phenomenology of propagating phonons (*18*), which can also be strongly scattered from static nanostructure fluctuations (*11*), both extended and localized acoustic modes combining with an excess density of optical modes (*19*). Experimentally, the magnitude of the BP is found to be greatest for strong glasses such as silica (*11, 20*) and to decline in strength as fragility increases (*21*). When the density of silica is reduced, however, the intensity of the BP increases further (*9, 10*), suggesting that the strength of the glass may also be increasing.

BP behavior has recently been observed in zeolite crystals (*9, 22*). These strong open-framework tetrahedral silicates have vast internal surfaces and are widely exploited in industry (*23*). Their low-density crystalline structures are constructed from a variety of secondary building units (SBUs), the most common being α cages, β cages, and double six rings (D6Rs) (*23*). Zeolite crystals are stabilized by water, which congregates mainly in the α cage, but once dehydrated, the low-density ordered structure is vulnerable to thermal and mechanical stress, disintegrating beyond a particular threshold (*24*). Zeolites are an excellent class of materials with which to examine catastrophic order-disorder transitions, because their crystalline structures, although complex, are now well-known (*25*), and the glasses and viscous melts into which they transform are also well-studied (*26*). We have reasoned that studies of the low-frequency vibrational properties of zeolites might provide insight into the structural origin of the characteristic features of glasses. To that end,

we have performed high-resolution inelastic neutron scattering (INS) studies of zeolite Y and of materials that form from it at different stages of amorphization.

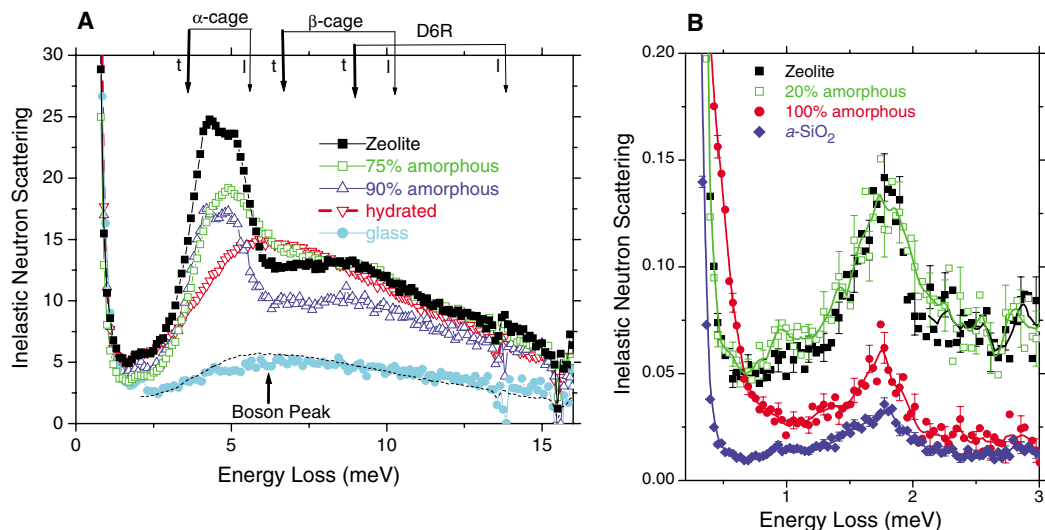
In zeolites, the compressive process that yields the amorphous state can be initiated by temperature or by pressure (*24*). The rate of zeolite collapse can be easily measured, increasing with the stress rate and revealing evidence of the presence of an intermediate low-density amorphous phase (LDA) before the final high-density amorphous phase (HDA) is reached. The coexistence of different glasses (or liquids) of the same composition but each having a different density—polyamorphism—has been advanced as the source of crystalline instability in amorphization (*27*). From in situ small and wide-angle x-ray scattering experiments, zeolite collapse appears to be followed by an LDA-HDA transition in the glassy state (*28*). In particular, the measured temperature dependence of the time for zeolites to collapse, τ_A , follows an Arrhenius dependence $\tau_A = \tau_0 e^{(H_A/k_B T)}$, where k_B is Boltzmann's constant and T is temperature. The activation energy H_A is approximately half that found in molten silica (*24*), which is indicative of a superstrong liquid. Moreover, the prefactor τ_0 lies between 10^{-11} and 10^{-12} s, suggesting that the zeolite structure may be destabilized by phonons with energies of a few milli-electron volts (*29*) that are in the low-frequency range where conventional glasses and crystals show marked differences (*4*).

Zeolite Y was thermally amorphized in three stages by heating at $10^\circ \text{ min}^{-1}$: first to 650°C (20%), then to 750°C (60%), and finally to 850°C (100%). The glass was made by quenching from the melt at 1300°C . A 90% amorphized specimen was fabricated in a multi-anvil press at 8 GPa for 5 hours. The degree of amorphization was obtained by comparing the intensity of x-ray diffraction powder patterns with that of the starting material. Before making INS measurements (*30*), specimens were dried at 300°C in a vacuum furnace for 5 hours.

INS spectra at 20 K with 0.8-meV resolution (Fig. 1A) compare zeolite Y with a glass of the same composition and with zeolite Y at different stages of thermal and pressure-induced amorphization. Zeolite Y exhibits a broad band centered around 6 meV, including a sharp doublet located at 4.5 meV and a wide maximum at around 9 meV. Both features are prominent in intermediate amorphized versions but are replaced in the glass by a BP with no sharp features. The spectrum for hydrated zeolite is also included in Fig. 1A, for which the 4.5-meV double peak in the anhydrous zeolite is absent, and the featureless band reaches a maximum around 6 meV. Indeed, if this band is rescaled downward, it provides an approximate envelope for the BP in the vitrified zeolite. A second feature is

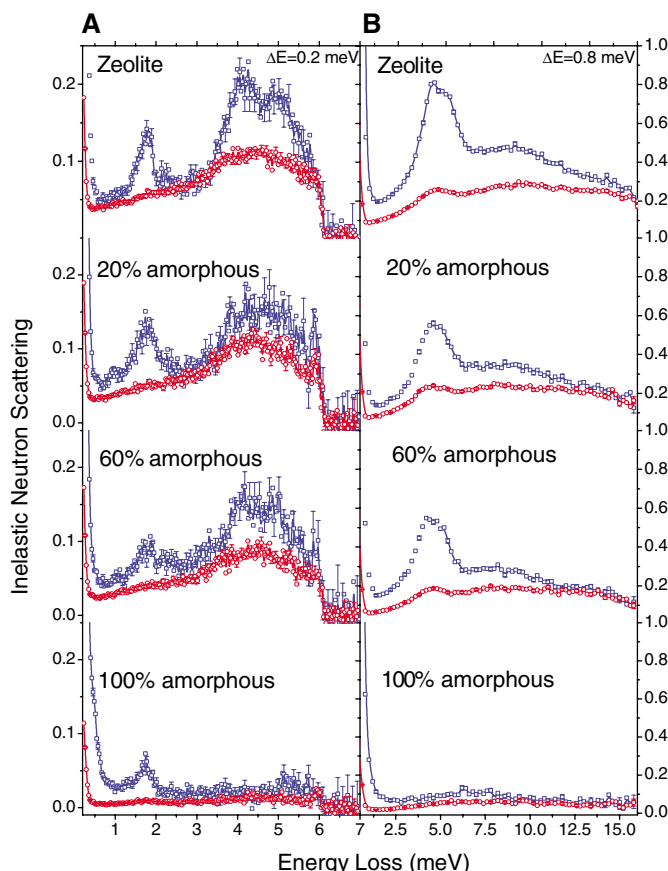
¹Institute of Mathematical and Physical Sciences, University of Wales, Aberystwyth, SY23 3BZ, UK. ²Netherlands Organisation for Scientific Research (NWO), DUBBLE CRG/ESRF, Post Office Box 220, F38043 Grenoble Cedex, France. ³Ecole Nationale Supérieure de Chimie de Paris, 11 rue Pierre et Marie Curie, 75231, Paris, France. ⁴ISIS Facility, Rutherford Appleton Laboratory, Chilton, OX11 0QX, UK.

Fig. 1. INS profiles at 20 K for anhydrous (black squares) and hydrated (red inverted triangles) Na zeolite Y ($\text{Na}_{56}\text{Al}_{56}\text{Si}_{136}\text{O}_{384}$) compared to partially amorphized anhydrous materials (green squares and purple triangles). Errors are given by the symbol size or plotted directly. **(A)** Data obtained using 17-meV neutrons with a Q range of 0.18 to 5.3 \AA^{-1} . All spectra are normalized by mass and the intensity scales with Q^2 , indicating sound-propagating acoustic modes. The full width at half maximum (FWHM) of the elastic line is 0.8 meV and defines the spectral resolution. The dispersed bands at 4.5 and 9 meV are absent from the hydrated zeolite as well as from the vitreous material (blue circles), which exhibits the BP expected in the glassy state, but are present even in the pressure-induced 90% amorphous material. The dotted curve is the featureless profile for hydrated zeolite scaled to the BP of the glass. The arrows indicate the fundamental transverse (t) and longitudinal (l) normal mode frequencies v_t/L and v_l/L for the SBUs in zeolite Y, where L is the circumference of the internal rings (20-fold, 12-fold, and 8-fold) and v_t and v_l are 3358 and 5181 ms^{-1} , respectively (32–35). **(B)** Data obtained using 8-meV neutrons with a Q range of 0.1 to 3.6 \AA^{-1} . All spectra are normalized by mass. The FWHM of the elastic line is 0.2 meV. INS intensities



of the 0.9- and 1.8-meV features scale with Q , which is indicative of nondispersed localized modes, which may correspond to eclipsed and staggered configurations. The integrated spectra of zeolites (black and green squares) change in strength with amorphization, with a significant component being retained once the material is 100% amorphized (red circles). A similar nondispersed band is also found in silica (blue diamonds). The 100% amorphized zeolite has a broader elastic line than the zeolite, suggesting an additional feature near 0.5 meV.

Fig. 2. Temperature dependence of INS profiles for Na zeolite Y and for various degrees of amorphization obtained using **(A)** 8-meV neutrons ($\Delta E = 0.2 \text{ meV}$) and **(B)** 17-meV neutrons ($\Delta E = 0.8 \text{ meV}$). All spectra are normalized by mass. The cutoffs at 6 meV in (A) and 12 meV in (B) relate, respectively, to the 8- and 17-meV neutrons used. Data were collected at 20 K (blue squares) and at 290 K (red circles) and were temperature-corrected for the Bose function. Error bars are shown at every fourth point or given by the symbol size. Where the BP in the amorphized zeolite scales closely with the Bose function, the other features in both dispersed and nondispersed bands do not, indicating substantial anharmonic character in the starting zeolite and during amorphization.



the strength of the low-frequency VDOS band in the starting zeolite as compared to the glass, the ratio in area being 8:1. Although this feature is reduced with increased amorphization,

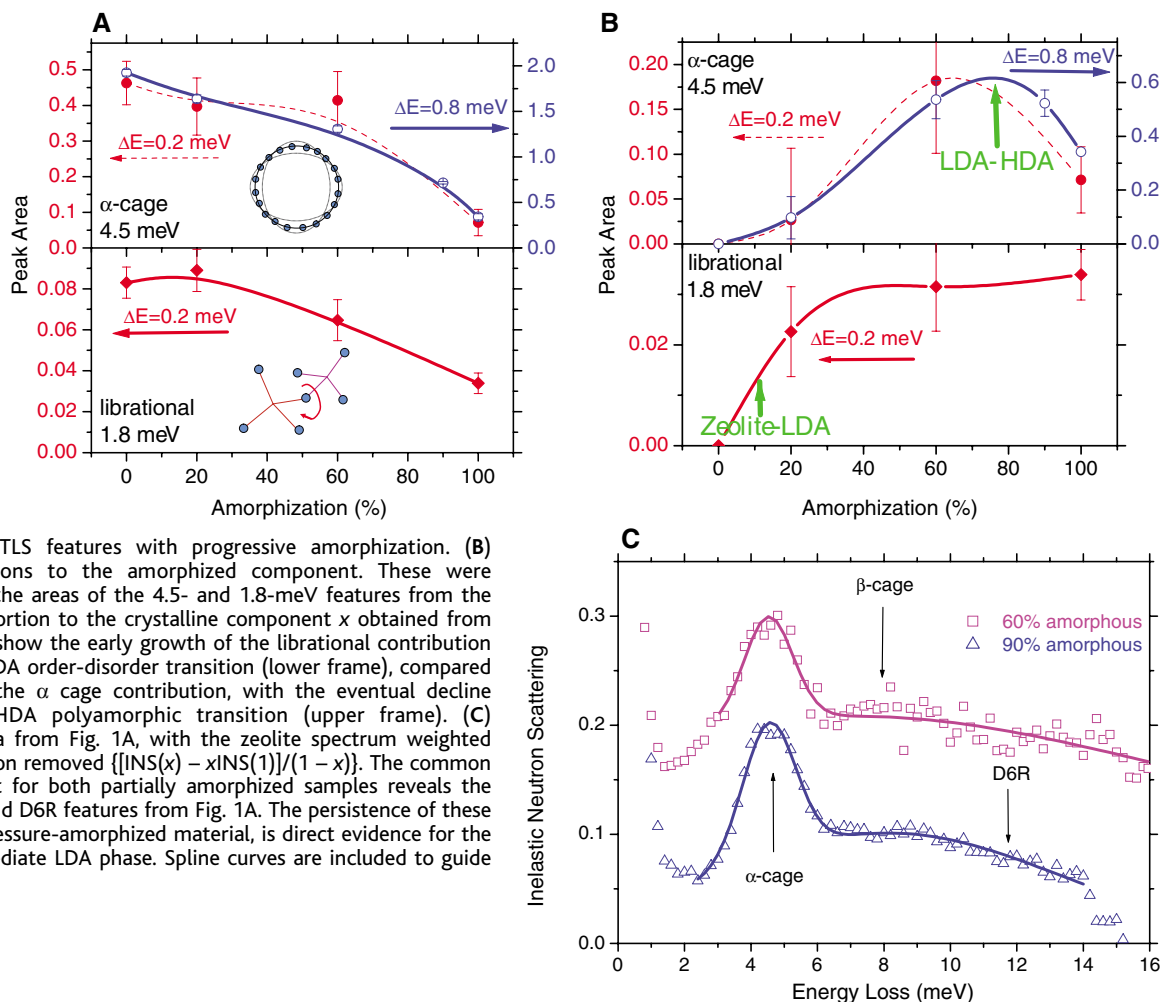
the enhancement is still more than 3:1, even when 90% of the zeolite has collapsed under pressure. Finally, all of the structure between 4 and 9 meV is highly dispersed, increasing

in intensity as Q^2 , where Q is the neutron momentum transfer.

Examples of INS spectra with higher resolution (0.2 meV) collected at 20 K from zeolite Y and amorphized versions are shown in Fig. 1B. These comprise a new and narrow band at 1.8 meV, with a shoulder at 0.9 meV: a splitting of 0.9 meV or 2 K. Furthermore, although this feature declines in strength with zeolite collapse by about a factor approaching 3, unlike the dispersed bands in Fig. 1A, the low-frequency structure in Fig. 1B can also be found in the 100% amorphized material. Moreover, we find similar nondispersed bands in silica, albeit further diminished in strength but, at 20 K, noticeably stronger than the corresponding BP. In contrast to the structure illustrated in Fig. 1A, which is dispersed, all of the features between 0.8 and 2.7 meV in Fig. 1B are strongly nondispersed, the scattered intensity increasing linearly with Q .

The temperature dependencies of low- and high-resolution INS spectra are shown in Fig. 2, where data collected at 20 and 290 K are compared after temperature correction. The BP in the fully amorphized zeolite approximately scales with the Bose function, reflecting the harmonic behavior reported for the BP in conventional glasses (3, 8), from which the BP gets its name. However, the enhanced features found at low temperatures in the zeolite or its intermediate amorphized versions scale far less rapidly with temperature, which indicates anharmonic character. Similar behavior occurs for the nondispersed band at 1.8 meV, which virtually disappears at 290 K.

Fig. 3. Nonlinear changes in the strength of the dispersed BP 4.5-meV band (upper frames) and the nondispersed TLS 1.8-meV band (lower frames) in Na zeolite Y. The behavior of the BP feature shown in the upper frames illustrates consistency between 0.2-meV- and 0.8-meV-resolution data: the dashed and solid curves, respectively. (A) Integrated areas under 4.5- and 1.8-meV peaks from Figs. 1 and 2, showing the nonlinear decline in the BP and TLS features with progressive amorphization. (B) Anharmonic contributions to the amorphized component. These were obtained by removing the areas of the 4.5- and 1.8-meV features from the starting zeolite in proportion to the crystalline component x obtained from x-ray diffraction. They show the early growth of the librational contribution related to the zeolite-LDA order-disorder transition (lower frame), compared to the slower rise in the α cage contribution, with the eventual decline pointing to an LDA-HDA polyamorphic transition (upper frame). (C) Normalized INS spectra from Fig. 1A, with the zeolite spectrum weighted by the crystalline fraction removed $\{[\text{INS}(x) - x\text{INS}(1)]/(1 - x)\}$. The common amorphized component for both partially amorphized samples reveals the same α -cage, β -cage, and D6R features from Fig. 1A. The persistence of these modes, even in 90% pressure-amorphized material, is direct evidence for the existence of an intermediate LDA phase. Spline curves are included to guide the eye.



The VDOS at high frequencies in silicates is dominated by the stretching and bending modes associated with nearest neighbors in corner-sharing tetrahedra (26), whereas the modes that contribute to the BP and TLS have been attributed to groups of tetrahedra and the linkages between them (4–9, 11, 13–17). In zeolites, the obvious candidates for these larger units are the SBUs that characterize the low-density structures and the oxygen bridges that link them. Because SBUs selectively adsorb small molecules, the absence of the sharp double peak at 4.5 meV in hydrated zeolite Y (Fig. 1A) is interesting, because clathrated water condenses in the α cages (23), where it is expected to stiffen the supercage structure. Thus, if the 4.5-meV feature in anhydrous zeolite Y is attributed to α -cage dynamics, the remaining low-frequency band out to 15 meV may reasonably be associated with oscillations in the β cage and D6R SBUs.

Clearer evidence for the assignments in Fig. 1A lie in the different sizes of SBUs. The SBU surfaces of zeolite Y are made up of planar fourfold and sixfold rings, but these units are circumscribed by much larger puckered rings, such as 20-fold, 12-fold, and 8-fold

rings for the α -cage, β -cage, and D6R units, respectively. To a first approximation, the frequencies of the fundamental normal modes for these large rings are given by v_t/L and v_l/L , where v_t and v_l are the transverse and longitudinal velocities of sound in the zeolite and L is the circumference of the ring. Ring frequencies for zeolite Y lie between 4 and 14 meV (35), as indicated in Fig. 1A. The association of the 4.5-meV doublet with α cages is confirmed, as are the peaks at 6, 9, and 14 meV with β cages and D6Rs. In zeolites, SBUs are not independent units but are interconnected, and so vibrations can be expected to be anharmonic, explaining the non-Bose temperature dependence of the low-frequency bands illustrated in Fig. 2.

With the assignments made in Fig. 1A, the decline in strength of the low-frequency structure can be used to follow the collapse of the SBUs to the silica-like structure of the vitreous zeolite when the baseline BP is reached (Fig. 2B). The weight of these features decreases nonlinearly, as exemplified by the reduction of the 4.5-meV peak area with amorphization (Fig. 3A, upper frame). The same data are replotted in Fig. 3B with the zeolite Y crystalline component removed.

The 4.5-meV peak reaches a maximum when more than 70% of the zeolite has collapsed, signifying the retention of α -cage units in the initial amorphous component. Corresponding spectra for the amorphous component remaining at intermediate stages of amorphization are shown in Fig. 3C. These spectra are identical within experimental error. The 4.5-meV peak remains prominent, as do the shoulders around 9 and 14 meV, which shows that in addition to the α cage, significant remnants of β -cage and D6R SBUs are also retained in the initial amorphous phase. Contrasting the spectra in Fig. 3C with the diminutive BP in the final amorphized product in Fig. 2, we see that at intermediate stages, the initial amorphized material incorporates low-density SBUs that eventually collapse when the final glass is formed. This result provides strong evidence for an intermediate LDA phase as well as for an LDA-HDA transition (24, 28, 29), as indicated in the upper frame of Fig. 3B.

Moreover, the assignment of the dispersed band between 4 and 15 meV with the large rings that define the zeolitic SBUs confers new meaning on the origin of the BP in the glassy state. From Fig. 1A, this feature can be attributed to the coupling of oscillations

between connected rings of many sizes, including the large 12-fold and 20-fold rings from the SBUs. In conventional ring-counting schemes, these are degenerate with the smaller four- and sixfold rings and would normally be ignored, but they explain the extension of the BP to lower frequencies. With smaller rings contributing to the higher frequencies, the variety of ring sizes is expected to result in inhomogeneities in strain across the amorphous network, an assumption frequently made in modeling the BP (13). Furthermore, the INS Q^2 dependence confirms the predominance of propagating acoustic phonons across the network and is also in agreement with the results of inelastic x-ray scattering experiments on simple glasses at BP frequencies (18).

Turning finally to the band of nondispersed oscillations shown in Fig. 1B, we attribute these features to librational modes between coupled tetrahedra predicted in silica glass at these frequencies (7). This interpretation is further supported by the linear INS Q dependence pointing to localization and the non-Bose temperature dependence indicative of anharmonicity. These properties, coupled with the acoustic phonon characteristics of the BP, also accord with an alternative view (11, 36, 37) that the BP maximum marks a Ioffe-Regel crossover (38) from localized band-tail states to propagating sound states. In the context of microporous silicate structures, librational modes will be particularly important at the linkages between SBUs and may create numerous sources of potential instability. Notably, the energy of the nondispersed band—1 to 2 meV—approximates to h/τ_0 (where h is Planck's constant) and therefore appears to be directly coupled with zeolite collapse. In particular, the decline in the strength of the 1.8-meV peak with amorphization is plotted in the lower frame of Fig. 3A and is clearly nonlinear but also different from the behavior of the 4.5-meV peak attributed to α -cage dynamics plotted above. The amorphous component obtained from Fig. 3A by removing the zeolite fraction shown in the lower frame of Fig. 3B rises rapidly to a plateau earlier than the growth of the 4.5-meV α -cage feature. This suggests that it is the librational modes that initiate the order-disorder transition of the zeolite to an LDA phase. Rotational motion promotes buckling in silicate glasses (7, 16) and in this zeolite-LDA transition should leave the ring topology of the SBUs initially intact, together with chemical ordering, which we have proposed elsewhere (24) characterizes the superstrong LDA phase in zeolite amorphization. Eventually, as amorphization advances, bonds will be broken in the transition to the final glass, chemical order will be lost, and the large rings of the SBUs will be subsumed into the three-dimensional network of the HDA phase,

with an accompanying fall in the size of the BP (Fig. 3B) and in the strength of the glass.

We believe that the low-frequency modes in zeolitic materials reported here offer insights into the way large density differences between crystalline and amorphous networks are correlated through ring topology and conformational dynamics. Moreover, because conventional glasses exhibit enhanced specific heat at very low temperatures (4), we anticipate that this effect will be dramatically enlarged in zeolites and the LDA phases that initially form during amorphization, the sharp librational modes cutting into the fluctuating microporous energy landscape (31, 39) to create anharmonic tunneling TLS states. More generally, we expect that giant soft phonon bands are a common feature of all microporous materials, crystalline or glassy, and lie at the heart of the nanoscale instabilities that threaten their functionality in industrial applications.

References and Notes

- M. Born, K. Huang, *Dynamical Theory of Crystal Lattices* (Clarendon, Oxford, 1954).
- S. R. Elliott, *Physics of Amorphous Materials* (Longman, New York, 1990).
- D. J. Wales, *Energy Landscapes* (Cambridge Univ. Press, Cambridge, 2003).
- W. A. Phillips, *Amorphous Solids: Low Temperature Properties* (Springer-Verlag, Berlin, 1981).
- P. W. Anderson, B. I. Halperin, C. M. Varma, *Philos. Mag.* **25**, 1 (1972).
- U. Buchenau, H. M. Zhou, N. Nücker, K. S. Gilroy, W. A. Phillips, *Phys. Rev. Lett.* **60**, 1318 (1988).
- U. Buchenau et al., *Phys. Rev. B* **34**, 5665 (1986).
- C. A. Angell, K. L. Ngai, G. B. McKenna, P. F. McMillan, S. W. Martin, *J. Appl. Phys.* **88**, 3113 (2000).
- J. Boerio-Goates, R. Stevens, B. Lang, B. F. Woodfield, *J. Therm. Anal. Calorimetry* **69**, 773 (2002).
- Y. Inamura et al., *J. Non-Cryst. Solids* **293-295**, 389 (2001).
- E. Courtens, M. Foret, B. Hehlen, R. Vacher, *Solid State Commun.* **117**, 187 (2001).
- At low temperatures T and frequencies ω , the Debye model (1) predicts that C_p/T^3 and $V\text{DOS}/\omega^2$ are constant, where C_p is the specific heat. The BP is observed as a broad feature reaching a maximum in silica glass around 10 K or 5 meV (11).
- S. R. Elliott, *Europhys. Lett.* **19**, 201 (1992).
- E. Duval, A. Boukenter, B. Champagnon, *Phys. Rev. Lett.* **56**, 2052 (1986).
- M. T. Dove et al., *Phys. Rev. Lett.* **78**, 1070 (1997).
- M. Nakamura, M. Arai, Y. Inamura, T. Otomo, S. M. Bennington, *Phys. Rev. B* **66**, 024203 (2002).
- C. A. Angell, *J. Phys. Condens. Matter* **12**, 6463 (2000).
- F. Sette, M. H. Krisch, C. Masciovecchio, G. Ruocco, G. Monaco, *Science* **280**, 1550 (1998).
- B. Hehlen et al., *Phys. Rev. Lett.* **84**, 5355 (2000).
- A. P. Sokolov et al., *Phys. Rev. Lett.* **78**, 2405 (1997).
- The fragility of supercooled glass-forming liquids can be judged from the steepness index $[\partial \ln \eta / \partial (T_g/T)]$ of the temperature dependence of the viscosity η , or the structural relaxation time τ , at glass transition temperature T_g (40). This follows the convention of scaling reciprocal temperature to T_g/T (41, 42) in order to obtain universal plots for different glass-forming liquids. Typically, the steepness index falls in the range from 0.2 for van der Waals glasses down to 0.05 for silica, with superstrong glasses being significantly lower (24).
- A. B. Mukhopadhyay, C. Oligschleger, M. Dolg, *Phys. Rev. B* **69**, 012202 (2004).
- A. Dyer, *An Introduction to Zeolite Molecular Sieves* (Wiley, New York, 1988).
- G. N. Greaves et al., *Nat. Mater.* **2**, 622 (2003).
- J. V. Smith, *ACS Symp. Ser.* **101**, 170 (1971).
- Reviews in Mineralogy*, vol. 32, *Structure, Dynamics and Properties of Silicate Melts*, J. F. Stebbins, P. F. McMillan, D. B. Dingwell, Eds. (Mineralogical Society of America, Washington, DC, 1995).

- E. G. Ponyatovsky, O. I. Barkolov, *Mater. Sci. Rep.* **8**, 147 (1992).
- F. Meneau, G. N. Greaves, *Nucl. Instrum. Methods B*, in press.
- G. N. Greaves, F. Meneau, *J. Phys. Condens. Matter* **16**, 1 (2004).
- X-ray diffraction powder patterns were obtained on the NWO beamline at the European Synchrotron Radiation Facility (ESRF) in order to determine the crystalline fraction x and hence the degree of amorphization $1-x$. INS experiments were performed on MARI at the ISIS spallation neutron source at Rutherford Appleton Laboratory. Two neutron energies were chosen to obtain different energy resolutions: 17 meV [$\Delta E = 0.8$ meV, where ΔE is the measured FWHM of the elastic line] and 8 meV ($\Delta E = 0.2$ meV). With machine currents of ~ 170 μA , data collection times were typically 12 hours. Data were collected at 20 K and also at 290 K; samples were placed in the cryostat within 5 min of being removed from the drying oven, in order to minimize water contamination. One undried specimen was also measured. For ordered crystals, the experimental geometry used was sensitive only to transverse phonons. However, for polycrystalline zeolites, where the charge-compensating cations are known to distort the framework (37), we can expect substantial coupling between longitudinal and transverse modes. The longitudinal and transverse sound velocities in isotropic materials, v_l and v_t , are directly related to the elastic stiffness coefficients c_{11} and c_{44} and the density ρ , by $v_l = \sqrt{c_{11}/\rho}$ and $v_t = \sqrt{c_{44}/\rho}$, respectively. Zeolites are micrometer-sized powders, making direct measurements of stress coefficients impracticable. For hydrostatic stress, though, the compressibility β , which equals $3/(3c_{11} - 4c_{44})$, can be determined with in situ x-ray diffraction. In particular, we have shown how $\beta(P)$ for zeolites decreases linearly with increasing pressure (24), from which values of $\beta(0) = 0.042 \pm 0.005$ GPa^{-1} can be obtained by extrapolation. Values for v_l and v_t of 5181 and 3358 ms^{-1} , respectively, have been computed for the orthorhombic zeolite ZSM-5 (32). With little anisotropy observed, these yield a figure for β of 0.047 GPa^{-1} in ZSM-5, in close agreement with our measurements of cubic zeolites. Accordingly, with only a 10% difference in density between ZSM-5 and zeolite Y, we have adopted the above values for v_l and v_t in analyzing the newly discovered bands of low-frequency modes.
- E. Dooryhee et al., *J. Phys. Chem.* **95**, 1229 (1991).
- These values of v_l and v_t were obtained from molecular dynamics calculations (33) using potentials designed by Vashishta (34), which have been shown to reproduce realistic physical constants for silicate systems.
- A. B. Mukhopadhyay, C. Oligschleger, M. Dolg, *Phys. Rev. B* **68**, 024205 (2003).
- P. Vashishta, R. K. Kalia, J. P. Rino, *Phys. Rev. B* **41**, 12197 (1990).
- Diameters D of 20-fold α -cage rings, 12-fold β -cage rings, and 8-fold rings in D6R SBUs are 11.8, 6.6, and 4.9 Å, respectively (23). Taking $v_t = 3358$ ms^{-1} and $v_l = 5181$ ms^{-1} (32), the corresponding normal modes of isolated rings $v_l r/\pi D$ are 3.7, 6.7, and 9.0 meV for transverse sound and 5.7, 10.3, and 13.9 meV for longitudinal sound, respectively, marked t and l in Fig. 1A.
- S. Taraskin, S. R. Elliott, *Europhys. Lett.* **39**, 37 (1997).
- S. Taraskin, S. R. Elliott, *Phys. Rev. B* **59**, 8572 (1999).
- A. F. Ioffe, A. R. Regel, *Prog. Semicond.* **4**, 237 (1960).
- K. D. Hammonds, H. Dong, V. Heine, M. T. Dove, *Phys. Rev. Lett.* **78**, 3701 (1997).
- R. Böhmer, C. A. Angell, in *Disorder Effects on Relaxation Processes*, R. Richert, A. Blumen, Eds. (Springer, Berlin, 1994), pp. 11–54.
- Von Werner Oldekop, *Glasstechnische Berichte* **30** (1957).
- W. T. Laughlin, D. R. Uhlmann, *J. Phys. Chem.* **76**, 2317 (1972).
- We thank the Council for the Central Laboratories for the Research Councils for providing inelastic neutron facilities on ISIS at the Rutherford Appleton Laboratories, UK. We are also grateful to NWO and the ESRF at Grenoble, France, for x-ray facilities on the DUBBLE beamline.

5 January 2005; accepted 4 April 2005
10.1126/science.1109411

The Importance of Threading Dislocations on the Motion of Domain Boundaries in Thin Films

Farid El Gabaly,¹ Wai Li W. Ling,² Kevin F. McCarty,²
Juan de la Figuera^{1*}

Thin films often present domain structures whose detailed evolution is a subject of debate. We analyze the evolution of copper films, which contain both rotational and stacking domains, on ruthenium. Real-time observation by low-energy electron microscopy shows that the stacking domains evolve in a seemingly complex way. Not only do the stacking boundaries move in preferred directions, but their motion is extremely uneven and they become stuck when they reach rotational boundaries. We show that this behavior occurs because the stacking-boundary motion is impeded by threading dislocations. This study underscores how the coarse-scale evolution of thin films can be controlled by defects.

Because of its technological importance, the growth of a crystalline material on top of a dissimilar crystalline material, heteroepitaxy (1), has been intensively investigated (2). To accommodate its physical differences with the substrate, films commonly develop spatial domains that differ somewhat from each other (3). Examples include rotational domains, which differ only in how a crystallographic direction within the plane of the film is oriented with respect to the substrate directions. For films of simple metals (4), additional domain types can be distinguished by the stacking sequence of the close-packed layers that lie parallel to the substrate. These stacking domains are separated by planar boundaries (stacking faults) lying within the film. Stacking- and rotational-domain boundaries can substantially degrade the properties of the film by, for example, scattering charge carriers, quenching excitations, or serving as pathways for enhanced mass transport (5–7). Although these defects can sometimes be healed (8, 9), this process is only partially understood.

Here we investigate how rotational- and stacking-domain boundaries in strained copper films move and interact with each other. We use the unique capabilities (10) of low-energy electron microscopy (LEEM) to follow the evolution in real time. Based on the known structure of the different boundaries, the experimental observations can be explained by the interactions of the dislocations present at the domain boundaries. The large-scale evolution of the thin film can be understood by considering the individual interactions

of the dislocations that form the different boundaries.

Thin films of Cu on Ru(0001) present both rotational and stacking domains (11–15). Typical grain sizes are on the order of hundreds of nanometers. The stacking domains can be observed with LEEM under bright-field conditions (16) as two different gray levels on a continuous two-monolayer (ML) film (Fig. 1A). In addition to the stacking domains, copper films two layers thick on Ru(0001) show an in-plane uniaxial relaxation. Given that the Ru(0001) substrate has threefold symmetry, domains occur where the relaxation direction lies in each of the three equivalent directions, giving rise to three rotational domains. Each rotational domain diffracts low-energy electrons in specific directions (fig. S1A). In a real-space LEEM image formed using the electrons diffracted from a given domain type, only film regions of that domain type appear bright (fig. S1B). By taking successive images with diffracted beams cor-

responding to the three different domains, the full rotational-domain microstructure of the film can be determined. To show the film's entire rotational-domain structure in one image, we color each rotational domain either red, green, or blue (Fig. 1B).

Because each of the three rotational domains can have two stacking domains, the complete microstructure has six types of domains. In Fig. 1C, the six different regions are coded by three colors (rotational domains) and two gray levels (stacking domains). The two types of domain boundaries, namely stacking and rotational boundaries, are distinct.

At temperatures below 350°C, the rotational domains do not evolve with time (17). We focus on the evolution of the stacking boundaries and their relationship with the rotational domains. The evolution of the stacking domains, as followed in real time in Fig. 2, A to C, is quite discontinuous; several minutes may elapse without changes. But sometimes the boundaries between stacking domains move very quickly, as shown by the blurred edges in Fig. 2B. When fast motion occurs, the stacking boundary moves along the unique in-plane direction of the rotational domain (Fig. 2D). Superimposing the rotational and stacking domains also shows that the fast motion of stacking-domain boundaries takes place within rotational domains. The slowing down of their motion, on the other hand, frequently occurs at the boundaries between rotational domains.

To further highlight the observed effect of the rotational-domain boundaries on stacking-boundary motion, we exposed the film to sulfur. Sulfur removes the rotational domains in the copper film (18, 19), changing its structure so that only a single rotational (orientational) domain occurs (figs. S3 and S4). The stacking domains are preserved (Fig. 3A and fig. S3). Without rotational domains, the stacking boundaries advance smoothly with time, in marked contrast to the clean Cu films.

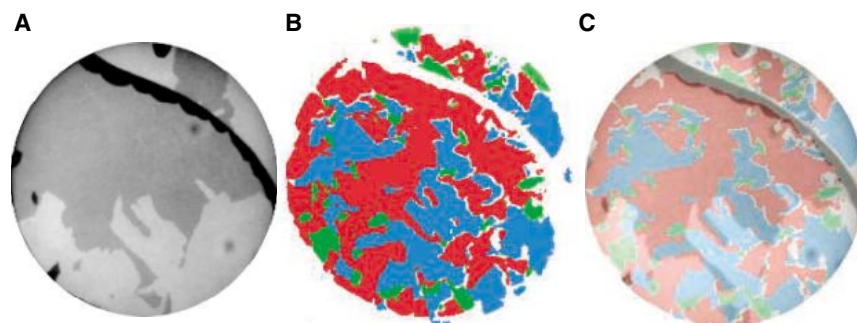


Fig. 1. Domains in two Cu layers on Ru(0001). The field of view of the LEEM images is 5 μm . (A) Bright-field LEEM showing the two different stacking domains, which correspond to the two gray levels in the image. The black areas are regions of the copper film that are three layers high. The incoming electron energy (38 eV) is selected to give good contrast between the stacking domains. (B) Composite color image obtained from the superposition of the three dark-field images of fig. S1, where the colors indicate the orientation of each rotational domain. The areas that are not shown in any color correspond to 3-ML Cu. (C) Full domain microstructure of two copper layers on Ru, obtained by superposition of the previous images.

¹Departamento de Física de la Materia Condensada, Universidad Autónoma de Madrid, Madrid 28049, Spain. ²Sandia National Laboratories, Livermore, CA 94550, USA.

*To whom correspondence should be addressed. E-mail: juan.delafiguera@uam.es

In addition, the stacking boundaries do not move in any preferred direction.

Hence, the rotational domains have a great influence on the evolution of the stacking domains—within a rotational domain, the stacking boundaries move rapidly. But at the rotational boundaries, the stacking boundaries

become impeded. This complicated behavior can be understood by considering the defects at the domain boundaries—the rotational boundaries contain threading dislocations that act as obstacles to the stacking-domain boundaries.

To understand why the observed evolution occurs, we need to describe the stacking and

the rotational domains in more detail. The rotational domains in clean 2-ML copper films are caused by the uniaxial relaxation of Cu atoms in a nearest-neighbor direction through the introduction of parallel arrays of misfit dislocations at the Cu/Ru interface (15, 20). At the boundaries of the rotational domains, there are arrays of edge dislocations (20) that thread out from the substrate/film interface to the film/vacuum interface. Within the rotational domains, no such “threading” dislocations occur. The threading dislocations, which are only two atoms long, are marked in Fig. 4, A to C, and fig. S2C by yellow “T” symbols.

The second Cu layer of a 2-ML film can be located in two different positions that avoid unfavorable on-top positions. These two different stacking sequences give rise to the two stacking domains (15). Although the two domains should have different energies, the energy difference is too small to be reliably determined by ab initio methods (<4 meV per atom, as estimated by density functional theory calculations) (15). Because this energy difference is small, however, islands of both stacking types can nucleate. Indeed, when 2-ML Cu islands grow on top of a complete 1-ML film at our growth temperature, both stacking types occur with about equal probability. Following the growth in real time with LEEM shows that individual islands retain their stacking character until a continuous 2-ML film is formed by island coalescence. The boundaries separating coalesced islands of unlike stacking then move because even a small difference in energy per atom represents a strong driving force to convert the higher-energy stacking domain into the lower-energy one by moving the boundary between them. The boundary separating domains of different stacking sequence is a Shockley partial dislocation located between the two Cu layers (shown as a gray line in Fig. 4, A to C). This directed motion is in contrast to the dislocation motion on 1-ML Cu on Ru(0001) (21). In this case, the Shockley partial dislocations undergo thermal fluctuations because no driving force to push the dislocations exists.

The domain evolution can be interpreted in terms of the dislocation structures of the stacking and the rotational domains described above. The stacking-boundary dislocation can glide within rotational boundaries without encountering intersecting (threading) dislocations (Fig. 4, A and B). Because the energy (Peierls) barrier needed to move such a dislocation is small [<0.25 meV/Å, as estimated by embedded atom method calculations (22, 23)], such glide motion is expected to be very fast. We observe that the stacking boundaries can move as fast as $\sim 10^3$ nm/s.

When moving across rotational domains, however, the stacking-boundary dislocation must cross the threading dislocations present at the rotational boundaries (fig. S2). Given the

Fig. 2. (A to C) Evolution of the stacking-domain structure at 250°C. The size of the images is 1.8 μm by 1.3 μm . From image (A) to image (B), 30 s have elapsed. Image (B) appears blurred at the end of the advancing stacking boundary because of the temporal averaging used (1 s). The fast motion direction is aligned with the underlying rotational domain, as indicated schematically in (D). The time difference between images (B) and (C) is 5 s.

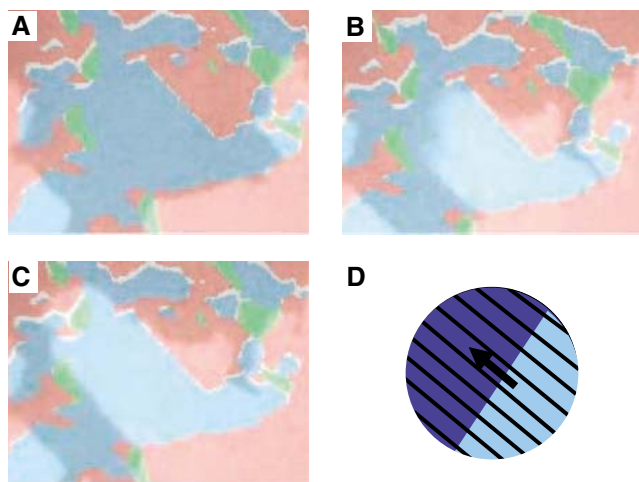


Fig. 3. Evolution of stacking domains in a 2-ML Cu film modified by sulfur. The bright-field LEEM images were taken at 38 eV and are 1.4 μm by 1.9 μm in size. Image (A) was taken at 135°C after the sulfur exposure. Images (B) and (C) were taken at 152°C. The stacking-domain boundaries do not move in preferred directions, unlike sulfur-free films, which contain rotational domains.

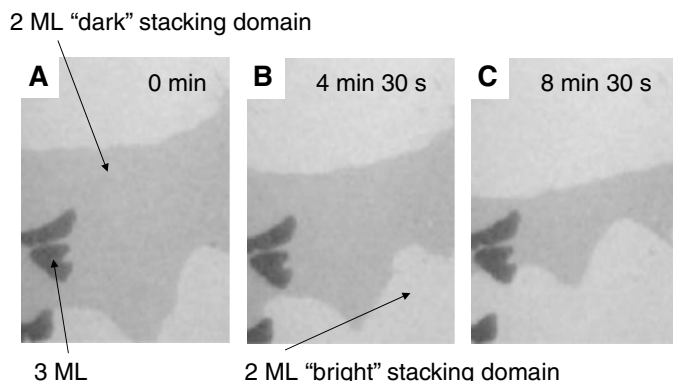
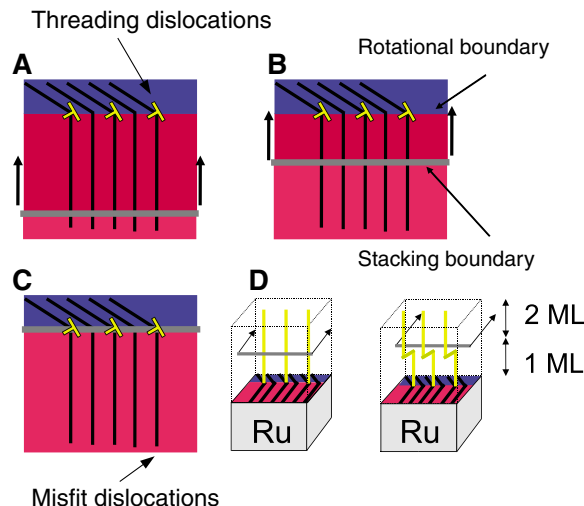


Fig. 4. Explanation of stacking-boundary motion. (A and B) Fast motion of the stacking boundary is observed within rotational domains because the dislocation (boundary), marked by the gray line, can move by glide because no threading dislocations are encountered. (C) Schematic of a stacking boundary crossing between rotational domains. (D) Three-dimensional schematic of the crossing of the rotational boundaries by a stacking boundary. The Cu film (outlined cubes) lies on the Ru substrate (light gray). The misfit dislocations, located at the Ru-Cu interface, are shown as black lines. The stacking boundary, a dislocation within the Cu film between the two copper layers, is shown before and after crossing the threading dislocations present at the rotational boundary. After the crossing (right drawing), jogs are left on each threading dislocation (marked by dark yellow). The corresponding kinks on the stacking boundary are not drawn.



Burgers vectors of the involved dislocations (24), a jog is produced on each threading dislocation when the stacking boundary crosses the “forest” of threading dislocations (Fig. 4D). In turn, the stacking-boundary dislocation acquires a kink for each crossing. The production of a jog on each threading dislocation costs energy, and the total energy barrier of all the needed crossings is much larger than the Peierls glide barrier encountered for pure glide within a rotational domain. Thus, the threading dislocations impede the stacking-boundary motion. Because the threading dislocations only occur at the rotational-domain boundaries, we explain the experimental observation that the stacking boundaries become stuck at the rotational boundaries. The crossing of the threading dislocations is temperature activated: The lower the temperature, the longer the stacking boundaries are pinned at the rotational boundaries. In contrast, the glide motion within rotational boundaries is independent of temperature in the observation range.

We can also understand why stacking boundaries preferentially advance (Fig. 2) along the unique direction of the misfit dislocations within each rotational domain. The array of misfit dislocations within each rotational domain constitutes a periodic array of obstacles for stacking-boundary motion unless, as observed, the stacking-boundary dislocation moves along the misfit dislocations themselves.

The experiments under sulfur exposure can also be explained by the atomistic details of the dislocation structures. When sulfur is deposited on a 2-ML Cu/Ru(0001) film, the striped pattern of misfit dislocations responsible for the rotational domains breaks down (fig. S3), and a well-ordered triangular pattern appears (18, 19) that lacks rotational domains (fig. S4B). The unit cell of this pattern (fig. S4) is a small triangular unit with sides composed of misfit dislocations and threading dislocations at the three corners (18). Nevertheless, the stacking domains still persist and are observed as before in bright-field conditions (Fig. 3). As in 2-ML Cu/Ru(0001) without sulfur (Fig. 1A), there are still two different possibilities for stacking the second Cu layer on top of the first. However, the threading dislocations are now uniformly distributed within the film. The stacking boundary dislocations now encounter a closely spaced (<7 nm apart) distribution of threading dislocations, so the stacking domains evolve smoothly at our observation scale, which is larger than the film's threading dislocation spacing (the LEEM resolution is ~10 nm). Therefore, the stacking boundaries move smoothly with no preferred directions (Fig. 3).

In summary, we have shown how observing thin-film microstructure evolution in real time and in real space can determine what process controls the healing of crystallographic defects.

In the Cu on Ru system, all the microstructure interactions can be observed and understood; it serves as a model of thin-film evolution in which the detailed interactions can be fully modeled (25). Given the ubiquity of dislocations in heteroepitaxial films, we anticipate that our key finding, that dislocations interactions control the rate at which extended defects heal themselves, will hold in many other metal and nonmetal systems.

References and Notes

1. W. Cochrane, *Proc. Phys. Soc.* **48**, 723 (1936).
2. E. Bauer, *Appl. Surf. Sci.* **11**, 479 (1982).
3. O. L. Alerhand, D. Vanderbilt, R. D. Meade, J. D. Joannopoulos, *Phys. Rev. Lett.* **61**, 1973 (1988).
4. R. Q. Hwang, M. C. Bartelt, *Chem. Rev.* **97**, 1063 (1997).
5. O. Rodríguez de la Fuente *et al.*, *Phys. Rev. Lett.* **88**, 036101 (2002).
6. J. de la Figuera *et al.*, *Mat. Sci. Forum* **426-432**, 3421 (2003).
7. F. El Gabaly, R. Miranda, J. de la Figuera, *Phys. Rev. B* **70**, 012102 (2004).
8. R. Phillips, *Crystals, Defects and Microstructures: Modeling Across Scales* (Cambridge Univ. Press, Cambridge, 2001).
9. C. Busse, T. Michely, *Surf. Sci.* **552**, 281 (2004).
10. E. Bauer, *Rep. Prog. Phys.* **57**, 895 (1994).
11. C. Günther, J. Vrijmoeth, R. Q. Hwang, R. J. Behm, *Phys. Rev. Lett.* **74**, 754 (1995).
12. C. Ammer, K. Meinel, H. Wolter, A. Beckmann, H. Neddermeyer, *Surf. Sci.* **375**, 302 (1997).
13. H. Zajonz, D. Gibbs, A. P. Baddorf, V. Jahns, D. M. Zehner, *Surf. Sci.* **447**, L141 (2000).
14. H. Zajonz, A. P. Baddorf, D. Gibbs, D. M. Zehner, *Phys. Rev. B* **62**, 10436 (2000).

15. J. de la Figuera, A. K. Schmid, N. C. Bartelt, K. Pohl, R. Q. Hwang, *Phys. Rev. B* **63**, 165431 (2001).
16. Materials and methods are available as supporting material on Science Online.
17. T. Giessel, A. K. Schmid, N. C. Bartelt, J. de la Figuera, R. Q. Hwang, *18th European Conference on Surface Science*, Vienna, 21 to 24 September 1999 (European Physical Society, Paris, 1999), abstr. Th-P-151.
18. J. de la Figuera *et al.*, *Surf. Sci.* **433-435**, 93 (1999).
19. J. Hrbek *et al.*, *J. Phys. Chem. B* **103**, 10557 (1999).
20. C. B. Carter, R. Q. Hwang, *Phys. Rev. B* **51**, 4730 (1995).
21. J. de la Figuera *et al.*, *Phys. Rev. Lett.* **86**, 3819 (2001).
22. M. S. Daw, S. M. Foiles, M. I. Baskes, *Mat. Sci. Rep.* **9**, 251 (1993).
23. S. M. Foiles, M. I. Baskes, M. S. Daw, *Phys. Rev. B* **33**, 7983 (1986).
24. J. P. Hirth, J. Lothe, *Theory of Dislocations* (Krieger, Malabar, FL, 1992).
25. S. J. Zhou, D. L. Preston, P. S. Lomdahl, D. M. Beazley, *Science* **279**, 1525 (1998).
26. This research was partly supported by the Office of Basic Energy Sciences, Division of Materials Sciences, U.S. Department of Energy, under Contract DE-AC04-94AL85000, by the Comunidad Autónoma de Madrid through Project 07N/0041/2002, and by the Spanish Ministry of Science and Technology through Project MAT2003-08627-C02-02. J.d.l.F. gratefully acknowledges additional support through a “Ramón y Cajal” contract from the Spanish Ministry of Science and Technology.

Supporting Online Material

www.sciencemag.org/cgi/content/full/308/5726/1303/DC1

Materials and Methods
Figs. S1 to S4
Movies S1 and S2

18 January 2005; accepted 23 March 2005
10.1126/science.1109889

A Microbial Arsenic Cycle in a Salt-Saturated, Extreme Environment

Ronald S. Oremland,^{1*} Thomas R. Kulp,¹ Jodi Switzer Blum,¹ Shelley E. Hoefft,¹ Shaun Baesman,¹ Laurence G. Miller,¹ John F. Stolz²

Searles Lake is a salt-saturated, alkaline brine unusually rich in the toxic element arsenic. Arsenic speciation changed from arsenate [As(V)] to arsenite [As(III)] with sediment depth. Incubated anoxic sediment slurries displayed dissimilatory As(V)-reductase activity that was markedly stimulated by H₂ or sulfide, whereas aerobic slurries had rapid As(III)-oxidase activity. An anaerobic, extremely haloalkaliphilic bacterium was isolated from the sediment that grew via As(V) respiration, using either lactate or sulfide as its electron donor. Hence, a full biogeochemical cycle of arsenic occurs in Searles Lake, driven in part by inorganic electron donors.

The microbial life that exists in brines of exceptionally high salinity has been a topic of fascination to microbiologists (1, 2). Primary productivity in hypersaline ecosystems

is driven by oxygenic photosynthesis, as typified by salt-adapted microbes like *Dunaliella parva* that provide the organic carbon needed to sustain a microbial food chain. Typical heterotrophs obtained from such locales are either obligate aerobes or fermentative anaerobes (3). Some also have the ability to respire nitrate, but the importance of this scarce anion as a respiratory electron acceptor in high-density brines has not been studied. In extremely hypersaline environments that have

¹U.S. Geological Survey, ms 480, 345 Middlefield Road, Menlo Park, CA 94025, USA. ²Department of Biological Science, Duquesne University, Pittsburgh, PA 15282, USA.

*To whom correspondence should be addressed.
E-mail: roremilan@usgs.gov

salt concentrations that approach saturation (e.g., ≥ 300 g/liter), the otherwise ubiquitous process of sulfate reduction is either notably absent or greatly diminished (4–6). Likewise, methanogenesis is either feeble (7) or undetectable (6). The most likely reason for this is that the metabolic pathways of these two processes generate insufficient energy to meet the higher requirements of maintaining an internal osmotic gradient against the strong external salt milieu (4). Hence, any anaerobe

with a respiratory metabolism that can live at extremely high salinities must be able to link its oxidation of carbon substrates to biological oxidants considerably stronger than sulfate or carbonate so as to yield more energy. For example, the selenate-respiring bacterium, *Selenihalanaerobacter shriftii*, was isolated from Dead Sea sediments (8), but the scarcity of this element in the brine means that this process is probably not of quantitative importance to the biogeochemical cycling of carbon.

In comparison to sulfate ($\text{SO}_4^{2-}/\text{HSO}_3^-$: electrochemical potential $E_o' = -516$ mV) (9) or carbon dioxide (CO_2/CH_4 : $E_o' = -244$ mV) (9), arsenate [As(V)] reduction to arsenite [As(III)] is a more robust bio-oxidation (10), with a much higher electrochemical potential (arsenate [HAsO_4^{2-}]/arsenite [H_2AsO_3^-]: $E_o' = +60$ mV) (11). Although arsenic is usually thought of only for its toxic properties, several prokaryotes metabolize arsenic oxyanions to gain energy for growth. Arsenate respiration and chemoautotrophic arsenite oxidation occur in prokaryotes from broadly diverse phylogenetic groups and a variety of environments (12).

Relatively high concentrations of arsenic oxyanions occur in several soda lakes of the western United States (13), originating from hydrothermal springs that are common in this volcanically active region. Arsenate acts as an important respiratory electron acceptor in Mono Lake, second only to sulfate, for the oxidation of organic carbon by anaerobic bac-

Fig. 1. Searles Lake vertical sediment depth pore-water profiles of (A) arsenate [As(V)] and arsenite [As(III)] and (B) sulfide, methane, and ammonia.

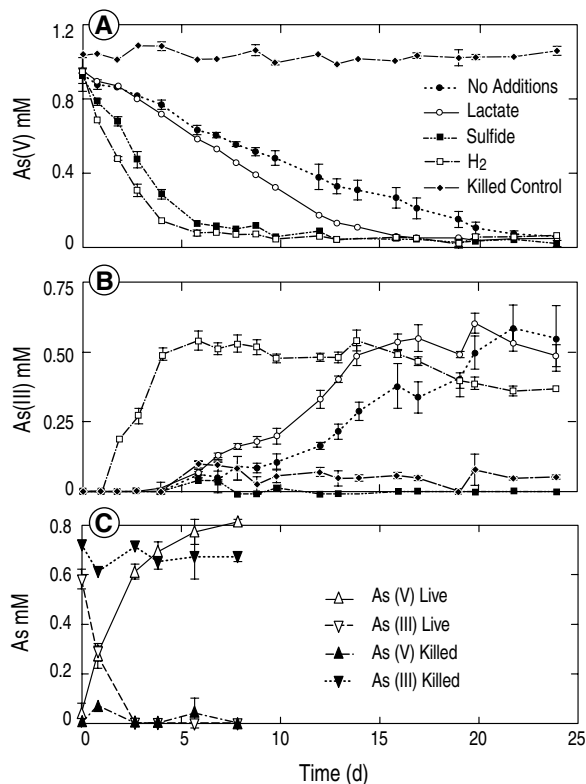
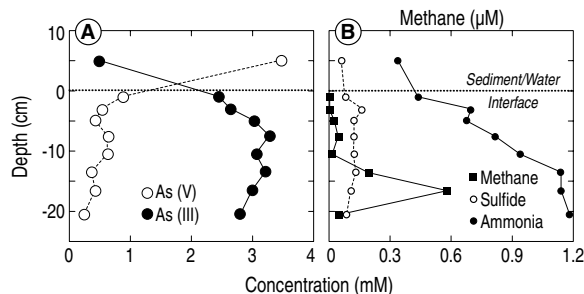
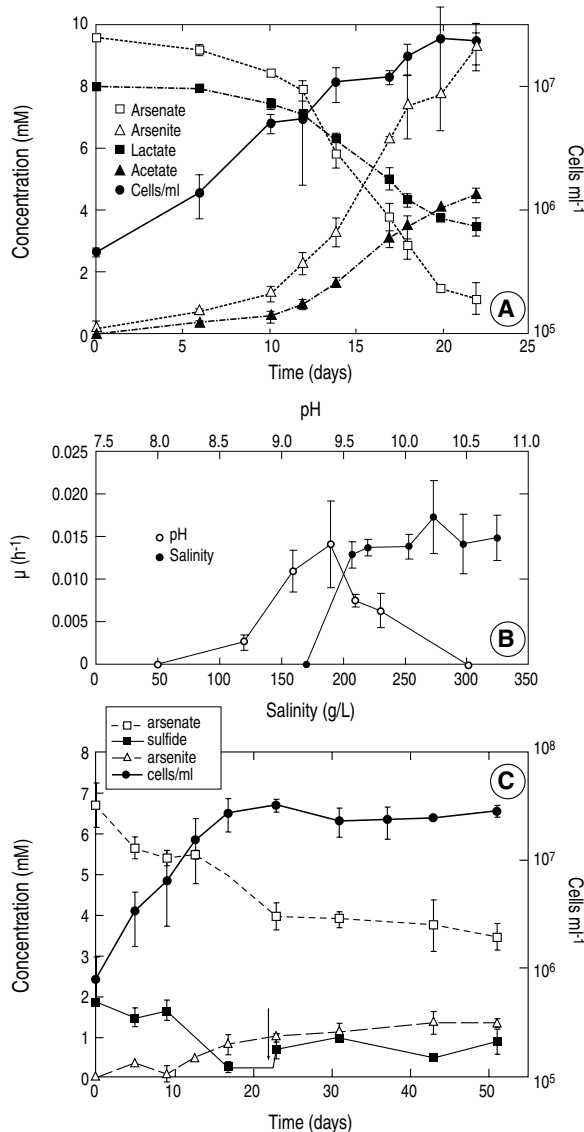


Fig. 2. (left) Incubation experiments with sediment slurries from Searles Lake under anoxic (A and B) or oxic (C) conditions. (A) Reduction of arsenate; (B) formation of arsenite; (C) oxidation of arsenite to arsenate. Symbols represent the mean ± 1 SD of three slurries. **Fig. 3.** (right) (A) Anaerobic growth of strain SLAS-1 on lactate plus arsenate at a salinity of ~ 330 g/liter and pH 9.8. (B) Salinity and pH range for growth of strain SLAS-1. (C) Anaerobic growth of strain SLAS-1 with sulfide as the electron donor. Arrow indicates addition of more (0.5 mM) sulfide to samples after 23 days of incubation. In all of the panels, symbols represent the mean ± 1 SD of three experimental growth cultures.



teria (14). Searles Lake is located in the Mojave Desert about 270 km south-southeast of Mono Lake. The major ionic constituents of the Searles Lake subsurface brine are (given as molality, *m*; moles per kilogram of solvent) Na⁺ (7.43), K⁺ (0.78), HCO₃⁻ + CO₃²⁻ (0.64), Cl⁻ (5.25), SO₄²⁻ (0.73), and BO₃³⁻ (0.46), as reported previously (15, 16).

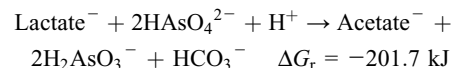
Searles Lake surface brine is unusually enriched in arsenic [ΣAs = ~ 3.9 mM; for methods, see (17)]. In a sediment core pore-water profile, the speciation of dissolved arsenic oxyanions changed from predominantly As(V) (88%) in the overlying water to predominantly As(III) (84%) by 7-cm sediment depth (Fig. 1A). The As(V) + As(III) content of the pore waters ranged from 84 to 97% of the overlying water, indicating that only minor loss of arsenic oxyanions was attributable to the formation of thioarsenites (18, 19), by adsorption onto mineral surfaces or by chemical precipitation as a mineral phase (e.g., arsenopyrite). Other relevant major anionic brine constituents were chloride (range = 4.7 to 5.0 *m*), sulfate (range = 0.66 to 0.79 *m*), and phosphate (range = 16 to 20 mM), but none displayed any trended variation with core depth (20). Nitrate was not detected, but traces of sulfide, methane, and ammonia were present (Fig. 1B), indicating generally reducing conditions in the sediments, which contrasted with the slightly oxic conditions (dissolved

oxygen = 6.3 μM) found in the overlying water. For comparison, the sulfide and methane concentrations were roughly a factor of 10 and 100 less, respectively, than what we reported in the anoxic bottom waters of Mono Lake (14), and a factor of 10 to 100 less for the methane concentrations in Mono Lake sediments (21). This supports Oren's hypothesis (4) of a near-absence of sulfate reduction and methanogenesis in salt-saturated (i.e., Searles Lake), anoxic environments (6). The arsenic speciation patterns in Searles Lake sediments were consistent with our observations of the stratified water column of Mono Lake, which were attributable to microbial reduction of As(V) in the anoxic zone and oxidation of As(III) in regions where dissolved oxygen, or nitrate, were present (14, 22, 23). To test whether the pore-water arsenic speciation observed in Searles Lake sediments was also attributable to microbiological processes, we conducted sediment incubation experiments (17).

Anaerobic sediment slurries reduced As(V) to As(III), whereas no activity was noted in autoclaved controls (Fig. 2, A and B). Addition of lactate, an electron donor used by many As(V) respirers (10, 12), modestly increased the rate of As(V) reduction. When inorganic electron donors sulfide or hydrogen were added, As(V) reduction was even more rapid, suggesting that these may be important in situ lithotrophic electron donors in this system,

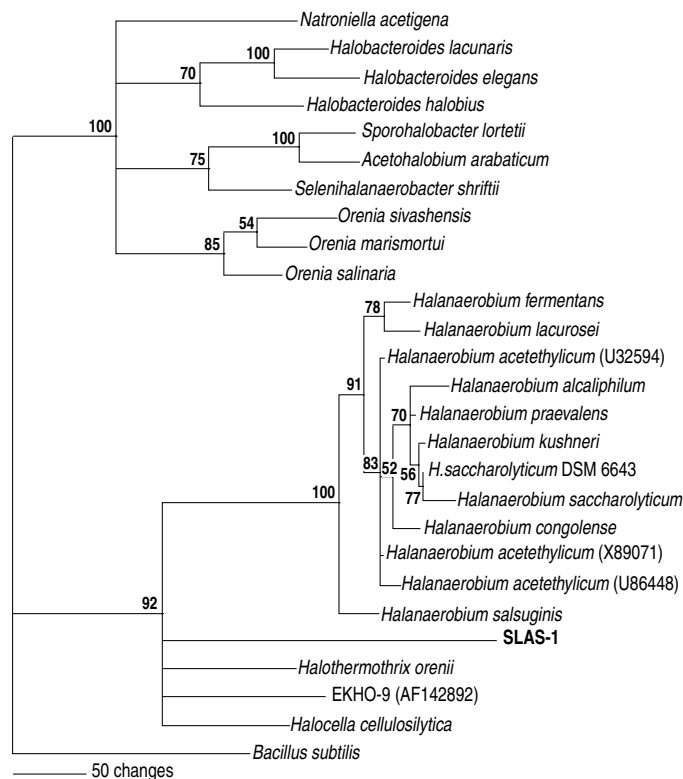
similar to other extreme systems (18, 24). Recovery of As(III) from added As(V) was generally only about 60 to 70% and was only ~10% in the slurries amended with sulfide (Fig. 2B), because of the formation of thioarsenites (20), which are soluble in alkaline, carbonate-rich solutions (18, 19). Live aerobic slurries rapidly oxidized As(III), whereas no oxidation occurred in the killed controls (Fig. 2C). Thus, a full biogeochemical cycling of arsenic occurs in Searles Lake, mediated by microbial aerobic oxidation of As(III) and anaerobic reduction of As(V).

We cultivated enrichments of anaerobic, As(V)-respiring prokaryotes adapted to the "extreme" conditions of Searles Lake by using our artificial brine (17) plus As(V) as the electron acceptor. Because this study preceded the sediment slurry investigations, we did not attempt to cultivate enrichments of cultures using inorganic electron donors. We used lactate as the electron donor based on our earlier success at isolating As(V)-respiring heterotrophs from Mono Lake (25). Over the course of 1 year, a stable population grew that was transferred every other week into fresh medium and subsequently purified by serial dilution. The isolate, strain SLAS-1, was a curved, motile rod that grew (doubling time ~48 hours) by oxidizing lactate to acetate plus HCO₃⁻ while reducing As(V) to As(III) (Fig. 3A), according to the stoichiometry noted previously (25) but recalculated for the actual concentrations used in the medium (17):



Strain SLAS-1 did not grow at salinities below 200 g/liter and had roughly equivalent growth rates at salinities >200 g/liter (Fig. 3B). Optimal growth was at pH 9.5, with little growth below pH 9.1 (Fig. 3B). Thus, strain SLAS-1 was well adapted to the extreme chemical conditions of Searles Lake. We also demonstrated that strain SLAS-1 could grow by using sulfide as its electron donor with As(V) as its electron acceptor (Fig. 3C). We noted, but did not quantify, the production of thioarsenites during this growth. Thioarsenites probably accounted for half of the reduced form of arsenic (+3 oxidation state) present by the end of growth because the ratio of As(V) consumed to As(III) produced was 2:1 rather than the expected 1:1. Hence, this microbe has a capacity for either heterotrophy or lithotrophy with regard to its ability to use either an organic (lactate) or inorganic (sulfide) electron donor to sustain its growth while respiring As(V). Further proof that strain SLAS-1 was able to grow as a chemolithoautotroph came from its ability to carry out dark HCO₃⁻ fixation into cell material when grown on sulfide plus As(V). Dilute washed suspensions (2.2 × 10⁷ cells ml⁻¹) of sulfide-grown

Fig. 4. Phylogenetic tree of Halanaerobiales showing the affiliation of SLAS-1 based on 16S rRNA gene sequence (920 bases) using maximum parsimony analysis (28). The species of Halanaerobiales used for the tree (with their GenBank accession numbers in parentheses) were *Halanaerobium congolense* (U76632), *Halanaerobium salsuginis* (L22890), *Halanaerobium kushneri* (U86446), *Halanaerobium alcaliphilum* (X81850), *Halanaerobium praevalens* (AB022035), *Halanaerobium saccharolyticum* (L37424, X89069), *Halanaerobium lacurosei* (L39787), *Halanaerobium fermentans* (AB023308), *Halobacteroides halobius* (U32595), *Halobacteroides lacunaris* (U32593), *Halanaerobium acetethylicum* (U32594, X89071, U86448), *Halobacteroides elegans* (AJ238119), *Halocella cellulositylica* (X89072), *Halothermothrix orenii* (L22016), *Orenia salinaria* (Y18485), *Orenia sivashensis* (AF152595), *Orenia marismortui* (X89073), *Natroniella acetigena* (X95817), *Sporohalobacter lortetii* (M59122), and *Acetohalobium arabaticum* (X89077). Bootstrap numbers are given at the branch nodes.



cells (17) fixed $^{14}\text{C-HCO}_3^-$ into cell carbon (2051 ± 1282 dpm; $n = 3 \pm 1$, mean \pm SD) when provided with both sulfide and As(V), whereas no activity occurred with live controls incubated without sulfide (80 ± 69 dpm; $n = 2$) or in a heat-killed control containing both sulfide and As(V) (30 dpm). Strain SLAS-1 was unable to metabolize H_2 ; however, we have subsequently cultivated enrichments from Searles Lake sediments that use H_2 as an electron donor to support chemolithoautotrophic growth on As(V) (20).

Phylogenetic alignment by 16S ribosomal RNA (rRNA) gene sequences taxonomically assigned strain SLAS-1 within the order *Halanaerobacteriales* in the Domain Bacteria (Fig. 4). With the exception of the selenate-respiring *Selenihalanaerobacter shriftii* isolated from the Dead Sea (8), all other strains are moderate or extremely halophilic, fermentative anaerobes. Strain SLAS-1 was only remotely related to these other species, having the closest sequence similarity to *Halothermothrix orenii* (83.9%) and *Halocella cellulytica* (83.5%). Clearly, strain SLAS-1 is sufficiently genetically distant from these other strains to merit eventual designation as a new species.

Our results show that a full biogeochemical arsenic cycle is operative in the sediments of this salt-encrusted lake, and we have isolated at least one bacterium that can account for some of these observed dynamics. Our demonstration that the abundant As(V) oxyanions present in the brine can be used as a

terminal electron acceptor broadens our understanding of the types of processes occurring in such extreme environments, which has implications for possible exobiological life in dense brines (26). However, basic research can also aid our interpretation of the interaction of hydrologic and microbial processes affecting arsenic solubility and partitioning in less extreme environments, such as drinking-water aquifers (27).

References and Notes

- B. Javor, *Hypersaline Environments* (Springer, Berlin, 1989).
- A. Oren, in *Microbiology and Biogeochemistry of Hypersaline Environments*, A. Oren, Ed. (CRC Press, Boca Raton, FL, 1999), pp. 1–12.
- A. Oren, *Adv. Microb. Ecol.* **10**, 193 (1988).
- A. Oren, *Microbiol. Mol. Biol. Rev.* **63**, 334 (1999).
- K. K. Brandt, F. Vester, A. N. Jensen, K. Ingvorsen, *Microb. Ecol.* **41**, 1 (2001).
- K. B. Sørensen, D. E. Canfield, A. Oren, *Appl. Environ. Microbiol.* **70**, 1608 (2004).
- M. A. Marvin-DiPasquale, A. Oren, Y. Cohen, R. S. Oremland, *Microbiology and Biogeochemistry of Hypersaline Environments*, A. Oren, Ed. (CRC Press, Boca Raton, FL, 1999), pp. 149–159.
- J. Switzer Blum, J. F. Stolz, A. Oren, R. S. Oremland, *Arch. Microbiol.* **175**, 208 (2001).
- R. K. Thauer, K. Jungerman, K. Decker, *Bacteriol. Rev.* **41**, 100 (1977).
- D. K. Newman, D. Ahmann, F. M. M. Morrell, *Geomicrobiol. J.* **15**, 255 (1998).
- A. J. Bard, R. Parsons, J. Jordan, *Standard Potentials in Aqueous Solutions* (Dekker, New York, 1985).
- R. S. Oremland, J. F. Stolz, *Science* **300**, 939 (2003).
- R. S. Oremland, J. F. Stolz, J. T. Hollibaugh, *FEMS Microbiol. Ecol.* **48**, 15 (2004).
- R. S. Oremland et al., *Geochim. Cosmochim. Acta* **64**, 3073 (2000).
- G. I. Smith, *U.S. Geol. Surv. Prof. Pap.* **1043**, 143 (1979).

- A. R. Felmy, J. H. Weare, *Geochim. Cosmochim. Acta* **50**, 2771 (1986).
- Materials and methods are available as supporting material on Science Online.
- S. E. Hoefft, T. R. Kulp, J. F. Stolz, J. T. Hollibaugh, R. S. Oremland, *Appl. Environ. Microbiol.* **70**, 2741 (2004).
- J. T. Hollibaugh et al., *Geochim. Cosmochim. Acta* **69**, 1925 (2005).
- T. R. Kulp, unpublished data.
- R. S. Oremland, L. G. Miller, M. J. Whitticar, *Geochim. Cosmochim. Acta* **51**, 2915 (1987).
- S. E. Hoefft, F. Lucas, J. T. Hollibaugh, R. S. Oremland, *Geomicrobiol. J.* **19**, 1 (2002).
- R. S. Oremland, S. E. Hoefft, N. Bano, R. A. Hollibaugh, J. T. Hollibaugh, *Appl. Environ. Microbiol.* **68**, 4795 (2002).
- A. E. Liu, E. Garcia-Dominguez, E. D. Rhine, L. Y. Young, *FEMS Microbiol. Ecol.* **48**, 323 (2004).
- J. Switzer Blum, A. Burns Bindi, J. Buzzelli, J. F. Stolz, R. S. Oremland, *Arch. Microbiol.* **171**, 19 (1998).
- P. W. J. J. van der Wielen et al., *Science* **307**, 121 (2005).
- R. S. Oremland, J. F. Stolz, *Trends Microbiol.* **13**, 45 (2005).
- J. Felsenstein, *Annu. Rev. Genet.* **22**, 521 (1988).
- We are grateful to D. Hamel, J. Fairchild, C. Hartwig (Searles Valley Minerals Corp., Trona, CA) and to M. Phillips for assistance with access, sampling, and logistics at Searles Lake. We thank H. Dalton, C. Murrell, A. Oren, R. Tabita, and M. Levandowski for constructive criticism of an earlier draft of this manuscript, and H. Cook for initiating our interest in Searles Lake. This work was supported by the U.S. Geological Survey National Research Program and by a grant from NASA's Exobiology Research Program. The GenBank accession number for strain SLAS-1 is AY965613.

Supporting Online Material

www.sciencemag.org/cgi/content/full/308/5726/1305/DC1
SOM Text
Materials and Methods
References

8 February 2005; accepted 22 March 2005
10.1126/science.1110832

Physical Limits and Design Principles for Plant and Fungal Movements

Jan M. Skotheim^{1,2} and L. Mahadevan^{2,3*}

The typical scales for plant and fungal movements vary over many orders of magnitude in time and length, but they are ultimately based on hydraulics and mechanics. We show that quantification of the length and time scales involved in plant and fungal motions leads to a natural classification, whose physical basis can be understood through an analysis of the mechanics of water transport through an elastic tissue. Our study also suggests a design principle for nonmuscular hydraulically actuated structures: Rapid actuation requires either small size or the enhancement of motion on large scales via elastic instabilities.

From the twirling circumnutation of growing tendrils to the opening and closing of stomata to the growth of fungal hyphae (1), plants and fungi are moving all of the time, often too slowly to notice. Rapid movements, though rarer, are used by many plants in essential functions such as seed or sporangium dispersal (Dwarf mistletoe, *Hura crepitans*, and the fungus *Pilobolus*); pollen emplacement (*Catsetum* orchids and *Stylidium* trig-

gerplants); defense (*Mimosa*); and nutrition (Venus flytrap, carnivorous fungi). The mechanisms involved in these movements are varied: *Hura crepitans* (2) uses explosive fractures to disperse seeds at speeds as great as 70 m/s, the Venus flytrap (3) uses an elastic buckling instability to catch insects in 0.1 s, and the noose-like carnivorous fungus *Dactylaria brochophaga* (4) traps nematodes in less than 0.1 s by swelling rapidly.

The diversity of these nonmuscular hydraulic movements, often referred to as nastic movements, raises two related questions: Is there a physical basis for their classification? What, if any, are the principles underlying the biological designs for rapid movements in plants and fungi? To address these, we note that plants and fungi have a common feature that allows us to consider them together here: a cell wall that allows their cells to sustain a large internal (turgor) pressure of up to 10 atmospheres that can be harnessed for growth and motion. Indeed, movements are eventually driven by differential turgor, which may be regulated actively [e.g., by osmotic control as in stomata (5)] or passively [e.g., by differential drying as in *Hura crepitans* (2)]. In either case, the speed is limited by the rate of fluid transport. Thus, a biophysical charac-

¹Department of Applied Mathematics and Theoretical Physics, Centre for Mathematical Sciences, University of Cambridge, Cambridge CB3 0WA, UK. ²Division of Engineering and Applied Sciences, Harvard University, Pierce Hall, 29 Oxford Street, Cambridge, MA 02138, USA. ³Department of Organismic and Evolutionary Biology, Harvard University Biological Laboratories, 16 Divinity Avenue, Cambridge, MA 02138, USA.

*To whom correspondence should be addressed. E-mail: lm@deas.harvard.edu.

terization of these movements requires knowledge of both the duration of the movement τ and the distance through which the fluid is transported L , which is usually the smallest macroscopic dimension of the moving part. In Fig. 1, we plot τ vs. L and see two categories of movements dominated either by swelling or by elastic instabilities, separated by a dashed line.

To understand this boundary, we recall the physics of water movements through a porous elastic material such as plant tissue. One limit to the speed of movement is determined by the time taken to transport water across the tissue, of characteristic thickness L . Because the fluid and the tissue material are approximately incompressible, the movement of water is compensated by that of the tissue relative to it. Consequently, a flow across a tissue will expand the cells on one side and contract the cells on the other, thereby creating a differential strain. If the typical tissue displacement is denoted by u , the typical fluid velocity field is denoted by v , and the volume fraction of fluid is denoted by ϕ , the continuity relation embodied in the previous statement reads as $\phi v = -(1 - \phi)\partial_t \mu \sim -[(1 - \phi)u]/\tau_p$, where τ_p is the characteristic time for this movement, which is to be determined. Furthermore, the velocity v of the interstitial fluid of viscosity μ in the porous tissue with hydraulic permeability k obeys Darcy's law (6), which states that the fluid velocity relative to the medium is proportional to the fluid pressure gradient. Then, if the pressure in the fluid (7) p varies over a characteristic length L , we may write $\phi[v - (u/\tau_p)] \sim kp/\mu L$. This flow is coupled to the tissue elastic stress so that a local balance of forces in the fluid-infiltrated medium yields $Eu/L \sim \phi p$, where E is the elastic modulus of the tissue (8). Substituting the latter expression for the pressure in the expression for the fluid velocity and using the continuity relation written earlier, we find a time scale known as the poroelastic time (9, 10)

$$\tau_p \sim \mu L^2 / kE \quad (1)$$

The poroelastic time characterizes the time for the diffusive equilibration of pressure via fluid transport in soft, wet tissues and is thus of crucial importance in determining the rate of hydraulic actuation in these systems. In Fig. 1, the dotted line corresponds to $\tau_p/L^2 = 1.6 \text{ s/mm}^2$, consistent with typical values for soft plant tissue (3, 11). This line separates all naturally occurring movements into two categories: slow movements ($\tau > \tau_p$), whose duration is limited by fluid transport; and rapid movements ($\tau < \tau_p$), which rely on elastic instabilities to cross the boundary $\tau = \tau_p$.

The elastic instabilities used by plants and fungi can be divided into two broad categories: snap-buckling and explosive fracture. To sufficiently understand the instability mecha-

nism a particular plant uses requires a detailed study of its geometry [for example (3)]. The main difference between these two instabilities is the release mechanism: Snap-buckling involves the rapid geometric changes associated with the buckling of thin shells, whereas explosive fracture involves the rapid geometric changes due to tearing the plant tissue.

The boundary $\tau = \tau_p$ separating the two categories of movement is clearly length-scale dependent and provides a significant barrier for rapid large-scale movements. Elastic instabilities provide the only way to cross the line $\tau = \tau_p$. To illustrate this, we compare *Aldrovanda* (12) (circled 1 in Fig. 1) with the closely related Venus flytrap (circled 2 in

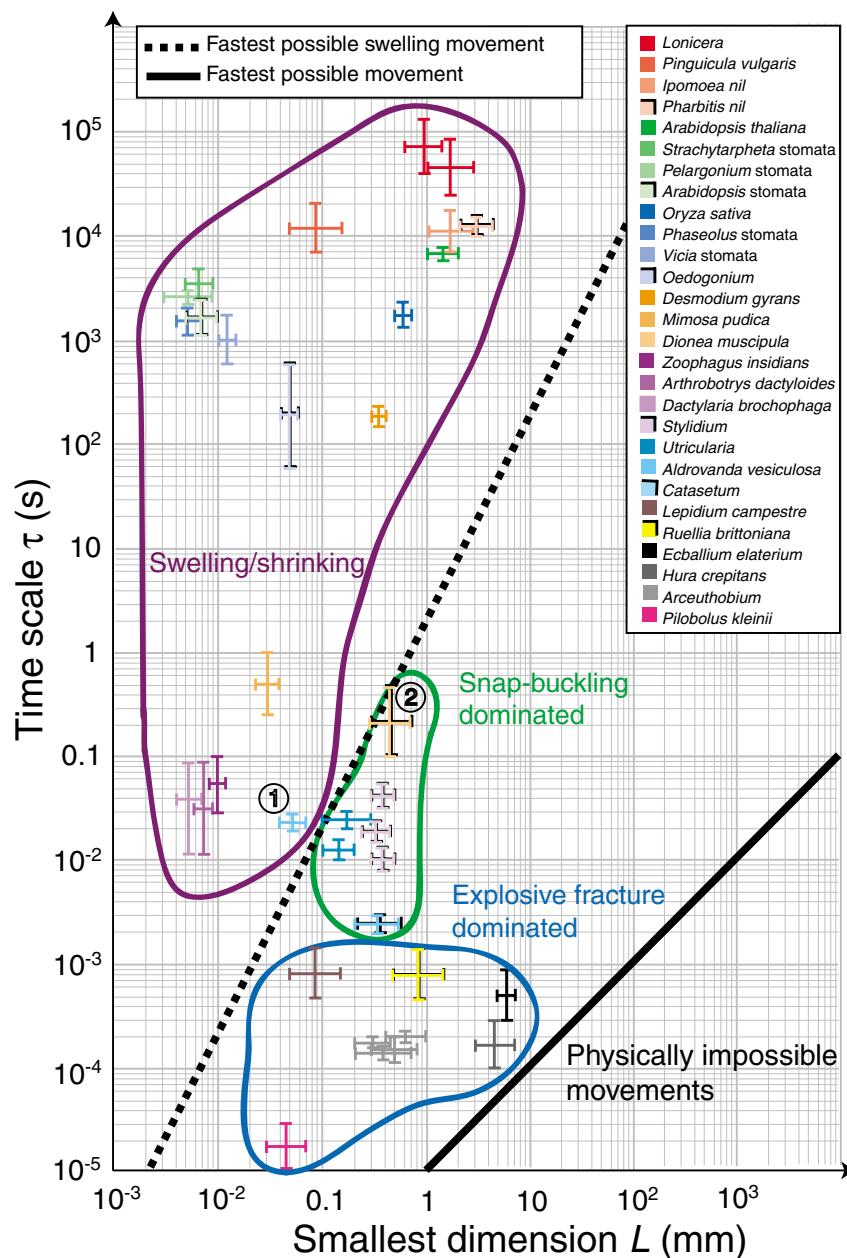


Fig. 1. Classification of plant and fungal movements. The duration of the movement τ is plotted as a function of L , the smallest macroscopic dimension of the moving part (see SOM for detailed references). The dashed line $\tau_p = 1.6 L^2 \text{ s/mm}^2$ characterizes the poroelastic time, whereas the solid line $\tau_i = 10^{-5} L \text{ s/mm}$ characterizes the inertial time. These lines set performance limits on plant and fungal movements while classifying them into two categories: those limited by fluid transport, i.e., $\tau_p < \tau$, and those that use elastic instabilities to go beyond, eventually limited by inertia, i.e., $\tau_i < \tau < \tau_p$. The elastic instabilities can be further categorized as either snap-buckling or explosive fracture. Both types of instabilities rely on geometries capable of gradually storing elastic energy and suddenly releasing it. The difference between the two groups is a matter of how the energy is released: Snap-buckling is associated with a rapid geometric change of a thin shell that does not rupture; explosive fracture involves a rapid geometric change from tissue tearing. The order of the labels in the figure legend coincides with their order in the figure from top to bottom.

Fig. 1), both of which close their leaves rapidly to capture prey; *Aldrovanda* closes its leaves in ~ 0.02 s, whereas the Venus flytrap closes in ~ 0.2 s. However, although the leaves of the Venus flytrap snap by reversing their curvature, *Aldrovanda*'s leaves are already initially curved inward so that closure does not produce a snap. To understand how the snapless *Aldrovanda* can be more rapid than the snapping Venus flytrap, we use Eq. (1) for the poroelastic time: for a Venus flytrap leaf of typical thickness $L = 0.5$ mm, $\tau_p = 1.6$ s/mm² $(0.5 \text{ mm})^2 \sim 0.4$ s, whereas for an *Aldrovanda* $L = 0.05$ mm, the value of τ_p is ~ 0.004 s. Because an *Aldrovanda* leaf is about 1/10th the size of the Venus flytrap, it can be actuated 100 times more rapidly and does not require an elastic instability to catch prey, whereas the Venus flytrap does, which is consistent with our classification.

The absolute physical limit of motion in self-actuated mechanical systems is determined by the speed of elastic waves in them, which propagate at a speed that scales as $\sqrt{E/\rho}$. This yields an estimate for the inertial time given by

$$\tau_i \sim L\sqrt{(\rho/E)} < \tau \quad (2)$$

The inertial time scale characterizes the time for wave propagation in mechanical

signalling in systems and must be less than τ , the time scale of the motion. In Fig. 1, the solid line denotes $\tau_i/L \sim 10^{-5}$ s/mm, consistent with typical values for soft plant tissue (3, 11), beyond which there can be no natural nastic movements. For the fungus *Pilobolus*'s sporangium discharge (13), $L \sim 0.05$ mm, so that $\tau_i \sim 10^{-7}$ s $< 10^{-5}$ s $\sim \tau$, whereas for fruit of *Hura crepitans* (2), $L \sim 5$ mm, so that $\tau_i \sim 10^{-5}$ s $< 10^{-4}$ s $\sim \tau$, as shown in Fig. 1. These explosive movements characterize Nature's best attempts to reach the physical limits of autonomous motion in elastic tissues.

In conclusion, we see that the size-dependent inertial-elastic time τ_i and the poroelastic time τ_p given by Eqs. (1) and (2) provide us with a physical basis for the classification of the hydraulic movements in plants and fungi and yield limits on their performance. This implies that the engineering of soft, nonmuscular hydraulically actuated systems for rapid movement requires either small size or the enhancement of motion on large scales via elastic instabilities. Nature has already implemented many such designs exquisitely; we simply need to follow her lead.

References and Notes

1. D. Attenborough, *The Private Life of Plants* (BBC Books, London, 1995).
2. M. D. Swaine, T. Beer, *New Phytol.* **78**, 695 (1977).

3. Y. Forterre, J. M. Skotheim, J. Dumais, L. Mahadevan, *Nature* **433**, 421 (2005).
4. J. Comandon, P. de Fonbrune, *C.R. Soc. Biol. Paris* **129**, 620 (1938).
5. O. V. S. Heath, *New Phytol.* **37**, 385 (1938).
6. This is a reasonable first approximation when the pore size does not change much and when the fluid is Newtonian. Then, the fluid shear viscosity, which characterizes the resistance of the fluid to shear, is a constant. For a simple derivation of Darcy's law in the context of poroelasticity, see (9); for a discussion of its implications in confined geometries, see (10).
7. The pressure, which has the units of force per unit area, characterizes the local isotropic component of the stress.
8. E is the drained elastic bulk modulus of the tissue, which characterizes the response of the tissue when the fluid is equilibrated. u denotes the typical tissue displacement, i.e., the distance a point in the tissue has moved from its initial position. We have assumed that the material behaves linearly, i.e., that the elastic stress is proportional to the strain. This assumption is usually a good one because the typical strains involved are of the order of a few percent at most.
9. M. A. Biot, *J. Appl. Phys.* **12**, 155 (1941).
10. J. M. Skotheim, L. Mahadevan, *Proc. R. Soc. Lond. A Math. Phys. Eng.* **460**, 1995 (2004).
11. J. French, E. Steudle, *Plant Physiol.* **91**, 719 (1989).
12. J. Ashida, *Mem. Coll. Sci. Kyoto Imp. Univ. B IX*, 141 (1934).
13. R. M. Page, *Science* **146**, 925 (1964).

Supporting Online Material

www.sciencemag.org/cgi/content/full/308/5726/1308/DC1

SOM Text
Table S1

29 November 2004; accepted 15 March 2005
10.1126/science.1107976

The Effects of Artificial Selection on the Maize Genome

Stephen I. Wright,^{1,3} Irie Vroh Bi,^{4*} Steve G. Schroeder,⁴ Masanori Yamasaki,⁴ John F. Doebley,⁵ Michael D. McMullen,^{4,6} Brandon S. Gaut^{1,2,†}

Domestication promotes rapid phenotypic evolution through artificial selection. We investigated the genetic history by which the wild grass teosinte (*Zea mays* ssp. *parviglumis*) was domesticated into modern maize (*Z. mays* ssp. *mays*). Analysis of single-nucleotide polymorphisms in 774 genes indicates that 2 to 4% of these genes experienced artificial selection. The remaining genes retain evidence of a population bottleneck associated with domestication. Candidate selected genes with putative function in plant growth are clustered near quantitative trait loci that contribute to phenotypic differences between maize and teosinte. If we assume that our sample of genes is representative, ~ 1200 genes throughout the maize genome have been affected by artificial selection.

Maize domestication has resulted in highly modified inflorescence and plant architecture (1). Improvement after domestication has also resulted in striking changes in yield, plant habit, biochemical composition, and other traits. At the genetic level, these phenotypic shifts are the result of strong directional (artificial) selection on target genes. With rare exceptions (2), targeted genes have not been identified.

Most domesticated plants and animals have experienced a "domestication bottleneck" that reduced genetic diversity relative to their wild ancestor (3). This bottleneck affects all genes

in the genome and modifies the distribution of genetic variation among loci. The magnitude and variance of the reduction in genetic diversity across loci provide insights into the demographic history of domestication. However, in genes targeted by artificial selection, genetic diversity is reduced above and beyond that caused by the domestication bottleneck (4). Selection is similar to a more severe bottleneck (5) that removes most (or all) of the genetic variation from a target locus.

Here, we report single-nucleotide polymorphism (SNP) diversity in 774 gene fragments

(100 to 900 base pairs) in a sample of 14 maize inbred lines (representing modern maize) and 16 inbred teosintes (tables S1 and S2). In this gene set, we have identified 3463 SNPs in maize and 6136 SNPs in teosinte. The polymorphism data are generally consistent with a population bottleneck during the domestication of maize.

Diversity, as measured by Watterson's estimator of the population mutation parameter θ (6), is reduced in maize relative to teosinte (Fig. 1). Our maize sample has about 57% of the variability found in its progenitor. This is somewhat lower than previous estimates that were based on a smaller number of genes (7, 8). The difference in part reflects differences in sampling and the presence of several loci with no polymorphism in maize; 65 maize genes in our data set contain no segregating sites.

¹Department of Ecology and Evolutionary Biology, ²Institute of Genomics and Bioinformatics, University of California, Irvine, CA 92697, USA. ³Department of Biology, York University, Toronto, Ontario M3J 1P3, Canada. ⁴Department of Agronomy, Plant Science Unit, University of Missouri, Columbia, MO 65211, USA. ⁵Department of Genetics, University of Wisconsin, Madison, WI 53706, USA. ⁶Plant Genetics Research Unit, USDA-Agricultural Research Service, Columbia, MO 65211, USA.

*Present address: Institute for Genomic Diversity, Cornell University, Ithaca, NY 14853, USA.

†To whom correspondence should be addressed. E-mail: bgaut@uci.edu

Linkage disequilibrium (LD) is increased in maize relative to teosinte. We have estimated the population recombination parameter ρ (9), which is inversely proportional to LD. The average estimate of ρ in maize is 17% that of teosinte (Fig. 1). Thus, estimates of ρ in maize have been reduced more drastically than estimates of θ , as expected under a recent population bottleneck (10). The ratio ρ/θ , the relative rate of recombination to mutation under the neutral equilibrium model, has declined sharply in maize relative to teosinte, from 4.5 in teosinte to 1.5 in maize. These results suggest that patterns of LD in maize are strongly influenced by population history, perhaps more so than by extant recombination rates.

Finally, the frequency distribution of polymorphisms, as measured by Tajima's D , has shifted between maize and teosinte (Fig. 1). In teosinte, polymorphisms are skewed toward rare variants, and the average D (\bar{D}) across loci is -0.50 . In contrast, \bar{D} is slightly positive (0.04) in maize, indicating a shift toward higher frequency alleles. This frequency shift is also expected after a recent bottleneck (11), because increased rates of genetic drift during a bottleneck tend to remove rare variants preferentially.

Our genome-wide estimates of SNP diversity from maize and teosinte provide a basis to estimate the demographic history of maize and to test for selection. We used coalescent simulations to infer the severity of the domestication bottleneck. Our coalescent model incorporates information about maize, such as the domestication time ~ 7500 years ago (7, 12) and the inference of a single domestication event (13). The model also uses diversity data from teosinte to control for variation in stochastic effects, mutation rates, and recombination rates among loci. Our simulation method differs from previously published methods in the use of a rejection-sampling scheme, which fits simulated data to multiple summaries of the teosinte data. Our reasoning for the rejection-sampling approach is that the demographic history of teosinte is unknown but is reflected in sequence data. By conditioning simulated data on observed data, our simulations capture much of the historical features of each locus. In the rejection-sampling process, simulations that mimic teosinte data are retained, compared to maize data, and then interpreted in a likelihood framework for parameter estimation and model testing (14).

The primary parameter of interest is maize bottleneck severity (k), which is the ratio of the size of the bottlenecked population (N_b) to the duration of the bottleneck (d) in generations. To estimate k , we simulated teosinte and maize data for each of 774 loci, varying bottleneck severity for different sets of simulations to find the best fitting model. The multilocus data are most consistent with a domestication bottleneck of moderate size, with \hat{k} , the maximum likelihood (ML) esti-

mate of k , equal to 2.45 (Fig. 2A). This estimate is slightly smaller than a previous estimate based on 12 loci (7), but the inference is robust to variation in model parameters such as domestication time, size of the predomestication population, and size of the current maize population (fig. S2). With independent information about d , \hat{k} provides insight into the founding population of maize. For example, the archaeological record suggests that the

maximum estimate of d for the domestication of maize is ~ 2800 years (12), assuming one generation per year for an annual plant. Under this time scale, N_b is 6860 chromosomes, which implies that fewer than 3500 individuals, or $<10\%$ (15, 16) of the teosinte population, contributed to the genetic diversity captured in our maize sample.

How well do the observed data fit this simple bottleneck model? We generated a simu-

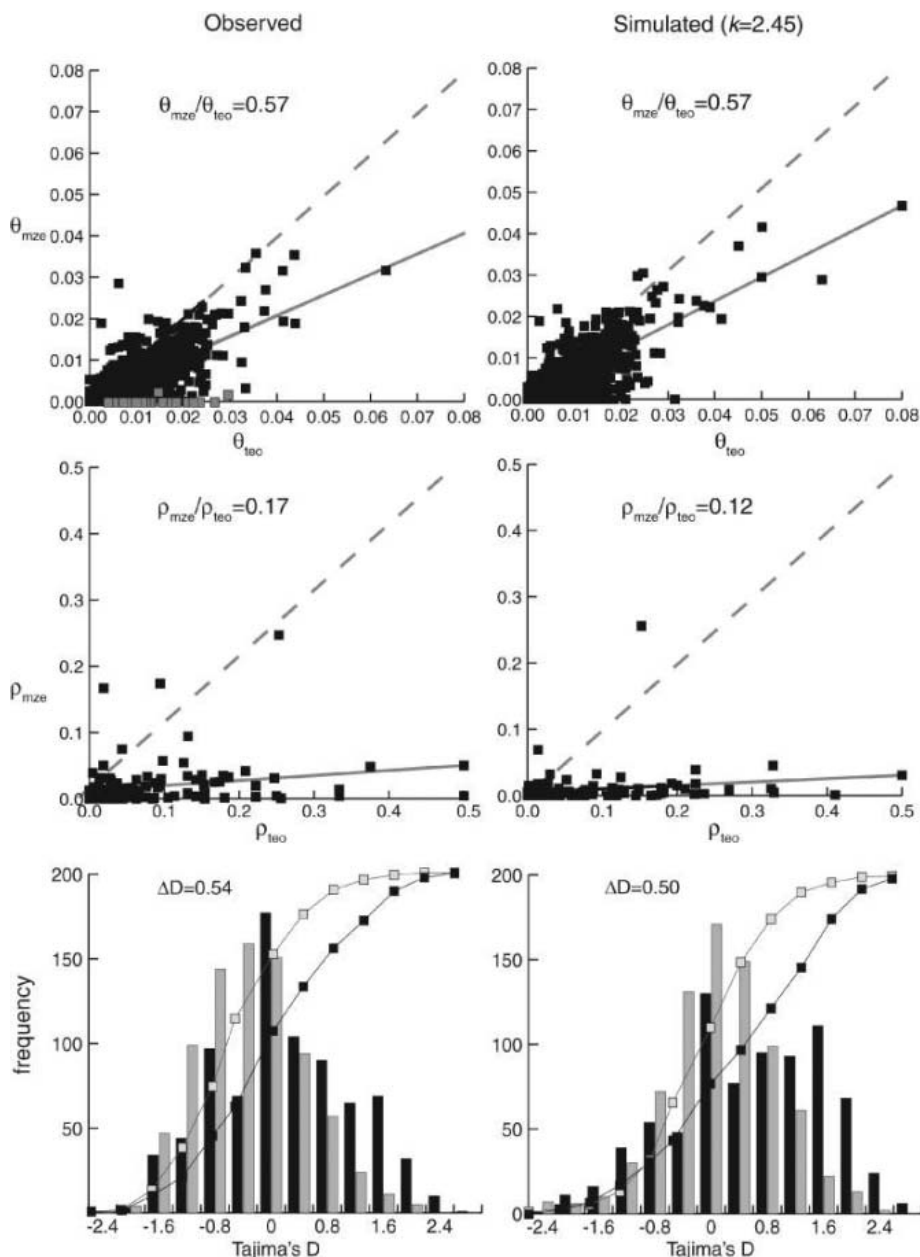


Fig. 1. Patterns of diversity in maize and teosinte at 774 gene fragments. The first column plots the observed data; the second column graphs a simulated data set with $k = 2.45$ (14). The first row illustrates the relationship between mean values of θ in teosinte (x axis) versus maize (y axis). Dashed diagonal lines have a slope of 1.0, representing equal diversity between taxa; solid lines are regression lines. Each square represents a single gene, with genes inferred to have been under selection in gray. The second row plots the relationship between estimates of the population recombination rate ρ in teosinte (x axis) versus maize (y axis) (14). Estimates of ρ were calculated using Hudson's (9) composite likelihood estimator. The third row shows a histogram of the frequency distribution of Tajima's D in maize (black) and teosinte (gray). The cumulative distribution of Tajima's D is also given. ΔD is the difference in average D values between maize and teosinte.

lated data set under the ML estimate of $\hat{k} = 2.45$ and compared simulated data to our observed data. The observed shifts in diversity (θ), frequency spectrum (D), and recombination (ρ) between teosinte and maize fit closely with simulated data (Fig. 1). However, the absolute values of D in simulated data do not fully agree with observed values, perhaps because of some feature of teosinte demographic history that is not fully captured by our model. Nonetheless, the most likely bottleneck model is generally consistent with observed patterns of sequence diversity.

Although there is a generally good fit of the bottleneck model, selection at some loci

can skew the distribution of polymorphism across loci. In particular, $\sim 10\%$ of our loci have zero diversity in maize; it is unclear whether a domestication bottleneck alone can explain this observation. To examine this, we developed a likelihood ratio (LR) test to determine whether the entire data set is consistent with a single domestication bottleneck or whether the multilocus data are better explained by two classes of genes—one consisting of nonselected genes that have experienced the domestication bottleneck (k_1), the other consisting of selected genes that have experienced a more severe bottleneck (k_2) that mimics selection. Our method simul-

taneously estimates the severity of both bottlenecks (k_1 and k_2) and also estimates the proportion of genes (f) that fit the severe bottleneck.

The LR test provides statistically significant support for the presence of two gene classes (LR = 5.8, df = 1, $P < 0.05$). The first class has experienced a domestication bottleneck of severity $\hat{k}_1 = 2.45$, and the second class has undergone a bottleneck of more than 10 times the intensity ($\hat{k}_2 = 0.15$). Under this model, the ML estimate of f is 0.02, indicating that 2% of our 774 maize genes are in the selected class. However, some of our 774 genes have low diversity in teosinte (Fig. 1). These genes provide little information to discriminate be-

Table 1. Candidate selected genes, sorted by posterior probability (PP).

Rank	Gene or locus	PP	Gene name or description	Putative gene function
1	<i>tb1</i>	0.87	Teosinte branched 1 (<i>tb1</i>)	Transcription factor
	AY112154	0.77	Ribosomal protein L28 family	Structural constituent of ribosome
2	AY105809	0.65	Acetyl transferase	Transferase activity
3*	AY107228	0.64	Dihydrodipicolinate synthase (DHPS)	Lysine biosynthesis
4*	AY106600	0.61	Adenylosuccinate synthetase	Purine biosynthesis
5	AY104983	0.59	Heat shock protein (hsp70)	Chaperone activity; protein folding
6†	AY105958	0.58	Auxin-induced protein	Transcription factor; response to sucrose
7	AY111546	0.57	Unknown	Unknown
8†	AY108246	0.55	Growth factor	
9	AY104090	0.54	Transmembrane protein	
10	AY111438	0.54	Glycosyltransferase	Transferase activity; carbohydrate biosynthesis
11	AY110082	0.53	Heat shock protein	Chaperone activity; protein folding
12†	AY104948	0.49	Auxin response factor (ARF1)	Transcription factor
13	AY106970	0.48	Unknown	
14	AY112083	0.47	Minichromosome maintenance factor 5	DNA-dependent ATPase activity; DNA replication initiation
15	AY106111	0.46	Hexokinase 1 (HXK1)	ATP binding
16	AY108481	0.45	Unknown	
17	AY104147	0.44	F-box family protein	
18*	AY107907	0.43	Chorismate mutase (CM2)	Aromatic amino acid biosynthesis
19*	AY105062	0.43	Microsomal signal peptidase (SPC25)	Peptidase activity
20*	AY107903	0.43	Ubiquitin C-terminal hydrolase family protein	Ubiquitin-dependent protein catabolism
21	AY104037	0.41	Aconitate hydratase	Aconitate hydratase activity
22	AY107173	0.40	Unknown	
23	AY103840	0.39	Ubiquitin/transferase family protein	Trichome branching; DNA endoreduplication
24	AY108543	0.38	Early responsive to dehydration protein	
25†	AY104065	0.36	Cell elongation protein DWARF1	Steroid biosynthesis; cell elongation; response to light
26*	AY104439	0.33	Indole synthase	Indole biosynthesis
27	AY108187	0.31	Unknown	
28	AY106496	0.30	Unknown	
29	AY104530	0.28	CBL-interacting protein kinase 3 (CIPK3)	Kinase activity; response to abiotic stimulus
30	AY107475	0.27	Basic endochitinase	Chitinase activity; anti-fungal peptide activity

*Genes with putative function in amino acid biosynthesis.

†Genes with putative function in plant growth.

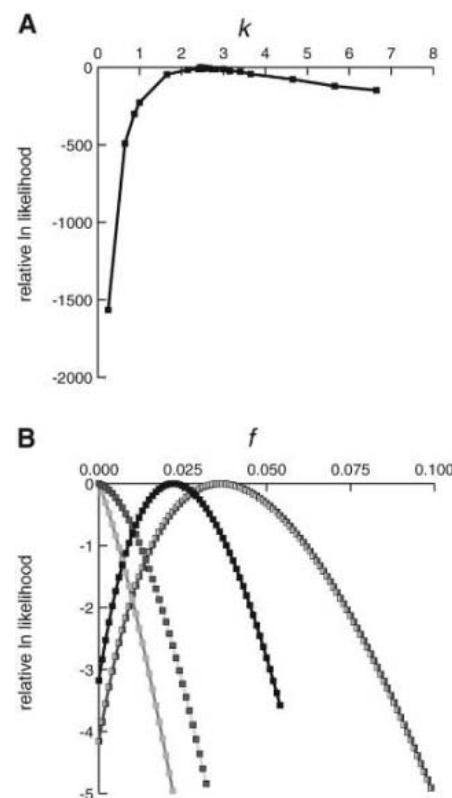


Fig. 2. Likelihood results fitting the population bottleneck. (A) Likelihood surface for the strength of the population bottleneck, k , based on all 774 loci. (B) The black points show the likelihood surface fitting f , the proportion of genes in the severe bottleneck (selected) class, using the most likely two-bottleneck model ($k_1 = 0.15$, $k_2 = 2.45$) and all 774 loci. The gray hatched curve to the right shows the likelihood surface fitting f using the most likely two-bottleneck model ($k_1 = 0.001$, $k_2 = 2.45$) and loci with 10 or more segregating sites in teosinte. The two curves on the left, both with an apex at $f = 0.00$, represent the likelihood surface for f based on analysis of data sets simulated with a single bottleneck using rejection sampling (14). The analysis correctly estimates f to be zero, as expected under neutrality. The light gray curve with apex at $f = 0.00$ is based on a simulated data set from one bottleneck that is also conditioned on the observed frequency spectrum (Tajima's D) in teosinte.

tween the two gene classes and therefore affect the estimation of f . When we conduct the LR test on 275 genes with relatively high polymorphism in teosinte (10 or more segregating sites), the proportion of genes under selection increases to $\hat{f} = 3.6\%$ (LR = 4.6, $P < 0.05$, $\hat{k}_1 = 2.45$, $\hat{k}_2 = 0.001$). Thus, our likelihood analysis estimates that 2 to 4% of maize genes have been selected during maize domestication and improvement. Note that nonzero estimates of f are not expected under a single, moderate population bottleneck, even when we account

fully for the skewed frequency distribution in teosinte (Fig. 2B).

Given these results, we used our likelihood framework to identify candidate selected genes by calculating the posterior probability (PP) that a gene is in the selected class (14). Table 1 shows the ranked PP for the top 4% of the candidate genes in our data set, as well as the PP for the *tb1* locus. *tb1* is included as a positive control because there is strong morphological and genetic evidence for selection on *tb1* during domestication (2, 17, 18). The

statistical power to detect selection may be higher for *tb1* than for most of our genes because the sequences are longer and the maize sample is larger. Nonetheless, our method correctly identifies *tb1* as a member of the selected class, with *tb1* assigned the highest PP (87%) among all genes.

The top candidate genes from our data set include genes known to be involved in plant growth and auxin response, which may contribute to the morphological differences between maize and teosinte (Table 1). In addition, our candidates identified a novel class of selected genes that function in amino acid biosynthesis and protein catabolism, suggesting selection for amino acid composition. Our inbred lines represent maize genetic diversity after domestication and breeding. We therefore cannot determine whether our high-PP genes were selected during the initial domestication event, during subsequent breeding and improvement, or both. However, amino acid composition is known to differ between maize and teosinte (19), and it is an important current target of selection for nutrition.

Previous studies (20, 21) have identified quantitative trait loci (QTLs) for phenotypic differences between maize and teosinte. We plotted the estimated map positions of these QTLs with the PP for each of the 638 mapped loci in our study (Fig. 3) (table S2). A number of high-PP genes map near QTLs, particularly on chromosomes 1 and 5, which suggests that we may have identified selected genes associated with these morphological differences. The average distance from estimated map positions of QTLs is significantly lower for the top 4% of the candidate genes than for the rest of our 638 loci (permutation test, $P < 0.05$), and thus our selected genes cluster near QTLs. However, these QTLs contribute to morphological differences between species, and some of our candidates appear to be associated with other types of selection, such as biochemical composition, that we do not expect to be associated with the QTLs. Accordingly, growth-associated candidate genes and QTL locations remain clustered ($P < 0.01$), but amino acid biosynthesis genes do not cluster with QTLs ($P = 0.66$). The distribution of candidate genes also suggests that a number of selected genes fall under a single QTL (Fig. 3); this implies that morphological differentiation at a given QTL may be caused by a cluster of loci in the same pathway, consistent with a long-standing hypothesis for maize evolution (1).

We estimate that 2 to 4% of maize genes were selected during domestication and subsequent improvement. If we assume that our sample of genes is representative of the genome as a whole and that maize contains 59,000 genes (22), our results suggest that a minimum of $59,000 \times 2\% \approx 1200$ genes throughout the genome have been targets of selection during

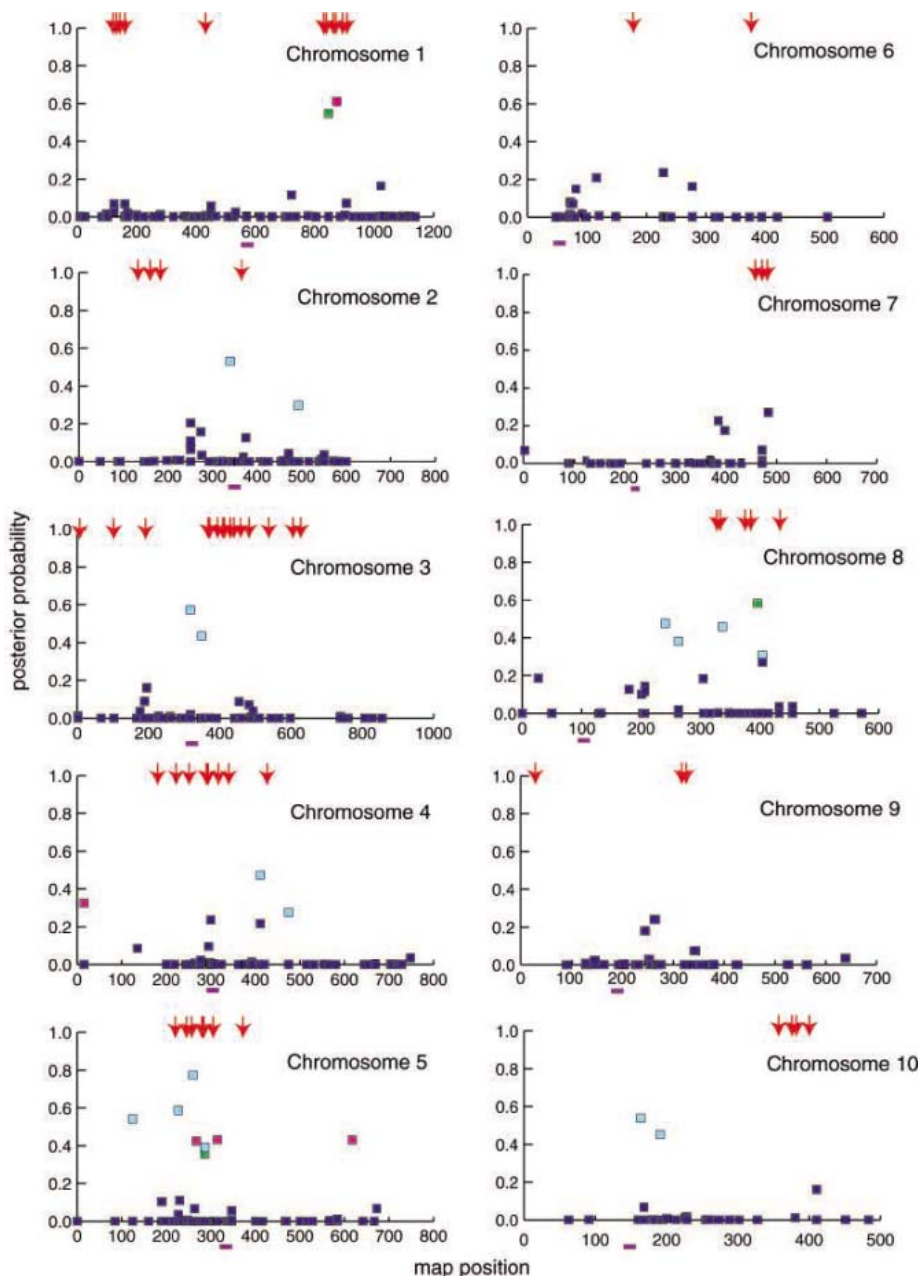


Fig. 3. Graphs of the posterior probabilities (PP) and map positions of 638 mapped genes (squares) against the estimated chromosomal locations of QTLs (red arrows) associated with a suite of morphological differences between teosinte and maize. Light blue, green, and magenta squares denote the top 30 high-PP genes listed in Table 1. Genes in green have a putative function in plant growth (genes 6, 8, 12, and 25 in Table 1). Genes in magenta putatively function in amino acid biosynthesis (genes 3, 4, 18, 19, 20, and 26 in Table 1). The centromeric position for each chromosome is identified by a purple line under the x axis. Chromosomal positions are roughly in units of 0.25 cM.

maize domestication and improvement. However, some of our candidate genes could be false positives, for three reasons. First, loci with very skewed frequency distributions in teosinte could lose more polymorphism during the domestication bottleneck than expected under our model, causing false inference of selection. Second, although our method confirms that the multilocus distribution of genetic diversity is inconsistent with a single bottleneck, any single gene could fall into the selected class by stochastic (nonselective) effects. Finally, rather than being the direct targets of selection, some loci could be hitchhiking with a site under selection. Indeed, candidate genes are significantly closer to the centromere than are non-candidates ($P < 0.05$), which suggests a greater chance of detecting selection in regions of reduced recombination, where hitchhiking should be more pronounced (23). Nonetheless, previous studies have shown that hitchhiked regions in maize tend to be relatively short (2, 24), and recombination in maize coding regions is sufficient to severely limit the physical extent of hitchhiking to one, or at most a few (25), genes. Additionally, the subset of candidates for growth and amino acid biosynthesis are not significantly closer than noncandidate genes to the centromeres ($P = 0.49$), which suggests that these candidates are direct targets of selection.

Despite these caveats, our estimate of 2 to 4% of genes having been under selection is likely conservative, for three reasons. First, if selection acted on moderate-frequency variants in teosinte, selection may have had little effect on diversity levels (4). In such cases, there is little power to detect selection. Second, our method assumes that selected genes are represented by a single severe bottleneck. This approach may not detect genes subjected to subtle selection regimes. Third, high recombination rates within maize genes could reduce the hitchhiking effect to the point that only short fragments within genes retain the footprint of selection. In *tb1*, for example, selection in the promoter region did not affect diversity in the coding region (2). It is thus possible that we sequenced a region within a bona fide selected gene, but our region did not retain evidence of selection.

Maize domestication prompted phenotypic change that is more extensive than in most domesticated plant species. It is thus possible that maize has a higher proportion of selected genes than most domesticates, but similar studies of additional domesticated species are required to address this issue. We have shown that our candidate genes are associated with QTL regions underlying phenotypic differences between maize and teosinte, which suggests that they contribute to traits selected during domestication. Note that these genes are depauperate for polymorphism in maize, and hence it is unlikely that they could have been

identified by methods that require segregating variation within maize, such as QTL or association analysis. The statistical methodology designed for this study will prove helpful both for identifying new candidates in maize and for application to other species, such as humans, where there is interest in selection on genes during the migration of modern humans out of Africa [e.g., (26)]. Finally, additional studies of our high-PP genes may provide important insight into the pathways and mutations responsible for maize evolution.

References and Notes

1. J. Doebley, *Annu. Rev. Genet.* **38**, 37 (2004).
2. R. L. Wang, A. Stec, J. Hey, L. Lukens, J. Doebley, *Nature* **398**, 236 (1999).
3. E. S. Buckler, J. M. Thornsberry, S. Kresovich, *Genet. Res.* **77**, 213 (2001).
4. H. Innan, Y. Kim, *Proc. Natl. Acad. Sci. U.S.A.* **101**, 10667 (2004).
5. N. Galtier, F. Depaulis, N. H. Barton, *Genetics* **155**, 981 (2000).
6. G. A. Watterson, *Theor. Popul. Biol.* **7**, 256 (1975).
7. M. I. Tenailon, J. U'Ren, O. Tenailon, B. S. Gaut, *Mol. Biol. Evol.* **21**, 1214 (2004).
8. L. Zhang, A. S. Peck, D. Dunams, B. S. Gaut, *Genetics* **162**, 851 (2002).
9. R. R. Hudson, *Genetics* **159**, 1805 (2001).
10. J. D. Wall, P. Andolfatto, M. Przeworski, *Genetics* **162**, 203 (2002).
11. F. Tajima, *Genetics* **123**, 597 (1989).
12. A. Eyre-Walker, R. L. Gaut, H. Hilton, D. L. Feldman, B. S. Gaut, *Proc. Natl. Acad. Sci. U.S.A.* **95**, 4441 (1998).

13. Y. Matsuoka et al., *Proc. Natl. Acad. Sci. U.S.A.* **99**, 6080 (2002).
14. See supporting data on Science Online.
15. H. Hilton, B. S. Gaut, *Genetics* **150**, 863 (1998).
16. Y. Vigouroux et al., *Mol. Biol. Evol.* **19**, 1251 (2002).
17. J. Doebley, A. Stec, C. Gustus, *Genetics* **141**, 333 (1995).
18. R. M. Clark, E. Linton, J. Messing, J. F. Doebley, *Proc. Natl. Acad. Sci. U.S.A.* **101**, 700 (2004).
19. R. Bressani, E. T. Mertz, *Cereal Chem.* **35**, 227 (1958).
20. J. Doebley, A. Stec, *Genetics* **134**, 559 (1993).
21. J. Doebley, A. Stec, *Genetics* **129**, 285 (1991).
22. J. Messing et al., *Proc. Natl. Acad. Sci. U.S.A.* **101**, 14349 (2004).
23. J. Maynard Smith, J. Haigh, *Genet. Res.* **23**, 23 (1974).
24. S. R. Whitt, L. M. Wilson, M. I. Tenailon, B. S. Gaut, E. S. t. Buckler, *Proc. Natl. Acad. Sci. U.S.A.* **99**, 12959 (2002).
25. K. Palaisa, M. Morgante, S. Tingey, A. Rafalski, *Proc. Natl. Acad. Sci. U.S.A.* **101**, 9885 (2004).
26. J. M. Akey et al., *PLoS Biol.* **2**, e286 (2004).
27. We thank P. Morrell, M. Clegg, T. Long, S. McDonald, M. Przeworski, and P. Andolfatto for comments and discussion; K. Houchins, L. Schultz, and N. Duru for technical assistance; and S. Frank and L. Donaldson for use of computer clusters. Supported by NSF grants DBI0096033, DBI9872655, and DBI0321467 and by the USDA–Agricultural Research Service.

Supporting Online Material

www.sciencemag.org/cgi/content/full/308/5726/1310/DC1
 Materials and Methods
 Figs. S1 and S2
 Tables S1 and S2
 References

24 April 2005; accepted 9 May 2005
 10.1126/science.1107891

Resting Microglial Cells Are Highly Dynamic Surveillants of Brain Parenchyma in Vivo

Axel Nimmerjahn,¹ Frank Kirchhoff,² Fritjof Helmchen^{1*}

Microglial cells represent the immune system of the mammalian brain and therefore are critically involved in various injuries and diseases. Little is known about their role in the healthy brain and their immediate reaction to brain damage. By using in vivo two-photon imaging in neocortex, we found that microglial cells are highly active in their presumed resting state, continually surveying their microenvironment with extremely motile processes and protrusions. Furthermore, blood-brain barrier disruption provoked immediate and focal activation of microglia, switching their behavior from patrolling to shielding of the injured site. Microglia thus are busy and vigilant housekeepers in the adult brain.

Microglial cells are the primary immune effector cells in the brain. In response to any kind of brain damage or injury, microglial cells become activated and undergo morphological as well as functional transformations. They are critically involved in lesions, neurodegenerative diseases, stroke, and brain tumors

(1–4). Resident microglial cells in the healthy brain are thought to rest in a dormant state, whereas activation is associated with structural changes, such as motile branches or migration of somata (5, 6). However, because most tissue preparations represent traumatic injuries by themselves, key aspects of microglia function have remained elusive.

Here, we investigated microglia behavior in intact adult brains both during the resting state and immediately after local injury by using in vivo two-photon microscopy (7). We used transgenic mice showing specific expression of enhanced green fluorescent protein

¹Abteilung Zellphysiologie, Max Planck Institut für Medizinische Forschung, Jahnstrasse 29, 69120 Heidelberg, Germany. ²Abteilung Neurogenetik, Max Planck Institut für Experimentelle Medizin, Hermann-Rein-Strasse 3, 37075 Göttingen, Germany.

*To whom correspondence should be addressed. E-mail: fritjof@mpimf-heidelberg.mpg.de

(EGFP) in resident microglia of the central nervous system (CNS). EGFP expression is achieved through placement of the EGFP reporter gene into the *Cx3cr1* locus encoding the chemokine receptor CX₃CR1 (8). Fluorescence images were acquired transcranially by using a thinned-skull preparation (fig. S1A) (9), except for cases that required direct access to the brain. Microglial cells had small rod-shaped somata from which numerous thin and highly ramified processes extended symmetrically (fig. S1B). Their three-dimensional distribution in vivo was rather homogeneous, displaying a territorial organization with typical cell-to-cell distances of 50 to 60 μm and volume densities of $6.5 \times 10^3 \pm 0.6 \times 10^3$ cells/ mm^3 and $6.4 \times 10^3 \pm 0.4 \times 10^3$ cells/ mm^3 in layer 1 and layer 2/3, respectively ($n = 6$ animals).

Time-lapse imaging experiments of up to 10 hours showed that somata of microglial cells generally remained fixed with only few signs of migration (5% of somata shifted their position by 1 to 2 μm per hour; 99 total cells; $n = 12$ animals). In contrast, microglial processes were remarkably motile, continuously undergoing cycles of de novo formation and withdrawal. These structural dynamics occurred on a time scale of minutes, leading to comprehensive changes in cellular morphologies within 1 hour except for a small scaffold of stable branches (Fig. 1A and movies S1 and S2). To quantify motility, we measured the velocity of length changes of individual processes. On average, extensions and retractions had similar velocities of 1.47 ± 0.10 $\mu\text{m}/\text{min}$ and 1.47 ± 0.08 $\mu\text{m}/\text{min}$, respectively (Fig. 1, B and C) (range from 0.4 to 3.8 $\mu\text{m}/\text{min}$; 95 extensions and 147 retractions in 14 cells; $n = 8$ animals; typically, thick branches were on the lower end of this range). Branch additions and losses occurred at every branch order and balanced each other (Fig. 1D).

Microglia processes also displayed highly motile filopodia-like protrusions of variable shape, typically forming bulbous endings (Fig. 1E and movie S3). Such protrusions transiently and sometimes repeatedly appeared at various locations along the main processes and at their terminal endings. Often protrusive activity stalled for several minutes before further extension (or retraction) occurred (Fig. 1F). Time-lapse imaging at high temporal and spatial resolution revealed a high turnover of protrusions with velocities of up to 4.1 $\mu\text{m}/\text{min}$ (extensions and retractions had similar rates: total average of 2.2 ± 0.2 $\mu\text{m}/\text{min}$, range from 0.6 to 4.1 $\mu\text{m}/\text{min}$, 22 extensions and 23 retractions on two cells in two animals). The average lifetime of such protrusions was 3.9 ± 0.2 min (Fig. 1, F and G) (72 protrusions in three cells; $n = 3$ animals; range from 1.7 to 8.3 min). Despite the constantly changing decoration of microglial processes with protrusions, the number of sites per cell showing

protrusive activity remained rather constant over time (fig. S2, A and B) (mean of 19.3 ± 5.3 for $n = 8$ cells), as did the average total length of microglial processes (fig. S2B).

Microglial processes and protrusions sampled the extracellular space in a seemingly random fashion and at a high turnover rate. To quantify the volume fraction surveyed by microglia per time, we analyzed cumulative maximum-intensity projections through time-

lapse recordings (9) (Fig. 2A), yielding a progressive filling rate of $14.4 \pm 1.6\%$ per hour ($n = 8$ animals) (Fig. 2B). Considering that the volume fraction of extracellular space is estimated to be about 20% (10), this suggests that the brain parenchyma is completely screened by resting microglia once every few hours. In doing so, microglial cells vary their territories. Border zones between neighboring microglial cells were mutable, and changes in favor of adjacent cells

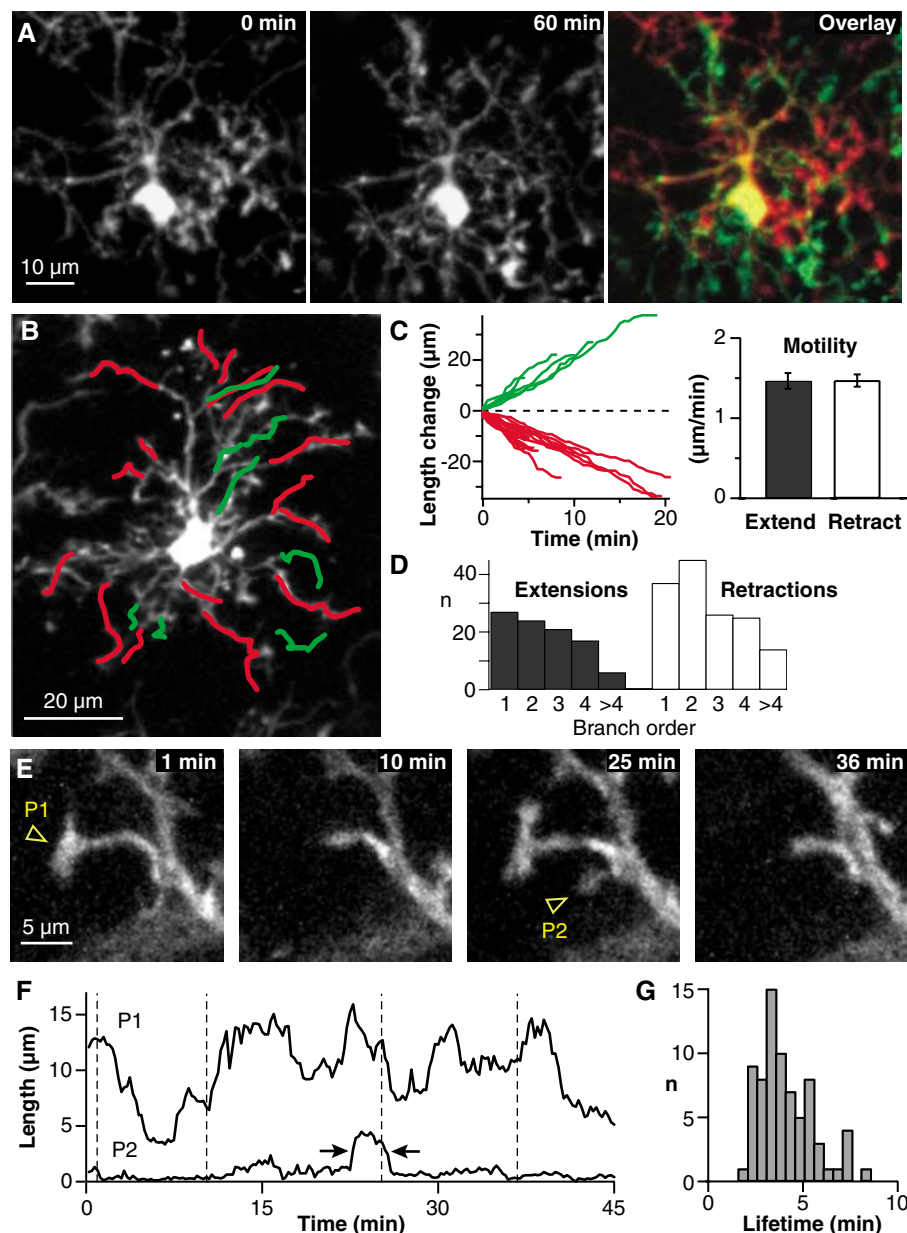


Fig. 1. Microglial cells are highly dynamic in the resting state in vivo. (A) Maximum-intensity projections of an individual microglial cell (45 to 75 μm below the pia) at the beginning (left) and 1 hour after (center) the start of a transcranial time-lapse recording. (Right) Overlay showing extensive formation (green) and deletion (red) of microglial processes. (B) Extensions (green) and retractions (red) of processes over the time course of 20 min. (C) Length changes of the processes shown in (B) as a function of time. (Right) Mean motility values in $\mu\text{m}/\text{min}$ for extensions and retractions. (D) Branch motility occurred at every branch order. (E) Example images of microglial protrusions (arrowheads) from a time-lapse recording. (F) Length changes over time of the two protrusions P1 and P2 indicated in (E). Vertical dashed lines mark the acquisition times of the images shown in (E). Arrows indicate protrusion lifetime (9). (G) Lifetime histogram of protrusions.

often occurred after retraction of thick processes in another cell. When processes of neighboring microglial cells encountered one other, endings mutually repelled each other.

This high resting motility may serve a housekeeping function, enabling microglial cells to effectively control the microenvironment and to clear the parenchyma of accumulated (low diffusible) metabolic products and deteriorated tissue components. Indeed, branch protuberances of microglial cells were short-lived and typically showed bulbous endings, indicating that tissue material had been collected. In a few cases, we observed spontaneous engulfments of tissue components, which subsequently were transported toward the soma (Fig. 2C and movie S4). To further reveal the interaction between microglia and other cortical elements, we counterstained astroglia with the red fluorescent dye sulforhodamine 101 (SR101) (11). Control imaging experiments before, during, and after SR101 application showed no adverse effects of SR101 itself on microglia motility ($n = 4$ animals). Unlike microglial cells, astrocytes showed no comparable restructuring of their processes. The SR101 counterstain also enabled us to visualize neuronal cell bodies and cortical blood vessels, which appear as unstained dark areas (Fig. 2D). Microglia processes and protrusions directly contacted astrocytes, neuronal cell bodies, and blood vessels, suggesting that in the healthy brain microglia dynamically interact with other cortical elements (Fig. 2D and movie S5). Because microglia are thought to monitor neuronal well-being through molecular changes in their microenvironment (12), we tested whether a change in the level of neuronal activity might affect microglia behavior. Surface application of the ionotropic γ -aminobutyric acid (GABA) receptor blocker bicuculline (BCC, 50 μ M) was found to significantly increase microglia volume sampling, whereas application of the sodium channel blocker tetrodotoxin (TTX, 25 to 50 μ M) had no significant effect [Supporting Online Material (SOM) Text, fig. S3, and movie S6].

Another likely function of the high resting microglia motility is to facilitate prompt reactions to brain injury (5). We therefore characterized microglia activation immediately after targeted disruption of the blood-brain barrier (BBB) at the level of individual capillaries (Fig. 3). Vessel outlines were visualized with the use of SR101 application. After a baseline imaging period, individual capillaries of about 6 μ m diameter were damaged by using highly localized laser lesions either through the thinned skull or through a small cranial window (Fig. 3A and movie S7). Disruption of the BBB was indicated by local tissue expansion and detachment of astroglial end feet. Laser lesions caused extravasation of dye in three experiments in which blood

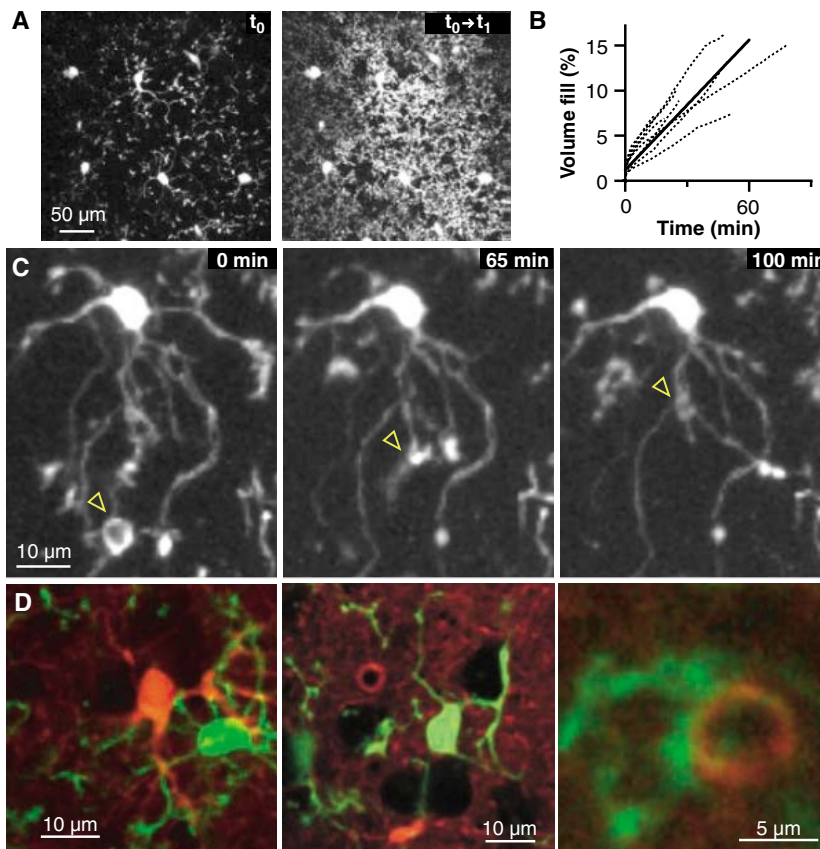


Fig. 2. Resting microglia continuously sample their microenvironment and dynamically interact with other cortical elements. (A) Example images illustrating cumulative volume sampling. (Left) Initial image at time t_0 . (Right) Cumulative projection at a later time point, t_1 (9). (B) Quantitation of volume sampling. Dashed lines, percentage increases for individual cells; solid line, average trace. (C) Example images from a time-lapse recording showing spontaneous engulfment and subsequent evacuation of tissue components by microglial processes (yellow arrowheads). (D) Example images showing how microglial processes and protrusions contact neighboring astrocytes (left), neuronal cell bodies (center; unstained dark areas), and the astrocytic sheath around a microvessel (right). Images are overlays of the green microglia and red SR101 stain.

plasma was stained via tail-vein injection of a dextran-conjugated fluorescent dye (movie S8). Laser lesions induced an immediate microglia response, indicated by a switch from undirected to targeted movement of nearby microglial processes toward the injured site (Fig. 3B and movies S7 and S9). The average velocity of extensions radially impinging on the injured site was similar to extension rates during the resting state (mean of 1.8 ± 0.3 μ m/min for $n = 5$ animals). Processes on the far side of activated microglial cells subsequently started to retract.

The number of responding microglial cells depended on the severity of the injury. In general, only microglial cells in the immediate vicinity of the microlesion were activated, whereas cells farther away (>90 μ m) did not or did not immediately respond. In two cases, laser lesions caused a transient activation of only a single microglial cell. In those cases, no measurable tissue expansion was observed, indicating only mild damage to the BBB. Yet in all lesion experiments, shielding of the injured area through accumu-

lation of microglial extensions was observed (Fig. 3B and movie S10). In cases of severe BBB disruption, multiple spherical-shaped inclusions started to form around 10 to 15 min after the lesion, indicating phagocytic activity by microglial processes. Inclusions were found within 15- to 25- μ m radial distances of the injured site, showing diverse dimensions with an average diameter of 4.6 ± 0.3 μ m (Fig. 3, C and D and movie S11) (range from 4.6 to 11.1 μ m; $n = 34$ inclusions in two animals). Inclusions were stable for several minutes (mean of 11.6 ± 1.9 min and range from 1.8 to 23.9 min) before they rapidly collapsed (mean of 2.0 ± 0.5 min; $n = 14$ inclusions in two animals) to around 40% of their initial size (Fig. 3E). Notably, the larger the inclusions, the shorter their lifetimes. Within the observation period (up to 5.5 hours), somata of microglial cells became more rounded. They did not, however, migrate toward the injured site. Interestingly, SR101-labeled astrocytes showed no morphological response to the laser-induced microstroke. A switch from undirected surveillance behavior to targeted

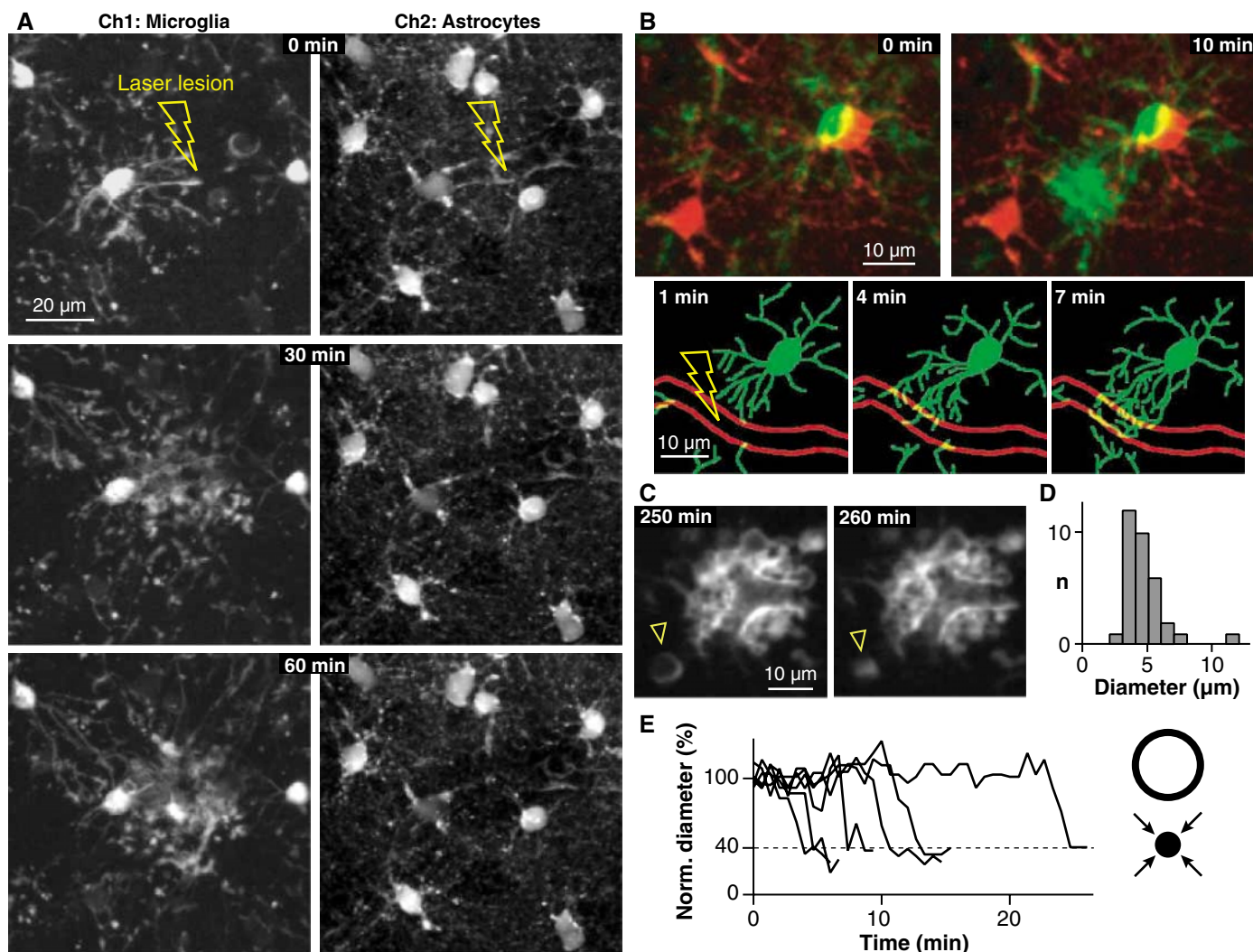


Fig. 3. Microglia are rapidly activated after local BBB disruption. (A) Fluorescence images of EGFP-expressing microglial cells (Ch1) and SR101 counterstained astrocytes (Ch2) before, 30 min, and 60 min after a targeted laser-induced microlesion. The disrupted blood vessel is apparent in Ch2 (yellow flashes indicate the site of injury). (B) Rapid shielding of a lesioned blood vessel section. (Top) Overlay of green microglia and red-stained astrocytes before and 10 min after the laser-induced lesion. (Bottom) Microglia morphology at intermediate time points showing rapid, targeted movement

of microglial processes toward the injured blood vessel (outlined in red; yellow flash indicates the site of injury). (C) Activated microglial processes at the site of laser lesion about 4 hours after injury. Several spherical engulfments are visible in the vicinity of the lesioned blood vessel arborization. Arrowhead points to an engulfment that collapsed within a few minutes. (D) Histogram of the diameter distribution of 33 postlesion engulfments. (E) (Left) Example time courses of spherical shaped engulfments. Diameters are normalized to initial values. (Right) Schematic illustrating the collapse of an engulfment.

movement of microglial processes was also observed in response to local lipopolysaccharide application (SOM Text).

Our results demonstrate that microglial cells are highly dynamic structures during the “resting” state *in vivo* and not only after activation. The extent of ongoing structural changes far exceeds what has been described for both neurons (13, 14) and astrocytes (15) on a similar time scale (SOM Text). The pronounced and ongoing structural changes of resting microglial cells presumably serve an immune surveillance function (SOM Text). In particular, microglia can sense subtle changes in their microenvironment through a variety of surface receptors, such as purino- and fractalkine receptors (12), receptors for complement fragments, immunoglobulins, ad-

hesion molecules, and inflammatory stimuli (16). In addition, microglia can respond to these changes, for example, through expression of neurotrophic factors or release of pro- and anti-inflammatory cytokines upon activation (12). Our experiments suggest that microglia perform this surveillance function by continuously sampling their environment with highly motile protrusions. These protrusions may also be involved in collecting tissue debris. Microglia motility most likely has its basis in actin, a cytoskeletal protein shown to be critically involved in growth and motility in many cells. Indeed, microglia contain high amounts of filamentous actin (17), and inhibitors of actin polymerization have been shown to affect the motility and migration of activated microglial cells (5).

Activated microglia are thought to exert neuroprotective as well as neurotoxic functions on neurons. Overall this effect may depend on both pathologic conditions and injury severity (12, 16). In our microlesion experiments, the shielding of injured sites indicated a neuroprotective role for microglia. Furthermore, the early formation of spherical-shaped inclusions suggests immediate phagocytic engulfment and removal of damaged tissue or leaked blood components. Together, this is consistent with the idea that microglia constitute the first line of defense against invading pathogens (12, 18). In conjunction with animal models of brain disease, our *in vivo* imaging approach presents the opportunity to study the role of microglia in various pathologies in the intact brain.

References and Notes

- G. W. Kreutzberg, *Trends Neurosci.* **19**, 312 (1996).
- G. Stoll, S. Jander, *Prog. Neurobiol.* **58**, 233 (1999).
- W. J. Streit, *Glia* **40**, 133 (2002).
- W. J. Streit, *J. Neurosci. Res.* **77**, 1 (2004).
- C. Nolte, T. Moller, T. Walter, H. Kettenmann, *Neuroscience* **73**, 1091 (1996).
- N. Stence, M. Waite, M. E. Dailey, *Glia* **33**, 256 (2001).
- W. Denk, K. Svoboda, *Neuron* **18**, 351 (1997).
- S. Jung et al., *Mol. Cell. Biol.* **20**, 4106 (2000).
- Materials and methods are available as supporting material on Science Online.
- A. Lehmenkuhler, E. Sykova, J. Svoboda, K. Zilles, C. Nicholson, *Neuroscience* **55**, 339 (1993).
- A. Nimmerjahn, F. Kirchhoff, J. N. D. Kerr, F. Helmchen, *Nat. Methods* **1**, 31 (2004).
- D. van Rossum, U. K. Hanisch, *Metab. Brain Dis.* **19**, 393 (2004).
- J. Grutzendler, N. Kasthuri, W. B. Gan, *Nature* **420**, 812 (2002).
- J. T. Trachtenberg et al., *Nature* **420**, 788 (2002).
- J. Hirrlinger, S. Hulsman, F. Kirchhoff, *Eur. J. Neurosci.* **20**, 2235 (2004).
- G. Raivich et al., *Brain Res. Rev.* **30**, 77 (1999).
- F. Capani, M. H. Ellisman, M. E. Martone, *Brain Res.* **923**, 1 (2001).
- F. Vilhardt, *Int. J. Biochem. Cell Biol.* **37**, 17 (2005).
- We thank S. Erdogan for help with the analysis, J. N. D. Kerr and G. W. Kreutzberg for comments on the manuscript, S. Jung and D. R. Littman for providing the green fluorescent microglia mouse line, and B. Sakmann for generous support. This work was sup-

ported by a predoctoral fellowship of the Boehringer Ingelheim Fonds to A.N.

Supporting Online Material

www.sciencemag.org/cgi/content/full/1110647/DC1
 Materials and Methods
 SOM Text
 Figs. S1 to S3
 References and Notes
 Movies S1 to S12

3 February 2005; accepted 17 March 2005

Published online 14 April 2005;

10.1126/science.1110647

Include this information when citing this paper.

Structural Bioinformatics-Based Design of Selective, Irreversible Kinase Inhibitors

Michael S. Cohen, Chao Zhang, Kevan M. Shokat, Jack Taunton*

The active sites of 491 human protein kinase domains are highly conserved, which makes the design of selective inhibitors a formidable challenge. We used a structural bioinformatics approach to identify two selectivity filters, a threonine and a cysteine, at defined positions in the active site of p90 ribosomal protein S6 kinase (RSK). A fluoromethylketone inhibitor, designed to exploit both selectivity filters, potently and selectively inactivated RSK1 and RSK2 in mammalian cells. Kinases with only one selectivity filter were resistant to the inhibitor, yet they became sensitized after genetic introduction of the second selectivity filter. Thus, two amino acids that distinguish RSK from other protein kinases are sufficient to confer inhibitor sensitivity.

Phosphorylation of serine, threonine, and tyrosine residues is a primary mechanism for regulating protein function in eukaryotic cells. Protein kinases, the enzymes that catalyze these reactions, regulate essentially all cellular processes and have thus emerged as therapeutic targets for many human diseases (1). Small-molecule inhibitors of the Abelson tyrosine kinase (Abl) and the epidermal growth factor receptor (EGFR) have been developed into clinically useful anticancer drugs (2, 3). Selective inhibitors can also increase our understanding of the cellular and organismal roles of protein kinases. However, nearly all kinase inhibitors target the adenosine triphosphate (ATP) binding site, which is well conserved even among distantly related kinase domains. For this reason, rational design of inhibitors that selectively target even a subset of the 491 related human kinase domains continues to be a daunting challenge.

Structural and mutagenesis studies have revealed key determinants of kinase inhibitor selectivity, including a widely exploited se-

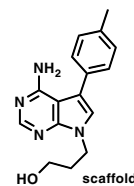
lectivity filter in the ATP binding site known as the "gatekeeper." A compact gatekeeper (such as threonine) allows bulky aromatic substituents, such as those found in the Src family kinase inhibitors, PP1 and PP2, to enter a deep hydrophobic pocket (4–6). In contrast, larger gatekeepers (methionine, leucine, isoleucine, or phenylalanine) restrict access to this pocket. A small gatekeeper provides only partial discrimination between kinase active sites, however, as ~20% of human kinases have a threonine at this position. Gleevec, a drug used to treat chronic myelogenous leukemia, exploits a threonine gatekeeper in the Abl kinase domain, yet it also potently inhibits the distantly related tyrosine kinase, c-KIT, as well as the platelet-derived growth factor receptor (PDGFR) (7).

We therefore sought a second selectivity filter that could be discerned from a primary sequence alignment. Among the 20 amino acids, cysteine has unique chemical reactivity and is commonly targeted by electrophilic inhibitors. In the case of cysteine protease inhibitors, the reactive cysteine is not a selectivity filter, because it is found in every cysteine protease and is essential for catalysis. Electrophilic, cysteine-directed inhibitors of the EGFR kinase domain have also been reported (8), but here again, the cysteine does not act as a selectivity filter, because neither the electrophile nor the reactive cysteine is required for potent, selective inhibition by these compounds. In this report, we describe the rational design of selective kinase inhibitors that require the simultaneous presence of a threonine gatekeeper and a reactive cysteine, which are uniquely found in the C-terminal kinase domain of p90 ribosomal protein S6 kinases (RSKs).

We used a kinomewide sequence alignment (1, 9) to search for cysteines that, together with a threonine gatekeeper, could form a covalent bond with an inhibitor in the ATP pocket. We focused on the conserved glycine-rich loop, which interacts with the triphosphate of ATP and is one of the most flexible structural elements of the kinase domain (10). A cysteine near this solvent-exposed loop is likely to have a lower pK_a and therefore to be more reactive than a cysteine buried in the hydrophobic pocket. Out of 491 related kinase domains in the human genome (1), we found 11 with a cysteine at the C-terminal end of the glycine-rich loop (Fig. 1A), a position usually occupied by valine. We next examined the gatekeeper in these

Table 1. Half-maximal inhibitory concentrations (IC_{50} in μM) for fmk and the pyrrolo[2,3-*d*]pyrimidine scaffold against the kinase activities of wild-type (WT) and mutant RSK2 CTDs. RSK2 CTDs were expressed in *E. coli* as His₆-tagged proteins and activated by incubation with bacterially expressed His₆-ERK2 and ATP. Kinase assay conditions: 30-min inhibitor pretreatment, 1 nM RSK2 CTD, 0.1 mM ATP, 0.1 mM "CTD-tide" substrate (14). WT and mutant CTDs had similar kinase activities.

	WT	C436V	T493M
fmk	0.015 ± 0.001	>10	3.4 ± 0.3
scaffold	1.2 ± 0.08	0.43 ± 0.14	>30



Program in Chemistry and Chemical Biology, and Department of Cellular and Molecular Pharmacology, University of California, San Francisco, CA 94143–2280, USA.

*To whom correspondence should be addressed. E-mail: taunton@cmp.ucsf.edu

kinases. Three closely related paralogs, RSK1, RSK2, and RSK4, have a threonine gatekeeper, whereas the remaining nine kinases, including RSK3, have larger gatekeepers (Fig. 1A). RSK1 and RSK2 are downstream effectors of the Ras-mitogen-activated protein kinase (MAPK) pathway and are directly activated by the MAPKs, ERK1 and ERK2 (11, 12). Mutations in the RSK2 gene cause Coffin-Lowry syndrome, a human disorder characterized by severe mental retardation (13). However, the precise roles of RSKs are poorly understood. All RSKs have two kinase domains. The regu-

latory C-terminal kinase domain (CTD) has the cysteine and threonine selectivity filters.

To exploit both selectivity filters in RSK family kinases, we needed a scaffold that could present an electrophile to the cysteine while occupying the hydrophobic pocket defined by the gatekeeper. Crystal structures of kinases with bound ATP analogs all reveal van der Waals contacts between a conserved valine, analogous to the cysteine we identified in RSKs (Fig. 1A), and the adenine C-8 position. We therefore designed and synthesized cmk and fmk (Fig. 1B), pyrrolopyrimi-

dines that contained a chloromethylketone and a fluoromethylketone, respectively. The *p*-tolyl substituent was designed to occupy the putative hydrophobic pocket. Structurally related pyrrolopyrimidines interact similarly with Src family kinases (4–6). We hypothesized that the electrophilic halomethylketones would be within striking distance of the key cysteine in RSK1, RSK2, and RSK4 and that kinases with only one of the two selectivity filters would be resistant to the inhibitors.

We first tested the electrophilic pyrrolopyrimidines against the RSK2 CTD in vitro (14). Both fmk (Table 1) and cmk (15) inhibited RSK2 CTD activity with similar potencies, but we focused on fmk because of its greater chemical stability. To test whether both selectivity filters were required for fmk sensitivity, we expressed two CTD mutants, C436V, in which Cys⁴³⁶ was replaced with Val, and T493M, in which Thr⁴⁹³ was replaced with Met. Fmk was a potent and selective inhibitor of wild-type (WT) RSK2 [half-maximal inhibitory concentration (IC₅₀) = 15 nM], with greater than 600- and 200-fold selectivity over the C436V and T493M mutants, respectively (Table 1). To test whether fmk forms an irreversible covalent bond with RSK2, we prepared a biotinylated derivative (see Supporting Online Material). Biotin-fmk reacted irreversibly with WT RSK2, but not with the selectivity filter mutants, as shown by denaturing gel electrophoresis and Western blot analysis with streptavidin-horseradish peroxidase (HRP) (Fig. 2A). ERK2, required to activate RSK2 in vitro, was not labeled by biotin-fmk, despite the presence of a solvent-exposed cysteine in its ATP pocket (16).

We next tested the selectivity of biotin-fmk in a human epithelial cell lysate containing thousands of potentially reactive proteins.

nonconserved cysteine		gatekeeper	
Src	[276] LGQCGFGEVVMGTWNG	[333] SEEP---	IYIVTEYMSKGSLS
RSK1	[424] IGVGSYSVCKRCVHKA	[480] DDGKH--	VYLVTLELMRGGEL
RSK2	[428] IGVGSYSVCKRCIHKA	[484] DDGKY--	VYVVTLELMKGGEL
RSK3	[421] IGVGSYSVCKRCVHKA	[477] DDGKF--	VYLVMELEMRGGEL
RSK4	[432] IGVGSYSVCKRCIHAT	[488] DDGRY--	VYLVTLELMKGGEL
MSK1	[432] LGEGSFISICRKCIVHKK	[489] HDQLH--	TFLVMELNNGGEL
MSK2	[395] LGQGSFVCRRCRQRQ	[452] HDQLH--	TYLVLELLRGGEL
PLK1	[59] LGKGGFAKCFEISDAD	[121] EDNDF--	VFVLELCRRRSL
PLK2	[88] LGKGGFAKCYEMTDLT	[150] EDKEN--	IYILLEYSRR-S
PLK3	[29] LGKGGFARCYEATDTE	[91] EDADN--	IYIFLELCSRK-S
NEK2	[14] IGTGSYGRCKIRRKS	[75] IDRTNTTLYIVMEYCEGDL	
MEKK1	[1300] IGLGAFSSCYQAQDVG	[1371] CEKSN--	YNLFIEWMAGGSV

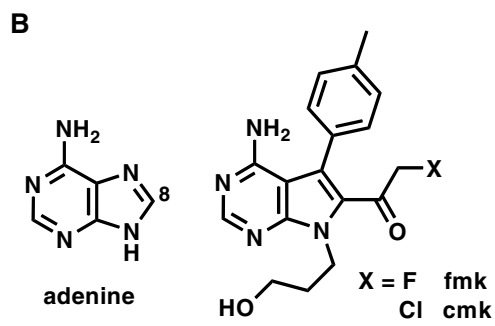


Fig. 1. Structural bioinformatics guides the design of electrophilic inhibitors of RSK family protein kinases. (A) Sequence alignment of the 11 human kinases with a cysteine selectivity filter at the C-terminal end of the glycine-rich loop. Of these 11, RSK1, RSK2, and RSK4 are the only kinases with a threonine selectivity filter in the gatekeeper position. Src, which has a threonine gatekeeper but lacks the cysteine, is shown for comparison. (B) Chemical structures of adenine and the rationally designed halomethylketone pyrrolopyrimidines, cmk and fmk.

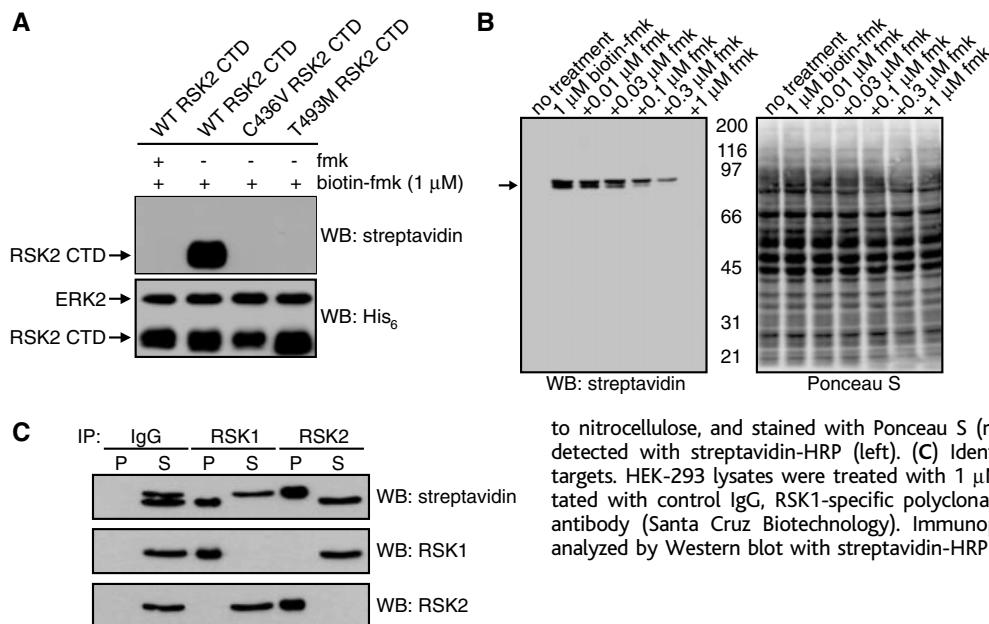


Fig. 2. Selective, irreversible targeting of RSK family kinases by fmk. (A) Covalent labeling of WT, but not mutant RSK2 by biotin-fmk. RSK2 with a hexahistidine tag (His₆-RSK2) CTDs were treated with 1 μM biotin-fmk in the presence of His₆-ERK2 for 1 hour. Proteins were resolved by SDS-polyacrylamide gel electrophoresis (SDS-PAGE) and detected by Western blot with streptavidin-HRP or antibodies to His₆. (B) Targeting of two ~90-kD proteins in human epithelial cell lysates by biotin-fmk. HEK-293 cell lysates were treated with the indicated concentrations of unlabeled fmk and then with 1 μM biotin-fmk. Proteins were resolved by SDS-PAGE, transferred to nitrocellulose, and stained with Ponceau S (right). Proteins labeled with biotin-fmk were detected with streptavidin-HRP (left). (C) Identification of RSK1 and RSK2 as biotin-fmk targets. HEK-293 lysates were treated with 1 μM biotin-fmk. Proteins were immunoprecipitated with control IgG, RSK1-specific polyclonal antibodies, or a RSK2-specific monoclonal antibody (Santa Cruz Biotechnology). Immunoprecipitates (P) and supernatants (S) were analyzed by Western blot with streptavidin-HRP and antibodies to RSK1 and RSK2.

Biotin-fmk (1 μ M) reacted with only two proteins, and labeling was abolished by pretreatment with 1 μ M fmk (Fig. 2B). These \sim 90-kD proteins were shown to be RSK1 and RSK2 by quantitative immunodepletion with specific antibodies (Fig. 2C). A cell-permeable, fluorescent derivative of fmk was also found to be highly selective toward RSK1 and RSK2 when added to cells growing in culture (15).

The only known substrate of the RSK2 CTD is Ser³⁸⁶ of RSK2 itself (17, 18). Phosphorylation of Ser³⁸⁶ creates a docking site for phosphoinositide-dependent kinase 1 (PKD1), which then phosphorylates and activates the N-terminal kinase domain (NTD) (19). The activated NTD then phosphorylates downstream substrates. Treatment of serum-starved COS-7 cells with EGF induced Ser³⁸⁶ phosphorylation of endogenous RSK2, which was inhibited by fmk with a half-maximal effective concentration (EC₅₀) of \sim 200 nM (Fig. 3A). Thus, the CTD appears to be the primary kinase responsible for EGF-stimulated Ser³⁸⁶ phosphorylation, consistent with results obtained with kinase-inactive mutants (17, 18). Fmk (10 μ M) had no effect on EGF-stimulated phosphorylation of ERK1 or ERK2 (Fig. 3B), the MAP kinases directly upstream of RSK2. This result further highlights the selectivity of fmk, as the signaling pathway leading to ERK activation involves at least three protein kinases (EGFR, Raf, and MEK), two of which (EGFR and Raf) have threonine gatekeepers, as well as potentially reactive cysteines, in their ATP binding pockets.

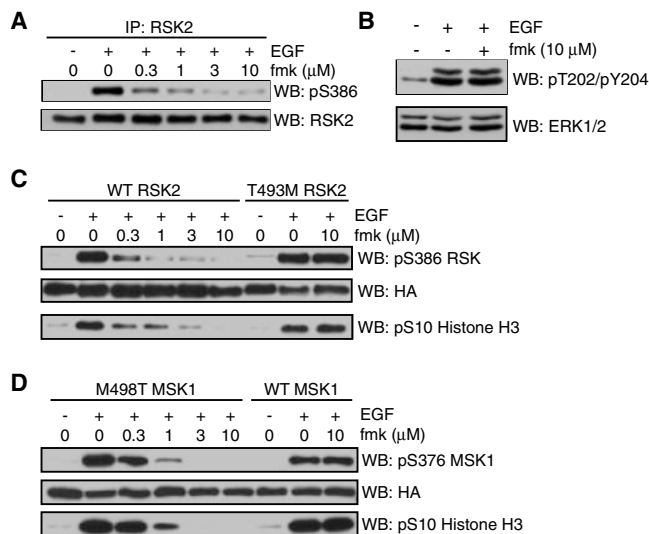
We next tested whether inhibition of the CTD by fmk could block signaling downstream of RSK2. In cells transfected with WT RSK2, treatment with EGF induced phosphorylation of histone H3 at Ser¹⁰, which was completely blocked by fmk (Fig. 3C). By contrast, H3 phosphorylation was unaffected by up to 10 μ M fmk in cells expressing the RSK2 gatekeeper mutant, T493M. Mutation of the cysteine selectivity filter to valine (C436V) also conferred complete resistance to fmk (fig. S1). Similar to RSK family kinases, the mitogen- and stress-activated kinases, MSK1 and MSK2, have two kinase domains. The CTD of MSK1 has a cysteine analogous to Cys⁴³⁶ of RSK2 (Fig. 1A), but unlike RSK2, MSK1 has a methionine gatekeeper. Fmk had no effect on H3 phosphorylation mediated by WT MSK1 (Fig. 3D). By contrast, an MSK1 mutant with a threonine gatekeeper was potently inhibited. Thus, despite having only \sim 40% sequence identity to RSK2, MSK1 became equally sensitive to fmk once the second selectivity filter was introduced. Fmk had no effect on phorbol ester-stimulated H3 phosphorylation in nontransfected fibroblasts (fig. S2), consistent with a dominant role for endogenous MSK1 and MSK2 in this pathway (20).

Pyrrolopyrimidines inhibit Src family kinases such as Fyn (21), which raises the possibility that they might be susceptible to reversible inhibition by cmk or fmk. WT Fyn was weakly inhibited by both compounds, with IC₅₀ values of \sim 4 μ M (compared with

an IC₅₀ value of 15 nM for fmk against RSK2). By contrast, cmk and fmk potently inhibited a Fyn mutant in which Val²⁸⁵ was replaced with Cys (IC₅₀ values of 1 nM and 100 nM, respectively). Similarly, at concentrations that completely inhibited RSK2 in cells, neither cmk nor fmk reversed the cellular phenotypes induced by v-Src (with a Thr in the gatekeeper position). By contrast, cmk (and less potently, fmk) promoted morphological reversion and reduced global tyrosine phosphorylation in cells expressing a v-Src mutant in which Val²⁸¹ was replaced with Cys (fig. S3).

In this study, we have rationally designed halomethylketone-substituted inhibitors whose molecular recognition by protein kinases requires the simultaneous presence of two selectivity filters: a cysteine following the glycine-rich loop and a threonine in the gatekeeper position. We estimate that \sim 20% of human kinases have a solvent-exposed cysteine in the ATP pocket. Because of the structural conservation of the pocket, it should be possible to predict the orientation of these cysteines. In addition, there are many reversible kinase inhibitors whose binding modes have been characterized by x-ray crystallography. The integration of both types of information should allow the design of scaffolds that exploit selectivity filters other than the gatekeeper, as well as the appropriate sites for attaching electrophilic substituents.

Fig. 3. Effect of fmk on EGF-activated RSK2 or MSK1. (A) Inhibition of EGF-stimulated RSK2 autophosphorylation by fmk. COS-7 cells were deprived of serum for 20 hours then treated with the indicated concentrations of fmk. Cells were stimulated for 10 min with EGF (1 ng/mL). RSK2 was immunoprecipitated and analyzed by Western blot with antibodies to phospho-Ser³⁸⁶ RSK (Cell Signaling Technology) and total RSK2. (B) Failure of fmk to inhibit EGF-stimulated activation of ERK1 and ERK2. Serum-starved COS-7 cells were treated with or without 10 μ M fmk, then stimulated with EGF as in (A). Doubly phosphorylated and total ERK1 and ERK2 were detected by Western blot (both antibodies from Cell Signaling Technology). (C) Inhibition of EGF-stimulated H3 phosphorylation in cells expressing WT RSK2, but not T493M RSK2. COS-7 cells were transfected with hemagglutinin (HA)-tagged WT or T493M RSK2. Twenty-four hours after transfection, cells were serum-starved for 3 hours then treated with the indicated concentrations of fmk. Cells were stimulated with EGF (150 ng/mL) for 25 min and subsequently lysed in Laemmli sample buffer. Proteins were resolved by SDS-PAGE and detected by Western blot with antibodies specific for phospho-Ser³⁸⁶ RSK, the HA epitope (Roche), or phospho-Ser¹⁰ H3 (Upstate). (D) Inhibition of MSK1 by fmk after mutation of Met⁴⁹⁸ to Thr. COS-7 cells were transfected with HA-tagged WT or M498T MSK1. MSK1 autophosphorylation and H3 phosphorylation were assessed as in (C).



References and Notes

- G. Manning, D. B. Whyte, R. Martinez, T. Hunter, S. Sudarsanam, *Science* **298**, 1912 (2002).
- B. J. Druker *et al.*, *Nat. Med.* **2**, 561 (1996).
- A. J. Barker *et al.*, *Bioorg. Med. Chem. Lett.* **11**, 1911 (2001).
- Y. Liu *et al.*, *Chem. Biol.* **6**, 671 (1999).
- T. Schindler *et al.*, *Mol. Cell* **3**, 639 (1999).
- X. Zhu *et al.*, *Structure Fold. Des.* **7**, 651 (1999).
- E. Buchdunger *et al.*, *J. Pharmacol. Exp. Ther.* **295**, 139 (2000).
- D. W. Fry *et al.*, *Proc. Natl. Acad. Sci. U.S.A.* **95**, 12022 (1998).
- O. Buzko, K. M. Shokat, *Bioinformatics* **18**, 1274 (2002).
- I. Tsigelny *et al.*, *Biopolymers* **50**, 513 (1999).
- T. W. Sturgill, L. B. Ray, E. Erikson, J. L. Maller, *Nature* **334**, 715 (1988).
- M. Frodin, S. Gammeltoft, *Mol. Cell. Endocrinol.* **151**, 65 (1999).
- A. Hanauer, I. D. Young, *J. Med. Genet.* **39**, 705 (2002).
- C. A. Chrestensen, T. W. Sturgill, *J. Biol. Chem.* **277**, 27733 (2002).
- M. S. Cohen, J. Taunton, unpublished data.
- B. J. Canagarajah, A. Khokhlatchev, M. H. Cobb, E. J. Goldsmith, *Cell* **90**, 859 (1997).
- T. A. Vik, J. W. Ryder, *Biochem. Biophys. Res. Commun.* **235**, 398 (1997).
- K. N. Dalby, N. Morrice, F. B. Caudwell, J. Avruch, P. Cohen, *J. Biol. Chem.* **273**, 1496 (1998).
- M. Frodin, C. J. Jensen, K. Merienne, S. Gammeltoft, *EMBO J.* **19**, 2924 (2000).
- A. Soloaga *et al.*, *EMBO J.* **22**, 2788 (2003).
- A. F. Burchat *et al.*, *Bioorg. Med. Chem. Lett.* **10**, 2171 (2000).
- This work was supported by the Searle Scholars Foundation (J.T.), the NIH (K.M.S.), and the ARCS Foundation (M.S.C.). We thank Y. Feng, T. Alber, K. Shah, T. Sturgill, C. Bjorbaek, M. Frodin, and M. Cobb

for reagents and S. Arriola for technical assistance. We thank W. Lim, H. Luecke, D. Morgan, B. Shoichet, H. Madhani, and E. O'Shea for advice on the manuscript and members of the Taunton and Shokat laboratories for many helpful discussions. Molecular interaction data have been deposited in the Bi-

molecular Interaction Network Database (BIND) with accession code 216037.

Supporting Online Material
www.sciencemag.org/cgi/content/full/308/5726/1318/DC1

Materials and Methods
Figs. S1 to S3
References and Notes

6 December 2004; accepted 23 February 2005
10.1126/science.1108367

Global Topology Analysis of the *Escherichia coli* Inner Membrane Proteome

Daniel O. Daley,^{1*} Mikaela Rapp,^{1*} Erik Granseth,² Karin Melén,²
David Drew,¹ Gunnar von Heijne^{1,2,†}

The protein complement of cellular membranes is notoriously resistant to standard proteomic analysis and structural studies. As a result, membrane proteomes remain ill-defined. Here, we report a global topology analysis of the *Escherichia coli* inner membrane proteome. Using C-terminal tagging with the alkaline phosphatase and green fluorescent protein, we established the periplasmic or cytoplasmic locations of the C termini for 601 inner membrane proteins. By constraining a topology prediction algorithm with this data, we derived high-quality topology models for the 601 proteins, providing a firm foundation for future functional studies of this and other membrane proteomes. We also estimated the overexpression potential for 397 green fluorescent protein fusions; the results suggest that a large fraction of all inner membrane proteins can be produced in sufficient quantities for biochemical and structural work.

Integral membrane proteins account for the coding capacity of 20 to 30% of the genes in typical organisms (1) and are critically important for many cellular functions. However, owing to their hydrophobic and amphiphilic nature, membrane proteins are difficult to study, and they account for less than 1% of the known high-resolution protein structures (2). Overexpression, purification, biochemical analysis, and structure determination are all far more challenging than for soluble proteins, and membrane proteins have rarely been considered in proteomics or structural genomics contexts to date.

In the absence of a high-resolution three-dimensional structure, an important cornerstone for the functional analysis of any membrane protein is an accurate topology model. A topology model describes the number of transmembrane spans and the orientation of the protein relative to the lipid bilayer. Topology models are usually produced by either sequence-based prediction or time-consuming experimental approaches. We have previously shown that topology prediction can be greatly improved by constraining it with an experimentally determined reference point, such as the location

of a protein's C terminus (3). For *E. coli* proteins, reference points can be obtained most easily through the use of topology reporter proteins such as alkaline phosphatase (PhoA) and green fluorescent protein (GFP). PhoA and GFP have opposite activity profiles: PhoA is active only in the periplasm of *E. coli* (4), whereas GFP is fluorescent only in the cytoplasm (5). When fused in parallel to the C terminus of a membrane protein, PhoA and GFP can accurately report on which side of the membrane the C terminus is located (6, 7). Here, we have applied the PhoA/GFP fusion approach to derive topology models for almost the entire *E. coli* inner membrane proteome.

Bioinformatic analysis of the *E. coli* proteome using the hidden Markov model topology predictor TMHMM (1) indicates that approximately 1000 of the 4288 predicted genes encode integral inner membrane proteins. We focused on the 737 genes that encode proteins longer than 100 residues with at least two predicted transmembrane helices. The second criterion was necessary to ensure that secreted proteins, whose hydrophobic signal sequence is often mistakenly predicted as a transmembrane helix, were not included.

Of the 737 selected genes, 714 were suitable for cloning into a standard set of *phoA* and *gfp* fusion vectors (8). We were able to obtain both fusions for 573 genes and one fusion for an additional 92 genes (Fig. 1, inset). By determining appropriate cutoffs (8), the C-terminal location (C_{in} , C_{out}) could be

assigned for 502 of the 665 cloned proteins by comparison of whole-cell GFP fluorescence and PhoA activity or, in a small number of cases, by either activity alone (Fig. 1).

To assign the location of the C terminus for the remaining proteins, we used the basic local alignment search tool (BLAST) (9) to search for homologs to the unassigned proteins among the 502 assigned proteins, imposing a strict E-value cutoff (10^{-4}) and the requirement that the BLAST-alignment should extend to within 25 residues of the C terminus of both proteins. We were able to assign C-terminal locations for an additional 99 proteins in this way, bringing the total number of assignments to 601 of the 737 proteins in the initial data set (table S1). Obviously, the same homology-based assignment scheme can be used to transfer the experimental data to other membrane proteomes.

The location of the C terminus for 71 of the 601 proteins was already known from published topology models (table S1) and was used to check the quality of our data. For all but two proteins, ArsB and YccA, our C-terminal assignment agreed with the published assignment. In the case of ArsB, the previous study (10) did not include experimental information on the location of the C terminus, and we suggest that our assignment is correct. For YccA, the reported experimental data on the location of the C terminus (11) contradicts our result; further studies will be required to resolve this discrepancy. In any case, it appears that

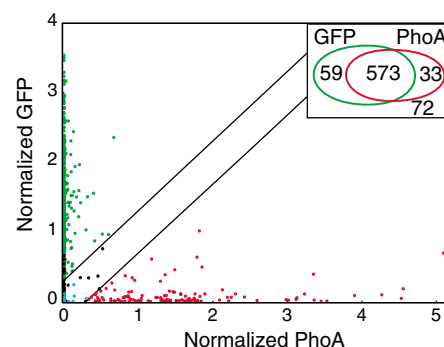


Fig. 1. Normalized PhoA and GFP activities. Cutoff lines for the assignment of C_{in} (cytoplasmic) and C_{out} (periplasmic) orientations are shown in black. Green and red dots: proteins assigned as C_{in} and C_{out} , respectively, based on the experimental data. Black and blue dots: proteins assigned as C_{in} and C_{out} , respectively, based on sequence homology to proteins with experimentally assigned C-terminal locations. (Inset) Venn diagram showing the number of proteins for which none, one, or both PhoA (red) and GFP (green) fusions were obtained.

¹Department of Biochemistry and Biophysics, Stockholm University, SE-106 91 Stockholm, Sweden.

²Stockholm Bioinformatics Center, AlbaNova, SE-106 91 Stockholm, Sweden.

*These authors contributed equally to this work.

†To whom correspondence should be addressed. E-mail: gunnar@dbb.su.se

Fig. 2. Functional categorization of the *E. coli* inner membrane proteome. (A) The fractions of the inner membrane proteome (737 proteins) assigned to different functional categories. (B) The number of proteins with assigned C-terminal location in each functional category for different topologies (601 proteins in total). C_{in} topologies are plotted upward, C_{out} downward. For C_{in} proteins, even numbers of transmembrane helices are three times as common as odd numbers; for C_{out} proteins, odd and even numbers of transmembrane helices are roughly equal.

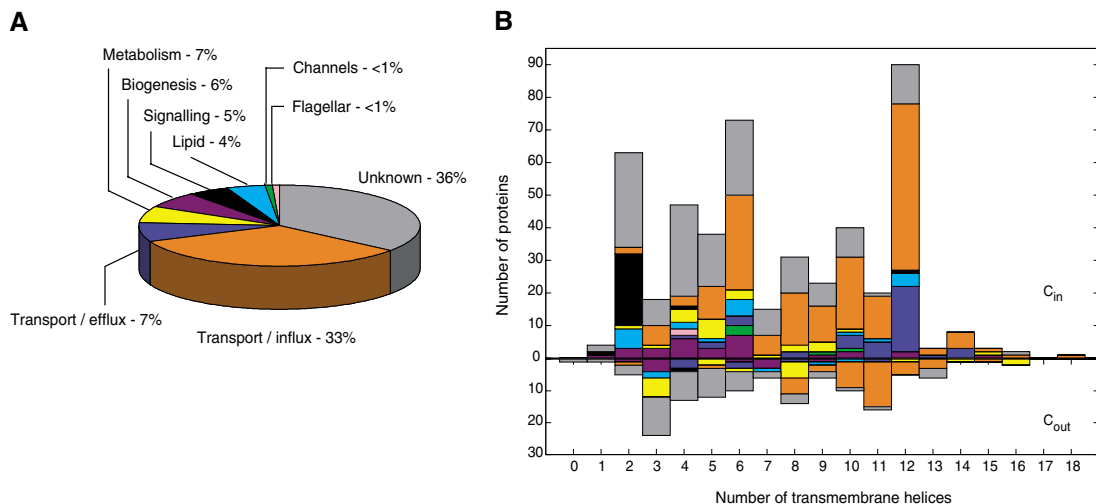
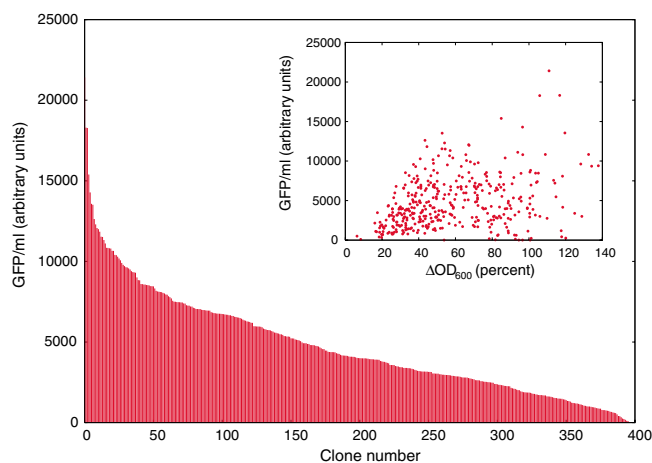


Fig. 3. GFP fluorescence for 397 C_{in} proteins. (Inset) Scatter plot with GFP activity plotted against the change in OD_{600} seen 2 hours after induction of protein expression compared with nontransformed cells grown under the same conditions [$100 \times \Delta OD_{600}$ (transformed cells) / ΔOD_{600} (nontransformed cells)].



the error rate in our C-terminal assignments is on the order of 1% or less.

Using the experimentally determined C-terminal locations as constraints for the TMHMM topology predictor (3), we generated experimentally based topology models for the 601 proteins, including 46 models from our previously published work (6, 7) (table S1 and www.sbc.su.se/~erikgr/tmhmm/index.html).

In the absence of experimental data, TMHMM alone predicts the correct C-terminal location for only 78% of the 601 proteins. By providing unambiguous C-terminal locations, the inclusion of experimental data thus leads to a major improvement in the overall quality of the topology models (illustrated in fig. S1). This is also reflected in the TMHMM reliability score (3); the score increases for 526 proteins and decreases for 75 proteins upon fixing of the C terminus.

To obtain a global view of the topologies within the proteome and how they relate to protein function, proteins were sorted according to known or predicted functional categories (Fig. 2). The most obvious trend is the predominance of $N_{in}-C_{in}$ topologies (57%

of all proteins), which suggests that pairs of closely spaced transmembrane helices (“helical hairpins”) may be a basic building block in membrane proteins. The largest functional category is transport proteins, many with 6 or 12 transmembrane helices. Most proteins with unknown function have ≤ 6 transmembrane helices, pointing to a systematic lack of studies of the smaller inner membrane proteins.

We have previously identified a case in which a gene duplication event has led to the formation of two separately expressed homologous proteins (YdgQ and YdgL) with opposite orientations in the membrane (12). To identify new instances of this kind, we searched for families of homologs that include pairs of proteins with the same number of predicted transmembrane helices but oppositely assigned C-terminal locations. Only the YdgE and YdgF proteins, both members of the small multidrug resistance (SMR) family of transporters (13), were found (fig. S2). The *ydgE* and *ydgF* genes overlap each other on the *E. coli* chromosome, and the two proteins catalyze drug efflux only when coexpressed (14), which suggests that they form

an antiparallel heterodimer (or higher oligomer) in the inner membrane.

EmrE, another member of the SMR family, has been suggested to adopt a dual topology in the inner membrane, where one $N_{in}-C_{in}$ molecule forms an antiparallel homodimer with one $N_{out}-C_{out}$ molecule (15–17). EmrE is assigned as C_{out} in our data set, but also has GFP fluorescence above background. Notably, EmrE contains very few positively charged residues, evenly distributed between the different loops, and thus lacks a clear “positive-inside” bias (18). We searched for additional candidate dual topology proteins with a weak charge bias and above-background PhoA and GFP activities. Five additional proteins emerged as possible dual topology proteins: SugE (a member of the SMR family), CrxB, YdgC, YnfA, and YbfB (fig. S2). Strikingly, all these proteins are small (around 100 residues) and have three or four strongly predicted transmembrane helices.

Although proteins with internal duplications in which the two halves of the protein have opposite orientations in the membrane are quite common among the *E. coli* inner membrane proteins (19–23), we conclude that homologs with opposite membrane orientations, as well as proteins with a dual topology, are exceedingly rare. Possibly, protein folding and assembly are more efficient when the two oppositely oriented halves are part of a single polypeptide chain than when they are expressed separately.

For the $\sim 80\%$ of the inner membrane proteome with a C_{in} orientation, the whole-cell GFP fluorescence provides a good estimate of the amount of fusion protein inserted into the membrane (24). Using standard overexpression conditions (8), we tabulated the GFP activity for the 397 proteins assigned as C_{in} (Fig. 3). We also assessed the effect of overexpression on cell growth, as determined by the change in optical density of the cell suspension after induction of membrane pro-

tein synthesis. Although a small number of proteins appeared toxic (Fig. 3, inset), the vast majority had only a limited effect on cell growth. Overexpression levels do not correlate with—and hence cannot be predicted by—obvious sequence characteristics such as codon usage, protein size, hydrophobicity, and number of transmembrane helices (table S2). The C-terminal His₆ tag and the tobacco etch virus (TEV) protease site present in the GFP fusions (8) make it possible to use an efficient, standardized purification protocol for the whole clone collection; yields of purified fusion protein are typically ≥ 1 mg per liter of culture (25). This sets a lower limit for what can be expected for individual proteins expressed, for example, without a GFP tag or using other expression vectors and growth conditions (26).

In conclusion, by analyzing a library of *E. coli* inner membrane proteins fused to PhoA and GFP, we have derived an experimentally based set of topology models for the membrane proteome and provide a large-scale data set on membrane protein overexpression. Our results provide an important basis for future functional

studies of membrane proteomes and will facilitate the identification of well-expressed targets for structural genomics projects.

References and Notes

1. A. Krogh, B. Larsson, G. von Heijne, E. Sonnhammer, *J. Mol. Biol.* **305**, 567 (2001).
2. S. H. White, *Protein Sci.* **13**, 1948 (2004).
3. K. Melén, A. Krogh, G. von Heijne, *J. Mol. Biol.* **327**, 735 (2003).
4. C. Manoil, J. Beckwith, *Science* **233**, 1403 (1986).
5. B. J. Feilmeier, G. Iseminger, D. Schroeder, H. Webber, G. J. Phillips, *J. Bacteriol.* **182**, 4068 (2000).
6. D. Drew *et al.*, *Proc. Natl. Acad. Sci. U.S.A.* **99**, 2690 (2002).
7. M. Rapp *et al.*, *Protein Sci* **13**, 937 (2004).
8. Materials and methods are available as supporting material on Science Online.
9. S. F. Altschul, W. Gish, W. Miller, E. W. Myers, D. J. Lipman, *J. Mol. Biol.* **215**, 403 (1990).
10. J. Wu, L. S. Tisa, B. P. Rosen, *J. Biol. Chem.* **267**, 12570 (1992).
11. A. Kihara, Y. Akiyama, K. Ito, *EMBO J.* **18**, 2970 (1999).
12. A. Sääf, M. Johansson, E. Wallin, G. von Heijne, *Proc. Natl. Acad. Sci. U.S.A.* **96**, 8540 (1999).
13. I. T. Paulsen *et al.*, *Mol. Microbiol.* **19**, 1167 (1996).
14. K. Nishino, A. Yamaguchi, *J. Bacteriol.* **183**, 5803 (2001).
15. I. Ubarretxena-Belandia, C. G. Tate, *FEBS Lett.* **564**, 234 (2004).
16. I. Ubarretxena-Belandia, J. M. Baldwin, S. Schuldiner, C. G. Tate, *EMBO J.* **22**, 6175 (2003).

17. C. Ma, G. Chang, *Proc. Natl. Acad. Sci. U.S.A.* **101**, 2852 (2004).
18. G. von Heijne, *EMBO J.* **5**, 3021 (1986).
19. B. van den Berg *et al.*, *Nature* **427**, 36 (2004).
20. D. Fu *et al.*, *Science* **290**, 481 (2000).
21. R. Dutzler, E. B. Campbell, M. Cadene, B. T. Chait, R. MacKinnon, *Nature* **415**, 287 (2002).
22. S. Khademi *et al.*, *Science* **305**, 1587 (2004).
23. T. Shimizu, H. Mitsuke, K. Noto, M. Arai, *J. Mol. Biol.* **339**, 1 (2004).
24. D. Drew, G. von Heijne, P. Nordlund, J. W. L. de Gier, *FEBS Lett.* **507**, 220 (2001).
25. D. Drew *et al.*, *Protein Sci*, in press.
26. S. Eshaghi *et al.*, *Protein Sci.* **14**, 676 (2005).
27. Supported by grants from the Swedish Research Council, the Marianne and Marcus Wallenberg Foundation, the Swedish Foundation for Strategic Research, and the Swedish Cancer Foundation to G.v.H., by the Swedish Knowledge Foundation to K.M., and by a European Molecular Biology Organization Long-Term Fellowship to D.O.D.

Supporting Online Material

www.sciencemag.org/cgi/content/full/308/5726/1321/DC1

Materials and Methods

Figs. S1 and S2

Tables S1 and S2

References

13 January 2005; accepted 14 March 2005

10.1126/science.1109730

Firearm Violence Exposure and Serious Violent Behavior

Jeffrey B. Bingenheimer,^{1*} Robert T. Brennan,² Felton J. Earls²

To estimate the cause-effect relationship between exposure to firearm violence and subsequent perpetration of serious violence, we applied the analytic method of propensity stratification to longitudinal data on adolescents residing in Chicago, Illinois. Results indicate that exposure to firearm violence approximately doubles the probability that an adolescent will perpetrate serious violence over the subsequent 2 years.

Within the past few decades, the popular notion that violence begets violence has come under scientific scrutiny. Early research by psychologists, criminologists, and others focused on the impact of being physically abused as a child on subsequent delinquency, community violence, and spouse and child abuse. Simple comparisons of violent offenders and nonoffenders showed that the former were more likely to report having been abused during childhood (1, 2). More carefully controlled prospective studies comparing abused and nonabused children confirmed these basic relationships (3) and provided insights into the cognitive and neurological mechanisms involved (4, 5).

Recently, interest has expanded to encompass exposure to violence occurring in community settings such as neighborhoods and schools. This change was spurred in part by elevated rates of violent crime, including firearm homicide, in American cities in the early 1990s (6, 7). In several studies conducted around that time, urban children and adolescents reported alarmingly high levels of exposure to community violence, both as witnesses and as victims (8–10). These findings raised troubling questions about the possible developmental ramifications of such widespread experience with violence.

Numerous recent investigations have revealed statistical associations between children's and adolescents' self-reports of exposure to community violence and concurrent or subsequent assessments of violence and aggression (11–14). Available estimates of these associations, however, do not adequately control for the possibility that a common set of personal characteristics and environment circumstances may jointly influence who is ex-

posed to community violence and who becomes a perpetrator of violent acts. The extent to which these statistical associations are attributable to cause-effect relationships therefore remains uncertain (15).

The randomized experiment is the scientific gold standard for causal inference, but in the instance of community violence is neither technically nor ethically feasible. We used the method of propensity score stratification (16–18) to approximate a randomized experiment in which exposure to firearm violence was the treatment variable and subsequent perpetration of serious violence was the outcome. This method is based upon counterfactual thinking and the framework of potential outcomes described by Rubin (19) and others (20). Investigators in economics (21), medicine (22), and other fields (23) are increasingly using propensity score matching and stratification to improve the credibility of estimates of cause-effect relationships obtained from observational data.

Propensity stratification views exposure allocation as a process involving both systematic and random components. First, personal and environmental characteristics of the individual determine systematically her or his probability π of exposure, called the propensity score. The individual then participates in a lottery in which the exposure is assigned with probability π , or nonexposure is assigned with probability $1 - \pi$. In theory, comparing individuals with identical propensity scores but different realized exposures is analogous to conducting a randomized experiment, and therefore provides a valid basis for measuring a cause-effect relationship between expo-

¹Department of Health Behavior and Health Education, 1420 Washington Heights, University of Michigan School of Public Health, Ann Arbor, MI 48109–2029, USA. ²Department of Social Medicine, Harvard Medical School, 1430 Massachusetts Avenue, 4th Floor, Cambridge, MA 02138, USA.

*To whom correspondence should be addressed. E-mail: bartbing@umich.edu

sure and outcome. The analytic strategy, then, has four stages: (i) Use all available preexposure information to derive an estimate $\hat{\pi}$ of each subject's propensity score; (ii) divide subjects into strata on the basis of $\hat{\pi}$; (iii) within each stratum, confirm that exposed and unexposed subjects are balanced on all measured preexposure covariates; and (iv) compute the mean difference between exposed and unexposed subjects on the outcome measure within these strata. This produces an unbiased estimate of the average causal effect of exposure under the assumption, termed "strongly ignorable treatment assignment" (16), that no measured or unmeasured preexposure characteristic predicts both exposure and outcome independent of estimated propensity scores. The greater the quantity and quality of preexposure information available to the analyst, the more precisely $\hat{\pi}$ will estimate π , and the more plausible the strongly ignorable treatment assignment assumption will become. Sensitivity analyses (24) enable the investigator to study the robustness of results to plausible violations of this assumption.

We analyzed data from a longitudinal cohort study of adolescents residing in 78 neighborhoods of Chicago, Illinois (Fig. 1) (25). The subjects ($N = 1517$) were aged 12 or 15 years at the beginning of the study (table S1). Subjects and their primary caregivers were each interviewed on three occasions over a period of 5 years. At Assessment 1, subjects and their caregivers provided detailed information about themselves. From these data we derived measures of 139 preexposure covariates falling into 10 domains: demographic background, family history and home environment, temperament, health and physical development, social support, peer influences, vocabulary and reading proficiency, school-

related factors, behavioral patterns, and previous exposure to violence (25) (table S2). Additionally, 14 neighborhood social and economic characteristics were quantified by means of census data and an independent survey of a probability sample of adult residents (26, 27), bringing the total number of preexposure covariates to 153 (25) (table S2).

At Assessment 2, subjects ($n = 1239$, 81.7% of the original sample) who could be located and who agreed to continue participating answered a series of questions regarding their exposure to firearm violence in the previous 12 months (25) (table S1). They were classified as exposed if they reported that they had been shot or shot at, or if they had seen someone shot or shot at, during that period. Those who reported none of these experiences were classified as unexposed. Fourteen subjects could not be classified due to missing or inconsistent data. Of those who could be classified, the majority ($n = 942$, 76.9%) were unexposed, and the remainder ($n = 283$, 23.1%) were exposed (25).

Subjects who reported exposure to firearm violence at Assessment 2 differed from unexposed subjects on many Assessment 1 covariates at the $\alpha = 0.01$ statistical significance level (Table 1; for more details see table S2). Compared with unexposed subjects, exposed subjects were more aggressive and reported committing more violent offenses. They tended to be non-white, male, from single-parent households, and receiving public assistance. In terms of temperament, exposed subjects were more impulsive and emotional and less inhibited than unexposed subjects. They were more likely to report having engaged in alcohol and drug use, truancy, general delinquency, and property crimes. Exposed subjects were more likely than unexposed subjects to

have family members with criminal records or legal problems. They were also more likely to have been corporally punished and physically abused and to have witnessed domestic violence in their households. Their peer groups were characterized by higher levels of aggressive and delinquent behaviors compared with the peer groups of unexposed subjects. Exposed subjects had lower scores on standardized tests of vocabulary and reading proficiency. Their neighborhoods of residence were characterized by more anomie, physical and social disorder, perceived violence, and concentrated disadvantage, and by lower levels of informal social control and satisfaction with policing, compared with the neighborhoods in which unexposed subjects resided. Many of these correlates of exposure to firearm violence are also well-established predictors of violent behavior (28, 29), substantiating the possibility that statistical associations between violence exposure and perpetration may be attributable in part to the joint influence of these factors on exposure and outcome status.

We used a maximum-likelihood logistic regression model to obtain an estimated propensity score $\hat{\pi}$ for each subject whose Assessment 2 exposure status was available. The model was constructed by an iterative stepwise selection procedure. The 153 Assessment 1 covariates, plus squared terms for the 92 covariates that were measured on continuous metrics, comprised the pool of candidate predictors. At each iteration, the procedure either (i) added to the model the single covariate that was most strongly associated with firearm violence exposure conditional upon the covariates already in the model, provided that the conditional association was statistically significant at the $\alpha = 0.10$ level, or (ii) removed from the model any covariate whose conditional association with gun violence exposure was no longer statistically significant at that level. The resulting model included 37 covariates. We modified this model by adding a squared term for each first-order continuous covariate selected by the procedure, and by adding a first-order term for each squared continuous covariate selected, bringing to 48 the total number of covariates included in the final model (25) (table S3).

Exposed and unexposed subjects had notably different probability densities of $\hat{\pi}$ (Fig. 2). The distribution for unexposed subjects was skewed sharply to the right, with nearly half ($n = 459$, 48.7%) having $\hat{\pi} < 0.10$ and none having $\hat{\pi} > 0.85$. In contrast, the probability density for exposed subjects was more nearly uniform, the only exception being that very few ($n = 3$, 1.1%) had $\hat{\pi} < 0.05$. We divided subjects into 12 strata on the basis of their estimated propensity scores (Table 2). Cut points were selected such that exposed and unexposed subjects had statistically indistinguishable mean estimated propensity scores

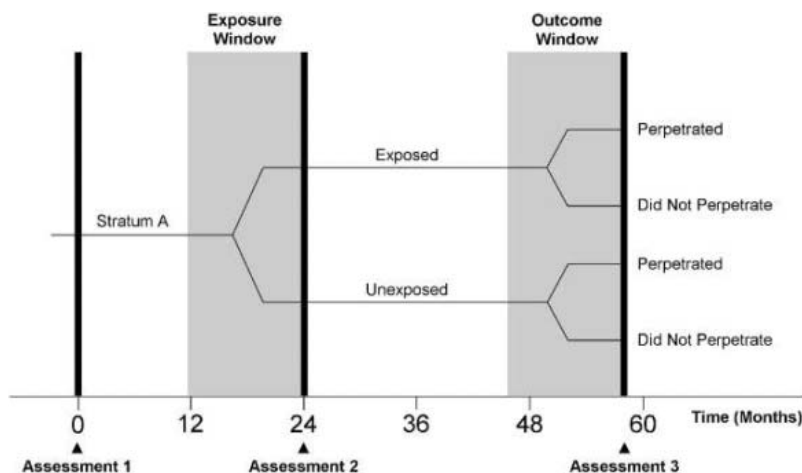


Fig. 1. Design of the propensity-stratified longitudinal study. This design was implemented for 12 propensity strata, 10 of which were used for estimating the cause-effect relationship between exposure to firearm violence (obtained at Assessment 2) and subsequent perpetration of serious violence (obtained at Assessment 3). Strata were defined on the basis of modeled probabilities of exposure at Assessment 2 conditional upon 153 covariates measured at Assessment 1. The placement of Assessments 2 and 3 on the horizontal axis is based upon the median time between interviews.

within each of the resulting strata. Satisfactory balance of unexposed and exposed subjects could not be achieved within the ranges $\hat{\pi} < 0.05$ and $\hat{\pi} > 0.75$. We therefore excluded the lowest and highest strata from the propensity-stratified analyses. Within each of the remaining 10 strata, exposed and unexposed subjects had nearly identical mean values of $\hat{\pi}$ [no statistical difference: $F(10,862) = 0.11, P = 0.9998$]. We also used statistical hypothesis tests to determine whether unexposed and exposed subjects had similar distributions of the Assessment 1 covariates within each of the 10 analytic propensity strata. We found no statistically significant ($\alpha = 0.01$) within-stratum differences between exposed and unexposed subjects on any of the 153 covariates (table S2), suggesting that our propensity model and stratification scheme adequately controlled selection on all measured preexposure covariates.

At Assessment 3, subjects who could again be located and who agreed to continue participating ($n = 984, 80.3\%$ of those whose Assessment 2 exposure status could be ascertained) answered questions about their perpetration of violent behavior in the previous 12 months (25) (table S1). Those reporting that they had carried a hidden weapon, attacked someone with a weapon, shot someone, shot at someone, or been in a gang fight in which someone was hurt or threatened with harm were classified as perpetrators of serious violence. Those reporting none of these five activities were classified as nonperpetrators. The majority of subjects ($n = 856, 87.0\%$) were classified as nonperpetrators, and a minority ($n = 122, 12.4\%$) were classified as perpetrators (25). A few ($n = 6, 0.6\%$) could not be classified due to incomplete or inconsistent responses.

We used a series of maximum-likelihood logistic regression models to obtain estimates of the statistical association and the cause-effect relationship between exposure to firearm violence and subsequent perpetration of serious violence (25). A model with no covariates revealed a strong statistical association; subjects who were exposed to firearm violence at Assessment 2 were much more likely than unexposed subjects to report perpetration of serious violence at Assessment 3 [odds ratio (OR) = 3.71, $\chi^2(1) = 41.99, P < 0.0001$]. Adjustment for race/ethnicity, age, sex, family socioeconomic index, and neighborhood of residence by regression methods attenuated this association only slightly (adjusted OR = 3.57, $t_{970} = 5.29, P < 0.0001$). Further adjustment for previous violence exposure, self-reported violent crime, and self- and caregiver-reported delinquency attenuated the association more substantially (adjusted OR = 2.47, $t_{966} = 3.64, P = 0.0003$).

Within the 10 analytic propensity strata, we found that subjects who were exposed to firearm violence at Assessment 2 were more

likely than unexposed subjects in the same stratum to report serious violence perpetration at Assessment 3 (common within-stratum OR = 2.43, $\chi^2(1) = 11.74, P = 0.0006$). Regression adjustment for race/ethnicity, age, sex, family socioeconomic index, and neighborhood of residence did not substantially alter this finding (adjusted common within-stratum OR = 2.62, $t_{677} = 3.039, P = 0.0025$), nor did further adjustment for previous violence exposure and violent and aggressive behaviors (adjusted common within-stratum OR = 2.76, $t_{673} = 2.721, P = 0.0067$). We also estimated a model in which the effect of firearm violence exposure was allowed to vary across the propensity strata, but comparison of this model with the original propensity-stratified model revealed that any heterogene-

ity in this effect was too small to be estimated reliably [no statistical difference: $\chi^2(9) = 15.12, P = 0.0877$].

Our estimate of the cause-effect relationship between firearm violence exposure and subsequent perpetration of serious violence represents an average treatment effect estimate. This estimate does not apply to individuals with very low or very high levels of propensity to be exposed. We did not estimate a cause-effect relationship outside the range $0.05 < \hat{\pi} < 0.75$ because of imbalance between exposed and unexposed subjects in the lowest and highest propensity strata.

Some sources of potential bias should also be noted. First, the subjects' exposure to firearm violence and subsequent perpetration of serious violence were both assessed by

Table 1. Comparison of exposed and unexposed subjects on select Assessment 1 covariates. Unless otherwise noted, covariates are measured on a continuous scale and standardized to unit variance; differences are standardized mean comparisons; and test statistics are $F(1,1223)$.

Preexposure covariate	Difference	Test statistic	P value
<i>Demographic characteristics</i>			
Male sex*	1.199	7.37	0.0066
Minority race/ethnicity†	–	38.55	<0.0001
Receiving public assistance*	1.664	24.34	<0.0001
Single-parent family structure†	–	28.52	0.0002
<i>Temperament</i>			
Impulsivity	0.298	19.63	<0.0001
Inhibitory control	0.218	10.43	0.0013
Sensation-seeking	0.341	25.91	<0.0001
Emotionality	0.203	9.00	0.0028
<i>Antisocial behaviors</i>			
Self-reported aggression	0.315	22.00	<0.0001
Caregiver-reported aggression	0.349	27.14	<0.0001
Violent offenses	0.619	89.19	<0.0001
Alcohol use*	1.540	19.31	<0.0001
Cigarette use*	1.508	15.48	<0.0001
Marijuana use*	2.550	39.41	<0.0001
Truancy	0.118	20.00	<0.0001
School drop-out*	0.977	12.14	0.0005
Self-reported delinquency	0.398	35.40	<0.0001
Caregiver-reported delinquency	0.471	50.27	<0.0001
Property crimes	0.375	31.36	<0.0001
<i>Family environment</i>			
Family members with criminal records*	1.407	12.98	0.0003
Family members with legal problems*	1.620	13.39	0.0003
Corporal punishment	0.244	13.10	0.0003
Physical abuse	0.299	19.80	<0.0001
Witnessing domestic violence	0.240	12.60	0.0004
<i>Peer group characteristics</i>			
Aggressive behaviors	0.567	74.13	<0.0001
Property crimes	0.358	28.52	<0.0001
Drug use	0.397	35.17	<0.0001
Drug selling	0.173	35.02	<0.0001
Sexual activity	0.373	81.76	<0.0001
<i>Indicators of intelligence</i>			
Vocabulary	–0.233	11.90	0.0006
Reading proficiency	–0.181	7.17	0.0075
<i>Neighborhood characteristics</i>			
Anomie	0.352	27.56	<0.0001
Social disorder	0.359	28.73	<0.0001
Perceived violence	0.265	15.45	<0.0001
Concentrated disadvantage	0.529	64.16	<0.0001
Informal social control	–0.190	7.95	0.0049
Satisfaction with policing	–0.269	15.92	<0.0001

*Measured dichotomously; differences are relative risks and test statistics are $\chi^2(1)$. †Measured nominally with more than two categories; reported differences are too complicated to tabulate here, but test statistics are $\chi^2(5)$ for race/ethnicity and $\chi^2(7)$ for family structure.

Fig. 2. Probability densities of estimated propensity scores.

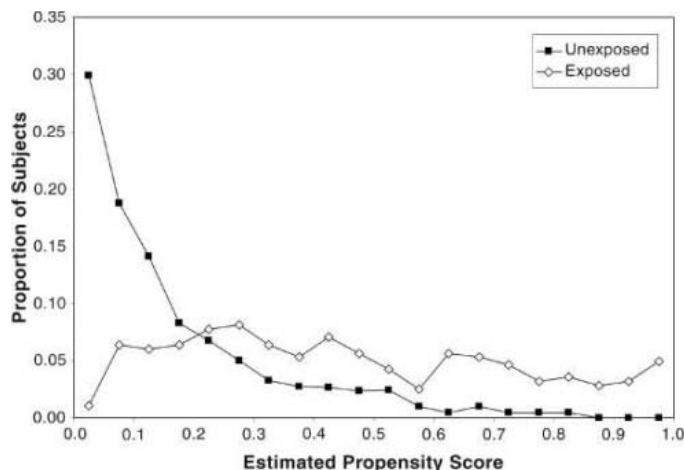


Table 2. Distribution of Assessment 3 serious violence perpetration, by propensity stratum and Assessment 2 firearm violence exposure status. Columns labeled "No" contain subjects who denied serious violence perpetration at Assessment 3; columns labeled "Yes" contain subjects who reported serious violence perpetration; columns labeled "?" contain subjects who were lost to follow-up or whose responses to Assessment 3 questions about violence perpetration were inconsistent.

Propensity stratum	Unexposed (N = 942)			Exposed (N = 283)		
	No	Yes	?	No	Yes	?
0.0000 – 0.0500*	224	12	46	3	0	0
0.0500 – 0.0875	96	5	24	8	3	2
0.0875 – 0.1250	85	10	17	4	0	7
0.1250 – 0.1625	82	5	16	7	3	6
0.1625 – 0.2000	35	0	13	8	1	4
0.2000 – 0.2500	44	6	14	10	9	3
0.2500 – 0.3375	58	8	9	19	3	9
0.3375 – 0.4375	31	8	10	25	6	10
0.4375 – 0.5375	26	6	13	20	6	4
0.5375 – 0.5875	6	1	5	2	3	2
0.5875 – 0.7500	12	3	4	22	9	15
0.7500 – 1.0000*	2	3	3	27	12	11
Total	701	67	174	155	55	73

*These strata are excluded from propensity-stratified analyses of covariate balance and treatment effects.

self-report, which implies that correlated misclassification on exposure and outcome status may have occurred, but the magnitude and direction of the resulting bias cannot be determined. Differential attrition of subjects between assessments is another potential source of bias. We found, however, that attrition was not strongly related to baseline covariates (25) (table S1), suggesting that any bias resulting from this may have been of minor importance.

Furthermore, we cannot rule out the possibility that unmeasured preexposure characteristics may have jointly influenced both exposure status at Assessment 2 and perpetration at Assessment 3. Yet, the omission of such variables from our analyses would constitute a violation of the assumption of strongly ignorable treatment assignment only to the extent that their influences were independent of estimated propensity scores. This would be most likely in the case of an omitted variable that was uncorrelated with the 153 covariates used in developing and testing our propensity model, but could occur under other circum-

stances as well. Sensitivity analyses (24, 25) (table S4) showed that these independent influences on both exposure and perpetration would need to be very strong to reduce substantially our estimate of the effect of firearm violence exposure on subsequent violent perpetration.

In conclusion, our focus on firearm violence exposure provided an operational definition of the treatment and control conditions and facilitated the assessment of each subject's exposure status. The longitudinal structure of the investigation established the temporal ordering of preexposure covariates, realized exposure status, and the behaviors comprising the focal outcome. We had access to a large and diverse set of well-measured preexposure covariates obtained from multiple sources, including subjects, their caregivers, neighborhood residents, and census data. We used this information to develop a model of how subjects' personal characteristics and environmental circumstances systematically influenced their probability of being exposed to firearm

violence. Stratifying on estimated propensity scores derived from this model provided statistical balance on all 153 measured preexposure covariates, suggesting that we succeeded in isolating the random part of the exposure allocation process, and thereby adequately approximated a randomized experiment. Our results thus provide a more credible basis for the conclusion that exposure to violence is causally related to violent behavior. Specifically, we estimate that being exposed to firearm violence approximately doubles the probability that an adolescent will perpetrate serious violence over the 2 subsequent years.

References and Notes

1. L. B. Silver, C. C. Dublin, R. S. Lourie, *Am. J. Psychiatry* **126**, 404 (1969).
2. J. J. Spinetta, D. Rigler, *Psychol. Bull.* **77**, 296 (1972).
3. C. S. Widom, *Science* **244**, 160 (1989).
4. K. A. Dodge, J. E. Bates, G. S. Pettit, *Science* **250**, 1678 (1990).
5. A. Caspi *et al.*, *Science* **297**, 851 (2002).
6. L. A. Fingerhut, D. D. Ingram, J. J. Feldman, *JAMA* **267**, 3048 (1992).
7. L. A. Fingerhut, D. D. Ingram, J. J. Feldman, *JAMA* **267**, 3054 (1992).
8. J. E. Richters, P. Martinez, *Psychiatry* **56**, 7 (1993).
9. H. Schubiner, R. Scott, A. Tzelepis, *J. Adol. Health* **14**, 214 (1993).
10. M. E. Schwab-Stone *et al.*, *J. Am. Acad. Child Adol. Psychiatry* **34**, 1343 (1995).
11. D. Gorman-Smith, P. Tolan, *Dev. Psychopathol.* **10**, 101 (1998).
12. L. Song, M. I. Singer, T. M. Anglin, *Arch. Pediatr. Adol. Med.* **152**, 531 (1998).
13. L. S. Miller *et al.*, *J. Clin. Child Psychol.* **28**, 2 (1999).
14. C. A. Halliday-Boykins, S. Graham, *J. Ab. Child Psychol.* **29**, 383 (2001).
15. S. L. Buka, T. L. Stichick, I. Birdthistle, F. J. Earls, *Am. J. Orthopsychiatry* **71**, 298 (2001).
16. P. R. Rosenbaum, D. B. Rubin, *Biometrika* **70**, 41 (1983).
17. P. R. Rosenbaum, D. B. Rubin, *J. Am. Stat. Assoc.* **79**, 516 (1984).
18. D. B. Rubin, *Ann. Intern. Med.* **127**, 757 (1997).
19. D. B. Rubin, *J. Educ. Psychol.* **66**, 688 (1974).
20. P. W. Holland, *J. Am. Stat. Assoc.* **81**, 945 (1986).
21. D. J. Benjamin, *J. Public Econ.* **87**, 1259 (2003).
22. K. He *et al.*, *JAMA* **288**, 3130 (2002).
23. J. L. Skeem, E. P. Mulvey, *J. Consult. Clin. Psychol.* **69**, 358 (2001).
24. J. Cornfield *et al.*, *J. Natl. Cancer Inst.* **22**, 173 (1959).
25. Materials and methods are available as supporting material on Science Online.
26. R. J. Sampson, S. W. Raudenbush, F. J. Earls, *Science* **277**, 918 (1997).
27. S. W. Raudenbush, R. J. Sampson, *Soc. Methodol.* **29**, 1 (1999).
28. J. D. Hawkins *et al.*, in *Serious and Violent Juvenile Offenders: Risk Factors and Successful Interventions*, R. Loeber, D. P. Farrington, Eds. (Sage, Thousand Oaks, CA, 1998), chap. 7.
29. D. P. Farrington, in *Youth Violence*, M. Torny, M. H. Moore, Eds. (Chicago Univ. Press, Chicago, 1998), pp. 421–475.
30. We thank J. Brooks-Gunn, R. J. Sampson, and S. W. Raudenbush for insight and advice. This work was funded in part by grants from the John D. and Catherine T. MacArthur Foundation, the National Institute of Justice, and the National Institute of Mental Health.

Supporting Online Material
www.sciencemag.org/cgi/content/full/308/5726/1323/DC1
 Materials and Methods
 Tables S1 to S4

24 January 2005; accepted 30 March 2005
 10.1126/science.1110096

NEW PRODUCTS

<http://science.labvelocity.com>

Polymerase Chain Reaction Reagents

Four new reagents kits are available for performing quantitative polymerase chain reaction (PCR) and reverse transcription PCR (RT-PCR). Sensitive, stable, and easy-to-use, &GO Mastermixes simplify the accurate, real-time analysis of DNA, complementary DNA (cDNA), and RNA, and are supplied as complete 5X mastermixes. This format minimizes pipetting to save time and minimize risk of contamination. Two kits are available for quantifying DNA and cDNA in thermal cyclers that use plasticware: qPCR ROX-&GO for analyses employing fluorescently labeled, sequence-specific probes, and qPCR ROX-&GO Green, which contains a fluorescent intercalating dye (SYBR Green). Both mastermixes contain ROX dye to normalize non-PCR related background fluorescence. The qPCR-&GO Green and qRT-PCR1-&GO Green mastermixes are intended for use with thermal cyclers that use glass capillary systems.

MP Biomedicals/Qbiogene For information 800-854-0530 www.qbiogene.com

ROX-Free PCR Kit

The BD Qtaq ROX-Free DNA Polymerase Kit not only provides the sensitivity and specificity needed in real-time quantitative polymerase chain reaction (qPCR), it also provides the ability to adjust the passive reference dye concentration. Because the ROX dye is provided separately, the kit allows the user to determine the best passive reference dye concentration for the experiment or to omit ROX altogether. The kit features a robust and sensitive full-length Taq DNA polymerase designed for high efficiency and yield in qPCR reactions.

BD Biosciences Clontech For information 800-662-2566 www.clontech.com

Labeled Lectin

Texas-Red-conjugated tomato lectin is now available. Tomato lectin (from *Lycopersicon esculentum*) is an effective marker of blood vessels and microglial cells in rodents. Conjugation of the lectin with a fluorophore facilitates fast, one-step detection and visualization using intravascular perfusion methods or direct application to tissue sections. The red color provides contrast to green or yellow fluorescence in double-label studies.

Vector Laboratories

For information 650-697-3600

www.vectorlabs.com

Diamond Trimming Tools

A family of diamond trimming tools is available for the trimming of blocks at room and cryogenic temperatures. The CTT-90 is a 90-degree trimming tool, so the sample remains a consistent width during sectioning. The CTT-45 produces blocks that are pyramidal in shape. The UltraTrim allows for the trimming of blocks quickly and easily without the need for razor blades or other hand-held or mechanical trimming devices.

Diatome For information 215-412-8390 www.emsdiasum.com

Automated Plant DNA

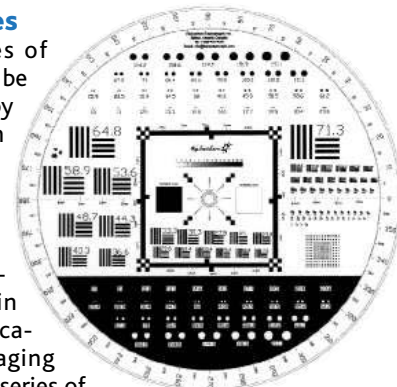
The BioSprint DNA Plant Kits enable rapid and cost-effective automated purification of high-quality plant DNA using BioSprint workstations. The automated procedure completely removes all contaminants and enzyme inhibitors, and the purified DNA is suit-

able for use in demanding downstream applications, such as polymerase chain reaction (PCR), real-time PCR, genotyping, and microsatellite analysis.

Qiagen For information 800-426-8157 www.qiagen.com

Microscope Test Slides

The Generation 3 series of microscope test slides can be used in confocal microscopy and light microscopy in brightfield, darkfield, or Hoffman contrast modes. The slides allow the user to take magnification, image resolution, and shape identification to new levels in even the highest magnification microscope and imaging system. They offer a large series of scales, gratings, squares, targets, and circles. Users can quickly identify any visual problems in an instrument, including astigmatism, barrel effect, aberrations, and more.



Electron Microscopy Sciences For information 215-412-8400

www.emsdiasum.com

Cell Culture Perfusion

A new line of disposable spinfilters has been developed for medium perfusion in cell culture processes. The Spinfilter P is constructed from precision-woven, open-mesh polyethylene terephthalate polyester (PETP) fabric on a polycarbonate body. This highly specialized monofilament fabric is characterized by precisely controlled pore sizes with tight tolerances. The material provides consistent and even surface properties for highly reproducible results. Standard pore sizes are 10, 20, and 40 μm with custom sizes also available. The disposable Spinfilter P line is available for vessels

ranging from 1 to 500 liters and can be used with a variety of stirrer shaft diameters by using the appropriate mounting adaptors.

Sartorius BBI Systems For information

800-258-9000 www.sartorius-bbi-systems.com

Literature

Worthington Biochemical Company 2005 Product Catalog features enzymes, biochemicals, and primary cell isolation kits for applications in life sciences research, diagnostics, and biotechnology. New and traditional products are included with applications in primary cell isolation and cell culture, protein research diagnostic enzymology and reagent production, and molecular biology.

Worthington Biochemical For information 800-445-9603

www.worthington-biochem.com

For more information visit **GetInfo**,
Science's new online product index at
<http://science.labvelocity.com>

From the pages of GetInfo, you can:

- Quickly find and request free information on products and services found in the pages of *Science*.
- Ask vendors to contact you with more information.
- Link directly to vendors' Web sites.

Newly offered instrumentation, apparatus, and laboratory materials of interest to researchers in all disciplines in academic, industrial, and government organizations are featured in this space. Emphasis is given to purpose, chief characteristics, and availability of products and materials. Endorsement by *Science* or AAAS of any products or materials mentioned is not implied. Additional information may be obtained from the manufacturer or supplier by visiting www.science.labvelocity.com on the Web, where you can request that the information be sent to you by e-mail, fax, mail, or telephone.



“Labelling molecules was as hard as writing on grains of dust with a pencil – until recently.”

In my biochemistry course about 25 years ago I used to study molecules by the diagram of biochemical paths. Today, I can watch some of these old acquaintances at work and see them wandering from one living cell to the next and influencing cellular functions. Labelling molecules is now no longer a problem – using a research or confocal microscope of the Leica Fluorescence Microscopy range. Leica also offers me top-precision image analysis systems for their subsequent quantification.

Prof. Dr. H. J. Tanke, Leiden University Medical Centre, The Netherlands
Prof. Tanke works with Leica research and confocal microscope systems.

 www.leica-microsystems.com

Leica
MICROSYSTEMS

» advances in:

Proteomics

Puzzling Out Proteins' Structures To determine the structures of large numbers of proteins, researchers rely on updated versions of well-tried experimental techniques. But the new approach of computer modeling has started to gather momentum. **BY PETER GWYNNE AND GARY HEEBNER**

Proteins have complex, three-dimensional structures whose dynamic twists and turns ultimately determine their function. They exist in huge numbers; each human cell typically contains 100,000 or more proteins. Not surprisingly, then, characterizing the structures of all the proteins in existence demands an eclectic mix of tools and technologies.

Proteins differ widely in the degree of difficulty that scientists encounter when they try determine their structures. "Assuming that the protein is of a suitable size and well behaved, it's quite straightforward," says Douglas Meinhart, product manager, NMR product lines and manager of the analytical laboratory at **JEOL USA**. "But the interesting ones are not well behaved." Determining the structures of badly behaved proteins "is still difficult to do," adds Carsten Mang, product manager for proteomics at **Hamilton Life Science Robotics**. "It's more an art than a science. But the tools are getting better."

The basic approaches to determining proteins' structures are familiar to bench scientists. "The technologies have been around for many years," says Nigel Darby, vice president of R&D for protein separations at **GE Healthcare**. "They have been applied to small molecules. But proteins are bigger and orders of magnitude more complex than small molecules." To permit them to tackle proteins, vendors have had to upgrade those methods. "The improvements in tools and technologies for protein

structure determination have been absolutely essential for the ability of the structural biology community to produce protein structures," says Lance Stewart, vice president of **deCODE biostructures**.

Data Driven Research

The large numbers of samples and conditions involved in these experiments require not only automated techniques but also powerful computers and software programs to make sense of all the information they create. After all, this is a data driven – rather than a hypothesis driven – field of research. "The data flood is incredible," declares Rudy Potenzzone, senior vice president for product management at **Ingenuity Systems**. "Without software," adds Thomas Billert, CEO of **Jena Bioscience**, "you could not solve a protein structure."

Experimental means of determining proteins' structures rely on diffraction techniques. "X-ray crystallography and NMR are the two main methods," Meinhart says. "You'll also run across people doing it with neutrons and even electron beams." X- **MORE >>>**

This is the third of four special supplements this year on Advances in Proteomics. The first two appeared in the 25 March and 29 April issues of Science and the final one will appear in the 16 September issue.

Inclusion of companies in this article does not indicate endorsement by either AAAS or Science, nor is it meant to imply that their products or services are superior to those of other companies.

In this issue:

- > Protein expression
- > Protein crystallization
- > X-ray crystallography
- > NMR spectroscopy
- > Software for structure determination
- > Computer modeling

» advances in: Proteomics

ray crystallography, which accounts for about 85 percent of known protein structures, “is the only method that can rapidly produce high resolution structures,” Stewart adds. NMR, however, has the advantage of investigating proteins in their natural environments, in solution, rather than in the solid state.

A significant new approach promises to complement those techniques. “The whole field of protein structure determination has been entirely experimental up to now,” explains Ying Xu, professor of biochemistry and molecular biology at the **University of Georgia**. “Until very recently the cost per structure determination was over \$100,000. Even a recent reduction to \$50,000 to \$70,000 means that it’s still very expensive. So we need another way.” That way is computer modeling. “We’re working on computational approaches to solving proteins’ structures that complement experimental techniques,” Xu states.

Purifying Proteins

For X-ray crystallography, the first step involves obtaining enough purified protein to allow analytical methods to be applied. That isn’t always easy. Scientists need a method that will produce a protein with the correct functional properties as well as one that they can crystallize successfully. Sometimes they need to test several expression constructs and expression systems before they find the combination that yields enough protein to move to the next phase: growing a crystal.

The situation has improved markedly in recent years. “The whole area of protein expression and purification, which had been a bottleneck, has undergone tremendous advances in the past 10 to 15 years,” says GE’s Darby. Several companies, including **Invitrogen**, **MP Biomedicals**, and **Sigma-Aldrich**, have developed novel protein expression and purification systems based on inserting small peptide sequences into a specific protein that can be identified with a molecule that recognizes the tag.

Before they can analyze a protein sample, scientists must purify it to remove contaminating substances. Desalting columns that use gel filtration methods and dialysis, from such companies as Sigma-Aldrich and **Stratagene**, provide effective tools to clean up protein samples.

GE Healthcare’s ÄKTApur automated, fully integrated chromatography system provides parallel, multidimensional, high throughput purification of tagged proteins. The system integrates hardware, software, and chromatography media in a user-friendly automated system. “The whole idea is to make a formidable operation – purifying proteins in parallel via multiple steps – a plug and play operation,” Darby says.

An Esoteric Bottleneck

As its name indicates, X-ray crystallography requires crystals – preferably extremely pure – of the entity under examination. “It’s still the main bottleneck – the most esoteric part of the whole process,” says Billert of Jena

Visit <http://www.science-benchtop.org> to find an expanded version of this article.

Bioscience. “You need to screen a very large number of conditions before you end up with microcrystals of an unknown protein. This may take just a couple of days, but if you’re unlucky it may take years.”

A good crystal usually has an extremely regular crystalline structure (referred to as low mosaicity) and a diameter of the order of several hundreds of microns. Crystallographers can deal with smaller crystals (down toward 50 microns diameter), but they need higher level sources of X-rays, such as synchrotrons, for structural analysis.

Companies such as **Emerald Biosystems**, **Hampton Research**, and Jena Bioscience offer supplies for screening and optimizing the crystallization conditions for proteins. “We are trying to become a one-stop shop for crystallography,” says Billert. “We offer screens, kits for crystal optimization and protein surface engineering, crystallization plates, and much more.” Several of the company’s products are also designed for high throughput work.

Other suppliers present a different way to simplify scientists’ lives. Several companies market automated workstations and robots to help with the repetitive work required to set up large numbers of sample replicates in varying conditions. Manufacturers such as **Apogent** (now a part of Fisher Scientific), **Caliper**, **Emerald Biosystems**, and **PerkinElmer Life and Analytical Sciences** offer a range of systems that scientists can adapt to routine laboratory procedures and studies of protein crystallization.

All Types of Liquids

Hamilton Life Science Robotics has designed its MICROLAB STAR automated workstation specifically for protein crystallization. It helps to meet researchers’ needs for high throughput screening of various conditions for protein crystallization, and can provide large, high-quality crystals suitable for X-ray diffraction. “It can handle all types of liquids, polar and nonpolar,” Mang says. “Our robots work like handheld pipettes, with which scientists are familiar in the lab. There are no syringes, no pumps, and no tubing. All problems related to dilution of samples with system liquids are gone. This technology also allows us to monitor each pipetting step, therefore achieving previously unknown process control.”

X-ray crystallography uses X-rays to determine the precise arrangements of atoms in crystalline specimens. Crystallographic systems generally include dedicated computers with associated hardware and software for instrument control, data reduction, solution and refinement of molecular structures, and the display and plotting of final results.

The approach can provide reliable answers to several structure related questions, from the nature of protein folds to the atomic details of bonding. The method has no limit on the size of the molecule or complex under study. “And once a reasonable crystal form has been worked out for the protein of interest, then the determination of protein-drug complexes can be worked out almost as fast as the diffraction data can be collected,” deCODE biostructures’ Stewart says.

Thermo Electron (formerly Applied Research Laboratories) offers a line of X-ray instruments for seamless integration into laboratory and total automation solutions. Several firms, including **Cengent Therapeutics** and **Rigaku**, grow crystals as a service for researchers. **MORE >>>**

GetInfo – Improved online reader service!

Search more easily for *Science* advertisers and their products. Do all your product research at – [science.labvelocity.com](http://www.science.labvelocity.com)

Visit <http://www.science-benchtop.org> to find this article as well as past special advertising sections.

Takara


PROTEIN EXPRESSION AT **COLD** TEMPERATURES **SHOCKING!!!**

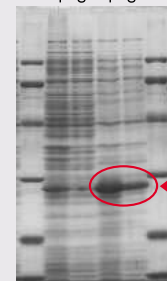


Takara's **pCold Vectors (I-IV)**

Takara's pCold Vectors (I-IV) offer Cold Shock expression technology for high purity-high yield protein expression. Robust expression of many proteins is possible, including proteins previously unable to be expressed using convention systems.

Comparison with a conventional expression system

T7		pCold	
T	S	T	S
			
T: Total protein S: Soluble protein			
Higher yield is observed with the pCold Expression System than T7 System.			
(CBB staining)			



T: Total protein
S: Soluble protein

Higher yield is observed with the pCold Expression System than T7 System.

(CBB staining)

High Purity-High Yield Recombinant Protein: Up to 60% of expressed intracellular protein is target protein; 50-400 mg protein/1 liter culture

Wide Range of *E. coli* Hosts:

Highly suitable for most *E. coli* strains

Radioisotope Labeling:

For labeling of human gene products, >90% of labeled expressed cellular protein is of target protein

Compatible with Chaperone Plasmid Vectors: Can be used with one of Takara's Chaperone Plasmids to further increase the amount of recoverable soluble protein

Products: •pCold I DNA •pCold II DNA •pCold III DNA •pCold IV DNA

pCold Vectors are covered by U.S. Patents No. 6479260, which are owned by TAKARA BIO, and the U.S. Patents, 5981280, 6686174, 6333191, which are exclusively licensed to TAKARA BIO. Protein Purification Technology of His-Tag used in pCold I and pCold II DNA is licensed from Hoffmann-La Roche, Inc., Nutley, NJ and/or Hoffmann-La Roche Ltd., Basel, Switzerland and is provided only for the use in research. Information about licenses for commercial use is available from QIAGEN GmbH, Qiagen Strasse 1, D-40724 Hilden, Germany.

Really **COOL** Technology for Protein Expression.

TAKARA BIO INC. Otsu, Shiga, Japan
The Biotechnology Company™ Phone: +81-77-543-7247 Fax: +81-77-543-9254

USA: Takara Mirus Bio Inc. Phone: +1-888-251-6618 Fax: +1-608-441-2845
Europe: Takara Bio Europe S.A. Phone: +33-1-4147-2370 Fax: +33-1-4147-2371
Korea: Takara Korea Biomedical Inc. Phone: +82-31-739-3300 Fax: +82-31-739-3311

For more information and a list of Takara distributors worldwide, please visit our website today! www.takara-bio.com

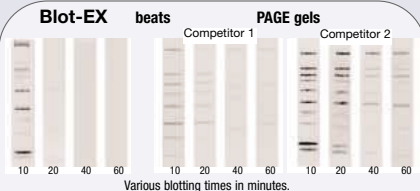
Blot-EX

For Western Blotting



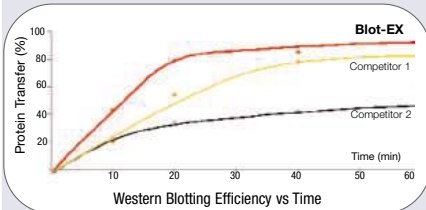
Drastically enhance performance in **protein recovery**

Don't Leave Money in your gel!



Less protein in the gel is best! This is your money in the gel.

Blot-EX Maximizes Protein Recovery



Greatest Protein Recovery

– greater than 90% overall recovery

Unsurpassed Transfer Efficiency

– 5 times greater transfer efficiency

Accelerated Transfer

– high transfer achieved in less than 20 min

Safe for Users

– NON acrylamide, non-toxic hydrogel



Need more information?

Call us. +41 41 747 25 50

E-mail us. info@elchrom.com

Fax us. +41 41 743 25 36

Order your Blot-EX starter kit today!

and visit our website

www.elchrom.com

GetInfo

science.labvelocity.com



Get the lab product info you need — FAST



Science announces a new online life science product information system, **GetInfo**, powered by **LabVelocity**

- Quickly find and request free information on products and/or services found in the pages of *Science* magazine
- Ask vendors to contact you with more information
- View detailed product information
- Link directly to vendors' websites

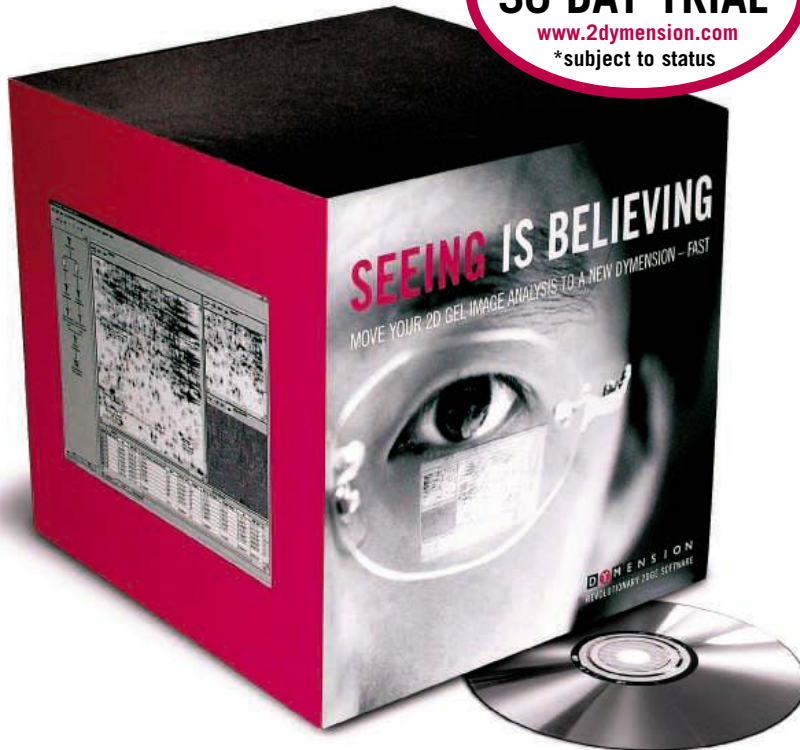
Visit GetInfo today at science.labvelocity.com



MOVE YOUR 2D GEL IMAGE ANALYSIS TO A NEW DYMENSION...FAST

FREE*
30 DAY TRIAL

www.2dymension.com
*subject to status



R A P I D

- Instant warping
- Impressively fast spot detection
- Spot matching in seconds

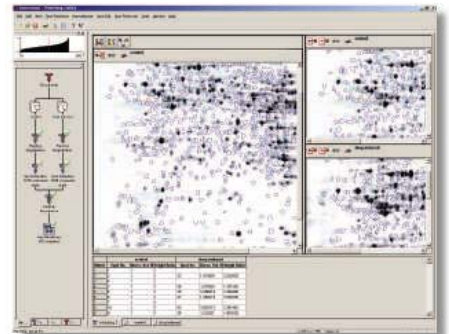
P R E C I S E

- Razor sharp warping, spot detection and matching
- Negligible post editing
- Supremely accurate

S I M P L E

- Easy to use interface
- Clear Process Flow chart
- Minimal training required

D I M E N S I O N overturns the accepted conventions of 2D gel electrophoresis analysis. This revolutionary new software will enable you to complete all procedures crucial to comprehensive 2D image analysis, at the touch of a button. Warping, spot detection and spot matching – tasks that once took hours – can now be performed within seconds.



Find out more at: www.2dymension.com

**Syngene Europe and
International Headquarters**
Beacon House Nuffield Road
Cambridge CB4 1TF UK
Tel: +44 (0) 1223 727123
Fax: +44 (0) 1223 727101
Email: sales@2dymension.com

Syngene USA Headquarters
5108 Pegasus Court Suite M
Frederick MD 21704 USA
Tel: 800 686 4407/301 662 2863
Fax: 301 631 3977
Email: ussales@2dymension.com



GenoMouse

For Mouse Background Analysis



Achieve fast, **clean mouse background**

Service and Kits for mouse:

Speed congenics

Strain and substrain identification

Service and Kits are offered for the following standard mouse strains:

B6, DBA/2, 129



FVB, Balb/c, NOD



Custom service is offered for other mouse strains on request.

Information Quality

– specific, reproducible, reliable

Traceability

– Automatic data capture, storage, processing

Speed

– High throughput

Cost effective

– Lower initial investment and operating costs

Ease of Use

– using standard methods



Need more information?

Call us. +41 41 747 25 50

E-mail us. info@elchrom.com

Fax us. +41 41 743 25 36

Order GenoMouse today!

and visit our website
www.elchrom.com

IT TAKES BOTH SIDES OF THE BRAIN.



CALL FOR ENTRIES

Science & Engineering Visualization Challenge

When the left brain collaborates with the right brain, science merges with art to enhance communication and understanding of research results—illustrating concepts, depicting phenomena, drawing conclusions.

The National Science Foundation and *Science*, published by the American Association for the Advancement of Science, invite you to participate in the annual *Science and Engineering Visualization Challenge*. The competition recognizes scientists, engineers, visualization specialists, and artists for producing or commissioning innovative work in visual communications.

ENTRY DEADLINE:

May 31, 2005

AWARDS CATEGORIES:

Photos/Still Images, Illustrations, Explanatory Graphics, Interactive Media, Non-interactive media

COMPLETE ENTRY INFORMATION:

www.nsf.gov/od/lpa/events/sevc/

Awards in each category will be published in the September 23, 2005 issue of *Science* and *Science Online* and displayed on the NSF website.



Accept the challenge. Show how you've mastered the art of understanding.



From research to quality control – base your decisions on the best

For more than 15 years Biacore has been supplying the life science market with a growing range of advanced systems for protein interaction analysis. Unique, high-quality data generated from each instrument supports the many critical decisions that lead to increased productivity in academic and pharmaceutical environments.

Biacore® systems define proteins in terms of their concentration, their specificity of interaction with other molecules, the rates at which they interact, how tightly they bind to another molecule and the thermodynamics involved – all without the use of labels.

Data you can depend on – from the unrivalled global leader in protein interaction analysis.

Protein interaction analysis in:

- **Disease mechanisms**
- **Antibody characterization**
- **Proteomics**
- **Lead selection**
- **Immunogenicity**
- **Biotherapeutic development**

Define • Decide

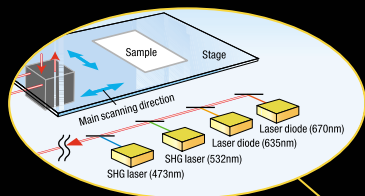


BIACORE

www.biacore.com

Introducing Fujifilm's new FLA-5100 Advanced Imaging System.

THE FUTURE OF SCIENCE IMAGING IS IN THE DETAILS.



Four Internal Lasers Available

Wavelength 473, 532, 635, 670nm.
Wide range of applications.



FLUOR Stage

Watertight, washable.



Filter Module

Easy to access,
changeable by users.

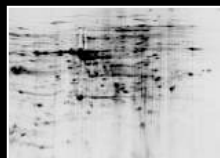


IP Stage

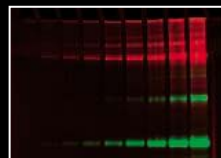
For phosphor imaging plate,
scanning area 40 X 46cm.

APPLICATION VERSATILITY

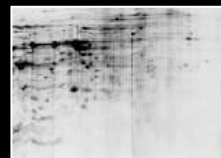
The new FLA-5100 imaging system allows imaging of fluorescent, radioisotopic, stained and chemiluminescent samples. This system is especially suitable for fluorescent (SYPRO® Ruby) detection or digitizing (CBB, silver stain) protein detection in the proteomics field.



Fluorescent SYPRO Ruby stain of 2D gel electrophoresis of Sake yeast.



2-Laser-2-Image overlap image with pseudocolor.



Fluorescent CBB stain detection by 670nm optional laser.

FEATURES

- Scanning area 46 X 40cm
- 2 Laser, 2 Image detection by dual PMT
- Fluorescent / Radioisotopic / Digitize / Chemiluminescent
- FLUOR / IP / MULTI Stage
- Pixel size – user choice of 10, 25, 50, 100, 200 microns
- Highly sensitive ³H detection by BAS-TR IP

» advances in: Proteomics

Contract Research Services

DeCODE biostructures provides contract research services related to the use of X-ray crystallography to determine the structures of protein-ligand complexes. "The gene-to-structure collaborative services we offer are of great benefit to startup or young organizations that want to apply structure-based drug designs in their product development plans but would rather not outlay the capital investments needed to install the capability for determining crystal development structure," Stewart says.

NMR, discovered in 1945, uses radio waves to induce transitions between energy levels in atomic nuclei. "You have to interpret the NMR spectra and perform a guess of the family structure to which the protein belongs and feed those coordinates into molecular modeling that runs them around and aims to minimize the energy and compare them with the NMR data," JEOL's Meinhart explains. "That can all be done in computers, but it still takes a matter of weeks or months computer time."

Companies that offer NMR systems include **Bruker AXS** and **Varian**, in addition to JEOL. "We supply our ECA instrument at various field strengths for protein structural work," Meinhart says. "It can accommodate up to six radio frequency channels; for protein work you typically need four. We also use our Delta NMR processing software – a full featured package for multidimensional data. You can walk in with your sample, put it in the magnet, get a full suite of calibrations, and go into the protein data collection automatically."

Ingenuity Systems applies two products, its Pathways Analysis solution and its Pathways Knowledge Base, to work on protein structures. "We come in at the functional studies stage," Potenzzone says. "Once you've determined what protein is relevant, we capture information about what it's doing, where it's located, what its binding modes are, and what kind of compounds interact with it. In effect, this is the next stage of determination beyond the structure. If you have similarly acting proteins, we might be able to give you some clues as to where else to look. It's like a dynamic database."

The Next Major Advance

Databases and information technology have also smoothed the way to the next major advance in determining proteins' structures: computer modeling. The University of Georgia's Xu explains the basis of the approach. "People have found that in nature the number of unique protein folds is quite small – perhaps a few thousand fold families," he says. "So if you solve one structure in a fold family, you can model the structures of the others in the family, using the solved structure as a structural template. People have found that about 90 percent of the struc-

tures solved in the past three years fall into fold families at least one of whose members have had their structures previously solved."

The process of modeling proteins' structures has only just started, and it still relies heavily on experimental structure determination. "Theoretically, once you know the structure of a member of your folding family you can model other family members' structures," Xu notes. "But the larger number of accurate structures you can get for a family, the better will be the accuracy of your modeling prediction." Computational structure predictions still have a long way to go to reach the accuracy level of experimental structure solutions such as X-ray crystallography and NMR. "We are probably still years away from consistently reaching the accuracy level of 1.5 Å obtained by experimental structures," Xu estimates. Nevertheless, he adds, "The economic argument is that this method has to work because it costs too much per structure to do it experimentally. The scientific argument is that it will work."

Peter Gwynne (pgwynne767@aol.com) is a freelance science writer based on Cape Cod, Massachusetts, U.S.A. Gary Heebner (gheebner@cell-associates.com) is a marketing consultant with Cell Associates in St. Louis, Missouri, U.S.A.

ADVERTISERS

Biacore AB

systems for protein interaction analysis in basic research, drug discovery and development
+46 18 675700, <http://www.biacore.com>

Elchrom Scientific AG

separation and purification products for genomics and proteomics research
+41 41 747 25 50, <http://www.elchrom.com>

Fuji Photo Film Co., Ltd. –

Life Science Products Division

QuickGene-810 nucleic acid isolation system, and BAS, LAS, and FLA imaging systems
+81 3 3406 2201, <http://lifescience.fujifilm.com>

Leica Microsystems AG [Germany]

instruments and systems for imaging analysis, digital cameras
+49 6441 290, <http://www.leica-microsystems.com>

Leica Microsystems [USA] 847-405-0123

Syngene [Europe]

digital imaging and analysis products for 2-D gel electrophoresis
+44 (0)1223 727123, <http://www.2dymension.com>

Syngene [USA] 301-662-2863

Takara Bio, Inc.

kits and reagents for molecular biology research, including genomics and proteomics
+81 77 543 7247, <http://www.takara-bio.com>

FEATURED COMPANIES

Apogent Technologies, Inc. (a Fisher Scientific Company), automated workstations, <http://www.apogent.com>

Bruker AXS, NMR spectrometers, <http://www.bruker-axs.de>

Caliper Life Sciences, automated workstations, <http://www.caliperls.com>

Cengent Therapeutics, Inc., crystallographic services, <http://www.cengent.com>
deCODE biostructures (a subsidiary of deCODE Genetics), proteomics services – protein structure determination, <http://www.decodebiostructures.com>

Emerald Biosystems, Inc., protein crystallization kits and reagents, <http://www.emeraldbiostructures.com>

GE Healthcare, protein separation and purification systems, <http://www.gehealthcare.com>

Hamilton Life Science Robotics, laboratory automation systems, <http://www.hamiltonrobotics.com>

Hampton Research Corporation, protein crystallization kits and reagents, <http://www.hamptonresearch.com>

Ingenuity Systems, scientific software, <http://www.ingenuity.com>

Invitrogen Corporation, protein expression systems, <http://www.invitrogen.com>

Jena Bioscience GmbH, protein crystallization kits and reagents, <http://www.jenabioscience.com>

JEOL-USA, Inc., NMR spectrometers, <http://www.jeol.com>

MP Biomedicals, protein expression systems, <http://www.mpbio.com>

PerkinElmer Life and Analytical Sciences, automated workstations, <http://las.perkinelmer.com>

Rigaku/MSK, X-ray systems [for protein crystallography, <http://www.rigakumsc.com>

Sigma-Aldrich Corporation, protein expression systems, <http://www.sigma-aldrich.com>

Stratagene, protein purification kits and reagents, <http://www.stratagene.com>

Thermo Electron Corporation, X-ray systems for protein crystallography, <http://www.thermo.com>

University of Georgia, university, <http://www.uga.edu>

Varian, Inc., NMR spectrometers, <http://www.varianinc.com>

Classified Advertising

Albert Einstein
1879-1955



ALBERT EINSTEIN and related photos by UC of The Museum of Modern Art, used under license. Reprinted by The Roger Sherman Agency, Inc. - www.albert-einstein.net

For full advertising details, go to www.sciencecareers.org and click on **How to Advertise**, or call one of our representatives.

United States & Canada

E-mail: advertise@sciencecareers.org
Fax: 202-289-6742

JILL DOWNING

(CT, DE, DC, FL, GA, MD, ME, MA, NH, NJ, NY, NC, PA, RI, SC, VT, VA)

Phone: 631-580-2445

KRISTINE VON ZEDLITZ

(AK, AZ, CA, CO, HI, ID, IA, KS, MT, NE, NV, ND, OR, SD, TX, UT, WA, WY)

Phone: 415-956-2531

KATHLEEN CLARK

Employment: AR, IL, LA, MN, MO, OK, WI, Canada; Graduate Programs; Meetings & Announcements (U.S., Canada, Caribbean, Central and South America)

Phone: 510-271-8349

EMNET TESFAYE

(Display Ads: AL, IN, KY, MI, MS, OH, TN, WV; Line Ads)

Phone: 202-326-6740

BETH DWYER

(Internet Sales Manager)

Phone: 202-326-6534

Europe & International

E-mail: ads@science-int.co.uk

Fax: +44 (0) 1223-326-532

TRACY HOLMES

Phone: +44 (0) 1223-326-525

HELEN MORONEY

Phone: +44 (0) 1223-326-528

CHRISTINA HARRISON

Phone: +44 (0) 1223-326-510

JASON HANNAFORD

Phone: +81 (0) 52-789-1860

To subscribe to Science:

In U.S./Canada call 202-326-6417 or 1-800-731-4939
In the rest of the world call +44 (0) 1223-326-515

Science makes every effort to screen its ads for offensive and/or discriminatory language in accordance with U.S. and non-U.S. law. Since we are an international journal, you may see ads from non-U.S. countries that request applications from specific demographic groups. Since U.S. law does not apply to other countries we try to accommodate recruiting practices of other countries. However, we encourage our readers to alert us to any ads that they feel are discriminatory or offensive.

POSITIONS OPEN

ASSISTANT/ASSOCIATE PROFESSOR OF ANATOMY

Kansas City University of Medicine and Biosciences (KCUMB) seeks candidates for the position of Assistant or Associate Professor of Anatomy. The successful candidate must have a Ph.D. in anatomy, or related discipline, and experience teaching histology and human gross anatomy. Duties will include teaching cell biology, histology, and full-dissection gross anatomy for medical students. The successful applicant may also elect to participate in teaching within graduate programs in the College of Biosciences. Successful applicants will be expected to maintain ongoing, productive scholarly activity. History of successful extramural funding is desirable. For additional information, contact: **Robert E. Stephens, Ph.D., Professor and Chair, Anatomy.** Telephone: 1-800-234-4847, extension 2244 or telephone: 816-283-2244; e-mail: rstephens@kcumb.edu.

KCUMB is Missouri's largest medical school with a new College of Biosciences and Biosciences' Research building. Competitive pay is complemented by an exceptional benefits package. KCUMB is located in the historic Northeast part of Kansas City, Missouri, near downtown and collaborating academic institutions.

To apply, send a letter of interest for job #05-11, curriculum vitae, a statement regarding scholarly activity, teaching goals and philosophies, and contact information for three references to: **Susan M. Schmidt, Assistant Director of Human Resources, 1750 Independence Avenue, Kansas City, MO 64106-1453.** Telephone: 800-234-4847, extension 2229 or telephone: 816-283-2229; e-mail: employment@kcumb.edu (Word or PDF format only please); or fax: 816-283-2285. Pre-employment drug screen and background check required. Must be authorized to work in the United States. Website: <http://www.kcumb.edu>. KCUMB is committed to being a key stakeholder and integral part of the Kansas City Area Life Sciences Institute. Website: <http://www.kclifesciences.org>.

Equal Opportunity Employer.

ASSOCIATE, ASSISTANT PROFESSORS
Viral Oncogenesis/Molecular Virology

The Department of Microbiology and Immunology of The Chicago Medical School, Rosalind Franklin University of Medicine and Science, located in the northern suburbs of Chicago, invites applications for full-time, tenure-track appointments at the Associate and Assistant Professor levels in viral oncogenesis. We seek candidates to join a significant expansion of the Department in a newly built research building with state-of-the-art laboratories and facilities. Core resources include confocal, live-cell and electron microscopy facilities, and a structural biology and proteomics center.

Candidates must have a Ph.D. or M.D. degree with training in viral oncogenesis and molecular virology. Candidates at the Associate Professor level must have a currently funded research program and a track record of federal funding. Candidates at the Assistant Professor level should show evidence of productive research accomplishments and demonstrated ability to pursue an independent research program. Successful candidates will receive competitive salaries, attractive startup packages, and are expected to develop and maintain an externally funded research program and teach at the medical and graduate level. Interested applicants should submit their curriculum vitae, description of current and future research plans, copies of recent representative publications, and names and contact information of at least three references to: **Bala Chandran, Ph.D., Chair, Department of Microbiology and Immunology, The Chicago Medical School, Rosalind Franklin University of Medicine and Science, 3333 Green Bay Road, North Chicago, IL 60064.** Review of applications will begin immediately and will continue until the positions are filled. *Rosalind Franklin University of Medicine and Science is an Equal Opportunity/Affirmative Action Employer.*

POSITIONS OPEN

ASSISTANT, ASSOCIATE, FULL PROFESSOR

The Department of Pathology at the University of California, San Diego (UCSD) (website: <http://medicine.ucsd.edu/Pathology>) announces an open search for outstanding investigators. Appointment at rank (tenured/tenure track) will be determined by skills and qualifications. Salary based on University of California pay scales. Applicants should have an M.D. and/or Ph.D., significant postdoctoral research experience, and the drive to develop a successful extramurally funded research program. The search is not limited to a specific research field; however, preference will be given to candidates in areas of cell biology relevant to pathology, such as cell-signaling, cell adhesion, and migration, growth and development, and the cytoskeleton. Board-certified/eligible pathologists, who are prepared to contribute to our clinical enterprise, in addition to establishing independent research, are particularly encouraged to apply. Successful candidates will occupy newly renovated laboratories and receive startup packages. Opportunities are available to participate in our teaching and highly regarded graduate education programs. Please forward curriculum vitae, names/addresses of at least three references, and a one-page description of your research plan to: **Dr. Steven L. Gonias, Search Committee Chair, c/o Ms. Judy Riddle, Search Coordinator, Department of Pathology 0717, University of California, San Diego School of Medicine, 9500 Gilman Drive, La Jolla, CA 92093-0717.** Applications are acceptable to e-mail: jriddle@ucsd.edu. Review of applications will begin June 22, 2005, and will continue until the position is filled. *UCSD is an Affirmative Action/Equal Opportunity Employer with a strong institutional commitment to excellence through diversity.*

TENURE-TRACK FACULTY POSITION
Molecular Oncology, Department of Medicine
Washington University, St. Louis

The Division of Oncology invites applications for full-time, tenure-track appointment at the rank of ASSISTANT PROFESSOR. Candidates must have a Ph.D., M.D., or equivalent degree, relevant postdoctoral experience, and a strong record of research accomplishment. We are seeking candidates with an interest in basic molecular oncology using innovative approaches in developmental, molecular or cell biology, biochemistry, or biophysics. The successful candidate will be expected to establish and maintain a vigorous, independently funded research program. Competitive salary, ample startup packages, and first-class laboratory space will be provided.

Please provide (1) current curriculum vitae, list of publications, and grant support, (2) a brief statement of research interests, and (3) contact information for three references. Send applications to: **Dr. Lee Ratner, Chair of the Search Committee, Division of Oncology, Campus Box 8069, 660 S. Euclid Avenue, Washington University, St. Louis, MO 63110** or to e-mail: lratner@im.wustl.edu.

ASSISTANT DIRECTOR
Instructional Development Program

Required: Ph.D., Ed.D., or terminal degree; two years' experience consulting with post-secondary faculty about teaching and learning issues; experience in developing and conducting workshops on college teaching and learning; demonstrated knowledge of educational psychology, learning theory, evaluation and instructional methodology; excellent writing skills; strong interpersonal skills. Preferred: college teaching experience; experience working with diverse groups. Visit our website: http://www.uri.edu/human_resources for a complete job description. Review of applications will begin on June 16, 2005, and continue until filled. Please submit (no e-mail or faxes, please) a resume, cover letter, and a list of three references to: **Lynn Pasquerella, Search Chair (Req #SM011032), University of Rhode Island, P.O. Box G, Kingston, RI 02881.** *University of Rhode Island is an Affirmative Action/Equal Employment Opportunity Employer and values diversity.*

small-company environment

big-company impactSM

Anthony, Research & Development

Anthony thrives in the friendly atmosphere of a small-company environment. He also benefits from the career flexibility that a big company offers.



Jane, Research & Development

Jane appreciates her big company's impact on global health care. She is also energized by the teamwork and cooperation of her small-company environment.

Who says you have to choose?

It's not about compromise—it's about realizing your vision.

You're an achiever who is passionate about the way you spend your days. You demand more from yourself and bring more to your job, your team, and your organization. You'd love to find a small-company environment where you can see and touch the bottom line. Yet you hunger for big-company impact, with world-class leadership and global achievement.

Within the Johnson & Johnson Family of Companies we celebrate and promote small-company environments that support the needs of individuals and teams. Our decentralized, adaptive organization has grown to become the world's most broadly based health care company. Through more than 200 operating units in 57 countries, we bring real, in-depth solutions to nearly every corner of global health care.



Johnson & Johnson
PHARMACEUTICAL RESEARCH
& DEVELOPMENT, L.L.C.

Johnson & Johnson Pharmaceutical Research & Development, L.L.C., a global leader in pharmaceutical R&D, develops treatments that improve the health and lifestyles of people worldwide. Research areas include psychiatry, gastroenterology, oncology, anti-infectives, central nervous system, diabetes, hematology, immunology/inflammation, and women's health.

Principal Scientist/Research Fellow— Antimicrobial Agents

Raritan, NJ (Req. 0505114)

Ph.D. in Microbiology or related field with 12+ years pharmaceutical experience in a microbiology Drug Discovery or Drug Development program. Will assume the major responsibility for the daily activities required to bring a late-stage beta-lactam antibiotic to market. Must be skilled in microbiology research techniques, with experience in the *in vitro* evaluations of antimicrobial agents. Will interact with outside investigators and will supervise associates in conducting MOA and resistance studies. Knowledge of microbiology requirements for IND, NDA and CLSI submissions is essential. Leadership skills in directing both Ph.D. and non-Ph.D. scientists are critical.

Assoc. Scientist/Sr. Assoc. Scientist— Antimicrobial Agents

Raritan, NJ (Req. 0506300)

MS, BA or BS in Microbiology, Molecular Biology or Biochemistry with 3 to 5 years pharmaceutical experience in a microbiology Drug Discovery program for an MS candidate; 5-7 years experience for a BA/BS candidate. Strong biochemistry background with experience in enzymology. Performs microbiology, biochemistry and/or molecular biology experiments to identify new antibacterial agents. Develops and executes primary and secondary screening assays for new antibacterial agents. Examines mechanisms of antibacterial action and resistance for lead compounds. Experience in working with *in vivo* infection models is an asset.

Research Asst./Research Assoc.— Antimicrobial Agents

Raritan, NJ (Req. 0505121)

MS in Biochemistry, Microbiology or Molecular Biology; BA or BS in Biochemistry is acceptable; 2 years pharmaceutical experience in a Drug Discovery program or in an academic laboratory for an MS candidate; 1 to 3 years in the pharmaceutical industry or in an academic laboratory for a candidate with a BA or BS. Purifies proteins for use in assay development and screening. Conducts primary and secondary screening assays for new antibacterial agents under supervision. Experience with and a working knowledge of bacterial pathogens is helpful.

Visit www.jnj.com/careers to establish a career profile or to forward your resume toward a posted position. Please reference company and requisition code with all specific applications. For these positions, please also email your resume to JJRDS@corus.jnj.com.

Look deeper at the Johnson & Johnson Family of Companies.



Johnson & Johnson Pharmaceutical Research & Development, L.L.C.
is a member of the Johnson & Johnson Family of Companies.

find more
www.jnj.com/careers

©Johnson & Johnson Pharmaceutical Research & Development, L.L.C. 2005.
An equal opportunity employer. SMALL-COMPANY ENVIRONMENT/
BIG-COMPANY IMPACT is a service mark of Johnson & Johnson.

Johnson & Johnson
Family of Companies

small-company environment
big-company impactSM



NATIONAL INSTITUTE OF DIABETES AND DIGESTIVE AND KIDNEY DISEASES (NIDDK) POSTDOCTORAL FELLOWSHIPS IN THE GENETICS & BIOCHEMISTRY BRANCH AND LABORATORY OF MOLECULAR BIOLOGY

We are a group of molecular and structural biologists who share state-of-the-art facilities on the main intramural campus of the NIH in Bethesda, Maryland. The intramural program of the NIH offers an outstanding research environment and many opportunities for collaborations. Applications are invited from individuals of the highest caliber with Ph.D., M.D., or M.D.-Ph.D degrees. Salary and benefits will be commensurate with the experience of the candidate. Please send a letter and CV to the following email addresses or mail to the appropriate investigator(s) at: National Institutes of Health, Building 5, Room 201, 9000 Rockville Pike, Bethesda, MD 20892-0538

- Mechanisms of protein transport across the ER and bacterial inner and outer membranes. (PNAS (2001) 98: 3471; EMBO J. (2001) 20: 6724; PNAS (2005) 102: 221). Harris Bernstein: harris_bernstein@nih.gov
- Structural biology of integral membrane proteins. (J. Mol. Biol. (2003) 332: 353; Mol. Microbiol. (2004) 51: 1027; FEBS Lett. (2004) 564: 294). Susan Buchanan: skbuchan@helix.nih.gov
- Mouse meiosis (Mol. Cell (2000) 6:975; Dev. Cell (2003) 4: 497; Nature Struct. Mol. Biol. (2005) 12: 449) and evolutionary genomics (Nature Genet (2004) 36: 642). Dan Camerini-Otero: camerini@ncifcrf.gov
- Molecular mechanism of retroviral integration. Biochemical and functional analysis of HIV integrase. <http://orac.niddk.nih.gov/www/craigie/crahome.html>. Bob Craigie: bobc@helix.nih.gov
- Structural biology of the ectodomains of the Toll-like receptors of the innate immune system. (Trends in Immunology (2003) 24: 528). David Davies: david.davies@nih.gov
- Structural biology of DNA recombination. (Nature (2004) 432: 995; Mol. Cell (2002) 10: 327; (2004) 13: 403; Mol. Cell (2000) 5: 1025; EMBO J. (2004) 23:2972). Fred Dyda: Fred.Dyda@nih.gov
- Chromatin structure/function; histone modifications; boundary elements. (Science (2001) 293: 2453-2555; EMBO J. (2004) 23: 138-149; Mol. Cell (2004) 13: 291-298). Gary Felsenfeld: gary.felsenfeld@nih.gov
- Biochemistry and molecular biology of gene rearrangement in the immune system. (EMBO J. (2002) 21: 6625; PNAS (2003) 100: 15446). Marty Gellert: gellert@helix.nih.gov
- Molecular mechanisms of DNA mismatch repair. (Nature (2000) 407: 703; J. Mol. Biology (2003) 334: 949; PNAS (2003) 100: 14822). Peggy Hsieh: ph52x@nih.gov
- Transcriptional regulation of development. Molecular and genetic analysis of the transcriptional control of development in *C. elegans* (Development (2005) 132: 1795). Michael Krause: mwkrause@helix.nih.gov
- Single-molecule biochemical study of macromolecular complex assembly/disassembly dynamics involved in a variety of cellular processes. (Mol. Cell (2002) 10: 1367). Kiyoshi Mizuuchi: kmizu@helix.nih.gov
- Structural and functional studies of DNA repair (Mol. Cell (2001) 7: 1; EMBO (2000) 19: 5962), and replication. (Nature (2003) 424: 1083; Mol. Cell (2004) 13: 751). Wei Yang: wei.yang@nih.gov
- Role of the ubiquitin-proteasome system in ER quality control (Nature 2001, 414: 652-656; J. Cell Biology 2003, 162: 71-84; Nature 2004, 429: 841-847). Yihong Ye: yihongy@mail.nih.gov



Tenure-Track Positions in Basic/Clinical Neurobiology

The Laboratory of Neurobiology in the Division of Intramural Research is recruiting Tenure-Track Investigators to establish high-quality independent research programs on fundamental problems in cellular and molecular neurobiology with the potential to identify and prevent environmental disruption of human cognitive potential at any life stage, including early development, childhood learning, or neurodegenerative processes associated with aging. Applicants should have an M.D., Ph.D., M.D.-Ph.D. or equivalent doctoral degree with 3 or more years of postdoctoral research experience and a strong publication record. Physician-scientists with a significant clinical component to their research proposal and investigators using genetic model organisms to understand human neurological disorders are especially encouraged to apply, but all outstanding applicants will be considered. Excellent start-up funds, salary, and benefits package will be provided. In addition the applicant will have access to state-of-the-art equipment and research core facilities at the NIEHS. Interested persons should send their curriculum vita with a statement of research accomplishments and plans, and arrange for three letters of recommendation to be submitted to the following address. **For general information concerning the Laboratory of Neurobiology, access website <http://dir.niehs.nih.gov/dirln/>. For general information about these positions, contact Perry J. Blackshear, M.D., D.Phil., Search Committee Chair at black009@niehs.nih.gov.** Applications received by **July 1, 2005**, will be given first consideration. Applications received after that date will be considered only if the position has not been filled.

Ms. Cindy Garrard (DIR05-06)
National Institutes of Health
National Institute of Environmental Health Sciences
P.O. Box 12233, Maildrop A2-06
111 Alexander Drive, Room A206
Research Triangle Park, NC 27709
E-mail: dir-appls@niehs.nih.gov



WWW.NIH.GOV

**NATIONAL
CANCER
INSTITUTE**



**DHHS, NIH, AND
NCI ARE EQUAL
OPPORTUNITY
EMPLOYERS**

Be an NCI Cancer Prevention Fellow

The Cancer Prevention Fellowship Program provides training for individuals from the health professions and biomedical sciences to become leaders in the field of cancer prevention and control. The Program is sponsored by the Department of Health and Human Services, the National Institutes of Health, the National Cancer Institute (NCI), and the Division of Cancer Prevention.

What will I get out of the program?

- Master of Public Health (M.P.H.) degree
- NCI Summer Curriculum in Cancer Prevention
- Mentored research opportunities at the NCI or at the Food and Drug Administration (FDA)
- Professional development and leadership training

What areas of cancer prevention research are available?

- Chemoprevention
- Clinical cancer prevention
- Development and research-related review of drugs, biologics, or medical devices
- Epidemiology (environmental, genetic, molecular, nutritional)

- Ethics and evidence-based decision making
- Laboratory-based research
- Screening and early detection
- Social and behavioral research
- Statistical methodology

Am I eligible?

You must have a doctoral degree (M.D., Ph.D., J.D., or equivalent). Foreign education must be comparable to that received in the United States.

You must also be a citizen or permanent resident of the United States at the time of application (September 1).

How long is the program?

The typical duration is 3 years (year 1: M.P.H.; years 2-3: NCI Summer Curriculum in Cancer Prevention and mentored research).

How do I obtain more information?

Visit our website <http://cancer.gov/prevention/pob> or request a catalog.

To receive a catalog*, contact:

Douglas L. Weed, M.D., M.P.H., Ph.D.
Director, Cancer Prevention Fellowship Program
National Cancer Institute
6130 Executive Boulevard (EPN)
Suite 321, MSC 7361
Bethesda, MD 20892-7361

* Please provide home address, telephone, e-mail, and where you heard about the Program.

How do I apply?

Apply online at <http://cancer.gov/prevention/pob> or send your application materials directly to the Cancer Prevention Fellowship Program Director, as described on our website and in our catalog.

When are applications due?

Applications are due September 1 for entry into the Program the following July 1.

Further inquiries:

Program Coordinator
Cancer Prevention Fellowship Program
Phone (301) 496-8640
Fax (301) 402-4863
E-mail: cpfpcoordinator@mail.nih.gov

Selection for these positions will be based solely on merit, with no discrimination for non-merit reasons, such as race, color, gender, national origin, age, religion, sexual orientation, or physical or mental disability. NIH provides reasonable accommodations to applicants with disabilities. If you need reasonable accommodation during any part of the application and hiring process, please notify us. The decision on granting reasonable accommodation will be handled on a case-by-case basis.

NATIONAL RESEARCH COUNCIL

OF THE NATIONAL ACADEMIES

NIH/NIST Joint Postdoctoral Program: Interfaces between the Biological and Physical Sciences

The National Research Council of the National Academies is accepting applications for the Joint Postdoctoral Program for research in residence at the National Institutes of Health (NIH) and the National Institute of Standards and Technology (NIST). The goal is to cultivate a scientific work force competent in both the biological and the physical sciences. The research opportunities will emphasize interdisciplinary research at the interface of the biological and physical sciences including, but not limited to, structural and computational biology, medical and bioinformatics, genomics and proteomics, tissue engineering, single molecule detection, nanotechnology, and imaging techniques. Each Postdoctoral Associate will have two Advisers, one at the NIH and one at NIST, and the Associate is expected to spend time at both the NIH and the NIST laboratories during the course of the two-year award. The NIH laboratories are located in Bethesda, Rockville, Frederick, and Baltimore, in Maryland; and in Research Triangle Park, North Carolina. The NIST laboratories are in Gaithersburg, Maryland, and in Boulder, Colorado.

Five awards will be made in 2005 with the competition being open to both U.S. and non-U.S. citizens. The application deadline date is August 1, 2005. Awards will be made in late September. Ph.D. recipients within five years of the doctorate at the time of application are eligible to apply. The award offers an annual stipend of \$55,000 plus relocation expenses, health insurance coverage, and limited professional travel.

For additional information, including specific research opportunities, refer to the NIH/NIST Joint Postdoctoral Program on the National Research Council Web site at: www.national-academies.org/rap

Application instructions can also be found on the NRC Web site. Questions should be directed to the NRC at 202-334-2760 (tel) or rap@nas.edu
Contact: NIST: Dr. Claire M. Saundry, E-mail: claire.saundry@nist.gov, Telephone: (301) 975-2386.

THE NATIONAL ACADEMIES

Advisers to the Nation on Science, Engineering, and Medicine

DEAN SCHOOL OF SCIENCE

Rensselaer Polytechnic Institute, the nation's oldest technological institute and a top-ranked private research university, seeks a highly accomplished, scientific leader to serve as Dean of the School of Science. The Dean will be the administrative head of the School, lead its academic and operational planning, and work to secure the necessary resources to fulfill its ambitions.

In May 2000, under the leadership of new President, the Honorable Shirley Ann Jackson, Ph.D., the Board of Trustees of Rensselaer Polytechnic Institute adopted The Rensselaer Plan, setting a bold course of action and signaling a new era in the distinguished history of the Institute. The Plan has launched a dramatic transformation at Rensselaer. With an emphasis on biotechnology and information technology, research funding has more than doubled in five years, faculty has been significantly expanded, student enrollment and quality are up, and an unprecedented building boom is underway. In September 2004, Dr. Jackson and Rensselaer announced the largest capital campaign in the University's history, with a goal of raising \$1 billion by the campaign's end in 2008.

At this time of unprecedented growth and vision, Rensselaer seeks an energetic and innovative leader to drive the School of Science's ascension in research and academic standing. Reporting to the Provost, the Dean will work to catalyze expanded research in fundamental as well as applied sciences; raise academic quality, ranking, and visibility across all departments; and increase undergraduate and Ph.D. enrollments. The Dean has an opportunity – building on the Institute's core strengths and extraordinary momentum – to lead the School of Science to a further enhanced position of national and international prominence.

Rensselaer seeks a Dean with broad intellectual interests, top-tier scientific credentials, and the leadership and managerial capacity to actualize a bold vision for the future of the School of Science. The position requires a leader with strategic capacity, a track record of excellence in research, outstanding communication skills, and entrepreneurial capacity to inspire and galvanize the Rensselaer School of Science.

All inquiries, nominations, and applications should be sent in confidence to: John Muckle, Isaacson, Miller, 334 Boylston Street, Suite 500, Boston, Massachusetts, 02116; Fax: 617.262.6509; email: 3016@imsearch.com.

Interested applicants are strongly encouraged to send resumes with cover letters via electronic mail.

Rensselaer Polytechnic Institute has a strong institutional commitment to diversity and is an Equal Opportunity/Affirmative Action employer.



PROFESSOR AND CHAIR DEPARTMENT OF VETERINARY PATHOBIOLOGY UNIVERSITY OF MISSOURI, COLUMBIA

The University of Missouri-Columbia College of Veterinary Medicine invites applications and nominations for the position of Professor and Chair of the Department of Veterinary Pathobiology. The Pathobiology Department, housed in recently renovated research and teaching facilities, consists of 43 faculty, 41 graduate students and postdoctoral fellows, and over 100 staff. Two administrative units reside in the department: the Research Animal Diagnostic Laboratory (RADIL) and the Veterinary Medical Diagnostic Laboratory (VMDL). The Department has a strong comparative medicine program, including three NIH Resource and Research Centers (mutant mouse, rat, and swine) and a T32 Comparative Medicine Training program. There is also a strong infectious disease research component, including the Regional BL3 Biocontainment Facility, under construction and a combined graduate program with the Molecular Microbiology and Immunology Department in the School of Medicine. The University of Missouri-Columbia campus offers unique opportunities for collaborations and multidisciplinary research including inter-disciplinary programs bridging to the College of Agriculture, Food and Natural Resources, Life Sciences Center, and the School of Medicine. Candidates for this position must be scholars of international or national stature with an earned doctorate. The individual selected must possess excellent interpersonal skills, communication skills, proven leadership abilities, and the vision to lead the diverse research, service and educational missions of this department. The Department Chair reports directly to the Dean and is a member of the College Executive Committee that advises the Dean and helps formulate College policy. He/She is expected to maintain a prominent level of scholarly activity and stimulate faculty toward high scholarly achievement. Preference will be given to individuals with proven leadership experience, a sustained record of extramural support, and an appreciation of the importance of the service components of the department.

Applicants should submit a letter of application, statement of goals, curriculum vitae, and the names and contact information of at least three references. Consideration of applications will begin **July 1, 2005** and will continue until the position is filled. Nominations and applications should be sent to: **Dr. M. Harold Laughlin, Chair of the Biomedical Sciences Department and Chair of the Veterinary Pathobiology Search Committee, ATTN: Ms. Jennifer Sonnenberg, W203 Veterinary Medicine Building, College of Veterinary Medicine, University of Missouri, Columbia, MO 65211. Telephone: (573) 882-3768.** Additional information is available at <http://www.cvm.missouri.edu/cvm/positions/pathobiology.html>.

The University of Missouri-Columbia is an Affirmative Action/Equal Opportunity Employer and complies with the guidelines of the Americans with Disabilities Act of 1990. If you have special needs as addressed by the ADA and need assistance with this or any portion of the application process, notify us at the address or telephone number above as soon as possible. Reasonable efforts will be made to accommodate your special needs.

eikones[®]

UNIVERSITÄT BASEL

NCCR Iconic Criticism. Understanding the Power and Meaning of Images

Iconic Criticism is one of the six recently launched National Centres of Competence in Research (NCCR) of the Swiss National Science Foundation. Home base is the University of Basel. This interdisciplinarily designed project of maximum duration of 12 years centers itself around the core questions of: How does the image generate meaning — in science, in the ordinary, in art? What influences the image and what is its influence? Where is the image's innate and irreplaceable might?

Attempts to clarify these unanswered questions come from the Humanities, the Natural Sciences as well as Technology. NCCR Iconic Criticism is building bridges between the disciplines within the responsible University of Basel as well as in various Swiss and international universities, colleges, research institutions, museums and collections.

NCCR Iconic Criticism is structured in 6 thematic modules: The Power of Images – Image Politics / Image, Architecture and Word / Time in the Image – Liveliness and Temporality / The Image of Writing / The Literary Text as Iconic Criticism / The Epistemic Image: Visualization in Science, Technology and Humanities as well as in a Postgraduate Research Group on the question of "Image and Knowledge".

Interested?

We advertise the first positions and grants starting 1 October 2005 :

- **20 positions for young academics**
 - **12 three-years doctoral grants for participation in the Postgraduate Research Group**
- Young academics (postdoctoral fellows, as well as doctoral candidates) from the fields of Image Studies, Language and Literature, Scientific History, Natural Sciences who have already excelled in their field are invited to apply.

Deadline for submissions 18 June 2005

Detailed descriptions of the positions can be found at: www.eikones.ch or through Helen Dunkel, phone ++41 61 267 1803, helen.dunkel@unibas.ch
eikones – NCCR Iconic Criticism, Universität Basel, Rheinsprung 11, CH 4051 Basel, Switzerland





Health Research in a Changing World

Fighting Diseases and Improving Lives

DEPARTMENT OF HEALTH AND HUMAN SERVICES NATIONAL INSTITUTES OF HEALTH NATIONAL INSTITUTE OF ALLERGY AND INFECTIOUS DISEASES

With nationwide responsibility for improving the health and well-being of all Americans, the National Institutes of Health (NIH) and the National Institutes of Allergy and Infectious Diseases (NIAID) conducts and supports a global program of research aimed at improving diagnosis, treatment and prevention of immunologic, allergic and emerging infectious diseases. NIAID's mission is driven by a strong commitment to basic research, which incorporates the complementary fields of vaccine research, immunology, microbiology and infectious diseases.

NIAID is a world leader in medical research and is on the cutting edge of medical and scientific research/discovery, including areas of biodefense (i.e., small pox and anthrax), HIV/AIDS research worldwide, vaccine research (i.e., Ebola), asthma and allergic diseases and other advances of medical and scientific research. NIAID has state-of-the-art equipment, facilities and laboratories and a highly trained staff with the potential and desire to find a cure/vaccine for some of the deadliest infectious diseases known to mankind.

The NIAID is committed to maintaining its stature as a premier research institution by building an inclusive workforce through the Workplace Diversity Initiative and Affirmative Action programs. The NIAID's commitment to equal opportunity and diversity in recruiting, hiring and career development will help ensure the continued output of excellent science.

Are you ready for an exciting career that could help improve millions of lives around the world? Then consider joining the scientific and medical forces at NIAID. The NIAID, NIH, DHHS offers competitive salaries and a comprehensive benefits package. Most job opportunities are conveniently located in Bethesda, Maryland within minutes of thousands of cultural, recreational, entertainment and educational centers. Positions are also available in Hamilton, Montana.

We invite you to explore job opportunities and submit your resumes online at: <http://healthresearch.niaid.nih.gov/Science>. Whether you are a scientist, nurse, health specialist or have a background in other support disciplines such as finance, communications and administration, your individual talents are needed to support our mission. Do not delay. Medical history won't wait. NIAID is currently searching for qualified Medical Officers, Nurse Consultants, Scientific Review Administrators, Senior Regulatory Affairs Specialists and Health Specialists.

We are happy to respond to your questions, and you may contact us toll-free at 888-798-4991.

**Please visit us at the American Society for Microbiology 105th General Meeting in Atlanta, GA
June 5-9 at booth #1008**

Please reference "Science" on your resume.



Department of Health and Human Services
National Institutes of Health
National Institute of Allergy and Infectious Diseases

Proud to be Equal Opportunity Employers

**Baylor College of Medicine
Children's Nutrition Research Center
Department of Pediatrics
POSITION DESCRIPTION**

Position: Assistant or Associate Professor of Exercise Science

The Children's Nutrition Research Center (one of six USDA funded Human Nutrition Research Centers across the US) is looking to expand its faculty to include an Assistant or Associate Professor of Exercise Science or Kinesiology. This is a 12 month, tenure track position. The primary responsibility of the successful candidate is to establish a highly successful program of externally funded research on physical activity among children, with an emphasis on obesity prevention. The primary methods could include epidemiological, behavioral and/or interventional approaches to enhancing physical activity in children.

The CNRC includes more than 55 faculty who engage in research on various aspects of nutrition, including exercise science. Twelve of these faculty are currently engaged in research on behavioral and related aspects of children's diet and physical activity. There will be substantial opportunity to collaborate with scientists with expertise in pediatric behavior, genetics, molecular biology, endocrinology, body composition, energy expenditure and other disciplines. The successful candidate will be invited to collaborate on several existing intervention studies. For more information on faculty interests at the Center, visit the CNRC faculty page at <http://www.kidnutrition.org/faculty/listing.htm>.

The successful candidate will have a track record of funding for research and a corresponding record of related publications in top-tier, peer reviewed journals. The position requires a doctoral degree in exercise science (or a closely related field) and, preferably, post-doctoral training with at least two years of research experience. Pediatricians with specialized training in exercise science and the above funding and publication accomplishments are also qualified to apply. Salary will be competitive and commensurate with qualifications.

Houston is the fourth largest city in the US with an ethnically diverse population. Houston contains all the educational, cultural, and sports amenities. The Gulf Coast and the beaches at Galveston are only 50 mins away.

Please submit a letter of application, a full CV (including the Science Citation Index for the 10 most frequently cited publications), copies of three best publications, and three letters of reference addressing the candidate's research, creativity and productivity, and ability to establish an internationally recognized program of externally funded research to: **Tom Baranowski, Ph.D., Professor of Pediatrics (Behavioral Nutrition and Physical Activity), Children's Nutrition Research Center, Department of Pediatrics, Baylor College of Medicine, 1100 Bates Street, Room 2038, Houston, TX 77030-2600; 713-798-6762 (phone); 713-798-7098 (fax); tbaranow@bcm.tmc.edu.**

Baylor College of Medicine is an Equal Opportunity/Affirmative Action/Equal Access Employer.

COASTAL WETLANDS ECOLOGIST

The Department of Marine Biology at Texas A&M University at Galveston (TAMUG) invites applications for a 9 month tenure-track position in coastal wetlands ecology at the assistant or associate professor level. The successful applicant is expected to teach at the undergraduate and graduate levels, advise graduate students, and develop an externally funded research program. Applicants must have a PhD, with post-doctoral experience. Areas of specialization include but are not restricted to ecosystem modeling, spatial analyses with GIS, land use, fisheries, restoration, and sea grass ecology. A commitment to excellence in teaching is required and prior teaching experience is desirable. The applicant is also expected to work with the Outreach Program for wetlands education and take a leading role in the maintenance and utilization of a newly constructed wetlands center. Competitive start-up funds are available.

TAMUG, with a current enrollment of approximately 1600 undergraduates and 75 graduate students, is the coastal branch campus of Texas A&M University (TAMU), and all students at TAMUG are enrolled in marine or maritime degree programs. The main campus has a current enrollment of approx. 44,000 students, and TAMU is the Land, Sea and Space Grant University of Texas. Graduate degrees pursued by TAMUG students at College Station include Biology, Oceanography, Ocean Engineering, Rangeland Ecology and Management, and Wildlife and Fisheries Sciences. Marine Biology (MARB) is the largest department at TAMUG, with approximately 500 undergraduates and 40 graduate students. TAMUG, as TAMU's 'window to the sea,' houses the Texas Maritime Academy, which operates the T/S TEXAS CLIPPER II. TAMUG is headquarters for the Texas Institute of Oceanography (TIO), Laboratory for Environmental Research (LOER), and the Institute of Marine Life Sciences (IMLS). Additional information about TAMUG and the Marine Biology Department may be found at <http://www.tamug.edu>.

Applications will be reviewed beginning **July 1, 2005**, and will continue until the position is filled. Applicants should submit curriculum vitae, statements of interest in teaching and research, and full contact information for four references. All materials should be mailed to: **Dr. Jay Rooker, Wetlands Search Chair, Marine Biology Department, Texas A&M University at Galveston, Galveston, Texas 77553-1675 USA.**

Texas A&M University is an Equal Opportunity/Affirmative Action Employer that accommodates individuals with disabilities. Individuals requesting a disability accommodation should contact the Human Resources Department. Proper documentation of identity and employability are required at the time of employment. Official transcript required for the application of employment.

**Join the Program of Excellence
in Nanotechnology for Vulnerable
Plaque Funded by the National Heart,
Lung and Blood Institute**

The physical rupture of atherosclerotic plaques and the resulting myocardial infarcts cause thousands of sudden cardiac deaths per year. Importantly, only certain subsets of plaques are vulnerable or rupture prone. The long-term objective of this Program of Excellence is to design nanodevices for the analysis, diagnosis, monitoring and treatment of vulnerable atherosclerotic plaques. By working at the interface of biochemical design and nanoscience, researchers will create novel, diagnostic therapies for atheroma. This Program of Excellence is a partnership between The Burnham Institute, The Scripps Research Institute, and The California Nano Systems Institute at the University of California Santa Barbara. The principal investigators in this program include:

- **Jeffrey W. Smith, Ph.D.**
Associate Professor/The Burnham Institute
Protein engineering, phage display, adhesion biology, vascular biology
- **Erkki Ruoslahti, Ph.D., M.D.**
Distinguished Professor/The Burnham Institute
Homing peptides for vascular targeting, phage display, drug targeting
- **Francesca Marassi, Ph.D.**
Assistant Professor/The Burnham Institute
Structural biology, NMR, solid-state NMR
- **Zaverio Ruggeri, M.D.**
Professor/The Scripps Research Institute
Vascular biology, platelet function, sheer stress, platelet adhesion proteins
- **Mark Yeager, M.D., Ph.D.**
Professor, Department of Cell Biology/ Scripps Research Institute; Professor, Department of Cardiology/Scripps Clinic
Protein structure, Cryo-EM
- **Samir Mitragotri, Ph.D.**
Assistant Professor of Chemical Engineering/ University of California Santa Barbara
Targeted drug delivery of nanoparticles, oral protein delivery, transdermal drug delivery
- **Joseph Zasadzinski, Ph.D.**
Professor of Chemical Engineering and Materials/University of California Santa Barbara
Polymers, biomimetic self-assembly, vesosomes, microscopy
- **Matthew Tirrell, Ph.D.**
Professor, Chemical Engineering, Materials and Biomolecular Science and Engineering/ University of California Santa Barbara
Self-assembling polymers and amphiphiles, frictional behavior
- **Patrick Daugherty, Ph.D.**
Assistant Professor/University of California Santa Barbara
Protein engineering through computational design and phage display
- **Andrew Cleland, Ph.D.**
Professor of Physics/ University of California Santa Barbara
Nanolithography, nanomachining and nanoelectronics

We are seeking postdoctoral candidates with expertise in biology, chemistry, engineering or physics to join us in this developing field. Applicants should submit via email a letter of application, a brief description of career interests, and a curriculum vitae and bibliography to: **The Burnham Institute, humanresources@burnham.org**

OPEN TO

TRANSATLANTIC BONDS

Connect with your future. At Novartis UK.

We currently have opportunities for talented PhD and postdoctoral chemists at our award-winning research facility in Horsham, England. [We welcome UK scientists home.](#)

To view descriptions of all open positions and to apply, visit www.nibr.novartis.com and follow the links to Careers and Job Opportunities.

Novartis is committed to embracing and leveraging diverse backgrounds, cultures, and talents to achieve competitive advantage.
Novartis is an equal opportunity employer. M/F/D/V



www.nibr.novartis.com
© 2005 Novartis AG



Issue date 1 July 2005
Reserve ad space by 14 June 2005

Celebrate 125 Years of Science

We're honoring *Science's* 125th anniversary in the 1 July issue with great recruiting opportunities

- Post your job openings for 8 weeks on ScienceCareers.org from 1 July–15 July for just \$125 per posting.
- 125 days of free access to ScienceCareers.org's Resume/CV Database when you run a print ad in the 1 July issue of *Science*.
- Added bonus distributions to 7 major shows in 2005: Drug Discovery Technology™, American Chemical Society, NIH Research Festival, Biotechnica, American Society of Human Genetics, Neuroscience, and American Society for Cell Biology

For more information, contact

U.S. Daryl Anderson
phone: 202-326-6543
e-mail: danderso@aaas.org

Europe and International
Tracy Holmes
phone: +44 (0) 1223 326 500
e-mail: ads@science-int.co.uk

Japan Jason Hannaford
phone: +81 (0) 52 789-1860
e-mail: jhannaford@sciencemag.jp

ScienceCareers.org
We know science AAAS



The
University
Of
Sheffield.

The
Achievement
Of
Excellence.

Department of Animal and Plant Sciences

Senior Lecturer/Reader/Professor

Salary £37,558 - £42,573 per annum (SL). By agreement (PROF)

The Department has an outstanding international reputation for research (5* RAE 2001) and teaching (QAA 24/24) and now seeks to appoint an outstanding individual to complement one or more of our key five research themes: evolution and behaviour; population and community ecology; biodiversity and conservation; global change biology; and plant molecular science. Informal enquiries may be addressed to the Head of Department, Professor Malcolm Press (m.c.press@sheffield.ac.uk).

Closing Date: 30 June 2005 Ref. R3677

Committed to equality through diversity.

For full details and application pack visit:

www.sheffield.ac.uk/jobs or e-mail:

jobs@sheffield.ac.uk Tel: 0114 222 1631 (24 hrs)

Please quote Ref. in all enquiries.



SCOTT & WHITE



College of Medicine
The Texas A&M University System
Health Science Center

Pediatric Hematology-Oncologist

The Section of Pediatric Hematology/Oncology at **Scott and White Clinic** and the **Texas A&M University System Health Science Center College of Medicine** (TAMUS HSC-COM) are seeking a clinician scientist with current research grants for a faculty position in a rapidly growing program. The candidate should be BE/BC in pediatric oncology and committed to an academic career. The successful candidates will join and enhance ongoing efforts in basic and translational research, with an institutional commitment to building a world-class experimental therapeutics program. An outstanding start-up package includes high quality laboratory space, excellent benefits and competitive salaries commensurate with academic qualifications. The position guarantees 75% protected time for research activities.

Scott & White Clinic is a 500+ physician directed multi-specialty group practice that is the leading provider of cancer care in Central Texas. Scott and White Clinic and the 486 bed tertiary Scott & White Memorial Hospital is the main clinical teaching facility for TAMUS HSC-COM. Outstanding clinical practice and laboratory facilities on campus that perform state of the art molecular and cellular biology research, flow cytometry, genomics and biostatistics are in place to support the research effort.

Please contact: **Don Wilson, M.D. Professor and Chairman, Department of Pediatrics, Scott & White, 2401 S. 31st, Temple, TX 76508. (800)725-3627 dwilson@swmail.sw.org Fax (254) 724-4974.**

For more information about Scott & White, please visit www.sw.org For Texas A&M www.tamhsc.edu. Scott & White is an equal opportunity employer.



Pacific Northwest National Laboratory

...delivering breakthrough science and technology

Senior Scientist V, VI - Microbial Pathogenesis

Pacific Northwest National Laboratory is seeking a Senior Scientist with expertise in microbial pathogenesis, including but not limited to host-pathogen interactions, genetics and proteomics of virulence, mechanisms of virulence and resistance, and biomedical effects of biofilms. The applicant will have the opportunity to build a program in microbial pathogenesis supported by a strong cadre of microbiologists with experience in environmental microbiology, microbial ecology, and the application of high throughput biology to microbial systems. This position features collaborative access to global proteomics, microarray facilities, metabolomics, imaging, and computational modeling. Resources will be available for growth of the program.

Minimum Requirements: PhD in Microbiology, Virology, Cell Biology, or related discipline and 7+ years' relevant experience. A substantial track record of peer-reviewed publications in appropriate journals and peer-reviewed funding from NIH and/or DHS are position prerequisites.

Qualifications: The ideal candidate will demonstrate an interest in multi-disciplinary, systems biology-based approaches to problem solving. The successful candidate will have a demonstrated record of strong leadership qualities, scientific talent, team building and motivation skills, and managing to outcomes, as well as a proven commitment to the mentoring and development of junior scientific staff. The candidate will participate in setting the national and/or international research agenda and will have obtained recognition via publications, awards, citations, or other honors. To allow participation in related national security research that requires a security clearance, U.S. citizenship is preferred.

Position is located in Richland, WA. Relocation support, as well as a competitive compensation and benefits package, is available.

• About Systems Biology at PNNL - <http://www.sysbio.org>

Apply online: www.jobs.pnl.gov. Reference job requisition # 109332. Please submit your curriculum vitae, a list of professional references and publications, and a cover letter detailing your research interests and experience in staff development.

For more information, contact: **Mariah Martin – Human Resources; mariah.martin@pnl.gov**



The University of Texas Medical Branch

Senior Faculty Position in Immunology

The University of Texas Medical Branch (UTMB) at Galveston seeks an accomplished immunologist (MD and/or PhD) for a tenured/tenure-track faculty position at the rank of Professor/Associate Professor. Candidates with proven abilities in research relating to immune mechanisms controlling infectious diseases, including demonstrated success in attracting extramural research funding and a strong publication record, are encouraged to apply. UTMB offers an outstanding environment to undertake research in the broad area of infection and immunity and is home to the future Galveston National Laboratory and the NIH-funded Western Regional Center of Excellence in Biodefense and Emerging Infectious Diseases. UTMB's programs include over 150 scientists conducting research in the area of infection and immunity in multiple medical school departments, supported by unique BSL-3 and BSL-4 containment laboratories and a broad array of state-of-the-art research core facilities. More information can be found at www.utmb.edu/gnl.

Interested candidates should send a C.V., outline of research interests and names of potential references to:

**Immunology Search Committee
Institute for Human Infections and Immunity
Department of Microbiology and Immunology
The University of Texas Medical Branch
301 University Blvd
Galveston, TX 77555-0428**

Further information and informal inquiries can be made to **Chair, Search Committee** (email: ihii.web@utmb.edu; telephone: (409) 747-6500).

UTMB is an Equal Opportunity/Affirmative Action University that proudly values diversity. Candidates of all backgrounds are encouraged to apply.



LOUISIANA STATE UNIVERSITY
Research and Economic
Development
Baton Rouge, Louisiana 70803

VICE CHANCELLOR FOR RESEARCH AND ECONOMIC DEVELOPMENT

Reporting to the Executive Vice Chancellor and Provost, the Vice Chancellor for Research and Economic Development serves as the Chief Research Officer of Louisiana State University A&M (www.lsu.edu). The Vice Chancellor for Research & Economic Development will take a leadership role in national and international activities regarding research policy and will guide LSU in defining, prioritizing, and energizing emerging research opportunities. This individual will provide the vision, energy and leadership for LSU's research and economic development agenda as it pursues further advancement within the ranks of America's public research universities, a quest that is articulated by LSU's National Flagship Agenda (www.lsu.edu/flagship). The Vice Chancellor will provide research leadership for the State of Louisiana by developing excellent relationships with University stakeholders, including government, business and industry, leaders at all levels of the education, arts, scientific and cultural communities, as well as with faculty, staff, students and alumni. Important elements of the research agenda include promotion of interdisciplinary and cross-disciplinary research and scholarship, promotion and facilitation of technology transfer and economic development, affirmation of the integrity of all research processes and policies, establishment of regional, national and international cooperative research ventures, and coordination of activities that promote broad participation in research, scholarly and creative work that continuously expands and strengthens LSU's research agenda.

Required Qualifications: strong background in a research-intensive discipline; demonstrated ability to build a nationally and internationally competitive research program; qualify for a tenured appointment in an appropriate academic unit.

Applications may be electronically submitted to: vcresearch@lsu.edu. Application deadline will be **July 29, 2005** or until a candidate has been selected. Further details about the position are available at <http://vcresearch.lsu.edu>. Applicants should send a letter of application, their curriculum vitae or resumes (including email addresses) to:

Vice Chancellor for Research Search Committee
c/o LSU Academic Affairs
135 Thomas Boyd Hall
Louisiana State University
Ref: #003690
Baton Rouge, LA 70803

*LSU IS AN EQUAL OPPORTUNITY/
EQUAL ACCESS EMPLOYER.*

Our client is the Swiss based headquarter of one of the world's most prominent life science companies, ranking in the top ten of pharmaceutical enterprises world wide. We are seeking you as the

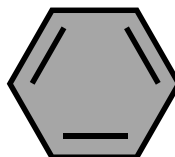
Unit Head Translational Biology

In the area of **Psychiatry**, with the responsibility for your team of around 40 co-workers, you are the interface between research and development. By stipulating, verifying, and elucidating psychiatric disease processes by the means of in vivo models, your contribution is key to the finding and development of new psychiatry drugs. As an

innovative out-of-the-box thinker

you search and walk new and creative pathways to find valuable results that push forward the specific research in your area. Based on your background with an MD or PhD in Biology, behavioural Pharmacology or a related area, you acquired at least five years of working experience in pharmaceutical industry. You are a specialist in behavioural Pharmacology and/or Physiology (focus on brain function). In parallel, you have a proven track record of team leadership for scientific teams. Ideally, you are familiar with CNS imaging techniques. English is a prerequisite, other languages are considered a plus.

If you are the driver to successfully fill this position, and you have a clear will to win, please send in your application with CV and testimonials to:



PP PHARMA PLANING
Bergauer + Partner AG
International Health Care Recruitment

attn. Mr Dieter Hubmann, PhD,
direct dial: +41-61-261 94 64
Gerbergässlein 41, 4051 Basel,
(Switzerland)
Tel. +41-61-261 94 93
e-mail: d.hubmann@pp-pharma-plan.com

www.pp-pharma-plan.com
www.pharma-career-box.com

Your application will be treated with strict confidentiality.


NIOSH
Molecular Toxicologist

The National Institute for Occupational Safety and Health (NIOSH) in the CDC announces recruitment for a full-time Project Leader in the area of Molecular Toxicology in Morgantown, WV. The position is in the

Toxicology and Molecular Biology Branch which is responsible for conducting laboratory-based research to help prevent or control occupational related diseases. The laboratory facility is located in close proximity to the West Virginia University Medical School, in a recently constructed state-of-the-art research facility. The branch presently comprises faculty experienced in cardiovascular toxicity, chronic stress, carcinogenesis, pulmonary diseases, musculoskeletal diseases, neurotoxicity and receptor-mediated toxicity.

We seek an experienced research scientist with a background in toxicology research. Interested candidates should have a Ph.D. (or equivalent) and a minimum of three years postdoctoral experience. Preference will be given to individuals who have initiated a strong research program in (1) molecular epidemiology, (2) dermatology or (3) ocular biology.

A competitive salary will be offered commensurate with qualifications and experience. The laboratory will have a fully funded annual operating budget and the successful candidate will have an opportunity to recruit technical and postdoctoral support staff.

Interested individuals should submit a letter of interest, current CV and a list of three references to: **Michael I. Luster, Ph.D., Chief, Toxicology and Molecular Biology Branch, National Institute of Occupational Safety and Health, 1095 Willowdale Rd, Morgantown, WV 26505** or by email (preferred) to: **RLanciotti@cdc.gov**.



*NIOSH is an Affirmative Action/
Equal Opportunity Employer.*

**C.W. Kearns, C.L. Metcalf and W.P. Flint
Endowed Chair in Insect Toxicology**

**Department of Entomology
School of Integrative Biology
University of Illinois at Urbana-Champaign**

The Department of Entomology and the School of Integrative Biology at the University of Illinois in Urbana-Champaign seek a highly qualified candidate for the **C.W. Kearns, C.L. Metcalf and W.P. Flint Endowed Chair in Insect Toxicology**. This is a full-time position at the rank of professor and with tenure. The starting date is negotiable after the closing date of the search. Candidates should exemplify the qualities demonstrated by Professors Kearns, Metcalf, and Flint in their long and distinguished careers: outstanding research with significant impact in insect toxicology, defined broadly. Experimental approaches can be at any level from molecular to environmental. The successful candidate must have a Ph.D. or equivalent and an internationally recognized, externally funded research program. Responsibilities also include teaching and participation in graduate and undergraduate training.

The Chair holder will have the opportunity to be part of dynamic and well-established communities of scientists in the Department of Entomology, the School of Integrative Biology, and in other life science units on campus. The presence of the Institute for Genomic Biology, the Beckman Institute for Advanced Science and Technology, the W.M. Keck Center for Comparative and Functional Genomics, the National Center for Supercomputing Applications and many interdisciplinary programs for graduate training, make this campus an especially vibrant place to conduct research. Salary will be commensurate with experience. Minorities, women, and members of other designated groups are encouraged to apply.

To ensure full consideration, nominations should be received by **September 30, 2005**. Evaluation of candidates will begin immediately. No final decision will be made prior to the closing date, and the search will continue until a suitable candidate is identified. Nominations (including self nominations) should include a CV. Materials should be sent to: **Dr. May R. Berenbaum, Chair, Search Committee, School of Integrative Biology, University of Illinois, 286 Morrill Hall, 505 S. Goodwin Ave., Urbana, IL 61801** (phone: 217/333-3044; fax: 217/244-1224; email: sib@life.uiuc.edu).

The University of Illinois is an Affirmative Action, Equal Opportunity Employer.


**Massey Cancer Center
Molecular Radiobiology**

The Department of Radiation Oncology at Virginia Commonwealth University is offering a tenure-track position at the level of Assistant or Associate Professor in its Molecular Radiobiology Division. The Department of Radiation Oncology, a component of the NCI-designated Massey Cancer Center, supports a highly integrated program studying cellular radiation responses spanning radiation-induced protein modifications, signal transduction responses and DNA damage processing funded by R01 and P01 grants from the NCI (www.radonc.vcu.edu). The successful candidate's research interests should complement existing expertise and he/she should be interested in collaborative research with other members of the Division. The Division is well-equipped for modern cell and molecular biology studies with translational emphasis including an ABI QStarXL mass spectrometer for protein sequencing and deconvolution fluorescence microscopy for 3D image analysis. Cancer center-sponsored core facilities for virus production, flow cytometry, DNA sequencing and synthesis, and structural biology (x-ray crystallography and NMR) are also available. Support will be provided for at least three years after which extramural research funding is expected. Qualifications: A Ph.D., M.D., or MD/Ph.D. with at least 3 years of post-doctoral research experience. To qualify for Associate Professor level position, extra-mural (NIH or similar) funding is required with significant peer-reviewed publications in his/her field.

Interested candidates should submit a CV, detailed research plan and three references to:

**Susan Kelly, Search Committee Administrator
VCU Department of Radiation Oncology
P.O. Box 980058
Richmond, VA 23298-0058
email: swkelly@vcu.edu
Fax: (804) 828-6042**

VCU is an EEO/AA Employer. Women, minorities, and persons with disabilities are encouraged to apply.


**Science and Regulatory Policy Leader,
Human Health**

Provides leadership and organization for science and regulatory policy issues in the area of human health on behalf of CropLife America. Responsible for monitoring, review and analysis of all relevant regulatory initiatives, including the identification of emerging policy issues, that impact the crop protection industry. Leads the development and implementation of effective strategies in support of CropLife America's objectives, including preparation of public comments in response to regulatory proposals. Reports to the Vice President of Science and Regulatory Affairs.

Candidates must possess strong analytical and interpretive skills; a strong scientific background in the area of human health and safety; and demonstrate a strong grasp of risk assessment principles and methodologies (toxicology, epidemiology and exposure assessment). Candidates must have excellent oral and writing skills and experience in submission of technical comments in response to federal regulatory proposals. Experience with the regulatory approval processes of the Environmental Protection Agency or the Food and Drug Administration is strongly preferred. An advanced degree in toxicology, pharmacology, physiology, chemistry or a related discipline is required.

Interested persons should contact:

**Karen McEvoy, Human Resources Manager
CropLife America
1156 15th Street, NW, #400
Washington, D.C. 20005
E-mail: kmcevoy@croplifeamerica.org
Tel: (202) 872-3858**

Deadline to Apply: **June 20, 2005**

CropLife America is an Equal Opportunity/Affirmative Action Employer.

Departments of Biochemistry (University of Leicester) and Paediatrics (Imperial College London)

Two Senior Postdoctoral Research Scientists

Salary range £29,699 - £39,094 (Research Fellow - Imperial College)

Salary Range £27,116 - £35,883 (Research Associate - University of Leicester)

We are seeking two postdoctoral research positions to join groups working on the development of novel therapies based on targeted stimulation of splicing. This is a Wellcome Trust-supported collaboration between groups with expertise in RNA splicing and neuromuscular biology and disease. The groups are based at the Hammersmith Campus of Imperial College London and the University of Leicester and one post would be based in each group. The two groups have recently demonstrated that it is possible to rescue inefficient splicing of the SMN2 gene in cultured fibroblasts from patients with Spinal Muscular Atrophy, one of the major lethal genetic diseases of young children (Skordis *et al.*, Proc. Natl. Acad. Sci. USA vol. 100, pp 4114-4119; 2003). The aim of this research is to develop the method further as a potential therapy for this and other diseases. The programme will involve fundamental research into the mechanisms by which splicing can be enhanced and the development of strategies for successful application *in vivo*.

The posts are fixed-term for four years.

Candidates should have a relevant PhD. with high-level experience of productive research in molecular biology and gene expression or cell biology.

Informal enquiries may be made to Prof Ian Eperon (eci@le.ac.uk tel 0116 252 3482) or Prof Francesco Muntoni (f.muntoni@imperial.ac.uk tel 020 8383 3295).

An application form may be obtained from the following web link <http://www.imperial.ac.uk/employment/index.htm> Alternatively, for an application pack please contact the Human Resources Division, Imperial College London, Hammersmith Campus, Commonwealth Building, Du Cane Road, London W12 0NN, quoting reference number HJ 825.

Closing date: 13 June 2005.

Valuing diversity and committed to equality of opportunity



www.ars.usda.gov

Research Leader

Supervisory Research Physical Scientist/Supervisory Research Chemist/Supervisory Microbiologist GS-14/15

Salary Range \$85,123 to \$130,173

The National Center for Agricultural Utilization Research, Bioproducts and Biocatalysis Research Unit, Peoria, IL, is seeking a permanent full-time Research Leader. The mission of the Bioproducts and Biocatalysis Research Unit is to develop processes for the conversion of agricultural commodities into biofuels, chemicals, enzymes, and polymers. Research is focused on the biochemistry, physiology, ecology, and genetics of microorganisms to develop new fermentation and enzyme technologies to produce value-added products. The Research Leader coordinates the Unit's research with other governmental, industrial, and university partners to achieve the goals of the assigned research program, supervises a group of 7 scientists and 10 support personnel and conducts a personal research program. The incumbent has responsibility to conceive, plan, and conduct research while managing fiscal, physical, and human resources. A degree in chemistry, microbiology, or physical sciences; in addition to knowledge of biochemistry, physiology, ecology, and genetics of microorganisms to develop new fermentation and enzyme technologies is required.

For details and application directions, visit the website <http://www.afm.ars.usda.gov/hrd> - refer to announcement ARS-X5W-0292. To receive a printed copy by mail, call 301-504-1482. U. S. citizenship and pre-employment background investigation required. Application must be postmarked by **July 1, 2005**.

USDA/ARS is an Equal Opportunity Employer and Provider.



TENURE TRACK FACULTY POSITIONS DEPARTMENT OF BIOCHEMISTRY CELLULAR AND MOLECULAR SIGNALING INITIATIVE Virginia Commonwealth University School of Medicine

The Department of Biochemistry at Virginia Commonwealth University School of Medicine has developed a strong program in molecular and cellular signaling. Virginia Commonwealth University is an ethnically and culturally diverse institution of higher learning located in Richmond, Virginia. We invite applications from outstanding individuals with expertise and interest in molecular signaling for several tenure-track and collateral faculty positions at Assistant/Associate/Professor levels. Successful applicants, with a Ph.D. and/or M.D. degree and several years of post-doctoral experience, are expected to develop a vigorous, externally funded research program and participate in the teaching mission of the Department. Applications from individuals with expertise in Proteomics, Lipidomics, Metabolomics, Enzymology, System Biology, or Signal Transduction are of special interest. In addition, applicants with other interests that complement existing departmental strengths will be considered.

Applications should include a CV, a brief statement of research plans, and three letters of recommendation; include information on extramural funding and teaching. This material should be sent to: **Dr. Robert Diegelmann, Chair, Search Committee, Department of Biochemistry, Virginia Commonwealth University School of Medicine, Richmond, VA 23298-0614** or e-mail directly to rdieglm@hsc.vcu.edu.

*Virginia Commonwealth University is an Equal Opportunity/
Affirmative Action Employer. Women, persons with disabilities,
and minorities are encouraged to apply.*

Postdoctoral Fellow/ Research Scientist

The Leon H. Charney Division of Cardiology of the Department of Medicine at the New York University School of Medicine seeks a Post Doctoral Fellow/Research Scientist to join our growing research staff.

The selected individual will participate in all aspects of ongoing studies in cardiovascular science and must have extensive experience in molecular biology, tissue culture, biochemical and histological techniques. Prior experience with animal surgery is desired. Candidate must be able to work independently, but also function well in an interactive laboratory group.

Applicants should send a letter of interest and CV to: **David E. Gutstein, M.D., Leon H. Charney Division of Cardiology, Department of Medicine, VAMC/NYU School of Medicine, 423 E. 23rd St., New York, NY 10010.** Email: David.Gutstein@med.nyu.edu. NYU School of Medicine is an Affirmative Action, Equal Opportunity Employer.



MASSACHUSETTS GENERAL HOSPITAL HARVARD STEM CELL INSTITUTE



is recruiting faculty in **Stem Cell Biology** for a newly created, multi-disciplinary **Center for Regenerative Medicine and Technology (CRMT)** and the affiliated **MGH-HMS Center for Nervous System Repair (CNSR)**. The successful candidates will also be members of the new Harvard Stem Cell Institute and faculty members of Harvard Medical School. One to three Assistant Professor level positions are available with one specifically focused on Neural Precursor/Stem Cell Biology.

The goal of the CRMT is to provide detailed analyses of tissue development for the purpose of modeling disease states and creating practical methods of tissue regeneration, replacement or repair. It incorporates developmental biology, ES and adult stem cell biology, bioengineering, imaging and computational expertise to understand the complex relationships of primitive cells with their microenvironment. The CNSR emphasizes applying elements of neuronal differentiation, precursor/stem cells, neurogenesis, axonal outgrowth, transplantation, and oligo differentiation to repair in the CNS. The centers participate fully in the larger Harvard University-wide stem cell research efforts and graduate programs; both are in new space on the MGH main campus. The HSCI is a major new university-wide, interdisciplinary endeavor with substantial resources to speed progress in the field. We are seeking Ph.D., M.D., or M.D./Ph.D. scientists with a history of innovative, interactive research using mammalian or non-mammalian systems.

Candidates should send a letter of interest including research plans, c.v. and 3 letters of support to: **Dr. David Scadden, c/o Chris Pasker: cpasker@partners.org and Dr. Jeffrey Macklis, c/o Anita Mohan: agmohan@partners.org.**

TEL AVIV UNIVERSITY



Sackler School of Medicine Tenure-Track Position

The Sackler School of Medicine seeks outstanding candidates to fill a tenure track position at the level of Lecturer, Senior Lecturer or Associate Professor in the areas of Microbiology and/or Immunology. Candidates must possess Ph.D. or M.D. degree and have postdoctoral experience. The candidates are expected to exhibit capability of developing an independent, vigorous research program in Microbiology and/or Immunology.

An appropriate start-up package will be offered.

Applicants should send electronic version of their Curriculum Vitae and list of publications, a statement of research program and addresses of 3 references, till **August 31, 2005** to the address below:

The Search Committee secretariat
Mrs. Gaby Mor
E mail: gabym@post.tau.ac.il

Human Oncology and Pathogenesis

A postdoctoral position is immediately available to investigate mechanisms of lung tumorigenesis, with particular emphasis on mechanisms of sensitivity and resistance to targeted therapies in human lung cancer, utilizing various molecular techniques, human specimens, and mouse models. Applicants should be highly motivated individuals who have a PhD and/or MD degree, background in molecular biology, interest in cancer biology; a working knowledge of xenografts and transgenic mouse models would be an advantage. The Fellow will be part of a strong collaborative and multidisciplinary research team at Memorial Sloan-Kettering Cancer Center.

Please send curriculum vitae and names of three references to:

William Pao, MD, PhD
Thoracic Oncology Service
Memorial Sloan-Kettering Cancer Center
1275 York Avenue
Box 62
New York, NY 10021

E-mail: paow@mskcc.org

*Memorial Sloan-Kettering Cancer Center
is an Equal Opportunity/Affirmative Action
Employer.*

FEATURED EMPLOYER

Search a
comprehensive list
of job postings from
this employer on
ScienceCareers.org.
Listings updated
three times a week.

Pfizer, Inc.
www.pfizer.com

If you would like to be a featured
employer, call 202-326-6534.

ScienceCareers.org
We know science



**Director, Center for Diabetes and Obesity Research
Robert C. Byrd Health Sciences Center
and
West Virginia University School of Medicine**

West Virginia University (WVU) is seeking an established investigator for **Professor and Director, Center for Diabetes and Obesity Research**. The Director will participate in the implementation of a new **Strategic Research Plan (SRP)** (*Science* 3/12/04) that includes extensive faculty recruitment in interdisciplinary focus areas of research, which includes diabetes and obesity. The **SRP** is designed to expand research as well as doctoral research training. Preference will be given to candidates with a research background in physiology, biochemistry or neuroscience who have a research program in adipose tissue biology, metabolic disorders, lipid transport, atherosclerosis or regulation of food intake using molecular-genetic techniques. The Director will coordinate the recruitment of new investigators and facilitate collaboration between newly recruited investigators and current faculty interested in lipid biochemistry, cardiovascular disease, fatty acid metabolism, molecular genetics as well as neuroendocrinology and diabetes. Priority will be given to candidates with experience in multidisciplinary research initiatives such as NIH Program Project or NIH Center Grants. Excellent opportunities also exist for collaboration with basic and clinical faculty involved in population based research, epidemiology and prevention research as related to diabetes, obesity and cardiac disease.

Candidates should have a transferable NIH funded research program with credentials for appointment as a tenured Professor in either a basic science or clinical department in the School of Medicine. Position includes a competitive salary, laboratory space, startup package, administrative support and resources to recruit additional faculty to the Center who will also have academic tenure-track departmental appointments.

West Virginia University is a land grant Carnegie-designated Doctoral Research/Extensive institution, with approximately 25,000 undergraduate and 5,500 graduate/professional students. WVU Health Sciences Center includes the Schools of Medicine, Pharmacy, Dentistry, and Nursing, each with health professional and graduate programs. Morgantown has 55,000 residents and is rated as one of the best small towns in the U.S., with affordable housing, excellent schools, a picturesque countryside and many outdoor activities.

Qualifications: Ph.D. or M.D. with outstanding research credentials and excellent leadership skills. Submit curriculum vitae and three references, in confidence to: **Diabetes and Obesity Search Committee, WVU Health Sciences, PO Box 9000, Morgantown, WV 26506**. Review of applicants will continue until the position is filled. CV's submitted by e-mail should be sent to **cbsmith@hsc.wvu.edu**.

West Virginia University is an Affirmative Action/Equal Opportunity Employer.



**Tenure-Track Assistant/Associate
Professor
Department of Anatomy
and Cell Biology
Oklahoma State University
Center for Health Sciences
Tulsa, Oklahoma**

The Department of Anatomy and Cell Biology seeks applications for a tenure-track faculty position. Candidates will be expected to develop a strong, independent research program that leads to external funding; startup funds available. Teaching medical students histology and/or gross anatomy is required; additional teaching opportunities are available in the biomedical sciences graduate program. Applicants must possess a Ph.D. or equivalent degree and have postdoctoral experience. Candidates must be eligible for employment under Immigration Reform and Control Act and must provide verification of highest degree.

Send curriculum vitae, statement of research interests, and three letters of reference to: **Director of Human Resources, Oklahoma State University, Center for Health Sciences, Main Hall 1405, 700 N. Greenwood, OK 74106**.

*OSU is an Affirmative Action/
Equal Opportunity Employer.*

**Tufts University School of Medicine
New England Eye Center
Department of Ophthalmology
Exciting Opportunities in Vision
Research at Tufts University
School of Medicine**

New England Eye Center and the Department of Ophthalmology, Tufts University School of Medicine, invite applications from outstanding vision scientists. Candidates must have an M.D. and/or Ph.D. degree. Strong preference will be given to candidates with funded, active research programs in molecular mechanisms leading to the development of glaucoma and retinal diseases. Appointments at the Assistant and Associate Professor levels will be made commensurate with qualifications; competitive salary and startup funds will be offered. Opportunities exist for secondary appointments with basic science departments and collaborative research between the basic and clinical sciences, particularly in the area of retinal cell biology, vascular biology and tissue repair and regeneration. These hires represent continued commitment to excellence in basic and translational sciences at the Boston Campus of Tufts University – New England Medical Center. Faculty will be members of the Tufts Center for Vision Research (www.tevr.org).

Please send a *curriculum vitae*, a statement of research interests and future aims, and the names of three references to: **Dr. Noorjahan Panjwani, Director of Research, Department of Ophthalmology, Tufts University School of Medicine, 136 Harrison Ave., Boston MA 02111, e-mail: noorjahan.panjwani@tufts.edu**.

*Tufts University School of Medicine is an
Affirmative Action/Equal Opportunity Employer.*



**Director
Stem Cell
Research**

**Children's Research Institute
Children's National Medical Center
(CNMC)
Washington, DC**

Children's Research Institute (CRI) at CNMC is seeking applications for Director of its new Stem Cell Research Program. CRI has strong research programs in neurodevelopment, immunology, cancer biology, genetic medicine and neural/muscle degenerative diseases. CNMC is one of the leading research institutions in the Washington, DC area with over \$50 million annually in research funding, and is undergoing a major expansion of research space.

The candidate must have: (1) established a nationally/internationally recognized research program in stem cell biology; (2) a successful track record in obtaining external funding, (3) the ability to coordinate with clinical programs that bring potential therapies to trial. The position includes a package of support and an endowed chair together with a Tenured Associate or Full Professor appointment at the George Washington University School of Medicine.

Applications should be sent by **August 1, 2005** and include a cv, a letter summarizing qualifications and three references to: **Vittorio Gallo, Ph. D., Children's Research Institute, 111 Michigan Ave. NW, Washington, DC 20010**.

POSITIONS OPEN



ENDOWED CHAIR FOR OHIO EMINENT SCHOLAR

**Case Western Reserve University
Center for Stem Cell and Regenerative Medicine**

Case Western Reserve University and the Center for Stem Cell and Regenerative Medicine invite applications for a newly formed position for the Ohio Eminent Scholar endowed chair. Candidates should be established leaders in stem cell science with an outstanding record preferably in targeted areas that will augment the Center's strengths in hematopoietic, neuroscience, musculoskeletal, and orthopedic research. The successful candidate is expected to have a productive research program in fundamental or translational aspect of stem cell biology and a vision for contributing to the leadership of this unique stem cell center, which is a state and federally funded collaborative among Case, University Hospitals of Cleveland, the Cleveland Clinic, and corporate partners. Experience or interest in technology transfer and links to biotechnology commercial entities is desirable. Please send curriculum vitae, a list of three or more references, and a cover letter outlining research focus and interests to:

Stanton Gerson, M.D.
Director, Center for Stem Cell
and Regenerative Medicine
11100 Euclid Avenue, Wearn 151
Cleveland, OH 44106-5065

Case is an Affirmative Action/Equal Opportunity Employer. Minorities and women are encouraged to apply.

ENDOWED CHAIR: GI CANCER RESEARCHER

Indiana University Cancer Center, Indiana University School of Medicine, seeks applications for a **TENURE-TRACK ASSOCIATE or FULL PROFESSOR** position to hold an Endowed Chair in gastrointestinal cancer research and lead a gastrointestinal cancer research program. The successful applicant will have a Ph.D. or M.D. degree or equivalent. This individual is also expected to have established an independent, high-quality, extramurally funded research program. The applicant will have a primary appointment in an appropriate clinical or basic department. Collaboration with basic, behavioral, or clinical investigators is required.

Applicants should send curriculum vitae and description of research and arrange for three letters of recommendation to be forwarded to:

Stephen D. Williams, M.D., Director
Indiana University Cancer Center
535 Barnhill Drive, Room RT 455
Indianapolis, IN 46202

Indiana University is an Equal Employment Opportunity/Affirmative Action Employer, Minorities/Females/Persons with Disabilities.

TWO TENURE-TRACK FACULTY POSITIONS

The University of Illinois College of Medicine at Rockford, Department of Biomedical Sciences seeks two tenure-track faculty members, one in the area of neuroscience and the other in microbiology. An M.D. and/or Ph.D., demonstrated excellence in research, and transferable extramural funds are required. Successful candidates will participate in team teaching to medical students in either pharmacology or microbiology. Rockford is a pleasant four-season city with affordable housing. Submit curriculum vitae, a short statement of research interests, and the names and addresses of three references to: **Janet Stull-Snow, Department of Biomedical Sciences, University of Illinois College of Medicine at Rockford, 1601 Parkview Avenue, Rockford, IL 61107-1897.** Review of applications will begin August 1, 2005, until the position is filled. *The University of Illinois is an Equal Opportunity/Affirmative Action Employer.*

POSITIONS OPEN

**CHAIR, DEPARTMENT OF NEUROBIOLOGY
University of Alabama
at Birmingham**

The University of Alabama at Birmingham (UAB) School of Medicine is seeking applications and nominations for the position of **PROFESSOR** and Chair of the Department of Neurobiology. Successful candidates should be internationally recognized as leaders with demonstrated success in teaching, research, and administration in academic institutions. The successful candidate will be expected to provide inspired leadership and develop a strategic vision for the Department in conjunction with the strategic plan for the school. A clear commitment to academic excellence is required. The Department of Neurobiology is currently ranked seventh in NIH funding, and has consistently ranked in the top ten. UAB is a comprehensive urban university and medical center enrolling 16,000 plus students in 12 schools on its 75-block campus. It is a Doctoral/Research Universities-Extensive institution with awards exceeding \$260 million. The School of Medicine is ranked 16th in NIH funding (2003). The University is the state's largest employer with more than 16,000 employees and a \$1.2 billion annual budget. Nominations and applications should include curriculum vitae, bibliography, and the names and addresses of at least three references and should be submitted electronically (preferably) or mailed to:

Dale J. Benos, Ph.D.
Chair, Department of Physiology and Biophysics
Chair, Search Committee
1530 3rd Avenue South, MCLM 704
Birmingham, AL 35294-0005
E-mail: benos@physiology.uab.edu

Additional information is available via our websites: UAB (website: <http://www.uab.edu>), the School of Medicine (website: <http://www.uab.edu/uasom>), and the Department of Neurobiology (website: <http://www.neurobiology.uab.edu>).

The University of Alabama at Birmingham is an Affirmative Action/Equal Opportunity Employer.

**RESEARCH ASSISTANT PROFESSOR/
POSTDOCTORAL RESEARCH SCIENTIST**

Successful candidate is sought for a joint position (Research Assistant Professor/Postdoctoral Research Scientist) to work on a project funded (National Cancer Institute) through a Long Island University (LIU)/Columbia University (CU) partnership grant (U54). This two-year position will be a joint appointment in which the recruited scientist will be a research assistant professor at LIU and a post-doctoral research scientist at CU Medical Center, College of Physicians and Surgeons. Focus is on research related to ongoing projects in the laboratory of **Dr. P. B. Fisher (CU)**, aspects of which will be the focus of the collaboration with **Dr. A. DePass (LIU)**. Information regarding ongoing projects/directions may be gleaned from Dr. Fisher's recent publications on Pub-Med. E-mail curriculum vitae and list of references to: **Dr. A. DePass (e-mail: adepass@liu.edu)** or **Dr. P. B. Fisher (e-mail: pbfl@columbia.edu)**.

Columbia University is an Affirmative Action/Equal Opportunity Employer.

**COLUMBIA UNIVERSITY MEDICAL CENTER
Department of Pathology**

Positions available for qualified individuals at levels of **POSTDOCTORAL RESEARCH SCIENTIST** and **ASSOCIATE RESEARCH SCIENTIST**. Latter requires at least three years of experience. Must have M.D. or Ph.D. with experience in cell or molecular biology or biochemistry. Preference given to candidates with experience with live cell imaging or immunofluorescence microscopy, since focus of research is on cell migration or mitosis. Send curriculum vitae to: **Dr. E. Marcantonio, Department of Pathology, Columbia University Medical Center, 630 W. 168th Street, New York, NY 10032.** *Columbia University takes Affirmative Action toward Equal Employment Opportunity.*

POSITIONS OPEN



The Department of Medicine at the University of Chicago is seeking a Chief for the Section of Endocrinology, to be appointed at the rank of **ASSOCIATE or FULL PROFESSOR**, commensurate with years of experience and accomplishments. The Section Chief will be responsible for implementing new research programs and expanding current research strengths, further developing clinical opportunities, and enhancing education programs. The successful candidate must have demonstrated professional distinction in research, have an active ongoing research program which has attracted national funding, and have demonstrated effectiveness in mentorship, teaching, administration, and interpersonal skills. Applicants should submit curriculum vitae to: **Dr. Joe G.N. Garcia, Chairman, Department of Medicine, The University of Chicago, 5841 South Maryland Avenue, MC6092, Chicago, IL 60637.** *Affirmative Action/Equal Opportunity Employer.*

**ASSISTANT PROFESSOR OF
RHEUMATOLOGY**

The Division of Rheumatology of the Department of Medicine at New York University (NYU) School of Medicine is recruiting a physician/scientist for a tenure-track position. Individuals with expertise in the area of cell/molecular biology of cartilage/synovium are encouraged to apply. In addition to the facilities of the Department of Medicine and the General Clinical Research Center at NYU School of Medicine, the Division offers support through extensive translational research programs in arthritis based at the Hospital for Joint Diseases. Candidates should have an M.D. or M.D./Ph.D., and have demonstrated the capacity to secure extramural grant funding for research.

Applicants should send a letter of interest and curriculum vitae to:

Steven Abramson, M.D.
Director, New York University
Division of Rheumatology
The Hospital for Joint Diseases
301 East 17th Street
New York, NY 10003
E-mail: stevenb.abramson@nyumc.org

DERMATOLOGY

A **POSTDOCTORAL POSITION** is immediately available to investigate melanocytic tumor progression and tumor cell-immune cell interactions *in vivo*, utilizing novel optical imaging techniques (e.g., *in vivo* confocal and reflectance microscopy). Fellow will be part of a strong collaborative and multidisciplinary research team at Memorial Sloan-Kettering Cancer Center. Applicants should have a Ph.D. and/or M.D. degree, with extensive background and interest in histology, pathology, and biology. Knowledge in immunology and experience with optical imaging techniques are desirable. Please send curriculum vitae and names of references to: **Allan C. Halpern, M.D., Dermatology Service, Memorial Sloan-Kettering Cancer Center, 1275 York Avenue, Box 158, New York, NY 10021.** E-mail: halperna@mskcc.org. *Memorial Sloan-Kettering Cancer Center is an Equal Opportunity/Affirmative Action Employer.*

POSTDOCTORAL ISLET RESEARCHER

A Postdoctoral position is available to study mitochondrial signals for insulin secretion in the pancreatic beta cell. Research will analyze cells with lowered levels of enzymes induced by RNA interference. Ph.D. in cell molecular biology or biochemistry is required. Salary midpoint is \$44,750. Send curriculum vitae to: **Michael J. MacDonald, University of Wisconsin Medical School. E-mail: mjmacdon@wisc.edu.** *UW-Madison is an Equal Opportunity Employer.*

**Associate Chief of Staff for Research and Development
WJB Dorn Veterans Affairs Medical Center**

William Jennings Bryan Dorn Department of Veterans Affairs Medical Center (VAMC) is recruiting an Associate Chief of Staff for Research and Development who will be responsible for oversight and promotion of all research efforts at the VAMC. We are affiliated with the University of South Carolina (USC) School of Medicine (USCSM). USC is the state's flagship research university, with Schools of Public Health (SOP), Nursing, Pharmacy, and an active Graduate School. Dorn VAMC is the major teaching hospital for USCSM, serving the midlands and upper part of South Carolina with a large primary care network; we are the tertiary care referral site for the area's large veteran population. We are a 2-hour drive from both the coast of SC and the NC mountains; we are part of Veterans Integrated Service Network 7 (VISN7), which is extremely supportive of VA Research and Development (R&D). A VISN-wide R&D Service Line supports a Career Development Program for VISN 7 medical centers. Additionally, USC has begun a new initiative to support biomedical research under the direction of the USC Vice President for Research and Health Sciences, with Dorn VAMC playing a major role.

The successful candidate is expected to develop a research program compatible with this new visionary approach to University-wide growth in biomedical research. Qualified candidates have a PhD or MD degree with experience in basic research and/or clinical research and funding, and will contribute meaningfully to these ongoing centers of biomedical research: (1) Public Health and Health Outcomes Research (SOP, VA); (2) Cancer (SC Cancer Center, COBRE colon cancer group, VA clinical trials and basic research, SOP epidemiology, and/or (3) Neurosciences Biology (USC, VA COBRE neurodevelopment group, HIV dementia). USC core research facilities will support each of these groups. Candidates should also have previous experience in administrative and leadership positions, preferably within the DVA system, and a record of research and academic excellence in their field, to qualify for the level of Associate Professor or Professor in a relevant school at USC. Send curriculum vitae to: **Donald Powell, Ph.D., Acting ACOS/R&D and Chairman, ACOS/R&D Search Committee, R&D Service Line (151), Dorn VA Medical Center, 6439 Garners Ferry Road, Columbia, SC 29209.** Review of applications commences on **June 30, 2005.**

An Equal Opportunity Employer.

CONFERENCE

**The Third International Conference
Ubiquitin, Ubiquitin-Like
Proteins, and Cancer**

February 9-11, 2006

The University of Texas M. D. Anderson Cancer Center
Houston, Texas

Organized by Edward T.H. Yeh

Confirmed Speakers

James Chen	Hsing-Jien Kung	Ze'ev Ronai
Mary Dasso	Christopher D. Lima	Brenda Schulman
George N. DeMartino	Leroy F. Liu	William P. Tansey
Raymond J. Deshaies	Michael J. Matunis	Ning Wei
Ronald T. Hay	Frauke Melchior	Allan M. Weissman
Avram Hershko	Kim Orth	Yue Xiong
Erica Johnson	Michele Pagano	Dong-Er Zhang
Peter-M. Kloetzel	Cam Patterson	Yanping Zhang



For information visit:
www.sentrin.org

WORKSHOPS

The Berkeley PGA presents:

**Comparative Genomics
in Biomedical Research**

Principles and Applications of Computational and
Experimental Genomic Tools to Biomedical Problems



Topics

1. Data Retrieval from UCSC and ENSEMBL Browsers
2. VISTA Tools for Comparative Genomics Analysis
3. Applications of Genomic Tools to Clinically Relevant Problems
4. Hands-on Tutorials

This course provides a detailed introduction to using genome sequences and comparative genomics to solve problems of interest to biomedical investigators. Sessions include a combination of technical lectures, scientific testimonials and hands-on computer classes. Ample time will be dedicated to the analysis of the students' favorite genes.

Who should attend:

Graduate students, post-doctoral, junior and senior investigators interested in learning how to leverage genomic resources to understand the mechanisms of disease.

This workshop is accredited with ACCME

For information visit: <http://pga.lbl.gov/Workshop>

October 17-19, 2005
Lawrence Berkeley National Laboratory
Berkeley, California

Great jobs
don't just fall
from the sky. Let
ScienceCareers.org
help.



- Save multiple resumes and cover letters to tailor job search
- Apply online to job postings
- Saved job searches update automatically
- Search by city/state or city/country
- And much more

ScienceCareers.org

We know science



POSITIONS OPEN

FACULTY POSITION, Department of Biology—Temple University's Department of Biology is anticipating openings for full-time, nontenure-track positions starting August 2005. The appointment is for one year and is not tenure track. However, the position may be renewable without limit. Primary teaching assignments will include courses in immunology and genetics, some at a suburban campus. Experience in anatomy and physiology is desirable. Additional assignments may include interdisciplinary and other courses, development of new course, and other activities determined by programmatic needs. Requires a Ph.D. in biological sciences. Candidates may send resume, letter of interest, three letters of recommendation, and transcript of highest academic degree to: **Dr. Shohreh Amini, Chair, Biology Department, Attn: Faculty Search, Temple University, 1900 N. 12th Street, Biology Life Sciences Building, Room 255, Philadelphia, PA 19122. Website: <http://www.temple.edu>.** *Applications from women and underrepresented minorities are especially encouraged. Temple University is an Affirmative Action Employer.*

TENURE-TRACK FACULTY POSITIONS
Wayne State University
School of Medicine

The Departments of Anatomy and Cell Biology and the Kresge Eye Institute of Wayne State University invite applications for joint appointment, tenure-track positions at the rank of **ASSISTANT PROFESSOR** or higher. Candidates should have current external funding and interest including, but not limited to, uveitis, macular degeneration, inherited retinal diseases, or glaucoma. Successful candidates will be expected to participate in teaching, contribute to the growth of a strong vision science research group, and will have access to an expanded pool of talented Ph.D. students. Information on the Departments can be found at **websites: <http://www.med.wayne.edu/anatomy/> and <http://www.med.wayne.edu/kresgeeye>.** Positions include a competitive recruitment package, salary, and comprehensive benefits. Interested applicants should respond to posting #031819 and apply online at **website: <http://jobs.wayne.edu>.** *Wayne State University is an Equal Opportunity Employer.*

BIOINFORMATICS DEVELOPER

WiCell Research Institute is seeking a qualified individual to act as our Bioinformatics Developer. This position will provide programming support to researchers studying gene expression and transcriptional regulation in embryonic stem cells and their differentiated derivatives. Please go to **website: <http://www.wicell.org>** for a complete position description. Please submit a cover letter, curriculum vitae, and list of three references to: **Susan Carlson, Business Manager, WiCell Research Institute, P.O. Box 7365, Madison, WI 53707-7365 or e-mail: susan@wicell.org.** *WiCell is a nonprofit research institute directed by Dr. James Thomson and is an Equal Opportunity/Affirmative Action Employer.*

DATABASE DEVELOPER, BIOINFORMATICS

WiCell Research Institute is seeking a qualified individual to provide database programming support to researchers studying gene expression and transcriptional regulation in embryonic stem cells and their differentiated derivatives. Please go to **website: <http://www.wicell.org>** for a complete position description. Please submit a cover letter, curriculum vitae, and list of three references to: **Susan Carlson, Business Manager, WiCell Research Institute, P.O. Box 7365, Madison, WI 53707-7365 or e-mail: susan@wicell.org.** *WiCell is a nonprofit research institute directed by Dr. James Thomson and is an Equal Opportunity/Affirmative Action Employer.*

POSITIONS OPEN

MEDICAL MICROBIOLOGY COURSE DIRECTOR—The Department of Microbiology at U.T. Southwestern Medical Center at Dallas seeks a full-time (12-month) Director for its medical microbiology course for sophomore medical students. The course (systems based) is integrated with other second-year medical school courses and encompasses immunology, bacteriology, virology, mycology, and parasitology, and consists of lectures, small-group conferences, and laboratory exercises. The candidate will be part of a team of Course Directors who will plan, coordinate, and implement all aspects of the course. This will include the identification and recruitment of faculty and other instructors for all phases of the course, planning of the schedule, preparation of the course syllabus (hard copy and electronic formats), implementation of examinations, monitoring of the course by attending all lectures, delivering didactic lectures, and review sessions as needed. The Director will make recommendations to the Chair of microbiology regarding course content and implementing guidelines from the curriculum committee. The ideal candidate will have an M.D., Ph.D., or M.D./Ph.D., excellent organization skills, and a commitment to medical student education with evidence of excellence as a teacher or prior experience as a course director. Please send curriculum vitae and three letters of recommendation to: **Dr. Michael Norgard, Chair, Department of Microbiology, U.T. Southwestern Medical Center, 5323 Harry Hines Boulevard, Dallas, TX 75390-9048. Fax: 214-648-5905; e-mail: michael.norgard@utsouthwestern.edu.** *U.T. Southwestern Medical Center is an Equal Opportunity/Affirmative Action Employer.*

POSTDOCTORAL RESEARCH ASSOCIATE
Center for Neurodynamics
University of Missouri at St. Louis

A Postdoctoral position in experimental and computational neurophysiology is available in the Center for Neurodynamics at the University of Missouri at St. Louis. Research will involve in vivo imaging of neocortical seizures in the rat, using various imaging methods (intrinsic optical signal, calcium dye imaging, voltage sensitive dye imaging), as well as analysis of patterns of seizure spread using nonlinear-dynamics-based techniques. Research may also include computational studies of synchronization in neural systems. We are seeking a highly motivated scientist with expertise in at least two of the following areas: (1) experimental neuroscience and brain imaging, (2) experimental electrophysiology, (3) nonlinear dynamics in biological systems. A Ph.D. in physics, neuroscience, or related field is required. Salary will be competitive and commensurate with experience. Applications, including curriculum vitae, description of research interests, PDF files of representative publications, and the names of three references, should be sent to: **Dr. Sonya Bahar at e-mail: bahars@umsl.edu.** *The University of Missouri-St. Louis is an Affirmative Action/Equal Opportunity Employer committed to excellence through diversity.*

COLUMBIA UNIVERSITY
Center for Radiological Research

Research positions at several levels (**POSTDOCTORAL RESEARCH SCIENTIST, ASSOCIATE RESEARCH SCIENTIST, STAFF ASSOCIATE**) available immediately for Ph.D.s with training in cellular, molecular, and free radical biology to work on projects involving (1) mitochondrial DNA mutations in environmental cancers; (2) mechanisms of nontargeted radiation effects (adaptive response, bystander response, genomic instability); (3) radiation cytogenetics; (4) mechanisms of environmental carcinogenesis using human cell cultures. For program information, please refer to **website: <http://www.crr-cu.org/index.htm>.** Send curriculum vitae and names of three references to either: **Professor Tom K. Hei (e-mail: hz63@columbia.edu) or Professor Charles R. Geard (e-mail: gej2s@columbia.edu), Center for Radiological Research, Columbia University, 630 West 168th Street, New York, NY 10032.** *Columbia University is an Affirmative Action/Equal Opportunity Employer.*

POSITIONS OPEN



U.S. Department of Agriculture (USDA)/Agricultural Research Service (ARS), Western Human Nutrition Research Center at the University of California, Davis, is seeking a **POSTDOCTORAL RESEARCH ASSOCIATE** (Research Molecular Biologist). The incumbent will serve as part of a team conducting research to investigate the roles of dietary fatty acids and phytochemicals in modulating inflammatory responses and chemoprevention. Successful candidate will require hands-on experience in molecular biological techniques including transgenic mice, bioinformatics, and gene manipulation. A strong background in molecular biology is highly desirable. Recent Ph.D. in biological sciences is required. Salary range is \$52,708.00 to \$68,521.00 per annum, plus benefits. *There are some citizenship restrictions.* Refer to **website: <http://www.ars.usda.gov>** for the full text announcement (RA-05-076L) and for complete application instructions. Send application materials and references to: **Dr. Daniel Hwang, U.S. Department of Agriculture/Agricultural Research Service, 430 G Street, #4160, Davis, CA 95616-4160. Telephone: 530-754-4838; e-mail: dhwang@whnrc.usda.gov.**

USDA/ARS is an Equal Opportunity Provider and Employer.

FACULTY POSITIONS
University of Pennsylvania
School of Medicine

The Department of Psychiatry at the University of Pennsylvania School of Medicine is seeking highly qualified candidates for several faculty positions. The faculty appointments will be at either the **ASSISTANT, ASSOCIATE, or FULL PROFESSOR** rank and in the tenure track. Rank will be commensurate with experience. The successful applicants will have experience in the fields of neuroscience, neurobiology and behavior, addictions research, neuropharmacology, genetics, genetics of epilepsy, and mathematical genetics depending on the specific qualifications for each position. Applicants must have an M.D. or Ph.D., or M.D./Ph.D. degree. For a specific description of each faculty position, please see "Job Opportunities" at **website: <http://www.med.upenn.edu/fapd/>.** For information about the Psychiatry Department, please visit **website: <http://www.med.upenn.edu/psychiatry.html>.** Please submit curriculum vitae, a letter of interest, three reference letters, and indicate Job Reference Number to: **Dwight L. Evans, M.D., c/o Ava Plotnick, Department of Psychiatry, University of Pennsylvania School of Medicine, 305 Blockley Hall, 423 Guardian Drive, Philadelphia, PA 19104. E-mail: plotnick@mail.med.upenn.edu.**

The University of Pennsylvania is an Equal Opportunity/Affirmative Action Employer. Women and minority candidates are strongly encouraged to apply.

POSTDOCTORAL FELLOW to study marine biofouling, including microbiology, and molecular approaches to invertebrate larval biology. The role of biofilm bacteria in recruitment of macroinvertebrates and algae may develop into a personal research program. See **website: <http://www.hawaii.edu/other.pho>.** Send application with resume, reprints, and three letters of recommendation to: **M.G. Hadfield, Kewalo Marine Laboratory, Pacific Biosciences Research Center, University of Hawaii, 41 Ahui Street, Honolulu, HI 96813; e-mail: hadfield@hawaii.edu.** Closing date: June 30, 2005.

PeprTech, Inc., a New Jersey-based biotech company, is seeking a senior **MICROBIOLOGIST** for a full-time position. The candidate should have extensive industrial experience of at least six years in both large-scale fermentation and mammalian-cell culturing. Education: the candidate must have a Master's degree in microbiology.



Please send resumes to: **PeprTech, Inc., 5 Crescent Avenue, Rocky Hill, NJ 08553-0275.**

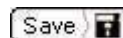
Post or update your resume/CV on ScienceCareers.org and enter to win an iPod shuffle.

When you update your resume/CV between now and 17 June, your name will be entered in a drawing to win 1 of 5 iPod shuffles being given away by ScienceCareers.org.*

* 5 names will be drawn on 20 June and the winners will be notified via email.

It's easy to do:

1. Visit ScienceCareers.org and click on [Log in to my account](#).
2. Either log in to your account or create a new account.
3. Click on  in the tool bar at top or [Post Resume](#) on the left side list.
4. Click the edit icon. 
5. Make any necessary changes OR simply click the save button at the bottom of the page.



This will post/update your resume and reflect that day's date.

ScienceCareers.org
We know science 

SEB_{at} Barcelona2005

SEB_{at} Barcelona2005

Monday 11th - Friday 15th July 2005

Register before 17th June 2005 at www.sebiology.org

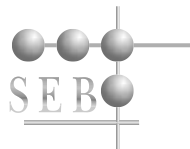
Join the SEB for 5 days of cutting edge science at the Universitat Autònoma de Barcelona.

Cell Biology: Salinity, Mechanisms of Thermal Limits, Plasticity to Temperature in Ectotherms: Genes to Organisms, NO signalling, Cyto and Nucleo Skeleton

Plant Biology: Cereal genomics, Phloem-insect interactions, Leaf metabolism in development, NO signalling, General plant biology, Plant proteomics, Protein: protein interactions, Below-ground processes (soil-root interface biology), Drought tolerance

Education: Science communication: Publishing your research a future perspective, Science communication: Communicating effectively with non-academic audience, Teaching Technology Posters

Animal Biology: Genomics in Mediterranean aquaculture, Insect physiology, General biomechanics, Developmental phylogeny, Neuropeptide structure, function and evolution, Environmental constraints on locomotion and energetics in aquatic locomotion, The comparative physiology of the cardiovascular and respiratory systems: A tribute to E.W. (Ted) Taylor, A tribute to Bob Bouillier - Whole organism to mitochondria, Comparative genomics, proteomics and identification of new molecular targets for drug action, Non-Steady Locomotion, General animal biology



Universitat
Autònoma
de Barcelona

POSITIONS OPEN

POSTDOCTORAL AND CLINICAL FELLOWSHIPS

at the
National Institutes of Health
U.S. Department of Health
and Human Services

Website: <http://www.training.nih.gov>
*NIH is dedicated to building a diverse
community in its training and employment
programs.*

POSTDOCTORAL POSITION
Diabetes and Metabolism

We seek a Postdoctoral Fellow with a strong background in molecular and cell biology. Our research focuses on the pathogenesis of insulin resistance, type 2 diabetes, and related conditions. We offer an exciting, multidisciplinary, team-oriented research environment with multiple ongoing studies. Our human metabolic research unit is fully equipped for performing state-of-the-art in vivo metabolic and vascular function studies. Our research laboratory is also fully equipped with new equipment and computers for performing all aspects of molecular/signaling analyses in human tissue and cell culture systems. This position is specially suited for individuals interested in doing translational research relevant to diabetes and insulin resistance.

Nestled in the Texas Hill Country, just three hours drive from the Gulf of Mexico, San Antonio offers an attractive multicultural lifestyle with a warm and sunny climate. All postdoctoral appointments are designated as security-sensitive positions. Please contact: **Ralph A. DeFronzo, M.D.** or **Nicolas Musi, M.D.**, The University of Texas Health Science Center at San Antonio. Telephone: 210-358-7350; e-mail: musi@uthscsa.edu.

The University of Texas Health Science Center at San Antonio is an Equal Employment Opportunity/Affirmative Action Employer.

TWO POSTDOCTORAL POSITIONS available at the Hormel Institute, University of Minnesota, Austin, Minnesota, to study the molecular and cellular biology in ocular diseases and carcinogenesis. We are seeking self-motivated Ph.D.s with experience in biochemistry, molecular and cellular biology, cancer biology. Experience in microarray, signal transduction, apoptosis, RNA interference, transgenic mice, or proteomics is a plus. Please send your curriculum vitae and the names and telephone numbers of three references to: **Dr. David W. Li, The Hormel Institute, University of Minnesota, 801 16th Avenue, NE, Austin, MN 55912.** Fax: 507-437-9606; e-mail: dwlil688@hotmail.com.

The University of Minnesota is committed to the policy that all persons shall have equal access to its programs, facilities, and employment without regard to race, color, creed, religion, national origin, sex, age, marital status, disability, public assistance status, veteran status, or sexual orientation.

POSTDOCTORAL POSITION available immediately for modeling Down syndrome in mice. We have recently generated a new mouse model of Down syndrome using chromosome engineering and are in the process of generating a mouse model trisomic for all human chromosome 21 syntenic regions. The candidates should have prior experience in rodent behavioral phenotyping and/or molecular biology techniques. Interested applicants should e-mail curriculum vitae, statement of scientific interests and career goals, and contact information of three references to: **Dr. Eugene Yu, Assistant Member, Genetics Program, Roswell Park Cancer Institute at e-mail: yucjin.yu@roswellpark.org.**

CHEMICAL ENGINEERING AND PUBLIC POLICY

FACULTY OPENING Carnegie Mellon University. Details at website: <http://www.epp.cmu.edu>. Resume, references, and research interests to: **Granger Morgan, EPP, Carnegie Mellon University, Pittsburgh, PA 15213.**

POSITIONS OPEN

POSTDOCTORAL POSITIONS
NEUROSCIENCE

Two positions for a Postdoctoral Fellow in the Neuroscience Group at the University of South Dakota (USD) School of Medicine are available immediately to study the cellular mechanisms underlying learning and memory in an in vitro model of eyeblink classical conditioning in turtles. An M.D. and/or Ph.D. is required. Experience in intracellular recording techniques is required for one position and experience in electrophysiology, immunocytochemistry, and molecular approaches is desired for all applicants. The Neuroscience Group is funded by an NIH Center of Biomedical Research Excellence award which provides for many opportunities for Postdoctoral Fellows. The Group is highly interactive and there is ample opportunity for collaboration. Information about the Group can be found at website: <http://www.usd.edu/med/biomed/faculty/biosketch/joycekeifer.cfm>.

Interested candidates should send a cover letter with statement of research experience and interests, curriculum vitae, and names of three references to: **Joyce Keifer, Ph.D., Neuroscience Group, Division of Basic Biomedical Sciences, University of South Dakota School of Medicine, 414 E. Clark Street, Vermillion, SD 57069-2390.** E-mail: jkeifer@usd.edu. Review of applications will begin June 27, 2005, until the positions are filled. USD is an Equal Opportunity/Affirmative Action Employer.

FACULTY POSITION, IMMUNOLOGY
Department of Microbiology and Immunology
Vanderbilt University
School of Medicine

We invite applications for a tenure-track faculty position in immunology at the ASSISTANT or ASSOCIATE PROFESSOR level. We seek an individual with research interests that complement the ongoing research in our Department (website: <http://www.mc.vanderbilt.edu/microbio/>). Target areas include, but are not restricted to immune memory and vaccines, stem cell biology, epigenetic regulation of immune responses, neuro-immunology, and innate, mucosal, and tumor immunology. Applicants should send curriculum vitae, a statement of current and future research interests, and three letters of recommendation to: **Luc Van Kaer, Chair, Search Committee, Department of Microbiology and Immunology, Vanderbilt University School of Medicine, Room A-5301, MCN, 1161 21st Avenue South, Nashville, TN 37232.** Inquiries, applications, and recommendation letters can be directed via e-mail: luc.van.kaer@vanderbilt.edu. The deadline for receipt of applications is August 31, 2005. *Vanderbilt University is an Affirmative Action/Equal Opportunity Employer. Women and minority candidates are encouraged to apply.*

A POSTDOCTORAL POSITION is available immediately at the Research Institute for Children, a division of Children's Hospital to investigate bacterial species composition and polymicrobial diseases using molecular analyses. Visit our website: <http://www.chnola-research.org/faculty/ferris/index.htm>, for additional information regarding this research. Applicants should have a terminal degree (Ph.D., M.D., etc.) with a background in microbiology, molecular biology, and phylogenetic analysis. Interested applicants should (1) complete an application form, which can be found at website: <http://www.chnola.org>, and (2) send the application, curriculum vitae, and the names of three references by e-mail: tpierce@chnola-research.org or mail: **Mr. Tim Pierce, The Research Institute for Children, Children's Hospital, 200 Henry Clay Avenue, New Orleans, LA 70118.** *Equal Employment Opportunity.*

Additional job postings not featured in this issue can be viewed online at website: <http://www.sciencecareers.org>. New jobs are added daily!

POSITIONS OPEN

The University of Oklahoma
HEALTH SCIENCES CENTER

POSTDOCTORAL POSITION available immediately to study mechanisms of autoimmunity, molecular mimicry, and infection and/or the pathogenesis of inflammatory heart disease. Experience in immunology required. Opportunities in NIH Immunology Training Program at the University of Oklahoma Health Sciences Center (OUHSC). Submit curriculum vitae and names of three references to: **Dr. Madeleine Cunningham, Department of Microbiology and Immunology, University of Oklahoma Health Sciences Center at fax: 405-271-2217 or e-mail: madeleine-cunningham@ouhsc.edu; or mail to: Madeleine W. Cunningham, Ph.D., George Lynn Cross Research Professor, Microbiology and Immunology, University of Oklahoma Health Sciences Center, Biomedical Research Center, Room 217, 975 NE 10th Street, Oklahoma City, OK 73104. Telephone: 405-271-3128; laboratory: 405-271-1147; fax: 405-271-2217.**

ASSISTANT PROFESSOR/RESEARCH
ASSISTANT PROFESSOR
Department of Physiology
The Chinese University of Hong Kong
(05/084(540)/2) (18 June 2005)

Applicants should have (i) a relevant Ph.D. degree; (ii) three to four years' postdoctoral experience; and (iii) a strong research track record in one of the following areas: (a) neurosciences and brain research; (b) cardiovascular biology and medicine; (c) stem cell biology and molecular endocrinology. Applicants with strong molecular background and/or experience with systems-level function, stem cell biology, and electrophysiological techniques are particularly welcome. The appointee will (i) teach undergraduate and postgraduate courses; and (ii) apply his/her expertise in one of the aforementioned areas so as to complement and strengthen the Department's existing research and teaching activities. Appointment will initially be made on a fixed-term contract basis for up to two years from August 2005 or as soon as possible thereafter, renewable subject to mutual agreement.

Salary and fringe benefits: Salary will be highly competitive, commensurate with qualifications and experience. The University offers a comprehensive fringe benefit package including medical care, a contract-end gratuity for an appointment of two years, and housing benefits for eligible appointees.

Further information about the University and the general terms of service for appointments is available at website: <http://www.cuhk.edu.hk/personnel>.

The terms mentioned herein are for reference only and are subject to revision by the University.

Application procedure: Please send full resume, copies of academic credentials, a publication list, and/or abstracts of selected published papers, together with names, addresses, and fax numbers/e-mail addresses of three references to whom applicants' consent has been given for their providing references (unless otherwise specified) to: **Personnel Office, The Chinese University of Hong Kong, Shatin, New Territories, Hong Kong (fax: 852-2603-6852)** on or before 18 June 2005. The Personal Information Collection Statement will be provided upon request. Please quote the reference number and mark Application-Confidential on cover. Note: The University reserves the right not to fill the post or to fill the post by invitation.

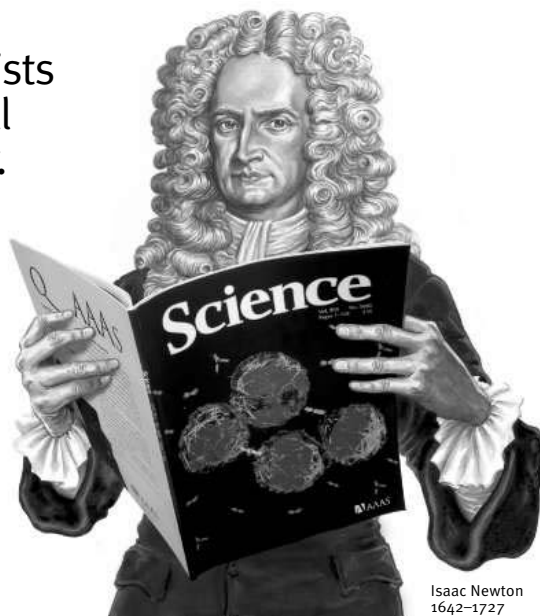
SAN FRANCISCO, CALIFORNIA

POSTDOCTORAL RESEARCH FELLOW position available at University of California San Francisco Division of Nephrology. *Must be U.S. citizen or permanent resident and eligible for NIH training grant.* Please send curriculum vitae to: **Dr. Stephen L. Gluck, 513 Parnassus Avenue, Box 0532, San Francisco, CA 94143-0532 or e-mail: glucksl@medicine.ucsf.edu.**

Great scientists
don't just fall
from the sky.



Post your jobs on
ScienceCareers.org
with **Post and Go.**



Isaac Newton
1642–1727

- Jobs are posted within one business day and stay up for 8 weeks.
- Applicable jobs are also searchable on the following websites:
 - Biocompare
 - National Postdoctoral Association (NPA)
 - Stanford University School of Medicine
 - *Science's* Signal Transduction Knowledge Environment (STKE)
 - *Science's* Aging Knowledge Environment (SAGE)
 - *Science's* Next Wave
- ScienceCareers.org averages over 1 million page views and over 75,000 unique visitors each month.¹
- All jobs are included in our Job Alerts e-mail system.

All this exposure means you can find the right scientist for your vacancy quickly and inexpensively.

For more information,
contact Beth Dwyer
Phone: 202-326-6534
E-mail: bdwyer@aaas.org

ScienceCareers.org

We know science



¹ *Science* Webtrends Reports.

Q
Who's making
Science a
household name?



Photo: Planet Photo Studio, Milan, Italy

“ I read my *Science* undisturbed and absorbed at home. Thank you, *Science*, for being so informative, knowledgeable, and abreast of times, and for giving me the intellectual stimulation I crave. ”

AAAS member Professor Fioretta Benedetto Mattia

AAAS is committed to advancing science and giving a voice to scientists around the world. Helping our members stay abreast of their field is a key priority.

One way we do this is through *Science*, which features all the latest groundbreaking research, and keeps scientists connected wherever they happen to be.

To join the international family of science, go to www.aaas.org/join.



ADVANCING SCIENCE. SERVING SOCIETY

www.aaas.org/join

MARKETPLACE

**Custom Peptides
& Antibodies**

Best Service & Price! Compare and Save!
Free Sequence and Antigenicity Analyses
Alpha Diagnostic (800) 736-5777
www.4adi.com service@4adi.com

**Diverse Small Molecules
Ready for Screening**

Upwards of 200,000
Compounds
Pre-Plated in DMSO
Very Competitively
Priced
Next Day Delivery*

**ChemBridge
Corporation**



Website: www.chembridge.com
Email: sales@chembridge.com

(800) 964-6143 or (858) 451-7400 Fax: (858) 451-7401
* Limited to 100,000

Molecular Cloning Laboratories

High throughput DNA sequencing
Gene synthesis \$2/bp any size
Protein expression & purification
Yeast 2 hybrid/phage displaying

www.mclab.com, 888-625-2288

POLYMORPHIC
Polymorphic DNA Technologies, Inc.

SNP Discovery
using DNA sequencing
\$.01 per base.

Assay design, primers,
PCR, DNA sequencing
and analysis included.

888.362.0888

www.polymorphicdna.com • info@polymorphicdna.com

The World of Science Online

SAGE KE
E-Marketplace
ScienceCareers.org
Science's Next Wave
Science NOW
STKE

Science
www.scienceonline.org

CUSTOM ANTIBODIES

Over 15 Years Experience Unlimited Flexibility

ABR

ABR--Affinity BioReagents

800.527.4535 www.antibodyondemand.com

**Anti Asialo GM1
For NK Cell Depletions**

Wako

Wako BioProducts
www.wakousa.com
(877) 714-1920

MARKETPLACE

**GET RESULTS FAST...
PEPscreen®
Custom Peptide Libraries**

DELIVERY IN 7 BUSINESS DAYS!

- QC: MS supplied for all peptides
- Amount: 0.5 - 2 mg
- Length: 6-20 amino acids
- Modifications: Variety available
- Format: Lyophilized in 96-tube rack
- Minimum order size: 48 peptides
- Price: \$50.00 per peptide (unmodified)

SIGMA
GENOSYS

www.sigma-genosys.com/MP

North America and Canada • 1-800-234-5362
Email: peptides@sial.com

DNA Peptide

Free Setup and
Desalting Call and Compare

**GENE Synthesis, Site Mutagenesis,
Protein Expression and more**
Compare and Save

DNA Sequencing \$10 EACH

Custom Anti-peptide Antibody
(Including peptide synthesis)
\$850

Genemed Synthesis

800.344.5337 Fax: 650.952.9540

WebSite: www.genemedsyn.com

Widely
Recognized
Original &
Guaranteed

KlenTaq I 8¢/u

Truncated
Taq DNA
Polymerase
Withstand 99°C

US Pat # 5,436,149

Call: **Ab Peptides** 1•800•383•3362
Fax: 314•968•8988 www.abpeps.com

Design
tagged primers for
Expression cloning
In vitro expression

**Xpression
Primer 3**

www.PremierBiosoft.com 650-856-2703

Pep-T-Topes

~1 mg crude (70% ave.)
1-15 mers, @ ≥ 96 peptides

PEPSCAN

\$35 / peptide

www.pepscan.com

Grasp the Proteome™

Protein Purification/Detection



Still using Streptavidin?

NeutrAvidin™ Protein offers ultra-low nonspecific binding at an *unbelievably* low price

NeutrAvidin™ Protein offers the highest possible specificity for biotin, yielding the lowest nonspecific binding. NeutrAvidin™ Protein provides exceptional performance for both purification and detection of biotin-labeled proteins. If you're still using Streptavidin, it's time to discover the advantages of NeutrAvidin™ Tools.

Advantages over streptavidin:

- Highest specificity for biotin binding
- No nonspecific binding to cell-surface proteins
- High signal-to-noise ratio in detection systems
- Saves money without sacrificing quality

Properties of biotin-binding proteins

	Avidin	Streptavidin	NeutrAvidin™ Protein
Molecular Weight	67K	53K	60K
Biotin-binding Sites	4	4	4
Isoelectric Point (pI)	10	6.8-7.5	6.3
Specificity	Low	High	Highest
Affinity for Biotin (K_d)	10 ⁻¹⁵ M	10 ⁻¹⁵ M	10 ⁻¹⁵ M
Nonspecific Binding	High	Low	Lowest

Available in bulk quantities and in the following convenient formats:

- Immobilized NeutrAvidin™ Protein on Agarose
- UltraLink® Immobilized NeutrAvidin™ Protein
- Soluble NeutrAvidin™ Protein
- HRP- and Alkaline Phosphatase-labeled NeutrAvidin™ Protein
- Fluorescein-labeled NeutrAvidin™ Protein
- Maleimide-activated NeutrAvidin™ Protein
- 96- and 384-well NeutrAvidin™ Plates

FREE Avidin-Biotin Handbook from Pierce, the leader in avidin-biotin products! Visit the Pierce web site at www.piercenet.com/ab95d or call 800-874-3723 to request your copy today.



www.piercenet.com/neu22d

PIERCE



Tel: 815-968-0747 or 800-874-3723 • Fax: 815-968-7316

Technical Assistance E-mail: TA@piercenet.com • Customer Assistance E-mail: CS@piercenet.com

Outside the United States, visit our web site or call 815-968-0747 to locate your local Perbio Science branch office (below) or distributor

Belgium & Dist.:
Tel +32 53 85 71 84
euromarketing@perbio.com

China:
Tel +86 10 8049 9033
support@perbio.com.cn

France:
Tel 0800 50 82 15
euromarketing@perbio.com

Germany:
Tel 0228 9125650
de.info@perbio.com

Hong Kong:
Tel 852 2753 0686
SalesHK@perbio.com

The Netherlands:
Tel 076 50 31 880
euromarketing@perbio.com

United Kingdom:
Tel 0800 252185
uk.info@perbio.com

Switzerland:
Tel 0800 56 31 40
euromarketing@perbio.com

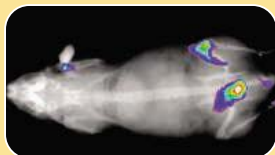
© Pierce Biotechnology, Inc., 2005. Pierce products are supplied for laboratory or manufacturing applications only. NeutrAvidin™ and UltraLink® are trademarks of Pierce Biotechnology, Inc.

96
PERBIO

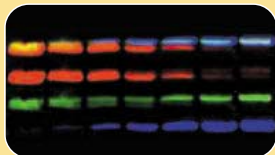
Supplied with all
new **KODAK** Molecular
Imaging Software

IT'S THE NEW IRONMAN OF MOLECULAR IMAGING.

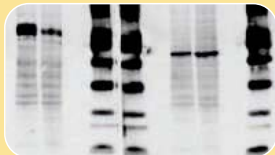
Kodak is a trademark. © Eastman Kodak Company, 2005
Qdot is a registered trademark of Quantum Dot Corporation.
SuperSignal is a registered trademark of Pierce Biotechnology, Inc.



Near-IR fluorescence and digital
x-ray overlay



Multiplexed fluorescence imaging of
Western blots using Qdot® Conjugates



Chemiluminescent imaging of Western blots
using Pierce SuperSignal West Pico Substrate

INTRODUCING THE KODAK IMAGE STATION 4000 DIGITAL IMAGING SYSTEM. WITH SUPERIOR RESOLUTION, ENHANCED SENSITIVITY, AND OUTSTANDING VERSATILITY, IT OUTPERFORMS THE COMPETITION EVERY TIME.

Multi-wavelength fluorescence illumination, radioisotopic imaging capability, and an optional X-ray Imaging Module make it the most versatile platform for *in-vitro* and *in-vivo* imaging. With 4-million pixel resolution (10 μ /pixel) and true 16-bit imaging, it resolves features and measures intensity more accurately than other systems. And it's **5x more sensitive** than our currently available *in-vitro/in-vivo* CCD imaging systems. All that, plus

Kodak's proven track record of delivering unmatched convenience and ease of use.

It's got the strength and power to go the distance, wherever your research takes you.



U.S. 1-877-SIS-HELP, exp. code 25
O.U.S. +1-203-786-5657
www.kodak.com/go/imagestation

KODAK MOLECULAR IMAGING SYSTEMS

